

Nqobile Khani

Influence of Airport Factors and Mission Fuel
Burn Optimised Aircraft Trajectories on Severity
and Engine Life

School of Aerospace, Transport and Manufacturing

PhD Thesis

School of Aerospace, Transport and Manufacturing

Propulsion Engineering Centre

PhD Thesis

Academic Year: 2013/2014

Nqobile Khani

Influence of Airport Factors and Mission Fuel
Burn Optimised Aircraft Trajectories on Severity
and Engine Life

Supervisors: Doctor Vishal Sethi and Professor Pericles Pilidis

20th June 2014

© Cranfield University, 2014. All rights reserved. No part of this publication may be reproduced without the written permission of the copyright holder.

Abstract

The continuous growth of air transport has raised concerns about global aircraft fuel consumption, emissions and noise. Industry's efforts have identified that to reduce future emissions and the impact of aircraft operations on the environment will require contribution from: a) New technologies with better efficiency b) Improved asset management and c) Greener manufacturing and recycling processes. This research falls under asset management and involves aircraft trajectory optimisation. Most aircraft trajectory optimisation studies concentrate on optimising fuel burn, emissions and noise. Fuel burn is the dominant contributor to operating costs. During the course of this work, no work was found to better understand from an operator's perspective how the optimal solutions for minimising fuel burn and protecting the environment will impact on engine useful life and the engine operating costs. Also no work was found to understand how engine component degradation will impact on the optimised solutions for fuel burn and engine life.

The contribution to knowledge from this research is a) the assessment of the impact of airport severity factors on engine life consumption and aircraft performance and b) the assessment and quantification of the change in engine life usage when optimising for flight mission fuel burn and the change in flight mission fuel burn when optimising for engine life usage; in both cases the effects of engine component degradation are considered and assessed.

The trade-offs between mission fuel burn and engine life optimised trajectories are presented here for a clean (new) engine for three routes (London–Madrid, London–Ankara and London–Abu Dhabi). The engine life calculated was the HPT blade life and HPT disc life due to creep, fatigue and oxidation failure modes independent of each other. Mission fuel burn and engine life trajectory optimisation assessments were conducted to incorporate the effects of degradation after 3000, 4500 and 5250cycles of operation. Further assessments were made linking aircraft performance to airport severity factors for the clean engine, after 3000cycles and after 5250cycles. A techno-economic environmental risk assessment approach was used.

The results indicate that airports at higher altitudes e.g. Cairo, suffer more severity due to higher operating temperatures, but benefit from less climb fuel burn and lower operating costs. The severity and fuel burn for take-off at airports with higher ambient temperatures was found to be more due to the higher operating temperatures required. The operating cost at these airports was thus higher. The fuel burn optimised trajectories were found to be achieved at higher operating temperatures with reduced blade life (due to creep, fatigue and oxidation). In particular, for London–Madrid, the blade creep and blade oxidation lives were found to reduce by -3.4% and -2.1% respectively. The blade oxidation life optimised trajectories showed increase in fuel burn of +3.6% and +4.9% for London–Madrid and London–Ankara respectively. The blade creep life optimised trajectories for London–Abu Dhabi were found to benefit from less fuel burn during climb. The disc creep life optimised trajectories showed benefit in fuel burn for London–Ankara and London–Abu Dhabi.

The conclusions from the study are:

- High OAT and high altitude airports such as Abu Dhabi require higher operating temperatures which have severe consequences on the engine component life, fuel burn and emissions.
- Fuel burn optimised trajectories have a negative effect on the blade life due to creep, fatigue and oxidation due to higher maximum operating temperatures. However, the reduction in fuel burn outweighs the drop in life, thus benefitting to the operating costs.
- Optimising for blade creep life benefits the fuel burn for London–Abu Dhabi due to less fuel burn at climb
- The blade oxidation life optimised trajectories are detrimental to the fuel burn due to slower cruise speeds and more time spent at cruise and descent
- The disc creep life optimised trajectories benefit the fuel burn for London – Ankara and London–Abu Dhabi due to flying at higher cruise altitudes and burning less fuel.

The recommendations from this research include making improvements to the framework such as a) Integrating the lifing methodologies because in reality the failure modes are not entirely independent of each other but do interact b) Develop and incorporate a diagnostics and prognostics tool to predict levels of degradation c) Using actual waypoints and incorporate horizontal trajectory profiles d) Future studies can include noise as an objective, which though mentioned has not been within the scope of this work. e) A key driver to lower operating costs is a considerable reduction in fuel burn. Maintenance costs will inevitably rise with engine life consumption. Further study of the trade-offs between fuel burn and engine life is therefore recommended.

Acknowledgements

First of all I thank my Lord and Saviour Jesus Christ, God my Father and the Holy Spirit for His infinite grace and mercy that have made it possible for me to fulfil my purpose and pursue my desires, to Him I give the glory.

It is with love that I am most grateful to my family. To my mum Elidah Khani, thank you for the sacrifices you make to see me succeed and fulfil my dreams; to my brother Lungelo for taking time off your accounts to proof read my first chapter; to my daughter Noluthando for being my inspiration to succeed and to my sister Florence and all of my family, my brothers and sisters for your encouragement. To my aunts and uncles, I extend my love.

Throughout this research, I have been blessed to meet various people who have been of invaluable assistance and guidance to me. The few I mention here do well to represent them all. I give a big thank you to my supervisor Dr Bobby Sethi for supporting me not only with the research but also with personal issues.

My sincere gratitude goes to Professor Pericles Pilidis, Professor Riti Singh and the late Dr Kenneth Ramsden for providing technical support and guidance. I extend my gratitude to my learned friends, Dr Devaiah Nalianda Karumbaiah, Dr Hugo Pervier and Dr Uyioghosa Igie for the many times you exchanged ideas with me and challenged my thinking. I am grateful to Dr Stephen Ogaji (Verity Concepts), Dr Georgios Doulgaris (Alstom), Dr Fernando Colmenares (University of Colombia) and Dr George Panagiotou (Alstom) for their support and technical expertise in helping my understanding.

I thank Messrs Matthew Sammut and Matthew Xuereb from the University of Malta and Mr Jonathan Haynes from the Cranfield University IT Department for helping me with my software and programming issues. I also thank the Cranfield University IT department for their support in getting me up and running all the times when my laptop packed up and failed.

I extend a profound thank you to all my friends and colleagues past and present who worked with me and to those who gave their advice, input and support, particularly to Abu Abdullahi Obonyegba, Emanuelle Pagone, Benjamin Venediger, Rukshan Navaratne, Clara Segovia, Subramanian Chandran, Wequin Gu, Barinyima Nkoi, Thierry Sibilli, Alex Nind, Tashfeen Mahmood, Panos Giannakakis and Christos Tsoskas.

I also thank the administrative staff of the Cranfield University Propulsion Engineering Centre: Mrs. Gillian Hargreaves, Mrs. Nicola Datt, Mrs. Sheila Holroyd, Mrs. Claire Bellis and Mr. Josh Redmond for their incredible support throughout the course of this PhD.

Lastly but not least I thank Miss Miriam Burrell for being a blessing to me. And thank you to Pastor Kunle Anderson for your prayers; brother Darlington for always having a word of encouragement and blessing, and to brother Isaiah Allison and family for your incredible support.

It is with gratitude that I acknowledge the financial support from Cranfield University and the European Union CLEANSKY project.

Table of contents

| | |
|---|-------------|
| ABSTRACT..... | III |
| ACKNOWLEDGEMENTS..... | V |
| TABLE OF CONTENTS..... | VII |
| LIST OF FIGURES..... | XIII |
| LIST OF TABLES | XIX |
| NOMENCLATURE..... | XX |
| CHAPTER 1..... | 1 |
| INTRODUCTION..... | 1 |
| ABSTRACT | 1 |
| 1.1 BACKGROUND | 1 |
| 1.2 CONTEXT | 2 |
| 1.3 REVIEW OF PAST STUDIES | 4 |
| 1.4 CONTRIBUTION TO KNOWLEDGE | 23 |
| 1.5 RESEARCH OBJECTIVES..... | 23 |
| 1.6 METHODOLOGY: STEPS TO COMPLETE THE RESEARCH | 23 |
| 1.6.1 Establishing the Focus of the Study | 24 |
| 1.6.2 Identifying the Specific Objectives of the Study..... | 25 |
| 1.6.3 Selecting the Research Method | 25 |
| 1.6.4 Developing the Research Framework | 25 |
| 1.6.5 Carrying Out the Assessments..... | 27 |
| 1.6.6 Results and Analysis | 28 |
| 1.6.7 Writing Up | 28 |
| 1.6.8 Enabling Dissemination..... | 28 |
| 1.7 THESIS STRUCTURE | 28 |
| 1.8 ADDITIONAL WORK UNDERTAKEN DURING RESEARCH..... | 31 |
| FIGURES FOR CHAPTER 1..... | 32 |
| REFERENCES FOR CHAPTER 1 | 61 |
| CHAPTER 2..... | 65 |
| ENGINE AND AIRCRAFT PERFORMANCE..... | 65 |
| ABSTRACT | 65 |
| 2.1 INTRODUCTION | 65 |
| 2.2 AIRCRAFT TECHNOLOGY | 65 |
| 2.2 AIRCRAFT CHARACTERISTICS | 66 |
| 2.3 ENGINE PERFORMANCE | 66 |
| 2.3.1 Thermal Efficiency..... | 67 |
| 2.3.2 Propulsive Efficiency | 67 |
| 2.2.3 Overall Efficiency..... | 68 |
| 2.4 GAS TURBINE ENGINE DEGRADATION | 68 |
| 2.4.1 Mechanisms of Engine Degradation..... | 68 |
| 2.4.1.1 Common Causes of Performance Deterioration | 69 |

| | |
|---|-----------|
| 2.4.1.2 Evolution of Degradation | 72 |
| 2.4.1.3 Gradual and Rapid Degradation | 72 |
| 2.4.1.4 Engine Rating | 72 |
| 2.4.2 Engine Component Degradation | 73 |
| 2.4.2.1 Airfoils | 73 |
| 2.4.2.2 Compressor | 74 |
| 2.4.2.3 Combustion System | 74 |
| 2.4.2.4 Turbine | 74 |
| 2.4.3 Effect of Degradation on the Engine | 75 |
| 2.4.3.1 Component Performance Degradation | 76 |
| 2.4.3.2 Influence of Component Performance Degradation | 76 |
| 2.5 AIRCRAFT PERFORMANCE | 77 |
| 2.6 ENGINE PERFORMANCE MODEL | 78 |
| 2.6.1 Engine Design Point Validation | 79 |
| 2.6.2 Off - Design Performance | 80 |
| 2.6.3 Engine Degradation Modeling | 81 |
| 2.6.4 Degraded Engine Performance | 81 |
| 2.7 AIRCRAFT PERFORMANCE MODEL | 82 |
| 2.7.1 Aircraft Performance Validation - Payload Range Diagram | 83 |
| 2.7.2 Aircraft Performance (Degraded Engine) | 84 |
| 2.8 SUMMARY AND CONCLUSIONS | 84 |
| FIGURES FOR CHAPTER 2 | 86 |
| REFERENCES FOR CHAPTER 2 | 93 |
| CHAPTER 3 | 95 |
| GAS TURBINE AERO - ENGINE LIFING | 95 |
| ABSTRACT | 95 |
| 3.1 INTRODUCTION | 95 |
| 3.2 GAS TURBINE ENGINE LIFE LIMITED PARTS | 95 |
| 3.3 GAS TURBINE ENGINE LIFE USAGE | 96 |
| 3.3.1 Engine Life Limiting Failure Modes | 96 |
| 3.3.1.1 Damage Due to External Factors | 96 |
| 3.3.1.2 Damage Due to Operating Conditions | 97 |
| 3.3.1.2.1 Creep | 97 |
| 3.3.1.2.2 Fatigue | 97 |
| 3.3.1.2.3 Oxidation | 98 |
| 3.3.2 Potential Engine Failure Modes | 98 |
| 3.3.2.1 Combined Modes | 99 |
| 3.3.3 Engine Flight Mission | 99 |
| 3.4 ENGINE LIFING MODEL | 100 |
| 3.4.1 The Structure of the Lifing Model | 100 |
| 3.4.1.1 Stress Analysis | 101 |
| 3.4.1.1.1 Blade Stress Analysis | 101 |
| 3.4.1.1.2 Disc Stress Analysis | 101 |
| 3.4.1.2 Creep Analysis | 102 |
| 3.4.1.3 Low Cycle Fatigue Analysis | 102 |
| 3.4.1.4 Oxidation Analysis | 102 |

| | |
|---|------------|
| 3.4.1.5 Cooling Module..... | 103 |
| 3.4.2 Engine Lifting Module Verification and Validation | 103 |
| 3.5 SUMMARY AND CONCLUSIONS | 103 |
| FIGURES FOR CHAPTER 3..... | 105 |
| REFERENCES FOR CHAPTER 3 | 110 |
| CHAPTER 4..... | 111 |
| GAS TURBINE AERO - ENGINE EMISSIONS..... | 111 |
| ABSTRACT | 111 |
| 4.1 INTRODUCTION | 111 |
| 4.2 GASEOUS EMISSIONS | 111 |
| 4.2.1 NO _x Emissions..... | 113 |
| 4.3 AVIATION EMISSIONS AND LEGISLATION..... | 113 |
| 4.4 CONTRIBUTION OF AVIATION TO EMISSIONS | 114 |
| 4.5 EMISSIONS PREDICTION MODELING | 116 |
| 4.5.1 Emissions Model Validation and Verification..... | 118 |
| 4.6 SUMMARY AND CONCLUSIONS | 118 |
| FIGURES FOR CHAPTER 4..... | 119 |
| REFERENCES FOR CHAPTER 4 | 122 |
| CHAPTER 5..... | 123 |
| ENGINE OPERATING COSTS | 123 |
| ABSTRACT | 123 |
| 5.1 INTRODUCTION | 123 |
| 5.2 POWER BY HOUR (PBH) – TOTAL CARE PACKAGE | 123 |
| 5.2.1 Operator’s Perspective..... | 124 |
| 5.2.2 Engine Manufacturer’s Perspective..... | 124 |
| 5.2.3 Rolls-Royce Engine Support | 124 |
| 5.3 ECONOMICS (DOC) MODEL | 125 |
| 5.3.1 Economic Model Validation and Verification | 126 |
| 5.4 SUMMARY AND CONCLUSIONS | 126 |
| FIGURES FOR CHAPTER 5..... | 128 |
| REFERENCES FOR CHAPTER 5 | 131 |
| CHAPTER 6..... | 133 |
| AIRCRAFT TRAJECTORY OPTIMISATION | 133 |
| ABSTRACT | 133 |
| 6.1 INTRODUCTION | 133 |
| 6.2 DEFINITION OF FLIGHT PHASES..... | 134 |
| 6.2.1 Take – Off and Initial Climb | 135 |
| 6.2.2 Climb | 135 |
| 6.2.3 Cruise..... | 136 |
| 6.2.4 Descent..... | 137 |
| 6.2.5 Approach and Landing | 138 |

| | |
|---|------------|
| 6.3 AIRCRAFT TRAJECTORY OPTIMISATION..... | 138 |
| 6.3.1 Numerical Methods for Trajectory Optimisation | 139 |
| 6.3.1.1 Hill Climbing Methods | 140 |
| 6.3.1.2 Random Search Methods | 140 |
| 6.3.1.3 Evolutionary Methods | 141 |
| 6.3.2 Trajectory Optimisation Technique Selection | 141 |
| 6.3.2.1 Genetic Algorithm Based Optimisation | 141 |
| 6.3.2.2 Optimiser Validation and Verification | 142 |
| 6.4 SUMMARY AND CONCLUSIONS | 143 |
| FIGURES FOR CHAPTER 6..... | 144 |
| REFERENCES FOR CHAPTER 6 | 152 |
| CHAPTER 7..... | 153 |
| CASE STUDY: AIRPORT SEVERITY FACTORS | 153 |
| ABSTRACT | 153 |
| 7.1 INTRODUCTION | 153 |
| 7.2 OPERATIONAL SEVERITY | 154 |
| 7.2.1 Factors Influencing Severity | 155 |
| 7.2.1.1 Flight Time | 155 |
| 7.2.1.2 Take-Off Derate | 155 |
| 7.2.1.3 Outside Air Temperature | 155 |
| 7.2.1.4 Altitude..... | 156 |
| 7.2.1.5 Environment..... | 156 |
| 7.2.2 Operational Severity Estimation | 156 |
| 7.2.2.1 Damage Calculation | 156 |
| 7.2.2.2 Severity Calculation | 157 |
| 7.3 CASE STUDIES: AIRPORT SEVERITY FACTORS | 158 |
| 7.3.1 Severity Estimation Process..... | 158 |
| 7.3.2 Operational Factors..... | 160 |
| 7.3.2.1 Clean Engine Performance..... | 160 |
| 7.3.2.2 Degraded Engine Performance | 161 |
| 7.3.2.3 Discussion of the Results | 162 |
| 7.3.2.3.1 Effects of Degradation..... | 162 |
| 7.3.2.3.2 Effects of Take-Off Derate..... | 162 |
| 7.3.2.3.3 Effects of Outside Air Temperature | 163 |
| 7.3.2.3.4 Effects of Airport Altitude..... | 165 |
| 7.3.3 Airport Severity Factors..... | 166 |
| 7.3.3.1 Clean Engine Performance..... | 168 |
| 7.3.3.2 Degraded Engine Performance | 170 |
| 7.3.3.3 Discussion of the Results | 171 |
| 7.4 SUMMARY AND CONCLUSIONS | 173 |
| FIGURES FOR CHAPTER 7..... | 177 |
| REFERENCES FOR CHAPTER 7 | 192 |
| CHAPTER 8..... | 195 |

| | |
|--|------------|
| CASE STUDY: FLIGHT MISSION FUEL BURN AND ENGINE LIFE OPTIMISED AIRCRAFT TRAJECTORIES..... | 195 |
| ABSTRACT | 195 |
| 8.1 INTRODUCTION | 195 |
| 8.2 AIRCRAFT TRAJECTORY DEFINITION | 196 |
| 8.3 CASE STUDIES: AIRCRAFT TRAJECTORY OPTIMISATION | 198 |
| 8.3.1 Route 1: London – Madrid | 201 |
| 8.3.1.1 Effects of Ageing and Engine Degradation | 202 |
| 8.3.1.2 Fuelburn Optimised Trajectory..... | 203 |
| 8.3.1.3 Blade Creep Life Optimised Trajectory | 204 |
| 8.3.1.4 Blade Fatigue Life Optimised Trajectory | 205 |
| 8.3.1.5 Blade Oxidation Life Optimised Trajectory..... | 207 |
| 8.3.1.6 Disc Creep Life Optimised Trajectory | 207 |
| 8.3.2 Route 2: London – Ankara | 208 |
| 8.3.2.1 Effects of Ageing and Engine Degradation | 209 |
| 8.3.2.2 Fuelburn Optimised Trajectory..... | 209 |
| 8.3.2.3 Blade Creep Life Optimised Trajectory | 211 |
| 8.3.2.4 Blade Fatigue Life Optimised Trajectory | 212 |
| 8.3.2.5 Blade Oxidation Life Optimised Trajectory..... | 213 |
| 8.3.2.6 Disc Creep Life Optimised Trajectory | 213 |
| 8.3.3 Route 3: London – Abu Dhabi | 214 |
| 8.3.3.1 Effects of Ageing and Engine Degradation | 215 |
| 8.3.3.2 Fuelburn Optimised Trajectory..... | 215 |
| 8.3.3.3 Blade Creep Life Optimised Trajectory | 217 |
| 8.3.3.4 Blade Fatigue Life Optimised Trajectory | 218 |
| 8.3.3.5 Blade Oxidation Life Optimised Trajectory..... | 219 |
| 8.3.3.6 Disc Creep Life Optimised Trajectory | 219 |
| 8.4 SUMMARY AND CONCLUSIONS | 220 |
| FIGURES FOR CHAPTER 8..... | 222 |
| REFERENCES FOR CHAPTER 8 | 237 |
| CHAPTER 9..... | 239 |
| CONCLUSIONS AND RECOMMENDATIONS..... | 239 |
| 9.1 INTRODUCTION | 239 |
| 9.2 ACHIEVEMENTS | 240 |
| 9.3 CONCLUSIONS AND DISCUSSIONS | 241 |
| 9.3.1 Airport Severity Factors..... | 241 |
| 9.3.1.1 Operational Factors | 241 |
| 9.3.1.1.1 Clean Engine Performance | 241 |
| 9.3.1.1.2 Degraded Engine Performance (After 3000 cycles) | 242 |
| 9.3.1.2 Airport Severity | 243 |
| 9.3.1.2.1 Clean Engine Performance | 243 |
| 9.3.1.2.2 Degraded Engine Performance..... | 245 |
| 9.3.2 Flight Mission Fuel Burn and Engine Life Optimised Aircraft Trajectories | 246 |
| 9.3.2.1 Clean Engine | 246 |

| | |
|---|------------|
| 9.3.2.2 After 3000 cycles | 251 |
| 9.3.2.3 After 4500cycles | 255 |
| 9.3.2.4 After 5250 cycles | 259 |
| 9.3.3 Conclusion | 262 |
| 9.3.3.1 Airport Severity Factors | 263 |
| 9.3.3.2 Trajectory Optimisation Studies | 264 |
| 9.4 RECOMMENDATIONS FOR FUTURE WORK | 265 |
| APPENDICES | 266 |
| APPENDIX 1 | 266 |
| APPENDIX 2 | 267 |
| APPENDIX 3 | 268 |
| APPENDIX 4 | 270 |
| APPENDIX 5 | 272 |

List of Figures

| | |
|---|----|
| Figure 1.1: Optimised flight trajectories | 32 |
| Figure 1.2: Fuel burn delta for the optimised flight trajectories relative to the baseline trajectory | 32 |
| Figure 1.3: Effect of 2% component degradation on blade creep life | 33 |
| Figure 1.4: Effect of 2% component degradation on disc creep life | 33 |
| Figure 1.5: Effect of 2% component degradation on blade fatigue life | 34 |
| Figure 1.6: Effect of 2% component degradation on blade oxidation life | 34 |
| Figure 1.7: Variation of fuel and time with altitude and Mach number for a short range aircraft | 35 |
| Figure 1.8: Variation of fuel and TBO with altitude and Mach number for a short range aircraft | 35 |
| Figure 1.9: Technical approach for historical data collection and analysis | 36 |
| Figure 1.10: Engine performance deterioration diagnostic technique | 36 |
| Figure 1.11: Estimated overall performance loss for fan | 37 |
| Figure 1.12: Estimated overall performance loss for LPC | 37 |
| Figure 1.13: Estimated overall performance loss for HPC | 38 |
| Figure 1.14: Estimated overall performance loss for LPT | 38 |
| Figure 1.15: Estimated overall performance loss for HPT | 39 |
| Figure 1.16: Change in total fuel used (expressed as a percentage of total fuel used with clean engines) for a 10% deterioration of stipulated components | 40 |
| Figure 1.17: Change in net thrust available from engine (expressed as a percentage of net thrust available from clean engine) for a 10% deterioration of stipulated components | 40 |
| Figure 1.18: Blade's predicted changes in creep life for engines with a 10% fouling index for the LPC and HPC, and a 10% erosion index for the LPT and HIPT separately, compared with those for a clean engine | 41 |
| Figure 1.19: Blade's predicted LCF life consumption for engines with a 10% fouling index for the LPC and HPC separately, and a 10% erosion index for the LPT and HPT separately | 41 |
| Figure 1.20: Blade's predicted change in the relative severity of thermal fatigue for engines with a 10% fouling index for the LPC and HPC, and a 10% erosion index for the LPT and HPT separately | 42 |
| Figure 1.21: Pareto fronts of fuel carried, LTO NOx, and cumulative certification noise vs. operating cost | 42 |
| Figure 1.22: Comparison of single-objective optimisation results | 43 |
| Figure 1.23: Pareto front of non-dimensional block fuel vs. LTO NOx | 43 |
| Figure 1.24: SFC versus time for take-off, climb and cruise | 44 |
| Figure 1.25: Engine speed versus time for take-off, climb and cruise | 44 |
| Figure 1.26: TET versus time for take-off, climb and cruise | 45 |
| Figure 1.27: Results of optimum trajectories relative to baseline | 45 |
| Figure 1.28: Baseline versus optimum trajectories | 46 |
| Figure 1.29: Optimum trajectory solutions for fuel burn and NOx | 46 |
| Figure 1.30: Optimum trajectory solutions for fuel burn and time | 47 |
| Figure 1.31: Fuel-time Pareto fronts for the long range flight | 47 |

| | |
|--|----|
| Figure 1.32: Optimised trajectory for minimum fuel and minimum time | 48 |
| Figure 1.33: Mission fuel versus NOx | 48 |
| Figure 1.34: Fuel-Time Pareto fronts for a medium range flight | 49 |
| Figure 1.35: Comparison of Fuel vs. Time optimum trajectories for a medium range flight | 49 |
| Figure 1.36: Fuel-NOx Pareto fronts for a medium range flight | 50 |
| Figure 1.37: Comparison of Fuel vs. NOx optimum trajectories for a medium range flight | 50 |
| Figure 1.38: Fuel vs. Time Pareto front | 51 |
| Figure 1.39: Fuel vs. Time flight trajectory | 51 |
| Figure 1.40: Time vs. NOx Pareto front | 52 |
| Figure 1.41: Time vs. NOx flight trajectory | 52 |
| Figure 1.42: Engine flight mission fuel flow (clean and degraded) | 53 |
| Figure 1.43: Engine flight mission TET (clean and degraded) | 53 |
| Figure 1.44: Pareto Front: Fuel vs. Time | 54 |
| Figure 1.45: Pareto Front: Fuel vs. NOx | 54 |
| Figure 1.46: Fuel-Time Pareto Front: for a long range flight | 55 |
| Figure 1.47: Optimised fuel and time trajectories for a long range flight | 55 |
| Figure 1.48: Fuel-NOx Pareto Front: for a long range flight | 56 |
| Figure 1.49: Optimised fuel and NOx trajectories for a long range flight | 56 |
| Figure 1.50: The variation of the fuel consumption according to the cruise altitude, Trondheim – Oslo | 57 |
| Figure 1.51: The accumulated fuel consumption according to the cruise altitude, Trondheim – Oslo | 57 |
| Figure 1.52: Cyclic to steady state usage severity relationships | 58 |
| Figure 1.53: Elements of severity estimation | 58 |
| Figure 1.54: Engine characteristics for variation in TO derate (a) EGT (b) Shaft speed scaling vector (c) Blade severity (d) Disc severity | 59 |
| Figure 1.55: Engine characteristics for variation in OAT (a) EGT (b) Shaft speed scaling vector (c) Blade severity (d) Disc severity | 59 |
| Figure 1.56: Engine characteristics for variation in airport altitude (a) EGT (b) Shaft speed scaling vector (c) Blade severity (d) Disc severity | 60 |
| Figure 1.57: Short haul flight engine severity sensitivity for operational factors (a) Blade severity (b) Disc severity (c) HPT severity | 60 |
| Figure 2.1: Sulphidation attack of a turbine blade | 86 |
| Figure 2.2: Mechanical damage caused by ingested foreign material on the leading edge of a compressor blade | 86 |
| Figure 2.3: Changes in compressor characteristics, running line and operating point due to fouling | 86 |
| Figure 2.4: Effect of Flight Mach number and Altitude on Net thrust (fixed TET= 1510K)..... | 87 |
| Figure 2.5: Effect of flight Mach number and altitude on SFC (fixed TET = 1510K)..... | 87 |
| Figure 2.6: Effect of ambient temperature and TET on net thrust (fixed flight speed at Mn = 0.785). | 88 |
| Figure 2.7: Effect of Altitude on net thrust and SFC (fixed TET = 1510K and changing flight speed). | 88 |

| | |
|--|-----|
| Figure 2.8: Effect of ambient temperature on net thrust and SFC (TET changing and fixed flight speed at $M_n = 0.785$) | 89 |
| Figure 2.9: Effect of ambient temperature and TET on SFC (fixed flight speed at $M_n = 0.785$) | 89 |
| Figure 2.10: The effect on performance characteristics of a degraded booster compressor with 1% reduction in efficiency and 2% reduction in flow capacity. | 90 |
| Figure 2.11: The effect on performance characteristics of a degraded booster compressor with 1% reduction in efficiency and 2% reduction in flow capacity. | 90 |
| Figure 2.12: The net thrust performance for a booster (LPC compressor) with reduced isentropic efficiency and reduced flow capacity (i.e. same level of degradation for both). | 91 |
| Figure 2.13: HERMES flow diagram | 91 |
| Figure 2.14: Payload-Range diagram for Boeing 737- 800 aircraft. | 92 |
| Figure 2.15: The effect of individual component degradation (2% reduction in flow capacities and 1% reduction in efficiency) on mission fuel burn. | 92 |
| Figure 3.1: Creep damage in a blade | 105 |
| Figure 3.2: Fatigue crack initiating (blade trailing edge) | 105 |
| Figure 3.3: The lifing model | 106 |
| Figure 3.4: Blade stress analysis module | 106 |
| Figure 3.5: Disc stress analysis module | 107 |
| Figure 3.6: Creep analysis module | 107 |
| Figure 3.7: The low cycle fatigue (LCF) module | 108 |
| Figure 3.8: The oxidation module | 109 |
| Figure 3.9: The cooling module | 109 |
| Figure 4.1: ICAO Technology Goals for NO _x | 119 |
| Figure 4.2: Global Transportation's and Global Aviation's Contributions to Carbon Dioxide Emissions, 2004 | 119 |
| Figure 4.3: Reactor layout for the emissions model | 120 |
| Figure 4.4: Results of NO _x emission prediction for various engines | 120 |
| Figure 4.5: CFM56-7B27 (CUCCTF model) NO _x emissions prediction..... | 121 |
| Figure 5.1: Maintenance costs as part of an aircraft engine's DOC | 128 |
| Figure 5.2: Components of an aircraft's MRO | 128 |
| Figure 5.3: Components of the DOC | 129 |
| Figure 5.4: Cost of maintenance for short range engines currently in use .. | 130 |
| Figure 5.5: Cost of maintenance for long range engines currently in use | 130 |
| Figure 6.1: A typical civil transport aircraft flight profile | 144 |
| Figure 6.2: Genetic algorithm optimisation flowchart | 145 |
| Figure 6.3: Pareto fronts obtained in GA optimiser benchmarking studies ... | 146 |
| Figure 6.4: Convergence metric for ZDT1, ZDT3 and ZDT6 test functions .. | 147 |
| Figure 6.5: Diversity metric for ZDT1, ZDT3 and ZDT6 test functions | 148 |
| Figure 6.6: Constraint altered Pareto front for CONSTR function | 149 |
| Figure 6.7: CONSTR function Pareto front reached by algorithm | 149 |
| Figure 6.8: Constrained TNK function Pareto curve | 150 |
| Figure 6.9: TNK function Pareto curves reached by algorithms | 150 |
| Figure 6.10: Fuel-Time Pareto fronts for a medium range flight | 151 |
| Figure 6.11: Comparison of optimum trajectories for a medium range flight | 151 |

| | |
|--|-----|
| Figure 7.1: Simplified flow diagram of multi-disciplinary framework | 177 |
| Figure 7.2: Typical degradation profile for a health parameter. Most health parameters decrease with wear, turbine flows increase with wear | 177 |
| Figure 7.3: a) Maximum operating temperature (TO TET) and b) EGT with varying TO derate for clean engine and after 3000cycles. | 178 |
| Figure 7.4: Severity with varying TO derate: a) clean engine and b) after 3000cycles. | 178 |
| Figure 7.5: TO fuel burn with varying TO derate for the clean engine and after 3000cycles. | 178 |
| Figure 7.6: a) ICAO LTO and b) TO NO _x emissions with varying TO derate for the clean engine and after 3000cycles. | 179 |
| Figure 7.7: Total flight NO _x emissions with varying TO derate for the clean engine and after 3000cycles. | 179 |
| Figure 7.8: HPT blade fatigue life with varying TO derate for the clean engine and after 3000cycles. | 180 |
| Figure 7.9: HPT blade oxidation life with varying TO derate for the clean engine and after 3000cycles. | 180 |
| Figure 7.10: Engine DOC per flight with varying TO derate for the clean engine and after 3000cycles. | 181 |
| Figure 7.11: a) Maximum operating temperature (TO TET) and b) EGT with varying OAT for a clean engine and after 3000cycles. | 181 |
| Figure 7.12: Severity with varying OAT: a) clean engine and b) after 3000cycles. | 181 |
| Figure 7.13: TO fuel burn with varying OAT for the clean engine and after 3000cycles. | 182 |
| Figure 7.14: ICAO LTO NO _x with varying OAT for the clean engine and after 3000cycles. | 182 |
| Figure 7.15: a) TO and b) Total flight NO _x with varying OAT for the clean engine and after 3000cycles. | 183 |
| Figure 7.16: HPT blade fatigue life with varying OAT for the clean engine and after 3000cycles. | 183 |
| Figure 7.17: HPT blade oxidation life with varying OAT for the clean engine and after 3000cycles. | 184 |
| Figure 7.18: Engine DOC per flight with varying OAT for the clean engine and after 3000cycles. | 184 |
| Figure 7.19: a) Maximum operating temperature (TO TET) and b) EGT with varying TO derate for clean engine and after 3000cycles. | 185 |
| Figure 7.20: Severity with varying altitude: a) clean engine and b) after 3000cycles. | 185 |
| Figure 7.21: a) TO and b) Climb fuel burn with varying altitude for the clean engine and after 3000cycles. | 185 |
| Figure 7.22: Total flight fuel burn with varying altitude for the clean engine and after 3000cycles. | 186 |
| Figure 7.23: a) ICAO LTO and b) TO NO _x with varying OAT for the clean engine and after 3000cycles. | 186 |
| Figure 7.24: a) Climb and b) Total flight NO _x emissions with varying altitude for the clean engine and after 3000cycles. | 186 |

| | |
|---|-----|
| Figure 7.25: HPT blade fatigue life with varying altitude for the clean engine and after 3000cycles. | 187 |
| Figure 7.26: HPT blade oxidation life with varying altitude for the clean engine and after 3000cycles. | 187 |
| Figure 7.27: DOC with varying altitude for the clean engine and after 3000cycles. | 188 |
| Figure 7.28: a) Maximum operating temperature (TO TET) and b) EGT variation against departure airport for clean engine, after 3000 and 5250cycles. | 188 |
| Figure 7.29: Severity with varying airport: a) clean engine and b) after 3000cycles. | 188 |
| Figure 7.30: a) TO and b) Climb fuel burn with varying airport for the clean engine, after 3000 and 5250cycles. | 189 |
| Figure 7.31: Total flight mission fuel burn with varying airport for the clean engine, after 3000 and 5250cycles. | 189 |
| Figure 7.32: a) ICAO LTO, b) TO, c) Climb and d) Total flight NO _x with varying airport for the clean engine, after 3000 and 5250cycles. | 190 |
| Figure 7.33: HPT blade fatigue life with varying airport for the clean engine, after 3000cycles and 5250cycles. | 190 |
| Figure 7.34: HPT blade oxidation life with varying airport for the clean engine, after 3000cycles and 5250cycles. | 191 |
| Figure 7.35: DOC with varying airport for the clean engine, after 3000cycles and 5250cycles. | 191 |
| Figure 8.1: Multi-disciplinary optimisation framework. | 222 |
| Figure 8.2: Baseline trajectory profiles for each chosen representative route. | 222 |
| Figure 8.3: London – Madrid Optimised flight trajectories a) clean b) 3000cycles c) 4500cycles and d) 5250cycles | 223 |
| Figure 8.4: London – Madrid Flight mission fuelburn for the baseline (clean), 3000, 4500 and 5250cycles of operation. | 223 |
| Figure 8.5: London – Madrid Total severity for the baseline (clean), 3000, 4500 and 5250cycles of operation. | 224 |
| Figure 8.6: London – Madrid HPT Life for the clean engine a) blade creep b) disc creep c) blade fatigue d) blade oxidation. | 224 |
| Figure 8.7: London – Madrid HPT Life for the 3000cycles engine a) blade creep b) disc creep c) blade fatigue d) blade oxidation. | 225 |
| Figure 8.8: London – Madrid HPT Life for the 4500cycles engine a) blade creep b) disc creep c) blade fatigue d) blade oxidation. | 225 |
| Figure 8.9: London – Madrid HPT Life for the 5250cycles engine a) blade creep b) disc creep c) blade fatigue d) blade oxidation. | 226 |
| Figure 8.10: London – Madrid Engine DOC per flight for the baseline (clean), 3000, 4500 and 5250cycles of operation. | 226 |
| Figure 8.11: London – Madrid: a) ICAO LTO NO _x and b) Total flight NO _x for the baseline (clean), 3000, 4500 and 5250cycles of operation. | 227 |
| Figure 8.12: London – Ankara Optimised flight trajectories a) clean b) 3000cycles c) 4500cycles and d) 5250cycles | 227 |
| Figure 8.13: London – Ankara Flight mission fuelburn for the baseline (clean), 3000, 4500 and 5250cycles of operation. | 228 |

| | |
|--|-----|
| Figure 8.14: London – Ankara Total severity for the baseline (clean), 3000, 4500 and 5250cycles of operation. | 228 |
| Figure 8.15: London – Ankara HPT Life for the clean engine a) blade creep b) disc creep c) blade fatigue d) blade oxidation. | 229 |
| Figure 8.16: London – Ankara HPT Life for the 3000cycles engine a) blade creep b) disc creep c) blade fatigue d) blade oxidation. | 229 |
| Figure 8.17: London – Ankara HPT Life for the 4500cycles engine a) blade creep b) disc creep c) blade fatigue d) blade oxidation. | 230 |
| Figure 8.18: London – Ankara HPT Life for the 5250cycles engine a) blade creep b) disc creep c) blade fatigue d) blade oxidation. | 230 |
| Figure 8.19: London – Ankara Engine DOC per flight (relative to the baseline) for the optimised baseline (clean), 3000, 4500 and 5250cycles. | 231 |
| Figure 8.20: London – Ankara a) ICAO LTO NO _x and b) Total flight NO _x for the baseline (clean), 3000, 4500 and 5250cycles. | 231 |
| Figure 8.21: London – Abu Dhabi Optimised flight trajectories a) clean b) 3000cycles c) 4500cycles and d) 5250cycles. | 232 |
| Figure 8.22: London – Abu Dhabi Flight mission fuelburn (relative to the baseline) for the optimised baseline (clean), 3000, 4500 and 5250cycles. | 232 |
| Figure 8.23: London – Abu Dhabi Total severity for the baseline (clean), 3000, 4500 and 5250cycles of operation. | 233 |
| Figure 8.24: London – Abu Dhabi HPT Life for the clean engine a) blade creep b) disc creep c) blade fatigue d) blade oxidation. | 233 |
| Figure 8.25: London – Abu Dhabi HPT Life for the 3000cycles engine a) blade creep b) disc creep c) blade fatigue d) blade oxidation. | 234 |
| Figure 8.26: London – Abu Dhabi HPT Life for the 4500cycles engine a) blade creep b) disc creep c) blade fatigue d) blade oxidation. | 234 |
| Figure 8.27: London – Abu Dhabi HPT Life for the 5250cycles engine a) blade creep b) disc creep c) blade fatigue d) blade oxidation. | 235 |
| Figure 8.28: London – Abu Dhabi Engine DOC per flight for the baseline (clean), 3000, 4500 and 5250cycles of operation. | 235 |
| Figure 8.29: London – Abu Dhabi a) ICAO LTO NO _x and b) Total flight NO _x for the optimised trajectories for the baseline (clean), 3000, 4500 and 5250cycles of operation. | 236 |

List of Tables

| | |
|---|-----|
| Table 1.1: Trajectory variation for the clean and degraded cases | 5 |
| Table 1.2: Major engine performance loss mechanisms for each module | 9 |
| Table 1.3: Summary of module degradation levels simulated | 9 |
| Table 1.4: Summary of the effects of degradation on rotating LCF and pressure LCF | 10 |
| Table 1.5: Summary of the effects of degradation on thermal fatigue and on creep | 11 |
| Table 1.6: Comparison of the effects of single and multiple component degradations | 11 |
| Table 1.7: Optimisation variable bounds | 16 |
| Table 1.8: Engine severity estimation for the reference mission | 19 |
| Table 1.9: Summary of previous work done..... | 20 |
| Table 2.1: CUCCTF (twin spool turbofan) engine data from | 79 |
| Table 2.2: CUCCTF (Simulated Engine) DP (ToC) data..... | 80 |
| Table 2.3: Public domain data vs. CUCCTF engine simulation results..... | 80 |
| Table 5.1: The economics model comparing against the Roskam method .. | 126 |
| Table 6.1: Flight segments characteristics | 134 |
| Table 7.1: Projected thrust requirements relative to reference (ISA SLS) requirements. | 154 |
| Table 7.2: Degradation level for health parameters as a % deviation from clean | 160 |
| Table 7.3: Airport environmental conditions | 167 |
| Table 7.4: Performance parameter sensitivity analysis..... | 168 |
| Table 7.5: Airport performance ranking per parameter. | 174 |
| Table 8.1: Optimisation variable bounds..... | 197 |
| Table 8.2: London – Madrid engine/aircraft performance changes with increasing cycles of operation relative to baseline. | 202 |
| Table 8.3: London – Madrid optimised trajectory results. | 204 |
| Table 8.4: London – Ankara engine/aircraft performance changes with increasing cycles of operation relative to the baseline. | 209 |
| Table 8.5: London – Ankara optimised trajectory results. | 210 |
| Table 8.6: London – Abu Dhabi aircraft performance changes with increasing cycles of operation relative to baseline. | 215 |
| Table 8.7: London – Abu Dhabi optimised trajectory results..... | 216 |
| Table 9.1: Key Conclusions | 263 |

Nomenclature

| SYMBOL/ ABBREVIATION | MEANING | SI UNITS |
|--|---|----------------------------------|
| ACARE | Advisory Council for Aeronautical Research in Europe | |
| AFR | Air Fuel Ratio | |
| ALT | Altitude | m |
| ATC | Air Traffic Control | |
| ATM | Air Traffic Management | |
| BADA | Base of Aircraft Data | |
| BPR | By-Pass Ratio | |
| C | Constant | |
| CAEP | Committee on Aviation Environmental Protection | |
| CAS | Calibrated Airspeed | knots (m s^{-1}) |
| CG | Centre of Gravity | |
| CI | Cost Index | |
| CO ₂ | Carbon Dioxide | |
| CO | Carbon Monoxide | |
| C _p | Specific Heat at Constant Pressure | $\text{J kg}^{-1} \text{K}^{-1}$ |
| CS | Cyclic Severity | |
| CUCCTF | Cranfield University Current Conventional TurboFan | |
| CUSMSA | Cranfield University Short Medium range Single Aisle aircraft | |
| C _v | Specific Heat at Constant Volume | $\text{J kg}^{-1} \text{K}^{-1}$ |
| D _{ci} | Cyclic Damage Fraction | |
| (D _{cyclic}) _{new} | Cyclic Damage Fraction for New | |
| (D _{cyclic}) _{ref} | Cyclic Damage Fraction for Reference | |
| DfT | Department for Transport | |
| DOC | Direct Operating Costs | US\$ |
| D _p | Total Grammes of Emissions Produced in LTO cycle | g |
| DP | Design Point | |
| D _{si} | Steady State Damage Fraction | |
| (D _{steadystate}) _{new} | Steady State Damage Fraction for New | |
| (D _{steadystate}) _{ref} | Steady State Damage Fraction for Reference | |

Nomenclature

| | | |
|---------------------|---|--|
| $(D_{total})_{new}$ | Total Damage Fraction for New | |
| $(D_{total})_{ref}$ | Total Damage Fraction for Reference | |
| EAS | Equivalent Airspeed | knots (m s^{-1}) |
| EDS | Environmental Design Space | |
| EFC | Engine Flight Cycles | cycles |
| EFH | Engine Flight Hours | hrs |
| EGT | Exhaust Gas Temperature | K |
| EGTM | Exhaust Gas Temperature Margin | K |
| EI | Emissions Index | g kg^{-1} |
| EIS | Entry Into Service | year |
| ETRW | Energy To Revenue Work | |
| FAA | Federal Aviation Authority | |
| FAR | Fuel Air Ratio | |
| FHV | Fuel Heating Value | J kg^{-1} |
| FN | Nett Thrust | N (kN) |
| FN/m | Specific Thrust | N kg^{-1} (kN kg^{-1}) |
| Foo | Sea Level Static Maximum Thrust | kN |
| FOD | Foreign Object Damage | |
| FPR | Fan Pressure Ratio | |
| GA | Genetic Algorithm | |
| GATAC | Green Aircraft Trajectories under ATM Constraints | |
| GRD | Ground | |
| H ₂ O | Water | |
| HCF | High Cycle Fatigue | cycles |
| HP | High Pressure | Pa |
| HPC | High Pressure Compressor | |
| HPT | High Pressure Turbine | |
| IAS | Indicated Airspeed | knots (m s^{-1}) |
| ICAO | International Civil Aviation Organisation | |
| IPCC | International Panel on Climate Change | |
| IOC | Indirect Operating Costs | US\$ |
| ISA | International Standard Atmosphere | |

Nomenclature

| | | |
|----------------|---|--------------------|
| ITD | Integrated Technology Demonstrator | |
| JTI | Joint Technology Initiative | |
| LCC | Life Cycle Costs | US\$ |
| LCF | Low Cycle Fatigue | cycles |
| LCV | Lower Calorific Value | J kg ⁻¹ |
| LLP | Life Limited Part | |
| LMP | Larson Miller Parameter | |
| LP | Low Pressure | Pa |
| LPC | Low Pressure Compressor | |
| LPP | Lean Prevaporised Premixed | |
| LPT | Low Pressure Turbine | |
| LTO | Landing and Take Off | |
| m | Mass | kg |
| MDO | Multidisciplinary Design Optimisation | |
| MSL | Mean Sea Level | m |
| MFC | Maximum Fuel Capacity | kg |
| Mn | Mach Number | |
| MRO | Maintenance Repair and Overhaul | |
| MTBR | Mean Time Between Removals | hrs |
| MTOW | Maximum Take Off Weight | kg |
| MUS | Method of Universal Slope | |
| MZFW | Maximum Zero Fuel Weight | kg |
| N ₂ | Nitrogen | |
| NASA | National Aeronautics Space Agency | |
| NGV | Nozzle Guide Vane | |
| n _i | Number of Cycles | cycles |
| N _i | Average Number of Cycles to Failure | cycles |
| NO | Nitric Oxide | |
| NOx | Nitrogen Oxides | |
| NSGAI | Non-dominated Sorting Genetic Algorithm | |
| O ₂ | Oxygen | |
| OAT | Outside Air Temperature | K (°C) |

Nomenclature

| | | |
|------------------|--|------------------------------------|
| OD | Off Design | |
| OEM | Original Equipment Manufacturer | |
| OEW | Overall Empty Weight | kg |
| OPR | Overall Pressure Ratio | |
| OPSEV | Operational Severity Analysis | |
| p | Static Pressure | Pa |
| P | Total (Stagnation) Pressure | Pa |
| P&WA | Pratt and Whitney Aircraft | |
| PaSR | Partially Stirred Reactor | |
| PARTNER | Partnership for AiR Transportation Noise and Emissions Reduction | |
| PBH | Power By Hour | |
| P _{in} | Pressure at Inlet | Pa |
| P _{out} | Pressure at Outlet | Pa |
| PLA | Power Lever Angle | ° |
| PR | Pressure Ratio | |
| PSR | Perfectly Stirred Reactor | |
| PSRS | Series of Perfectly Stirred Reactors | |
| R | Specific Gas Constant of Pure Air | J kg ⁻¹ K ⁻¹ |
| rpm | Revolutions Per Minute | min ⁻¹ |
| SFC | Specific Fuel Consumption | kg N ⁻¹ s ⁻¹ |
| SL | Sea Level | m |
| SLS | Sea Level Static | |
| SOT | Stator Outlet Temperature | K |
| SOx | Oxides of Sulphur | |
| SS | Steady State Severity | |
| t | Static Temperature | K |
| T | Total (Stagnation) Temperature | K |
| TAS | True Airspeed | knots (m s ⁻¹) |
| TBO | Time Between Overhaul | cycles (hrs) |
| TBC | Thermal Barrier Coating | |
| TERA | Techno-economic Environmental and Risk Assessment | |
| TET | Turbine Entry Temperature | K |

Nomenclature

| | | |
|---------------------------------|---|----------------------|
| TGO | Thermally Grown Oxide | |
| TMF | Thermal Fatigue | cycles |
| t_i | Time at stress level | hrs |
| t_f | Time to failure | hrs |
| TO | Take Off | |
| ToC | Top of Climb | |
| ToD | Top of Descent | |
| UHC | Unburnt Hydro-Carbons | |
| UN | United Nations | |
| V_{mcg} | Ground Minimum Control Speed | knots ($m s^{-1}$) |
| V_j | Jet Velocity | $m s^{-1}$ |
| V_{LOF} | Lift Off the Ground Speed | knots ($m s^{-1}$) |
| V_o | Flight Velocity | $m s^{-1}$ |
| VOC | Volatile Organic Compounds | |
| W | Mass Flow Rate | $kg s^{-1}$ |
| W_{ff} | Fuel Flow Rate | $kg s^{-1}$ |
| x | Carbon Coefficient in Chemical Formula for Fuel | moles |
| y | Hydrogen Coefficient in Chemical Formula for Fuel | moles |
| z | Sulphur Coefficient in Chemical Formula for Fuel | moles |
| $\gamma = C_p/C_v$ | Specific Heat Ratio | |
| η_o | Overall Efficiency | |
| η_{prop} | Propulsive Efficiency | |
| η_{th} | Thermal Efficiency | |
| $(\lambda_{cyclic})_{new}$ | Cyclic Severity for New Mission | |
| $(\lambda_{cyclic})_{ref}$ | Cyclic Severity for Reference Mission | |
| $(\lambda_{steadystate})_{new}$ | Steadystate Severity for New Mission | |
| $(\lambda_{steadystate})_{ref}$ | Steadystate Severity for Reference Mission | |
| $(\lambda_{total})_{new}$ | Total Severity for New Mission | |
| $(\lambda_{total})_{ref}$ | Total Severity for Reference Mission | |
| σ_i | Stress Amplitude | MPa |

Chapter 1

Introduction

Abstract

The aim of this chapter is to give the reader an understanding of the research undertaken and described in this thesis. The chapter provides the background and motivation of this research. A literature review from the earlier studies is presented and the work put into context. The objectives of the project are outlined and the major contributions from the research described in this thesis summarised.

1.1 Background

Aircraft contribute to the ever increasing concentrations of pollutant gases in the atmosphere by emitting greenhouse gases and other pollutant emissions. According to the Intergovernmental Panel on Climate Change (IPCC), the demand for air transport is expected to grow annually by 5% [1] in the next 20 years. This current and projected growth has brought to the fore environmental issues and the impact that fossil fuels have on the environment. The aviation industry is challenged to meet this expected growth in demand whilst ensuring the protection of the environment. This puts pressure on industry's efforts to provide economic, safe and environmentally-friendly air travel whilst reducing the environmental footprint. Many international organisations (and governments) such as ACARE (Advisory Council for Aeronautics Research in Europe) and ICAO (International Civil Aviation Organisation) have responded to the challenge to reduce future emissions by setting up goals and identifying ways to best reduce the impact of aircraft operations on the environment. ICAO has set up three environmental goals [2] for international aviation with the aim to: 1) reduce the number of people exposed to significant aircraft noise; 2) reduce the impact of aviation emissions on local air quality; and 3) reduce the impact of aviation emissions on the global climate. In line with the ICAO goals concerning the environment, ACARE have fixed goals for 2020 [3] to reduce CO₂ emissions by 50%, NO_x emissions by 80% and perceived noise by 50% (10dB) against the baseline set for the year 2000, and also to make substantial progress in reducing the environmental contribution and impact of aircraft (manufacture, maintenance and disposal) and associated products and systems. Further to and building on the 2020 vision, ACARE has laid out environmental targets for 2050 [4] relative to new aircraft capabilities for 2000 and these are: a 75% reduction in CO₂ emissions per passenger kilometre, a 90% reduction in NO_x emissions, a 65% reduction in the perceived noise emission of flying aircraft.

To offset the environmental impact of market growth, the challenge to the aviation industry's initiatives is to not only focus on the technical aspects of an engine and/or aircraft, but also to understand how the economic (or business)

model influences the choice when trading off between the environmental impact and the economic performance. Airlines (operators) need to know how aircraft contribute to emissions and noise in their bid to improve aircraft performance, and find good trade-off between performance improvements, operations and maintenance costs without incurring large operations costs. Research has indicated that to achieve the targets set by these organisations (ACARE and ICAO) will require contribution from:

- Technological improvements (better fuel efficiency and reduced emissions) related to engines, aircraft design and fuel sources.
- Operational improvements both on ground (taxiing) and in air (trajectory optimisation).
- Greener manufacturing and recycling processes including transportation (i.e. consideration of whole product cycle and not just mission consideration).

Technologies are expected to help reduce emissions growth, however, they present a range of challenges and further advances may come with high development costs. Improvements to reduce aircraft emissions face challenges, and adopting such improvements may depend on fuel prices and/or government policies that price emissions from aircraft. However, one most readily implementable contributor to achieving the ACARE targets is operational improvements which are financially viable whilst being cost effective for existing engines. The development of technologies to reduce emissions and noise in the way the aircraft manages its trajectory is an option.

1.2 Context

Aviation transport supports economic and social development worldwide, yet it contributes to the production of greenhouse gases i.e. about 2-3% [5] of human generated global carbon dioxide (CO₂) emissions and about 3% [5] of the potential warming effect of the total global emissions that can affect the earth's climate. Air transport is continuously growing, and is constantly making strides to reduce its carbon footprint by reducing fuel consumption through technological and operational advances. This rapid growth of the industry over the years and the forecasted growth have put environmental issues at the forefront of key industry drivers. Industry's concentrated effort to improve thermal efficiency (better fuel efficiency) has led to higher overall pressure ratios and turbine entry temperatures. Current effort is aimed at identifying ways to best reduce the impact of aircraft operations on the environment e.g. PARTNER (Partnership for AiR Transportation Noise and Emissions Reduction) [6] and the European Clean Sky JTI (Joint Technology Initiative) projects [7]. The Clean Sky JTI is aimed at developing, demonstrating and validating technologies to achieve the ACARE environmental targets.

However, with the anticipated growth of air transport, global aircraft fuel consumption and emissions are expected to increase every year. There is also one important aspect of aircraft engine operation, an inherent challenge to the industry's concentrated efforts; aero-engine components will during their life

time of service suffer the effects of degradation. The degradation of aero-engine components will cause changes in component characteristics, resulting in the overall performance deterioration of the aero-engine. Engine component degradation is caused by a combination of the flight-loads exerted, thermal distortions, erosion of airfoils, engine fouling, in-service damage and abuse, engine operation and deployment and the engine maintenance procedures employed. Deterioration can affect performance characteristics such as thrust (or power) and Specific Fuel Consumption (SFC). As a consequence of progressive performance loss, operation of the engine can become cost ineffective (e.g. leading to excessive SFC) or even unsafe (e.g. insufficient take-off thrust).

Aircraft take-off from a variety of geographical locations each demanding a different set of operational strategies and thrust requirements. The thrust requirements have a bearing on the engine degradation and engine life consumption and will affect the operational cost which is of concern to both the engine manufacturer and the operator. Airport severity is the relationship between the thrust requirement at take-off and the degree of engine life consumption. Each airport imposes a different thrust requirement due to the airport environment, Outside Air Temperature (OAT), altitude and other factors affecting engine performance. Airport severity estimation can serve as an aid when making decisions on operational strategies around different airports. This is because the airport environment influences the engine deterioration rate and the engine time on the wing, and the aero-engine operating costs are largely dependent on the life consumption of critical engine parts.

Performance is inseparable from the economic model and is pivotal to an engine's economic viability, both from the manufacturer and the operator's perspective. Performance measures such as fuel burn, engine life and maintenance requirements among others are all driven by the performance parameters, making it critical in the modern economic climate to understand how the economic (or business) model influences the choice of trade-offs between the environmental impact and the economic performance. In the context of increasing fuel costs and the competitive nature of the airline industry profitability and safety are critical for sustainability. Direct Operating Costs (DOC) become of concern to both the Original Equipment Manufacturer (OEM) and the airline, thus raising the need for the assessment of the engine and aircraft at mission level and the optimising of operational procedures. Cost effectiveness (making more money) is the perspective for both the OEM and the airlines. In view of the new model (known as total care packages or power by hour) contracts as opposed to the older model (time and materials) contracts, the OEM's key concern is to deliver good engines that are reliable and available, whilst remaining cost effective in terms of engine maintenance. The airlines' key concern is that to remain competitive, they have to operate at lower costs and within the constraints and operating guidelines imposed by the OEM. This brings to the fore, the importance of engine performance and engine life, because as an aero-engine degrades, the flight mission fuel burn increases and this translates into an increase in flight operating costs. Fuel burn is an important criterion that has to be satisfied to ensure the overall effectiveness of

an aircraft. Degraded engines burn more fuel (hence produce more CO₂), produce more NO_x, have less useful life and cost more to operate. In addition to more fuel costs, the weight of the additional fuel required can only be carried at the expense of the payload. Also, in view of the current power by hour contracts and the climate of fuel costs, a more efficient operation of aero-engines becomes of concern. According to ICAO [2]:

- On average, an aircraft will burn about 0.03kg of fuel for each kg carried per hour. This will be slightly higher for shorter flights and for older aircraft and slightly lower for longer flights and newer aircraft. This is assuming that 3.16 kg CO₂ is produced for every kg of fuel burnt.
- The total commercial fleet combined flies about 57 million hours per year; so, saving one kg on each commercial flight could save roughly 170,000 tonnes of fuel and 540,000 tonnes of CO₂ per year.
- Average fuel burn per minute of flight is 49 kg.
- Average of fuel burn per nautical mile (nm) of flight is 11 kg.

The literature reviewed (as detailed in next section) has shown that to date, much of the research effort has been aimed to better understand, assess and monitor the impact of flight operations on the environment, while developing green technologies, operational measures and related policies to reach an optimum balance between the growth of aviation and the need to protect the environment. Most of the work found and reviewed shows concentrated effort(s) on optimising fuel burn and emissions (reducing environmental impact). In addition to the work done as a collaborative effort by the author and Cranfield University MSc students [8] and [9], little or no work has been done to better understand how the optimal solutions for minimising fuel burn and protecting the environment together with engine degradation, will impact on the engine useful life and consequently the engine operating costs. This research introduces TERA type techno-economic assessments to understand the impact of engine component degradation and airport severity factors on flight mission fuel burn and engine useful life. The framework developed in this PhD research allows for engine/aircraft assessments to be made at mission level with a view of optimising operational procedures and minimising DOC. Optimum solutions for fuel burn and engine life are compared and the environmental impact and economic viability of such solutions assessed.

1.3 Review of Past Studies

This section is aimed at bringing into perspective the context of this work. A critical evaluation of the most relevant past work on aero-engine degradation, engine lifing, trajectory optimisation and operational severity and what others have contributed on the subject is presented.

In her work [8] an MSc student at Cranfield University uses a Techno-economic, Environmental, and Risk Assessment (TERA) type approach to make preliminary assessments on clean and degraded engine performance for short range missions. The work presented by [8] was a collaborative effort, with this author providing technical leadership and direction and has contributed to

the preliminary requirements of this research. [8] uses a multidisciplinary multi-objective optimisation framework developed in MATLAB to identify the optimum trajectories for the clean and degraded cases. [8] has carried out assessments on the effects of degradation on the high pressure turbine (HPT)'s creep life, Low Cycle Fatigue (LCF) life and oxidation life. The engine model used in these assessments is a typical twin spool high bypass turbofan engine similar to the CFM56-5B2/3 engine used to power an Airbus A320 aircraft. The design point for the engine model was set at Take-Off (TO) Sea Level Static (SLS) and International Standard Atmosphere (ISA) conditions. For the degraded engine and aircraft performance and lifing assessments, [8] introduced 2% degradation in efficiency and flow capacity across the compressors and turbines. The analyses were for single component degradation. The clean engine trajectory assessed at 10668m cruise altitude and 0.8 Mach number was set as the baseline (reference) trajectory against which the degraded and optimised trajectories were compared. For the optimisation assessments, full flight trajectories were assessed but the optimisation was only for the cruise segment. The bounds for the variables (cruise altitudes and cruise speeds (Mach number)) ranged from 10000 to 12000metres and 0.75 to 0.85 respectively. The climb and descent profiles were assumed to follow the same altitude and speed profiles as for the baseline trajectory.

The results of [8] compare well with those from the study by [9] cited below and show that degradation causes a drop in OPR, mass flow and net thrust. The results show an increase in SFC and fuel burn (and a reduced payload) for the same thrust requirements and trajectory flown due to the engine operating at higher spool speeds and higher turbine entry temperature (TET)'s. The results of [8] showing the effects of individual component degradation on mission fuel burn, HPT's life and the impact of component degradation on the fuel burn optimised trajectory are presented in table 1.1 and in figures 1.1 to figure 1.6.

Table 1.1: Trajectory variation for the clean and degraded cases [8].

| Engine Configuration | Baseline Fuel Burn Delta [%] | Optimum Fuel Burn Delta [%] | Optimum Cruise Altitude [m] | Optimum Cruise Mach Number [-] |
|----------------------|------------------------------|-----------------------------|-----------------------------|--------------------------------|
| Clean | 0 | -4.8 | 12000 | 0.77 |
| 2% Fan * | 11.9 | 5.3 | 11400 | 0.75 |
| 2% LPC * | 24.8 | 7.7 | 11900 | 0.75 |
| 2% HPC * | 13.3 | 4.7 | 11600 | 0.75 |
| 2% HPT * | 9.9 | 3.4 | 11600 | 0.75 |
| 2% LPT * | 9.9 | 4.9 | 11900 | 0.76 |

- Percentage represents level of degradation in efficiency and flow capacity

Table 1.1 and figure 1.1 show that the fuel burn optimised trajectory for the clean engine differs from that of the degraded engine(s). Figure 1.2 shows the variation (deltas) in mission fuel burn for the clean and degraded engine trajectories. Figures 1.3 to 1.6 show the variation in HPT life (blade and disc creep, blade fatigue and blade oxidation) for the clean and degraded cases.

The trajectory optimisation results of [8] compare well with those from earlier studies by [19] and [23] cited below and show that the optimised trajectory for minimum fuel burn is achieved at lower optimal speeds and higher flight altitudes (where the aircraft drag is less). [8] concludes that optimising for fuel burn gives more savings for the degraded engine than for the clean engine, savings which are likely to benefit the engine operating costs. The results of [8] demonstrate the importance of flying the optimised fuel burn trajectory since the economic impact will increase with the number of flights. The results of the lifing assessments of [8] are comparable with those presented by [12] cited below and show that engine component degradation will shorten the HPT useful creep life, LCF life and the oxidation life. The limitation of [8] is that the degradation levels have been arbitrarily assigned, and individual components have been degraded independent of each other, which is not so in practice. The optimisation has been limited to only the cruise phase, and the effects of flying fuel burn optimised trajectories on the HPT life have not been assessed by [8].

In his work [9] an MSc student at Cranfield University uses parametric analysis to assess the effects of engine degradation on engine and aircraft performance. In particular the work of [9] was to identify the optimised trajectories for fuel burn and (HPT) useful life by varying flight conditions at cruise. The work presented by [9] was a collaborative effort, with this author providing technical leadership and direction and has contributed to the preliminary requirements of this research. The engine model used in these assessments is a typical twin spool high bypass turbofan engine similar to the CFM56-7B27 engine used to power a Boeing 737-800 aircraft. The design point for the engine model was set at cruise altitude 10670m and 0.8 Mach number. [9] addresses the trade-offs between fuel burn and flight time, and between fuel burn and the life of the HPT (The HPT is identified as the most critical part, hence it's life is assumed to be the engine life). As with the work of [8] cited above, 2% degradation was introduced in efficiency and flow capacity across the compressors and turbines. The analyses were for single component degradation. The clean engine trajectory assessed at 10668m cruise altitude and 0.8 Mach number was set as the baseline (reference) trajectory against which comparison was made. The parametric analyses were done by varying the cruise altitude from 9000 to 12000meters and the Mach number from 0.75 to 0.8. The results of [9] showing the variation in fuel burn, engine life and flight time with cruise altitude and Mach number are presented in figures 1.7 and 1.8. The results of [9] for fuel burn and flight time compare well with those from earlier studies by [8] cited above and by [19] and [23] cited below, and show higher altitudes and lower speeds for the fuel burn optimised trajectory; lower altitudes and higher speeds for the time optimised trajectory and the optimum for engine life is achieved at higher altitudes and slower speeds. As with the results presented by [8], [9] also shows that the optimised fuel burn trajectory for the clean engine is different from that of the degraded engine. As with the work by [8] cited above and [22] cited below, the limitation of this work is that the degradation levels have been arbitrarily assigned, and individual components have been degraded independent of each other, which is not so in practice. The search space explored by [9] has also not been extensive.

In their work [10] researchers at the National Aeronautics Space Agency (NASA) do a study on the JT9D engine, paying particular attention to performance losses and the mechanisms of degradation that are responsible for the losses. Their study was based on historical records and data acquired from various sources including airlines, airframe manufacturers and Pratt & Whitney Aircraft (P&WA). The purpose of their study was to:

- 1) Collect, document and establish trends in performance loss in relation to engine and component usage for the JT9D engine.
- 2) Quantify the levels of performance degradation and the actual contribution to the degradation of each engine component.
- 3) Identify the causes for the performance losses.

In order to understand the role of each cause against engine usage [10] developed performance degradation models at the engine and component/module level. Large quantities of data were collected, documented and analysed by [10] to provide the underlying support for the performance degradation analysis. The data available were:

- 1) Airline engine flight performance and operating data correlated with engine utilisation (in hours or cycles).
- 2) Engine maintenance procedures (part replacement and repair rates) of particular operators.
- 3) Test data showing particular (single) engine performance levels and production performance records showing engine performance degradation.
- 4) Inspection results showing and relating the condition of uninstalled engine parts to length of service usage.

Figure 1.9 shows the technical process and associated actions undertaken by [10] to complete their study. This technique was used to bridge the gap existing in the data spectrum between the airline specific overall average engine performance data and the specific components from specific engines data. Engine performance data reduction and averaging (left column of figure 1.9) were employed by [10] to define the overall engine performance loss. To estimate module performance degradation as a function of module age, engine and component utilisation data and component condition data were used (right columns in figure 1.9). The estimate was used to model the overall engine degradation in an engine simulation and the results compared with the airline average engine experience as ascertained from the overall engine performance data. The performance degradation models they [10] developed were validated using the "top-down" and "bottom-up" techniques summarised in figure 1.10. In the top down approach, the airline's performance data was used to model and simulate the engine. This step involved using the engine data to establish an average engine performance trend and define the average engine degradation at selected number of engine cycles for each airline. The engine simulation is then used iteratively to estimate equivalent levels of individual module performance degradation. In the bottom up approach, the engine simulated was based on the airline's component condition data. This step involved the determination of the possible effects of the degradation of individual

components on module performance by analysing the component condition and maintenance data. Using simulation, the overall average engine performance loss was then predicted. The module and engine performance degradation were only modelled after comparison, reconsideration of assumptions and good agreement of the two models was reached.

The results of [10] show that engine performance degradation can be classed according to the time frame during which they occur:

- 1) Short term degradation occurring in the first few hundred flights after entry into service.
- 2) Long term degradation that progresses gradually with accumulating service hours.

The results show a performance loss of 1% in SFC on the first flight which grows to 1.5% by the 200th flight relative to the measured performance at SLS TO conditions. According to [9], performance losses of the Low Pressure (LP) spool (fan, LPC and LPT) contribute 55% of the SFC loss whereas 45% is due to performance losses of the High Pressure (HP) spool (HPC and HPT). In their conclusion [10] attribute the short-term performance losses to rubbing wear and increase in clearances due to contact between rotating and stationary parts. In contrast, the performance losses at the 3500 flights time frame are attributed largely to the HP spool than the LP spool.

[10], identifies four causes of engine component degradation:

- 1) The effect of flight loads which appear as engine casing distortion, produce rubbing and cause an increase in clearances.
- 2) Erosion of airfoils and seals which cause bluntness, reduce blade camber and blade length and increase clearances.
- 3) Thermal distortion due to changes in TET profiles which cause area changes, increase leakages, and alter clearances.
- 4) Operator maintenance procedures affect the level and rate of performance degradation, the time between repairs and overhaul and the level of performance before and after maintenance.

The work of [10] quantifies module performance loss mechanisms relative to usage and goes further to identify the dominant performance loss mechanism for each module. The major performance loss mechanisms for each module as presented by [10] are summarised in table 1.2. The estimated performance loss relative to engine flight cycles for each module is shown in figures 1.11 to 1.15. The limitation of [10] is that the studies were conducted on the JT9D family of engines. However, the trends established in [10] may be applicable to most turbofan engines. The work of [10] was therefore important to this research and contributed to the preliminary requirements of understanding the mechanisms that cause performance losses and the role of each mechanism as the engine ages. The engine component degradation trends established in [10] were used to generate the levels of degradation used in this work.

In his work [11] an MSc student at Cranfield University uses transient engine parameters to analyse the effects of engine degradation on the life usage of a

two spool military fighter aircraft engine, the F404-GE-400. The purpose of his study (relevant to this research) was to:

- 1) Determine the effects of individual component degradation on the major modes of engine failure.
- 2) Determine if the effects of individual component degradation are additive i.e. whether the effects of multiple component degradation can be determined by merely adding the known effects of single components.

Table 1.2: Major engine performance loss mechanisms for each module [10]

| Module | Performance Loss Mechanisms | |
|-----------|--|--|
| | Primary | Secondary |
| Fan | 1. Leading edge bluntness | 1. Airfoil roughness 2. Increased tip clearance |
| LPC | 1. Tip clearance increases | 1. Airfoil roughness |
| HPC | 1. Clearance increases 2. Increased roughness 3. Airfoil camber loss | |
| Combustor | No major direct effects but important indirect effects on turbine performance loss resulting from changes in TET pattern | |
| HPT | 1. Tip clearance increases | 1. Vane bow 2. Twisting |
| LPT | 1. Tip clearance increases | |

In his work [11] utilises an F404 transient engine simulation program to investigate the engine's life usage in terms of creep, LCF and thermal fatigue, and .simulates the component degradation as changes in flow capacity and efficiency. The representative values of degradation (shown in table 1.3) used by [11] were based on the analysis of [10] above but of higher magnitude to closely simulate the behaviour of engines used on fighter aircraft.

Table 1.3: Summary of module degradation levels simulated [11].

| Component | Efficiency % Delta | Flow Capacity % Delta |
|-----------|--------------------|-----------------------|
| LPC | -3.0 | -4.0 |
| HPC | -8.0 | -10.0 |
| HPT | -2.0 | +1.8 |
| LPT | -0.2 | +0.4 |

[11] uses the power lever angle (PLA) and thrust as control parameters providing input to the engine. [11] determined the effects of degradation on life usage by comparing the percentage levels of creep and fatigue against that

from a clean engine. The results from [11] are summarised in tables 1.4 to 1.6. They show that LPC degradations result in significant increases in creep and thermal fatigue due to an increase in TET, with marginal changes in the LCF. For the HPC degradation, [11] presents significant increases in both creep and thermal fatigue due to an increase in TET, whilst the impact on LCF (rotating and pressure) vary depending on the degraded performance parameter (flow capacity or efficiency). HPT degradations are reported to cause increase in both creep and thermal fatigue due to increases in TET, with effects on LCF inconclusive. LPT degradations are reported to have notable increases in rotating LCF and decrease in pressure LCF with negligible impact on creep and thermal fatigue. According to [11], the effects of flow capacity degradation are greater than those for efficiency degradation. The results of [11] show no identifiable correlation between the effects of single and multiple component degradation. The work of [11] was important to this research and contributed to the preliminary requirements of understanding the effects of engine component degradation on life usage as well as identifying any correlations between the effects of single and multiple component degradations. The limitation of [11] is that the studies were conducted on a military aircraft engine and no optimisation studies were conducted.

Table 1.4: Summary of the effects of degradation on rotating LCF and pressure LCF [11].

| Component | Effect of Efficiency on Rotating LCF [%] | | Effect of Flow Capacity on Rotating LCF [%] | |
|-----------|--|----------------|---|----------------|
| | PLA Control | Thrust Control | PLA Control | Thrust Control |
| LPC | 9 | Indeterminate | 5 | Inconclusive |
| HPC | -10 | -5 | 48 | 65 |
| HPT | Inconclusive | Inconclusive | Inconclusive | Inconclusive |
| LPT | 0 | 7.5 | 0 | 16.5 |
| Component | Effect of Efficiency on Pressure LCF [%] | | Effect of Flow Capacity on Pressure LCF [%] | |
| | PLA Control | Thrust Control | PLA Control | Thrust Control |
| LPC | -11.7 | 10.6 | Inconclusive | Indeterminate |
| HPC | -23.2 | -10 | Inconclusive | Inconclusive |
| HPT | 0.4 | Inconclusive | -10 | -21.7 |
| LPT | 0 | -7.1 | 0 | -12.5 |

Table 1.5: Summary of the effects of degradation on thermal fatigue and on creep [11].

| Component | Effect of Efficiency on Rotating LCF [%] | | Effect of Flow Capacity on Rotating LCF [%] | |
|-----------|--|----------------|---|----------------|
| | PLA Control | Thrust Control | PLA Control | Thrust Control |
| LPC | 21.5 | Indeterminate | 23.3 | 20.4 |
| HPC | 210 | 200 | 150 | 180 |
| HPT | 7.3 | 10.7 | 24 | 33.5 |
| LPT | 0.3 | 0.2 | -0.3 | 0.7 |
| Component | Effect of Efficiency on Creep [%] | | Effect of Flow Capacity on Creep [%] | |
| | PLA Control | Thrust Control | PLA Control | Thrust Control |
| LPC | 11.8 | 44.1 | 21.8 | 54.9 |
| HPC | 50 | 40 | 60 | 130 |
| HPT | Indeterminate | 9.5 | 50.3 | 42.7 |
| LPT | Inconclusive | Inconclusive | Inconclusive | Inconclusive |

Table 1.6: Comparison of the effects of single and multiple component degradations [11].

| Degraded Component | Rotating LCF | Pressure LCF | Creep | Thermal Fatigue |
|--|--------------|--------------|-------|-----------------|
| -3% LPC efficiency | 0.48 | 0.014 | 0.32 | 74.85 |
| -3% LPC flow | 0.66 | 0.016 | 0.32 | 70.51 |
| -5% HPC efficiency | 0.52 | 0.12 | 0.26 | 120.79 |
| -5% HPC flow | 0.98 | 0.014 | 0.36 | 82.47 |
| Combined -3% LPC efficiency and -3% LPC flow | 0.76 | 0.15 | 0.30 | 93.96 |
| Added individual -3% LPC efficiency and -3% LPC flow | 1.13 | 0.03 | 0.64 | 145.36 |
| Combined -5% HPC efficiency and -5% HPC flow | 0.67 | 0.011 | 0.33 | 207.97 |
| Added individual -5% HPC efficiency and -5% HPC flow | 1.51 | 0.026 | 0.62 | 203.26 |
| Combined -3% LPC flow and -5% HPC flow | 0.34 | 0.025 | 0.15 | 47.20 |
| Added individual -3% LPC flow and -5% HPC flow | 1.64 | 0.030 | 0.68 | 152.98 |

In his work [12] a PhD researcher at Cranfield University investigates the extents to which a military aircraft's engine degradation adversely affects the fuel, life-usage and the aircraft's operational-effectiveness. [12] uses computer modelling and simulation techniques to conduct analyses on the F404- GE-400 aero-engine used to power the McDonnell Douglas F- 18 aircraft. The research of [12] is useful to this research topic as it explores the implications of engine degradation on the aircraft's mission operational-effectiveness and on the fuel and life usage. [12] demonstrates that engine degradation adversely affects the performance and shortens the useful life of the engine, resulting in higher life cycle costs. The results of [12] for 10% component degradation are shown in figures 1.16 to figure 1.20. The results show the effects of individual component and whole engine degradation on net thrust, mission fuel burn and the variation in blade creep, LCF and thermal fatigue life. The limitation of [12] is that it was restricted to the analysis of a military aircraft (military engines are exposed to extremely severe manoeuvres compared to those experienced by civil aircraft), and no trajectory optimisation has been carried out.

The paragraphs that follow present a review of work from [13] to [25]. It is important at this juncture to highlight that the review of [13] to [25] serves to provide the context and significance of this PhD research. It highlights and shows that most work to date has been focused on optimising aircraft trajectories with respect to fuel burn, emissions, flight time and noise. No work has been found on engine degradation and the effects it has on DOC, emissions and the optimal solutions for fuel burn. No work found on the effect the optimal solutions for fuel burn have on engine useful life and DOC.

In their work [13] researchers at Stanford University explore the feasibility of integrating environmental performance as optimisation objectives at the aircraft conceptual design stage. The authors use a multidisciplinary multi-objective genetic algorithm to quantitatively address the trade-offs between aircraft noise, emissions and operating cost. The research undertaken by [13] is useful to this research topic as the authors use Multidisciplinary Design Optimisation (MDO) to resolve diverging (and conflicting) environmental objective requirements. [13] illustrates the ability of a conceptual tool to predict the consequences of design changes. Figure 1.21 shows the variation of fuel, Landing-Take-Off (LTO) NO_x and noise with operating cost. As with the later study by [14] cited below, the limitation of [13] is that it was restricted to aircraft design optimisation and not trajectory optimisation.

In his work [14] an MSc student at the University of Toronto uses MDO methods to simultaneously design and optimise aircraft airframes, engines and mission in developing environmentally friendly aircraft. The author performs single and multi-objective optimisations to assess the trade-offs between aircraft optimised for minimum LTO NO_x emissions, mission fuel burn, fuel burn per nautical mile flown and minimum cost. The work of [14] is useful to this research topic as it uses MDO to identify solutions for varying environmental objectives. The results of [15] demonstrate that multidisciplinary optimisation can be used as a tool to optimise aircraft (at the design stage) for minimum environmental

impact. The limitation of [14] is that it was restricted to aircraft design optimisation and not trajectory optimisation.

In his work [15] a PhD researcher at Cranfield University assesses the potential of different novel propulsion systems with enhanced propulsive efficiency and thermal efficiency to meet future environmental and economic goals. The author uses single and multi-objective optimisation to address the trade-offs to be made between noise, emissions, operating cost, fuel burn and performance at aircraft level in order to make aviation more sustainable environmentally and economically. [15] uses a multidisciplinary design framework to achieve this. The work of [15] is useful to this research topic as it uses TERA type techno-economic and environmental assessments, but has limitation in that it was restricted to aero-engine cycle optimisation rather than trajectory optimisation. Figures 1.22 and 1.23 show the single-objective and multi-objective optimisation results.

In their work [16] researchers from the National Technical University of Athens use an integrated aircraft mission analysis procedure incorporating engine deterioration to provide optimised flight trajectories for short – medium range missions. The authors use what is called the simplex downhill method in multi-dimensions to identify the optimum trajectories. [16] shows the mission characteristics cruise, altitude and speed for the optimum trajectories for engine deterioration, mission length and varying Take-Off Weight (TOW). The results of [16] show that for the same thrust requirements and trajectory flown, a degraded engine will operate at higher spool speeds; higher TET's and increased SFC and consequently burn more fuel. The results of [16] are shown in figures 1.24 to 1.26. The limitation of [16] is that the optimisation was for the climb and cruise segments.

In his work [17] a PhD researcher at Cranfield University evaluates engine/aircraft design trade-offs to be made when addressing the objective of delivering a low environmental impact at low operating costs. The author uses single-objective multidisciplinary genetic algorithm (GA) based optimisation to carry out aircraft trajectory (for short range missions) and engine cycle optimisations. The author addresses the trade-offs between flight time, fuel burn, and emissions (NO_x, CO₂ and H₂O) and the results shown in figure 1.27 and figure 1.28 compare well with those from later studies, notably by [18], [19], [20], [21] and [22] cited below. For minimising flight time, [17] suggests flying at the highest possible true airspeed and that in order to minimise fuel burn during a given flight profile, requires relative low speeds and high altitudes. The flight profiles optimised for minimum NO_x emissions are achieved similarly to the fuel optimised ones, i.e. at slower and higher than the minimum time flight profiles. [17] uses a multidisciplinary design framework to achieve this. The work of [17] is useful to this research topic as it employs TERA type techno-economic and environmental assessments and genetic based optimisers to determine and assess optimum and greener aircraft trajectories that will minimise the environmental impact of aircraft operations. The results from [17] demonstrate that by introducing changes in aircraft operational procedures, the environmental impact of commercial aviation may be reduced. The limitation of

[17] is that it was restricted to basic aircraft trajectories, thus the author's recommendation that more realistic aircraft trajectories need to be considered. The effects of engine degradation were not considered.

In his work [18] an MSc student at Cranfield University uses a multidisciplinary aircraft trajectory optimisation framework to identify "greener" trajectories. [18] carries out multi-objective optimisation case studies to minimise mission fuel burn, mission time and mission NO_x. The work of [18] is useful to this research topic as [18] uses TERA type techno-economic and environmental assessments to determine and assess optimum aircraft trajectories that will reduce the environmental impact of aircraft operations. The results of [18] as they are shown in figure 1.29 and figure 1.30 demonstrate that multidisciplinary optimisation can be used as a tool to identify flight trajectories for minimum environmental impact. As with some of the studies that have been cited, the limitation of [18] is that it was restricted to basic aircraft trajectories, thus the author's recommendation that more realistic aircraft trajectories need to be considered. No wind or other weather effects were taken into account in [18]. The effects of engine degradation were not considered.

In his work [19] an MSc student at Cranfield University uses the multidisciplinary Green Aircraft Trajectories under ATM Constraints (GATAC) model integration framework with a multi-objective genetic algorithm (GA) based optimiser to optimise aircraft trajectories for fuel burn, flight time and NO_x emissions for long range missions. The work of [19] is useful to this research topic as it uses the GATAC framework and optimiser which have been used in this research. The results from [19] demonstrate the benefit in fuel burn, NO_x and CO₂ emissions that can be attained when flying the optimised trajectories, and addresses the trade-offs between fuel burn and time and between fuel burn and NO_x emissions. As with some of the studies that have been cited, the limitation of [19] is that it was restricted to basic aircraft trajectories and did not consider Air Traffic Management (ATM) constraints, thus the author's recommendation that more realistic aircraft trajectories need to be considered. No wind or other weather effects were taken into account in [19]. The results of [19] shown in figures 1.31 to 1.33 compare well with those given by [19] and [21] cited below, and show that fuel burn and time are conflicting objectives, with the fuel burn optimised trajectory at higher altitudes and slower speeds, whereas the time optimised trajectory is at lower altitudes and faster speeds. [19] also shows that the fuel burn and NO_x emissions converge towards the same optimum conditions. The effects of engine degradation were not considered.

In their work, [20] researchers from Cranfield University and Airbus undertake preliminary studies to benchmark and validate a customised GA. The results of the benchmarking study establish the applicability of the customised GATAC GA optimiser as an optimisation tool and demonstrate it has the capability to evaluate optimised solutions in a complex design space which may include convex/concave and discontinuous Pareto optimal fronts. The validity and performance of the GATAC GA optimiser is established by applying it to simple trajectory optimisation cases to achieve multidisciplinary trajectory

optimisation objectives. The results presented by [20] highlight the trade-offs between mission fuel burn, mission time and mission NO_x produced for a short, medium and long range aircraft. Some of the results are shown in figures 1.34 to 1.37. The results of [20] compare well with those from studies by [8], [17], [19], [21] and [22]. [20] shows that for the flight time minimised trajectory, the GATAC GA optimiser suggests a solution where cruise altitude is minimised and flight speed maximised. The results of [20] suggest a fuel burn optimised trajectory at higher altitudes and slower cruise Mach, whereas the minimum NO_x trajectory is suggested at the maximum possible altitude and as slow as possible speed. The results of the benchmarking studies undertaken by [20] were useful for this research as they served to provide validation and performance integrity of the GATAC GA based optimiser that has been used in this work. As with some of the studies that have been cited, the limitation of [20] is that it was restricted to basic aircraft trajectories, and only the climb and cruise phases were optimised. No wind or other weather effects were taken into account in [20].

In his work [21] an MSc student at Cranfield University uses the multidisciplinary aircraft trajectory optimisation tool GATAC to assess the trade-offs between mission fuel burn, flight time and NO_x emissions, and the environmental trade-offs between direct flight trajectories and en-route stop missions for re-fuelling for long range missions. The work of [21] is useful to this research topic as [21] uses TERA type techno-economic and environmental assessments to determine and assess optimum aircraft trajectories that will reduce the environmental impact of aircraft operations. The results from [21] shown in figures 1.38 to 1.41 demonstrate that changing the way aircraft are operated is a possible solution to reduce the impact of aviation on the environment. As with some of the studies that have been cited, the limitation of [21] is that it was restricted to basic aircraft trajectories, thus the author's recommendation that more realistic aircraft trajectories need to be considered. No wind or other weather effects were taken into account in [21]. The effects of engine degradation were not considered.

In his work [22] an MSc student at Cranfield University investigates the effect of engine performance degradation on fuel burn and NO_x emissions. The author uses the generic multidisciplinary genetic algorithm based aircraft trajectory optimisation framework GATAC to identify the potential for optimised aircraft flight trajectories for short and medium range missions. The work presented by [22] is a result of a collaborative effort between this author and the MSc student, and has contributed to the preliminary requirements of this research. The engine model used in these assessments is a typical twin spool high bypass turbofan engine similar to the CFM56-5B3 engine used to power the Airbus A320 aircraft family. The design point for the engine model was set at Top of Climb (ToC). To model the effects of engine degradation 2% levels of degradation were made to the efficiencies and pressure ratios of key engine components such as the fan, LPC, HPC, LPT and HPT. The analyses were for single component degradation. The clean engine trajectory assessed at 10668m cruise altitude and 0.8 Mach number was set as the baseline (reference) trajectory against which the degraded and optimised trajectories were compared. Aircraft trajectory optimisation studies were conducted to

minimise mission fuel burn and mission time. For the optimisation assessments full flight trajectories were analysed but only the climb and cruise segments were the optimised. The variable bounds shown in table 1.7 were used. The take-off, descent, approach and landing segments were kept the same for all trajectories. The assessments made by [22] identify the trade-offs between fuel burn and flight time and between fuel burn and NOx emissions. The results of [22] are shown in figures 1.42 to 1.45 and show an increase in total mission fuel burn and NOx emissions because of degradation. The results of [22] compare well with those from previous studies by [8], [16] and [19] cited above, and by [23] cited below. The results show the fuel burn optimised trajectory burns less fuel and takes longer than the time optimised trajectory. Fuel burn and NOx converge towards one optimal solution. The optimised trajectories identified by [22] represent possible solutions with potential to reduce the environmental impact. The limitation of [22] is that the degradation levels have been arbitrarily assigned, and individual components have been degraded independent of each other, which is not so in practice. The optimisation has been limited to the clean engine and only for the climb and cruise phases. No wind or other weather effects were taken into account by [22]. The results of [22] have been beneficial to this work in the following regard: compared to the nominal (clean) engine, a degraded engine operates at greater airflow and fuel flow rates, increased turbine entry temperatures and spool speeds in order to meet the required thrust and aircraft performance. As a consequence, degraded engines burn more fuel and produce more NOx. The results of [22] further validate the use of the GATAC framework and optimiser in solving aircraft trajectory problems. [22] also shows the benefits of take-off derate in reducing fuel burn and NOx emissions.

Table 1.7: Optimisation variable bounds [22].

| Decision Variable | Lower Bound | Upper Bound |
|---------------------|-------------|-------------|
| Altitude 1 [m] | 458 | 1125 |
| Altitude 2 [m] | 1126 | 1792 |
| Altitude 3 [m] | 1793 | 2459 |
| Altitude 4 [m] | 2460 | 3126 |
| Altitude 5 [m] | 3127 | 3128 |
| Altitude 6 [m] | 3129 | 3130 |
| Altitude 7 [m] | 3131 | 3795 |
| Altitude 8 [m] | 3796 | 4462 |
| Altitude 9 [m] | 4463 | 5129 |
| Altitude 10 [m] | 5130 | 5796 |
| Altitude 11 [m] | 5797 | 6463 |
| Altitude 12 [m] | 6464 | 7130 |
| Altitude 13 [m] | 7131 | 7797 |
| Altitude 14 [m] | 7798 | 8464 |
| Altitude 15 [m] | 9465 | 9131 |
| Altitude 16 [m] | 9132 | 9999 |
| Altitude 17 [m] | 10000 | 11000 |
| Cruise Altitude [m] | 10001 | 11000 |
| Cruise Mach [-] | 0.75 | 0.85 |

In his work [23] an MSc student at Cranfield University uses the multidisciplinary GATAC framework and the GATAC GA based aircraft trajectory optimiser to make multi-objective assessments on the impact of aircraft operations (for short, medium and long range missions) on the environment and to address the trade-offs between fuel burn and flight time, and between fuel burn and NO_x emissions. The work of [23] is useful to this research topic as it uses the GATAC framework and TERA type techno-economic and environmental assessments to determine and assess optimum aircraft trajectories that will reduce the environmental impact of aircraft operations. The results from [23] are shown in figures 1.46 to 1.49 demonstrate that aircraft trajectory optimisation is a possible solution to reducing the environmental impact of aircraft operations. The limitation of the work of [23] is that it was restricted to basic aircraft trajectories, thus the author's recommendation that more realistic aircraft trajectories need to be considered. No wind or other weather effects were taken into account in the work of [23]. The effects of engine degradation were not considered. The work of [23] also serves to benchmark and test the GATAC GA based optimiser that has been adopted for use in this research.

In their work [24] researchers at the National Aeronautics Space Agency (NASA) and the University of California develop a flight trajectory optimisation algorithm to calculate a wind-optimal trajectory for cruising aircraft while avoiding the regions of airspace prone to persistent contrails formation. The authors use a non-linear optimal control with path constraints to make trade-offs between persistent contrails and fuel burn. The results of [24] demonstrate the complex relation between fuel efficiency and the impact on the environment. The limitation of [24] is that it was limited to only the cruise altitude as an optimisation variable. The work of [24] was useful for this research, as it provided useful supplementary information on employing operational strategies in air traffic management to potentially mitigate the environmental impact of aircraft operations.

In her work, [25], an MSc student at the Norwegian University of Science and Technology uses parametric analysis to identify 'greener sky' aircraft trajectories for reduced fuel burn and emissions for short, medium and long haul flights. The results presented by [25] and shown in figure 1.50 and figure 1.51 show the influence of climb and descent time and cruise altitude on the fuel consumption. The author shows how the different phases of the flight trajectory have to be optimised to reduce the fuel consumption. For the short haul flight mission [25] shows that the maximum fuel burn occurs during the climb phase. To reduce this consumption, [25] suggests decreasing the climb distance and the climb time. For the medium and long haul flight missions the author shows that the most fuel is consumed during the cruise phase, yet fuel burn per unit time remains higher during the climb phase. The results of [25] show that the optimal flight trajectory for the minimum fuel burn is obtained for a short climb phase and a long descent. The author also shows that fuel burn will benefit where the aircraft take-off weight has been reduced. In the current climate where flight operators' objective is finding solutions to reduce fuel burn, the results of [25] were useful for this research by providing useful information on

the influence the flight trajectory has on fuel burn and the importance of optimising the different phases of the trajectory. The limitation of the work of [25] is that the assessments were restricted to a clean engine and the effects of engine degradation were not considered.

In their work [26] researchers from Purdue University and Massachusetts Institute of Technology identify and systematically evaluate a comprehensive set of potential near-term operational mitigations across all flight phases. The authors use a rating system to perform an iterative evaluation of the mitigation options and determine for each, the relative environmental mitigation benefits and potential for successful implementation, and identifies possible barriers to implementation. The result of [26] is the evaluation of the mitigation's impact in fuel burn reduction, climate impact reduction, air quality impact reduction, and noise reduction. The work of [26] was useful for this research, by providing supplementary information on using operational procedures as one way of mitigating the environmental impacts of aviation. The limitation of the work of [26] is that no actual optimisation studies were carried out.

In their work [27] researchers at the General Electric Company and Wright Patterson Air Force Base do a study to evaluate the differences between engine design usage and actual flight usage and the effect these differences have on the relative durability and life of the engine's turbine components. Their studies were carried out on the CF6-50 and F101 engines for both commercial and military applications. Available engine flight usage data was used to relate engine operating conditions to flight conditions, effects of engine. The Operational Severity Analysis (OPSEV) computer program was used in the analyses to predict the relative usage severity of the engine and its components as a function of engine cycle, mission and component characteristics. For each major component, the cyclic and steady state damage rates were related to the specific engine parameters influencing their failure characteristics. Trade-off curves (derived using basic failure equations and experience) were used to predict the severity for each mission as seen by each component. The results of the studies by [27] show that military transport aircraft engine usage is more severe than commercial aircraft usage (figure 1.52). The increased usage severity is attributed to higher cyclic damage. The limitation of the work of [27] is that the effects of engine component degradation were not considered in the severity studies and the studies were restricted to severity due to the type of mission and not due to taking off from specific airports. The work of [27] was however important to this research and contributed to the preliminary understanding of severity as a measure of life consumption.

In his work [28] a PhD researcher at Cranfield University estimates the severity of a civil aero-engine as influenced by operational and technological factors for short and long haul flights. The purpose of his study (as relevant to this research) was to determine the effect of operational and technological factors on the severity of the HPT. [28] performed parametric analyses on the operational parameters: take-off, climb and cruise derate, OAT, airport altitude, cruise altitude and cruise Mach number, and on the technological parameters: cooling effectiveness, thermal barrier coating thickness, thermal conductivity of

the coating, pattern factor and profile. In order to estimate the severity, [28] defined the reference mission for the short and long haul as follows:

- Short range: 10% TO derate, 1.4hrs trip length, 18 °C OAT
- Long range: 10% TO derate, 4hrs trip length, 18 °C OAT

For different levels of thrust, [28] keeps with the definition of [27] on severity and expresses the level of damage as a ratio relative to the reference mission e.g. the reference mission has a severity equal to unity. Figure 1.64 shows the different elements employed by [28] in the severity estimation process. The life is estimated in terms of creep, LCF and oxidation. The results show that TO derate and OAT both have a dominating influence on engine severity, whereas employing derate during climb is more beneficial in lowering the severity of long haul flight engines. The effects of airport altitude could be reduced by using appropriate TO derate. Figures 1.53 to 1.56 show the effects of TO derate, OAT and airport altitude for the short haul case as presented by [28]. Figure 1.57 shows the variation in severity for increasing TO altitude by 500m, OAT by 5°C, TO derate by 5%, climb derate by 5%, cruise derate by 5%, cruise altitude by 500m and cruise Mach by 0.05. The results of [28] show (in table 1.8) that for short haul flights, engine severity is dominated by cyclic damage (due to LCF) for both the blades and the disc, whereas for long haul flights steady state damage (due to creep) is dominant for the blade and cyclic damage is dominant for the disc. The limitation of the work of [28] is that the severity studies were carried out for a clean engine, were restricted to different thrust engines and parametric analyses and not TO from specific airports and a constant offset in OAT with altitude is assumed. The work of [28] was however important to this research and as with [27] cited above, contributed to the preliminary understanding of severity as a measure of life consumption and establishing the characteristic trends associated with derate, OAT and airport altitude.

Table 1.8: Engine severity estimation for the reference mission [28].

| Trip Length [hrs.] | TO Derate [%] | Blade | | | Disc | | | Average | | |
|--------------------|---------------|-------|------|-------|------|------|-------|---------|------|-------|
| | | CS | SS | Total | CS | SS | Total | CS | SS | Total |
| 1.4 | 10 | 0.97 | 0.03 | 1.00 | 1.00 | 0.00 | 1.00 | 0.98 | 0.02 | 1.00 |
| 4 | 10 | 0.00 | 1.00 | 1.00 | 1.00 | 0.00 | 1.00 | 0.50 | 0.50 | 1.00 |

CS – Cyclic Severity

SS – Steady State Severity

Total – Total Severity

The work reviewed and the limitations of each is summarised in table 1.9.

Table 1.9: Summary of previous work done

| Reference | Main Objectives | Limitations | Addressed in Current Work |
|-----------|---|---|---|
| [8] | <ol style="list-style-type: none"> 1. Fuel burn optimised civil aircraft trajectories for clean and degraded engines 2. Degraded engine life assessments | <ol style="list-style-type: none"> 1. Single component degradation 2. Arbitrary assignment of degradation levels 3. Cruise segment optimisation | <ol style="list-style-type: none"> 1. Multiple component degradations 2. Degradation levels based on established trends 3. Full trajectory optimisation 4. Fuel burn and engine life optimised trajectories |
| [9] | <ol style="list-style-type: none"> 1. Best trajectory for fuel, time and engine life 2. Degraded engine life assessments | <ol style="list-style-type: none"> 1. Parametric analyses 2. Single component degradation 3. Arbitrary assignment of degradation levels 4. Cruise segment assessments | <ol style="list-style-type: none"> 1. Genetic Algorithm based optimisations 2. Multiple component degradations 3. Degradation levels based on established trends 4. Full trajectory optimisation |
| [10] | <ol style="list-style-type: none"> 1. Establish trends in performance loss 2. Quantify levels of degradation and contribution of each component 3. Identify causes of degradation | <ol style="list-style-type: none"> 1. Studies conducted on JT9D engines 2. No optimisation studies | <ol style="list-style-type: none"> 1. CFM56-7B27 engine studied 2. Fuel burn and engine life optimisation studies |
| [11] | <ol style="list-style-type: none"> 1. Effects of degradation on the major modes of engine failure 2. Determine if effects of individual component degradation are additive | <ol style="list-style-type: none"> 1. Study limited to military application 2. No optimisation | <ol style="list-style-type: none"> 1. Civil aircraft application studied 2. Fuel burn and engine life optimisation studies |
| [12] | <ol style="list-style-type: none"> 1. Effects of engine degradation on fuel burn, life-usage and aircraft operational-effectiveness | <ol style="list-style-type: none"> 1. Military aircraft application 2. No flight trajectory optimisation | <ol style="list-style-type: none"> 1. Civil aircraft application 2. Fuel burn and engine life optimised trajectories |
| [13] | <ol style="list-style-type: none"> 1. Quantitative analysis of the trade-offs between environmental performance and operating cost | <ol style="list-style-type: none"> 1. Aircraft design optimisation 2. No trajectory optimisation | <ol style="list-style-type: none"> 1. Fuel burn and engine life trajectory optimisation studies |
| [14] | <ol style="list-style-type: none"> 1. Potential of novel propulsion systems to meet future environmental and economic goals 2. Trade-offs between noise, emissions, operating cost, fuel burn and performance | <ol style="list-style-type: none"> 1. Engine cycle optimisation 2. No trajectory optimisation | <ol style="list-style-type: none"> 1. Fuel burn and engine life trajectory optimisation studies |

Table 1.9 Continued

| Reference | Main Objectives | Limitations | Addressed in Current Work |
|-----------|---|--|---|
| [15] | 1. Aircraft design optimisation to assess trade-offs between aircraft optimised for minimum LTO NOx emissions, mission fuel burn, fuel burn per nautical mile flown and minimum cost. | 1. Aircraft design optimisation 2. No trajectory optimisation | 1. Fuel burn and engine life aircraft trajectory optimisation studies |
| [16] | 1. Fuel burn optimised civil aircraft trajectories for clean and degraded engines 2. Degraded engine performance assessments | 1. Climb and cruise segments optimisation | 1. Fuel burn and engine life optimisation 2. Full flight trajectory optimisation |
| [17] | 1. Evaluate and optimise aircraft flight trajectories and aircraft engine cycles for performance, emissions and cost | 1. Effects of degradation not assessed | 1. Degraded engine assessments |
| [18] | 1. Fuel burn, time and NOx optimised civil aircraft trajectories for short, medium and long range aircraft | 1. Effects of degradation not assessed | 1. Degraded engine assessments |
| [19] | 1. Fuel burn, time and NOx optimised civil aircraft trajectories for long range aircraft | 1. ATM constraints not considered 2. Effects of degradation not assessed | 1. Aircraft trajectories under ATM constraints 2. Degraded engine assessments |
| [20] | 1. Benchmarking and validation of GATAC GA optimiser | 1 Climb and cruise segments optimised | 1. Full trajectory optimisation |
| [21] | 1. Fuel burn, time and NOx optimised civil aircraft trajectories for long range aircraft | 1. Effects of degradation not assessed | 1. Degraded engine assessments |
| [22] | 1. Fuel burn and NOx optimised civil aircraft trajectories for long range aircraft 2. Degraded engine assessments | 1. Single component degradation 2. Arbitrary assignment of degradation levels 3. Climb and cruise segment optimisation 4. Optimisation restricted to clean engine | 1. Multiple component degradations 2. Degradation levels based on established trends 3. Full trajectory optimisation 4. Fuel burn and engine life optimised trajectories |

Table 1.9 Continued

| Reference | Main Objectives | Limitations | Addressed in Current Work |
|-----------|---|--|---|
| [23] | 1. Impact of aircraft operations for short, medium and long range missions on the environment 2. Trade-offs between fuel burn, flight time and NOx emissions | 1.. Effects of degradation not assessed | 1. Degraded engine assessments |
| [24] | 1. Wind-optimal trajectory assessments 2. Trade-offs between fuel burn and contrails | 1. Cruise segment optimisation | 1. Fuel burn and engine life trade-offs |
| [25] | 1. Optimum aircraft trajectories for reduced fuel burn and emissions for short, medium and long haul flights. | 1. No engine degradation studies | 1. Degraded engine assessments |
| [26] | 1. Evaluation of potential near-term operational mitigations across all flight phases | 1. No optimisation studies performed | 1. Fuel burn and. engine life optimised trajectories |
| [27] | 1. Evaluate the effect of differences between engine design usage and actual flight usage on the relative durability and life of the engine components. | 1. Engine application and usage severity studies | 1. Airport specific severity studies |
| [28] | 1. Severity of a civil aero-engine due to operational and technological factors for short and long haul flights. | 1. Parametric studies 2. No effects of degradation considered | 1. Airport specific severity studies 2. Engine degradation assessments |

1.4 Contribution to Knowledge

The contribution to knowledge separates into two elements: engine degradation and airport severity factors. The first is the assessment of the effects of engine degradation on flight mission fuel burn and engine life. The emphasis towards this contribution is on the change in engine life usage when optimising for flight mission fuel burn and the change in flight mission fuel burn when optimising for engine life usage. The other is the assessment of the airport environment (e.g. sand) in addition to the airport OAT and altitude, and the impact on engine component damage and life consumption, and on engine/aircraft performance metrics such as flight mission fuel burn, engine life, operating costs and emissions among others. Reference is made to table 1.9.

1.5 Research Objectives

The main aims of this research are to provide a detailed understanding on the effects of engine degradation on flight mission fuel burn and engine life, and to present an assessment (by the author) of the implications of airport severity factors on aero-engine component life and on engine and aircraft performance. The primary objectives are to provide detailed descriptions of the change in engine life when flying fuel burn optimised trajectories and the change in flight mission fuel burn when flying engine life optimised trajectories. Additionally, the impact on direct operating costs and emissions are presented. The effects of airport severity factors are discussed with the aid of several case studies.

1.6 Methodology: Steps to Complete the Research

A global framework was developed for this work. The framework was modelled after the Techno-economic & Environmental Risk Assessment' (TERA), a concept developed at Cranfield University. TERA is a multidisciplinary optimisation tool that allows for risk assessment and the comparison and ranking of competing goal functions. The framework is made up of mathematical modules that can be used to simulate the performance of single standalone or a set of integrated technologies. This section and sub-sections describe and explain the steps taken to achieve the aims and objectives of this work and provides an overview of the multidisciplinary framework used. The framework has a modular structure consisting of the following set of mathematical modules coupled to an optimiser: engine and aircraft performance, engine degradation, lifing, emissions and operating cost.

In sections 1.1 to 1.5 the subject of this thesis was introduced, i.e. the assessment of the impact of airport severity factors on engine life consumption and aircraft performance and the assessment and quantification of the change in engine life usage when optimising for flight mission fuel burn and the change in flight mission fuel burn when optimising for engine life usage. The focus was particularly the influence of airport conditions and the environment on aircraft performance and the influence of fuel burn optimised trajectories on engine life and of engine life optimised trajectories on fuel burn. Additionally, the impact on

direct operating costs and emissions and the effects of engine component degradation was to be incorporated and assessed.

According to [31], “Performance comprises the power output delivered for a given fuel flow, life, weight, emissions, engine diameter and cost, while ensuring stable and safe operation throughout the operational envelope at all conditions.” Since performance is inseparable from the economic model, it is a fulcrum in the economic viability of any engine. In this current and modern economic climate, engine performance underlines the criticality of choosing between the environmental impact and the economic performance. Any mechanical device such as an aircraft gas turbine engine will in its lifetime of service show the effects of damage and deterioration which will affect engine performance (fuel burn, engine life, emissions and engine operating costs). It is therefore very useful to make preliminary assessments (at mission level) from an operator’s perspective that may be used to give a clear view and understanding of the relative risks and benefits of potential solutions early on in the development phase. A thorough assessment of a wide ranging and sometimes conflicting disciplines requires making simultaneous and consistent comparative assessments such as those offered by MDO and in particular by TERA type assessments [32] [33] and [34]. A multidisciplinary framework was developed to enable the comparison of optimised solutions for fuel burn and engine life whilst assessing their environmental and economic impact in terms of emissions and operating costs. The same framework was used to compare the aircraft performance at varying airports. The remaining sub-sections describe and explain the steps that were followed to undertake this research.

The following steps were identified as the stages of activity which needed to be worked through in carrying out and completing the research.

- 1) Establishing the focus of the study
- 2) Identifying the specific objectives of the study
- 3) Selecting the research method
- 4) Developing the research framework
- 5) Carrying out the assessments
- 6) Results and analysis
- 7) Writing up
- 8) Enabling dissemination

1.6.1 Establishing the Focus of the Study

The continuous growth of air transport has raised concerns about global aircraft fuel consumption, emissions and noise. Industry’s efforts have identified that to reduce future emissions and the impact of aircraft operations on the environment will require contribution from: a) New technologies with better efficiency b) Improved asset management and c) Greener manufacturing and recycling processes. This research falls under asset management and involves aircraft trajectory optimisation. Most aircraft trajectory optimisation studies concentrate on optimising fuel burn, emissions and noise. During the course of this work, no work was found to better understand from an operator’s perspective how the optimal solutions for minimising fuel burn and protecting

the environment together with engine degradation, will impact on the engine useful life and consequently the engine operating costs. In that context, the focus of this research thus became the assessment of the trade-offs between mission fuel burn and engine life and the implications on operating costs and emissions when considering the effects of engine degradation. This research also looked at the influence of airport severity factors on aircraft performance.

1.6.2 Identifying the Specific Objectives of the Study

Once the focus of the study had been established, the next step was to define the specific research objectives which would assist in choosing the research method. The initial reading and literature review influenced the formulation of the research objectives and contributed to the understanding of the mechanisms of degradation and engine life limiting failure modes. Reading was continuous throughout the research period to identify new publications which might significantly influence this work and its findings. In the literature review in section 1.3, an attempt has been made to provide context to the subject area being investigated.

1.6.3 Selecting the Research Method

Once the research objectives had been formulated, the research method was selected. A TERA type aero-engine multidisciplinary integration tool was identified and used in this work. This approach was chosen as it offers preliminary assessments of competing goal functions and allows the assessment of the trade-offs between the many different requirements whilst considering different disciplines simultaneously. A techno-economic type trajectory analysis offers a preliminary understanding of the impact of flying fuel burn optimised aircraft trajectories on engine life and the impact of flying engine life optimised aircraft trajectories on fuel burn. Additionally insight and understanding is offered on how aircraft TO performance varies and is influenced by the airport of departure. Such analyses will give indication of how aircraft trajectory management may be used to put constraints on those trajectories that have a strong impact on engine deterioration.

1.6.4 Developing the Research Framework

The models making up the tool were identified; each representing a discipline sought i.e. engine and aircraft performance, emissions prediction, engine lifing assessment and operating cost prediction. These models were chosen for their legacy (having been used in past European projects such as VITAL [32]), availability and access to source codes. The models adapted for this work were developed, verified and validated at Cranfield University. None of the models was modified, and for the purposes of this work, each model's performance was assessed and validated (where possible as described in chapters 2, 3, 4 and 5) against data available in literature. The initial assessments were undertaken with the aim of demonstrating the performance of the individual models and their suitability in satisfying the requirements and

aims of this research. The assessments were conducted (to show the effects of degradation on engine and aircraft performance (fuel burn, emissions, thrust output and engine life) and these showed consistency with trends identified in the literature (where available). The fidelity of each model was deemed adequate to show the relative changes to objectives against a baseline, without greatly impacting on the results. There are other methods and models available such as those for the Environmental Design Space (EDS) [35], but these were not chosen for the reasons mentioned above.

To study the effects of degradation and the influence of airport factors on aircraft performance, a multi-disciplinary design framework (shown in figure 7.2) was used. To make the optimisation assessments, the same framework was used coupled with an optimiser (shown in figure 8.3) and integrated within the GATAC [36] integration software. A computer program was written (in FORTRAN) by the author to integrate and interface the models. This allowed for automated communication between the modules i.e. the extraction of data from the output of one module and preparing input files (required by other modules in the framework) in the required format. For the optimisation assessments there were two options to integrate the modules, either inside of GATAC or outside of GATAC. The author chose to integrate the models outside of GATAC as there were challenges to integrating within GATAC. The challenges included:

- Required inputs from some of the models such as the aircraft performance were in more than one output file, and GATAC allows only one input and one output file to be specified from which the required data can be extracted.
- The integration of individual models within GATAC would require multiple loops (interfaces) mapping inputs and outputs to respective models, which would make troubleshooting cumbersome in the case of a process failure as each loop would need to be checked.
- Communication and data handling of inputs and outputs is via GATAC hence it would take longer for each evaluation to complete.

The merits of model integration outside of GATAC were:

- The computer program allowed every required input to be extracted from whichever output file it was located in.
- No hassle of multiple loops as the integrated models interfaced with GATAC as one model (all other models inside), only one interface/loop was needed.
- GATAC sees one model (integration framework) and handles inputs and outputs from this single model, allowing for quick communication and faster execution times.
- Data flow and communication handling between models within the integration framework and not through GATAC, allowing for easy troubleshooting.

Once integration was complete, the framework was tested and deemed suitable. The next stage was undertaking the research in the form of case studies.

1.6.5 Carrying Out the Assessments

The following outlined procedure was used (The optimiser was used only for the optimisation assessments and not the airport severity factors):

- The engine performance code TURBOMATCH is used to calculate the take-off thrust, flight segment spool speeds, operating temperatures and cooling flow temperatures and specific fuel consumption (SFC).
- The aircraft performance code HERMES is used to integrate the engine and aircraft and to calculate the flight performance in terms of total mission fuel burn and flight mission time.
- The lifing code is used to estimate the useful life of the HPT blade and disc (LCF, creep and oxidation) based on metal temperatures, stresses and material properties. The life estimates are converted to damage fractions using the linear damage rule as described in chapter 7.
- The damage fractions calculated by the lifing code are used to estimate the severity for the HPT blade and disc as described in chapter 7.
- The emissions prediction code HEHAESTUS is used to predict the emissions indices for CO₂, NO_x and H₂O for the flight mission.
- The economics model HESTA is used to translate the life estimation into engine/aircraft direct operating costs.
- The GA optimiser was used to determine the fuel burn and engine life optimised trajectories. The optimised flight profile phases are defined in terms of flight altitudes and speeds.

To model the effects of engine degradation changes were made to the flow capacities and efficiencies of key engine components such as Fan, LPC, HPC, LPT and HPT.

The studies for the airport severity factors were conducted in two parts:

- Parametric studies to investigate the effect of operational parameters (TO derate, OAT, altitude and environment)
- Airport severity factors to investigate the effect of taking off from different airports e.g. Abu Dhabi, Cairo and London Heathrow.

Parametric analyses were carried out by varying the TO derate from 0% to 30%, altitude from 0m to 1500m and OAT deviation from -20°C to +20°C. The reference airport was assumed at 0% derate and ISA SLS (15°C OAT, 0°C deviation and sea level). The baseline trajectory was assumed for a clean engine TO from the reference airport on a flight mission range of 3000km. The assessments were carried out for a clean engine and after 3000 cycles. To model the desert conditions at airports such as Abu Dhabi, Cairo and Riyadh, assessments were carried out for an engine after 5250 cycles. A sensitivity study was conducted after 4500, 5250 and 6000 cycles, to guide the choice leading to the 5250 cycles being used.

The optimisation studies were conducted on the three routes (London – Madrid, London – Ankara and London - Abu Dhabi) with the aid of the following case studies:

- Case 1: Aircraft performance calculation for the clean engine (to establish baseline trajectory performance). Calculate performances after 3000, 4500 and 5250cycles of operation along same trajectory
- Case 2: Aircraft trajectory optimised for fuel burn and engine life for the clean engine
- Case 3: Aircraft trajectory optimised for fuel burn and engine life after 3000cycles of engine operation
- Case 4: Aircraft trajectory optimised for fuel burn and engine life after 4500cycles of engine operation
- Case 5: Aircraft trajectory optimised for fuel burn and engine life after 5250cycles of engine operation

The clean engine aircraft performance was assumed as the baseline trajectory along each route.

1.6.6 Results and Analysis

The results were analysed against the aims of this research. The airport severity factors are presented in chapter 7 and the aircraft trajectory optimisation in chapter 8.

1.6.7 Writing Up

The aim at this stage was to summarise and communicate the research undertaken, the results and overall conclusions of the research in an appropriate form to a wider audience.

1.6.8 Enabling Dissemination

It was important to research an aspect that was topical and relevant to the aviation industry today. Another important part of the research process was to make the findings available to a wider audience. Consequently some of the findings, results and conclusions have been used by the author to make significant contributions to knowledge in conference (and in future journal) publications.

1.7 Thesis Structure

This thesis has a modular structure adopted to reflect the modular nature of the TERA type multidisciplinary framework used and consists of ten individual chapters: Each chapter is self-contained with chapter specific abstracts, related literature, technical assessments, results, conclusions and references.

Chapter 1 is the Introduction and Background. The chapter provides the background, context and motivation of this research. A summary of the literature review of related past research and studies, an outline of the project objectives and the major contributions from the research are provided. The chapter also describes the Methodology and Overview of the Framework, and explains the steps taken to achieve the aims and objectives of this work and

provides an overview of the multidisciplinary framework used in the assessments. The framework has a modular structure consisting of the following set of mathematical modules coupled to an optimiser: engine and aircraft performance, engine degradation, lifing, emissions and operating cost.

Chapter 2 is the Engine and Aircraft Performance. The chapter provides detailed descriptions of the engine performance code TURBOMATCH, an in house simulation and diagnostics code developed at Cranfield University that was used to model the engine by calculating and closely approximating the Design Point (DP) and Off-Design (OD) engine performance to the engine data found in the public domain. The chapter also provides detailed descriptions of the aircraft performance code HERMES that was used to integrate the engine and aircraft and to determine the aircraft performance in terms of flight mission fuel burn and flight mission time. The first part of the chapter is literature describing concepts relevant to engine performance, engine component degradation and aircraft performance. The second part of the chapter describes in detail the engine performance and aircraft performance modules. The results of the validation and verification of the engine and aircraft performance models are presented.

Chapter 3 is the Gas Turbine Aero - Engine Lifing. The chapter provides a detailed description of the lifing module that has been used to estimate the creep, fatigue and oxidation life of the HPT disc and blades through analysis over a full working cycle of the engine. The first part of the chapter is literature describing concepts relevant to engine life usage, and the major life limiting modes of failure. The second part of the chapter describes in detail the engine lifing module. The HPT's creep, LCF and oxidation life estimation approaches are discussed. The results of the validation and verification of the engine lifing model done by an MSc student at Cranfield University can be found in [36].

Chapter 4 is the Gas Turbine Aero - Engine Emissions. The chapter provides a detailed description of the emissions module HEPHAESTUS developed at Cranfield University and has been used to predict the LTO and total flight emissions. The first part of the chapter is literature describing concepts relevant to aero-engine emissions, legislation and the contribution of aviation to emissions. The second part of the chapter describes the working principles of the emissions module. The results of the validation and verification of the emissions code are presented.

Chapter 5 is the Engine Operating Costs. The chapter provides a detailed description of the economics module HESTA that was used to calculate the DOC of the engine as a function of maintenance cost, cost of taxes on emissions and noise, cost of fuel, cost of insurance and cost of interest paid on the total investment, and the DOC of the aircraft as a function of the cost of cabin and flight crew, cost of landing, navigational and ground handling fees. The first part of the chapter is a review on the new total care package (power by hour) business model. The second part of the chapter describes in detail the economics module. The results of the validation and verification of the economics model are presented.

Chapter 6 is the Aircraft Trajectory Optimisation. The first part of the chapter provides discussions on available optimisation methods and the benefits offered by aircraft trajectory optimisation as a financially viable option that can cost effectively and competitively improve aircraft operations and contribute towards the ACARE targets for existing engines and aircraft. The latter part of the chapter presents the optimiser that has been selected and used in this work: a genetic algorithm based multi objective optimiser which implements a Non-dominated Sorting Genetic Algorithm (NSGAI). The results of the validation and verification of the optimiser are presented.

Chapter 7 is the Case Study: Airport Severity Factors. The chapter presents a major contribution made by the author in the assessment of the impact of airport severity factors on aero-engine degradation, flight mission fuel burn and engine life. The chapter uses severity as a measure of life consumption and an assessment on the implications of airport factors on engine/aircraft performance metrics is presented. The first part of the chapter links engine damage with severity. The second part of the chapter presents the preliminary assessments carried out to establish how the major parameters influence operational severity. The results of parametric assessments on the life consumption (damage rate), operating conditions (TET and exhaust gas temperature (EGT)), DOC per flight, engine life, mission fuel burn and ICAO LTO and total flight emissions of civil aero-engines are presented. Additionally, the results of case studies carried out on specific airports are also presented.

Chapter 8 is the Case Study: Flight Mission Fuel Burn and Engine Life Optimised Aircraft Trajectories. The chapter presents another major contribution made by the author in the assessment of the trade-offs between mission fuel burn and engine life optimised aircraft trajectories and the impact of aero-engine component degradation. The results of aircraft trajectory optimisation assessments carried out at mission level for an engine and aircraft similar to the short to medium range single aisle Boeing 737-800 aircraft powered by a CFM56-7B27 engine are presented. The case studies described represent mission ranges of: 674nm, 1569nm and 2981 nm, corresponding to the city pairs: London – Madrid, London – Ankara and London – Abu Dhabi respectively. The results showing the effects on engine life (creep, fatigue and oxidation) when flying mission fuel burn optimised trajectories and the effects on mission fuel burn when flying engine life optimised trajectories are presented. Additionally, the life consumption (damage fraction), operating conditions (TET and EGT), DOC per flight, engine life, mission fuel burn and ICAO LTO and total flight emissions of civil aero-engines are presented.

Chapter 9 is the Conclusions and Recommendations. This is the final chapter of the thesis and provides an overall conclusion of the work presented in each of the individual chapters 7 and 8. The author's main contributions to knowledge in the area of aircraft operational procedures and trajectory optimisation are presented. The limitations of each of the varying analyses are highlighted and recommendations for further work appropriately made.

1.8 Additional Work Undertaken During Research

Apart from working on the research, the PhD has provided opportunity to closely work with and assist several MSc students with their research thesis (which is a major contributor to the MSc course). Technical leadership and support provided by the author, and the MSc work essentially used inputs from this PhD research and acknowledged its contribution in achieving the project aims and vice versa.

The author has also contributed towards conference publications. This section provides details of the conference publications and the contribution made to other research projects.

Published Papers:

1. *“Towards Development of a Diagnostic and Prognostic Tool for Civil Aero-Engine Component Degradation”* [29]

Conference: ASME India 2012

Paper Reference: GTIndia2012-9703

Authors: N. Khani, C. Segovia, R. Navaratne, V. Sethi, R. Singh and P. Pilidis

NB: The abstract of this publication is presented in Appendix 1.

2. *“Effects of Aero-Engine Component Degradation on Flight Mission Fuel Burn and NOx Emissions”* [30]

Conference: ISABE 2013

Paper Reference: ISABE-2013-1335

Authors: N. Khani, B. Venediger, C. Segovia, V. Sethi, P. Pilidis and Y. Li

NB: The abstract of this publication is presented in Appendix 2.

Contribution to Research Projects:

1. Segovia, C. (2012), *“Effect of engine degradation on fuel burn optimum civil aircraft trajectories”* [8].

NB: The abstract of this MSc thesis is presented in Appendix 3.

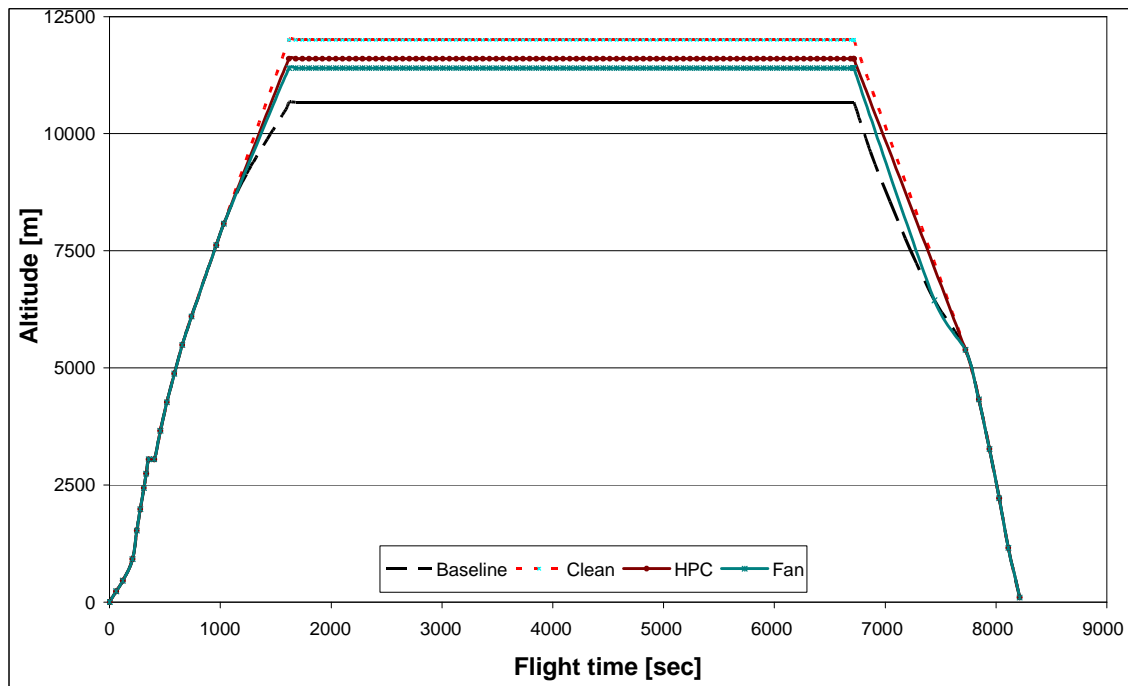
2. Venediger, B. (2013), *“Civil aircraft trajectory analyses: Impact of engine degradation on fuel burn and emissions”* [22].

NB: The abstract of this MSc thesis is presented in Appendix 4.

3. Chandran S. (2013), *“Effect of engine degradation on engine and aircraft performance”* [9]

NB: The abstract of this MSc thesis is presented in Appendix 5.

Figures for Chapter 1



Baseline - Trajectory for clean engine

Clean - Optimised trajectory for clean engine

HPC - Optimum trajectory for 2% degradation in both HPC efficiency and flow capacity

Fan - Optimum trajectory for 2% degradation in both fan efficiency and flow capacity

Figure 1.1: Optimised flight trajectories [8].

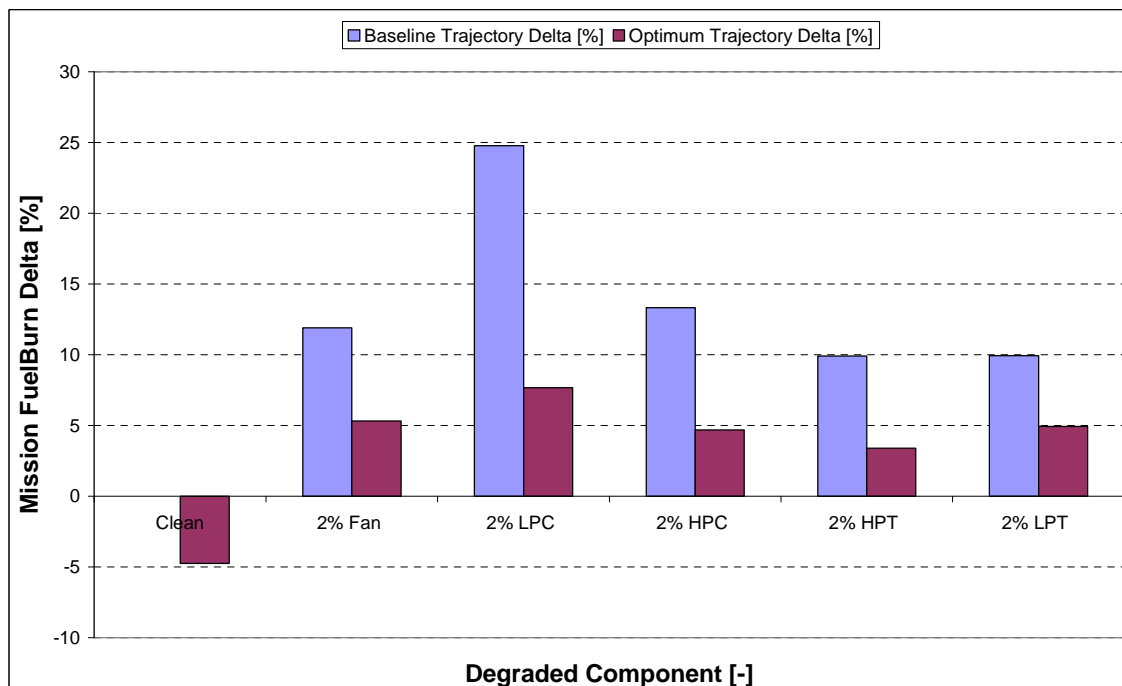


Figure 1.2: Fuel burn delta for the optimised flight trajectories relative to the baseline trajectory [8].

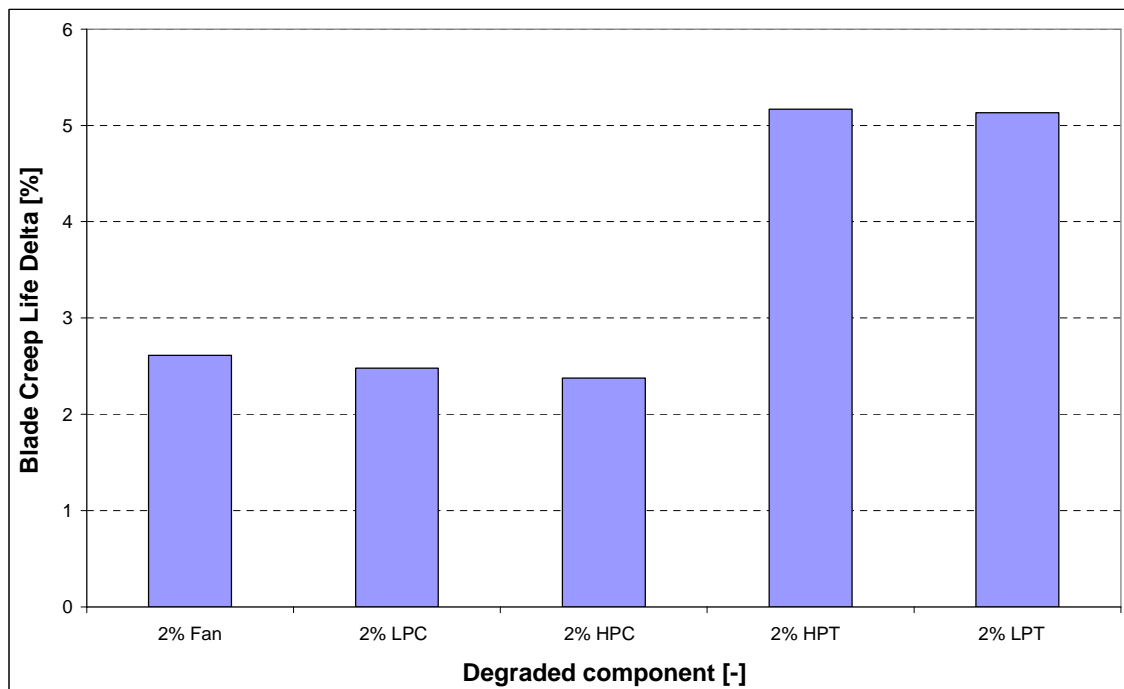


Figure 1.3: Effect of 2% component degradation on blade creep life [8].

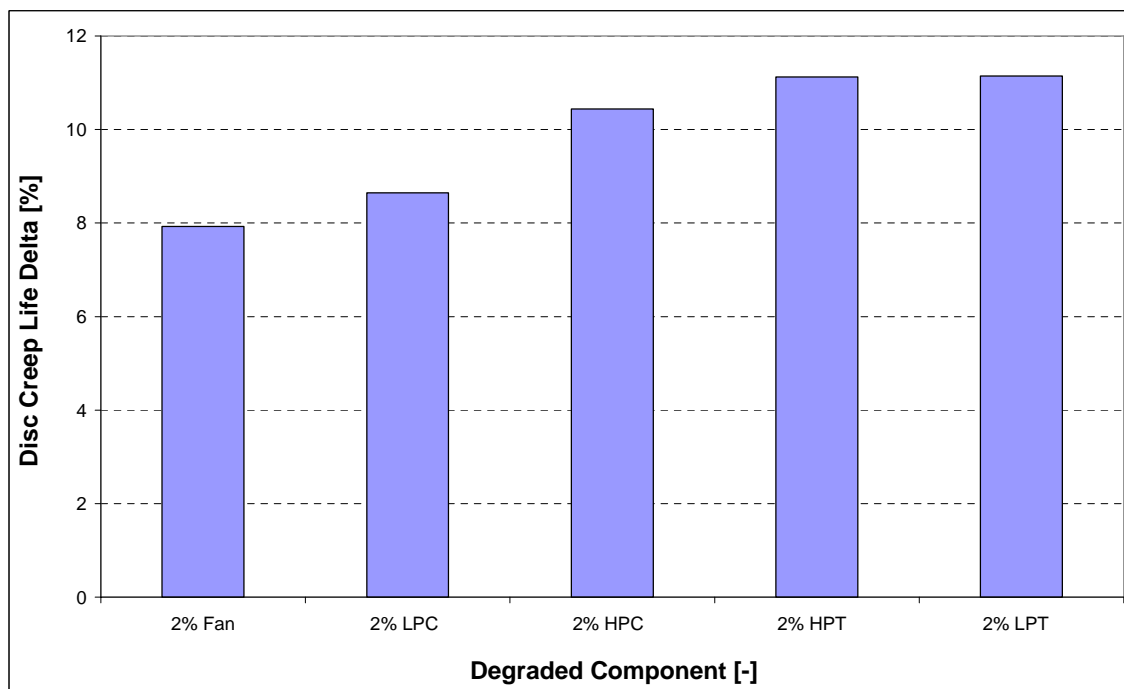


Figure 1.4: Effect of 2% component degradation on disc creep life [8].

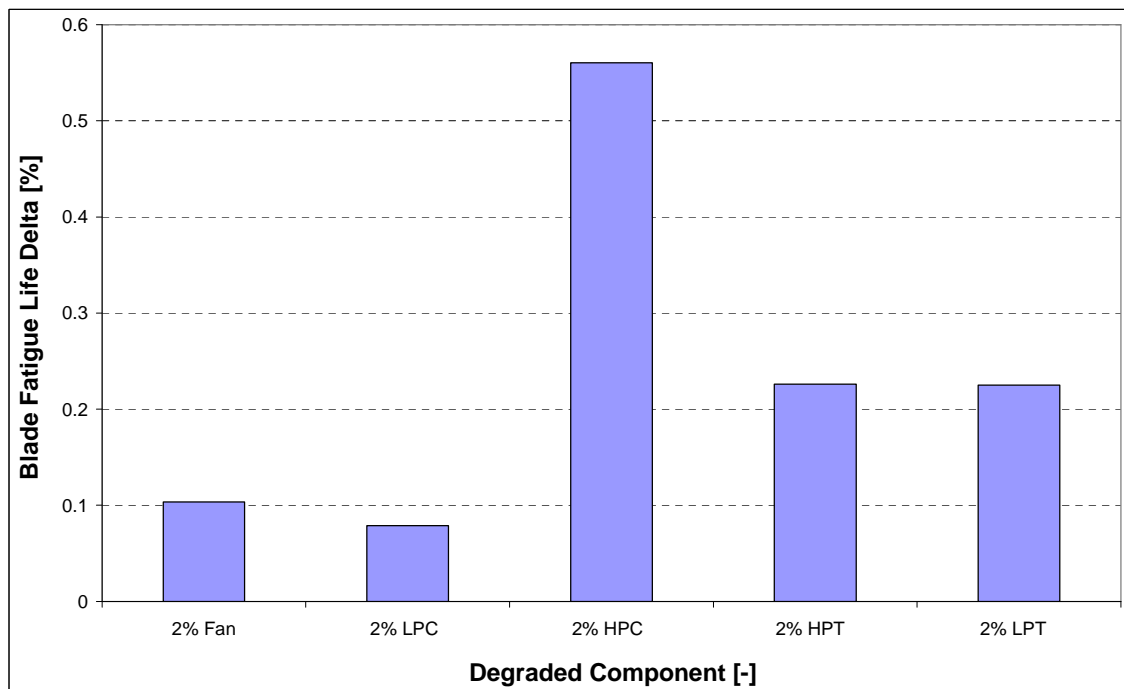


Figure 1.5: Effect of 2% component degradation on blade fatigue life [8].

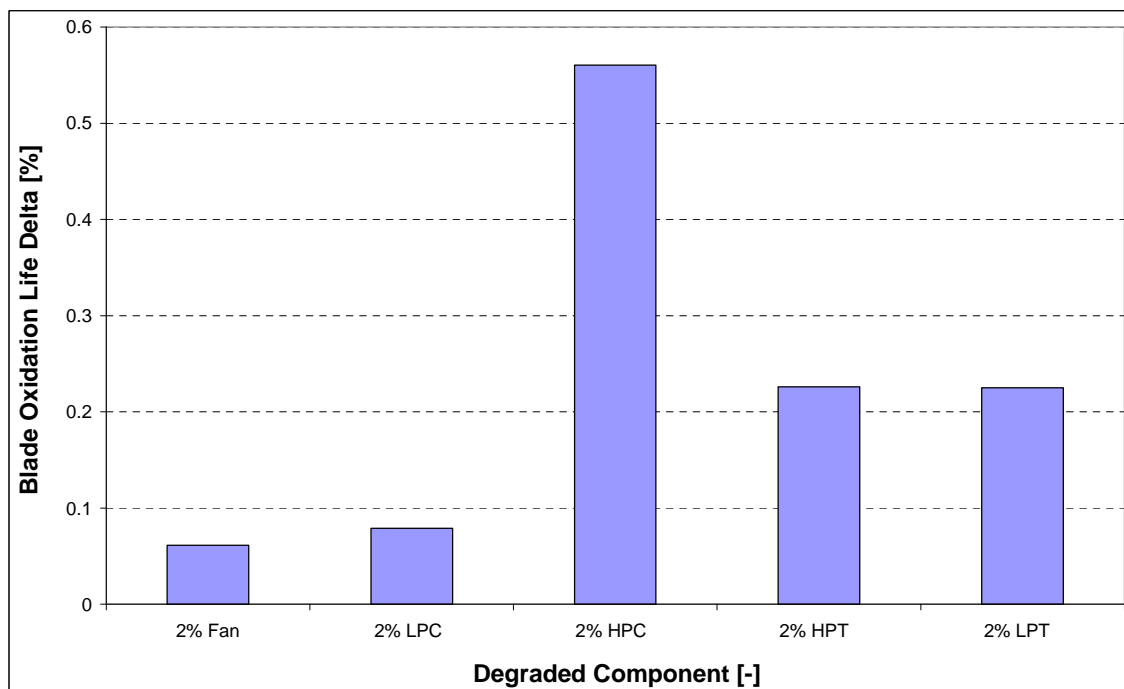


Figure 1.6: Effect of 2% component degradation on blade oxidation life [8].

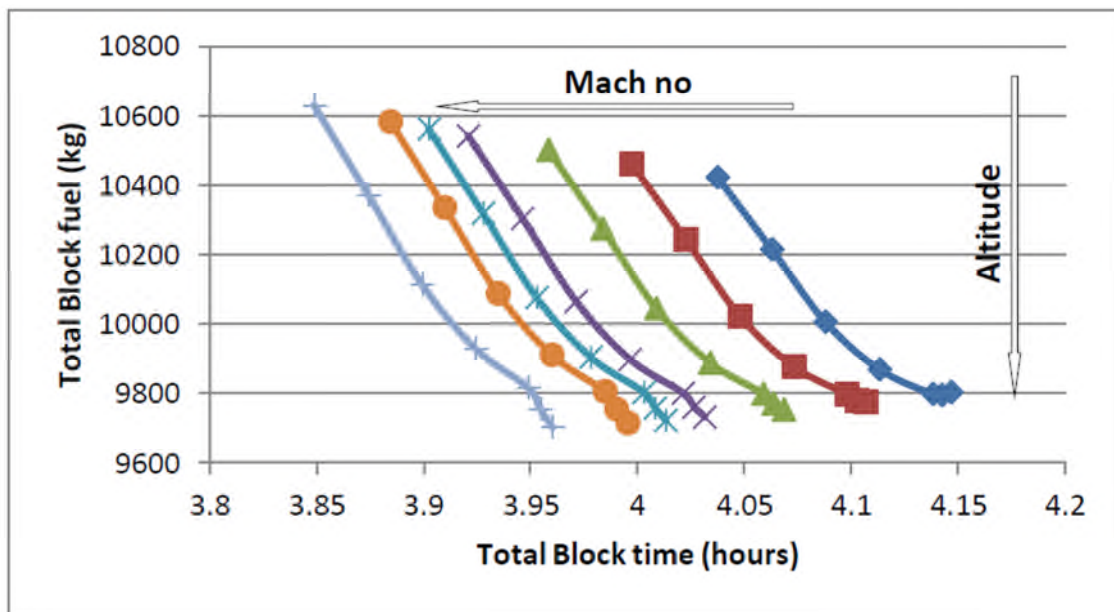


Figure 1.7: Variation of fuel and time with altitude and Mach number for a short range aircraft [9].

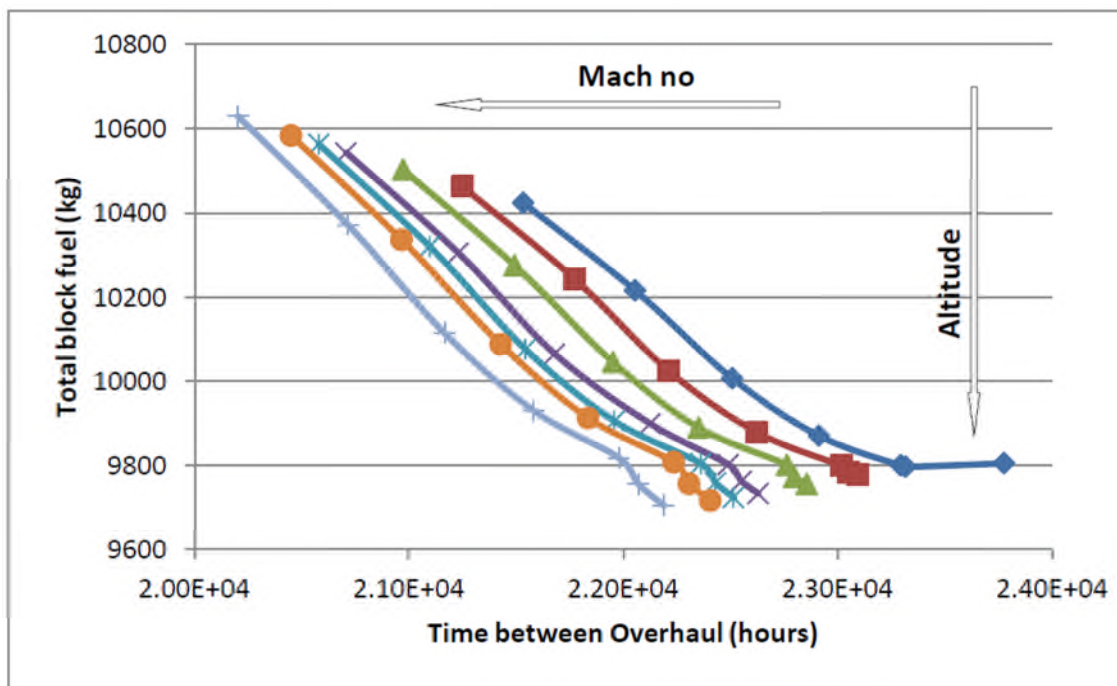


Figure 1.8: Variation of fuel and TBO with altitude and Mach number for a short range aircraft [9].

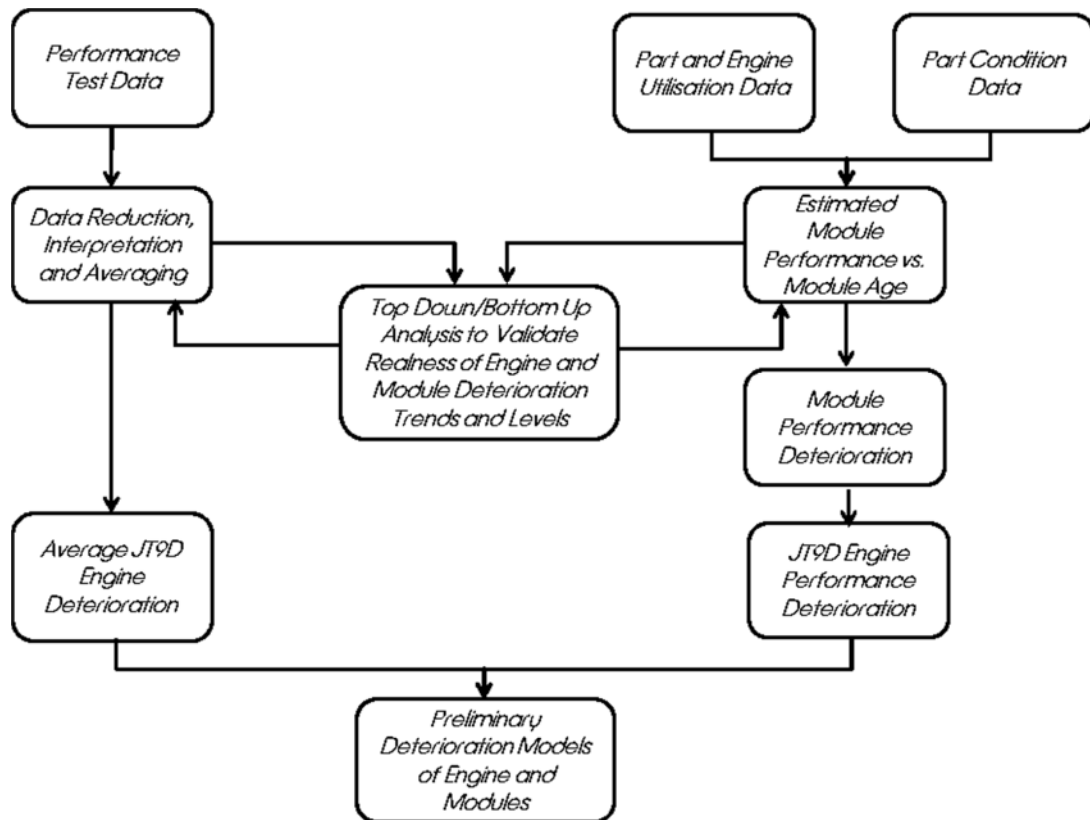


Figure 1.9: Technical approach for historical data collection and analysis [10].

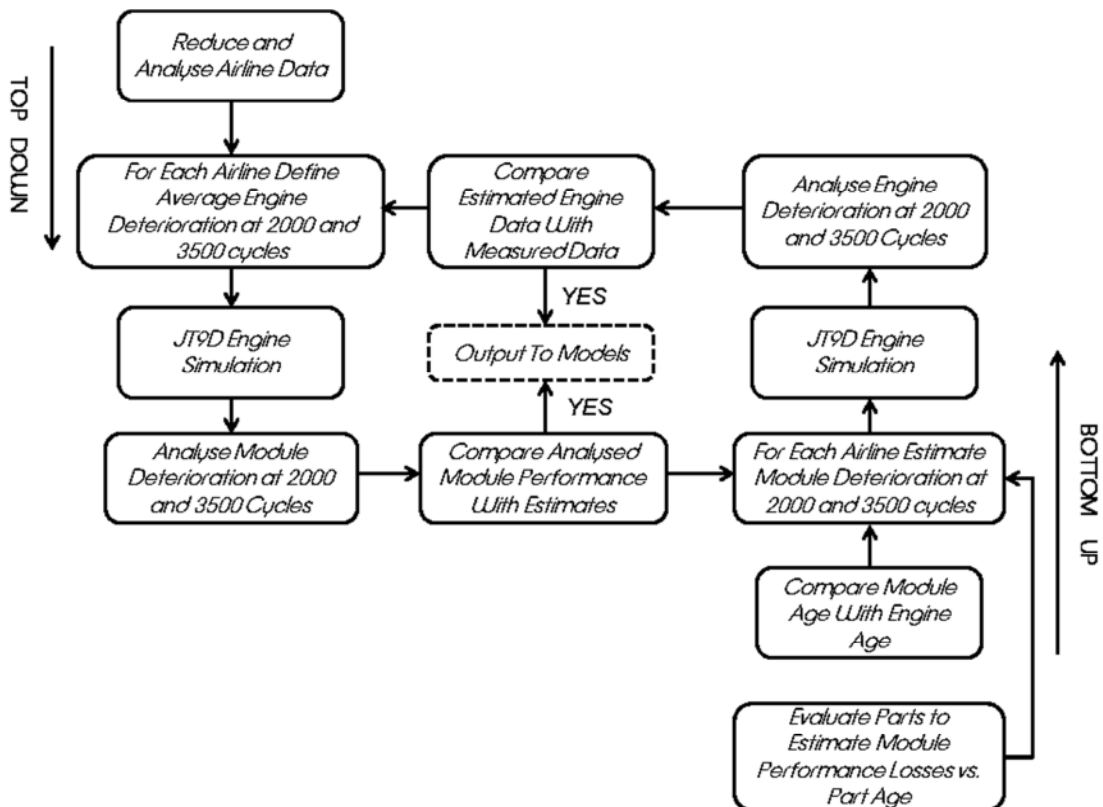


Figure 1.10: Engine performance deterioration diagnostic technique [10].

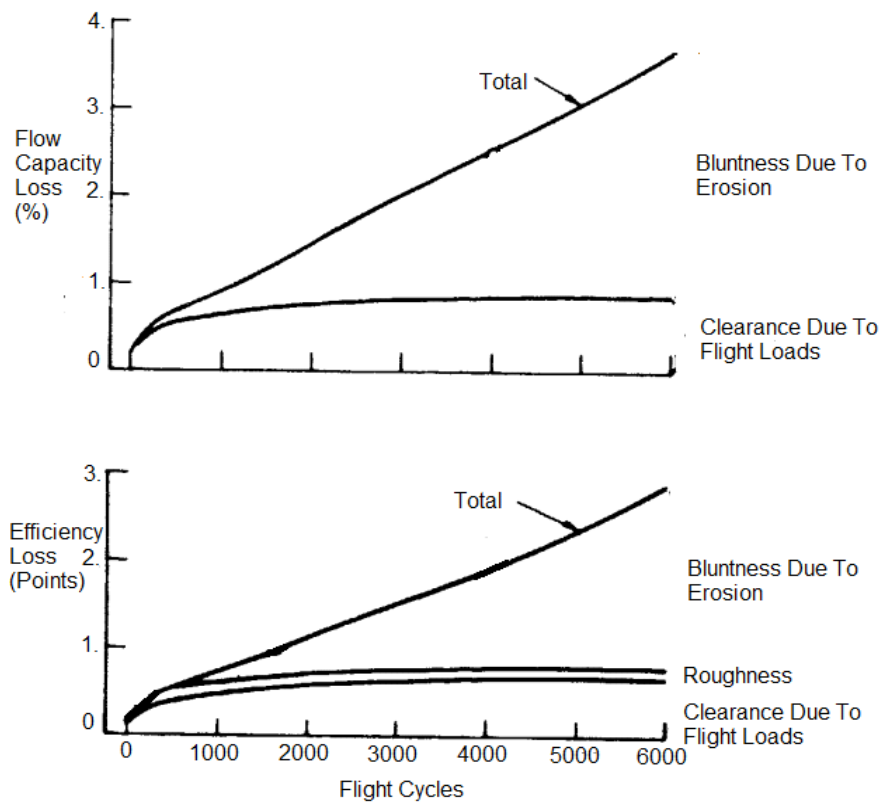


Figure 1.11: Estimated overall performance loss for fan [10].

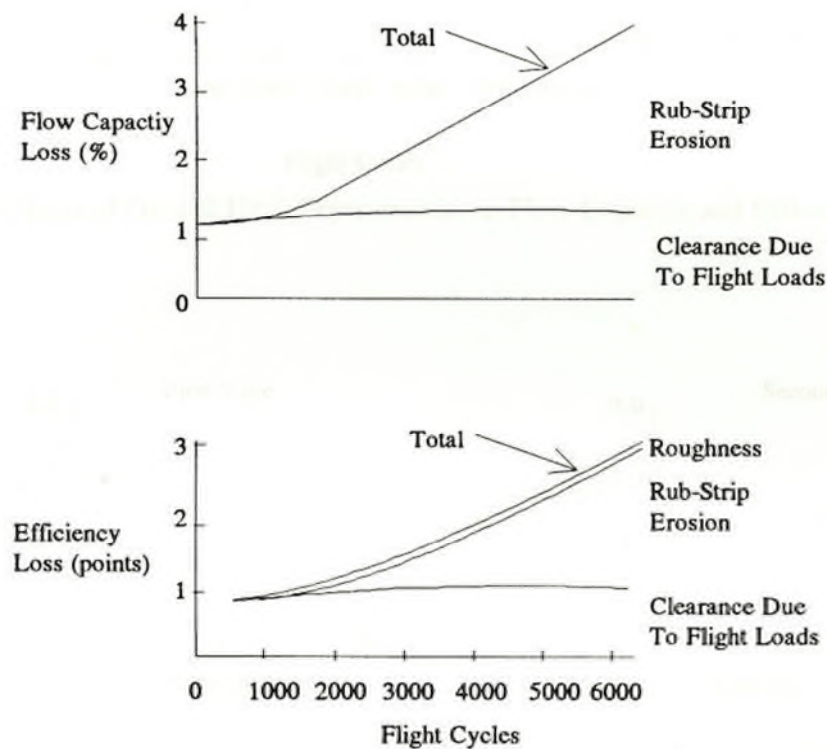


Figure 1.12: Estimated overall performance loss for LPC [10].

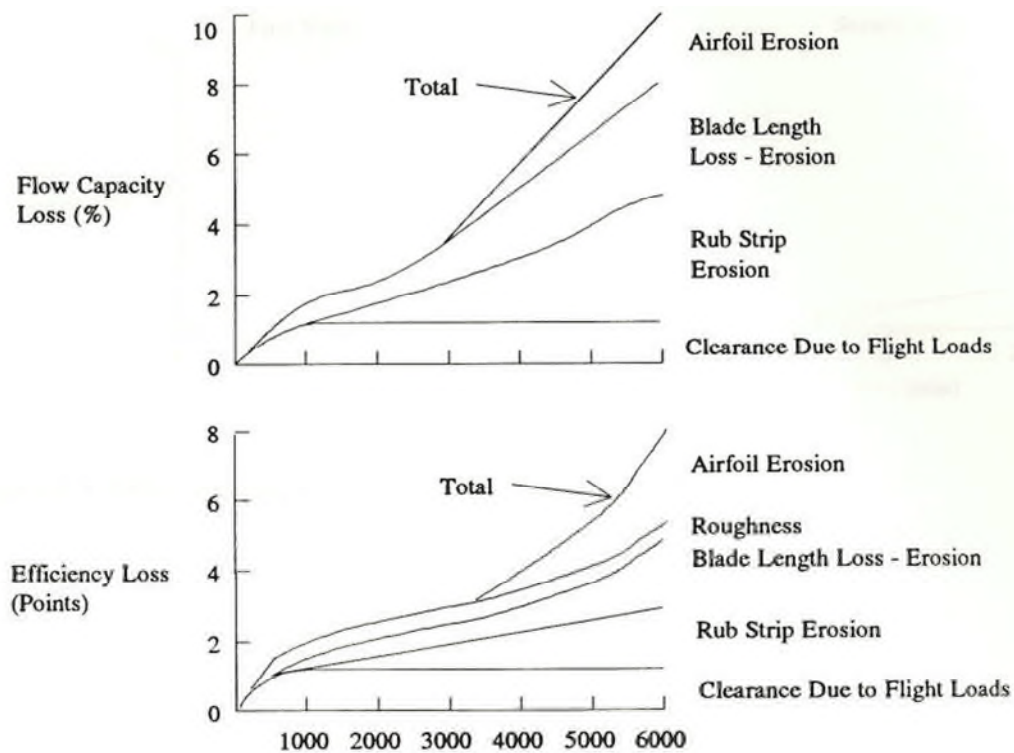


Figure 1.13: Estimated overall performance loss for HPC [10].

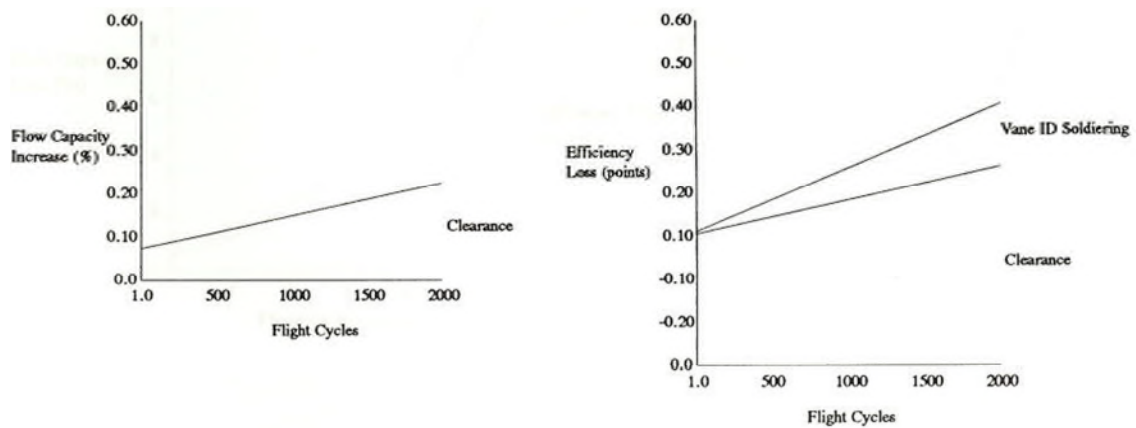


Figure 1.14: Estimated overall performance loss for LPT [10].

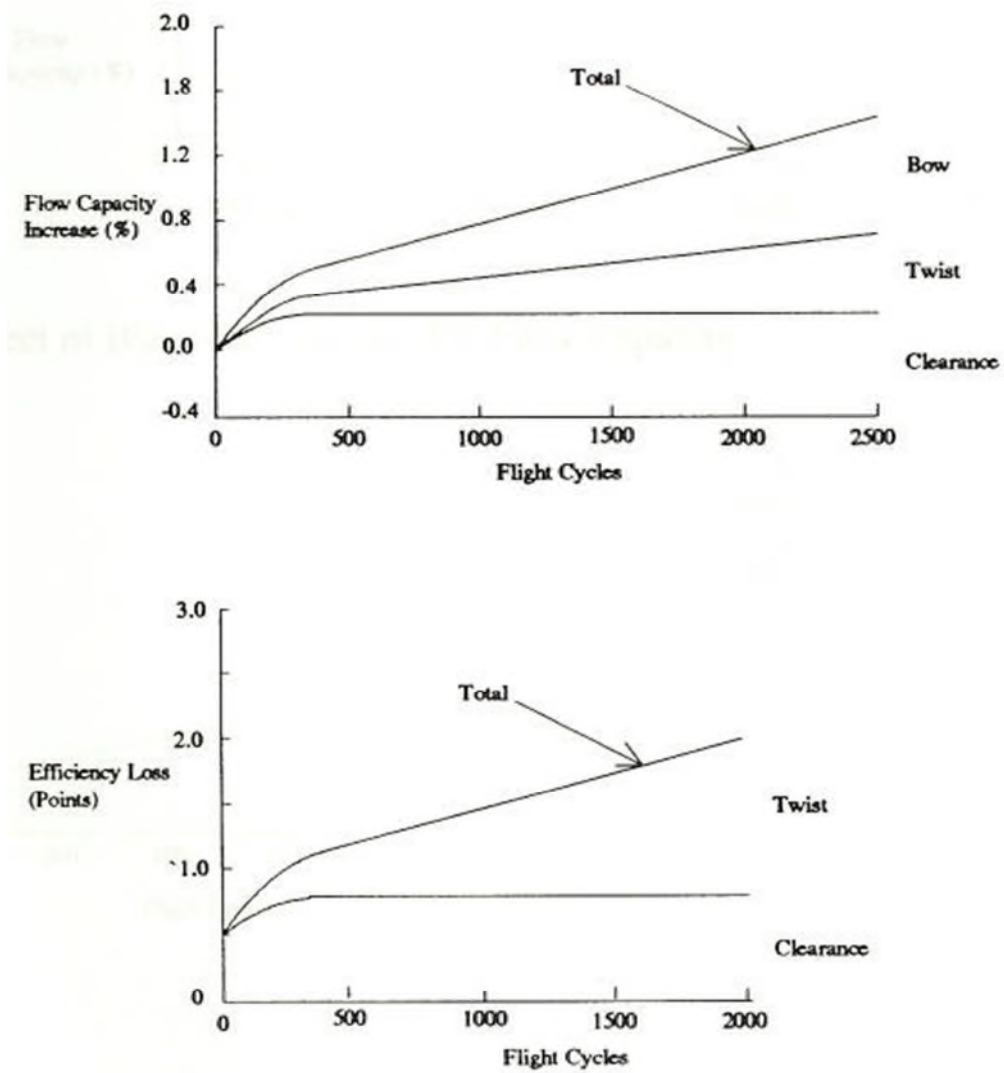


Figure 1.15: Estimated overall performance loss for HPT [10].

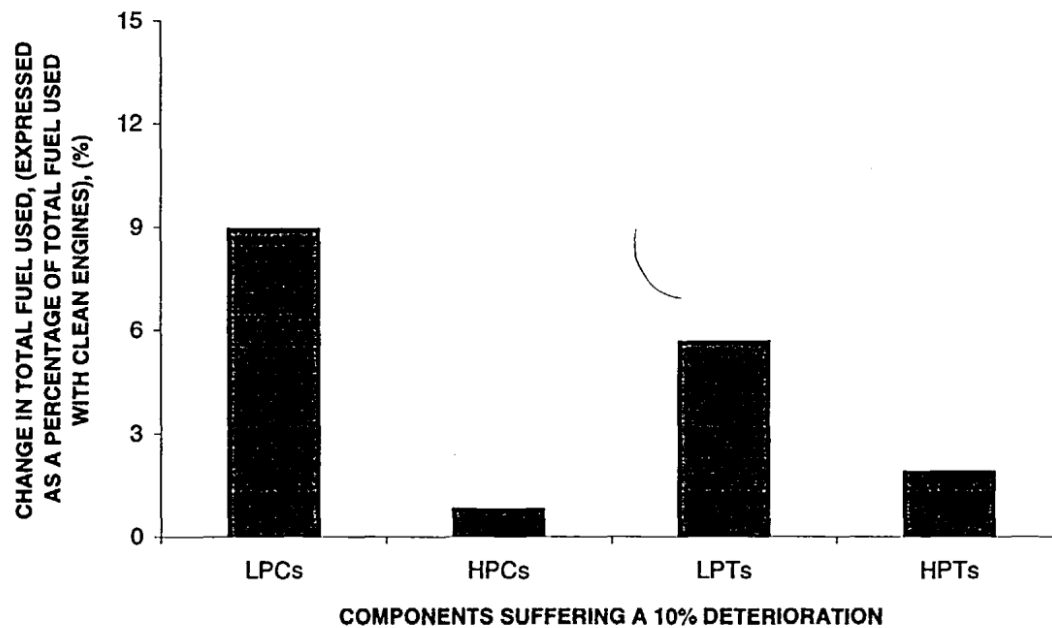


Figure 1.16: Change in total fuel used (expressed as a percentage of total fuel used with clean engines) for a 10% deterioration of stipulated components [12].

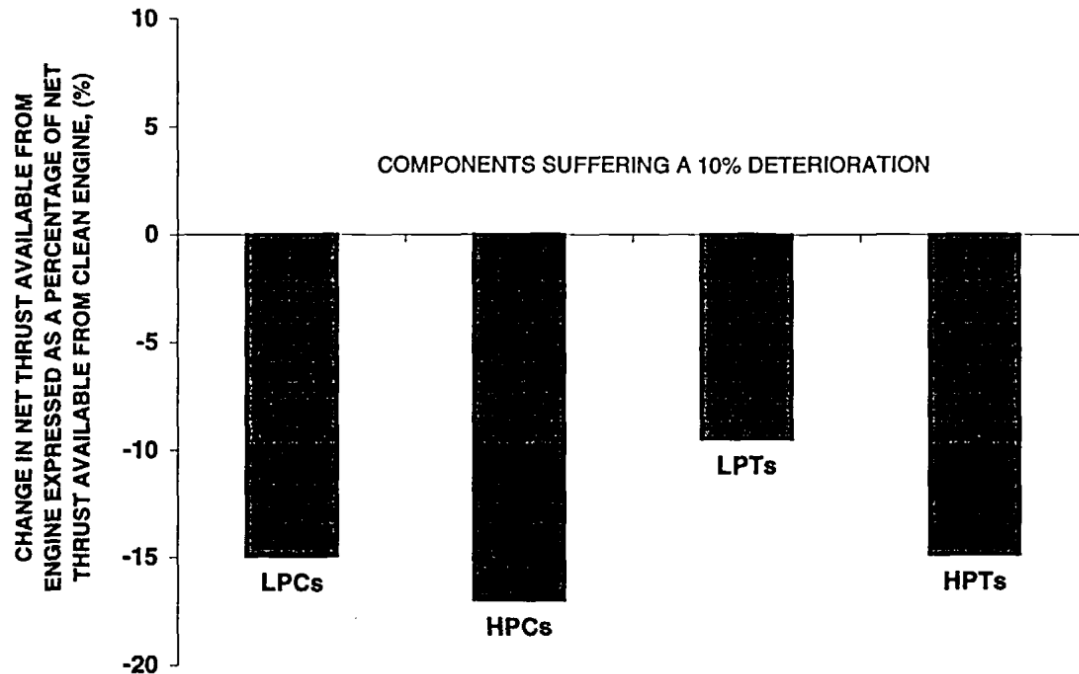


Figure 1.17: Change in net thrust available from engine (expressed as a percentage of net thrust available from clean engine) for a 10% deterioration of stipulated components [12].

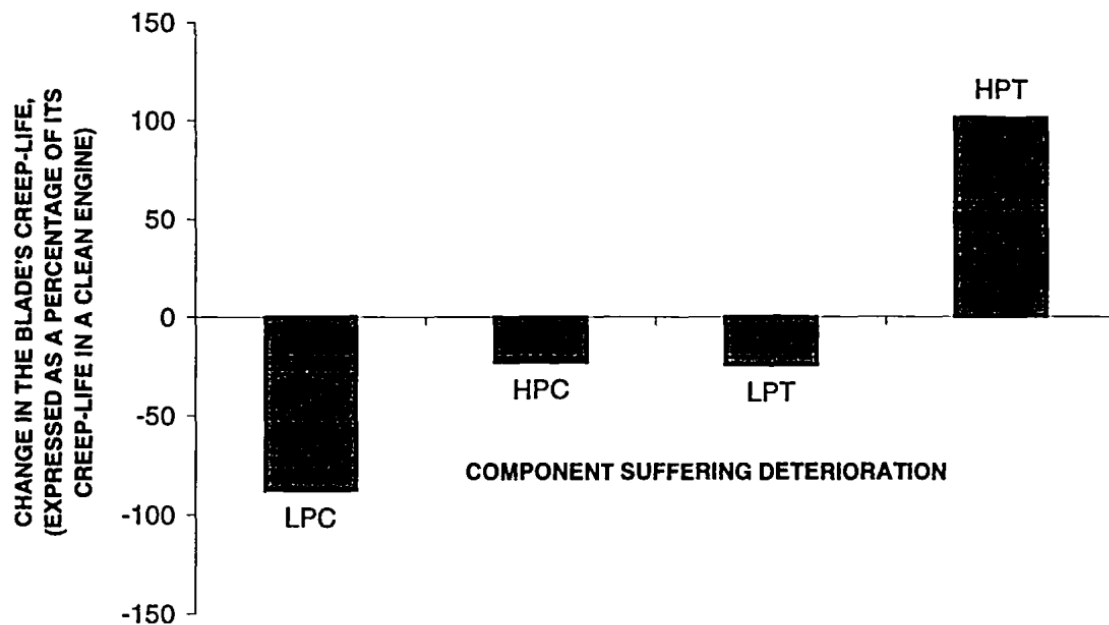


Figure 1.18: Blade's predicted changes in creep life for engines with a 10% fouling index for the LPC and HPC, and a 10% erosion index for the LPT and HIPT separately, compared with those for a clean engine [12].

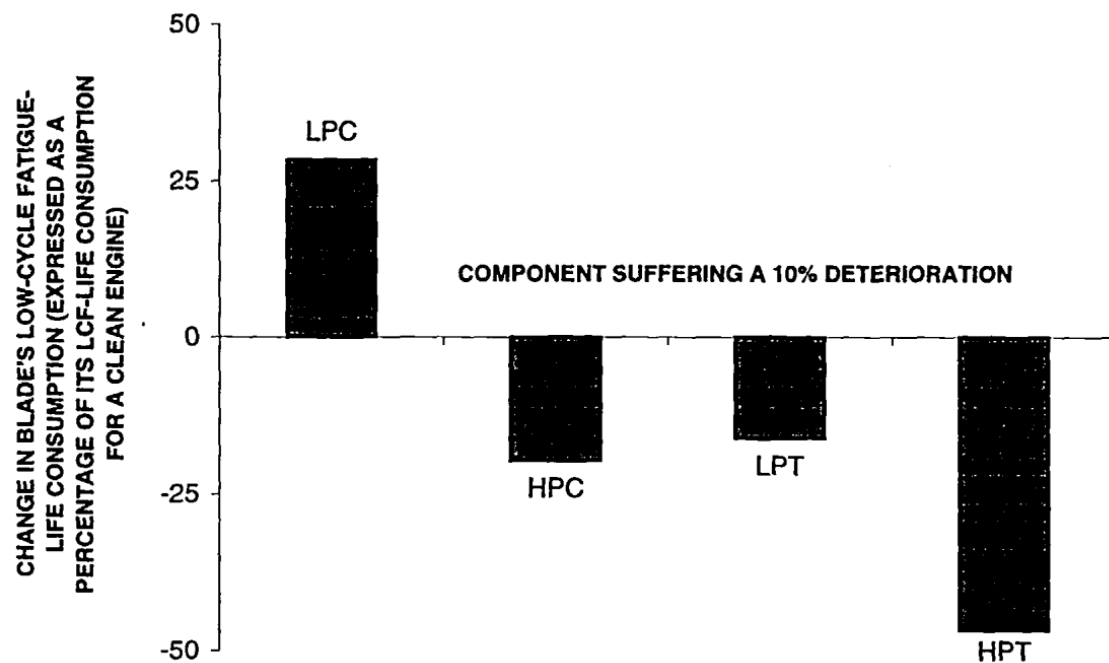


Figure 1.19: Blade's predicted LCF life consumption for engines with a 10% fouling index for the LPC and HPC separately, and a 10% erosion index for the LPT and HPT separately [12].

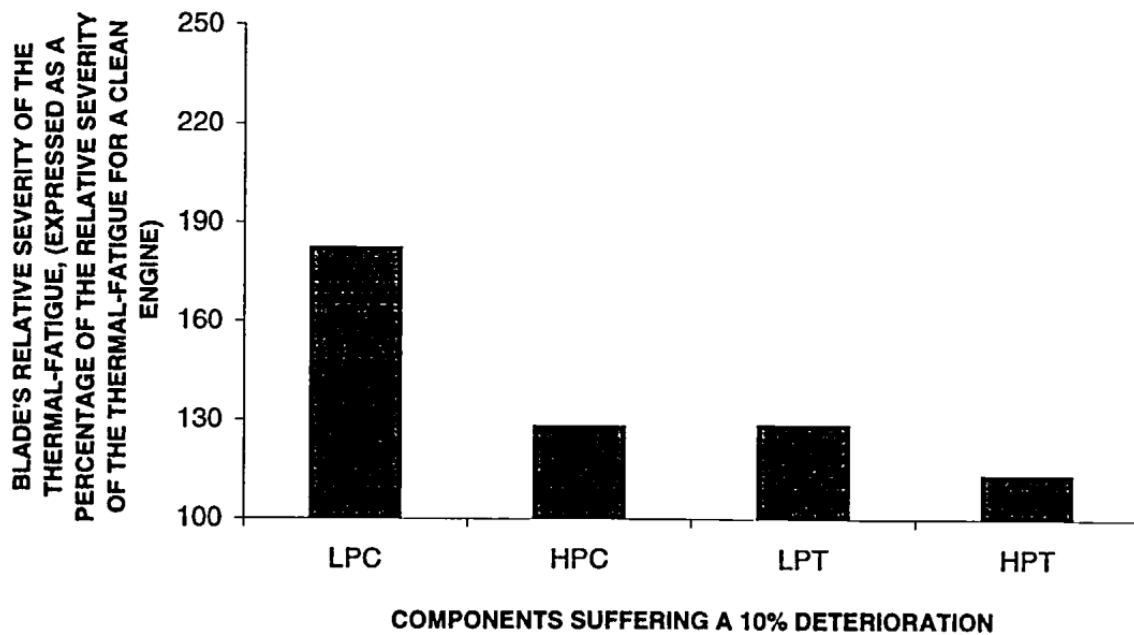


Figure 1.20: Blade's predicted change in the relative severity of thermal fatigue for engines with a 10% fouling index for the LPC and HPC, and a 10% erosion index for the LPT and HPT separately [12].

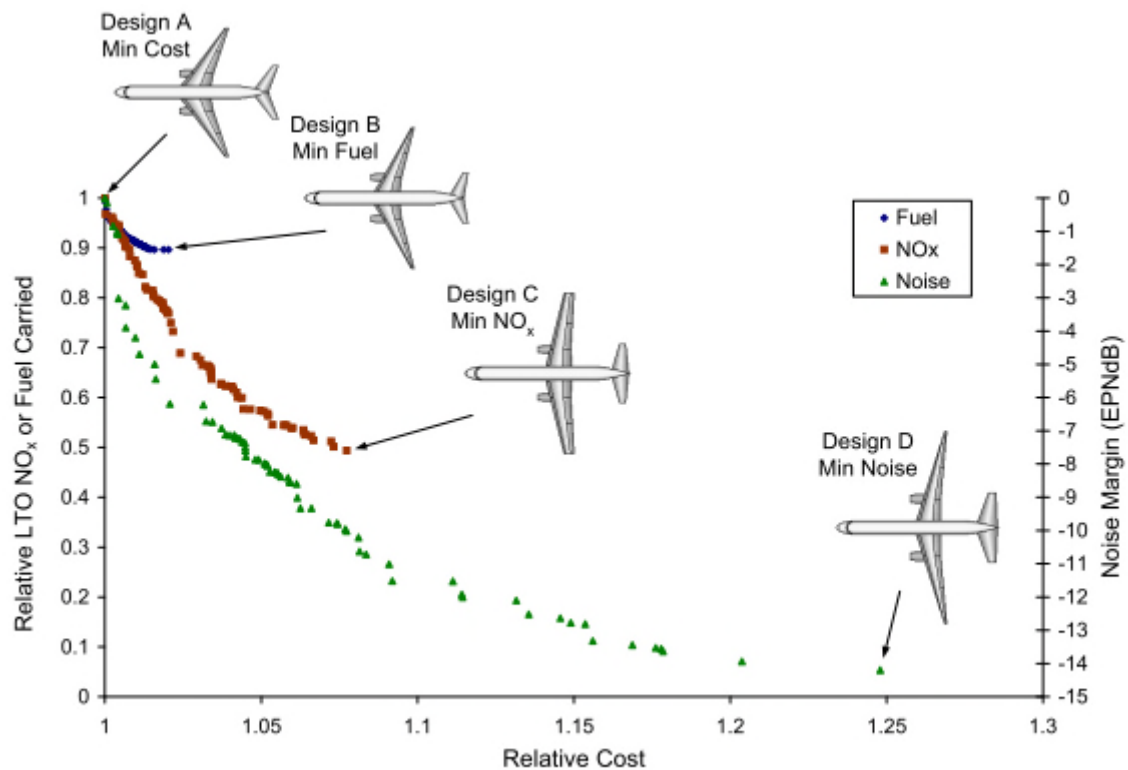


Figure 1.21: Pareto fronts of fuel carried, LTO NO_x, and cumulative certification noise vs. operating cost [13].

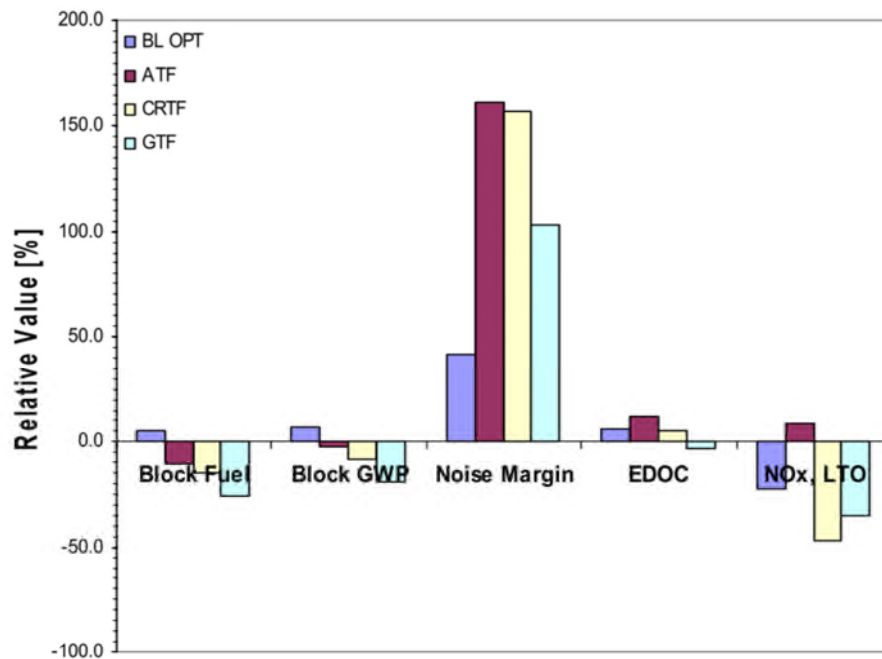
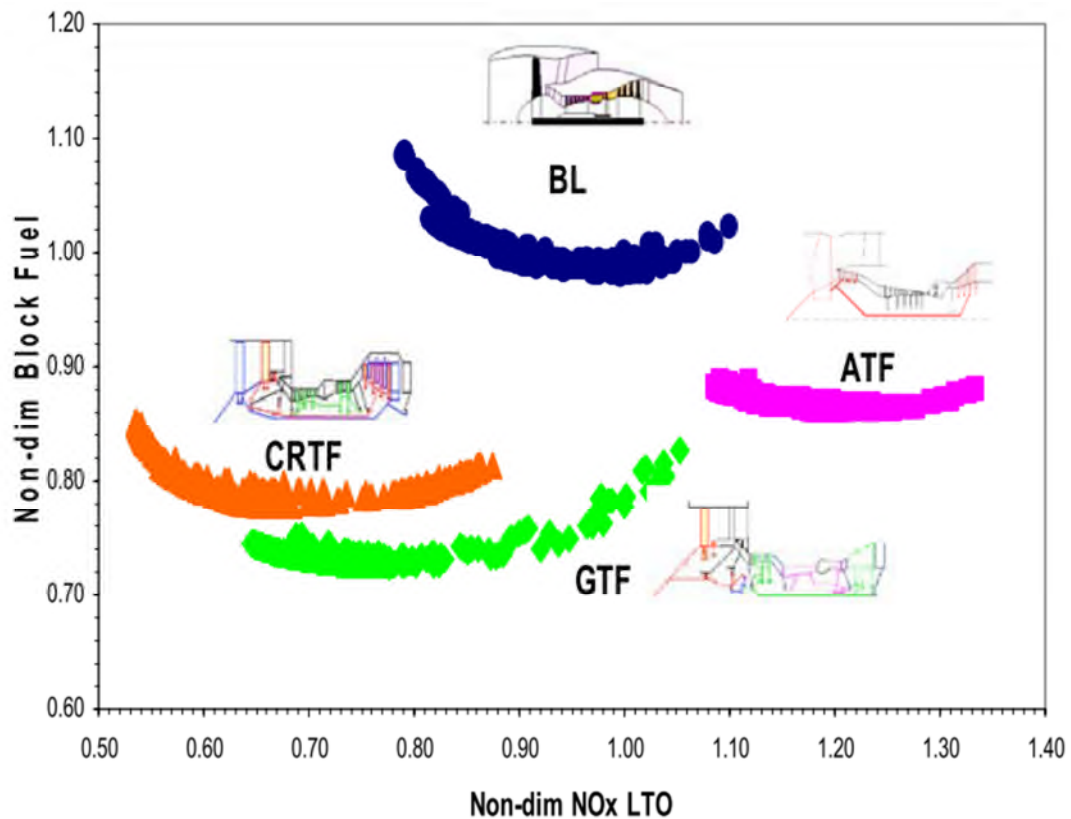


Figure of Merit

Figure 1.22: Comparison of single-objective optimisation results [15].



BL – Baseline; CRTF – Contra-Rotating Turbofan; GTF – Geared Turbofan; ATF – Advanced Turbofan

Figure 1.23: Pareto front of non-dimensional block fuel vs. LTO NOx [15].

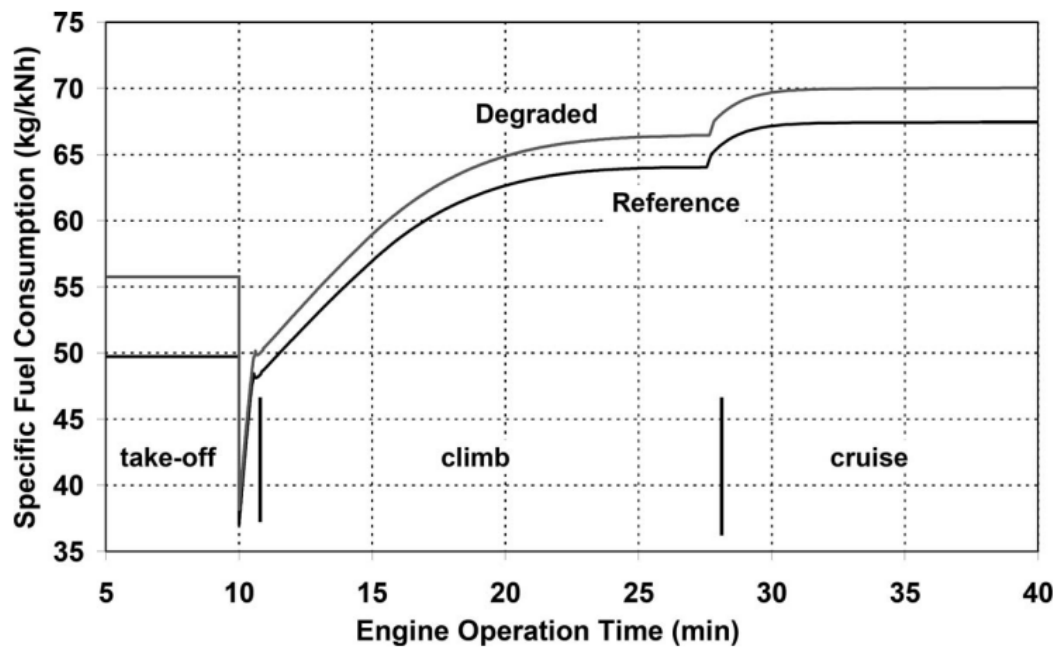


Figure 1.24: SFC versus time for take-off, climb and cruise [16].

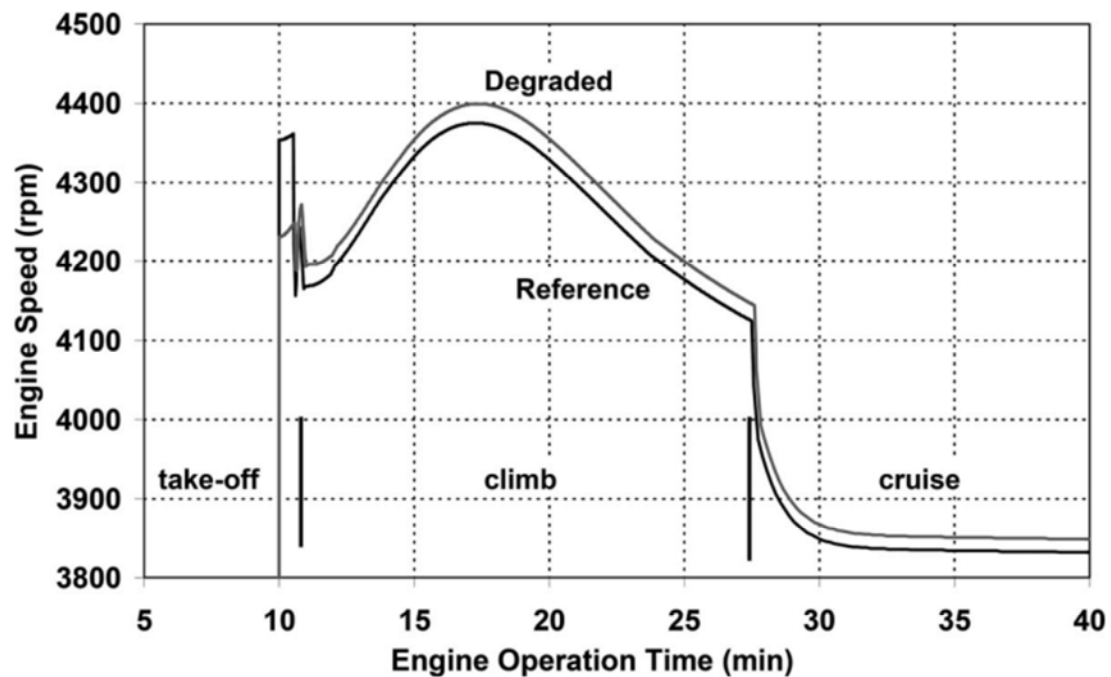


Figure 1.25: Engine speed versus time for take-off, climb and cruise [16].

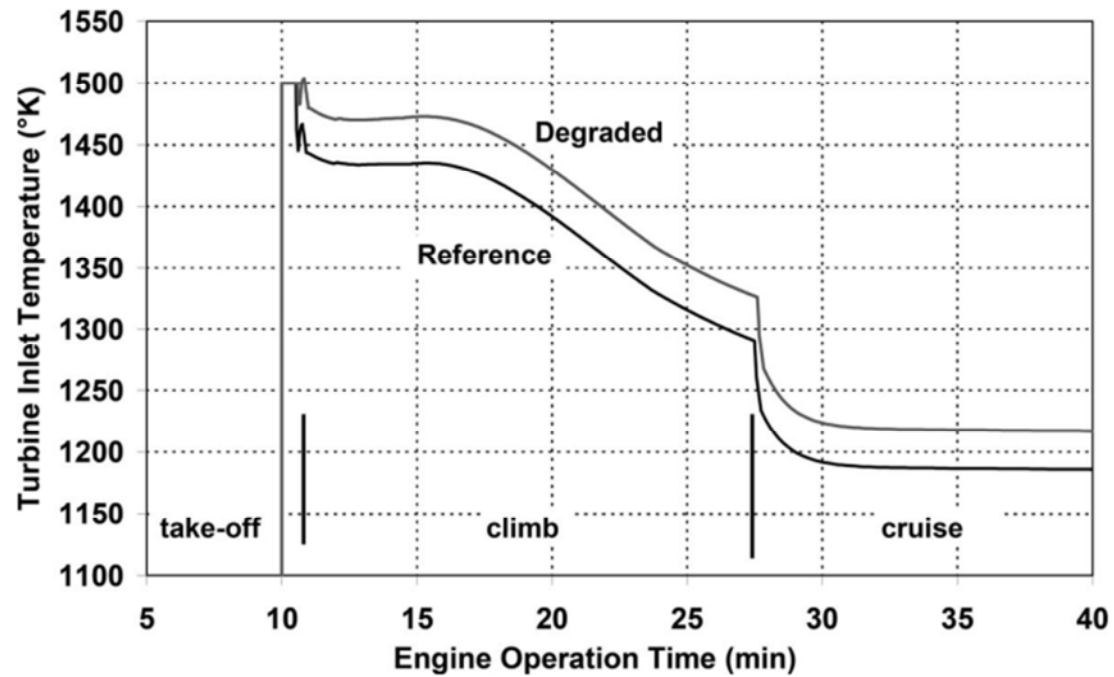


Figure 1.26: TET versus time for take-off, climb and cruise [16].

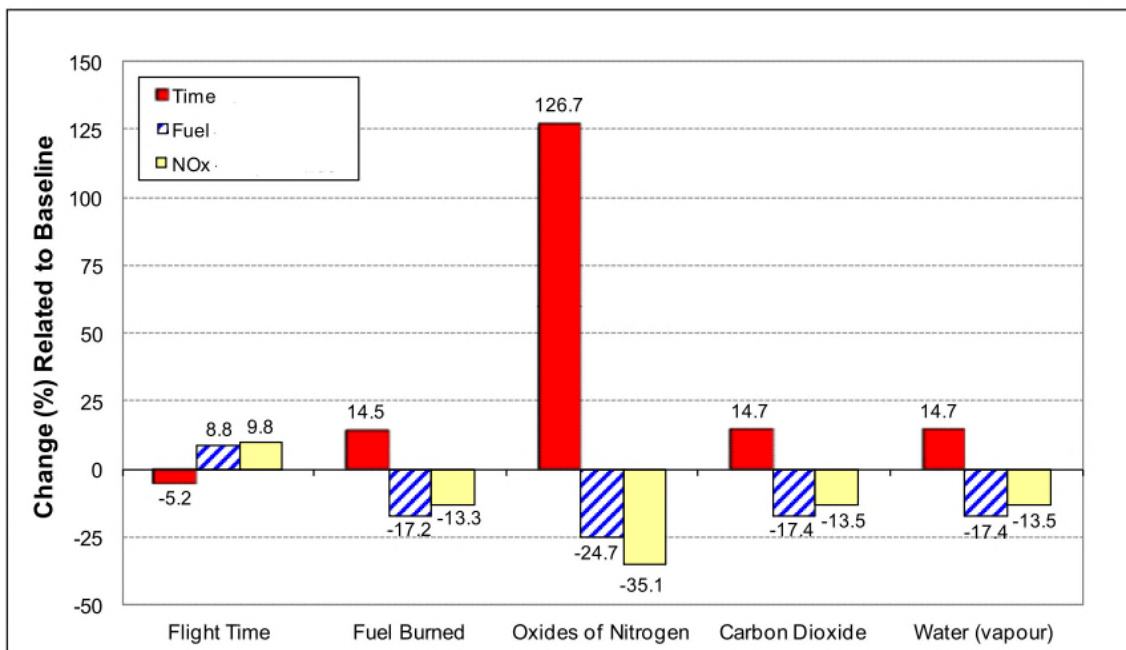


Figure 1.27: Results of optimum trajectories relative to baseline [17].

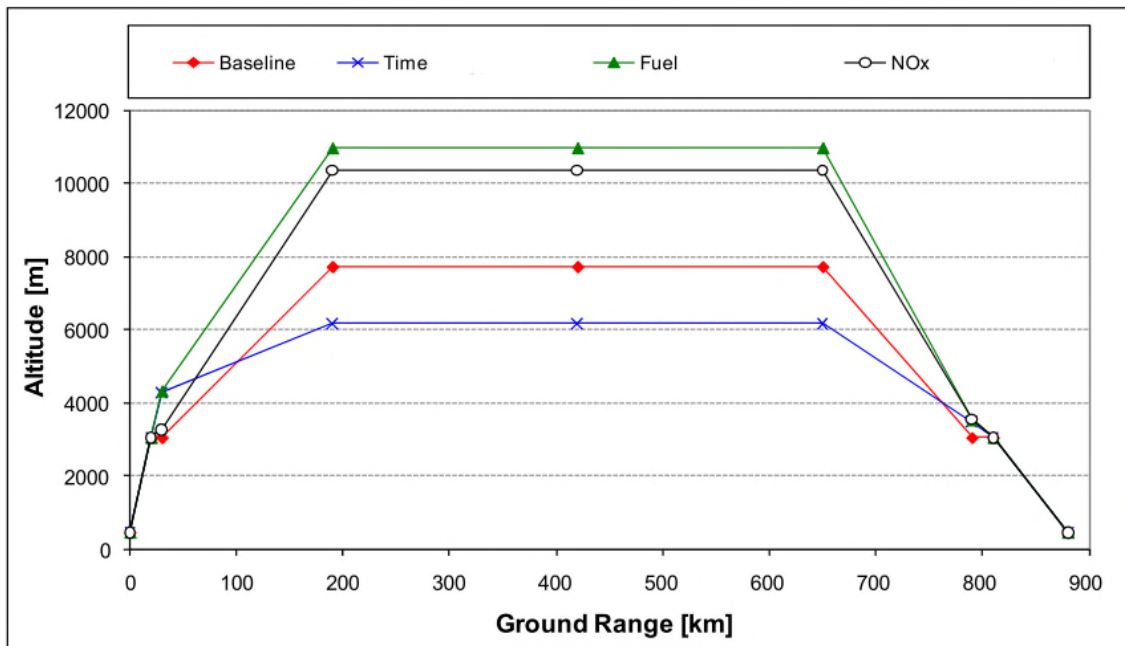
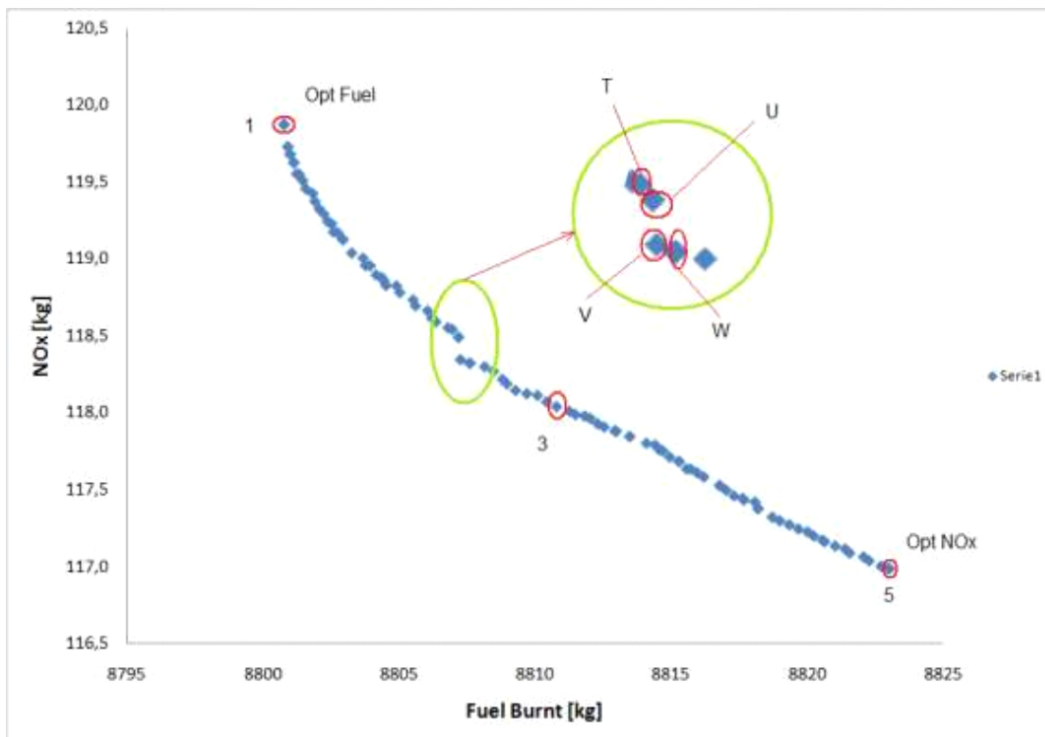
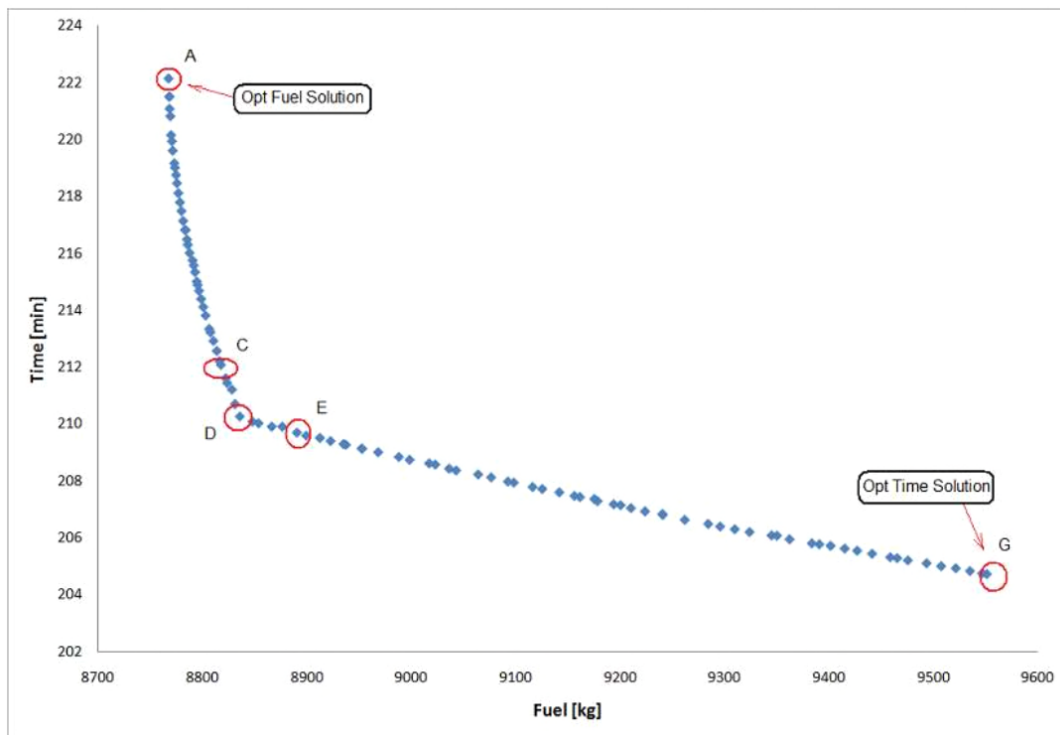


Figure 1.28: Baseline versus optimum trajectories [17].



T – At this and all points to the left the optimiser is seeking optimum for fuel burn
W – At this and all points to the right the optimiser is seeking optimum for NOx
U and V – Transition from seeking fuel burn optimum to seeking NOx optimum

Figure 1.29: Optimum trajectory solutions for fuel burn and NOx [18].



- C – Point close to the elbow of the Pareto between the crank and the optimum for fuel burn
- D – Crank point (elbow) between the two optimums
- E – Point close to the elbow of the Pareto between the crank and the optimum for time

Figure 1.30: Optimum trajectory solutions for fuel burn and time [18].

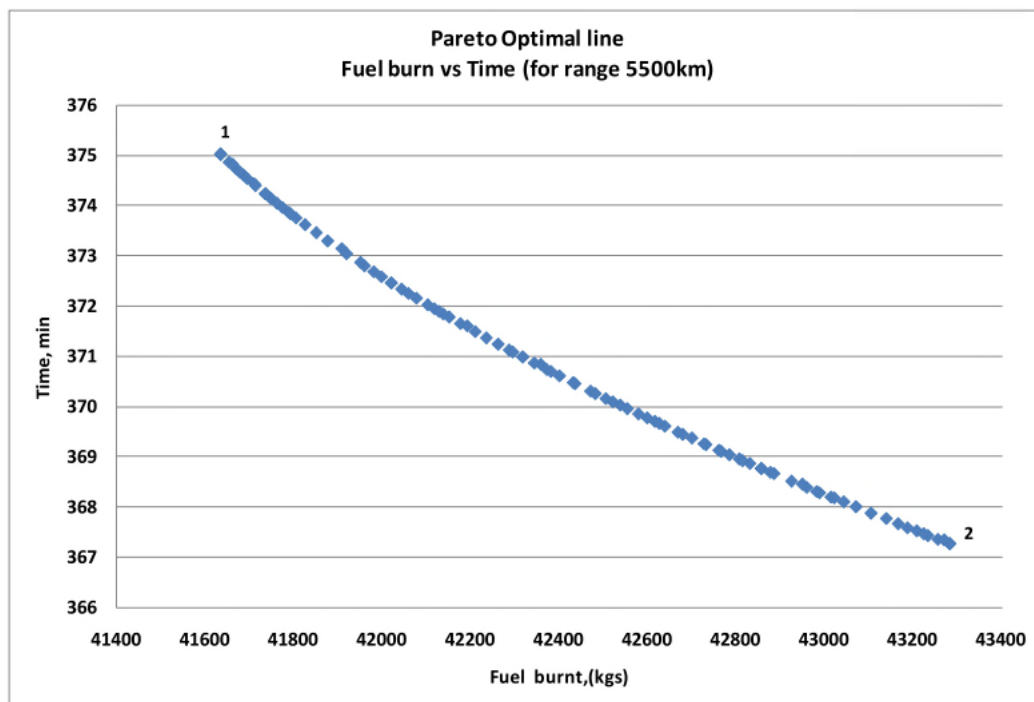


Figure 1.31: Fuel-time Pareto fronts for the long range flight [19].

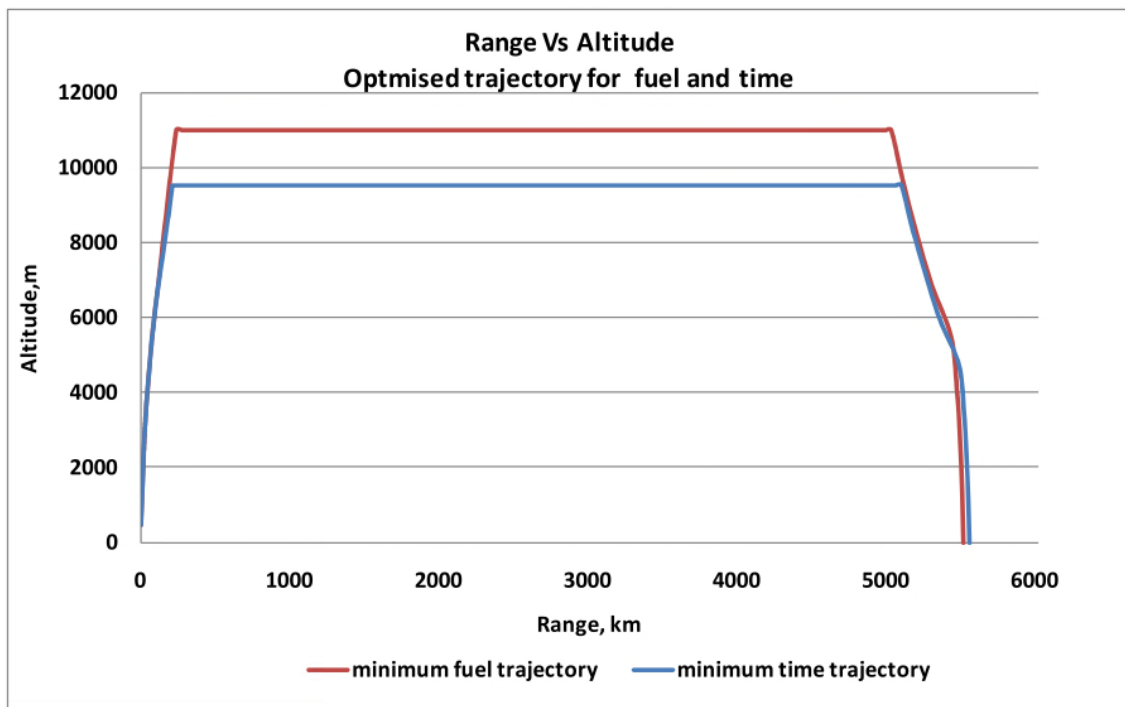


Figure 1.32: Optimised trajectory for minimum fuel and minimum time [19].

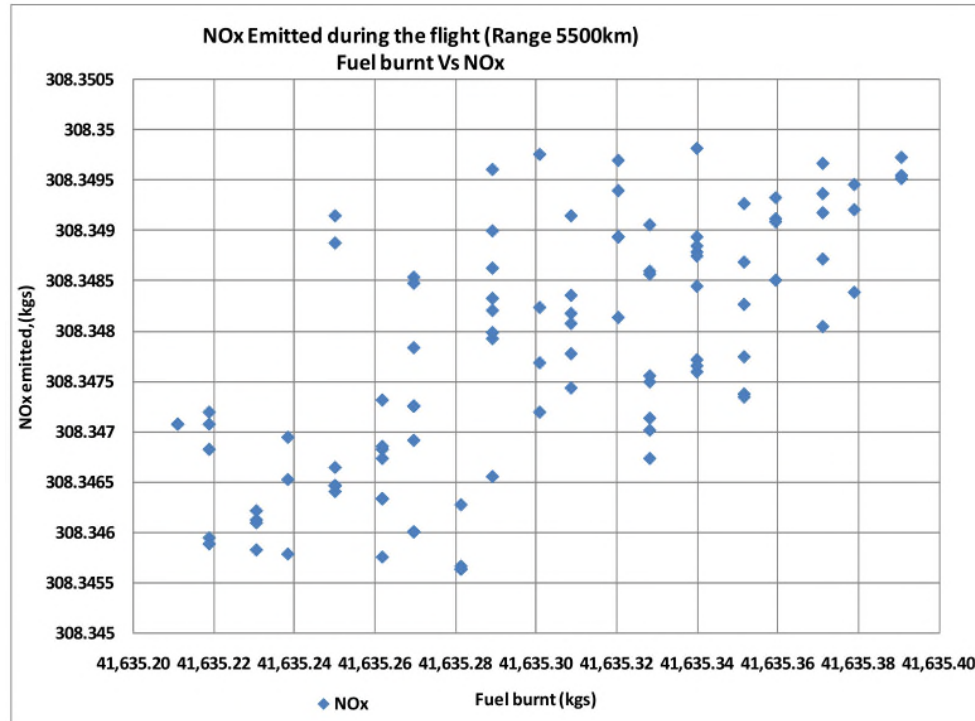


Figure 1.33: Mission fuel versus NOx [19].

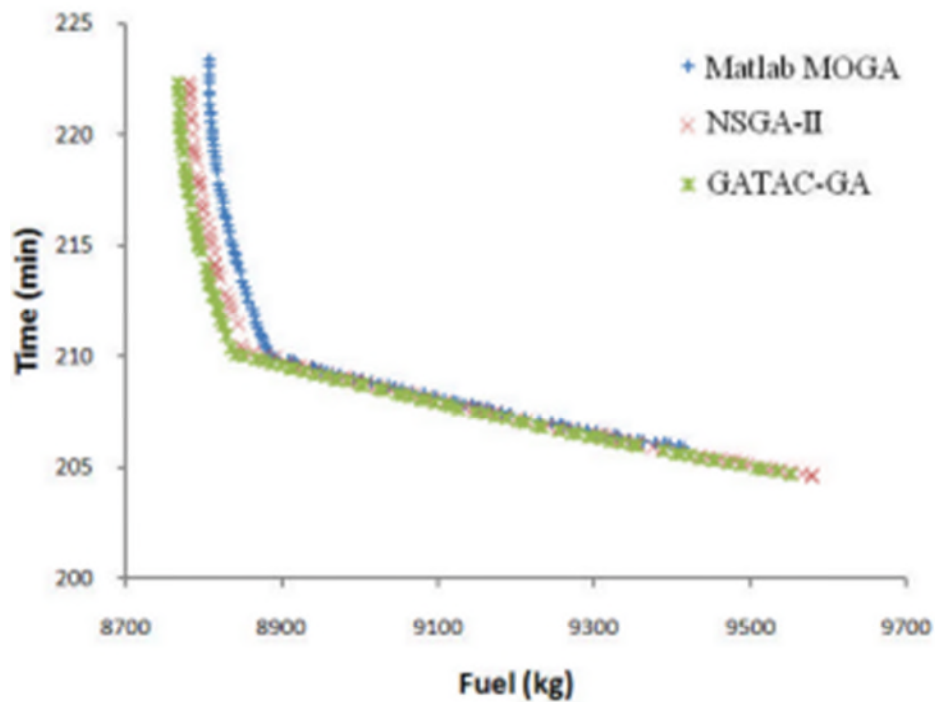


Figure 1.34: Fuel-Time Pareto fronts for a medium range flight [20].

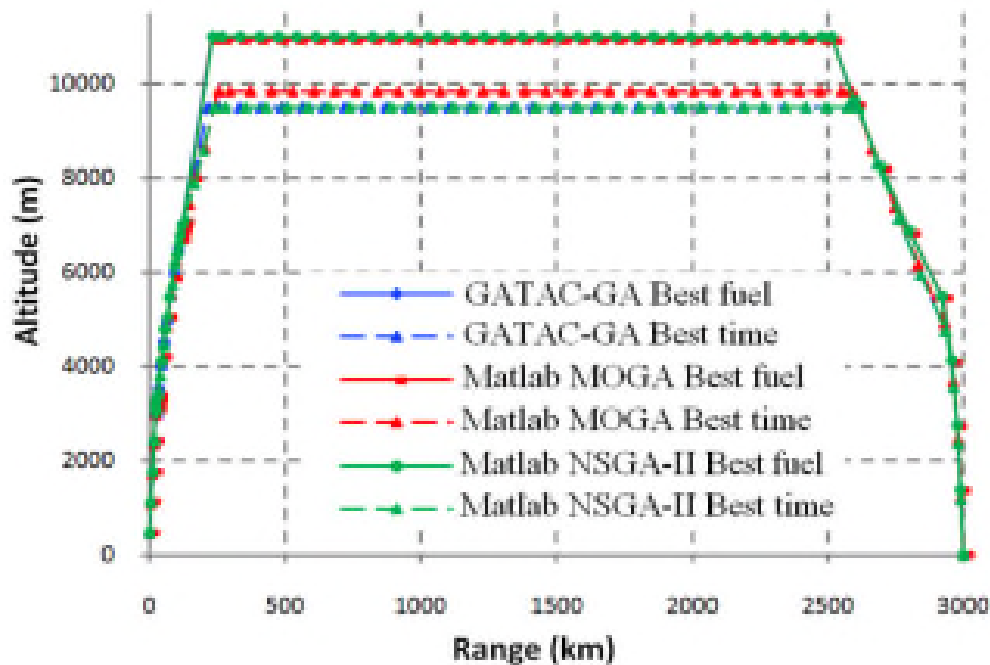


Figure 1.35: Comparison of Fuel vs. Time optimum trajectories for a medium range flight [20].

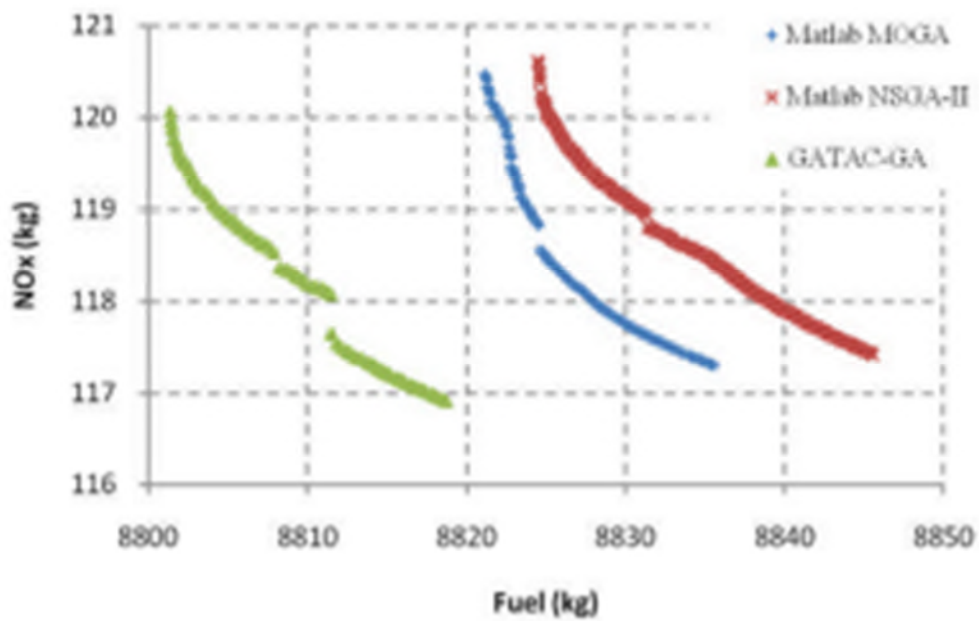


Figure 1.36: Fuel-NOx Pareto fronts for a medium range flight [20].

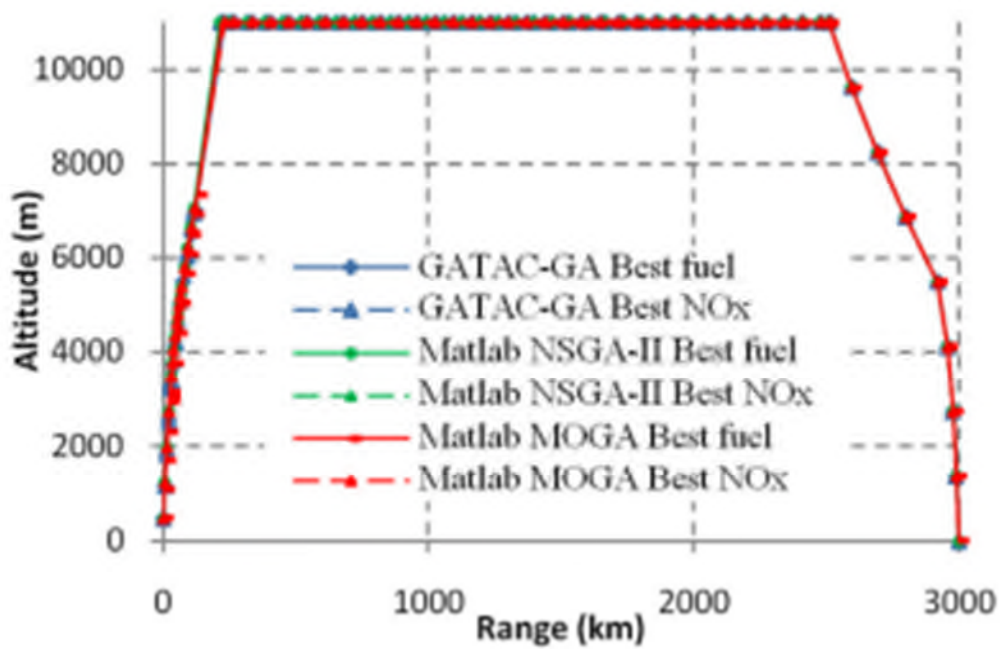


Figure 1.37: Comparison of Fuel vs. NOx optimum trajectories for a medium range flight [20].

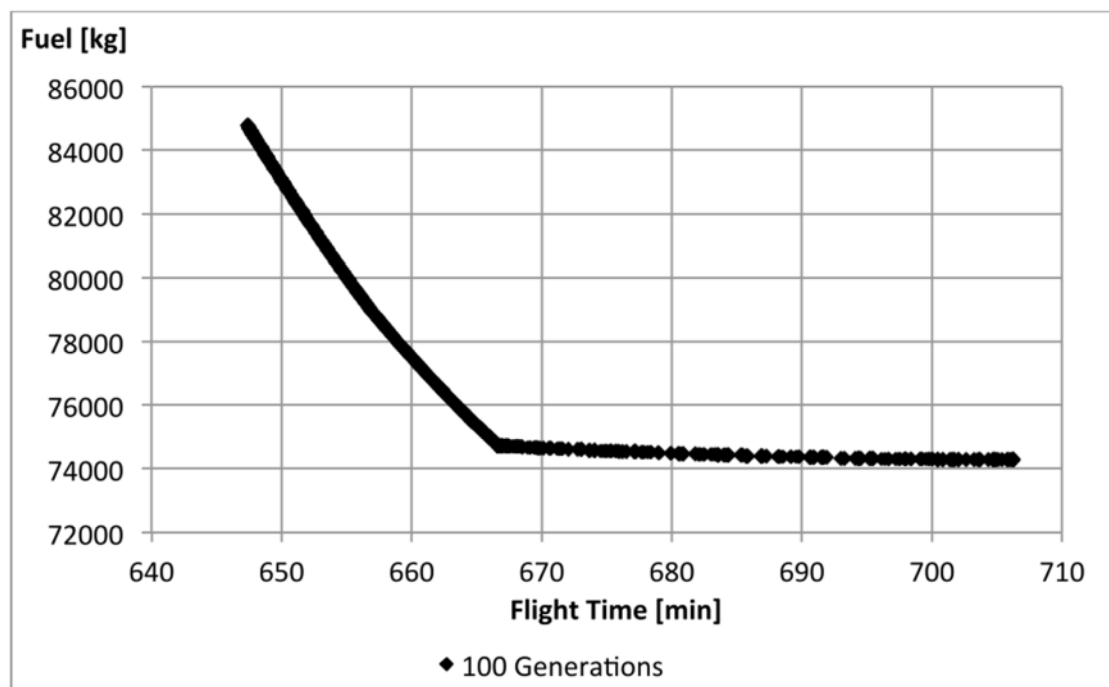


Figure 1.38: Fuel vs. Time Pareto front [21].

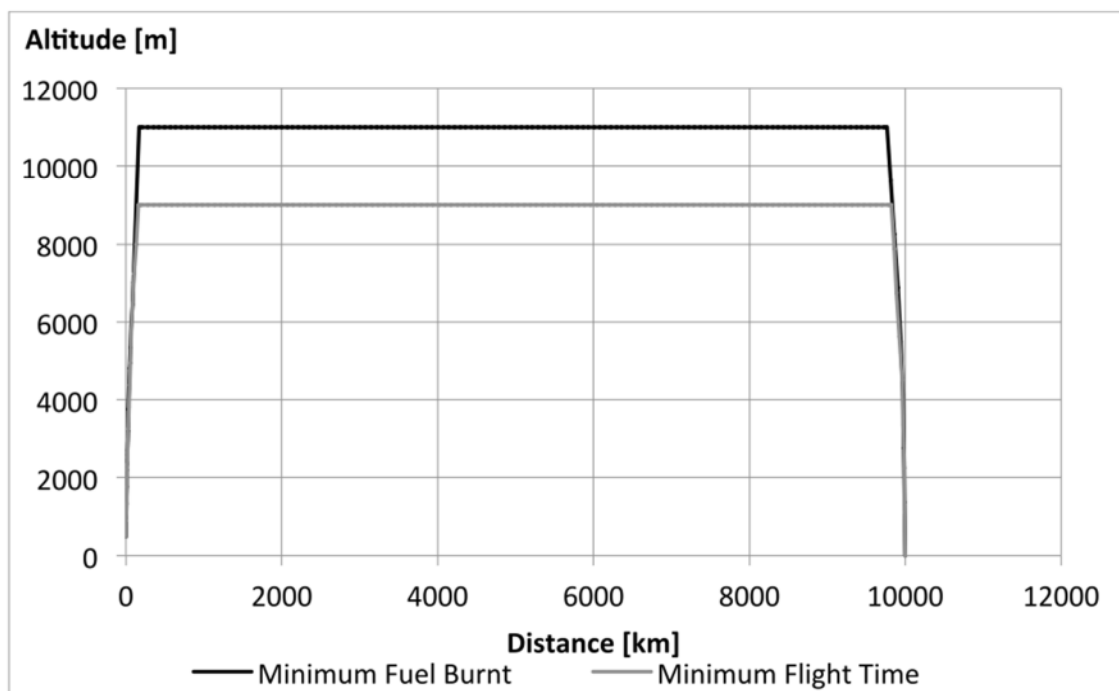


Figure 1.39: Fuel vs. Time flight trajectory [21].

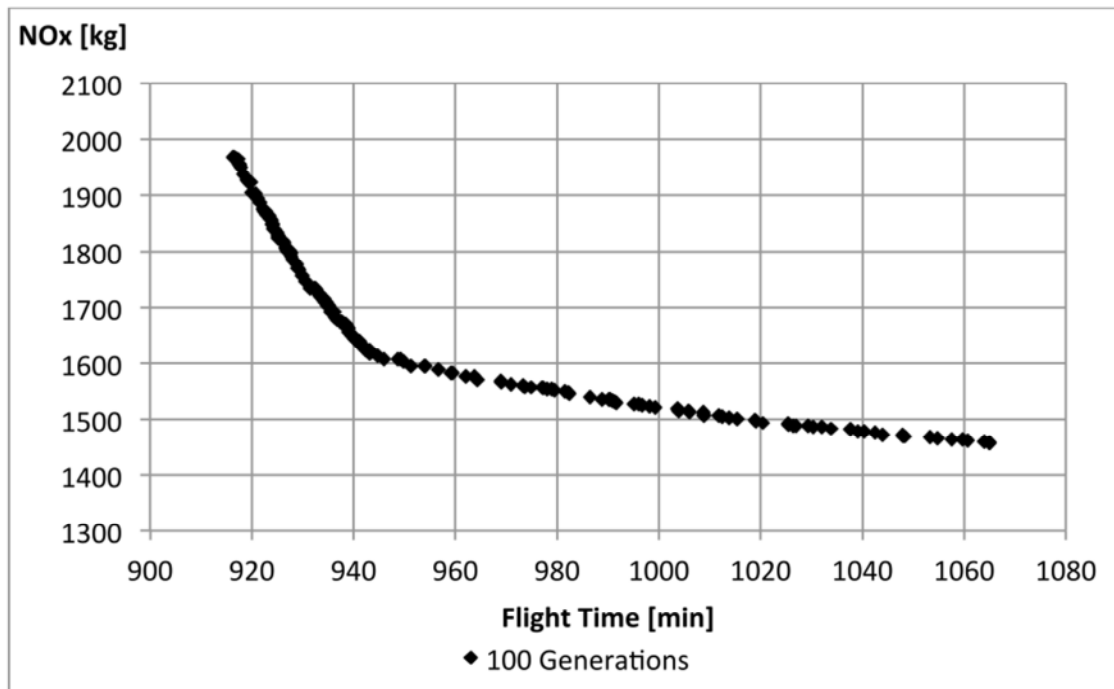


Figure 1.40: Time vs. NOx Pareto front [21].

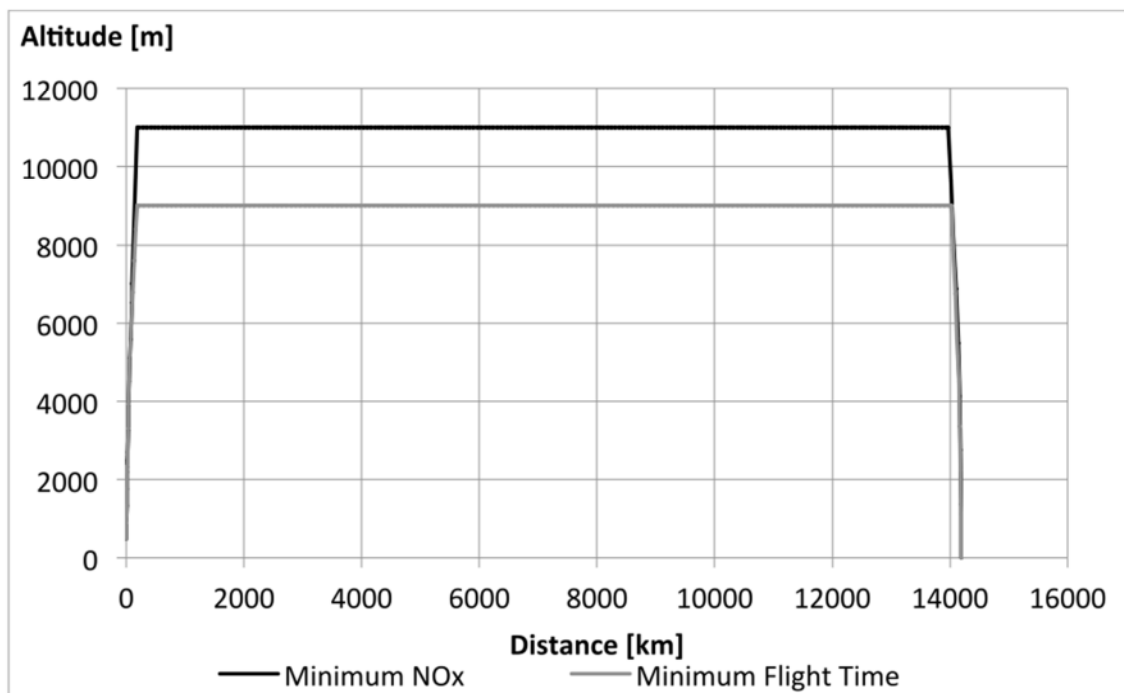


Figure 1.41: Time vs. NOx flight trajectory [21].

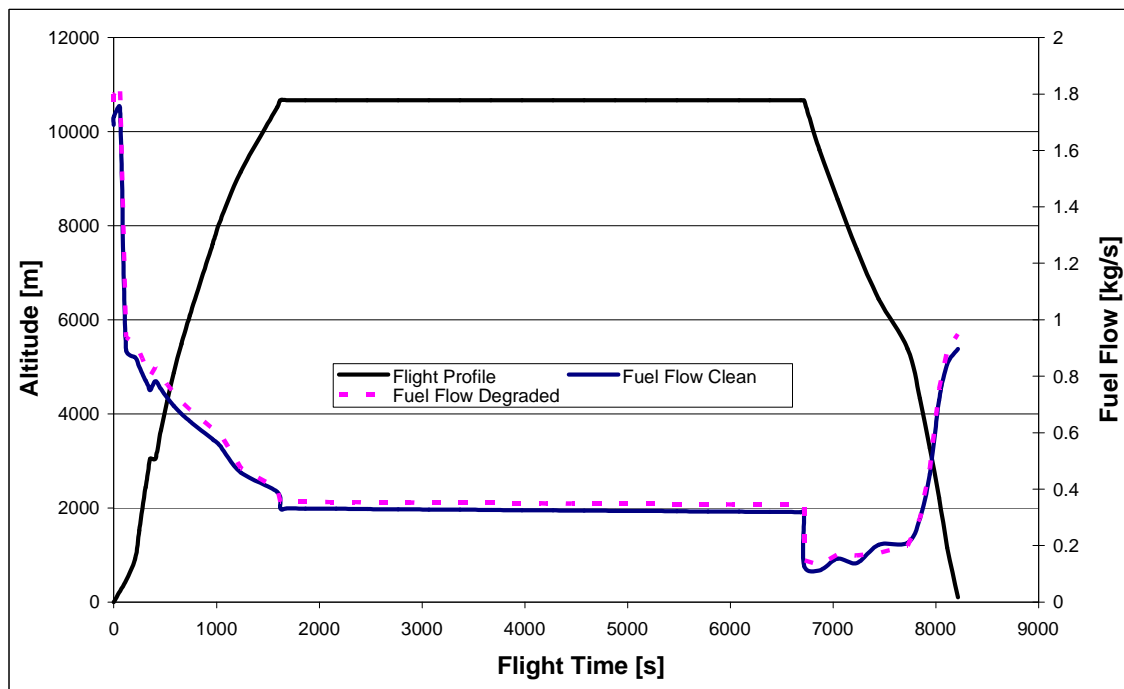


Figure 1.42: Engine flight mission fuel flow (clean and degraded) [22].

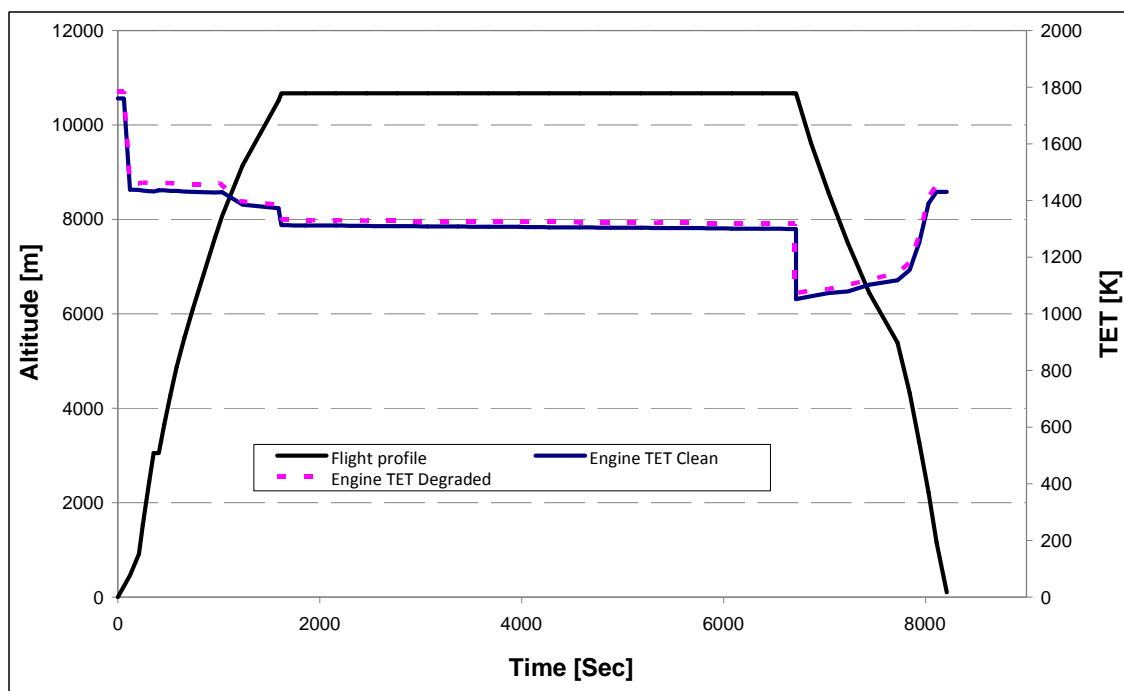


Figure 1.43: Engine flight mission TET (clean and degraded) [22].

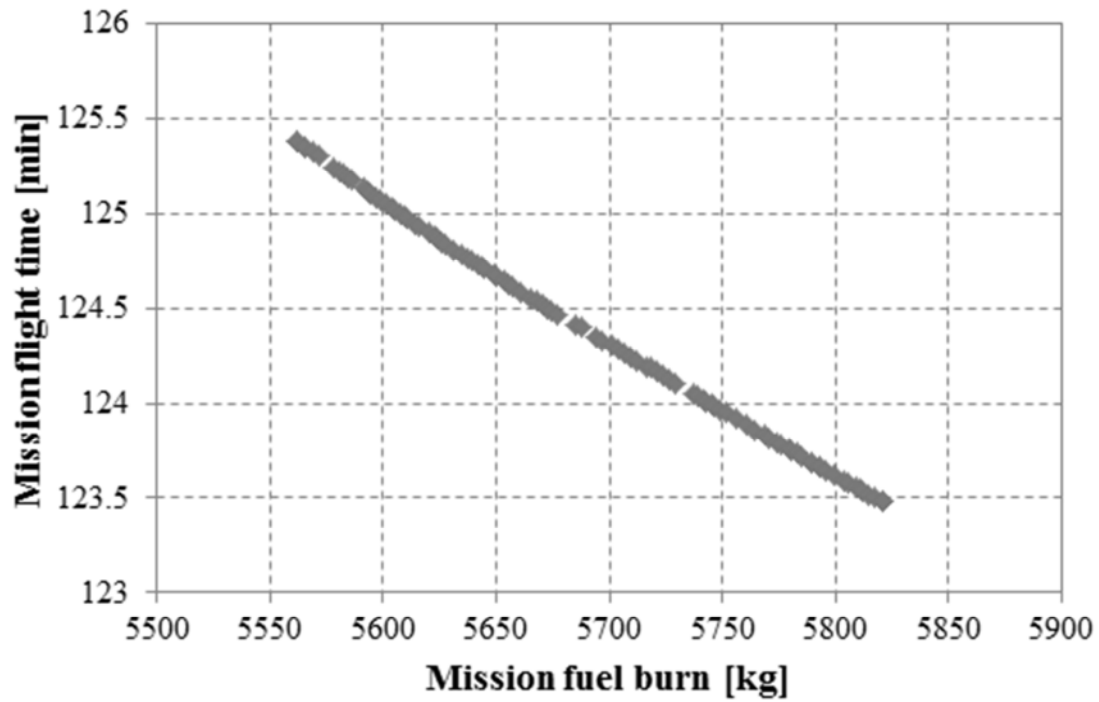


Figure 1.44: Pareto Front: Fuel vs. Time [22].

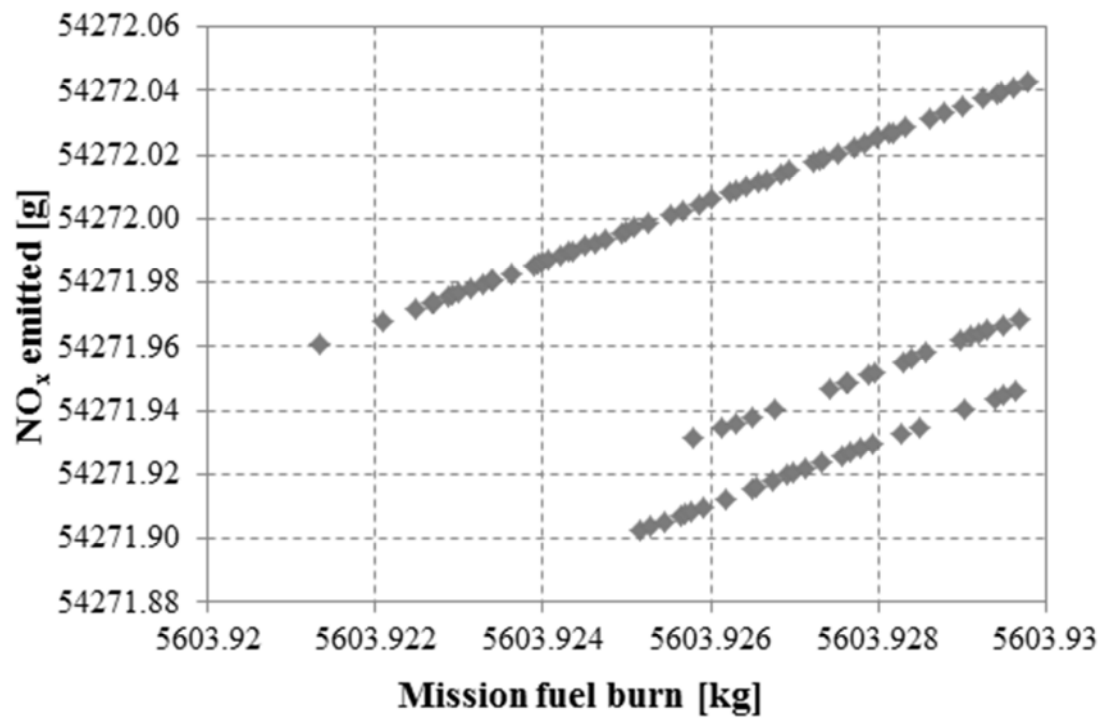


Figure 1.45: Pareto Front: Fuel vs. NOX [22].

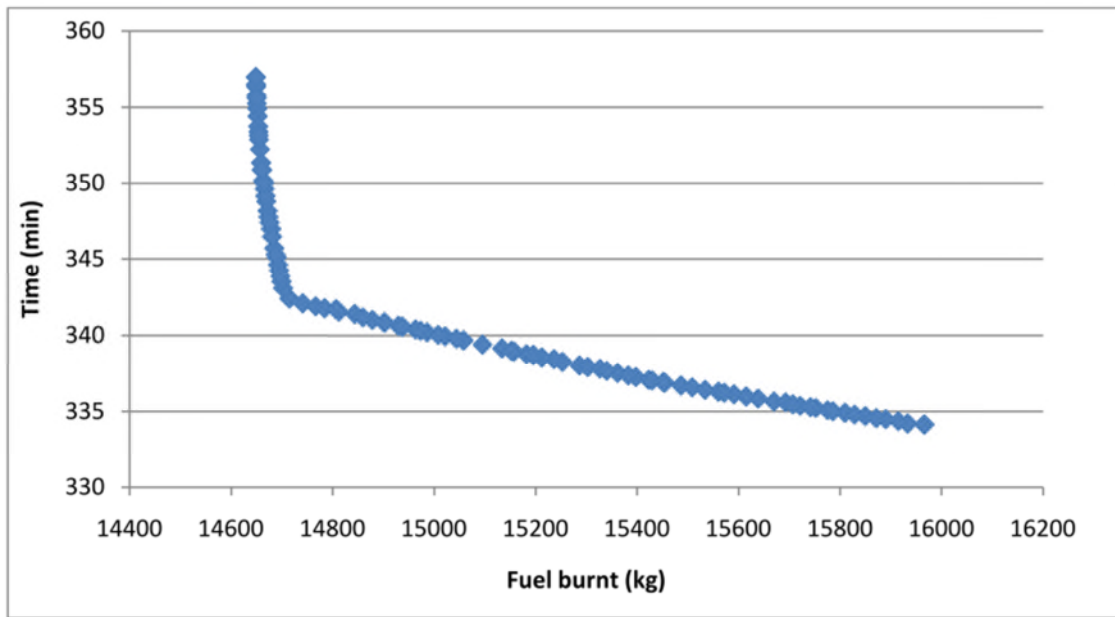


Figure 1.46: Fuel-Time Pareto Front: for a long range flight [23].

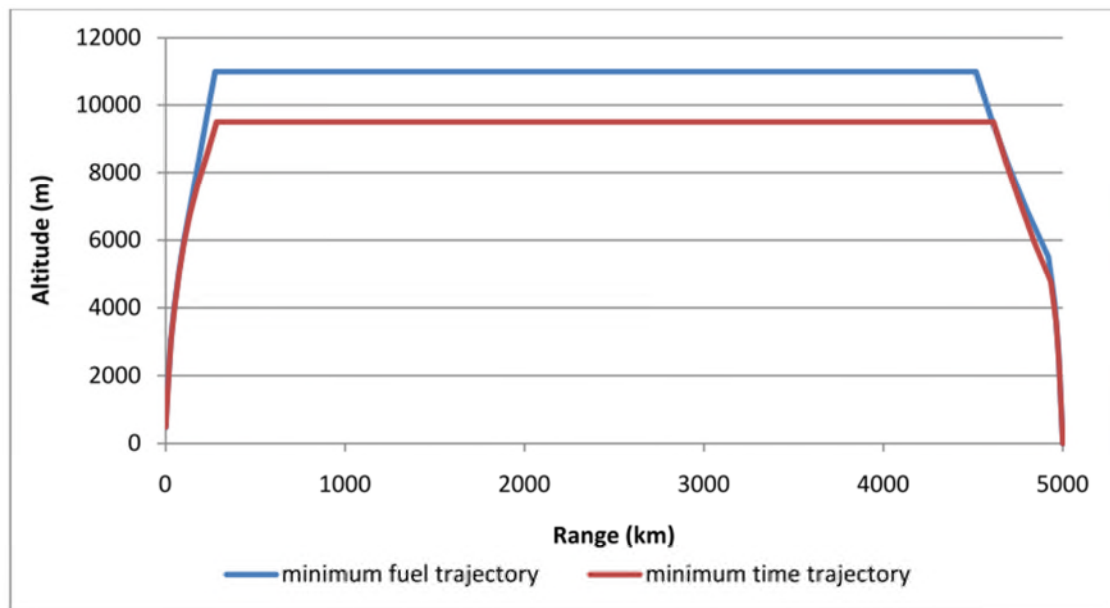


Figure 1.47: Optimised fuel and time trajectories for a long range flight [23].

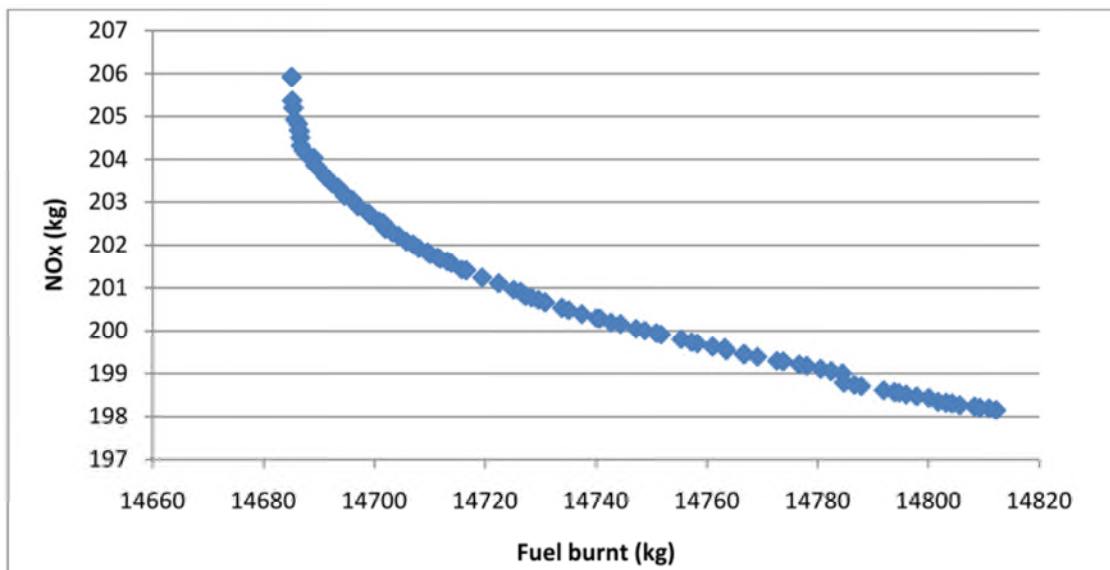


Figure 1.48: Fuel-NOx Pareto Front: for a long range flight [23].

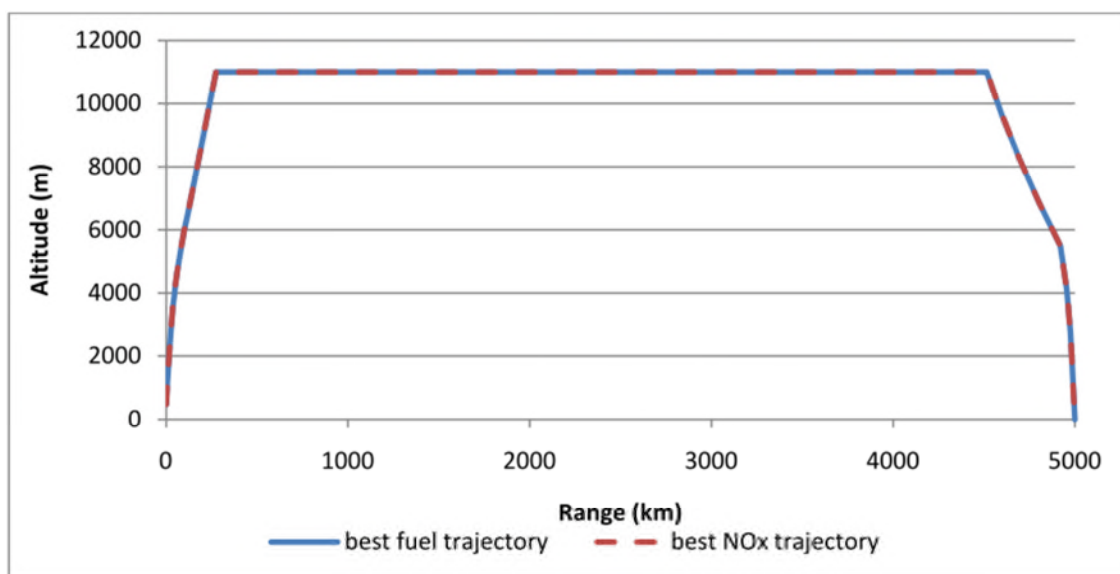


Figure 1.49: Optimised fuel and NOx trajectories for a long range flight [23].

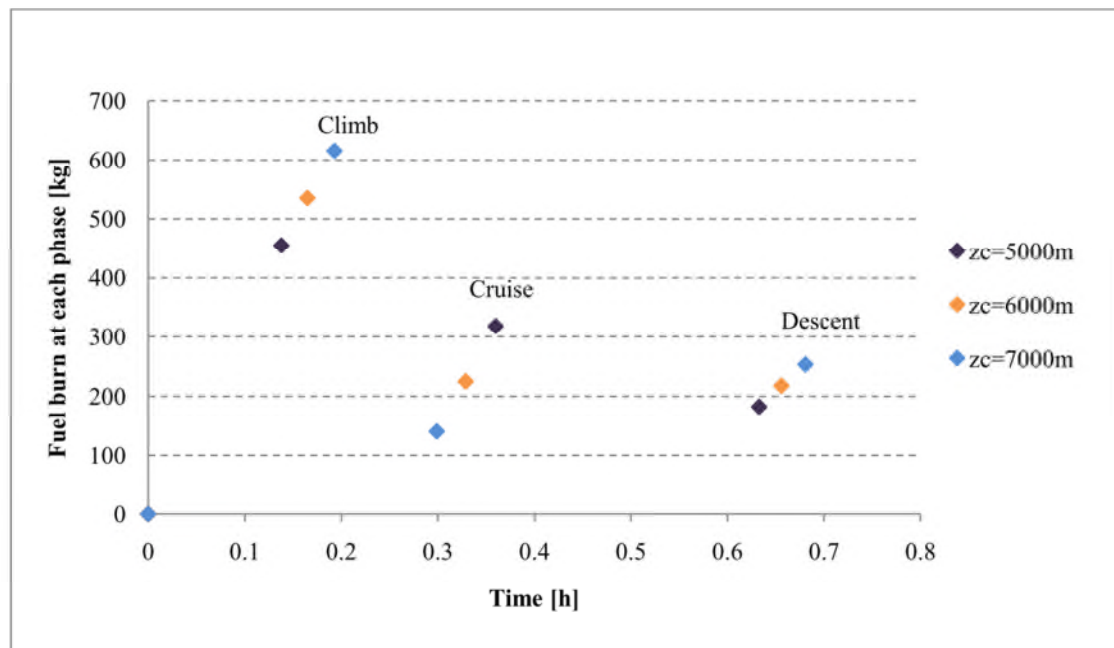


Figure 1.50: The variation of the fuel consumption according to the cruise altitude, Trondheim – Oslo [25].

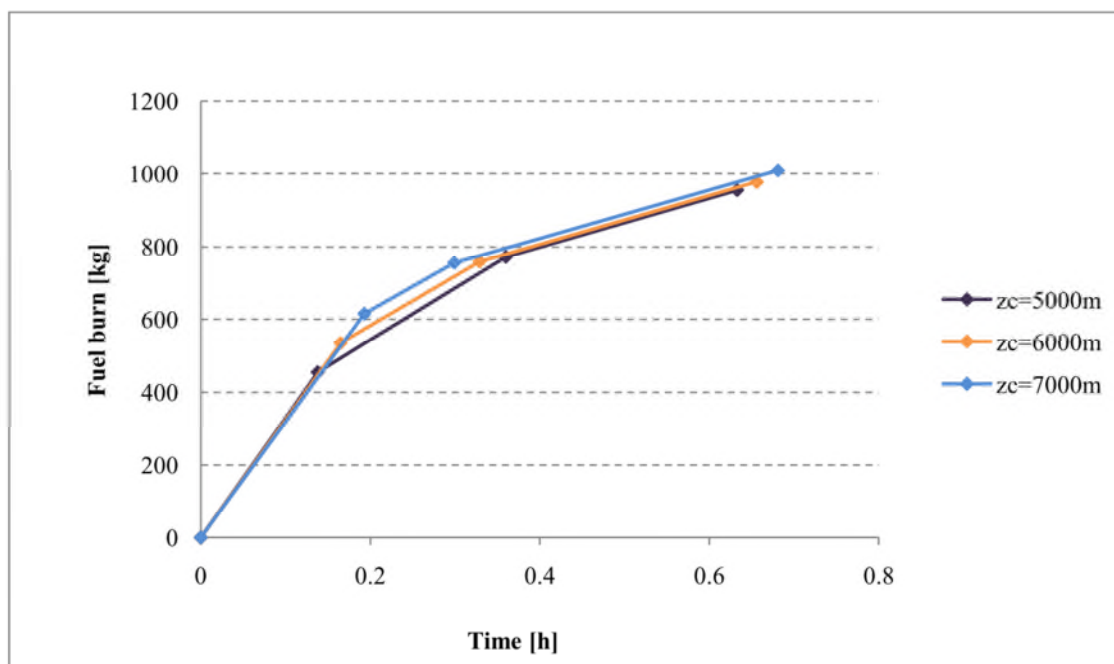


Figure 1.51: The accumulated fuel consumption according to the cruise altitude, Trondheim – Oslo [25].

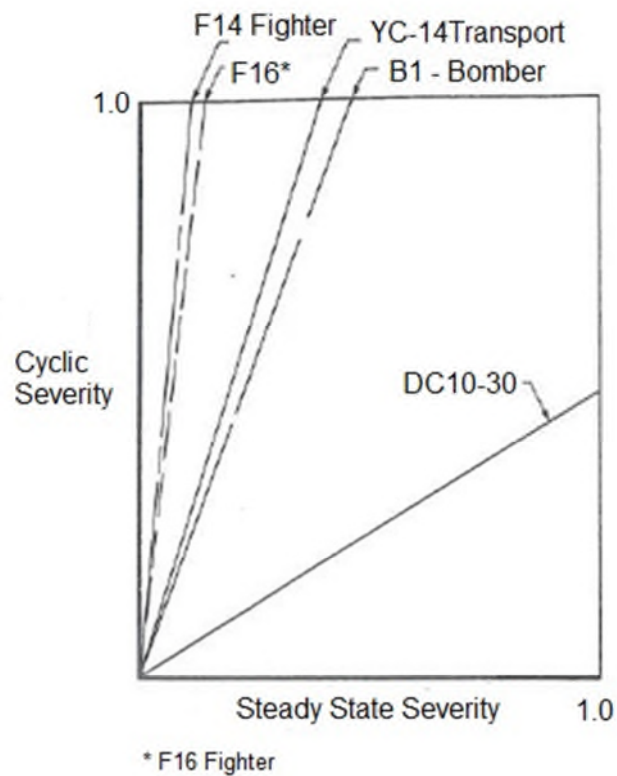


Figure 1.52: Cyclic to steady state usage severity relationships [27].

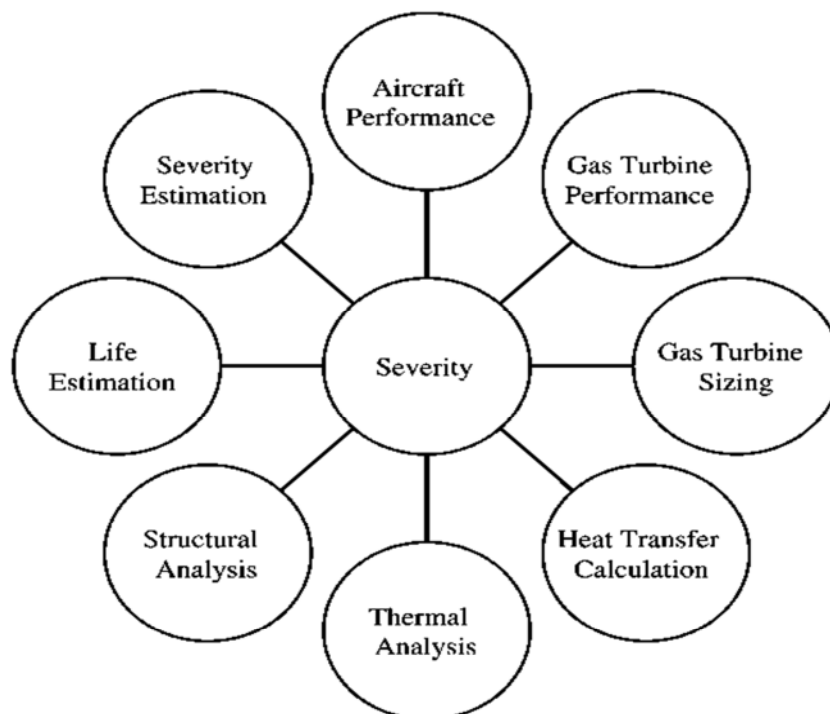


Figure 1.53: Elements of severity estimation [28].

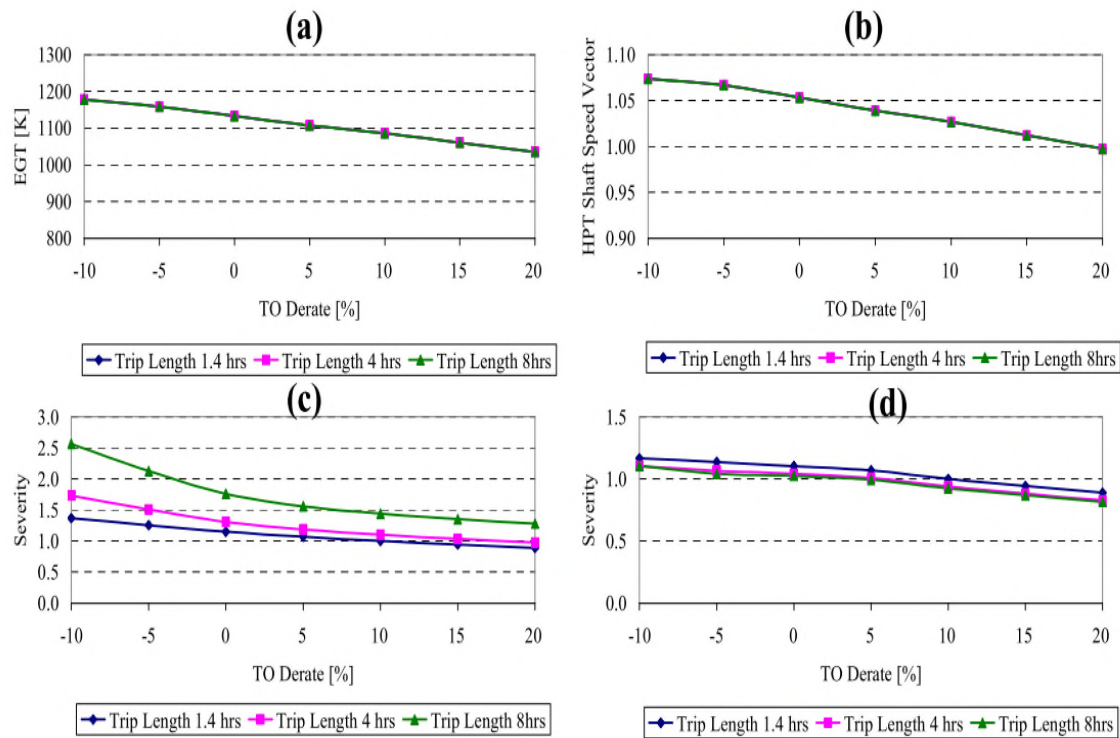


Figure 1.54: Engine characteristics for variation in TO derate (a) EGT (b) Shaft speed scaling vector (c) Blade severity (d) Disc severity [28].

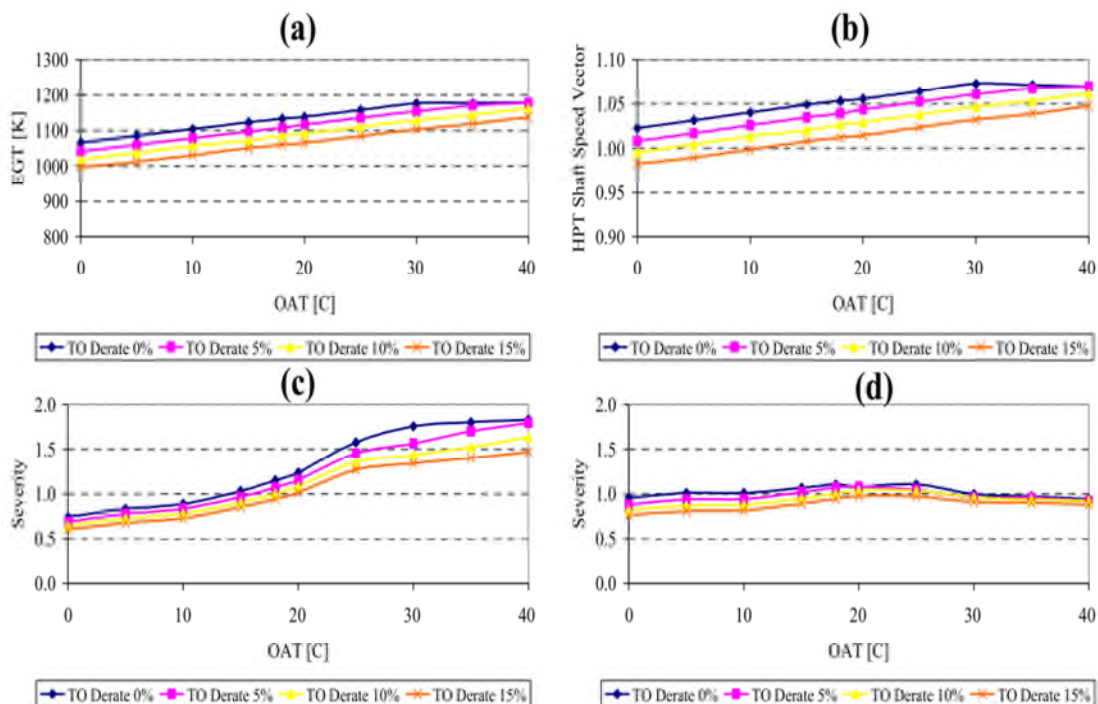


Figure 1.55: Engine characteristics for variation in OAT (a) EGT (b) Shaft speed scaling vector (c) Blade severity (d) Disc severity [28].

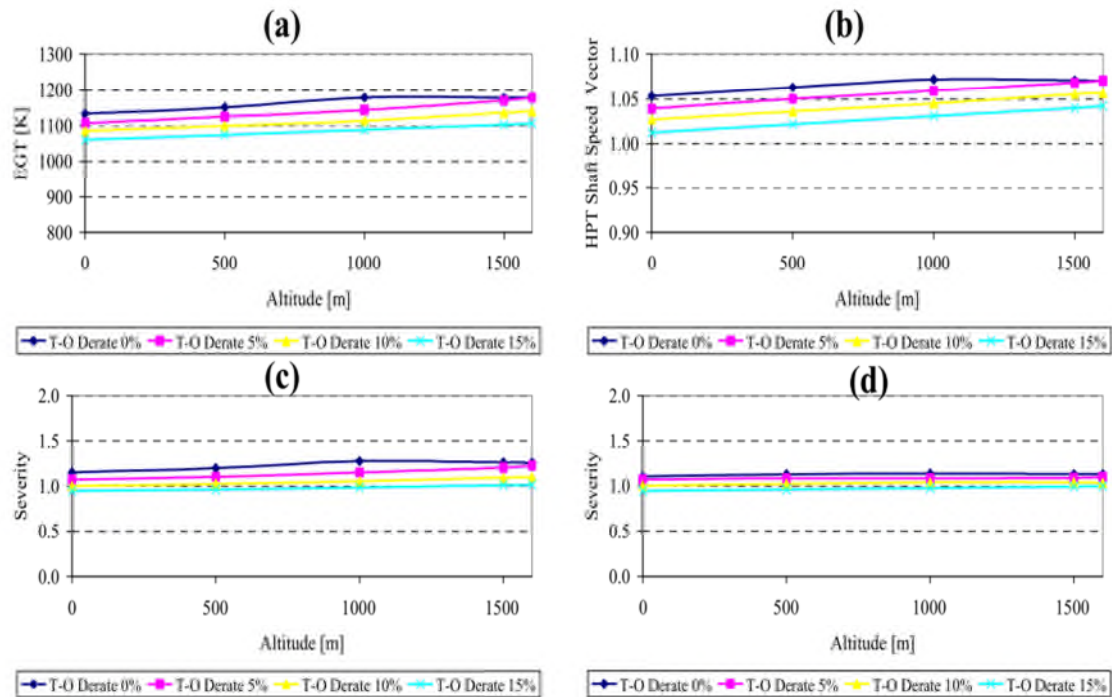


Figure 1.56: Engine characteristics for variation in airport altitude (a) EGT (b) Shaft speed scaling vector (c) Blade severity (d) Disc severity [28].

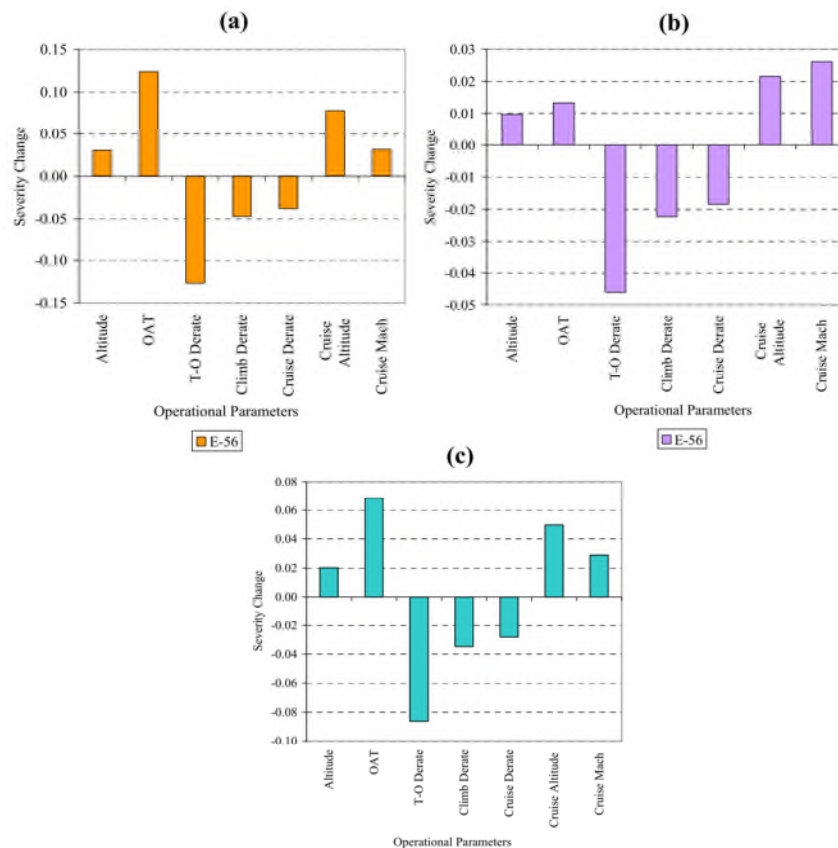


Figure 1.57: Short haul flight engine severity sensitivity for operational factors (a) Blade severity (b) Disc severity (c) HPT severity [28].

References for Chapter 1

- [1] Penner, J.E., Lister, D.H., Griggs, D.J, Dokken, D.J., McFarland, M. (1999). Aviation and the Global Atmosphere, IPCC special report, Intergovernmental Panel on Climate Change, Cambridge University Press, Cambridge, England
- [2] ICAO Environmental Report (2010). Environmental Branch, International Commercial Aviation Organisation, Montreal, Canada
- [3] Aeronautics and Air Transport: Beyond vision 2020 (Towards 2050) (2010). Report by Advisory Council for Aeronautics Research in Europe (ACARE)
- [4] Flightpath 2050: Europe's Vision for aviation maintaining global leadership & serving society's needs (2011). Report of the high level group on aviation research, European Commission
- [5] US Government Accountability Office (GAO) (2009). Aviation and Climate Change, GAO-09-554
- [6] PARTNER: Partnership for Air Transportation Noise and Emissions Reduction website (<http://partner.mit.edu/>).
- [7] Clean Sky Website (<http://www.cleansky.eu/>).
- [8] Segovia Blat C. M., (2012). Effect of engine degradation on fuel burn optimum civil aircraft trajectories, MSc Thesis, Cranfield University
- [9] Chandran S., (2013). Effect of engine degradation on engine and aircraft performance, MSc Thesis, Cranfield University
- [10] Sallee, G. P., (1978). Performance deterioration based on existing (historical) data-JT9D jet engine diagnostics program, NASA-CR-135448, Pratt and Whitney Aircraft Group
- [11] Little, P.D. (1994). The effects of gas turbine engine degradation on life usage, MSc Thesis, Cranfield University
- [12] Naeem M., (1999). Implications of aero-engine deterioration for a military aircraft's performance, PhD Thesis, Cranfield University
- [13] Antoine N. E., Kroo I. M., (2005). Framework for aircraft conceptual design and environmental performance studies, AIAA Journal, Vol. 43, No. 10, October 2005
- [14] Henderson R. P., (2009). Multidisciplinary design optimisation of airframe and engine for emissions reduction, MSc Thesis, University of Toronto
- [15] Colmenares Quintero R.F., (2009). Techno-economic and environmental risk assessment of innovative propulsion systems for short-range civil aircraft, PhD Thesis, Cranfield University

-
- [16] Kelaidis M., Aretakis N., Tsalavoutas A., and Mathioudakis K., (2009). Optimal mission analysis accounting for engine ageing and emissions, *Journal of Engineering for Gas Turbines and Power (ASME)*, Vol. 131, January 2009.
 - [17] Celis C., (2010). Evaluation and optimisation of environmentally friendly aircraft propulsion systems, PhD Thesis, Cranfield University
 - [18] Gherardi M., (2010). Development of engine performance models for MDO aircraft trajectory framework, MSc Thesis, Cranfield University
 - [19] Murugaiyan J., (2011). Multi-disciplinary civil aircraft trajectory optimisation studies, MSc Thesis. Cranfield University
 - [20] Pervier H., Nalianda D., Marzal Espi R., Sethi V., Pilidis P. Zammit-Mangion D., Rogero J-M., and Entz R., (2011). Application of genetic algorithm for preliminary trajectory optimisation, *SAE International* (2011), 2011-01-2594
 - [21] Tessaro M., (2012). Multi-disciplinary long-range aircraft trajectory assessments, MSc Thesis, Cranfield University
 - [22] Venediger B., (2013). Civil aircraft trajectory analyses – Impact of engine degradation on fuel burn and emissions, MSc Thesis, Cranfield University
 - [23] Marzal Espi R., (2010). Benchmarking and testing of different genetic algorithms for multi-disciplinary aircraft trajectory studies, MSc Thesis, Cranfield University
 - [24] Sridhar B., Chen N. Y., Ng H. K., (2010). Aircraft trajectory optimization and contrails avoidance in the presence of winds, *AAA Journal of Guidance, Control, and Dynamics*, Vol. 34, No. 5, September–October 2011.
 - [25] Merle D., (2011). Flight path optimisation for an airplane, MSc Thesis, Norwegian University of Science and Technology
 - [26] Marais K. B., Reynolds T. G., Uday P., Muller D., Lovegren J., Dumont J., and Hansman R. J., (2012). Evaluation of potential near-term operational changes to mitigate environmental impacts of aviation, *Journal of Aerospace Engineering (IMECHE)* 227(8), 1277-1299
 - [27] Troha, W., Stabrylla, R. (1980). Effect of aircraft power plant usage on turbine engine relative durability/life Report no: AIAA 80-1115, American Institute for Aeronautics and Astronautics (AIAA), Reston, Virginia
 - [28] Hanumanthan, H., Stitt, A., Laskaridis, P. and Singh, R. (2011). Severity estimation and effect of operational parameters for civil aircraft jet engines, *Proceedings of the Institution of Mechanical Engineers, Part G: Journal of Aerospace Engineering*
 - [29] Khani, N., Segovia, C., Navaratne, R., Sethi, V., Singh, R and Pilidis, P. (2012). Towards development of a diagnostic and prognostic tool for civil aero-engine component degradation, *GTIndia2012-9703*, ASME India 2012

- [30] Khani, N., Venediger, B., Segovia, C., Sethi, V., Pilidis, P. and Li, Y. (2012). Effects of Aero-Engine Component Degradation on Flight Mission Fuel Burn and NOx Emissions, ISABE-2013-1335, South Korea
- [31] Walsh, P.P., Fletcher, P., (1998), Gas turbine performance, Blackwell Science.
- [32] Ogaji, S.O.T, Pilidis, P. and Hales, R. (2007). TERA- A tool for aero-engine modeling and management, 2nd World Congress on Engineering Asset Management and 4th International Conference on Condition Monitoring, 11-14th June 2007, Harrogate, UK
- [33] Ogaji, S.O.T., Pilidis, P. and Sethi, V. (2009). Advanced power plant selection: The TERA (Techno-economic Environmental Risk Analysis) framework, ISABE 2009 Proceedings, ISABE-2009-1115
- [34] Kyprianidis, K.G., Di Lorenzo, G., Ogaji, S.O.T. and Pilidis, P. (2008). The TERA Approach – A methodology for techno-economical, environmental and risk analysis of multidisciplinary systems, Cranfield University Multi-Strand Conference, Cranfield
- [35] Kirby, M.R., Mavris, D. (2008). The environmental design space, 26TH International Congress of the Aeronautical Sciences, ICAS 2008
- [36] Chircop, K., Xuereb, M., Zammit-Mangion, D. and Cachia, E. (2010). A generic framework for multi-parameter optimisation of flight trajectories, 27th International Congress of the Aeronautical Sciences, ICAS 2010

Chapter 2

Engine and Aircraft Performance

Abstract

The engine performance code TURBOMATCH, an in house simulation and diagnostics code developed at Cranfield University is used to calculate the engine DP and OD thermodynamics when BPR, OPR and TET have been determined. The aircraft performance code HERMES is used to integrate the engine and aircraft and to determine the flight performance in terms of total fuel burn for the mission and the flight mission time. The first part of the chapter is literature describing concepts relevant to engine performance, engine component degradation and aircraft performance. The second part of the chapter describes in detail the engine performance and aircraft performance modules. The design point and off-design performance calculation procedures for the validation and verification of the engine model are discussed. The payload range diagram for the validation and verification of the aircraft performance model is also discussed. For each model a comprehensive list of assumptions, capabilities and limitations is provided. The results of preliminary assessments for both models are presented where relevant.

2.1 Introduction

Performance is inseparable from the economic model and is pivotal to an engine's economic viability. Performance measures such as fuel burn, life and maintenance requirements among others are all driven by the performance parameters, making it critical in the modern economic climate to understand how the economic (or business) model influences the choice of trade-offs between the environmental impact and the economic performance.

2.2 Aircraft Technology

Over the last 40 years the aircraft industry has developed to see an improvement in aircraft fuel efficiency of 70% [1], an improvement resulting from advances in airframe design, engine technology and rising load factors [1]. Most of the improvement has been attributed to better engine technology. The future predicts a continuation of these trends, with airframe improvements in efficiency, new materials and better control and handling systems expected to have more contribution to fuel efficiency improvements. Airframe fuel efficiency improvement up to the year period 2040-2050 is projected to be in the region of 25% [1]. Today's large conventional aircraft have design constraints, constraints which can be relaxed in future designs of larger aircraft such as with blended-wing or double-deck cabin. The fuel efficiency of a given fleet of aircraft is expected to improve slowly due to the low replacement rates; today's aircraft have lifetimes of up to 50 years; a trend expected to be maintained by rising

market demand [1]. A 40-50% improvement in fuel efficiency improvement is projected for new production aircraft by the year period 2040-2050 [1].

2.2 Aircraft Characteristics

The civil aviation industry has experienced many technology breakthroughs in the past 40 years. From propeller-powered aircraft through jet powered aircraft of the early 1960s, right up to the turbofans of the 1970s to 1990s. Ever powerful and fuel-efficient power plants have been developed with matching aerodynamic improvements and network reductions in baseline airframes. These improvements were, and continue to be driven by demand for better flight range, increased fuel efficiency, better capacity and greater speed. These are drivers with a positive market and economic impact as well as the environmental effect of aircraft. Fuel efficiency improvements averaging 1-2% annually have been realised since the introduction of the jet engine; advances that can be attributed to the integration of new engine and aircraft technology. Over this period, changes have been incremental and large scale representing improvement that has been relatively steady and continuous. Projecting forward to 2040-2050, the same trend is expected and adopted [1].

2.3 Engine Performance

Performance is the thrust power delivered for a given fuel flow, life, weight, emissions, engine diameter and cost, whilst ensuring stable and safe operation throughout the flight envelope at all steady state and transient conditions [2].

The main performance design drivers for the turbofan are the Turbine Entry Temperature (TET), Overall Pressure Ratio (OPR) and the Bypass Ratio (BPR). For a given set of BPR, OPR and TET there is an optimum Fan Pressure ratio (FPR) where SFC is a minimum and specific thrust is a maximum. At a fixed TET, OPR and BPR, as FPR increases, the fan thrust (and jet velocity of the bypass) will increase and the hot thrust (and jet velocity of the core) will decrease. This is due to an increase in the work extracted from the LP turbine. An increase in TET and/or OPR will increase the useful work and also improve the thermal efficiency and the optimum FPR. Increasing BPR will improve the propulsive efficiency and the fuel efficiency (hence a better SFC). Improvements in thermal efficiency and propulsive efficiency will give an increase in the overall efficiency. Whilst increasing BPR will improve the SFC, it will incur a significant reduction in the specific thrust. The specific thrust falls due to a fall in the core energy as the demand to drive the bypass gets bigger and the jet velocity decreases. The optimum FPR decreases with an increase in BPR. A significant reduction in SFC can be realised by optimising the key parameters.

Since the inception of the gas turbine as the source of propulsion in civil aviation, technological strides have been made which have influenced the key engine design and performance characteristics. Advances have been made in the aerodynamics of turbo-machinery, combustion, materials and turbine blade cooling. The civil aircraft engine has benefited from high bypass ratio engines,

which have lower fuel burn. Common practice dictates that engines are compared in terms of specific fuel consumption (SFC) [1]. However, the ultimate goal of aircraft engine design with respect to fuel economy is to minimise fuel burn per flight mission rather than SFC. The total fuel burn for a flight mission is influenced by the engine weight, installation drag and SFC. Engine weight for subsonic aircraft is about 10-15% of the empty aircraft weight. Savings on engine weight will benefit fuel burn reduction which equates to an increase in aircraft range.

2.3.1 Thermal Efficiency

The thermal efficiency for an aero-engine is a measure used to assess how effectively the chemical energy in the fuel is converted into mechanical work (increase the kinetic energy of the exhaust gases) by the thermodynamic cycle. It is dependent on pressures, temperatures, component efficiencies and other associated losses [2] [3]. To improve the thermal efficiency of an engine cycle, an increase in overall pressure ratio, temperature ratio and component efficiencies is necessary, resulting in an increase in jet velocity. It can also be improved by using better technology for cooling and sealing to minimise component losses or by using unconventional components to change the thermodynamic cycle such as the constant volume combustor (CVC), not investigated in this study. The thermal efficiency is best approximated using the representation in Equation 2.1.

$$\eta_{th} = \frac{V_j^2 - V_o^2}{FAR \times FHV} \quad (2.1)$$

Where, V_o is the flight velocity, and V_j is the jet velocity, and FAR is the fuel-air ratio and FHV is the fuel heating value.

2.3.2 Propulsive Efficiency

The propulsive efficiency for aero-engines is a measure of efficiency of the jet for aircraft propulsion. It accounts for the relationship between the thrust power and the increase in kinetic energy power through the engine [3]. An improvement in the propulsive efficiency is characteristically achieved when the bypass ratio is increased and the fan pressure ratio reduced resulting in the specific thrust and hence, the jet velocity to fall. The propulsive efficiency is best approximated by Equation 2.2.

$$\eta_{prop} = \frac{2V_o}{(V_o + V_j)} \quad (2.2)$$

Where, V_o is again the flight velocity, and V_j is the jet velocity.

2.2.3 Overall Efficiency

The overall efficiency of an aero-engine is the amount of mechanical energy produced by the thrust when fuel is burned to give energy. It is the product of the thermal efficiency and the propulsive efficiency as shown in Equation 2.3.

$$\eta_o = \eta_{th} \times \eta_{prop} \quad (2.3)$$

Increasing the overall efficiency will reduce the SFC. It can be improved by promoting thermal efficiency and/or propulsive efficiency. Further increases are possible by increasing the bypass ratio. However, there has to be trade-offs against increase in size, weight of the engine, and changes in drag. The drag and weight of the aircraft have an influence in the level of efficiency due to their effect on the fuel consumption. High efficiency is achieved by minimising fuel consumption via reductions in drag and weight. Low fuel consumption ensures a subsequent reduction in CO₂ and water output levels. The bypass engine in today's aircraft is a practical way of increasing overall efficiency by reducing the jet velocity and raising the propulsive efficiency. The high bypass ratio, high pressure ratio engine is the most fuel efficient in aviation industry today. These engines have high pressures and temperatures of combustion resulting in high NOx formation at take-off and cruise for the same combustor technology.

2.4 Gas Turbine Engine Degradation

The gas turbine is a system that functions as a result of the fine tuning and matching of a number of different components. Over time, any of the engine components can show the effects of degradation, which will affect the matching of the components and adversely affect the overall engine performance. The degradation of an engine will affect its economic performance since performance measures such as fuel burn, life and maintenance requirements are influenced by performance parameters. It is therefore essential when attempting to predict engine component degradation and remaining useful life, to understand the mechanisms that will cause degradation and to understand how the remaining useful life is changing as the engine degrades [4].

2.4.1 Mechanisms of Engine Degradation

There are several mechanisms that will cause engine degradation and following technical discussions with [5] these mechanisms have been broadly classified into the following three events:

1. Singular events: Events comprising “unique singular events” e.g. Foreign Object Damage (FOD), engine surge and foreign object ingestion (volcanic ash).
2. Benign events: Events associated with the natural ageing of the engine (and associated degradation) e.g. thermal distortion and flight loads.
3. “Not entirely benign” events: Events comprising of factors other than natural ageing of the engine which cause the engine to degrade e.g. engine flight operational procedures (harsh deployment of thrust

reversers, sharper take-off and climb manoeuvres) and maintenance procedures, engine fouling (e.g. sand ingestion) due to deposits within the engine, and the erosion of aerofoils (also caused by natural ageing and accelerated by fouling).

Due to the “unique” and largely unpredictable nature of singular events, they have not been considered within the scope of this work.

2.4.1.1 Common Causes of Performance Deterioration

Flight Loads and Thermal Distortion

The push for better engine performance has resulted in increased mass flows, pressure ratios, firing temperatures, improved efficiencies and reduced clearances and weight. Increasing the mass flows has resulted in a subsequent increase in engine size, and this coupled with smaller clearances has increased engine sensitivity to the loads exerted during flight manoeuvres. Flight manoeuvre loads affect each of the engine components, and the greatest impact is wear occurring between the rotor blades and the engine seals. During transient performance, the engine experiences rapid behavioural changes and exhibits its greatest expansion under the effects of increased flight loads. As the engine accelerates, the rotating parts expand to their greatest size causing maximum interaction and larger blade clearances than those expected under constant engine load. According to [7] studies on the effects of clearance increases have shown that an LPT increase of 0.010” in clearance results in a 0.5% decrease in isentropic efficiency and 0.83% decrease in flow capacity.

The effect of flight loads will also appear as engine casing distortion, which is more pronounced during critical flight conditions at take-off and landing. As the casing temperatures increase, the casing expands and distorts causing an increase in clearances [6] [7].

During the design phase, the engine stationary and rotating parts are thermally matched, an effort aimed at slowing degradation. This matching of the thermal growth of components is to ensure and maintain a constant running clearance during thermal cycles i.e. start and stop cycles or change of load. A distortion in thermal loading gives rise to differential thermal growth and subsequent mismatch in the thermal growth of components which enhances degradation. Under high temperatures and stress fluctuations, thermal distortions occur as primary twisting, bowing and soldering of turbine vanes. Changes in compressor and combustor performance give rise to changes in turbine entry conditions. In particular, changes in the combustor effect changes in the temperature profile at entry to the turbine and this could result in elevated local temperatures, variation in clearances and area, increased leakage and distortion. The efficiency and life of the turbine suffer with thermal distortions. The combustor also suffers from thermal distortion causing the components to fail prematurely and increasing life cycle costs. Thermal expansion causes blade tip and labyrinth seal wear [6] [7].

As the equipment ages, clearances between the rotating hub and stationary blades or between the rotating blades and stationary casing open up resulting in higher flow leakages and a reduction in the possible head capability and the efficiency of the components. The production losses occur due to intensive mixing of the leakage flows and the main flow, and also due to the leakage flows acting as a blockage across the flow area thereby reducing the effective through flow area [6] [7].

Engine Flight Operation and Maintenance Procedures

Taking into account that a gas turbine functions as a result of the interdependencies of various components, one major cause of engine degradation is the actual interaction of these components. The nature of engine operation will therefore affect the rate of degradation and the life of the components. Engine deployment does not always maintain steady state operations where the components interact with little rubbing, at times, rapid throttle movements are required giving rise to unequal growth and added rubbing. Some missions demand more in terms of fuel consumption due to flying at different altitudes, Mach numbers and power settings [6] [8].

The maintenance procedures employed on an engine will affect the level and rate of performance degradation and the time between repairs and overhaul. Maintenance standards vary from user to manufacturer to facilities, and are greatly influenced by understanding performance degradation and the factors that affect degradation. Studies have identified that maintenance practices could have differences in the degradation of engines amounting to as much as 13% [7], and have shown that engine efficiency can be improved by over 2% [7] through compressor washing and dressing of blades.

Fouling and Abrasion

Fouling is the degradation of flow capacity and efficiency due to contaminant particles adhering to airfoil and/or annulus surfaces in the presence of oil or water mists. Fouling will result in a reduced flow area; an increase in surface roughness and changes in the airfoil shape (which influence its aerodynamic behaviour). Fouling will also lead to a reduction in power output, efficiency drop and increased fuel consumption. Both compressors and turbines can be fouled; however compressor fouling is the more prevalent cause of performance deterioration and will increase both creep and fatigue as well as result in increases in turbine temperatures of as much as 15°C. Compressor fouling can cause flow reductions of up to 8% and efficiency reductions of 1% [6] depending on the operating condition and severity as well as cause increases in engine rotational speed. Turbine fouling of Nozzle Guide Vanes (NGVs) will result in approximately 2% reduction in flow capacity and 1% in efficiency. Particles also may plug the turbine blade cooling holes and promote damage due to overheating. The decrease in engine performance requires higher turbine entry temperatures and speeds to maintain the required power output. This results in reduced engine life and increased operating costs. Regular offline washing or in

combination with online washing to a large extent mitigates the effects of fouling [6].

Abrasion is the outcome when rotating parts rub on the stationary parts causing the seal and/or tip clearances to increase.

Hot Corrosion

Hot corrosion is material loss (and/or deterioration) when chemical reactions occur between certain contaminants such as salts, mineral acids or reactive gases and components in the flow path. When the products of such reactions adhere to the components, the result is scaling. Also, chemical reactions occur between the metal atoms of the components and oxygen that is found in the surrounding hot gaseous environment, causing high temperature oxidation [4].

Erosion and Corrosion

Erosion is the wearing of components (airfoil and seals) when hard or incompressible particles impinge on flow surfaces and remove material from the flow path by abrasion. It will occur in airfoils when foreign particles are ingested into the engine. Ingested particles can vary from items on the ground to environmental conditions (e.g. volcanic ash, hail, soot and pollution). Ingestion of particles can affect performance by causing the engine to stall, and also by eroding seals and blade material. Erosion can lead to permanent performance degradation and will produce stress risers which reduce engine life. It will blunt airfoils, reduce blade camber and blade length and increase clearances (causing an increase in blade tip leakages, change blade aerodynamics, increase pressure losses and cause blades to fail). In compressors, erosion will typically reduce flow capacity by 2% and isentropic efficiency by 1%. Erosion will affect the turbine by increasing the nozzle area and lowering its efficiency and typical effects are 2% increase in flow capacity and 1% reduction in efficiency. Erosion of the blades can lead to excessive blade metal temperatures and premature failures due to changes in the profile of the cooling holes which affects the effectiveness of cooling the blade [6].

Corrosion (figure 2.1) is the loss of material due to chemical reactions between contaminants in the air or fuel and the components. Another source of problems is when particles fuse onto hot surfaces and block cooling passages, alter the surface shape and interfere with heat transfer (resulting in thermal fatigue). Corrosion though having the same impact as erosion (with similar changes in flow capacity and efficiency) is more severe and cannot be stopped easily once it has started and will lead to premature engine (or component) failure [4].

Damage

Damage will occur when large foreign objects such as large birds strike the components in the flow path (figure 2.2). These objects may enter the engine with the intake flow or can be engine pieces that have broken off. Pieces of ice

breaking off the intake or carbon build-up breaking off from the fuel nozzles can also cause damage [4].

2.4.1.2 Evolution of Degradation

Gas turbine performance losses get progressively worse with time unless corrective action is taken. There is little quantitative information available publicly concerning degradation and how it evolves when an engine is in operation. According to [7] degradation can be separated according to time frames into:

- Short term (permanent) degradation that occurs rapidly during early stages (first few hundred flights) after entry into service.
- Long term degradation that progresses gradually with accumulating service hours.

Gas turbine degradation is not linear but logarithmic and the rate of degradation diminishes with time i.e. a new engine initially degrades more rapidly than it degrades after several thousand hours of operation [6] [7]. The main cause of degradation during its early life is increase in clearances. Once the clearances have been established, the rate of degradation reduces (unless harsh deployment and violent manoeuvres) as clearances no longer increase. After this initial phase, performance degradation is due to fouling, erosion and corrosion.

2.4.1.3 Gradual and Rapid Degradation

Further, degradation can be divided according to the rate of performance loss as gradual or rapid. Gradual degradations are those that occur slowly as a result of fouling, erosion, corrosion and rubbing wear. Rapid degradations are those that are instantaneous such as due to foreign (and domestic) object damage, faulty systems and sensors. Rapid degradations are not within the scope of this work as they are random and unpredictable in nature [9].

Some of the effects of degradation that have been mentioned can be mitigated by engine washing or cleaning, whereas others require the components to be re-adjusted, repaired or replaced. For this reason, mechanisms of degradation can also be identified as either recoverable or non-recoverable degradations. Degradations in which the performance loss can be mitigated through online and offline water washing of components are recoverable degradations. Non-recoverable degradations require engine overhaul as they cannot be mitigated by merely washing and or cleaning. Non-recoverable degradations include permanent degradations whereby the recovery of full performance is not possible even with overhaul.

2.4.1.4 Engine Rating

Engine rating also known as thrust rating is whereby the engine's performance is limited or a specified power setting (baseline value) adequate for a given set of flight conditions is selected. This allows the engine to operate

at lower temperatures and engine spool speeds (part load), hence a reduction in the centrifugal force and thermal expansion which increases engine life. Engine thrust rating reduces the life accumulation rates of an engine and will potentially reduce the Life Cycle Costs (LCC) [11].

A de-rated degraded engine will have a significantly lower loss in efficiency than when it is operating at full load. Thrust rating has minimal effect on LCF life and studies have shown an increase of 3-5% and 2.5% gain in the cold section and hot section LCF life respectively [6]. The hot section components mainly affected by thermal fatigue have shown significant benefit due to thrust rating. According to [6], the following life extensions have been achieved for a 100 hour Stator Outlet Temperature (SOT) adjustment interval:

1. Combustion chamber – 6%
2. HP turbine nozzle guide vanes – 11%
3. HP turbine rotor blades – 18%
4. IP turbine nozzle guide vanes – 17%
5. IP turbine blades – 31%

2.4.2 Engine Component Degradation

A combination of some or all of the mechanisms that have been discussed in section 3.4.1 will lead to engine component degradation.

2.4.2.1 Airfoils

Fouling and erosion will increase the blade surface roughness which in turn promotes frictional losses. Increased roughness also causes premature transition from laminar to turbulent boundary layers as well as premature flow separation, giving rise to production losses. Changes to the geometric shape of the airfoil will occur with erosion, deposits or damage to the airfoil and reduce the optimum performance of the airfoil. The exit angles change as the turbine blades deteriorate therefore reducing the work and increasing the losses. In blades which operate at or near transonic speeds, blade deposits and added roughness consequently lead to a thicker boundary layer and a subsequent reduction of flow capacity through the blade row. Erosion of the trailing edge increases the throat width of the blade allowing more flow but less work extraction. The blade leading edges are most significantly affected by erosion, and this has an effect on the location and extent of the transition of the boundary layer from laminar to turbulent. The heat transfer characteristics of a boundary layer are not only dependent upon the thickness, but also upon the state of boundary layer whether laminar, turbulent, and transitional or separated; hence erosion of the leading edge will influence the heat balance of the blade. In general, degradation (i.e. fouling, erosion, deposits, corrosion and other damage) of the airfoil creates higher losses and less turning, thus presenting the succeeding row of airfoils with different incidence angles, higher temperatures, lower pressures and densities for compressors and higher pressures and densities for turbines [6].

2.4.2.2 Compressor

There are three major effects that determine the performance deterioration of the compressor:

1. Increase in tip clearances
2. Airfoil geometry changes
3. Airfoil surface quality changes

The first two effects lead to non-recoverable degradation, whereas through compressor washing the latter effect can be partially recovered. A combination of the effects will lower the compressor flow capacity and its efficiency, and effectively reduce the compressor surge or stall margin. A further reduction in the surge margin, though maybe not directly affecting the steady state operation, may reduce the transient capabilities and cause damage. Compressor fouling will shift the equilibrium running line to both a lower mass flow rate and a lower pressure ratio (figure 2.3) [4]. This is because, at any given engine spool speed, the degraded compressor operates at a lower than design efficiency and at a non-optimum surge margin and reduced operating range. Fouling the first stage will have more impact on the overall compressor performance than similarly fouling a later stage. In addition to reduced stage performance, there will be additional losses and efficiency reductions due to individual stages operating at lower flow coefficients than for the clean engine. Since the operating point of the compressor is determined by the turbine flow capacity, the condition of the compressor will impact the turbine performance.

2.4.2.3 Combustion System

The combustion system will not directly lead to performance deterioration, and apart from severe combustor damage the combustion efficiency will normally not decrease. Combustor performance deterioration potentially leads to coking of fuel nozzles, changes in the fuel spray pattern and the temperature profile at the combustor exit becoming distorted. A variation in the exit temperature distribution will implicate on the turbine performance as the below points [4]:

1. Local temperature peaks cause turbine section damage.
2. The modified temperature profile increases secondary flow activity causing a reduction in turbine efficiency.
3. Due to measurements of the control temperature being taken at discrete circumferential points, the average measured temperature is different from the true average thermodynamic temperature.

2.4.2.4 Turbine

Turbine degradation will result in the following effects:

1. Increase in tip clearances
2. Airfoil geometry changes
3. Airfoil surface quality changes

An engine transiting from cold to accelerating to full load will experience extreme temperature changes; for this reason it is problematic to maintain tip clearances in the turbine section. In a large number of cases there is a different rate of expansion for the stationary components and the rotating components. Centrifugal and thermal loads exerted during transient operation and also engine casing distortion caused by flight loads will increase clearances. Clearances are proportional to the losses and the losses increase with flow increase. Added clearances reduce efficiency and also increase the axial flow blockage thus reducing the through flow and increasing the velocities in the main flow. Aerodynamic loads and thermal stresses distort the turbine inlet guide vanes allowing the cooling air into the main gas stream. This reduces the gas temperature and has a negative impact on the turbine efficiency [4].

Corrosion alters the flow path by increasing the surface roughness, causing thicker boundary layers on the blades and sidewalls. This has the effect of possibly reducing the flow capacity, more so at near choking conditions. Also, corrosion leads to material removal, particularly at the airfoil leading and trailing edges. The removal of material especially in the nozzle area has an opposite effect, it will result in increases in flow capacity for any given pressure ratio due to a larger effective throat area (a limiting factor in flow capacity of any nozzle) and also increases in the exit flow angle, thus reducing turning in the stator and rotor with a subsequent reduction in work extracted. Any change in the turbine flow capacity will impact the operating point of the compressor [4].

2.4.3 Effect of Degradation on the Engine

Engine component(s) degradation cause changes in the performance characteristics and hence a mismatch which gives a compound effect on the engine performance. A degraded engine will seek a different steady operating point in relation to that of a clean engine, and this variation in the engine's steady operating point causes changes in the SFC and/or fuel flow (W_{F}) [4] [8].

Compressor degradation affects the compressor pressure ratio, efficiency and flow capacity, and the type of degradation influences the level of impact. An engine with reduced compressor efficiency due to fouling will display momentous changes in pressure ratio and flow capacity. This type of degradation of the compressor will not alter the relationship between compressor flow capacity and pressure ratio as it is determined by the turbine, though the engine will run faster and the compressor consume more power. The engine exhibits a loss in power. An engine with reduced compressor flow capacity due to fouling or increased clearances will exhibit a power loss.

An engine with the turbine nozzle degraded by erosion or corrosion experiences a turbine pressure ratio and efficiency drop, leading to a reduction in engine speed. The effect this degradation has on overall engine performance depends on the compressor speed and if compressor efficiency does not change with speed there is a resulting drop in engine output and efficiency. TET is not measured directly in most engines but is calculated as a function of the Exhaust Gas Temperature (EGT). Because the measured EGT is not the thermodynamic average temperature, but rather the arithmetic average

temperature, engine degradation can lead to a shift in the true ratio between TET and EGT causing the engine to over fire or under fire; a shift caused by changes in flame patterns which result in changes in temperature patterns and also by changes in turbine efficiency or flow capacity.

In summary, the performance degradation mechanisms associated with the compressors reduce flow capacity and efficiency whereas those associated with the turbines largely increase flow capacity and reduce efficiency. The effects of performance degradation increase with increasing number of flight cycles for both the compressors and the turbines. The levels of degradation for a serviceable engine level off after a given number of flight cycles [4] [6] [7].

2.4.3.1 Component Performance Degradation

The performance characteristics of an engine component are determined by established performance parameters. These basic parameters are used when matching the components to ensure the functionality of an engine as a system. Some of the basic performance parameters are listed below:

- Compressor efficiency and flow capacity
- Combustor efficiency
- Turbine efficiency
- Area of nozzle guide vane
- Area of exhaust nozzle

A set of basic performance parameters also referred to as 'engine design parameters' fixes the geometry of the engine and will vary according to the engine configuration. Engine degradation will alter these basic design parameters and change the performance characteristics of components resulting in a mismatch. The performance characteristics that change with degradation are dependent upon the engine design parameters and these include:

- Fuel flow
- Thrust power
- Engine temperatures
- Engine pressures
- Rotational speeds

2.4.3.2 Influence of Component Performance Degradation

A turbine produces power of magnitude P as given in Equation 2.4.

$$P = WC_p(TET) \left[1 - \frac{1}{\left[\frac{P_{in}}{P_{out}} \right]^{\frac{\gamma-1}{\gamma}}} \right] \quad (2.4)$$

Equation 2.4 assumes constant fluid properties at inlet and outlet, no bleed and no cooling. In reality C_p and γ are a function of temperature and gas

composition and as described in [12] and [13] any assumptions made will affect the caloric properties and can yield significant inaccuracies in performance calculations.

The pressure at inlet to the HPT is the compressor delivery pressure less the combustor pressure drop. Since degradation causes the compressor flow capacity and delivery pressure to drop, the turbine work is reduced. To maintain the thrust requirement, the engine's fuel flow control system compensates for the effects of degradation by increasing the fuel flow rate which is matched by a corresponding increase in turbine entry temperature. The increase in TET increases the acceleration of the gases through the turbine giving a higher engine speed and a correspondingly greater airflow which increases the compressor delivery pressure. Because degradation causes the compressor efficiency to drop, the turbine must compensate by producing more work to maintain the fuel flow rate, higher compressor delivery pressure and engine performance output. This increased demand on the turbine results in more creep and fatigue damage which shortens the lives of the hot section components and increases the engine LCC [14].

From the preceding discussions, the TET (and/or EGT), fuel flow rate and engine power (thrust) output are identified as the main drivers that affect the evolution of the engine life potential. An increase in the magnitude of these drivers has detrimental effects on the engine life.

2.5 Aircraft Performance

In the past, concentrated effort to improve aerodynamic efficiency has been centred on the take-off/climb and the cruise phase of the aircraft mission profile and this has resulted in improvement in the lift and drag performance and hence fuel burn [1]. Also, by reducing the airframe weight due to available lighter and stronger materials for structural components, fuel burn has been reduced. For future designs, a greater understanding of the aerodynamic flow requirements around the airframe is needed.

Increasing bypass ratios has seen increase in the weight and drag of the nacelle. High bypass ratio engines in comparison to low by-pass ratio engines have, however, provided significant gains in fuel burn reduction per given flight mission. This has in turn given operators more performance flexibility when optimising range, take-off weight and payload. Local drag effects can be reduced by improving the aerodynamic nature of the engine-nacelle flows and changing the length and shape of the inlet. This has the added bonus of increasing efficiency [1] [15]. The operating empty weight is reduced by developing lighter materials and structures for the nacelle. Improving the efficiency of the thrust reverser enhances landing performance as well as reducing the nacelle package weight [1] [15]. Current and future designs have the limiting factor of having to satisfy noise regulations.

Interference drag problems arise when integrating the nacelle and the engine [16], and in future designs there needs to be consideration of trade-offs between higher drag and minimising interference for high bypass ratio engines

as well as noise impacts. An example is locating the nacelle closer to the wing without inducing interference; this will reduce the pylon weight and drag and the height and weight of the landing gear. The use of fly-by-wire and the lighter fly-by-light control systems in today's modern airframes has seen tremendous reduction in Operating Empty Weight (OEW). Engine fuel burn at cruise is reduced when engine bleed air is not required. It is reduced due to re-circulation of air for the cabin and conditioning requirements. This saving in fuel is limited by quality of air required for the cabin. Future fuel savings are possible with designs for high-lift systems that provide the same performance for lift versus drag at lower weight. Databus control systems technology has seen less wiring needed for modern electrical systems, reducing further airframe OEW [1].

There have been advances made in aerodynamic studies such as to improve wing tip structures to have smoother surfaces; better aircraft control systems and weight reduction. These can be adapted as derivatives for future aircraft technologies for better fuel efficiency.

2.6 Engine Performance Model

The engine performance model to be used is built using the gas turbine simulation and diagnostics software TURBOMATCH, an in-house engine performance code developed at Cranfield University to carry out DP and OD engine performance calculations. It has a modular structure that allows the user to use components (bricks) to assemble an engine configuration, thus allowing for use in modelling advanced propulsion cycles. TURBOMATCH uses component maps to carry out a mass and energy balance through iteration. Further details about TURBOMATCH can be found in [17].

Assumptions

To simplify the engine performance models the following blanket assumptions were made [18]:

- All the components are modelled as “bricks” with no consideration for variations in dimension.
- Fixed coefficients are given to every “brick”.
- Electrical components and mechanical components are not modelled.
- Component maps are used to determine compressor and turbine component behaviour.
- Overall pressure losses account for friction and heat transfer
- Isentropic relations model the modifications to airflow, and isentropic efficiencies cater for any adjustments.
- Bleed air extraction is located at a compressor exit rather than across the stages as in real engines.
- Similarly, the cooling air is delivered at the burner exit rather than across the turbine stages.
- Extraction of auxiliary power and bleed air for the cabin is not modelled.

- Interaction of the bypass exhaust jet and the core exhaust jet is not simulated.

Capabilities

- Parametric analysis
- Degradation modelling
- Transient performance calculations
- Modular structure allows coupling with other software

Limitations

- Extraction of auxiliary power and bleed air for the cabin is not modelled.
- Dynamic engine performance (e.g. flow behaviour, variable stator vane scheduling) not accounted for.

The flight mission spool speeds, operating temperatures, cooling flow temperatures and engine take-off thrust calculated by the engine performance model are used as input to the lifing module.

2.6.1 Engine Design Point Validation

The engine model used in this research is a typical twin spool high bypass turbofan engine similar to a CFM56-7B27 engine used to power a Boeing 737-800 aircraft. The design point for the engine model is set at Top of Climb (ToC). The performance of the model was calculated and matched to the performance data found in [19].

Table 2.1: CUCCTF (twin spool turbofan) engine data from [19].

| Engine Configuration | Twin Spool Turbofan |
|---------------------------------------|---------------------|
| Take-Off Thrust (kN) | 121.4 |
| Take-Off Mass Flow Rate (kg/s) | 354.8 |
| Take-Off Bypass Ratio (-) | 5.1 |
| Overall Pressure Ratio (Take-Off) (-) | 31.65 |
| Overall Pressure Ratio (ToC) (-) | 32.8 |
| Maximum Climb Thrust (kN) | 26.5 |
| Cruise Altitude (m) | 10668 |
| Cruise Mach Number (-) | 0.785 |
| Maximum Cruise Thrust (kN) | 24.4 |
| Fan Diameter (m) | 1.55 |

The data used for the engine design point as found in [19] is shown in table 2.1. From here on the simulated engine model will be referred to as the Cranfield University Current Conventional TurboFan (CUCCTF). The TET at ToC was determined from the thrust requirements and the OPR obtained from [19]. Component parameters such as pressure ratios, efficiencies and others were guessed to closely approximate the OD engine performance (at TO and cruise). The output parameters for the simulated engine are summarised in

table 2.2. Some of the engine simulation results which have been closely matched with the engine data from reference [19] are shown in table 2.3. The discrepancy for the TO mass flow rate of 3.4% is less than 5% therefore the simulated engine model is acceptable for the purposes of this research.

Table 2.2: CUCCTF (Simulated Engine) DP (ToC) data.

| Parameter | Value |
|-------------------------------|-------|
| Mass Flow (kg/s) | 366.8 |
| Bypass Ratio (-) | 4.9 |
| Overall Pressure Ratio (-) | 32.8 |
| Fan Pressure Ratio | 1.68 |
| Booster Pressure Ratio | 1.79 |
| HPC Pressure Ratio | 10.15 |
| Fan Efficiency (-) | 0.885 |
| Booster Efficiency (-) | 0.87 |
| HPC Efficiency (-) | 0.877 |
| HPT Cooling Flow (%) | 10% |
| Combustion Efficiency (-) | 0.999 |
| Combustor Pressure Loss (-) | 0.04 |
| Turbine Entry Temperature (K) | 1510 |
| HPT Efficiency (-) | 0.92 |
| LPT Efficiency (-) | 0.91 |
| Operating Altitude (m) | 10668 |
| Flight Mach Number (-) | 0.785 |

Table 2.3: Public domain data vs. CUCCTF engine simulation results

| Parameter | Required | Simulation | Delta [%] |
|--------------------------------|-----------|------------|-----------|
| Take-Off Thrust (kN) | 121.4 | 121.4 | 0.0 |
| Take-Off Mass Flow Rate (kg/s) | 354.8 | 366.8 | 3.4 |
| ToC Thrust (kN) | 26.5 | 26.5 | 0.0 |
| Cruise Thrust (kN) | 24.4 | 24.4 | 0.0 |
| BPR Take-Off (-) | 5.1 | 5.1 | 0.0 |
| SFC Take-Off (mg/Ns) | Not Known | 9.7 | - |
| SFC ToC (mg/Ns) | Not Known | 17.1 | - |

2.6.2 Off - Design Performance

The engine will not always operate at design point and operating conditions and thrust requirements will change across the flight envelope, and also airports are located at different geographical locations and altitudes and the ambient conditions vary from one place to another and in accordance with seasonal changes. In that context, and for the purposes of simulating and matching engine behaviour at those conditions, OD performance calculations were carried out and the results are presented here. Figures 2.4 – 2.9 show the variation of the engine performance parameters SFC and net thrust plotted against ambient temperature, altitude, flight Mach number and TET. The trends

shown are comparable to expected engine performance trends as found in [2] and [16]. It can be noted that at a fixed flight M_n the thrust decreases with increasing altitude and SFC also decreases. The SFC increases with rising M_n and the thrust falls with rising M_n . Net thrust increases with rising TET. Figure 2.9 shows the variation of SFC against TET at varying OATs. The figure shows a swap in the energy efficiency and SFC trend. At the higher OATs, as TET is increased, there is a reduction in SFC due to the effect of the thermal efficiency improving with TET much more rapidly than the fall in propulsive efficiency. At a certain point, the SFC starts to rise with increasing TET due to the fall in propulsive efficiency exceeding the benefit of any improvement in thermal efficiency. For the lower OATs, the SFC continuously rises with an increase in TET due to the propulsive efficiency falling much more rapidly than the rise in thermal efficiency. The outcome is there is an inflection point at 1600K such that the SFC decreases with OAT for low TETs and increases with reducing OAT at higher TETs.

2.6.3 Engine Degradation Modeling

To model the effects of engine degradation changes are made to the flow capacities and efficiencies of key engine components such as Fan, LPC, HPC, LPT and HPT. These component characteristics (flow capacities and efficiencies) are known as health parameters. The numerical values assigned to the engine components are a percentage deviation from the clean (nominal), where for each parameter, the nominal engine is at 100%. The degradation values used in this study (apart from those for the preliminary studies which were arbitrarily assigned) are derived from [8], an open literature source on engine performance degradation.

2.6.4 Degraded Engine Performance

Preliminary assessments (pilot studies) to illustrate the effects of degradation on the component performance characteristics were carried out. The levels of degradation investigated were arbitrarily introduced by the author and for the compressors were kept within the 3-8% reduction in flow capacity and 1% reduction in efficiency that typically occur with fouling (as discussed in section 2.4.1.1). For the turbines the levels of degradation introduced were kept within the 2% reduction/increase in flow capacity and 1% reduction in efficiency that typically occur due to fouling and erosion. The assessments were carried out for single and not multiple component degradation. Figure 2.10 shows the variation from clean, the performance characteristics of a degraded booster compressor with 2% reduction in flow capacity and 1% reduction in efficiency. The degraded compressor has a different steady state operating point and component map from that of a clean engine. This is because degradation affects the matching of the components causing the engine to seek an alternative steady state operating point away from that of the clean engine. For a given engine speed, an engine with a degraded compressor will operate at a lower than design efficiency (as shown in figure 2.11) and at a reduced surge margin and operating range.

The results also show (figure 2.12) that degradation will reduce the thrust output from the engine. This is because compressor degradation will cause the compressor delivery pressure to drop, resulting in a reduction in the turbine work and the thrust output. To maintain the thrust requirement, the engine's fuel flow control system has to compensate for the effects of degradation by increasing the fuel flow rate which is matched by a corresponding increase in turbine entry temperature [8]. The increase in TET increases the acceleration of the gases through the turbine giving a higher engine speed and an increase in the compressor delivery pressure.

2.7 Aircraft Performance Model

The aircraft performance model HERMES is used to integrate the engine and aircraft to determine the engine and aircraft performance. The code uses an engine performance input file generated by TURBOMATCH to give the total mission fuel burn and flight time. This allows for the optimisation of fuel burn rather than SFC and the fuel burn can be translated into the life and operational costs and hence the economic viability of the configuration being studied. Also, as fuel burn is proportional to CO₂ emissions, the impact on the environment can be incorporated into the design. The code uses aircraft theory to calculate the airframe aerodynamic values [20]. It implements TURBOMATCH and generates the engine performance data for the flight segments i.e. climb, cruise and descent. At each segment the code iterates to match the thrust requirement of the airframe with that of the engine, giving as output the mass of fuel burned and the difference from total aircraft mass. The code is described in depth in [21]. The geometric mission and engine specification file is the main input to the code; it gives the airframe geometry, flight mission altitude, and Mach number and engine power settings for all the flight segments. TURBOMATCH uses the same input file to calculate the thrust and SFC covering the entire flight envelope. The flow diagram of the code is shown in figure 2.13 [22].

Assumptions

- Aircraft is considered a punctual mass.
- Aerodynamics estimated (engine installation effects).

Capabilities

- Implements TURBOMATCH to provide engine performance data.
- Uses aircraft theory to calculate aerodynamic values of airframe.
- User defined mission profile (trajectory and diversion).
- Design optimisation using rubber wing scaling.
- Analysis of individual flight segments.
- Analysis of whole mission.

Limitations

- Engine position not accounted for.

- Uses constant values for taxi and contingency fuels
- Accounts for single type of engine mounting configuration.
- Does not account for varying airframe configurations.
- Manoeuvres during climb and approach not catered for.
- Amount of detail for TO and landing flight paths does not allow prediction of slow and steep TO and approach.

The Maximum Take-Off Weight (MTOW), flight mission fuel burn, total flight time, flight distance and the flight time at each segment calculated by the aircraft performance model are used as input to the lifing module.

At this point it is worth mentioning that the aims of this research were to assess and identify the effects of engine degradation on flight mission fuel burn and engine life, and to assess the implications of aero-engine component degradation and airport severity factors on engine and aircraft performance. The results (numerical values) required in the analyses were not definitive or absolute values but rather relative (and indicative) values showing the trends of the effects (which are important) and providing insight into how the engine performance and behaviour changes. Hence despite the limitations highlighted, the engine and aircraft models were suitable and able to satisfy the aims and achieve the purposes of this research.

2.7.1 Aircraft Performance Validation - Payload Range Diagram

The aircraft used in this study is a typical narrow body single-aisle aircraft similar to a Boeing 737-800 aircraft used in short to medium range applications. The aircraft model is created using data from [23]. From here on and for the purposes of this work the aircraft model will be referred to as the Cranfield University Short Medium range Single Aisle aircraft (CUSMSA). To validate the aircraft model, the performance of the integrated engine and aircraft has been assessed by plotting on and against a payload range chart of a Boeing 737-800 powered by a CFM56-7B27 engine. A payload range diagram represents the available trade-off between the aircraft's payload and its range performance. It is a useful tool used by operators to compare the operating economics of an aircraft and in decision making in the choice of an aircraft for a given mission.

The payload-range is plotted for the following critical points:

- The maximum payload range, the range over which the maximum structural payload can be transported.
- The maximum fuel range, the range over which the maximum disposable load can be carried, the payload being limited by fuel load.
- The ferry range, the range that can be achieved with full fuel and no payload.

A detailed methodology of how to calculate the payload-range diagram is described in [20]. The conditions for flight used to calculate the payload-range have been selected at an altitude of 35000ft and 0.785 Mach number.

The payload-range diagram in figure 2.14 has been obtained using data corresponding to the Boeing 737-800 obtained from [23] and [24]. The aircraft

performance model has been used to calculate the fuel needed to cover the range with the required payload. The boundaries and limitations of the payload-range diagram are as follows:

- At point A the aircraft is carrying its maximum payload and zero fuel. At maximum payload the aircraft capacity is limited by the Maximum Zero Fuel Weight (MZFW).
- Along points A to B fuel is added to allow the aircraft to fly a given range, and this line represents the range over which the aircraft is able to carry its maximum payload.
- Point B corresponds to the maximum range that can be flown with the aircraft carrying its maximum payload
- Along points B to C the payload is reduced in exchange for fuel and this allows longer ranges to be flown. Along this line, the aircraft capacity is limited by the MTOW
- Point C corresponds to the maximum range that can be flown with maximum fuel and associated payload whilst maintaining the aircraft MTOW
- Along points C to D the payload is reduced in order to allow greater ranges to be flown. Along this line, the aircraft capacity is limited by the Maximum Fuel Capacity (MFC)
- Point D corresponds to the range flown at maximum fuel and zero payload, otherwise known as the maximum ferry range. At this point the aircraft is at its OEW.

The code has also been verified and validated for different aircraft/engine combinations in the collaborative work done with MSc students and as outlined in [25], [26] and [27]. And considering the level of fidelity required for this research which is to present relative and not absolute values, the code is deemed suitable for the purposes of this research.

2.7.2 Aircraft Performance (Degraded Engine)

Preliminary assessments to illustrate the effects of individual engine component degradation on the aircraft's fuel burn performance were carried out. The levels of engine component degradation described and assessed in section 2.6.4 were used in the preliminary aircraft performance calculations. The results are presented in figure 2.15 and show that because a degraded engine will produce less thrust than the clean engine (figure 2.12); it will burn more fuel to achieve the same thrust output (and thrust requirements of the aircraft) as the clean engine.

2.8 Summary and Conclusions

This chapter has described the engine performance and aircraft performance modules, both of which have been validated against data available in the public domain. The results obtained in the validation have shown

adequacy and capability of the models to calculate engine and aircraft performance, and to provide the relative values required to meet the purposes of this work. The engine performance and aircraft performance modules are therefore deemed suitable for use in achieving the objectives of this work.

Figures for Chapter 2

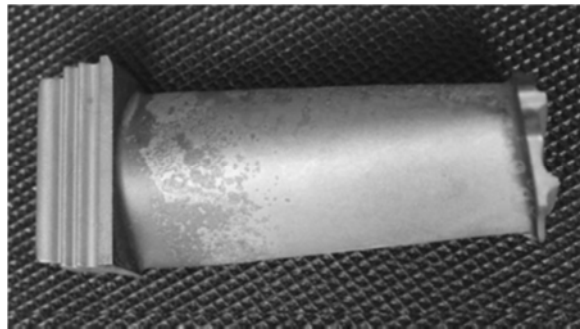


Figure 2.1: Sulphidation attack of a turbine blade [10].

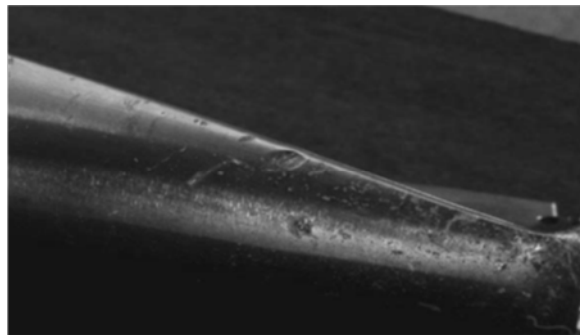


Figure 2.2: Mechanical damage caused by ingested foreign material on the leading edge of a compressor blade [10].

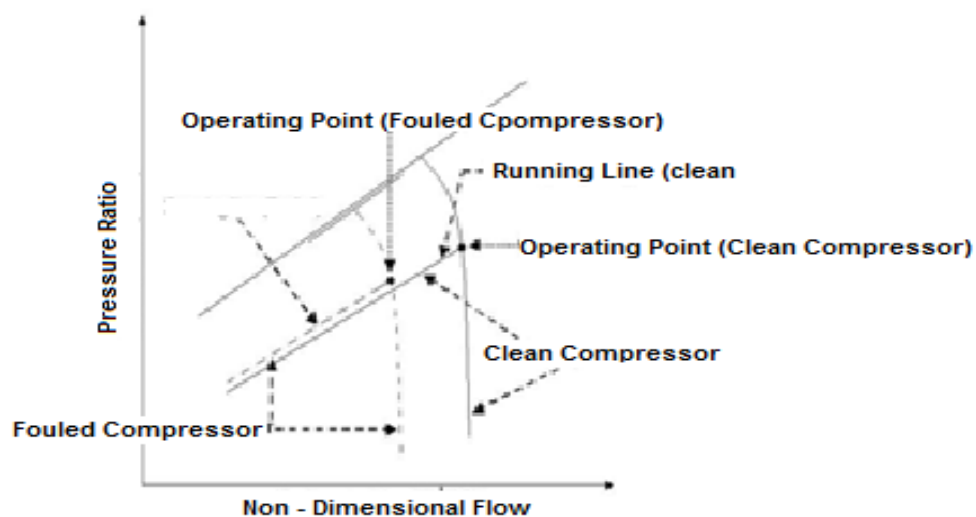


Figure 2.3: Changes in compressor characteristics, running line and operating point due to fouling [4].

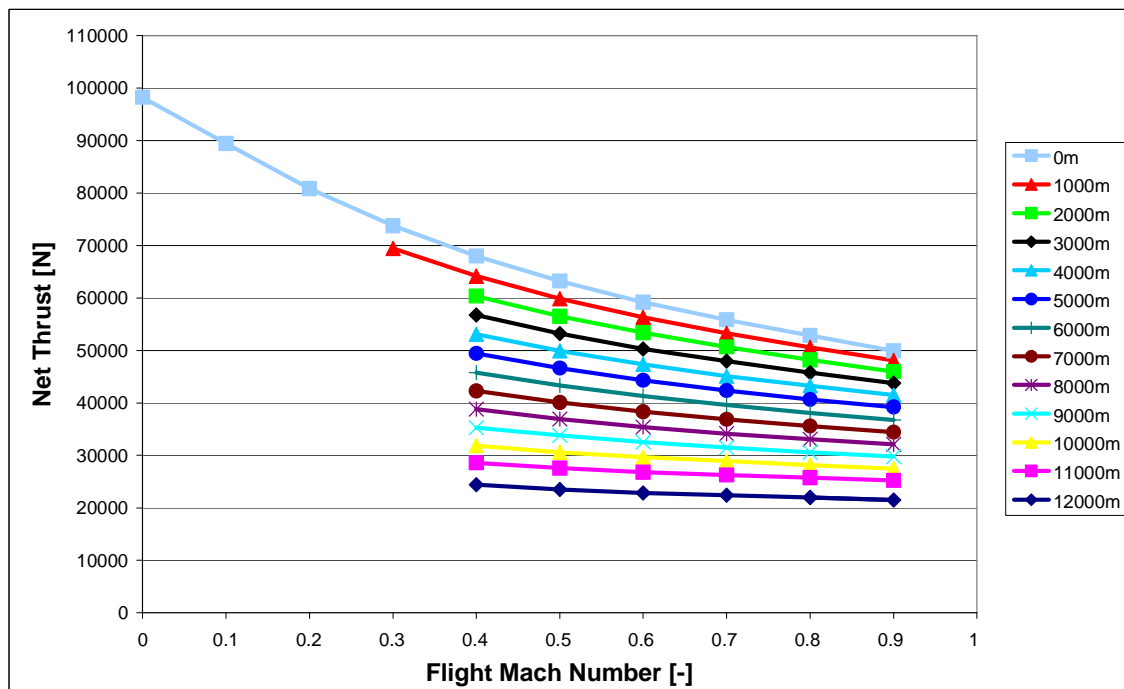


Figure 2.4: Effect of Flight Mach number and Altitude on Net thrust (fixed TET=1510K).

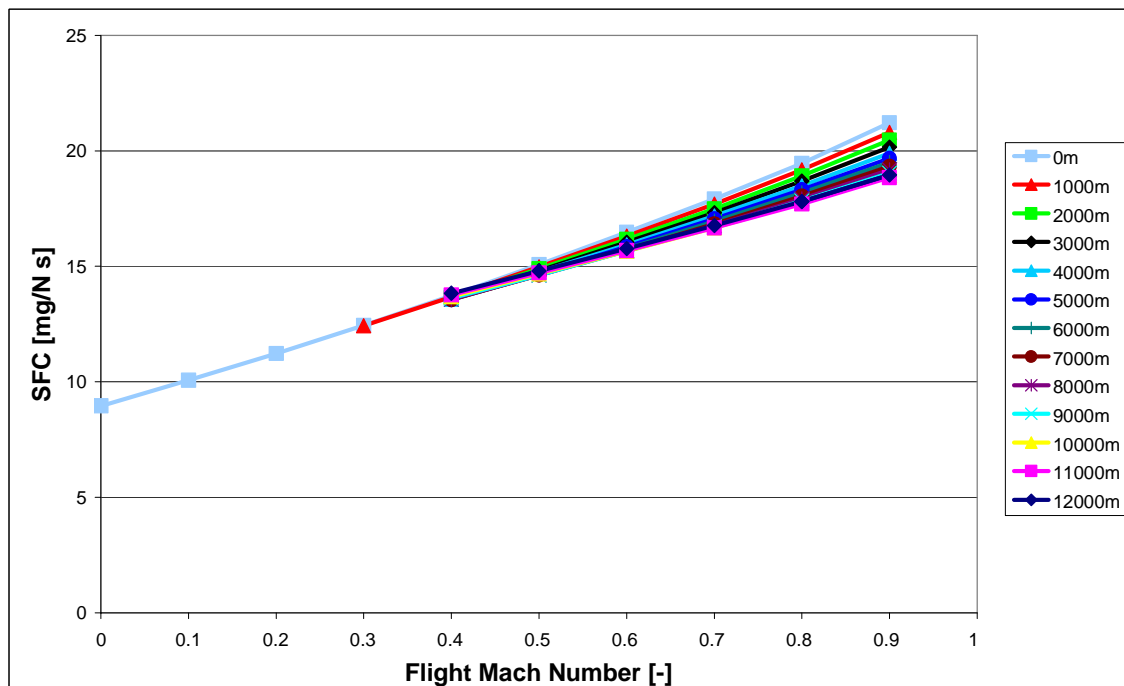


Figure 2.5: Effect of flight Mach number and altitude on SFC (fixed TET = 1510K).

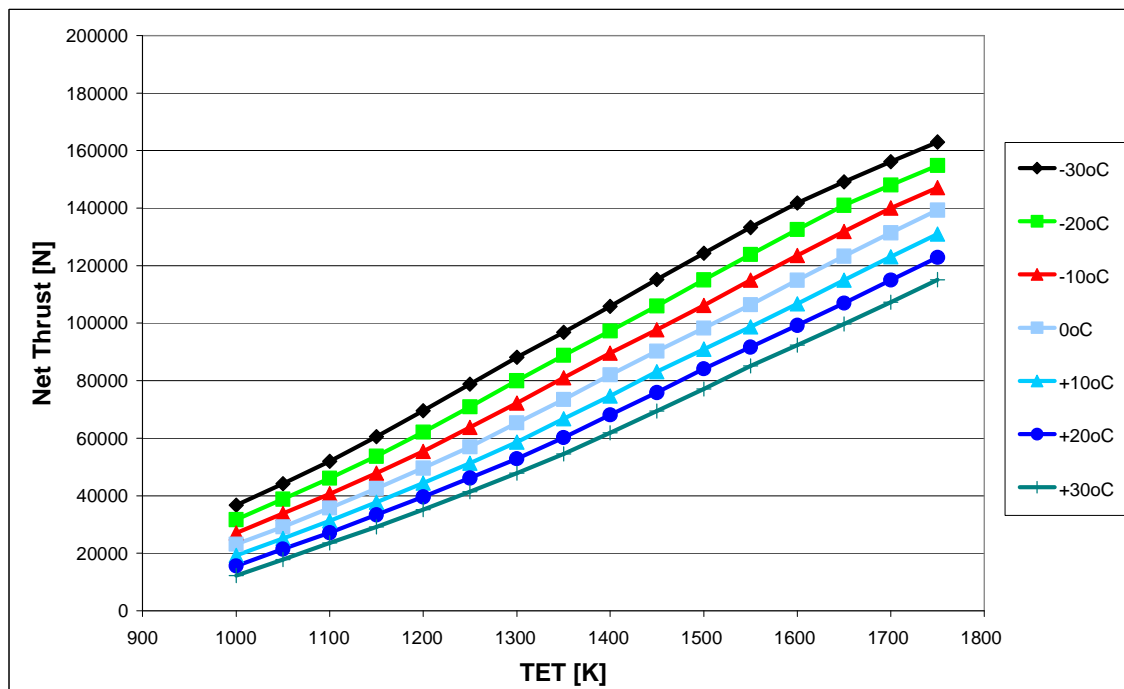


Figure 2.6: Effect of ambient temperature and TET on net thrust (fixed flight speed at $M_n = 0.785$).

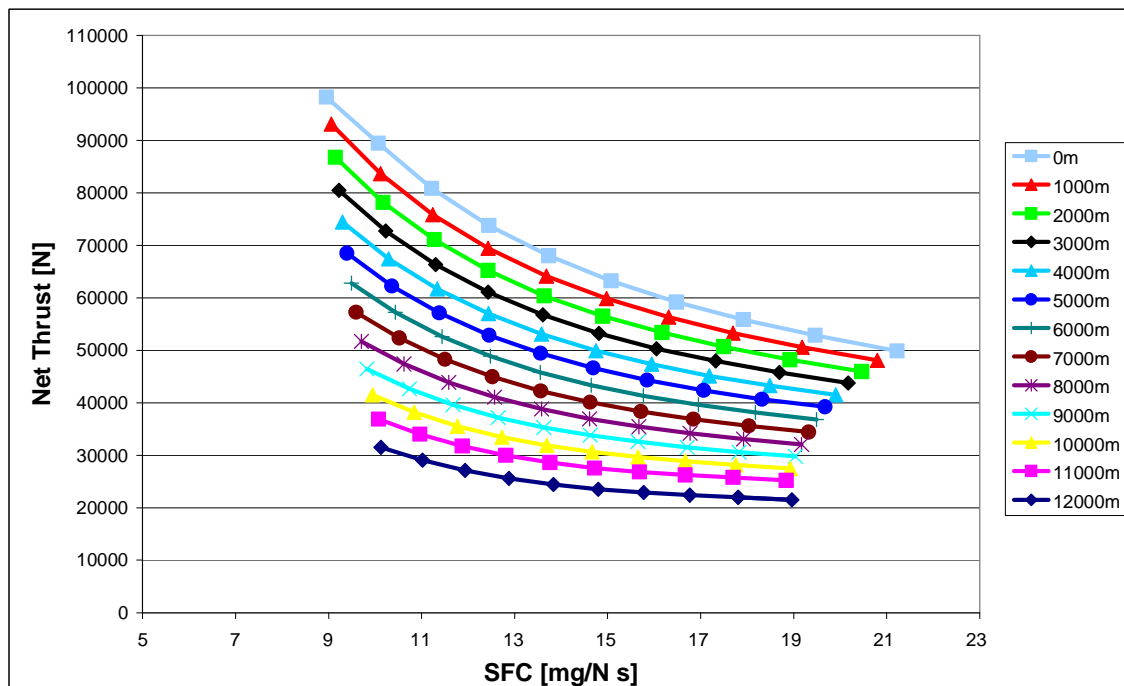


Figure 2.7: Effect of Altitude on net thrust and SFC (fixed TET = 1510K and changing flight speed).

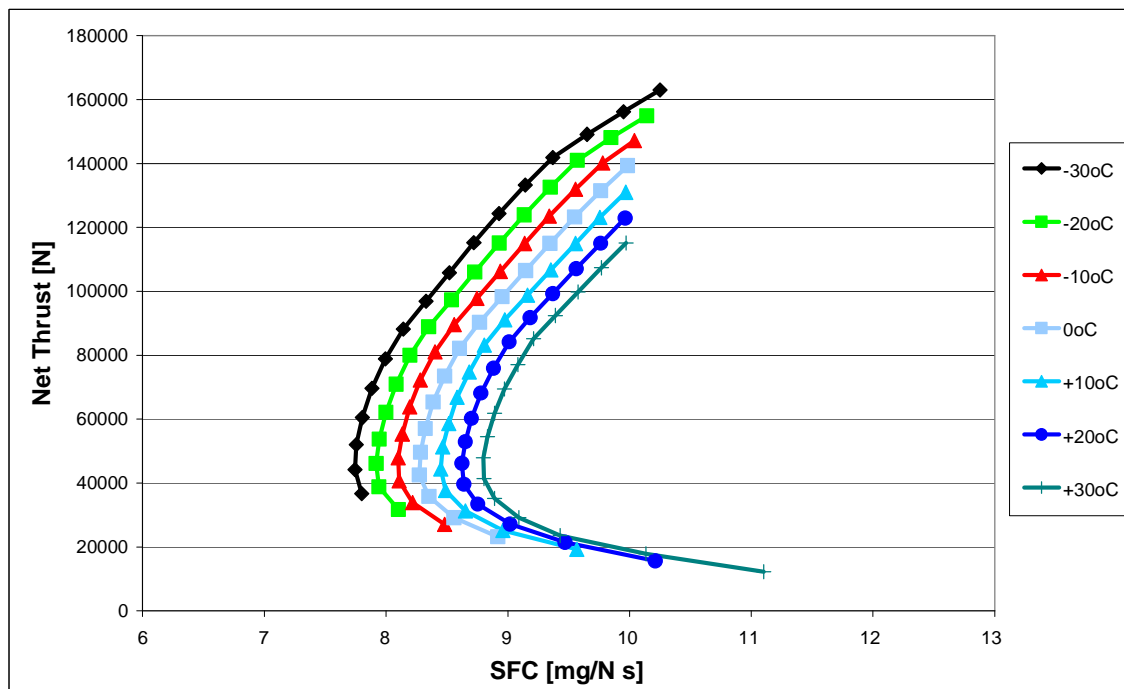


Figure 2.8: Effect of ambient temperature on net thrust and SFC (TET changing and fixed flight speed at $M_n = 0.785$)

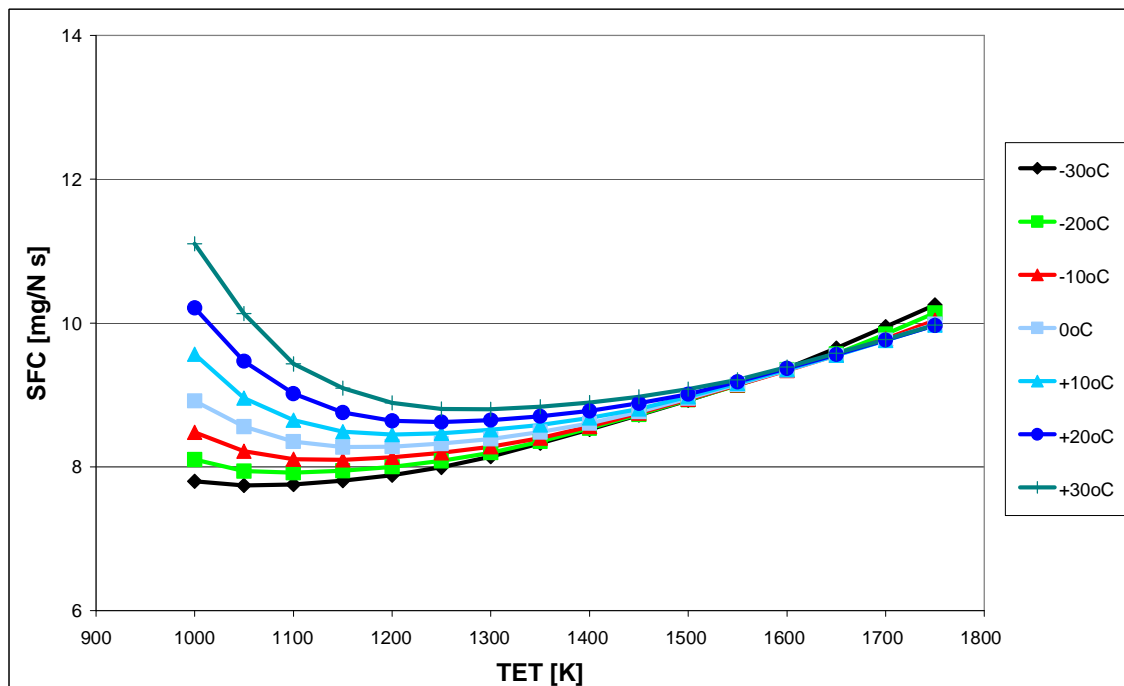


Figure 2.9: Effect of ambient temperature and TET on SFC (fixed flight speed at $M_n = 0.785$).

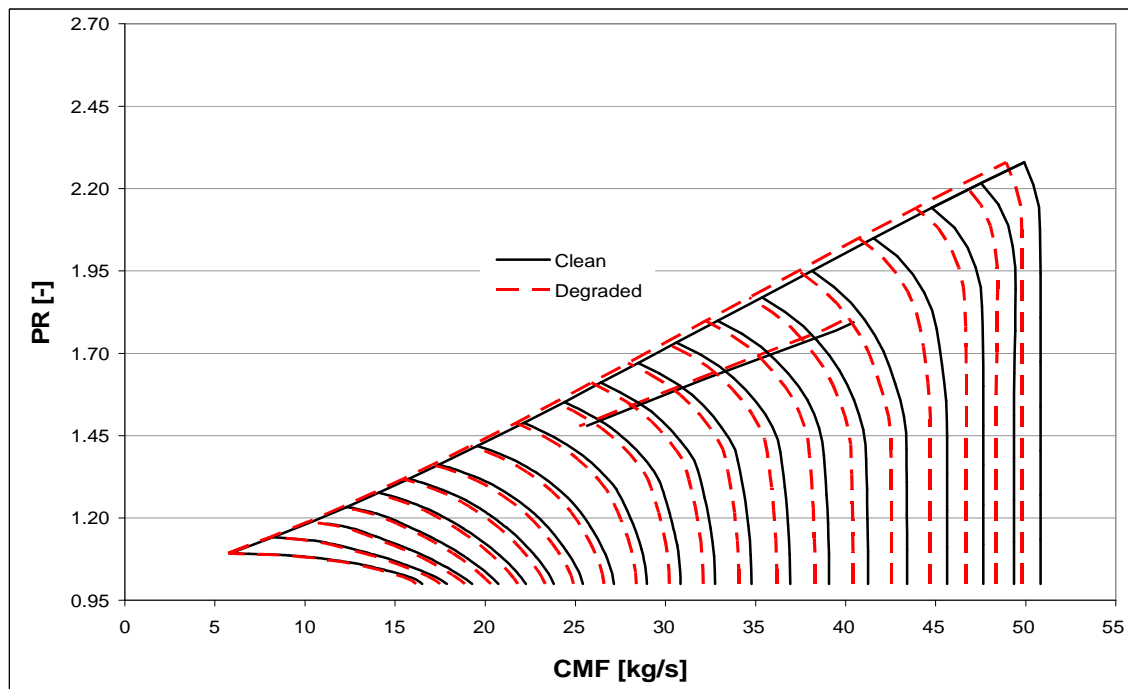


Figure 2.10: The effect on performance characteristics of a degraded booster compressor with 1% reduction in efficiency and 2% reduction in flow capacity.

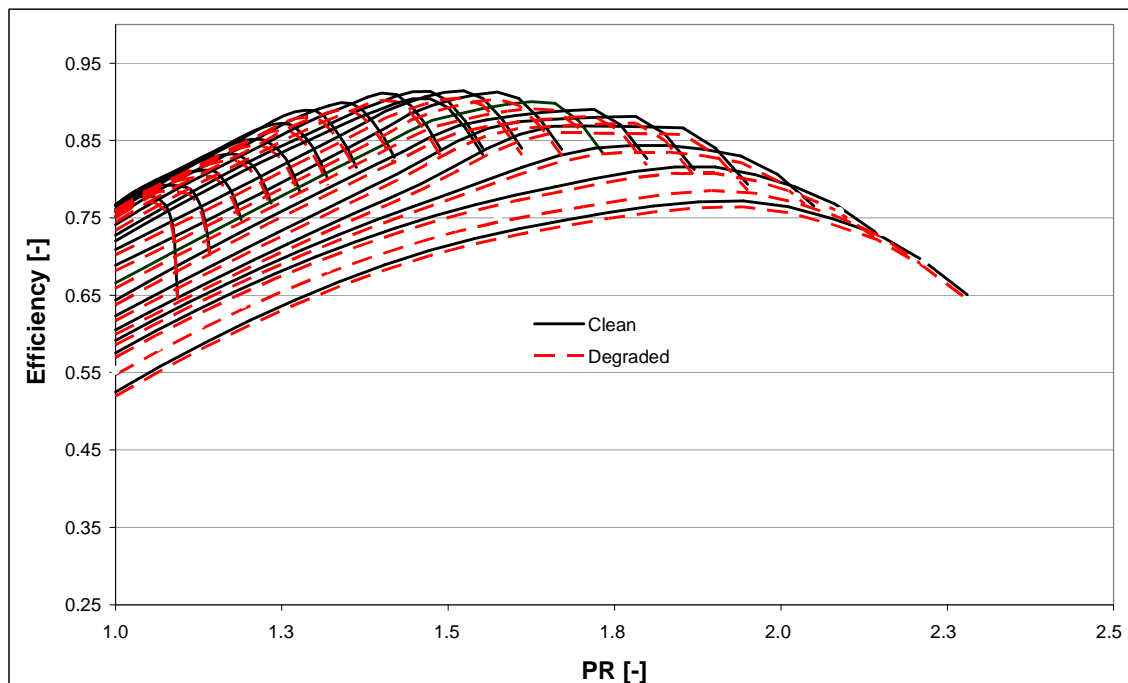


Figure 2.11: The effect on performance characteristics of a degraded booster compressor with 1% reduction in efficiency and 2% reduction in flow capacity.

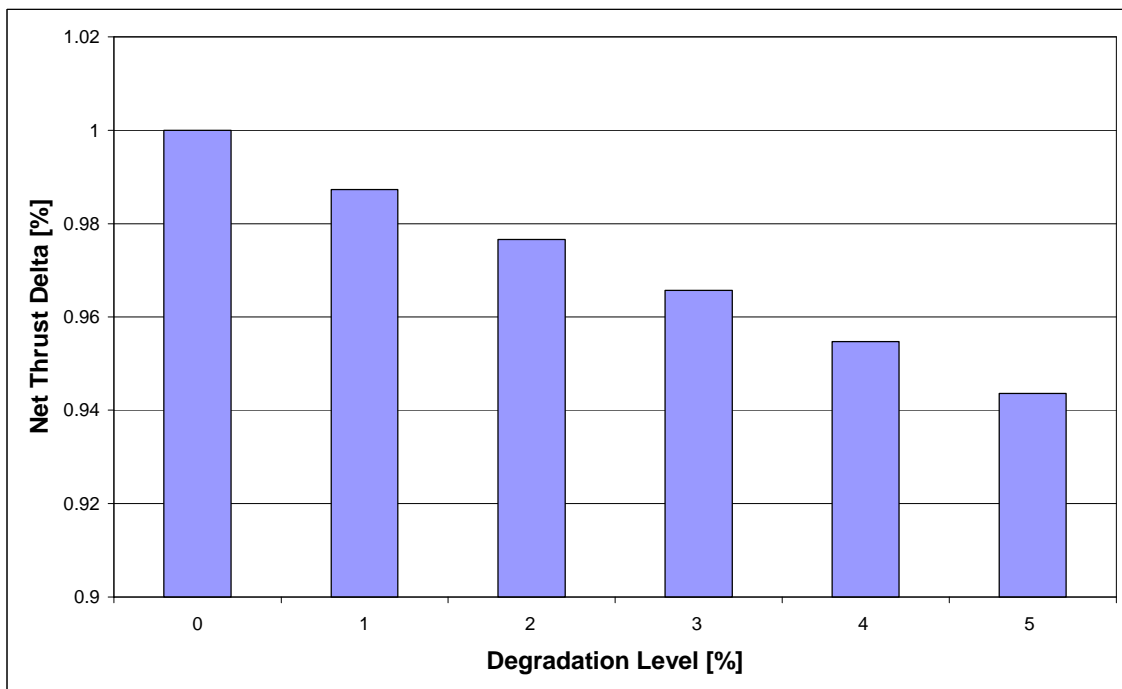


Figure 2.12: The net thrust performance for a booster (LPC compressor) with reduced isentropic efficiency and reduced flow capacity (i.e. same level of degradation for both).

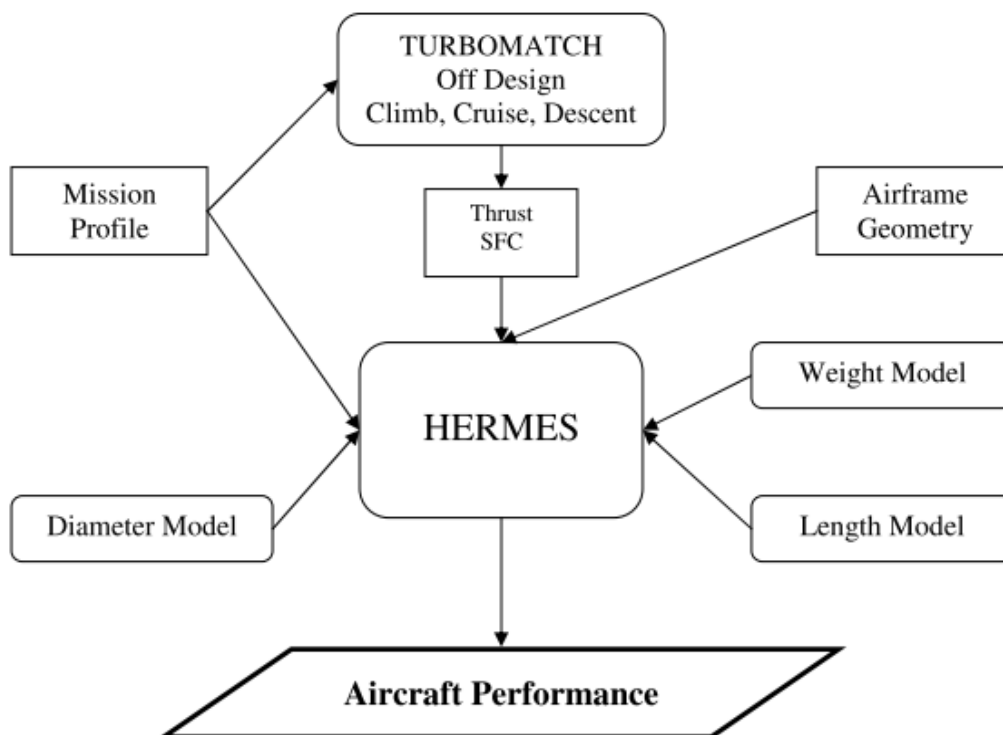


Figure 2.13: HERMES flow diagram (*Courtesy Hermes manual [22]*).

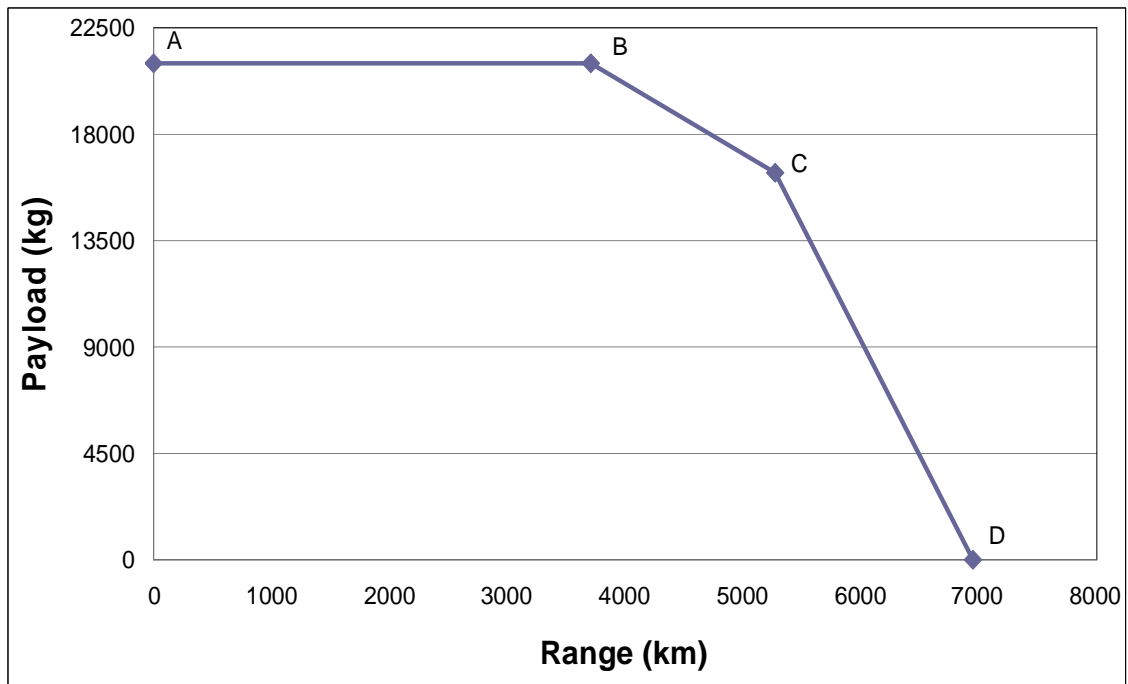


Figure 2.14: Payload-Range diagram for Boeing 737- 800 aircraft.

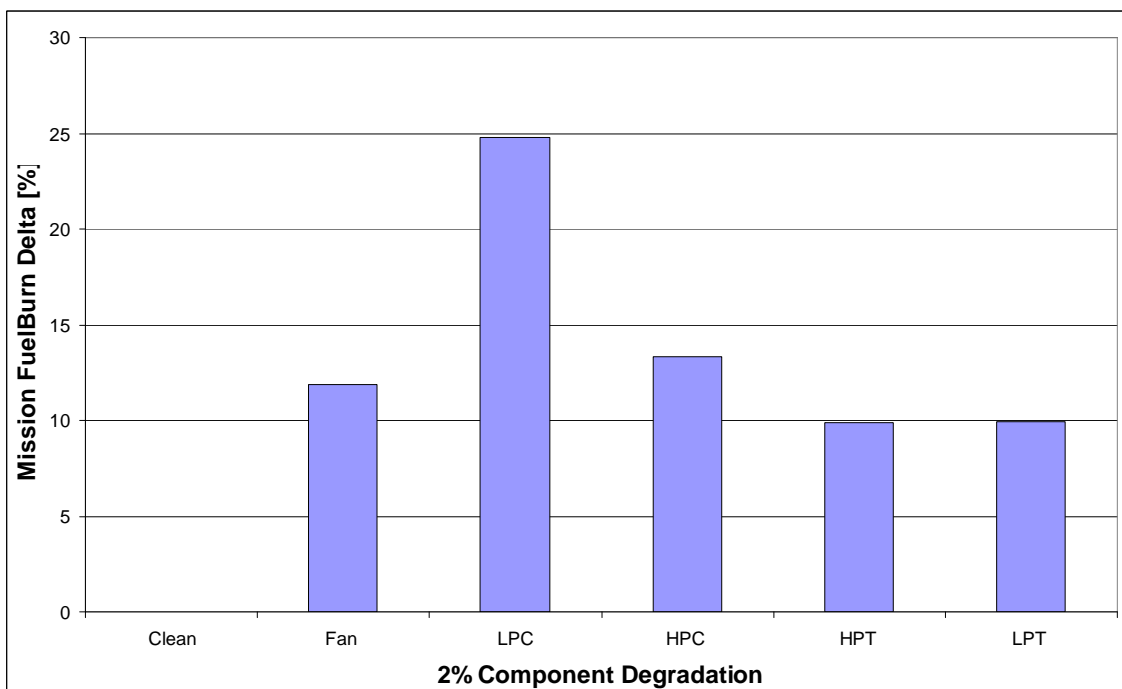


Figure 2.15: The effect of individual component degradation (2% reduction in flow capacities and 1% reduction in efficiency) on mission fuel burn.

References for Chapter 2

- [1] Penner, J.E., Lister, D.H., Griggs, D.J, Dokken, D.J., McFarland, M. (1999). Aviation and the global atmosphere, IPCC special report, Intergovernmental Panel on Climate Change, Cambridge University Press, Cambridge, England
- [2] Walsh, P.P., Fletcher, P. (1998). Gas turbine performance, Blackwell Science
- [3] Palmer, J.R. and Pilidis, P. (2008), Gas turbine theory and performance, MSc Course Notes, Cranfield University, UK
- [4] Kurz, R., Brun K. Gas Turbine Tutorial – Maintenance and operating practices, effects on degradation and life. Proceedings from the thirty sixth Turbomachinery Symposium (2007)
- [5] R. Singh. (2011). Events that cause aero-engine degradation, Technical Discussions, Cranfield University
- [6] Little, P.D. (1994). "The effects of gas turbine engine degradation on life usage" MSc Thesis, Cranfield University
- [7] Sallee, G.P. (1978). Performance deterioration based on existing (historical) data-JT9D jet engine diagnostics program, NASA-CR-135448, Pratt and Whitney Aircraft Group
- [8] Naeem, M. (1999). Implications of aero-engine deterioration for a military aircraft's performance, PhD Thesis, Cranfield University
- [9] Marinai, L. (2004). Gas-path diagnostics and prognostics for aero-engines using fuzzy logic and time series analysis, Ph.D. thesis, Cranfield University School of Engineering,
- [10] Carter, T.J. (2005). Common failures in gas turbine blades, Engineering Failure Analysis 12, pp. 237–247
- [11] Devereux, B. (1992). Improving life usage of the F404 engine through thrust rating. MSc Thesis, Cranfield University
- [12] Kyprianidis, K. G., Sethi, V., Ogaji, S. O. T., Pilidis, P., Singh, R. and Kalfas, A. I. (2009). Thermo-fluid modelling for gas turbines - Part I: Theoretical foundation and uncertainty analysis. ASME Turbo Expo, Orlando, Florida
- [13] Kyprianidis, K. G., Sethi, V., Ogaji, S. O. T., Pilidis, P., Singh, R. and Kalfas, A. I. (2009). Thermo-fluid modelling for gas turbines - Part II: Impact on performance calculations and emissions predictions at aircraft system level. ASME Turbo Expo, Orlando, Florida
- [14] Rolls Royce, (1986). The jet engine, 5th Edition

- [15] Lynch, F.T, and Crites, R.T. (1996). "Some constraints imposed on the aerodynamic development process by wind-tunnel circuit design characteristics", Advisory Group for Aerospace Research and Development, Moscow, Russia
- [16] Mattingly, J.D. (1996). Elements of gas turbine propulsion, McGraw-Hill series in aeronautical and aerospace engineering, McGraw-Hill book co., Singapore
- [17] Escher, P.C. (1995). PYTHIA: An object-oriented gas path analysis computer program for general applications, PhD Thesis, Cranfield University
- [18] Palmer, J.R. (1967). The turbocode scheme for the programming of the thermodynamic cycle calculations on an electronic digital computer, COA/AERO-198, College of Aeronautics, Cranfield Institute of Technology
- [19] CFM (2011). CFM technical specification engine database (<http://www.cfmaeroengines.com/engines/cfm56-7b>)
- [20] Jenkinson, L.R., Simpkin, P., Rhodes, D. (1999). "Civil jet aircraft design", Arnold, London
- [21] P. Lakaridis, P. Pilidis, P. Kotsiopoulos, An Integrated engine-aircraft performance platform for assessing new technologies in aeronautics, ISABE-2005-1165, Munich, Germany
- [22] Hermes Manual, Cranfield University, (2009)
- [23] Aircraft performance data Boeing 737-800 (http://www.boeing.com/assets/pdf/commercial/startup/pdf/737ng_perf.pdf)
- [24] Aircraft Commerce (2010) Operators and owners guide: 737NG family, Issue No. 70 • June/July 2010, 2010, Nimrod Publications Limited, United Kingdom
- [25] Segovia Blat C. M. (2011). Effect of engine degradation on fuel burn optimum civil aircraft trajectories, MSc Thesis, Cranfield University
- [26] Venediger B. (2013). Civil aircraft trajectory analyses – Impact of engine degradation on fuel burn and emissions. MSc Thesis. Cranfield University
- [27] Chandran S. (2013). Effect of engine degradation on engine and aircraft performance, MSc Thesis, Cranfield University

Chapter 3

Gas Turbine Aero - Engine Lifting

Abstract

One of the aims of this thesis is to give an understanding on the effects of engine component degradation on engine life. One primary objective being to provide detailed descriptions of the changes that occur in the engine life when flying fuel burn optimised trajectories. For that purpose, a lifing module is needed to estimate the engine life. In the context of this research, the life of the high pressure turbine (HPT) disc and blades estimated through the analysis of creep, fatigue and oxidation (over a full working cycle of the engine) is assumed to be the life of the engine. Basic theories of failure and the analysis of stress (based on operating conditions) are used in the module to estimate the life of an engine. Safety factors are used to account for uncertainty. This chapter describes gas turbine engine life usage and the mechanics of the lifing module used in this work. The first part of the chapter describes the concepts relevant to engine life usage, and the major life limiting failure modes that govern engine life. The second part of the chapter describes in detail the engine lifing module. The approaches used to estimate the HPT's creep, low cycle fatigue (LCF) and oxidation life are discussed. The validation and verification of the engine lifing model has been undertaken by an MSc student at Cranfield University as referenced. A comprehensive list of assumptions, capabilities and limitations of the model are provided.

3.1 Introduction

In an effort to move towards higher thermal efficiencies, both turbine blade tip speeds and turbine inlet temperatures have increased. In order to carry out a preliminary analysis with reasonable accuracy for aircraft mission engines, it is useful to identify the drivers that are most restrictive to the life of the component, causing failure after a certain amount of time.

3.2 Gas Turbine Engine Life Limited Parts

Engine Life Limited Parts (LLPs) are the major rotating and static structural engine parts whose failure is likely to be hazardous to the engine and/or aircraft. These are parts which cannot be contained upon failing and are critical to the mechanical integrity of the engine. Current Federal Aviation Administration (FAA) guidelines identify LLPs as those whose mechanisms of damage are governed by LCF. In the FAA guidelines, the critical engine's LLPs are mainly the rotating parts and consist of but are not limited to spools, shafts, seals and disks. Engines also contain static LLPs, which though not classified with the critical rotating parts, do fall under the category of parts whose failure could be hazardous to the aircraft. Static LLPs usually consist of but are not limited to

structural parts such as high-pressure cases, shrouds and non-redundant engine mount components. In accordance with the FAA guidelines, LLPs are identified by the aircraft manufacturer or production certificate holder and for each an operating life limit is defined. The life limit specifies the maximum permitted number of flight cycles the part should remain in service before it is removed. To prevent the risk of catastrophic failure occurring, the life consumption of the critical components needs to be monitored allowing for their retirement from service before the defined life is exceeded[1] [2].

3.3 Gas Turbine Engine Life Usage

The life expectancy of an engine and its components is governed by low cycle fatigue, thermal fatigue, damage due to creep and oxidation. It is impossible for an engine to exhibit the same level of performance throughout its time in service and engine components will experience degradation. Engine component degradation leads to performance deterioration and change (e.g. compressor and turbine efficiencies and flow capacities), requiring the engine to run faster and hotter so as to meet the required aircraft and thrust performance. The result is an increase in creep and fatigue damage to the hot section components and an increase in the engine LCC [3]. One way of reducing LCC is by better usage of the engine. This involves being certain about the life potential of the engine and its components and how this life evolves with use. Knowledge about the engine condition and the likely stresses to which it will be subjected is required to analyse engine component usage and:

- Reduce degradation
- Raise safe-life limits of components
- Reduce maintenance requirements

An understanding of the engine's operating environment and how in every component, damage is sustained and accumulated is vital in the prediction of engine components' life spans. To achieve a sound understanding of how the engine life evolves in service requires predicting the degree of degradation and the remaining life due to thermal fatigue, creep and low cycle fatigue (factors which are not a direct function of the engine operating time) [4].

3.3.1 Engine Life Limiting Failure Modes

The likely degradation of an engine and its components is determined by the environment within which the engine operates. It is very important to understand how an engine is used in service and to identify and know the main drivers that affect the engine potential life in order to predict how these drivers change with engine degradation and the consequent effect on engine life [4].

3.3.1.1 Damage Due to External Factors

A number of external factors can cause damage in the form of corrosion, erosion, fretting, material defects, wear, engine overstressing, uniform creep and FOD. Corrosion, erosion and FOD are influenced by the external

environment of the engine, and because a corrosive environment will increase the severity of fatigue, only corrosion affects failure due to LCF [5]. The occurrence of corrosion, erosion and FOD failure modes is difficult to predict because they are influenced by external factors. Uniform creep results when a steady load is applied to a component at high temperatures causing excessive distortion and failure by excessive rubbing.

3.3.1.2 Damage Due to Operating Conditions

Creep, fatigue and oxidation are the mechanisms of consequence that lead to damage due to the nature of the operating conditions. Studies have shown that due to the high frequency of start/stop cycles, low cycle fatigue is dominant in short range flight missions, whereas creep and oxidation are dominant in long range flight missions in which the engine components spend long periods of time at elevated temperatures. In medium range missions the three mechanisms of failure have a balanced influence on life [4].

3.3.1.2.1 Creep

Prolonged high temperature operation will cause plastic deformation, otherwise known as creep. Creep (figure 3.1 [6]) is time sensitive and thermally enhances material deformation under stress. Engine parts that are sensitive to creep are the hot section parts and the final stages of the compressor, the mid-span region of the airfoil (which experiences the highest temperature) and the disk rim region (time dependent plastic deformation due to high stresses and temperature). Creep life can be largely reduced by a slight increase in the operating temperature [7]. This is illustrated by the Larson Miller equation (equation 3.1):

$$\text{Log}t_f = \frac{1000LMP}{T} - C \quad (3.1)$$

Where t_f is the creep life, LMP is the Larson Miller parameter and C is a constant. Creep represents the biggest potential as an agent of degradation in applications of high temperature and high stress [7].

3.3.1.2.2 Fatigue

When fluctuating stresses arise due to varying loads applied to an engine component, the result is fatigue which leads to component failure (figure 3.2 [6]). Failure will not necessarily occur because the maximum stress limit has been reached, static loads with an average stress below the nominal strength of the material may cause failure [7].

High Cycle Fatigue (HCF)

High cycle fatigue is caused by aerodynamic excitations or by self-excited vibration and flutter which lead to high frequency load cycles. Though fluctuating stresses may be low, the maximum stress at resonance can be

dramatically high. Vibration is mainly caused by imbalances, misalignments, loose fitting installations and whirl. These causes can be introduced at various stages of the engine life i.e. at design, manufacture, repair or in service. There are difficulties associated with predicting and monitoring magnitudes and frequencies of vibration, hence there is no sufficient understanding of the relationship between vibration and HCF to allow the use of HCF analysis to calculate an engine component's life [7].

Low Cycle Fatigue (LCF)

Low cycle fatigue is associated with engines that have been in service for long periods of time and occurs due to machine cyclic loading (i.e. start/stop cycles). Failure is as a result of the growth of minute flaws into cracks. LCF is prevalent in the bolt-hole areas and bores of compressor and turbine disks which operate under centrifugal stresses. LCF is the most significant mechanism of degradation in engine operations that result in a large number of throttle movements [7].

Thermal Fatigue (TMF)

Rapid engine throttle movements result in thermal fatigue due to temperature gradients which are created within the components. Thermal stresses combine with mechanical stresses plus gas pressure stresses and cause local high transient strains, initiating surface cracks (that propagate through the blade). The severity of thermal fatigue as a mechanism of degradation increases exponentially with temperature and rapid throttle movements [7].

3.3.1.2.3 Oxidation

Oxidation is the formation of an oxide layer on the surface of the oxidising metal. Turbine blades oxidise at high temperatures by forming an oxide layer (i.e. a Thermally Grown Oxide (TGO)). When subjected to thermal mechanical cycling, the oxide layer undergoes microscale rupture which leads to spalling and progressive loss of material [8]. Oxidation has a large influence in high temperature applications and at temperatures in excess of 1050°C there is a rapid increase in material loss [8].

3.3.2 Potential Engine Failure Modes

The major modes of degradation and potential failure in aero-engines (and their components) are creep, fatigue and oxidation. The degree of deterioration and the life of an engine or component are determined by the long term failure mechanisms. Mechanical fatigue is the dominant mode of deterioration and failure at temperatures below 800°C, and in this temperature range, a second order influence is exerted by the environment. At temperatures above 1000°C, deterioration and failure is caused by creep, oxidation, thermal fatigue or a combination of the three, and in this temperature range the environment strongly influences the deterioration (and failure) mode. The temperature range

between 800°C and 1000°C is dominated by any one of mechanical fatigue, creep and thermal fatigue, depending on the material, component structure and engine cycle of operation [4].

3.3.2.1 Combined Modes

Due to the tendency towards higher thermal efficiencies, turbine components operate in hostile environments and severe operating conditions in which creep, oxidation, hot corrosion and thermal fatigue work together resulting in combined failure. This means that the Individual modes of failure are not entirely independent and can at times combine, reducing the engine component life to below that of the individual modes [8]. An example is stress corrosion fatigue in which the presence of corrosion reduces the fatigue life, and repeated stressing accelerates corrosive action. In this case an understanding of the interaction between these modes is required. Gas turbine engine hot section components operate at high temperatures, and changes in engine start-up, operating and shutdown conditions result in transient temperature gradients and differential thermal growth. A repeat of the transients results in thermally induced cyclic stresses. The resulting fatigue damage is dependent on the nature and frequency of the transients, the induced thermal gradients and the component material properties. Hence, the interaction between creep and fatigue can result in a considerable reduction in component life. Other examples would be loss of coating leading to substrate oxidation and cracking. Another example is local oxidation at high temperatures, which degrade the fatigue and creep resistance. High temperature oxidation accelerates crack initiation and propagation rates due to the loss of coating, and freshly exposed surfaces produced by local plasticity can rapidly oxidise [9].

Compound failure modes have not been considered in the lifing calculations carried out in this work.

3.3.3 Engine Flight Mission

The mission flown is important because it influences the LCF life and the creep life of an engine component. The LCF life of a component is determined by the number and the intensity of cycles the material has to endure, whereas the creep life of a component depends on the time it spends operating within the material's creep temperature range. The time that an engine must operate in various segments of the flight envelope is defined by the flight mission requirements. Engine usage varies from one mission profile to another, and the prediction of an engine component's life requires the correct definition of the mission profile. An engine duty cycle governs the frequency, the ordering and the magnitude of the engine setting (spool speed or power level angle) changes as functions of time, including the effects on the sizes and the changes in the turbine inlet pressures and temperatures which define the usage limits of each component. The changes in the duty cycle of an engine affect the life of the engine and its overall performance [5].

3.4 Engine Lifting Model

Whilst in service, the hot section components of an aero-engine are subject to different mechanisms of degradation due to the operating conditions and environment. Creep, thermal and mechanical fatigue, oxidation and hot corrosion are potential causes of hot section component failure. The life assessment of an engine requires expert knowledge in aerodynamics, thermodynamics, mechanical design, materials technology, fracture mechanics, metallurgy, engine operation and engine usage history. OEMs provide life limits which are based on the expected base load, calculated (or measured) stresses and temperatures depending on operating conditions, material response to operating conditions and safety factors to account for uncertainties. Uncertainties and different operating conditions for different engines mean that the OEM's estimated life may be conservative or unachievable.

The lifting model developed at Cranfield University uses basic theories of failure and the analysis of stress (based on operating conditions) to estimate the life of an engine whilst accounting for uncertainty by use of safety factors [10].

Assumptions

- Engine Life is the shorter life between creep, LCF and oxidation life.
- No interaction between the failure modes.

Capabilities

- Modular structure allows module to be run as a whole or each sub-module to be run independently.
- Uses basic theories of failure and stress analysis to calculate life.
- Uses LMP and Miner's law to estimate creep life.
- Uses Coffin-Manson rule and Neuber method to calculate fatigue life.
- Uses Miner's law to calculate the oxidation life of TBC.

Limitations

- Variable thickness discs are split into several constant thickness rings with hoop stress calculated iteratively with an initial guess.
- Does not calculate disc fatigue life.
- Assumes HPT turbine is life limiting part.
- Considers creep, fatigue and oxidation independent of each other.
- Limited material database (some missing LMPs).

3.4.1 The Structure of the Lifting Model

The lifting model consists of different modules for creep, low cycle fatigue and oxidation analysis. The structure of the module is shown in figure 3.3 [10]. The lifting module uses output from the other modules in the framework as follows:

- from the engine performance module: flight segment spool speeds, take-off thrust, flight segment operating temperature, flight segment cooling flow temperature.
- from the aircraft performance module: MTOW, fuel burn, total flight time, flight distance, flight time at each segment.
- from the emissions module: ICAO LTO cycle NO_x.

The lifing module gives as output the engine life which is used as input to the economics module. The module does not consider the influence of interaction between modes of failure, but calculates the component life as influenced by each mode independently. The creep module calculates the creep life for both the blades and the disc using performance data and the maximum stress applied. The low cycle fatigue module uses the material properties and the maximum temperature at start-up to calculate the fatigue life for both components. The oxidation module calculates the oxidation life of the TBC of the HPT blade, and uses this to predict the oxidation life of the HPT blades. The main algorithm of the lifing model then compares the creep life, the low cycle fatigue life and the oxidation life, taking the shorter life as the time between overhaul of the engine. The code uses safety factors to account for uncertainties.

3.4.1.1 Stress Analysis

Two modules are used to calculate the turbine blades' stresses and the turbine disc stress.

3.4.1.1.1 Blade Stress Analysis

The module is broken down as shown in figure 3.4. The module uses simple mathematical relations to calculate the centrifugal stresses acting on each section of the blade and thereafter the maximum stress at the blade root. The HP spool speed (rpm), the number of blade sections and the radius and cross-sectional area for each section are used as input into the code.

3.4.1.1.2 Disc Stress Analysis

The module is broken down as shown in the figure 3.5. The module calculates the maximum stress acting on the disc. The module has two approaches, depending on whether the disc is of constant or varying thickness. The rim diameter, bore diameter and disc thickness are input into the code, with the rim stress either being given as input or calculated (using number of blades, blade mass and radius of centre of gravity relative to the root of the blade). For a varying thickness disc, the disc is split into rings and each ring considered as a constant thickness ring. The stress distribution across the disc is found via the stress calculation across each ring. The code compares the calculated stress with the stress due to the blades and iteratively corrects for the hoop stress until parity is achieved [10].

3.4.1.2 Creep Analysis

The creep life of an engine component is calculated using the Larson-Miller parameter and Miner's cumulative creep law. To arrive at the creep life, the flight envelope is divided into segments namely climb, cruise and descent. The rpm and TET determine the operating condition and together with the time spent in each segment, are used to calculate the creep life. Because creep is a function of stress, the module first calculates the stress load on the blade and the disc and creates a matrix containing the stress, the time and temperature for each flight segment. Thereafter, the LMP values for each segment are either input directly where known or the Larson-Miller curve is input and the LMP values found by extrapolation. Miner's cumulative creep law is then used to calculate the creep life (in flight hours or cycles). The code does not take into account take-off and approach due to the short times spent at these two flight segments. The creep module is represented in figure 3.6 [10].

3.4.1.3 Low Cycle Fatigue Analysis

The low cycle fatigue module is shown in figure 3.7. The algorithm uses the Coffin-Manson rule and applies the Neuber method to cyclic loading to calculate the low cycle fatigue of engine components. This is a strain method based on the tolerance level of the component material to the start/stop cyclic loading it endures at start-up and take-off conditions at which the turbine experiences peak TET. The turbine experiences a temperature difference between ambient and TET at start-up and the module predicts the fatigue life under the thermal stresses arising in these conditions of temperature difference.

The thermal strain (temperature difference multiplied by linear coefficient of thermal expansion) and the maximum stress (thermal strain multiplied by material's elastic modulus) can be calculated when the material linear coefficient of thermal expansion is known and perfect elastic behaviour is assumed. The Neuber rule determines the tensile strain occurring at the tensile yield stress and the compressive strain that corresponds to the compressive stress. From the tensile and compressive strains, the total strain range is calculated. A method of universal slope (MUS) is then used to iteratively compute the strain range by guessing the total number of cycles to failure, until the values of the MUS strain range and the Neuber strain range are within 1% of each other, and the total number of cycles will have been found [10].

3.4.1.4 Oxidation Analysis

The oxidation module is shown in figure 3.8. The oxidation algorithm uses engine performance data and material properties to predict the oxidation life of engine components. It estimates the blade interface and the blade metal temperatures, applies a cooling mechanism and a temperature reduction due to the presence of a thermal barrier coating.

To arrive at the oxidation life, the flight envelope is divided into segments namely climb, cruise and descent, and the oxide thickness is calculated for at

each segment using the parabolic law of growth. The characteristics of each segment are operating temperature, cooling effectiveness, cooling flow temperature and the time spent in each segment. The code calculates the free elongation, mechanical strain and thickness of the thermally grown oxide (TGO), after which it uses the calculated values to estimate the breaking or splitting (i.e. spalling) of the TBC at each flight segment. The code uses Miner's cumulative law to calculate the oxidation life (in flight hours or cycles).

3.4.1.5 Cooling Module

The lifing model gives the user an option to use a blade cooling flow system which is available to the creep, low cycle fatigue and oxidation algorithms. The simple sub-module is represented in figure 3.9. The code uses a one dimensional model of cooling and assumes equilibrium in the transfer of heat into and out of the blade. The algorithm estimates the temperature of the cooled blade using the temperature of the air bled from the high pressure compressor, the gas temperature around the blades (i.e. the TET) and the cooling effectiveness as input by the user.

3.4.2 Engine Lifing Module Verification and Validation

The lifing code has been verified and validated by [10] and the details and results of the validation process can be found in [10]. The validation by [10] has been in two parts:

- Each module validated independently.
- Code validated as a whole.

The validation process involved calculating and matching the engine life data found in [7]. The lack of proprietary data for the HPT's blade and disk geometry meant the validation was limited to using flight plan and engine component life data provided by [7]. This lack of data in no way affects the implementation of the algorithms used in the code but rather impacts on the accuracy of the life estimate. The results obtained by [10] are in close agreement (less than 2% delta) with the results given in [7]. The results show that the lifing algorithms used were implemented correctly and the code is therefore deemed suitable for the purposes of this research.

3.5 Summary and Conclusions

The life of an engine is a useful parameter in determining the engine life cycle costs. The longer the engine stays on wing in between overhauls, the lower the engine operating costs. The life assessment of an engine is therefore useful in this regard and in assisting decision making in the way the engine is deployed. This chapter describes the engine lifing module which has been validated by the developer using data provided by Cranfield University. The failure modes have been considered independently and the implications identified with the lifing module are consistent with studies found in literature. The results obtained in the validation show good accuracy of the engine lifing

model in estimating the engine life. Since interaction will likely occur, the independent consideration of failure modes is a limitation of reality. However, the actual development of the code is beyond the scope of this work, and the objective has been to understand the physics, the maths and the appropriateness of the code to this research and use as is. Hence, despite this and the other limitations that have been highlighted, the engine lifing module is deemed suitable for use in achieving the objectives of this work. The purpose of using the lifing code and the analyses performed has been to assess and present relative values depicting trends (changes) in the engine life rather than presenting the absolute and accurate engine life values.

Figures for Chapter 3

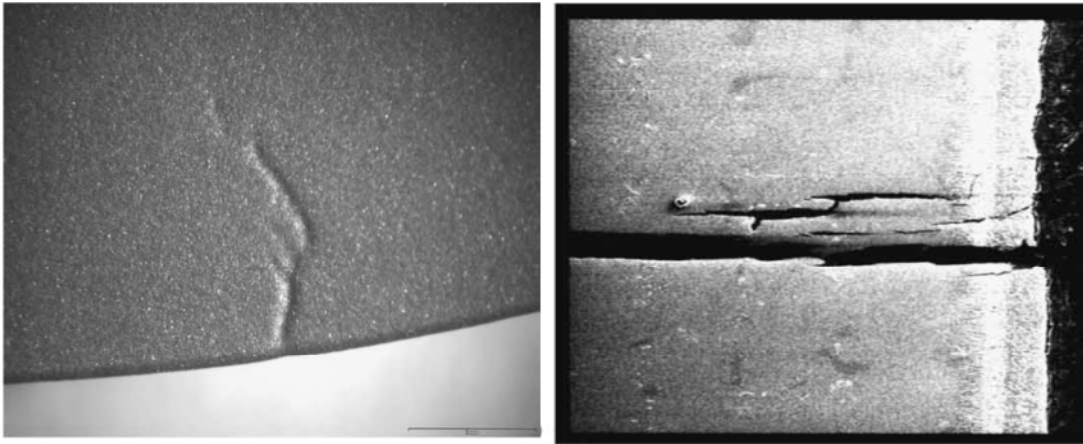


Figure 3.1: Creep damage in a blade [6]

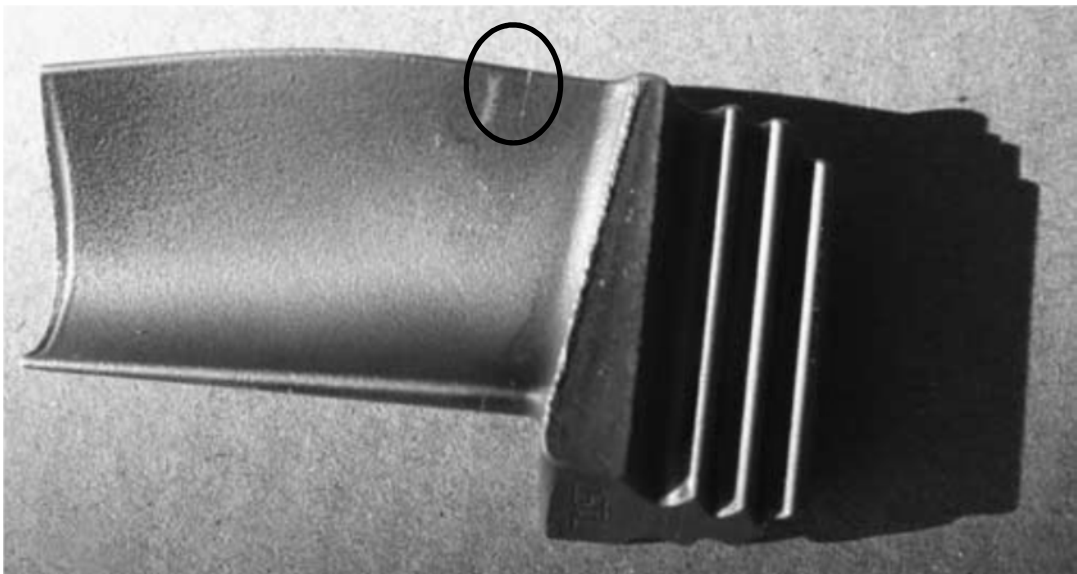


Figure 3.2: Fatigue crack initiating (blade trailing edge) [6]

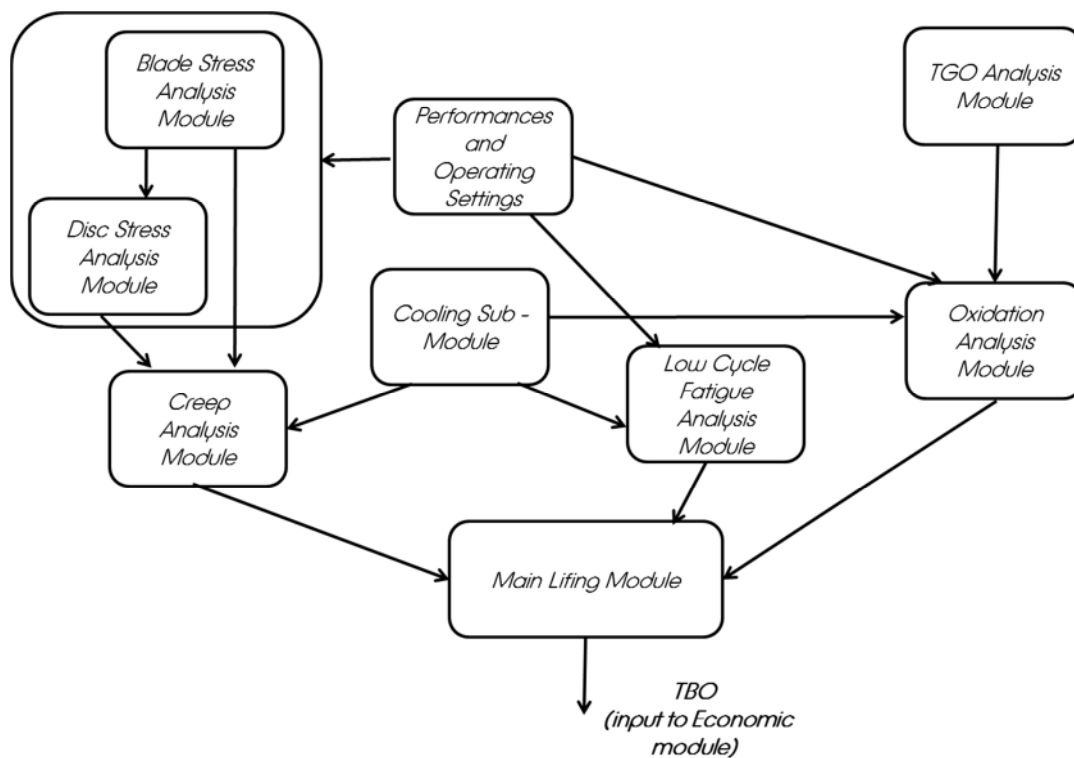


Figure 3.3: The lifing model [10]

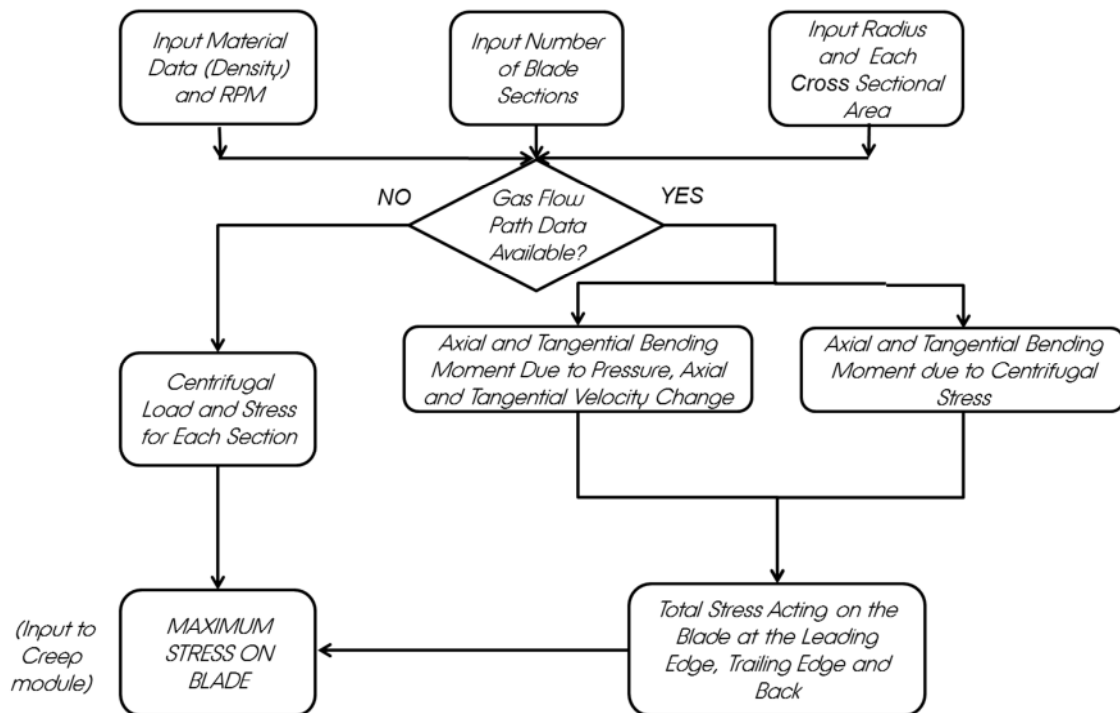


Figure 3.4: Blade stress analysis module [10]

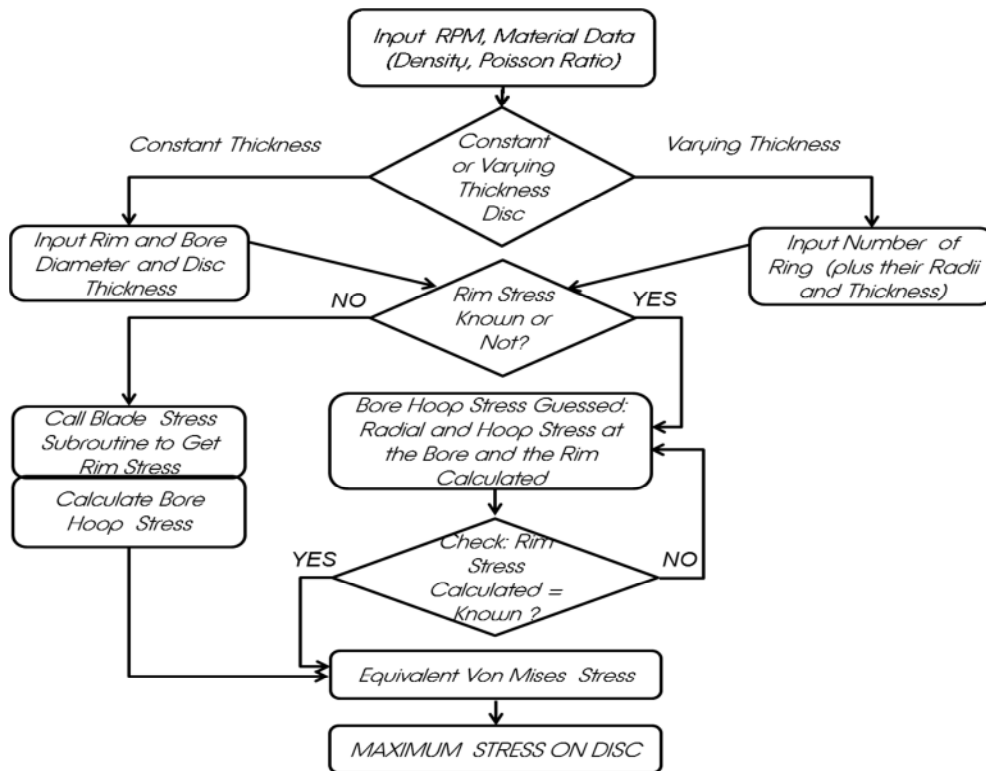


Figure 3.5: Disc stress analysis module [10]

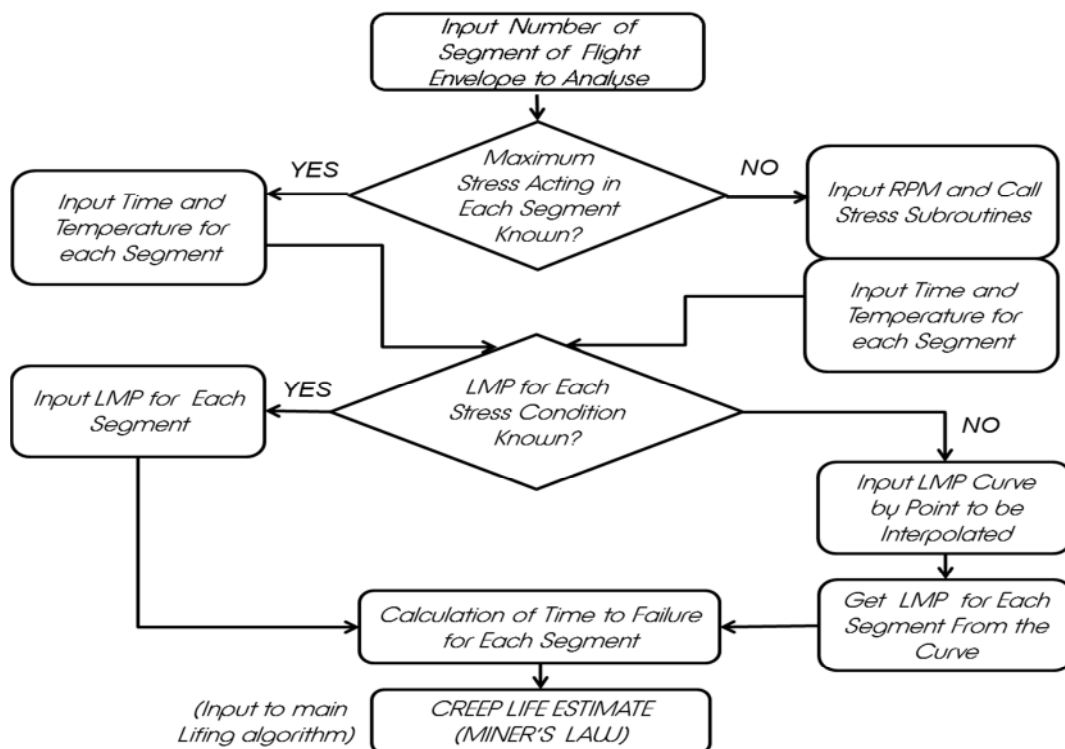


Figure 3.6: Creep analysis module [10]

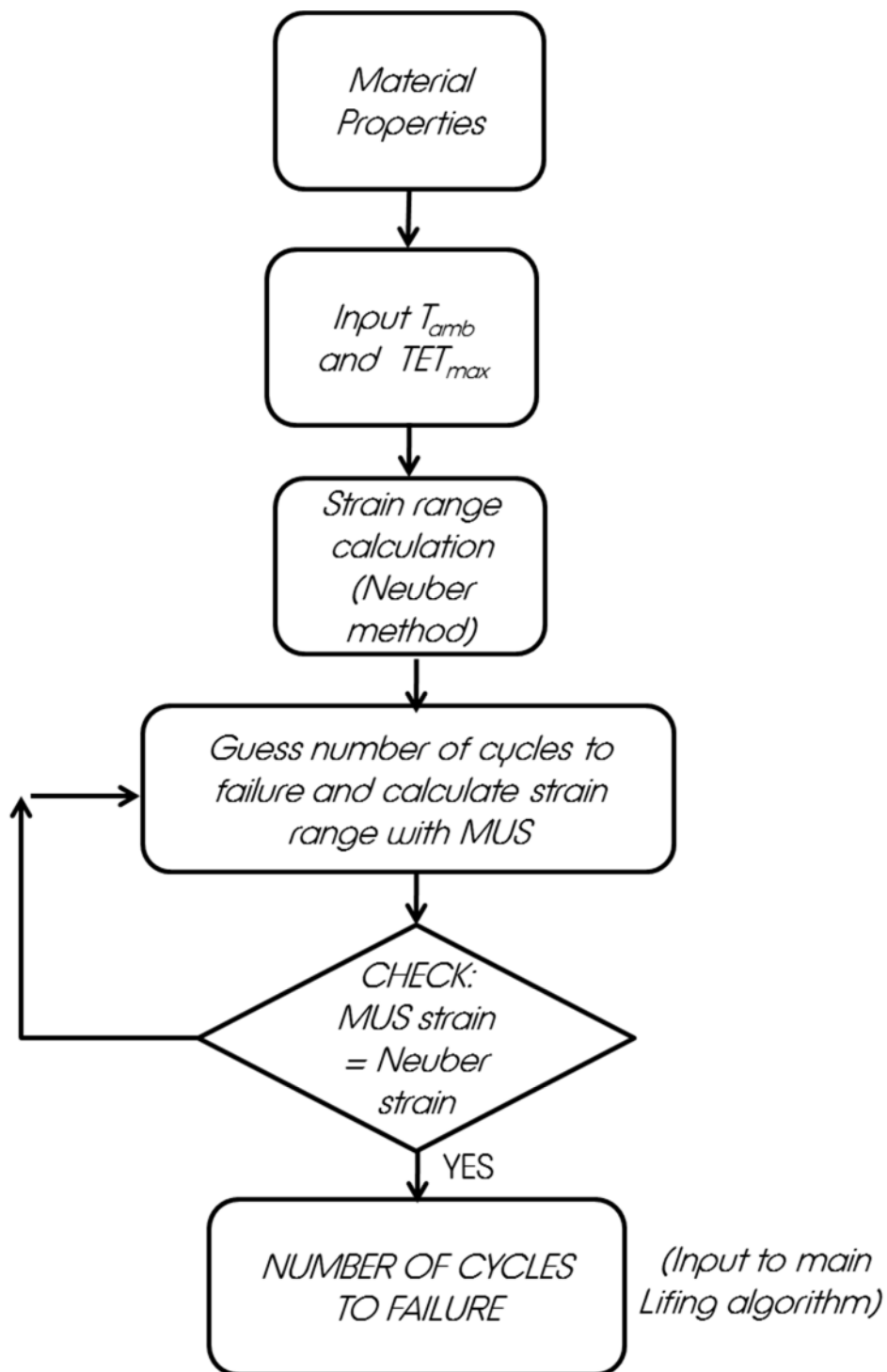


Figure 3.7: The low cycle fatigue (LCF) module [10]

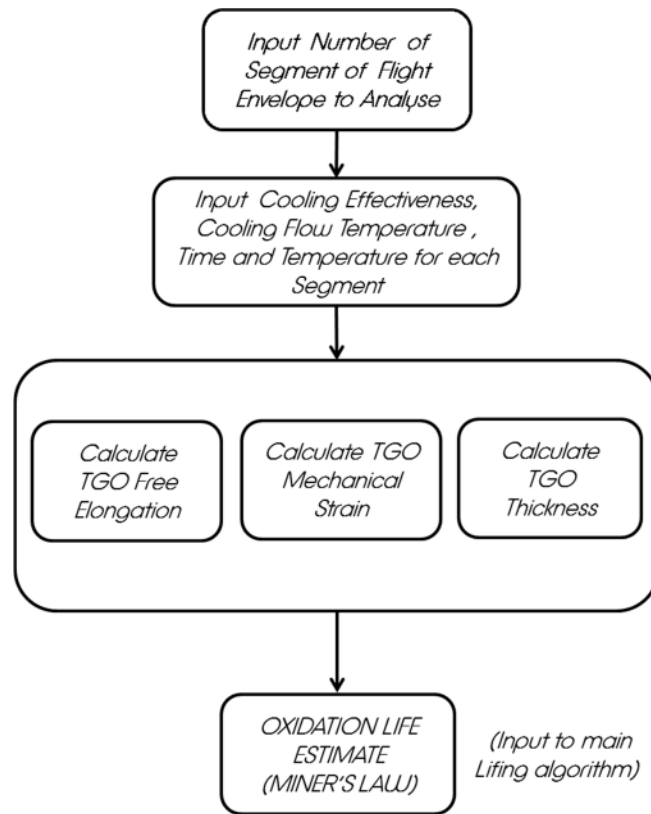


Figure 3.8: The oxidation module [8]

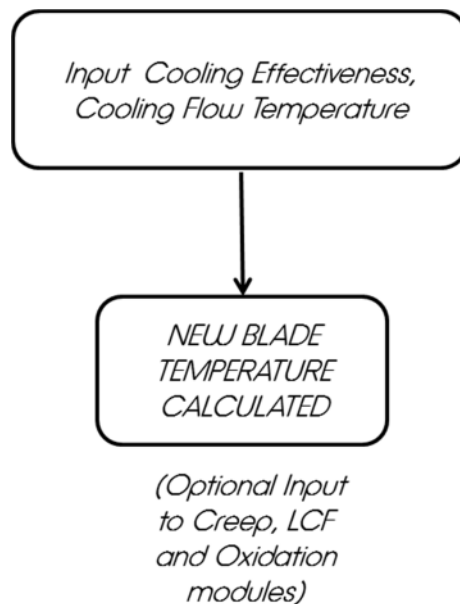


Figure 3.9: The cooling module [10]

References for Chapter 3

- [1] Federal Aviation Administration (FAA). (2009). Guidance material for aircraft engine life limited parts requirements. Advisory Circular 33.70-1
- [2] Ackert, S. (2011). Engine maintenance concepts for financiers: Elements of turbofan shop maintenance costs. Aircraft Monitor
- [3] Kurz, R., Brun K. Gas turbine tutorial – Maintenance and operating practices effects on degradation and life. Proceedings from the 36th Turbomachinery Symposium (2007).
- [4] Naeem, M. (1999). Implications of Aero-engine deterioration for a military aircraft's performance. PhD Thesis, Cranfield University.
- [5] Little, P.D. (1994). The effects of gas turbine engine degradation on life usage. MSc Thesis, Cranfield University
- [6] Carter, T.J. (2005). Common failures in gas turbine blades. Engineering Failure Analysis 12, pp. 237–247
- [7] Cookson, R. A., Haslam, A.S. (2008). Mechanical design of Turbomachinery. MSc Course Notes, Cranfield University
- [8] Bagnall, S. D., Shaw, D. L. and Mason-Flucke, J. C. (1999). Implications of power by the hour on turbine blade lifing. RTO AVT Specialists Meeting on Design for Low Cost Operation and Support, Ottawa, Canada
- [9] Beres, W. (2000). Mechanics of materials failure. Recommended Practices for Monitoring Gas turbine Engine Life Consumption, RTO-TR-28
- [10] Vigna Suria, O. (2006). A flexible lifing model for gas turbines: creep and low cycle fatigue approach. MSc Thesis, Cranfield University

Chapter 4

Gas Turbine Aero - Engine Emissions

Abstract

The emissions module HEPHAESTUS is a modelling tool developed at Cranfield University to predict the emissions from varying gas turbine engine configurations. The tool uses generic reactor models and its modularity and extensibility allows the prediction of emissions from current and potential future engines. The first part of the chapter is literature describing concepts relevant to aero-engine emissions, legislation and the contribution of aviation to emissions. The second part of the chapter describes the working principles of the emissions module. The emissions code has been developed, validated and verified by another PhD researcher Hugo Pervier at Cranfield University as referenced.

4.1 Introduction

Emissions from a variety of human-generated sources, including commercial aircraft contribute to climate change by trapping heat in the atmosphere. Aircraft emit greenhouse gases and other emissions during flight operations, including carbon dioxide (CO₂), nitrogen oxides (NO_x), soot, and water vapor. Aircraft CO₂ emissions are a direct result of fuel burn and for every gallon of jet fuel burned, about 21 pounds of carbon dioxide are emitted [1]. Reducing the amount of fuel burn per flight mission will therefore reduce the amount of CO₂ emitted. Water vapor emissions and certain atmospheric temperature and humidity conditions can lead to the formation of contrails, a cloudlike trail of condensed water vapor, and can induce the creation of cirrus clouds. Both contrails and cirrus clouds are believed to have a warming effect on the earth's atmosphere. Contrails modelling and prediction is not relevant to this study. Aircraft also emit other pollutants that affect local air quality.

4.2 Gaseous Emissions

Emissions are a primary impact of aviation on the environment. Aircraft engines produce carbon dioxide (CO₂), water vapour (H₂O), nitrogen oxides (NO_x), carbon monoxide (CO), oxides of sulphur (SO_x) and unburned or partially combusted hydrocarbons (UHC). Aircraft emissions are comprised of approximately 99.6% CO₂ and H₂O, with NO_x, CO, SO_x and UHC making up the remainder [1]. Emissions occurring at or near ground are considered local air quality pollutants whereas emissions occurring at altitude are considered greenhouse gases. At altitude, water in the aircraft exhaust may have a greenhouse effect, and occasionally this water will produce contrails, which also may have a greenhouse effect. About 10% of all aircraft emissions are

produced during airport ground level operations and during landing and take-off. 90% of aircraft emissions occur at higher altitudes [1] [2].

Carbon dioxide is the product of complete combustion of hydrocarbon fuel like jet fuel, and so too is water vapour. Nitrogen oxides are produced due to the high temperature/high pressure combustion which causes nitrogen and oxygen present in the air to combine forming NO_x. Unburned Hydrocarbons are produced when there is incomplete combustion of fuel which can result from either improper fuel/air mixing or insufficient air. They are also referred to as Volatile Organic Compounds (VOCs), and many VOCs are hazardous air pollutants. Carbon monoxide is formed due to the incomplete combustion of the carbon in the fuel. Sulphur oxides are produced during combustion when small quantities of sulphur which are present in essentially all hydrocarbon fuels, combine with oxygen from the air.

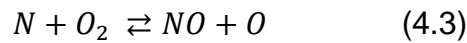
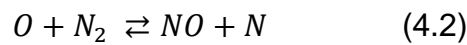
There are also small particles, small enough to be inhaled that are formed due to incomplete combustion, and these are referred to as particulates. Particulates can either be solid or liquid. One other important consideration in the environmental impact of aviation is ozone (O₃) which though not emitted directly into the air forms readily in the atmosphere when VOCs react with NO_x in the presence of heat and sunlight. Ozone is the primary constituent of smog. Operating procedures can have both direct and indirect influence on aircraft emissions. Some procedures affect the engine operating regime which directly influences the rate of pollutant emissions. The concentration levels of the emissions produced are proportionately influenced by the engine operating conditions, except the levels for CO₂ and water vapour which are dependent on the mission fuel burn. NO_x emissions are higher during high power operations such as TO when the combustor temperatures are high, whereas UHC and CO emissions are higher during low power operations such as taxiing at which the combustor temperatures are low and the engine is less efficient. Hence, flying derated and reducing engine power for a given operation such as TO and climb out will generally increase the rate of UHC and CO emissions and also reduce the rate of NO_x emissions, but will have little or no effect on CO₂ emissions.

Pressure, temperature and time are the principal conditions which affect the formation of pollutant emissions. In the primary zone the hydrocarbons are converted into carbon monoxide and smoke in the fuel rich regions. Dilution with fresh air in the dilution zone allows the carbon monoxide and the smoke to oxidize into carbon dioxide. Unburned hydrocarbons can also be reduced in this zone by allowing the combustion process to proceed to completion. However as already mentioned, the conditions that allow for the suppression of the other pollutants promote the formation of the oxides of nitrogen, hence it is desirable to cool the flame as quickly as possible and to reduce the time available for combustion. This conflict of conditions requires a compromise to be made. Nonetheless, continuing improvements in combustor design and performance has led to a substantially 'cleaner' combustion process [2].

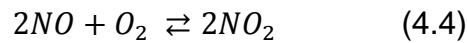
4.2.1 NOx Emissions

NOx is composed of Nitric Oxide (NO) and Nitrogen Dioxide (NO₂). The temperature range, stoichiometric ratio and type of nitrous species distinguish and influence the mechanisms of NOx formation. There are three recognised mechanisms and these are thermal, prompt, and fuel.

Thermal NOx: Thermal NOx is produced when atmospheric oxygen and nitrogen react at elevated temperatures. The set of reactions leading to thermal NOx are described by the Zeldovich mechanism shown in the equations 4.1 to 4.4 below [3]. These equations describe the NO formation at high temperatures.



At lower temperatures



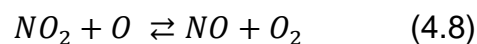
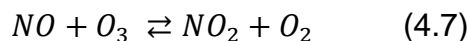
Prompt NOx: Prompt NOx is formed at low temperature and fuel rich flame conditions when hydrocarbon radicals react with nitrogen in the air. These reactions are complex and less well understood.

Fuel NOx: Fuel NOx is formed when organically bonded nitrogen in the fuel reacts with oxygen. This is not a problem in aero-applications as the levels of fuel bonded nitrogen in aviation fuel are low.

At ground level and in the troposphere (up to 10km above earth's surface), the presence of NOx results in an increase in ozone concentration (equations 4.5 and 4.6), causing respiratory illness and impaired vision [3].



In the stratosphere (10km – 50km above earth's surface), cruise NOx results in ozone depletion (equations 4.7 and 4.8) thus affecting climate change and consequently an increase in ultra-violet radiation which causes skin cancer and eye diseases.



4.3 Aviation Emissions and Legislation

The International Civil Aviation Organisation (ICAO) is responsible for the planning, implementation and coordination of civil aviation worldwide. ICAO is a

United Nations (UN) intergovernmental body responsible for setting emission standards for and evaluating the environmental performance of aircraft engines. The emissions standards set by ICAO form the basis of aircraft engine performance certification standards for national aviation authorities such as the Federal Aviation Authority (FAA) [2].

The main aviation pollutants legislated for by ICAO are smoke (carbon particles), unburned hydrocarbons (unburned fuel), carbon monoxide and oxides of nitrogen. The smoke number is used to measure smoke, whereas the gaseous emissions are quoted in terms of mass which is measured in grams. Legislation currently controls emissions below 3000ft in the landing and take-off (LTO) cycle, with no regulation for greenhouse gas emissions at cruise; future legislation will include emissions control at cruise. The ICAO emission points are at specified thrust settings ($100\%F_{oo}$, $85\% F_{oo}$, $30\% F_{oo}$ and $7\% F_{oo}$) which correspond to the four phases (Take-off, Climb, Approach, and Idle) of the ICAO reference LTO cycle. The legislative limits for NO_x emissions as per the ICAO Annex 16 volume II, as well as the medium term and long term technology goals set by the Committee on Aviation Environmental Protection (CAEP) are illustrated in figure 4.1. Since the original NO_x Standard was introduced in 1981, it has been made 50% more stringent [4]. The ICAO LTO NO_x legislative limits are quite strict for low OPR engines while providing a better LTO NO_x allowance for high OPR engines (allows for better thermal efficiencies at higher OPR and TET). In addition, engines are required to meet the current CAEP/6 standard, and those not meeting this standard can no longer be produced. Although NO_x Standards were initially intended to address local air quality, they also contribute to reducing the impact of aviation on climate (i.e. climb and cruise NO_x).

4.4 Contribution of Aviation to Emissions

Aviation emissions are a reflection of the overall activity level of aviation, and because air travel has grown rapidly in the past several decades, concerns about emissions from aviation activity have been raised as a result. Aviation emissions contribute a relatively small percentage to air quality concerns when compared with other sources, both in terms of local air quality and greenhouse gases. Aggregate aircraft emissions of air pollutants that are currently legislated against have declined over time when considered in terms of transporting one passenger one mile. Total aircraft emissions have however increased because of the growth in aviation over the same period.

In civil aero-engines, fuel efficiency has improved and carbon dioxide emissions have reduced over the last 40 years of aviation. This achievement is attributed to an increase in overall pressure ratio, higher turbine entry temperatures and advancement in materials and better cooling techniques, improved efficiency of turbo-machinery and high bypass ratio configurations, all of which have contributed to boost the thermal and propulsive efficiencies. In this era, Carbon Monoxide (CO) and un-burnt hydrocarbons as well as noise levels have been considerably reduced. Technological advancements during this time have seen engine performance optimised for minimum fuel burn, whilst

keeping within the legislative requirements for noise and other emissions. However, the increase in overall pressure ratio has resulted in an increase in the combustor inlet temperature, which in turn favours the production of Nitrogen Oxides (NO_x). The introduction of noise legislation has led to optimised solutions that impact on fuel efficiency in large aircraft, which is further marred by NO_x reducing targets that impinge on any further increases in pressure ratio. As the targets for CO₂, noise and NO_x become more interconnected, improvements on conventional engine architectures become ever increasingly challenging [2].

Although aviation has grown faster and outpaced other sources of emissions, its contribution to local air quality inventories has remained fairly modest when compared to other sources. This is because most of an aircraft's operations take place at altitude where the emissions do not affect the local air quality. As such, because most of aviation emissions occur at altitude, it results in the generation of greenhouse gases which have the potential of contributing to climate change. CO₂ and NO_x are the most relevant greenhouse gases from an aviation perspective. Over the past 10 years, greenhouse gas emissions from aviation have grown and are projected to continue to grow in the future. This projection in growth assumes a constant relationship between aircraft operations and greenhouse emissions and expects an increase of 60% in aircraft greenhouse gases [2].

The relative contributions to global carbon dioxide emissions and the relative contributions of the transport sector (aviation, road traffic and others) are illustrated in figure 4.2. According to estimates by the Intergovernmental Panel on Climate Change (IPCC), aviation currently contributes about 2% of human generated carbon dioxide emissions globally and global emissions of the world's aircraft fleet contribute approximately 3% potential warming effect of the total global emissions (greenhouse emissions) that affect the world's climate with the majority coming from commercial aviation. IPCC estimates forecast the global aviation industry (including aircraft emissions) to emit approximately 3% of global CO₂ and approximately 5% of the total global human-generated emissions by the year 2050 [2]. The IPCC forecasts for aviation's contribution to global emissions for 2050 are based on the assumption that emissions from other sources will continue to grow. The relative contribution of aviation could be greater if other sources make progress in reducing emissions and aviation emissions continue to grow; or it could be less than estimated if other sources do not make progress in reducing emissions. Technological improvements such as fuel efficient engines are currently relied upon by airlines to reduce emissions and these are limited in their potential to satisfy future targets in reducing emissions. A combination of technological, operational and fuel improvements are expected to help reduce aviation emissions in the future, with their availability, development and adoption partially influenced by the economic climate and the level and stability of fuel costs [2].

Contrails are also becoming of concern to the aviation industry because of their warming effect; they cool the climate by reflecting the solar radiation and

contribute to global warming by trapping heat on the earth. However, the magnitude of this effect remains uncertain.

4.5 Emissions Prediction Modeling

Combustion is a complex reaction flow process and there are challenges and limitations that make it difficult to accurately model the combustion process and predict emissions. The challenges to the accurate emissions prediction arise due to the relative difficulty in capturing the different aerodynamic and thermodynamic phenomena inside the combustion chamber. The inherent complexities in the combustion process make it difficult to accurately capture the mixing processes, recirculation, dilution and temperature fluctuations. Other imposing problems are in modelling the stability of a flame and the interaction between the turbulence in the flame and the chemical reactions. These challenges among others make it difficult to accurately predict the emissions. However despite the challenges and the limitations in the quantitative accuracy of the predictions, the qualitative information from the predictions are useful in capturing changes and trends rather than giving absolute values. There are three approaches that can be used to predict the emissions produced in a combustion chamber: empirical correlations, stirred reactor (physics based) and high fidelity models (comprehensive numerical models which include detailed Computational Fluid Dynamics (CFD) calculations).

Empirical correlations are simple and the creation of new databases is required for different concepts of combustion, and also coarsely represents the processes inside the combustor. This limits the use of the correlation based approach to current engine configurations with available data and it is not suitable for innovative engine designs with no available experimental data. Also because engine data is proprietary it may not be generally available further limiting the correlation approach. An example of the semi-empirical approach is the P3T3 method. This method is one of the methodologies offered in the Cranfield University emissions modelling tool HEPHAESTUS. The P3T3 is a method that predicts NO_x emissions by correlating the NO_x emission indices and the engine operating conditions. The method predicts the EINO_x levels at altitude by using the EINO_x levels at ground level and correcting them to the altitude condition. This is based on knowledge of the combustor inlet conditions at both ground level and altitude. The EINO_x levels at the ICAO certification points (found in reference [5]) are used as reference to plot EINO_x levels at ground level against the combustor inlet temperature. The combustor inlet pressure and Fuel-Air Ratio (FAR) are also plotted against combustor inlet temperature at ground level. The EINO_x plot is used to obtain the EINO_x at ground level that corresponds to the combustor inlet temperature at altitude. This EINO_x is then corrected for humidity and the differences in the combustor conditions (inlet pressure and FAR) at ground level and at altitude (equation 4.9) [6]. The amount of NO_x in kilograms is calculated for using equation 4.10.

$$EINO_{x(ALT)} = EINO_{x(GRD)} \left(\frac{P_{ALT}}{P_{GRD}} \right)^n \times \left(\frac{FAR_{ALT}}{FAR_{GRD}} \right)^m \exp(H) \quad (4.9)$$

$$NO_x = (w_f \times Time) \times EINO_x \quad (4.10)$$

A more detailed description of the P3T3 emissions model for NO_x prediction with validation model is found in [6]. The P3T3 uses the Fuel Composition Method (FCM) to calculate the CO₂ and H₂O emissions. These emissions are controlled by fuel composition and are proportional to fuel burn [7]. The EICO₂ and EIH₂O are estimated using equations 4.11 and 4.12. These equations calculate the pollutants per kilogram of fuel and assume stoichiometric combustion and that the fuel composition is represented by C_xH_yS_z (carbon, hydrogen and sulphur). Where x, y and z are the respective carbon, hydrogen and sulphur coefficient in moles in the fuel chemical formula.

$$EICO_2 = \frac{1000 \times x \times [12.011 + (2 \times 15.994)]}{(x \times 12.011) + (y \times 1.0079) + (z \times 32.06)} \quad (4.11)$$

$$EIH_2O = \frac{1000 \times \frac{y}{2} \times [(2 \times 1.0079) + 15.994]}{(x \times 12.011) + (y \times 1.0079) + (z \times 32.06)} \quad (4.12)$$

The high fidelity approach involving CFD calculations uses detailed simulation of the chemical reactions and the flow within the combustion chamber. It is however very expensive and time consuming requiring detailed simulation of the flow and the combustion chamber (which may not be freely accessible).

The third approach uses stirred reactors to predict combustion emissions. It is this approach that is used in the Cranfield University emissions modelling tool HEPHAESTUS and has been adopted for this work. This tool allows the prediction of emissions from current and future engine configurations in the presence of degradation. The schematic of the model is shown in figure 4.3. The tool uses three generic reactor models: a Perfectly Stirred Reactor (PSR) model, a series of Perfectly Stirred Reactor models (PSRS) and a Partially Stirred Reactor (PaSR) model, and its modularity and extensibility allows the prediction of emissions from potential future engines [8]. A detailed description of the reactor based emissions model with validation is found in [8].

Assumptions

- Complete combustion of combustion products.
- No impact of pollutant formation on combustion heat.
- Assumed equivalence ratio distribution of 0.9 at the flame front.

Capabilities

- Reactor (physics based) simulations.
- Conventional and LPP combustor emissions prediction.
- Emissions indices for: NO_x, CO₂, H₂O.
- Multi-fuel capabilities: Jet-A, Bio-fuel, natural gas.
- Fixed or variable combustor geometry for LPP.

Limitations

- Levels of accuracy.

The emissions module uses the ambient conditions (temperature, pressure, altitude), inlet conditions to the combustor (temperature, pressure, mass flow rate) calculated by the engine performance module, combustor geometry and fuel flow as input. The module gives the emission indices for CO₂, NO_x and H₂O as output, which are used in the framework integration code written by the author to calculate the emissions produced for each species.

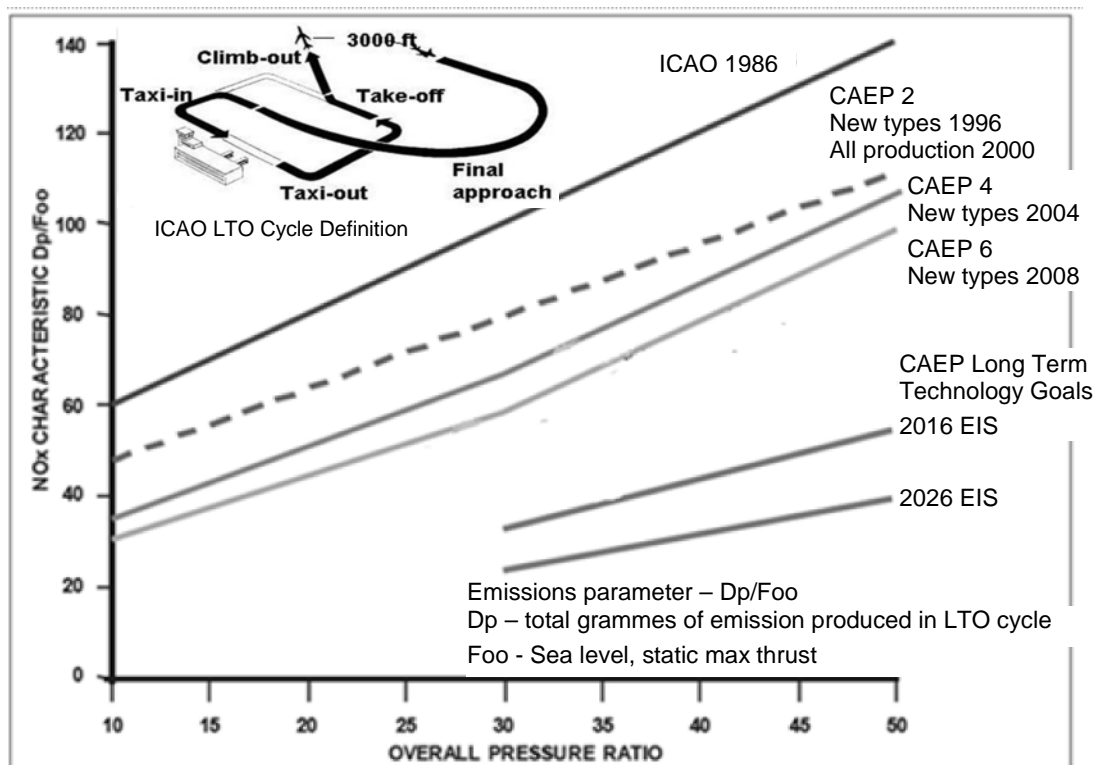
4.5.1 Emissions Model Validation and Verification

The validation and verification of the emissions model is outlined in [8]. The validation results from [8] are also reproduced here (figure 4.4). For the purposes of this research, the emissions prediction of the CUCCTF engine was compared against the emissions indices of the CFM56-7B27 engine as found in the ICAO databank [5]. The ICAO emission points are at specified thrust settings (0.7min at 100%F_{oo}, 2.2min at 85% F_{oo}, 4.0min at 30% F_{oo} and 26min at 7% F_{oo}) which correspond to the four phases (Take-off, Climb, Approach, and Idle) of the ICAO reference LTO cycle. The CUCCTF emissions indices' predictions (shown in figure 4.5) are in good agreement with those found in [5]. The code is therefore deemed suitable for the purposes of this research, considering the level of fidelity required which is to present relative and not absolute predictions of the emissions.

4.6 Summary and Conclusions

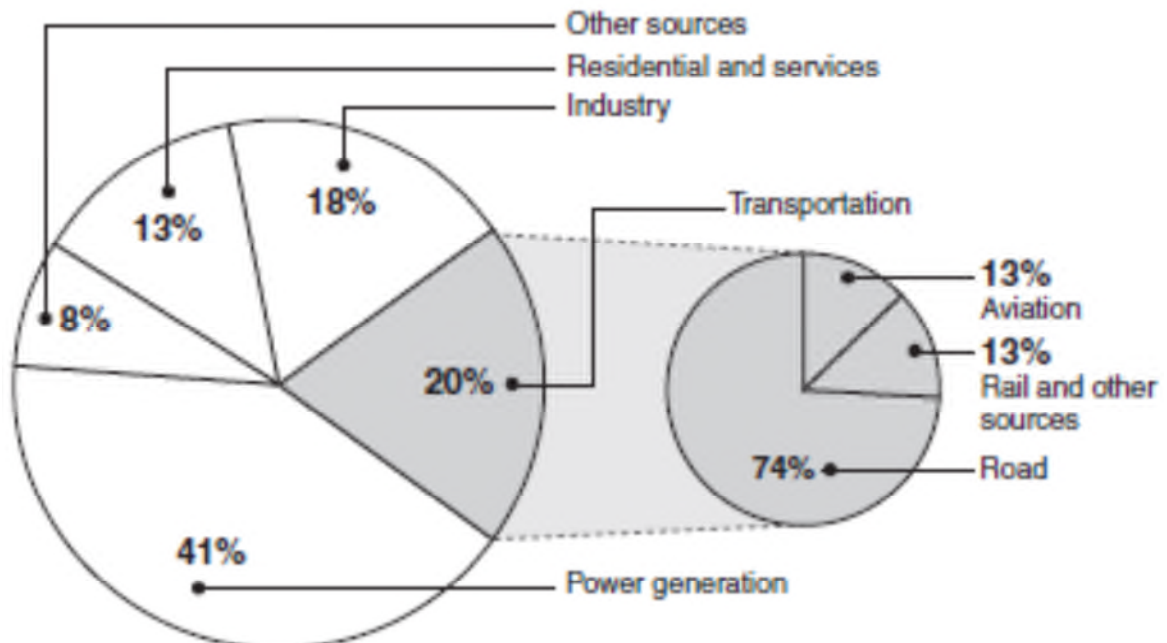
The prediction of aircraft flight mission emissions is useful in making decisions that will aid efforts to counteract the expected increases in emissions by offering means to identify operational practices that promote emissions production. This chapter has described the aircraft emissions prediction module which has been validated by the developer and this author using data available publicly. The results obtained in the validation have shown good accuracy and agreement (with available data) of the emissions model in estimating aircraft emissions. Considering the level of fidelity required which is to present relative values showing changes and trends rather than absolute values for the emissions, the module is deemed suitable for use in achieving the objectives of this work.

Figures for Chapter 4



CAEP: Committee on Aviation Environmental Protection

Figure 4.1: ICAO Technology Goals for NOx [4].



Sources: GAO presentation of International Energy Agency and IPCC data.

Figure 4.2: Global Transportation's and Global Aviation's Contributions to Carbon Dioxide Emissions, 2004 [1]

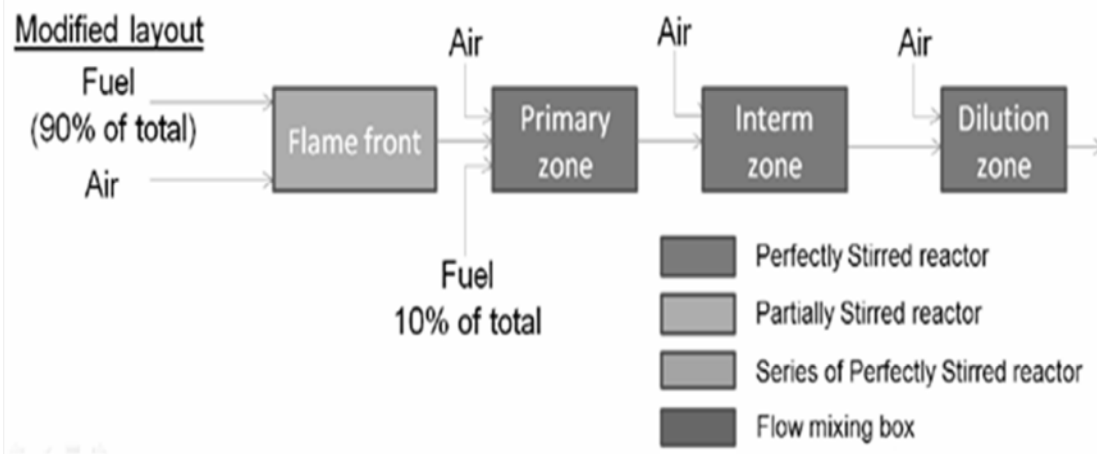


Figure 4.3: Reactor layout for the emissions model [8].

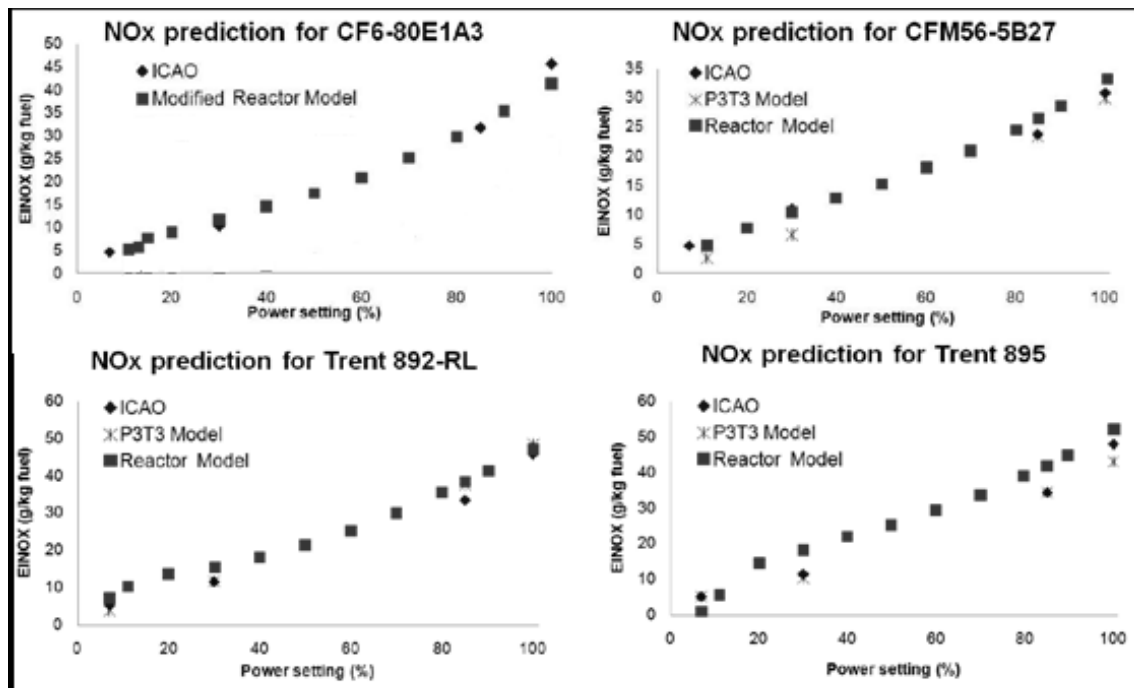


Figure 4.4: Results of NOx emission prediction for various engines [8]

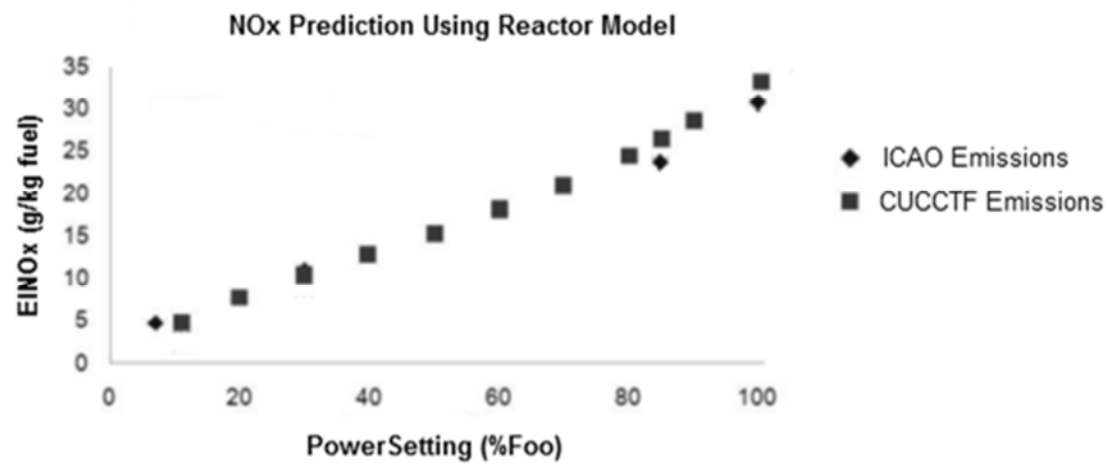


Figure 4.5: CFM56-7B27 (CUCCTF model) NOx emissions prediction.

References for Chapter 4

- [1] US Government Accountability Office (GAO) (2009). Aviation and climate change. GAO-09-554
- [2] Penner, J.E., Lister, D.H., Griggs, D.J, Dokken, D.J., McFarland, M. (1999). Aviation and the global atmosphere, IPCC special report, Intergovernmental Panel on Climate Change, Cambridge University Press, Cambridge, England.
- [3] Sethi, V. (2011), Presentation and overview of gas turbine generated pollutants, Cranfield University, Cranfield, England
- [4] CAEP IV & VI NOx emissions standards, Aircraft Commerce, Issue 64 June/July 2009, Nimrod Publications Limited, UK
- [5] ICAO Aircraft engine emissions databank (2012).
(<http://easa.europa.eu/environment/edb/aircraft-engine-emissions.php>)
(accessed in February 2012)
- [6] Norman, P. D., et al. (2003). Development of the technical basis for a new emissions parameter covering the whole AIRcraft operation: NEPAIR, Final Technical Report, NEPAIR/WP4/WPR/01, European Community under the 'Competitive and Sustainable Growth' Programme (1998-2002), United Kingdom
- [7] Nalianda D., K. (2012). Impact of environmental taxation policies on civil aviation: A techno-economic environmental risk assessment. PhD Thesis, Cranfield University
- [8] Pervier, H., (2013) Emissions modelling for engine cycle and aircraft trajectory optimisation. PhD Thesis, Cranfield University

Chapter 5

Engine Operating Costs

Abstract

The economics module HESTA uses the engine life estimate, the cost of labour and the cost of the engine (used to determine the cost of spares) to estimate the cost of maintenance of the engine. The Direct Operating Costs (DOC) of the engine are calculated as a function of maintenance cost, cost of taxes on emissions and noise, cost of fuel, cost of insurance and cost of interest paid on the total investment. The cost of cabin and flight crew, cost of landing, navigational and ground handling fees are included in the DOC of the aircraft. The first part of the chapter is a review on the new power by hour business model. The second part of the chapter describes in some detail the operating cost (economics) module. The economics model has been validated and verified at Cranfield University as referenced.

5.1 Introduction

The growth of the global market for passenger air transportation has been tremendous over the past decades and this is expected to continue well into the future. This has re-defined the industry's business model, airlines see themselves in a more competitive market environment, and the emerging number of low-cost-carriers has marked a turning point in the market structure. In the current competitive climate airlines need to continuously seek cost reduction potentials in order to stay competitive. This ambition is closely linked to evaluating new methodologies in the way an aircraft manages its trajectory and the possible contribution to reducing the long term operating life cycle costs. For the OEM, the increased competition has reduced the profits from engine sales giving more reliance on the aftermarket. Engine related operating costs (figure 5.1) contribute a considerable share of the DOC [1]. Engine Maintenance, Repair and Overhaul (MRO) make up a large share of the aircraft's MRO costs (figure 5.2) [2]. The engine MRO is therefore considered a cost driver and it is in the interest of aircraft operators to estimate the LCC related to the engine maintenance, when making decisions regarding the aircraft trajectory management. This has given rise to total support agreements/total care packages (between operators and OEMs or an MRO provider) referred to as power by the hour contracts [3].

5.2 Power by Hour (PBH) – Total Care Package

A PBH or total support agreement with the OEM or an MRO provider is one option for the operator, that would allow continued flying without assuming the responsibility of balancing maintenance costs against operational risks and determining the maintenance planning. A PBH contract is an agreement in

which the engine operator buys a fleet of engines, but will not buy spare engines and/or spares. The OEM consents to supplying spare engines and/or accessories (or modules) if and when required, and to perform all the maintenance requirements of the fleet of engines. The technical risk is transferred from the operator to the engine maker or MRO provider. The operator pays the OEM or MRO provider an individually arranged, flight hour-based rate for their technical support services (fleet management and engine aftercare) and concentrate on its main business of providing air transport. This new business model provides a win-win opportunity for both operators and OEMs.

5.2.1 Operator's Perspective

In the current economic climate and competitive nature of the airline industry, it is imperative for operators to focus on their core business activities, maximize operational reliability and minimize financial risk and costs. The key to addressing these issues lies in removing the technical and financial uncertainties associated with engine aftercare. The priority for the airlines is for high quality fleet management and comprehensive engine-aftercare service. The operator is released from the technical and financial problems of engine maintenance and management and the uncertain cost of ownership, which is transferred to the manufacturer for an agreed rate per engine flying hour [3] [4].

5.2.2 Engine Manufacturer's Perspective

In the old business model, the impact of the aftermarket for engine manufacturers was critical in that the aftermarket is more profitable than the original equipment sales, and while new equipment sales can be negatively impacted during economic downturns, the aftermarket may sustain the business until the next economic upturn. In the previous model of after-sales maintenance practice, prolonging an engine's life could lead to instances where the engine requires no major service during the aircraft's service life, resulting in the total or part loss of the engine-manufacturers' aftermarket business. In the new business model, the priority for the OEM is to provide engines with improved reliability and long life which gives benefit to the long-term maintenance contracts based on an agreed rate per engine flying hour [3] [4]. It is no longer just about selling products, it is now about maintaining the product at minimum cost, without lowering performance or safety.

5.2.3 Rolls-Royce Engine Support

Engine manufacturers provide continuous support and maintenance of their products after the original sale. An example is the TotalCare service agreement offered by Rolls Royce to its airline customers. TotalCare guarantees the customer lifetime engine support and covers key areas of engine management and maintenance. TotalCare benefits the customer in the following ways:

- Risks associated with time-on-wing and shop visit cost is transferred to Rolls-Royce.

- Allows customer to concentrate on core business activities.
- Costs are predictable, providing greater visibility and increased control of financial planning.
- Improved efficiency i.e. minimise operational disruptions.

TotalCare is about keeping the engine on-wing as long as possible and thus minimise the costs associated with removing an engine for maintenance. It rewards reliability, and by transferring the technical and financial risks associated with engine aftercare to the OEM, makes reliability and time on-wing drivers for profit for both Rolls-Royce and the airline customer [5].

5.3 Economics (DOC) Model

The economic module used has been adopted from previous research work conducted at Cranfield University and a detailed description can be found in [6]. It uses the engine life estimate together with the cost of labour and the cost of the engine (used to determine the cost of spare parts) to estimate the cost of maintenance of the engine. The DOC of the engine are calculated as a function of maintenance cost, cost of taxes on emissions and noise, cost of fuel, cost of insurance and cost of interest paid on the total investment. The cost of cabin and flight crew, cost of landing, navigational and ground handling fees are included in the DOC of the aircraft. The cost of aircraft maintenance is calculated (as a function of the cost of spares and the cost of labour) using the OEW and the MTOW.

The model is based on the methods outlined in [7] and [8]. The components of the DOC as outlined by [8] are shown in figure 5.3. The module uses the following inputs from the other modules in the framework:

- from the engine performance module: take-off thrust from which depend the maintenance hours needed by the engine.
- from the aircraft performance module: OEW to assess the maintenance hours needed by the airframe.
- from the aircraft performance module: fuel burn.
- from the lifing module: engine life.

In addition, the cost module uses the following elements: cost of aviation fuel, cost of maintenance hours, Interest rates, and noise charges at airports, carbon emission charges and NOx charges. The model accounts for a number of costs including:

- Time dependent costs related to the operation of the aircraft such as airframe and engine maintenance costs which are based on the frequency and regularity of maintenance routines.
- Standing charges related to the cost of depreciation, the cost of engine spares, and the cost of operational life.
- Fuel dependent costs which are related to the total amount of fuel burn per flight mission. The model allows fuel price forecasts.
- Emission dependent costs which are a function of the amount of fuel burn per flight mission..

A detailed account of these charges can be found in [7] and [9]. The module gives the following as outputs:

- DOC.
- Engine maintenance cost.
- Net present cost (NPC).
- Cost of taxes.
- Cost of airframe maintenance.
- The cost of labour and materials used in the overhaul.

5.3.1 Economic Model Validation and Verification

The validation and verification of the economics model is outlined in [6] and the results are reproduced here. The economic model was validated by the developer against airline information publicly available in [9] [10] [11] [12], and against already existing and well recognised methods [7]. The results are reproduced in table 5.1, figure 5.4 and figure 5.5. The results show that though the individual values maybe far apart, the model has an overall accuracy of 85% in estimating the DOC. The code is therefore deemed suitable for achieving deltas and for the purposes of this research.

Table 5.1: The economics model comparing against the Roskam method [6]

| Result (Unit of measure) | Roskam Method Value | Public Data Value | Economic Model Value |
|---|---------------------|-------------------|----------------------|
| Cost of Labour/Engine (€/Hr.) | 23.95 | 70 | 93.5 |
| Number of Engine Maintenance Hours Needed/ Block hour | 0.26 | 1.25 | 1.31 |
| Cost of Maintenance Materials/Engine/Block Hour (€/Hr.) | 173.66 | 80 | 59.76 |
| DOC of Maintenance /Engine/Block Hour ((€/Hr.) | 197.61 | 150 | 153.26 |

5.4 Summary and Conclusions

Direct operating costs become of concern to both the OEM and the airline, thus raising the need for the assessment of the engine and aircraft at mission level and the optimising of operational procedures. Cost effectiveness (making more money) is the perspective for both the OEM and the airlines. In view of the new model (power by hour) contracts as opposed to the older model (time and materials) contracts, the OEM's key concern is to deliver good engines that are reliable and available, whilst remain cost effective in terms of engine maintenance. The airlines' key concern is that to remain competitive, they have to operate cost effectively (i.e. lower operating costs) and remain within the constraints and operating guidelines imposed by the OEM. This brings to the fore, the importance of engine performance and engine life, because as the

engine degrades the flight mission fuel burn increases, in turn translating as an increase in operating costs.

This chapter has described the economic (DOC) module which has been validated by the developer using data available in the public domain and against already existing and well recognised methods. The results obtained in the validation show an 85% accuracy of the economic model in estimating DOC. The module is deemed suitable for use in achieving the objectives of this work as relative costs and not absolute costs are the important objectives of this research. The method is chosen to show the relative cost variation between different trajectories and not predict the actual cost as these vary so widely over different operational practices.

Figures for Chapter 5

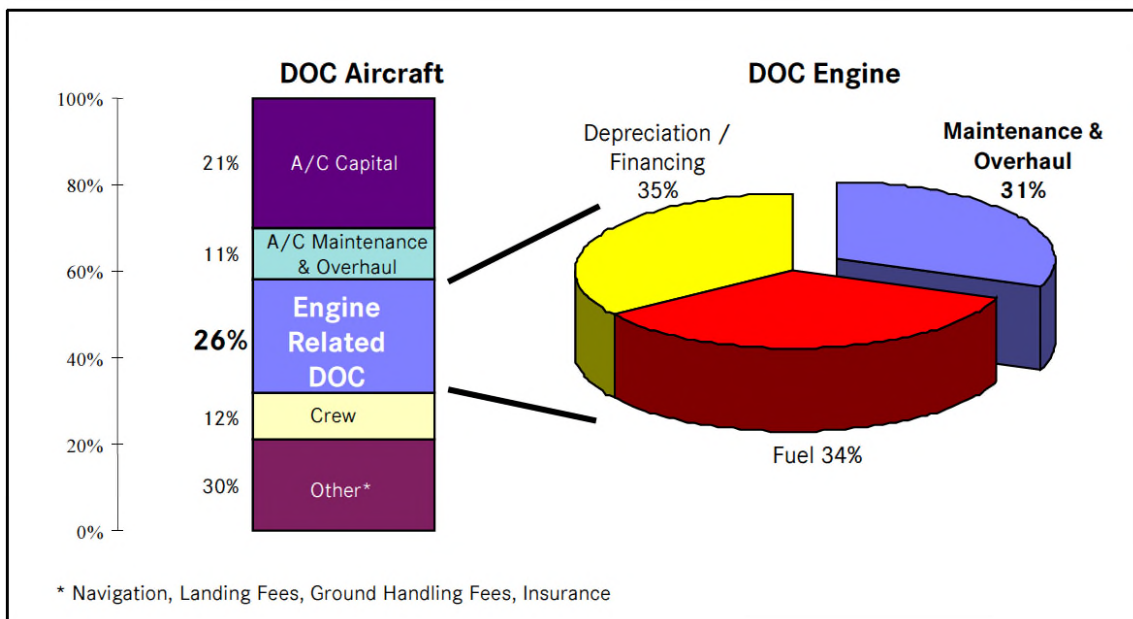


Figure 5.1: Maintenance costs as part of an aircraft engine's DOC [1]

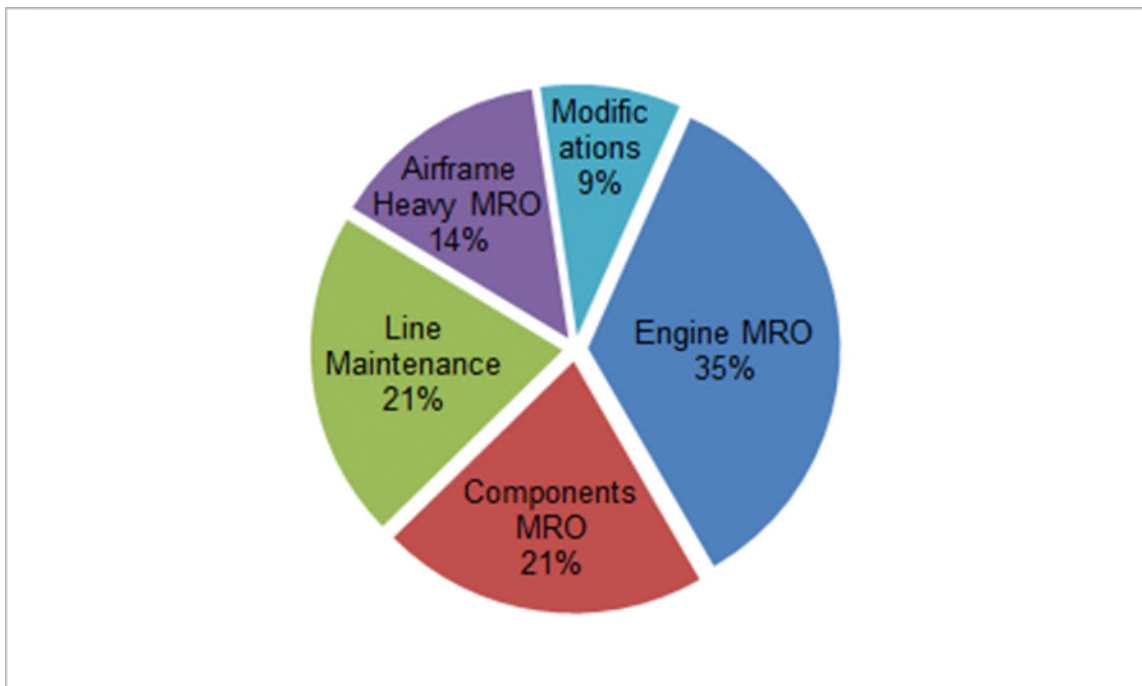


Figure 5.2: Components of an aircraft's MRO [2]

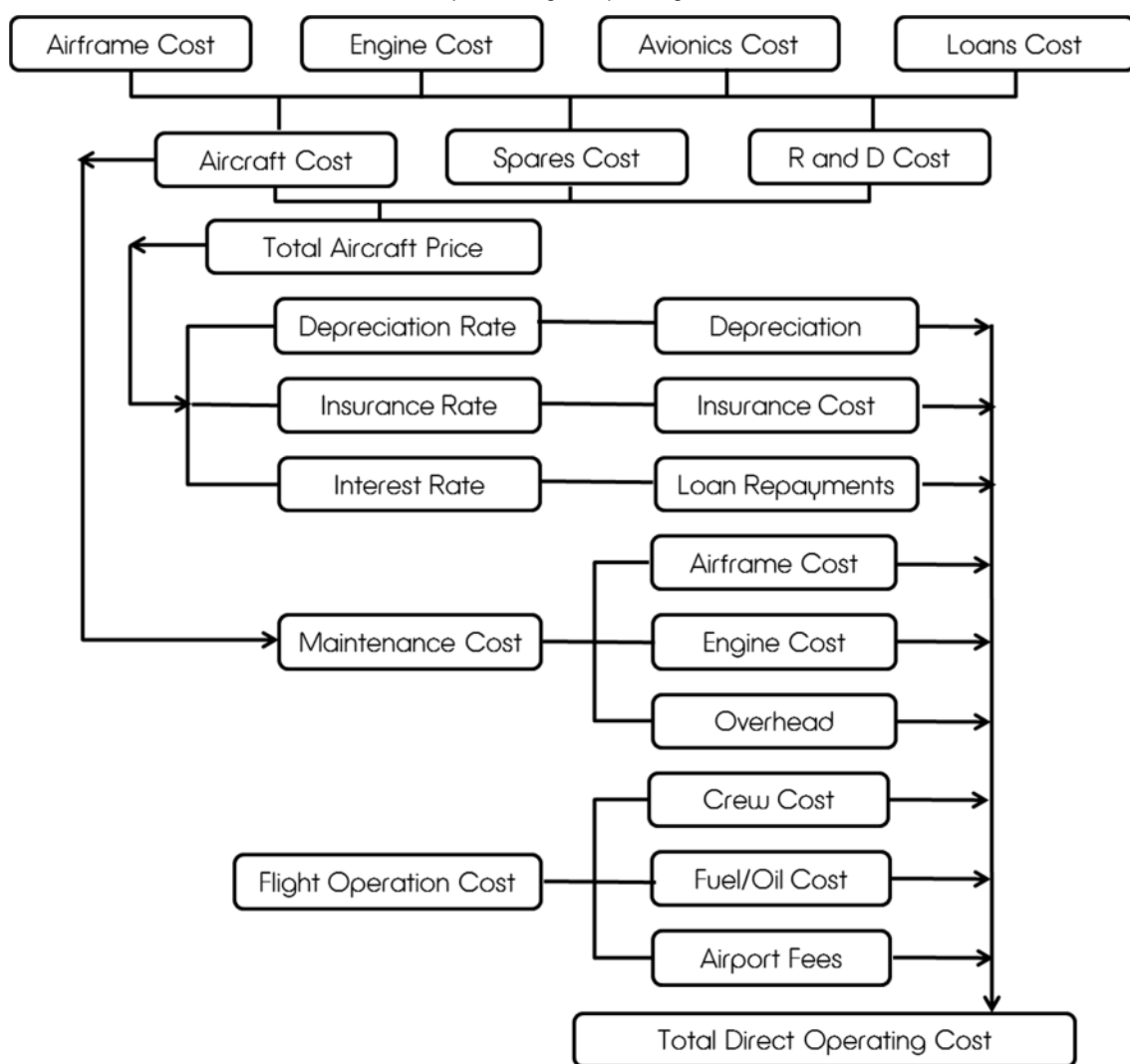


Figure 5.3: Components of the DOC [8]

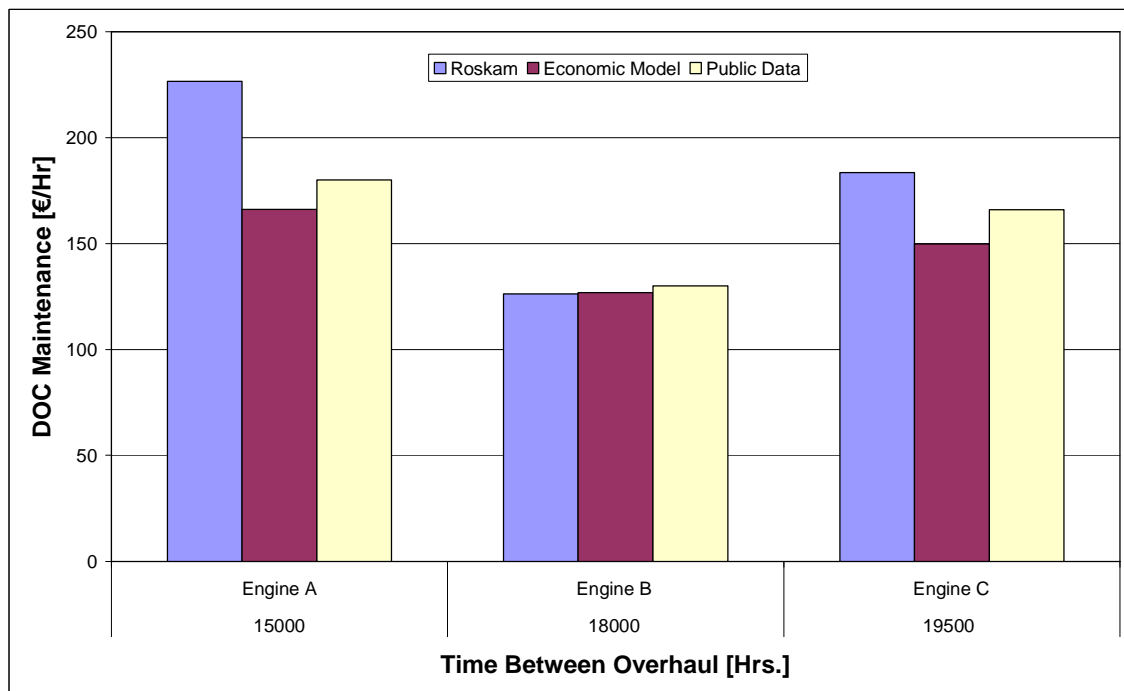


Figure 5.4: Cost of maintenance for short range engines currently in use [6]

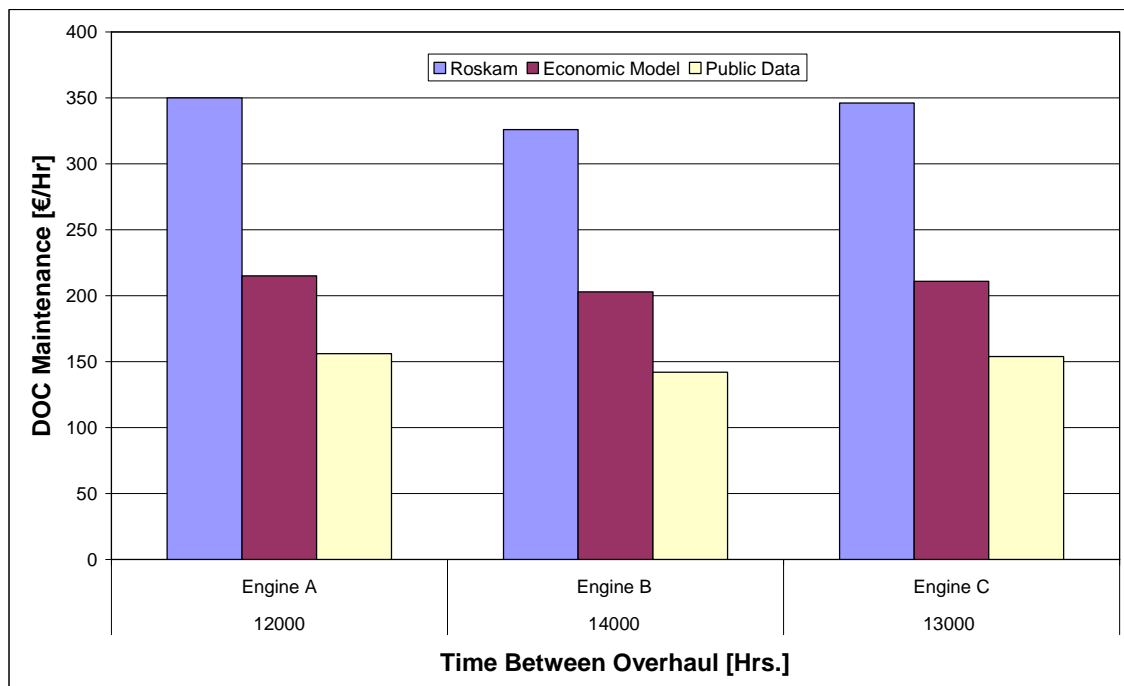


Figure 5.5: Cost of maintenance for long range engines currently in use [6]

References for Chapter 5

- [1] Rupp, O. (2002). Instandhaltungskosten bei zivilen strahltriebwerken, Hannover, Langenhagen, Germany, MTU Maintenance
- [2] Jet Engine Consulting: Our consultancy philosophy (2008), (http://www.jetengineconsulting.com/pdf/JEC_Consulting_Philosophy.pdf)
- [3] Holland, J., Gubisch, M., Derber, A. (2011). The engine year book: Aircraft technology's annual publication for the aero-engine professional, UBM Aviation Publications Ltd
- [4] Marinai, L. (2004). Gas-path diagnostics and prognostics for aero-engines using fuzzy logic and time series analysis, Ph.D. thesis, Cranfield University
- [5] <http://www.rolls-royce.com/civil/services/totalcare/> (accessed March 2014)
- [6] Pascovici, D. (2008). Climate thermo economic and risk analysis for advanced long range aero engines, PhD Thesis, Cranfield University
- [7] Roskam, J. (1990). Airplane design, Part VIII, Airplane cost estimation: design, development, manufacturing and operating, Ottawa, Kansas: Roskam Aviation and Engineering Corporation
- [8] Jenkinson, L.R., Simpkin, P., Rhodes, D. (1999). Civil jet aircraft design, Arnold, London
- [9] Aircraft Commerce: Issue No.5, 23, 30, 38, 39, 44
- [10] <http://www.icaodata.com/> (accessed December 2013)
- [11] Flight international: Issue no.5022-5052
- [12] Overhaul and Maintenance: An aviation week magazine

Chapter 6

Aircraft Trajectory Optimisation

Abstract

The ACARE environmental targets for 2020 (2050) are extremely challenging and aim to: reduce CO₂ emissions by 50% (75%), reduce NO_x emissions by 80% (90%) and reduce perceived noise by 50% (65%). Achieving these goals poses significant technical challenges requiring that trade-offs be addressed. Research has indicated that to achieve these targets will require contribution from technological improvements (15-20% related to engines, 20-25% to aircraft design), operational improvements (5-10% related to improved air traffic management and operational efficiency) and greener manufacturing and recycling processes including transportation. Technological improvements present a range of challenges and further advances may come with high development costs. Operational improvements are a most readily implementable contributor to achieving the ACARE targets. They are financially viable, cost effective and competitive for existing engines and aircraft. One option of operational improvements is aircraft trajectory optimisation. Optimisation provides methods that search for global (and or local) solutions to problems that contain multiple maxima or minima. In this chapter, the trajectory to be optimised is defined in terms of the flight phases that make up the trajectory. Optimisation problems, with a deliberate bias towards aircraft trajectory optimisation are discussed including methods and criteria used when classifying trajectory problems. The optimiser used in this work is a genetic algorithm based multi objective optimiser which implements a Non-dominated Sorting Genetic Algorithm (NSGAI). The optimiser was developed, tested, benchmarked and verified at Cranfield University as part of the Clean Sky project requirement for aircraft trajectory optimisation. The optimiser is described in detail in the latter part of the chapter. The optimiser was validated and verified by the developers as referenced.

6.1 Introduction

Optimisation provides methods that search for global (and or local) solutions to problems that contain multiple maxima or minima. It includes global search (and or local search), multistart, pattern search, genetic algorithm, and simulated annealing. These methods can be used to solve optimisation problems where the objective or constraint function is continuous, discontinuous, and stochastic, does not possess derivatives, or includes simulations or black-box functions with undefined values for some parameter settings. The methods are able to find optimal solutions to problems with or without constraints.

6.2 Definition of Flight Phases

A civil aircraft flight path consists of a number of phases or segments which make up the total flight mission. These are: take-off and initial climb, climb, cruise, descent, and approach and landing. A typical civil aircraft mission profile is shown in figure 6.1 [1].

Table 6.1: Flight segments characteristics [2] [3]

| Phase | Parameter | Start | End |
|-------------------------|------------------------|-----------------------|----------------------|
| Take Off | Speed | Zero | Initial climb |
| | Altitude | Ground | 35ft |
| | Aircraft Configuration | Take-Off ¹ | Take-Off |
| | Engine Power Settings | Take-Off | Take-Off |
| Initial Climb | Speed | Initial climb | Climb |
| | Altitude | 35ft | 1500ft |
| | Aircraft Configuration | Take-Off | Clean ² |
| | Engine Power Settings | Take-Off | Climb |
| Climb | Speed | 250kts CAS | Cruise Speed |
| | Altitude | 1500ft | Cruise Altitude |
| | Aircraft Configuration | Clean | Clean |
| | Engine Power Settings | Climb | Cruise |
| Cruise | Speed | Cruise Speed | Cruise Speed |
| | Altitude | Cruise Altitude | Cruise Altitude |
| | Aircraft Configuration | Clean | Clean |
| | Engine Power Settings | Cruise | Flight Idle |
| Descent | Speed | Cruise | 250kts CAS |
| | Altitude | Cruise Altitude | 10000ft |
| | Aircraft Configuration | Clean | Clean |
| | Engine Power Settings | Flight Idle | Flight Idle |
| Approach Landing | Speed | 250kts CAS | Zero |
| | Altitude | 10000ft | Ground |
| | Aircraft Configuration | Clean | Landing ³ |
| | Engine Power Settings | Flight Idle | Ground Idle |

1. Take Off configuration: Flaps, slats deployed, brakes released, gear down

2. Clean configuration: Flaps, slats and gear retracted

3. Landing configuration: High lift, high drag, gear down

Each of these phases can be analysed or optimised separately. This section provides a brief description of each of the flight phases used in this research representing a typical flight trajectory (or mission profile) and the Air Traffic Management (ATM) constraints governing each phase. In table 6.1 [2] [3] is given a summary of the conditions at the start and end of each phase.

6.2.1 Take – Off and Initial Climb

Take – Off: The take-off segment is the phase in which the aircraft is transferred from a stationary ground-borne state into a safe airborne state. In this phase, the aircraft is accelerated along the runway to a speed at which the lift produced exceeds the weight and it lifts off and begins to climb. The aircraft starts off at rest on the runway, with brakes released and engine settings at take-off thrust. During the ground run, the angle of attack is kept low so as to maximise the thrust available for acceleration. As the aircraft accelerates it progresses through the minimum control speed (ground) V_{mcg} , achieves rotation speed at which aircraft is rotated into nose up attitude that equals the required lift-off angle of attack, reaches the lift-off-speed V_{LOF} and becomes airborne. The take-off is complete when the aircraft clears a height of 35ft above the runway.

Initial Climb: The initial climb starts at 35ft above the runway and ends with the aircraft in a clean configuration (with flaps and landing gear retracted). It follows airport specific noise alleviation procedures and is constrained by other Air Traffic Control (ATC) regulations such as a speed limit of 250kts CAS at altitudes below 10000ft. This segment also involves acceleration to the en-route climb speed.

6.2.2 Climb

The climb flight segment is the phase in which the aircraft increases its altitude to the required cruise flight level. It begins at the end of the initial climb phase. During this phase, it is required that the propulsive thrust must exceed the airframe drag for the aircraft to climb. In a climb, the aircraft uses fuel energy, to achieve an increase in its potential energy. The climb performance is important for the economy of operation and for the safety of flight. Optimum economy of operation can be achieved by using the correct climb technique to minimise the amount of fuel used to reach a given altitude. Additionally, sufficient thrust must be available to ensure the aircraft safely climbs above every obstruction along the flight path. An aircraft's climb capability will be affected by the thrust, the weight, and the ratio of drag to lift. The climb phase is split into three parts: it starts from 1500ft to 10000ft at a constant equivalent airspeed (EAS) of 250kts with Mach number allowed to increase. (It is worth noting that at typical climbing speeds for civil aircraft, the scale-altitude correction is small and the CAS is close to the EAS). This state presents a constant angle of attack and constant lift to drag ratio. The next stage is acceleration from 10000ft until the cruise Mach transition altitude is reached. The last stage is a climb at constant Mach number and EAS decreasing until

the initial cruise altitude is reached. The aircraft climb performance is currently subject to and constrained by these specified air traffic regulations:

- The aircraft operational height must not exceed the maximum certified altitude.
- The aircraft must be flown below the maximum flight level of associated air routes.
- The aircraft must not fly at a speed that exceeds the limit for maximum operating calibrated airspeed (CAS).
- The aircraft must reach the selected ToC flight level with a flight speed equalling the optimal Mach cruise.
- The aircraft speed should not be lower than the stall speed.
- The aircraft speed must not exceed the limit for maximum operating Mach number.
- The aircraft operating speed must not be less than the minimum buffet speed.
- The aircraft speed Mach number must not exceed the maximum operating limit Mach number.
- The minimum climb gradient for a two-engine aircraft may not be less than 1.2% with one engine inoperative and the others operating at maximum continuous thrust.
- The engine rating should be lower than the maximum climb rating.

6.2.3 Cruise

The cruise flight segment is the phase between climb and descent. It begins at ToC and ends when the descent phase starts i.e. Top of Descent (ToD). The important parameters that define the cruise phase are the altitude (flight level) and the flight speed (Mach number), of which both are essentially constant. The cost of fuel and cost of time contribute to the cost of operation, and typically with the exception of short range flights, the largest percentages of trip time and trip fuel are consumed in this phase of flight. The selected cruise speed, altitude and Centre of Gravity (CG) will have an effect on the total flight time and fuel burn. The flight level and speed selection may be influenced by the following objectives:

- Maximise the range flown for a given amount of fuel.
- Minimise flight fuel burn for a given range flown.
- Minimise flight time.
- Minimise total flight operating cost.
- Maintain flight schedule.

In day to day flight operations, these objectives will not always be practicable and at times pilots may be forced to temporarily abandon their cruise strategy to deal with short term constraints that arise during a flight. Since an aircraft will usually spend a greater part of its mission in cruise flight, the cruise segment performance has a strong influence on the overall mission performance and the cost of operation of the aircraft. Cruise performance is therefore important to the overall balance between fuel burn and flight time and

the aircraft needs to be flown in a manner and at a flight level and speed that will optimise the overall operating cost. Achieving the optimum cruise performance is subject to operational constraints which are dependent on ATM regulations.

During the cruise phase, the aircraft is considered to be in steady (no unbalanced forces), level (constant altitude), straight (velocity vector parallel to the ground), symmetric flight with no acceleration (constant speed). There is an optimum altitude for cruise and this altitude increases as the fuel is burned and the aircraft weight decreases. The cruise trajectory is dependent on the flight mission range. For short range flights, the cruise trajectory is small or non-existent. For medium range flights, the cruise trajectory is assumed horizontal at constant cruise altitude. For long range flights, because the airplane weight changes significantly, the climb is continuous and the initial and final cruise altitudes are not the same. Due to constraints imposed by Air Traffic Control (ATC) regulations, the true optimum is not attainable, as the variable altitude or climbing cruise is not practical. There is need to provide and maintain vertical separation between flights in different directions and current air traffic control rules specify that aircraft must be flown at specific and constant flight altitudes that are compatible with other traffic on a specified route segment, and request ATC clearance to climb to the next highest available altitude when sufficient fuel is consumed.

6.2.4 Descent

The descent flight segment is the phase in which the aircraft decreases its altitude from cruise flight level to 10000ft above mean sea level. It begins at the end of the cruise phase. During this phase, it is required that the airframe drag exceeds the propulsive thrust for the aircraft to descend. Similar to the climb segment, the descent follows a specified airspeed schedule with speed limit restrictions at 10000ft. The initial part of the descent is at cruise Mach number, followed by descent at constant airspeed and in the final part of descent the aircraft slows down to an approach speed. A wide range of descent path profiles are available to the aircraft and these can be varied from a shallow descent to a very steep descent either by reducing the engine thrust or by increasing the airframe drag. The drag can be increased either by changing the aircraft configuration or by varying the airspeed. A gliding descent is achieved when there is no propulsive thrust and the lift-drag ratio determines the descent, however ATC restrictions and the need to maintain control of the flight path gradient require necessary use and changes in thrust. The choice of descent path will be affected by safety-related issues such as the aircraft attitude, rate of change of cabin pressure and the need for the engines to supply power or airframe services. To optimise the descent for fuel burn is not as straightforward as for climb. This is because in a descent, the aircraft operates at low thrust, low fuel flow and the economics are less critical than for the climb. The aircraft descent performance is currently subject to and constrained by these specified air traffic regulations:

- The aircraft must in compliance with ATC restrictions fly at a given airspeed and maintain traffic separation as it positions for final approach.
- The aircraft speed should not be lower than the stall speed.
- The aircraft speed must not exceed the limit for maximum operating Mach number.
- The aircraft operating speed must be within the limits for the maximum and minimum buffet speed.
- The aircraft speed at ToD must equal the optimum cruise Mach.
- At 10000ft and below, the aircraft must not fly at a speed that exceeds 250kts CAS.
- The engine rating should be higher than the idle rating.

6.2.5 Approach and Landing

Approach: The approach begins when the descending aircraft reaches 10000ft above mean sea level at airspeed of 250kts CAS and ends when the aircraft is 50ft above ground level. On final approach, the gradient of the flight path must be steep enough to exceed the limit imposed by the slope of the minimum obstacle but not too steep to for the flare to touchdown to require an excessive pitch attitude change.

Landing: The landing phase is when the aircraft is on a descending path towards the runway. It begins when the descending aircraft clears a height of 50ft above the landing surface and ends whet the aircraft is brought to a stop on the runway. As the aircraft approaches the runway the airspeed and rate of descent are reduced in the flare so that an acceptable touchdown is achieved. An acceptable touchdown requires the aircraft to be flying at low airspeeds and in a high lift, high drag and gear down configuration. The thrust is reduced to flight idle and the angle of attack progressively increased. After touchdown the aircraft decelerates, the nose is lowered onto the runway and the landing is completed when the aircraft comes to a stop.

The constraints to the approach and landing phase are as follows:

- The aircraft must not accelerate during approach.
- The aircraft must be flown at the lowest airspeed at which the safety margins can be met and at an attitude allowing for a smooth flare and touchdown.
- The aircraft flight airspeed must not be less than the minimum drag speed to maintain flight path control and stability.
- The final approach gradient must be 3° (equivalent to a 5% gradient).
- Aircraft speed should not be lower than the stall speed.
- The engines must operate at a fairly higher than idle thrust setting.

6.3 Aircraft Trajectory Optimisation

Optimisation can be defined as the process of finding a condition that gives a minimum or maximum of a given function. It can also be defined as the process of establishing the best possible solution to a given mathematical

problem within a set of circumstances or constraints [4] [5]. There is no single optimisation technique that will sufficiently cater for all optimisation problems, hence a number of optimisation techniques have been developed. One such group of developed methods is the mathematical programming techniques (optimum seeking solutions) which will establish the minimum value of a multi-variable function within a given set of constraints [5] [6]. This section looks at how mathematical programming techniques can be used in aircraft trajectory optimisation.

The aim of a design procedure is to find an acceptable design, which will satisfy the requirements of the problem. However, generally, there is more than one and the purpose of optimisation therefore becomes one of ascertaining (within a chosen criterion), the best acceptable design out of the many acceptable designs available. Optimisation problems can be classified according to the following methods and criteria as outlined in [5] [6]:

- Constrained or unconstrained: depends on existence of constraints in the problem.
- Parameter or trajectory: depends on whether time dependent or not.
- Optimal or non-optimal control: depends on physical nature of the problem.
- Nature of the equations involved (linear, nonlinear, geometric, and quadratic programming).
- Integer or real-valued programming: nature of values permitted.
- Deterministic or stochastic programming: nature of the variables permitted.
- Separable or non-separable: depends on whether objective function and constraints are separable.
- Single or multi-objective: depends on the number of objective functions.

In accordance with the above mentioned problem classifications, an aircraft trajectory optimisation problem can be classified as a multi-objective, constrained, dynamic, optimal control, non-linear, real-valued, deterministic, and non-separable problem. Since a number of parameters will be involved during the optimisation process, and it is assumed there are a number of local minima or maxima, the problem can also be classified as multi-dimensional and multi-modal.

6.3.1 Numerical Methods for Trajectory Optimisation

There are a number of mathematical programming techniques that can be used to find the minimum of a function within a given set of constraints. However, it is not within the intentions of this work to detail every technique available for aircraft trajectory optimisation methods, hence only those (hill climbing, random search and evolutionary methods) that have been widely used in aircraft trajectory optimisation are presented here.

6.3.1.1 Hill Climbing Methods

Hill climbing methods are described in [6] [7] as “the intuitive way by which a sightless climber feels his way from the valley to the tip of the mountain”, and are applicable to single (one) and multi-dimensional problems. Single dimensional problem solving methods are further classified as either sequential or simultaneous methods. Sequential methods carry out a number of trials sequentially to establish the minimum and uses intermediate results as input in the next trials. Simultaneous methods carry out trials simultaneously at a number of points to obtain the value of the objective function (at those points) and thus establish the minima or maxima. Multi-dimensional problem solving techniques generally extend the ideas used in single dimension methods into several dimensions. They can be classified as direct approach, gradient and newton methods.

Direct search methods are sometimes referred to as trial and error methods and follow a heuristic (non-optimal) path to fix the length and direction of subsequent steps. The objective function is used only during the optimisation process. These methods are simple and have proved a success in practical applications making them an attractive proposition. Examples of direct search methods are hill climbing search and simulated annealing search which are useful when it is irrelevant which path is followed to establish the optimal solution [6] [8].

The gradient method assumes the objective is continually differentiable and thus uses both the gradient function and its first partial derivative to seek the optimal solution. All hill climbing search methods that use the first partial derivative of the objective function to search for the optimum are called gradient methods [6] [7].

Newton methods are methods which use the second partial derivative of the objective function by exploiting the Taylor series. The optimisation process follows steps in which the first and second derivatives of the objective function are calculated and the Hessian matrix inverted. When the objective function is quadratic, a single step process is required otherwise process is iterative. Convergence problems will occur when the Hessian matrix cannot be inverted (is singular). The choice of starting point is critical for a successful search; a good knowledge of the objective function and the search space is essential when choosing a starting point [6 [7]]. Further information and description of hill climbing methods can be found in [6] and [7].

6.3.1.2 Random Search Methods

Random search methods are methods which randomly search (irrespective of the structure of the objective function) for the optimum by using parameters which vary along probabilistic rather than deterministic rules [6] [7]. These methods can be applied in all cases and are useful in situations where deterministic methods have been unsuccessful such as where the objective function is non-differentiable in which case information on the Hessian matrix

and gradient is not required. Their random nature of execution however makes them costly to implement. Further information on random search methods can be found in [6] and [7].

6.3.1.3 Evolutionary Methods

Evolutionary methods are problem solving techniques that are inspired by nature. They are based on principles of evolution by Darwin such as the reproduction cycle, natural selection, and diversity by variation [9]. Evolutionary programming, evolution strategies, genetic programming, and genetic algorithms are among the most important of evolutionary methods.

Evolutionary programming methods do not model any kind of recombination of different species [6] [9], whereas evolution strategies contain some form of recombination between solutions. Genetic programming methods use the current population to create new population of offspring programs through Darwin's principle of reproduction and natural selection (survival of the fittest) as well as the genetic operation of sexual recombination [6] [9].

Genetic Algorithms (GAs) are based on the principles of natural genetics (including reproduction, crossover, and mutation) and natural selection. GAs are the most extensively used of all the evolutionary techniques, and have had a profound impact on optimisation [6] [8]. GAs, are extremely robust and suited for problems in which the inputs and outputs relationship is unknown and may behave unexpectedly. In cases where the performance of standard nonlinear programming techniques is not satisfactory (are inefficient, computationally expensive, and converge at a relative optimum that is closest to the starting point), GA's have been found to be effective [6]. Further information about GAs and how they differ from traditional optimisation methods can be found in [5].

6.3.2 Trajectory Optimisation Technique Selection

For the purposes of this work, the genetic algorithm based optimiser is used for the reasons outlined in the proceeding sections.

6.3.2.1 Genetic Algorithm Based Optimisation

A genetic algorithm based optimiser NSGAMO II provided by [10] has been chosen to solve the aircraft trajectory optimisation problem for the following reasons:

- GAs are problem independent and do not use previously known domain-specific information to guide each step, rather they make random changes to their candidate solutions and using the fitness function then determine whether the changes produce an improvement. This is important in aircraft trajectory optimisation which involves multi-model integration, since the functions relating inputs to outputs are unknown. GAs are found to be effective in that the optimisation routines are both model and problem independent and allow the user to simultaneously

run different models and simulate different disciplines (e.g. aircraft and engine performance, emissions formation etc.).

- GAs perform well in problems where the candidate solutions are in a discontinuous and complex landscape with many local optima.
- GAs use a parallel process of search and explore for optimum solutions effectively reducing optimisation time. They explore the search space in multiple directions, proceeding only along those paths likely to yield a solution and are suitable for large search spaces such as are nonlinear problems.

The genetic algorithm can be customised by modifying initial population and fitness scaling options or by defining parent selection, crossover, and mutation functions. The genetic algorithm (figure 6.2) initiates the optimisation process by generating a set of random solutions (initial population) which is equivalent to the product of the initialisation factor and the user defined population size. The optimiser evaluates the initial population and trims it down to the user defined population size according to a fitness function (e.g. fuel burn, flight time). The process loops until certain criteria (defining the optimal solutions) are met. The criteria for stopping the process can include the maximum number of generations or the maximum fitness. The best solutions from the preceding generation are used to create the next generation, thus a smoother Pareto front is obtained with each generation [10].

6.3.2.2 Optimiser Validation and Verification

The performance of the genetic algorithm was benchmarked and tested for by [11] in three phases. Phase 1 involved performance testing using various mathematical functions otherwise known as the Zitzler-Deb-Thiele's (ZDT) test problems. These test problems were formulated by Zitzler et al. to assess the performance of a multi-objective optimisation algorithm for the following properties [12]:

- Ability of the algorithm to handle difficulties along the Pareto optimal front and find diverse Pareto optimal solutions.
- Ability of the algorithm to handle difficulties lateral to and converge to the true or global Pareto optimal front.
- Ability to handle different shapes of the Pareto optimal front and solve problems with convex, non-convex or discontinuous Pareto optimal fronts.

In phase 1 the ZDT1, ZDT3 and ZDT6 were used and the optimiser was tested for convergence, diversity and the number of evaluations required by the algorithm to converge to the Pareto optimal front. The ZDT1 tests the ability of the optimiser to handle problems with a large number of variables (30) with a convex Pareto optimal set. The ZDT3 tests the ability of the optimiser to handle problems with a large number of variables (30) and a set of discontinuous Pareto optimal fronts. The ZDT6 tests the ability of the optimiser to handle a multi-variable (10) problem with a non-convex Pareto optimal set and an adverse density of solutions across the Pareto optimal front. In phase 2 the

optimiser was tested for its constraint handling ability. The Constr-Ex and TNK test problems were used (as recommended by [12]). The Constr-Ex tests the ability of the optimiser to reach a solution when a part of the unconstrained Pareto optimal region is made infeasible by a constraint. The TNK tests the ability of the optimiser to reach a solution when the Pareto optimal region is discontinuous and falls entirely on the first constraint boundary. In phase 3, [11] established the validity and performance of the GA optimiser by applying it to simple trajectory optimisation cases to achieve multi-disciplinary trajectory optimisation objectives. The performance of the GA optimiser was comparable with that of other methods and commercially available optimisers [11] [13]. The optimiser showed good diversity, convergence and constraint handling ability. The results outlined in [11] establish the applicability of the GA optimiser as an optimisation tool and demonstrate it has the capability to evaluate optimised solutions in a complex design space which may include convex/concave and discontinuous Pareto optimal fronts. Some of the results of the validation are reproduced in this thesis and are shown in figures 6.3 to 6.11. For the criteria adopted and for a more elaborate description of the validation and results, the reader is referred to [3] and [11].

6.4 Summary and Conclusions

Operating costs are an important concern to airlines and engine manufacturers (OEMs). Fuel burn is a measure of an aircraft's mission flight performance. Flying the fuel burn optimum trajectory is beneficial to reducing the direct operating costs. A civil aircraft will spend most of its mission flight time at the cruise phase, more so for medium and long range flights, making the cruise performance of the aircraft strongly influential on the overall flight mission performance and operating costs because most of the fuel burn will occur during cruise.

Optimisation methods can be used to solve aircraft trajectory optimisation problems with or without constraints. The chapter has provided a definition of the flight phases that are part of a civil aircraft's flight path as well as detailed information on the optimiser. The chapter has described optimisation techniques and classification and in particular the NSGAMO II genetic algorithm based optimiser which has been adopted for the purposes of this research. The optimiser was validated, tested and benchmarked by the respective developers using data available in the public domain and against already existing and well recognised optimisation methods. Some of the results obtained in the validations have been presented in this chapter and show good accuracy and potential to solve the trajectory optimisation objectives of this work.

Figures for Chapter 6

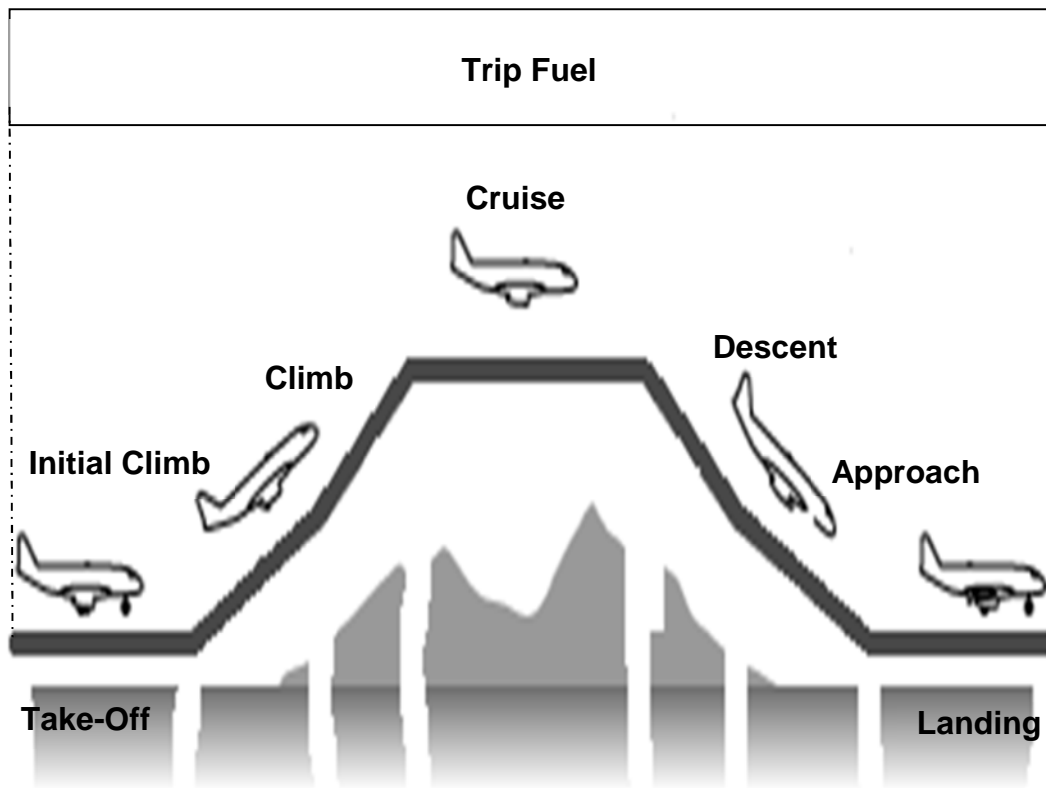


Figure 6.1: A typical civil transport aircraft flight profile [1]

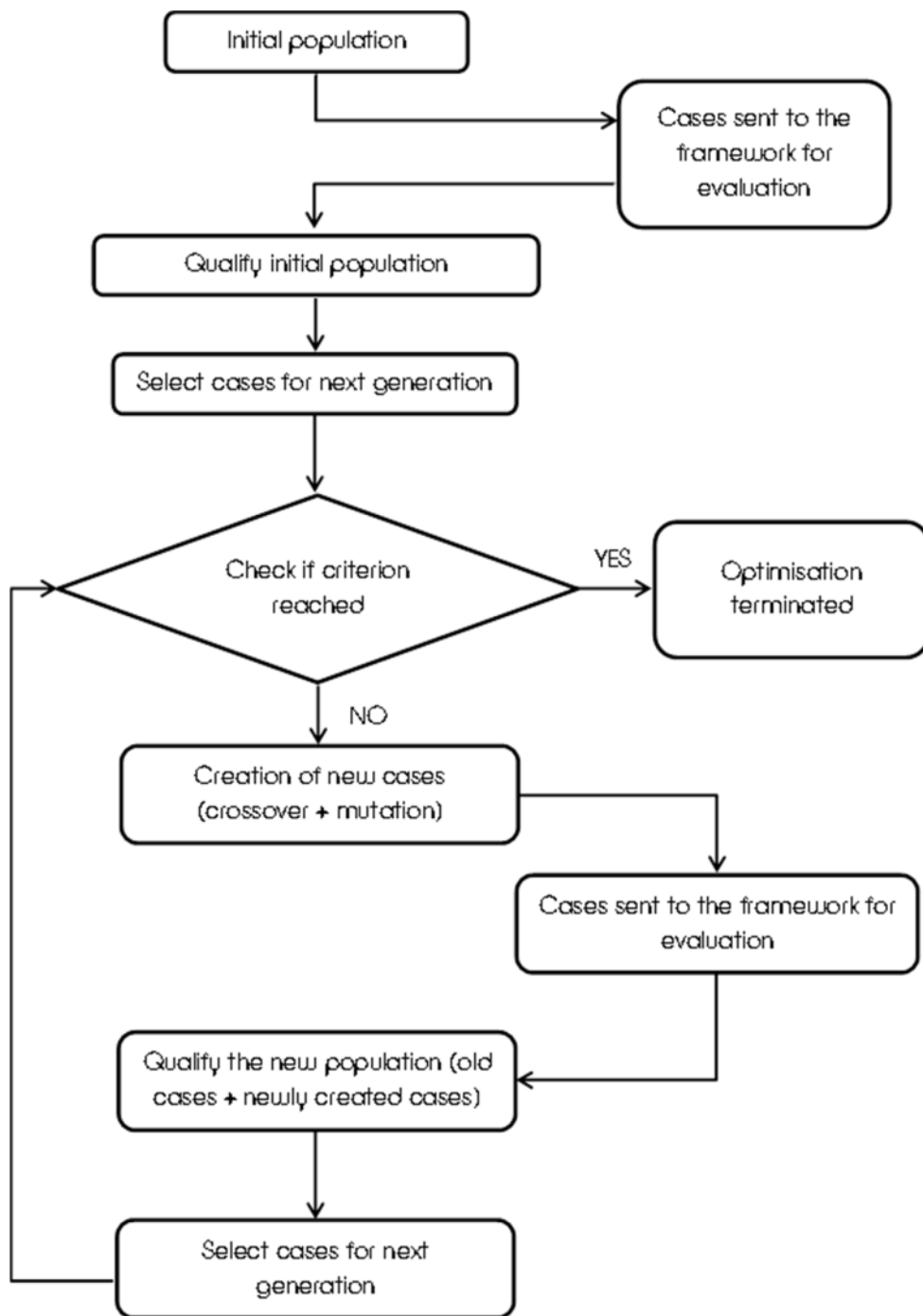


Figure 6.2: Genetic algorithm optimisation flowchart [10].

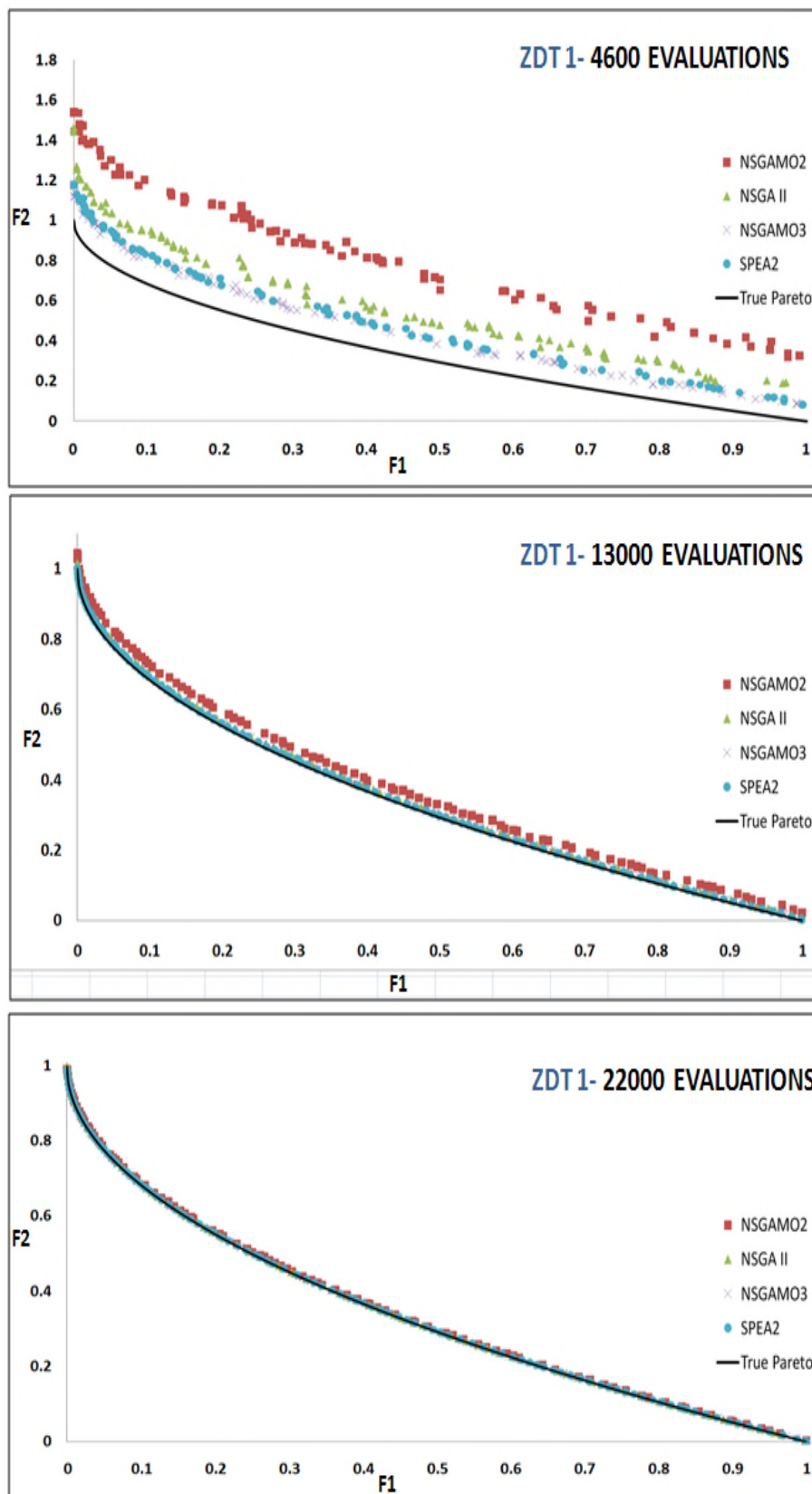


Figure 6.3: Pareto fronts obtained in GA optimiser benchmarking studies [11].

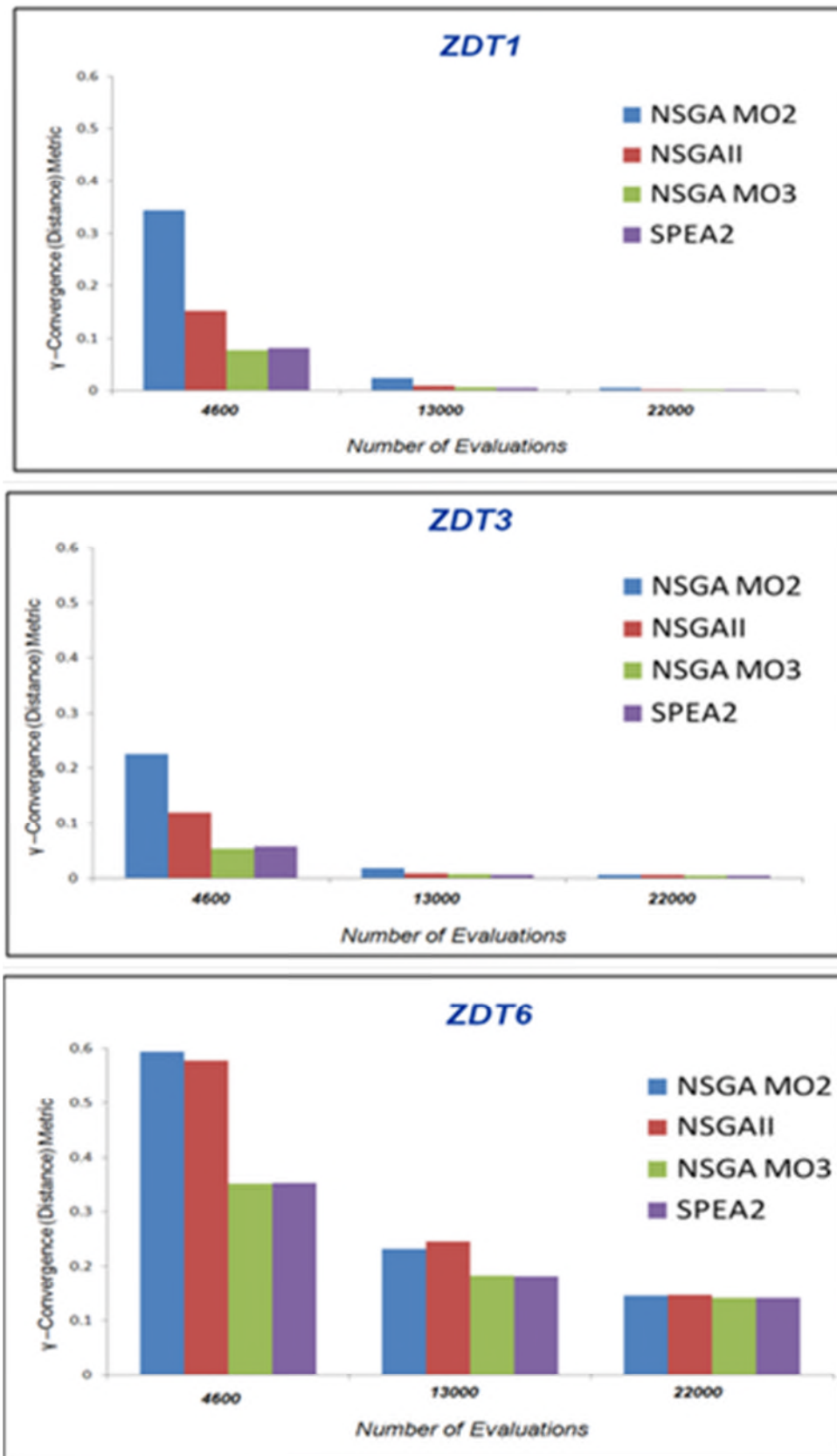


Figure 6.4: Convergence metric for ZDT1, ZDT3 and ZDT6 test functions [11].

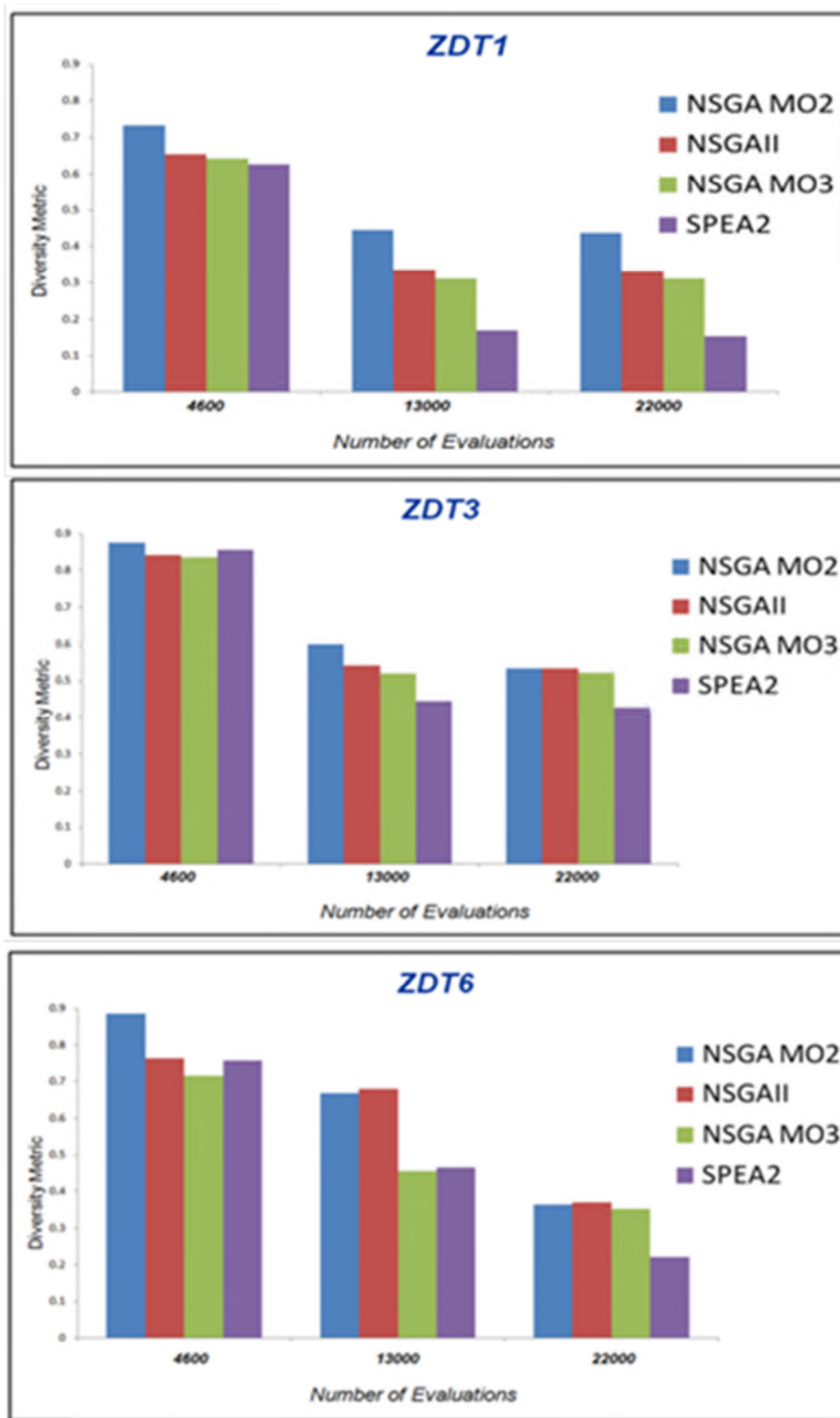


Figure 6.5: Diversity metric for ZDT1, ZDT3 and ZDT6 test functions [11].

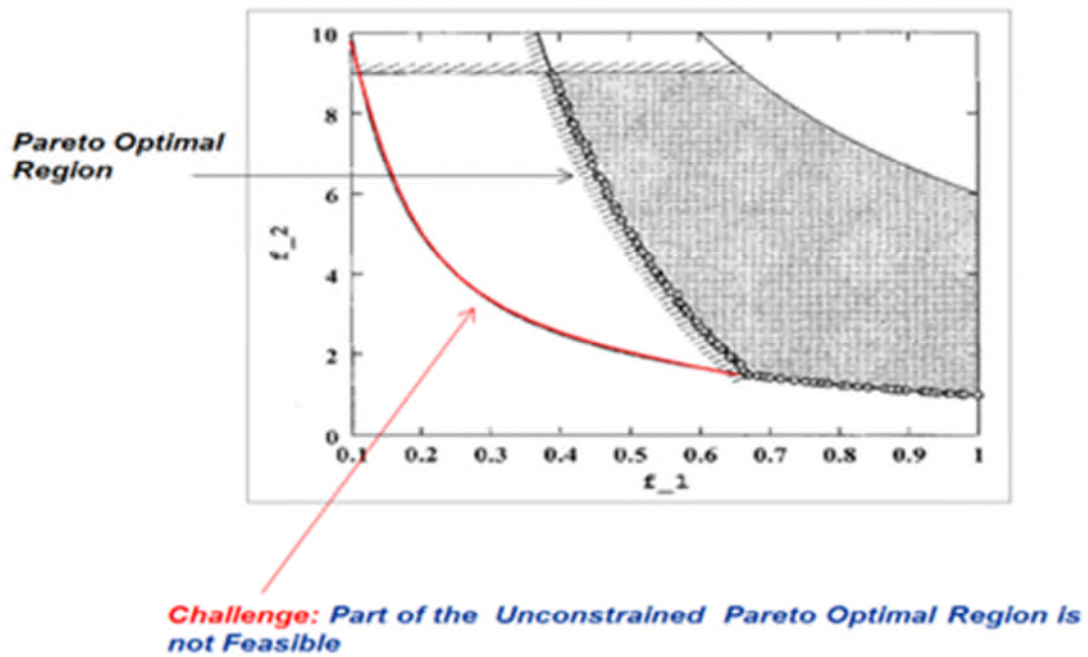


Figure 6.6: Constraint altered Pareto front for CONSTR function [3].

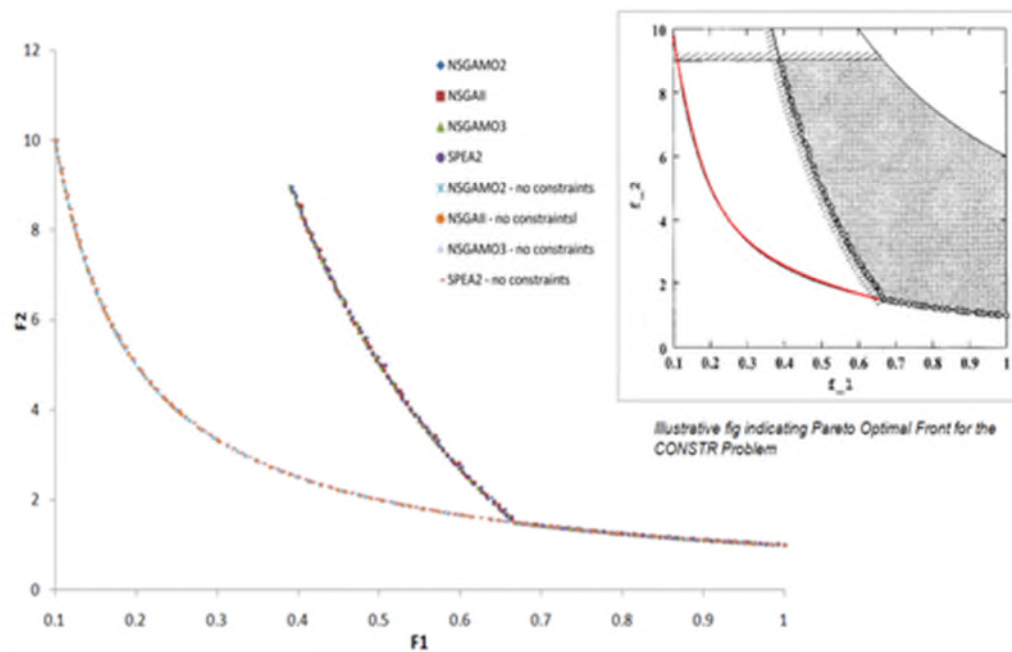


Figure 6.7: CONSTR function Pareto front reached by algorithm [3].

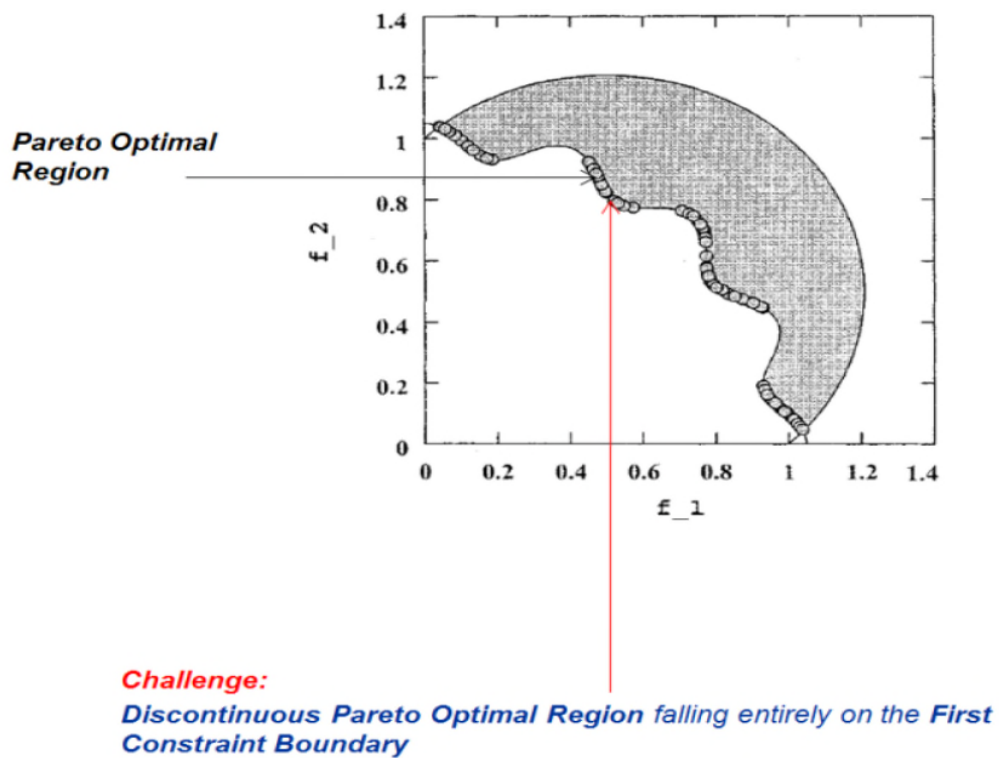


Figure 6.8: Constrained TNK function Pareto curve [3].

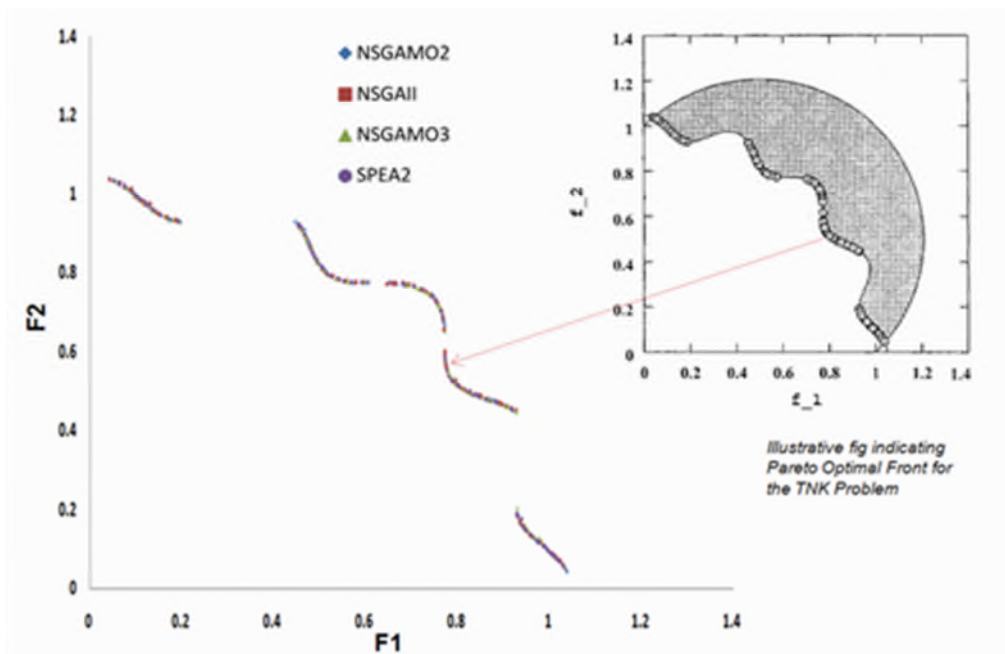


Figure 6.9: TNK function Pareto curves reached by algorithms [3].

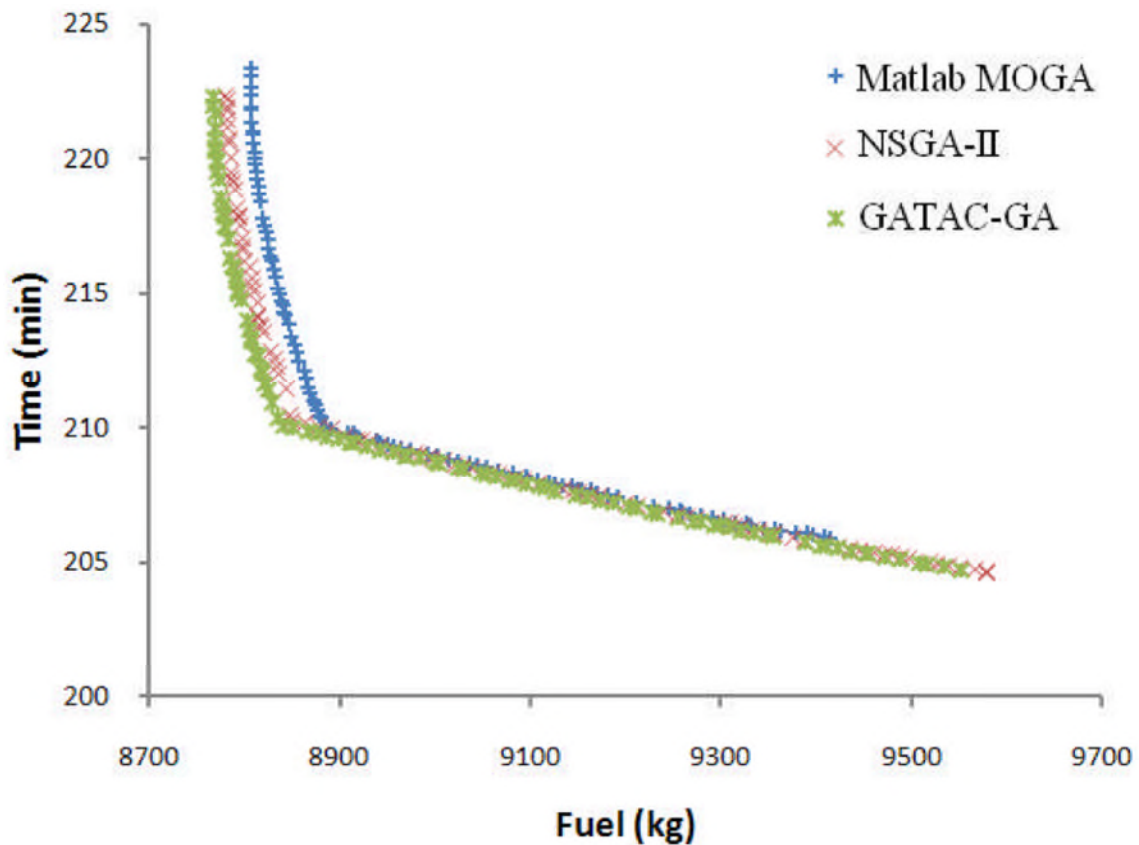


Figure 6.10: Fuel-Time Pareto fronts for a medium range flight [11]

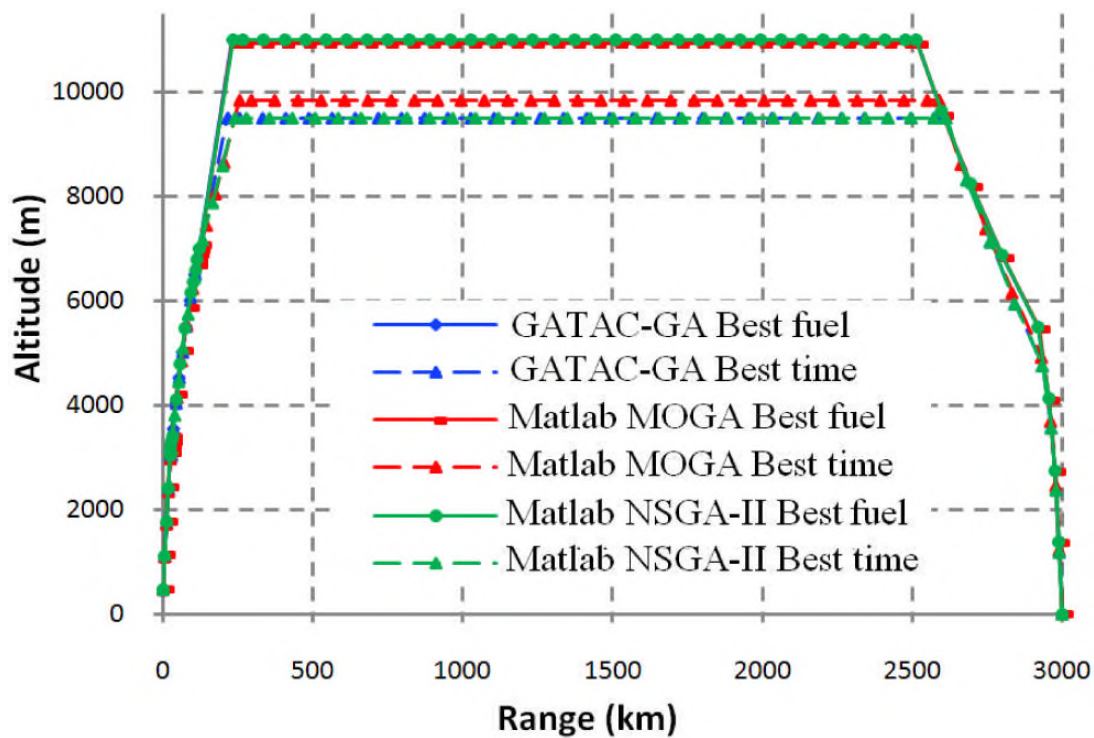


Figure 6.11: Comparison of optimum trajectories for a medium range flight [11].

References for Chapter 6

- [1] <http://science.howstuffworks.com/transport/flight/modern/air-traffic-control1.htm> (accessed December 2013)
- [2] Quaglia, D., Madani, I., Jia, H., Zammit-Mangion, D. (2011). Optimal Trajectories Concepts for Cycle 1, Report number O_3.2.2_3/ SGO-WP 3.2-C-U-OUT-0143, Project Clean Sky SGO ITD, TU Delft, Cranfield University, and University of Malta
- [3] Nalianda, D., K. (2012). Impact of environmental taxation policies on civil aviation – a techno-economic environmental risk assessment, PhD Thesis, Cranfield University
- [4] Fletcher, R. (1987). Practical methods of optimization, 2nd Edition, John Wiley, Chichester, UK
- [5] Rao, S. S. (1996). Engineering optimization: Theory and practice, 3rd Edition, John Wiley, New York, US
- [6] Schwefel, H. P. (1981). Numerical optimization of computer models, John Wiley, Chichester, UK
- [6] Celis, C. (2010). Evaluation and optimisation of environmentally friendly aircraft propulsion system, PhD Thesis, Cranfield University
- [8] Russell, S., and Norvig, P. (2003). Artificial Intelligence: A modern approach, 2nd Edition, Prentice Hall, New Jersey, US
- [9] Quagliarella, D. (1998). Genetic algorithms and evolution strategy in engineering and computer science, recent advances and industrial applications, John Wiley & Sons, Ltd., Chichester, UK
- [10] Sammut, M., Xuereb, M., Chircop, K., Camilleri, W., Dimech, E., Nalianda Karumbaiah, D. and Pervier, H. (2012). GATAC V3 Beta user manual, Clean Sky Report, University of Malta, Cranfield University
- [11] Pervier H., Nalianda D., Marzal Espi R., Sethi V., Pilidis P. Zammit-Mangion D., Rogero J-M., and Entz R., (2011). Application of genetic algorithm for preliminary trajectory optimisation, SAE International, 2011-01-2594
- [12] Deb, K.(2002). Multi objective optimisation using evolutionary algorithms, John Wiley and Sons, New York, USA
- [13] Seshadri, A. (2006). A fast elitist multi-objective genetic algorithm: NSGA-II, MATLAB Implementation

Chapter 7

Case Study: Airport Severity Factors

Abstract

Aircraft take-off from a variety of geographical locations each demanding a different set of operational strategies and power settings for the same TO thrust requirements. The thrust requirements have a bearing on the engine life consumption and in turn the operational cost which is of concern to both the engine manufacturer and the operator. One of the aims of this thesis is to present and give understanding on the implications of airport severity factors and aero-engine component degradation on engine and aircraft performance. The primary objectives are to provide detailed descriptions of the changes in engine life, flight mission fuel burn, DOC and emissions. The aim of this chapter is to present the effects of airport severity factors and engine degradation with the aid of several case studies. In this work, airport severity is the term for operational severity defined by the relationship between the thrust requirement at take-off and the degree of engine life consumption. Airport severity estimation can serve as an aid when making decisions on operational strategies around different airports. This is because the airport environment has a large influence on the engine deterioration rate and on the engine time on the wing. Also, aero-engine operating costs are largely dependent on the life consumption of critical engine parts. In this chapter, severity is calculated as a measure of life consumption and assessments on the implications of airport factors on engine/aircraft performance are presented. The first part of the chapter links engine damage with severity. The second part of the chapter presents the preliminary assessments done using the multidisciplinary framework (described in chapter 1) to establish how the major parameters influence operational severity, and case studies carried out on specific airports (e.g. London Heathrow, Madrid Barajas and Cairo International among others) are also presented. The results show that engine derate will reduce the rate of component damage and result in less flight operating costs. Airports at higher OATs were found to cause increase in the rate of component damage and operating costs per flight. Those at higher altitudes were found to cause increased damage, yet lower the costs. The results also show that degraded engines exhibit higher levels of damage which increases demand on the turbine, further reducing the useful engine life and increasing operating costs per flight.

7.1 Introduction

Aircraft take-off from a variety of geographical locations each demanding a different set off operational strategies and thrust requirements (shown in table 7.1). The thrust requirements have a bearing on the engine life consumption and in turn the operational cost which is of concern to both the engine manufacturer and the operator. Each airport imposes a different thrust

requirement due to the airport environment, outside air temperature (OAT), altitude and other factors affecting engine performance. In the context of the power by hour total care agreements, the manufacturer is in actuality selling component damage accumulation over the useful life of the component at an agreed rate. An understanding of the damage accumulation due to airport severity offers the operator a way of budgeting and making decisions in the operation of the aircraft. The operator can provide guaranteed availability of the engines and a continuous warranty whilst maximising the benefits from the contract.

Table 7.1: Projected thrust requirements relative to reference (ISA SLS) requirements.

| Take Off Airport | Delta from Reference | |
|------------------|----------------------|--------------------------------|
| | Max TO TET [K] | Projected Thrust @ ISA SLS [%] |
| Abu Dhabi | +68.1 | +8.5 |
| Ankara Esenboga | +20.4 | +2.7 |
| Beirut | +32.2 | +4.1 |
| Cairo | +47.5 | +6.0 |
| Dublin | -21.6 | -3.0 |
| London Heathrow | -39.8 | -5.6 |
| Madrid Barajas | +50.2 | +6.3 |
| Riyadh | +89.5 | +11.1 |
| Reference | = | = |

7.2 Operational Severity

Severity is the relative engine damage i.e. the ratio of engine damage for a new mission relative to a reference mission [1] [2]. It can be used as a measure of the life consumption of engine parts subjected to the life limiting modes LCF, creep and oxidation. Operational severity is the damage to the engine that is due to the manner in which the engine/aircraft is deployed (or operated). In this chapter, and for the purposes of this work (i.e. to identify the effects of TO from different airports), operational severity and airport severity will be used interchangeably to refer to the relative damage associated with taking off from different airports. It will be assessed in terms of the relationship between the thrust requirement at take-off and the degree of engine life consumption. Operating conditions considerably influence an engine's time on-wing. Rigorous and more demanding conditions will lead to greater stresses acting on the engine thereby increasing engine wear. The forces of lift, drag, weight and thrust govern the operational parameters. TET and shaft speed are the control parameters to achieve the required thrust at a given operating point. Thrust requirements change according to operational scenarios:

- constant speed level altitude
- constant speed changing altitude
- variable speed level altitude
- variable speed changing altitude

TO thrust is phenomenally high as the aircraft must reach a velocity that is beyond the stall velocity for lift off (need to counter large forces of drag and inertia).

7.2.1 Factors Influencing Severity

The major parameters that influence operating severity include [3]: flight time, TO derate, OAT, altitude and the environment.

7.2.1.1 Flight Time

The length of flight time an engine operates on-wing can be measured in Engine Flight Hours (EFH) and Engine Flight Cycles (EFC). A flight hour is equivalent to one hour of flight, and a flight cycle to one take-off and landing [4]. EFC is the more appropriate measure for engines operating on short-haul flights, whereas EFH are appropriate for engines that are operated on medium and long flight flights. According to [3], an engine operating on a short haul flight will suffer a more rapid performance deterioration, hence shorter shop visit intervals and higher engine maintenance costs per flight hour. Conversely, as the average flight time increases the engine experiences less wear and remains longer on wing with reduced maintenance costs. This is because longer stage length flights have less take-off and climb phases where the engine parts are exposed to particularly high stress levels due to high temperatures and pressures. According to [3], a CFM56-7B operating in the Indian sub-continent with a stage length of 2.2hrs has a Mean Time Between Removals (MTBR) of about 18500hrs whilst a stage length of 2.4hrs has a MTBR of about 20000hrs.

7.2.1.2 Take-Off Derate

Take-Off derate is the percentage reduction of maximum thrust at TO. Derate is a strategy used to lower the EGT thereby reducing the rate of engine component degradation, extending engine time on the wing and reducing engine maintenance costs. It is employed in any of the following situations: take-off weight is below the maximum take-off weight of the aircraft, a long runway is available or the ambient temperatures during take-off are relatively low [4]. TO derate is more beneficial for engines operated on short haul flights than those operated on long-haul flights.

7.2.1.3 Outside Air Temperature

The TO EGT is directly influenced by the outside air temperature. For a given thrust setting, the EGT increases constantly as the OAT increases. In other words, low ambient air temperatures result in low gas path temperatures

and reduced thermal stresses on the engine's hardware. In order to prevent the engine from operating at EGTs that could result in severe damage, flat rating is employed, and the EGT and the Exhaust Gas Temperature Margin (EGTM) are kept constant at all OATs above the flat rating OAT. Flat rating reduces the engine's thrust and prolongs the engine time on the wing [5] [6]. Without flat rating, the EGT would continue to rise with increasing OAT.

7.2.1.4 Altitude

The net thrust performance of an engine is affected by the altitude. As the altitude increases, the ambient static temperature falls linearly as do the ambient static pressure and density. At constant shaft speed, the result is a drop in mass flow which is the dominating influence on thrust. In other words, an engine will lose power with increasing altitude [7]. For the same TO requirements and thrust settings, the performance demand on the engine is to operate at higher spool speeds and higher operating temperatures. The higher speeds and operating temperatures mean the EGT and thermal stresses are also higher resulting in an increase in the rate of engine component damage and reducing the engine time on the wing. In order to prevent the engine from operating at temperatures and EGTs that could result in severe damage, flat rating is employed, and the EGT and the EGTM are kept constant when the aircraft ceiling altitude is reached. As previously mentioned, flat rating reduces the engine's thrust and prolongs the engine time on the wing [5] [6]. Without flat rating, the EGT would continue to rise with increasing altitude.

7.2.1.5 Environment

Environmental conditions contribute to the severity of an engine's operating procedures. Particulate matter such as: dust, sand, industry emissions or volcanic ash can erode compressor blades and block turbine vane/blade cooling holes. Salty environments in coastal areas accelerate corrosion and oxidation of the engine components [3]. Environmental conditions such as these can have a severe impact on the engine's hardware deterioration and thus, on the engine time on the wing. According to [3], an IAE V2500-D5 engine operating in the Middle East has a MTBR of about 4500hrs compared to about 8000hrs in less harsh conditions. The environmental conditions are therefore important for engine performance and deterioration.

7.2.2 Operational Severity Estimation

The severity estimation procedure takes into account the relative damage caused by each of the failure modes discussed in chapter 3.

7.2.2.1 Damage Calculation

A number of cumulative damage laws to determine the amount of damage caused by stress amplitudes are available in literature. The most widely used method and the one adopted for this research is the Palmgren-Miner Rule

(Miner's Law) [8]. The law assumes all the damage fractions add up to unity at which point failure occurs. The damage considered in this work is the sum of cyclic damage due to low cycle fatigue and steady state damage due to the combined effect of creep and oxidation. The damage fraction is defined as the ratio of the time (or cycles) at a given a given power setting to the time (or cycles) to failure at that power setting. Cyclic damage is expressed in terms of cycles to failure, whereas steady state damage is expressed in terms of time (hours) to failure. The damage fraction is expressed in equations 7.1 and 7.2.

$$D_{ci} = \frac{n_i}{N_i} \quad (7.1)$$

$$D_{si} = \frac{t_i}{t_f} \quad (7.2)$$

where

D = damage fraction
 ci = cyclic damage fraction
 si = steady state damage fraction
 n_i = number of cycles at stress amplitude σ_i
 N_i = average number of cycles to failure
 t_i = time at stress amplitude σ_i
 t_f = time to failure

The total damage fraction for TO from a reference and a new airport are given by equations 7.3 and 7.4:

$$(D_{total})_{ref} = (D_{cyclic})_{ref} + (D_{steadystate})_{ref} \quad (7.3)$$

$$(D_{total})_{new} = (D_{cyclic})_{new} + (D_{steadystate})_{new} \quad (7.4)$$

where

$total$ = total damage fraction
 ref = reference case
 new = new case

7.2.2.2 Severity Calculation

The severity is made up of two components: the cyclic part reflecting low cycle fatigue (power transients) and the steady state part reflecting the cumulative effect of creep and oxidation (time at a power condition) [3]. Since severity is relative damage, normalizing equations 7.3 and 7.4 by dividing both equations by the total reference damage fraction $(D_{total})_{ref}$ yields equations 7.5 and 7.6 which are the mathematical representations of severity for the reference and new missions respectively.

$$(\lambda_{total})_{ref} = 1 = (\lambda_{cyclic})_{ref} + (\lambda_{steadystate})_{ref} \quad (7.5)$$

$$(\lambda_{total})_{new} = (\lambda_{cyclic})_{new} + (\lambda_{steadystate})_{new} \quad (7.6)$$

where:

- λ_{total} = total severity
- λ_{cyclic} = cyclic severity
- $\lambda_{steadystate}$ = steady state severity
- $\lambda_{total})_{ref}$ = total severity for reference mission
- $\lambda_{total})_{new}$ = total severity for new mission

The damage pattern is dependent on and changes with engine operation. Cyclic damage is dominant for short haul flights which have frequent TO and landings, whereas steady state damage is dominant for long haul flights. A severity of less than unity means the damage is less and the engine life is longer than for the reference whereas a severity of more than unity means the damage is more and the engine life is shorter than for the reference. Severity is therefore the inverse of engine life. For the studies discussed in this thesis, the steady state severity is the sum total of the blade severity and disc severity i.e. severity due to blade creep, blade oxidation and disc creep, and the cyclic severity is that due to blade fatigue.

7.3 Case Studies: Airport Severity Factors

The purpose of this section is to present the results of studies conducted to identify the effect of changes to airport operational and environmental factors. The life consumption (damage fraction), operating conditions (TET and EGT), DOC per flight, engine life due to creep, fatigue and oxidation, mission fuel burn and ICAO LTO and flight emissions of civil aero-engines are presented. In this study the effect of TO derate, OAT, airport altitude and the airport environment (e.g. sand) on the performance of the HPT were evaluated. In the context of this work, airport severity factors refer to the airport conditions such as OAT, altitude and the environment that will influence the level of damage suffered by the engine. A multi-disciplinary framework (shown in figure 7.1) was used to relate engine operating conditions to flight conditions, translating the power settings imposed by varying airport operational conditions into DOC, emissions and engine life estimates (reflecting severity on the HPT life limiting part). The framework combines the engine performance, aircraft performance, emissions prediction, lifing analysis and economics mathematical models described in chapters 2, 3, 4 and 5.

7.3.1 Severity Estimation Process

The studies were conducted on the CUCCTF engine model and CUSMSA aircraft model described in chapter 2. The studies were conducted in two parts:

- Parametric studies to investigate the effect of operational parameters (TO derate, OAT, altitude and environment)..
- Airport severity factors to investigate the effect of taking off from different airports.

A reference airport at ISA SLS conditions (15°C OAT and sea level) was used in the studies. A mission range of 3000km (1620nm) was used. The flight mission for a clean engine taking off from the reference airport and flying this range (3000km) was assumed as the baseline trajectory. The cruise, descent and approach/landing profiles were kept the same for all the studies. The baseline was chosen to closely approximate and match the performance of the aircraft on the payload range chart [9]. In the context of this study, (airport) severity is defined as the ratio of the damage fraction of the flight mission when taking off from the current airport to the damage fraction of the flight mission when taking off from the reference airport. The following outlined procedure was used for both the parametric and the airport studies. In both cases, the prediction was related to the changes in take-off airport conditions and environment on engine performance:

- The engine performance code TURBOMATCH is used to calculate the take-off thrust, flight segment spool speeds, operating temperatures and cooling flow temperatures and SFC.
- The aircraft performance code HERMES is used to integrate the engine and aircraft and to calculate the flight performance in terms of total mission fuel burn and flight mission time.
- The lifing code is used to estimate the life of the HPT blade and disc (LCF, creep and oxidation) based on metal temperatures, stresses and material properties. The life estimates are converted to damage fractions using the linear damage rule as described in 7.2.2.1.
- The damage fractions calculated by the lifing code are used to estimate the severity for the HPT blade and disc as described in 7.2.2.2.
- The emissions prediction code HEHAESTUS is used to predict the emissions indices for CO₂, NO_x and H₂O for the flight mission.
- The economics model HESTA is used to translate the life estimation into engine/aircraft direct operating costs.

To model the effects of engine degradation changes are made to the flow capacities and efficiencies of key engine components such as Fan, LPC, HPC, LPT and HPT. These component characteristics (flow capacities and efficiencies) are known as health parameters because they indicate the degree of engine degradation. In this work the health parameters are assumed to follow an average degradation profile with a fast initial rise due to rub-in and related new engine degradation mechanisms [10] (Mechanisms of engine component degradation are described in chapter 2). As the engine ages, the health parameters tend towards linear degradation as shown in figure 7.2 [11] [12]. The health parameter values used in this research correspond to 3000, 4500, 5250 and 6000cycles of operation and are shown in table 7.2. These values of degradation represent percentage deviation from the clean (for each parameter the clean is 100%) and are derived from [9]. They correspond to those found in [13] and [14]. According to [13] and [14], these health parameter values assigned to the engine components correspond to moderate to severe degradation such as when the engine is due for overhaul or when the engine is

used in a harsh environment such as a sandy desert or an area of volcanic activity.

Table 7.2: Degradation level for health parameters as a % deviation from clean [13] [14].

| Flight Cycles | Fan | | LPC | | HPC | | HPT | | LPT | |
|---------------|----------|--------|----------|--------|----------|--------|----------|--------|----------|--------|
| | $\eta\%$ | Flow % | $\eta\%$ | Flow % | $\eta\%$ | Flow % | $\eta\%$ | Flow % | $\eta\%$ | Flow % |
| 0 | 0 | 0 | 0 | 0 | 0 | 0 | 0 | 0 | 0 | 0 |
| 3000 | -1.5 | -2.04 | -1.46 | -2.08 | -2.94 | -3.91 | -2.63 | 1.76 | -0.538 | 0.2588 |
| 4500 | -2.18 | -2.85 | -2.04 | -3.04 | -6.17 | -8.99 | -3.22 | 2.17 | -0.808 | 0.3407 |
| 5250 | -2.52 | -3.25 | -2.33 | -3.52 | -7.79 | -11.53 | -3.52 | 2.37 | -0.934 | 0.3880 |
| 6000 | -2.85 | -3.65 | -2.61 | -4.00 | -9.40 | -14.06 | -3.81 | 2.57 | -1.078 | 0.4226 |

7.3.2 Operational Factors

Severity of aero-engines is largely sensitive to operational parameters (such as TO derate and OAT) which directly impact the thermal and mechanical stresses acting on the engine. In the context of this work, studies were done for the purposes of identifying and quantifying the sensitivity of an engine's performance and engine damage to airport factors. Parametric analyses were carried out by varying the a) TO derate from 0% to 30%, b) altitude from 0m to 1500m and c) OAT from -20°C to +20°C. As mentioned earlier, the reference airport was assumed at 0% derate and ISA SLS (15°C OAT and sea level). A full flight mission analysis was carried out in all the case studies. The baseline trajectory was assumed for a clean engine TO from the reference airport on a flight mission range of 3000km. The studies were done for a clean engine and for the same engine with the health parameter values after 3000 cycles of operation. The aircraft performance was analysed in terms of maximum operating temperature, EGT, mission fuel burn, DOC per flight, engine life, ICAO LTO and flight mission emissions and severity. The results presented here are relative to the baseline and are summarised in the following sections. The results have shown that the engine is more likely to fail due to blade fatigue and blade oxidation than due to blade creep and disc creep. Hence only the deltas for the blade fatigue and blade oxidation are presented in these results. The results shown in parentheses (in the section on degraded engine performance) are for the TO from the reference airport after 3000cycles.

7.3.2.1 Clean Engine Performance

- Derated engines operate at reduced thrust levels. A 30% derated engine is found to have a -7.3% reduction in severity, a direct benefit from a -

181K reduction in the operating temperatures. The TO fuel burn reduces by -37.5% with a small benefit of -0.2% in flight operating costs. The derated engine demonstrates a higher blade and disc life, with discrepancies of +15.3% and +7.8% for the blade fatigue and oxidation lives respectively. The ICAO LTO and flight NOx reduce by -23.8% and -2.6% respectively.

- Engine thrust output reduces with rising OATs. A clean engine TO at an OAT deviation of +20°C was found to have a +6% penalty on severity caused by a +102K rise in operating temperatures. There is also a rise of +4.1% in TO fuel burn which contributes to a discrepancy of +0.3% in flight operating costs. The blade life due to fatigue and oxidation reduce by -30% and -5% respectively. The higher operating temperatures increase the ICAO LTO and flight NOx by +13% and +1.4% respectively. A TO at an OAT deviation of -20°C was found to have -10.2% reduction on severity caused by a drop in operating temperatures of -103K. There is also a drop of -4.2% in TO fuel burn and a discrepancy of -0.1% in flight operating costs. The discrepancy in the blade life due to fatigue and oxidation is +16.8% and +11.2% respectively. The lower operating temperatures reduce the ICAO LTO and flight NOx by -9.3% and -0.8% respectively.
- Engine thrust output reduces with increasing altitude. A clean engine TO from an airport 1500m above sea level was found to have a +4.8% and +7.1% increase in severity and TO fuel burn respectively, a consequence of a +109K increase in operating temperatures. Despite these penalties, the fuel burn at climb is -12.4% less and there is a small benefit of -0.5% on the flight operating costs. The blade life due to fatigue and oxidation reduce by -22.1% and -4% respectively. The discrepancy in the ICAO LTO and flight NOx is +2.5% and -4.2% respectively.

7.3.2.2 Degraded Engine Performance

- As expected of degraded engines, it was found that after 3000 cycles the engine operating temperatures are higher, having increased by +54K. In turn the engine severity and mission fuel burn increase by +56.8% and +3.5% respectively, translating into a rise of +1.2% in DOC. The blade life due to fatigue and oxidation reduce by -16.7% and -36.5% respectively. The higher operating temperatures increase the ICAO LTO and flight NOx by +26.1% and +31% respectively.
- A 30% derated engine is found to have -139K (+54K) discrepancy in the operating temperatures and severity of +44.6% (+56.8%). The TO fuel burn is -36.7% (+3.5%) less, which impacts on the flight operating costs by +0.9% (+1.2%). The blade life due to fatigue and oxidation has a discrepancy of +6.7% (-16.7%) and -31.3% (-36.5%) respectively. The ICAO LTO and flight NOx have a discrepancy of -7.8% (+26.1%) and +27.4% (+31%) respectively.
- A TO at an OAT deviation of +20°C was found to have a +71.2% penalty on severity caused by a +159K rise in operating temperatures. There is also a rise of +7.8% in TO fuel burn which contributes to a rise of +1.7%

in flight operating costs. The blade life due to fatigue and oxidation reduce by -47.5% and -39.4% respectively. The higher operating temperatures increase the ICAO LTO and flight NO_x by +44.2% and +32.8% respectively. A TO at an OAT deviation of -20°C was found to have -52K drop in operating temperatures and a +40% penalty on severity. There is also a drop of -0.8% in TO fuel burn and a rise of +1% in flight operating costs. The discrepancy in the blade life due to fatigue and oxidation is +10.6% and -29.1% respectively. The discrepancy in the ICAO LTO and flight NO_x is +13.1% and +29.6% respectively.

- A TO from an airport 1500m above sea level was found to have a +71.1% and +10.4% increase in severity and TO fuel burn respectively, a consequence of a +164K increase in operating temperatures. Despite these penalties, the fuel burn at climb is -8.6% less and there is an impact of +0.8% on the flight operating costs. The blade life due to fatigue and oxidation reduce by -41.6% and -38.9% respectively. The discrepancy in the ICAO LTO and flight NO_x is +32.5% and +25.7% respectively.

7.3.2.3 Discussion of the Results

7.3.2.3.1 Effects of Degradation

As previously discussed in the review of past work (section 1.3) and in chapter 2, engine component degradation has a negative impact on thrust power, specific fuel consumption and operating costs. The results presented in figures 7.3 to 7.27 are in conformity; degraded engines run at higher maximum operating temperatures (and EGTs), have a higher severity and burn more fuel. In addition they produce more emissions, have less time on wing and require maintenance and/or overhaul more frequently due to reduced component lives and cost more to operate.

7.3.2.3.2 Effects of Take-Off Derate

The results from the TO derate parametric analyses are presented in figures 7.3 to 7.10. The parameters are presented as normalised (i.e. divided by the value for the baseline) values, and the baseline is 1.0 in all the figures.

Figure 7.3 shows the engine maximum operating temperature and EGT as a function of varying TO derate. As highlighted above, it was observed that the engine operating temperatures reduce with increasing derate. This reduction may be explained by considering the fact that derate represents a percentage reduction of maximum thrust, and the TO is achieved at lower operating temperatures. The lower thrust requirements and lower operating temperatures translate into lower EGTs, and as shown in figure 7.3 the EGT also reduces with increasing derate.

Figure 7.4 shows the engine severity with varying TO derate. In this figure, the height of the bars represents the total engine severity; the blue shaded region represents the steady state severity contribution and the purple shaded

region the cyclic severity contribution. The results show that the severity reduces as the derate increases. This is largely due to the contribution of the reduction in the steady state severity by -7.2% and -7.6% and in cyclic severity by -10.5% and -21.7% for the clean and after 3000cycles respectively.

Figure 7.5 shows the TO fuel burn with varying TO derate. The results show that the TO fuel burn reduces with increasing derate. It is concluded that the lower thrust requirements and lower operating temperatures at TO result in reduced fuel burn. The taxi, climb, cruise, descent and approach/landing fuel burn remain essentially the same for all cases considered. The reduction in TO fuel burn manifests as a proportional reduction in CO₂ and H₂O emissions.

Figures 7.6 and 7.7 show the NO_x emissions (ICAO LTO and TO, and total flight respectively) with varying TO derate. The results show reductions in the emissions with increasing derate. The LTO and flight NO_x reduce due to the reduction in TO NO_x (by -57% (clean) and -46.5% (after 3000cycles)). The explanation of the reduction may be found in the fact that the production of thermal NO_x is promoted at elevated temperatures, therefore the lower operating temperatures achieved with derate give benefit to lower NO_x levels.

Figure 7.8 and 7.9 show the HPT blade fatigue life and blade oxidation life (respectively) with varying TO derate. The results show that the blade lives are longer with increasing derate. The explanation may be provided by considering the severity and the maximum operating temperatures. Severity as described in section 7.2 is the relative engine component damage for a given mission, and damage is the inverse of life. A key driver of engine life (or damage) is the maximum operating temperature. Therefore a reduction in operating temperatures implies reduced engine damage (hence reduced severity) which means a longer component life.

Figure 7.10 shows the engine DOC per flight with varying TO derate. The results show that there is reduction in the DOC as derate increases. The DOC is calculated as a function of emissions taxes, fuel and maintenance costs. The reduction in fuel costs, emissions taxes and the longer engine component lives therefore contribute to lowering the DOC.

7.3.2.3.3 Effects of Outside Air Temperature

Changes in inlet air conditions will change the level of thrust produced. To minimize engine damage: airliners use higher derate for areas with high OAT, and manufacturers use flat rating up to a certain OAT which allows the combustor temperature to offset the reduction in thrust (beyond flat rating temperature thrust reduces). The results from the OAT parametric analyses are presented in figures 7.11 to 7.18. The parameters are presented as normalised (i.e. divided by the value for the baseline) values, and the baseline is 1.0 in all the figures.

Figure 7.11 shows the engine maximum operating temperature and EGT with varying OAT. The results show that the inlet temperatures have a significant effect on the engine performance. The low ambient air temperatures tend towards lower gas path temperatures whereas the high ambient air

temperatures tend towards higher. The results show the maximum operating temperature rising with increasing OATs and falling with decreasing OATs. Considering a case where the engine is running at a constant shaft speed, the behaviour of the engine is such that, on a cold day (lower OAT) the engine will operate at a higher N/\sqrt{T} and therefore a higher pressure and temperature ratio than during a standard day. At a fixed TET, there will be an increase in the thrust output and thermal efficiency. The reverse is true on a hot day (higher OAT); the engine running at constant shaft speed will operate at lower N/\sqrt{T} (and therefore a lower pressure and temperature ratio) than during a standard day, thereby reducing the thrust output and thermal efficiency at fixed TET. It is concluded that for a given thrust setting, the engine operating temperature is reduced at lower OATs and increased at higher OATs. The lower operating temperatures at low OATs translate into lower EGTs, and the higher operating temperatures at high OATs translate into higher EGTs. These EGT trends are also shown in figure 7.11.

Figure 7.12 shows the engine severity with varying OAT. As with the TO derate, the height of the bars represents the total engine severity with the blue shaded region representing the steady state severity contribution and the purple shaded region the cyclic severity contribution. The results show that the severity rises with increasing OATs and falls with decreasing OATs. The reduction in severity at an OAT of -20°C is largely due to the contribution of the reduction in steady state severity by -10.1% and -10.5% and in cyclic severity by -15.8% and -26.1% for the clean and after 3000cycles respectively. The rise in severity at an OAT of $+20^{\circ}\text{C}$ is largely due to the contribution of the rise in steady state severity by $+3.3\%$ and $+10.5\%$ and in cyclic severity by $+42.1\%$ and $+59\%$ for the clean and after 3000cycles respectively.

Figure 7.13 shows the TO fuel burn with varying OAT. The results show that the TO fuel burn rises with increasing OAT. It is concluded that the lower thrust requirements and lower operating temperatures at the lower OATs result in reduced fuel burn, whilst the opposite is true at the higher OATs. The taxi, climb, cruise, descent and approach/landing fuel burn remain essentially the same for all cases considered. As explained in the discussion on TO derate, the CO_2 and H_2O emissions levels are proportional to the fuel burn.

Figures 7.14 and 7.15 show the NO_x emissions (ICAO LTO and TO and total flight respectively) with varying TO OAT. The results show a rise in the emissions with increasing OAT. The NO_x rises for the same reasons explained in the derate analysis. In this case, the TO NO_x for the clean and after 3000cycles rises by $+75.3\%$ and $+28.5\%$ respectively at an OAT of $+20^{\circ}\text{C}$ and reduces by -20.4% and -5.6% respectively at an OAT of -20°C .

Figures 7.16 and 7.17 show the HPT blade fatigue life and the blade oxidation life (respectively) with varying OAT. The results show that the blade and disc lives are reduced with increasing OAT. As explained with derate, the engine component lives are largely influenced by the maximum operating temperatures and severity. At lower OATs because the temperatures and severity are low (-103K and -10.2% respectively at -20°C OAT for a clean engine), the HPT fatigue (and oxidation) life is $+16.8\%$ ($+11.2\%$) longer. At

higher OATs the opposite is true, temperatures and severity are +102K and +6% higher respectively, the fatigue (and oxidation) life is -30% (-5%) shorter.

Figure 7.18 shows the engine DOC per flight with varying OAT. The results show that as the OATs reduce, the DOC reduces, and as the OATs rise, the DOC increases. As explained with the results on TO derate, the contribution to the DOC comes from the fuel costs, emissions taxes and the engine component lives; lower fuel costs, less emissions taxes and longer lives reduce DOC.

7.3.2.3.4 Effects of Airport Altitude

The results from the airport TO altitude parametric analyses are presented figures 7.19 to 7.27. As with the other studies already presented, the parameters are presented as normalised (i.e. divided by the value for the baseline) values and the baseline is 1.0 in all the figures.

Figure 7.19 shows the engine maximum operating temperature and EGT with varying airport altitude. As already presented prior, the results show the maximum operating temperature rising with increasing altitude. The reduction of thrust output with increase in altitude warrants higher operating temperatures to compensate a given thrust requirements. The higher operating temperatures translate into higher EGTs, and as shown in figure 7.19 the EGT also increases with increasing altitude.

Figure 7.20 shows the engine severity with varying altitude. The results are presented in the same manner as the other two case studies. The results show that the severity rises with increasing altitude. This increase is largely due to the increase in both the cyclic (+28.4% and +71.2%) and steady state severity (+4.4% and +71.3%) for the clean and after 3000cycles respectively. It is concluded that the higher operating temperatures and higher EGTs increase both the steady state and cyclic engine component damage fractions.

Figure 7.21 shows the TO and climb fuel burn with varying altitude. The results show that the TO fuel burn rises with increasing altitude. The rise is attributed to the higher operating temperatures needed to produce the required thrust at higher altitude. The climb fuel burn was found to be lower at higher TO altitude because for the same ToC (cruise altitude), the climb is shorter and less fuel is burned to reach ToC for the higher altitudes. The cruise, descent and approach/landing fuel burn remain essentially constant.

Figure 7.22 shows the total flight mission fuel burn with varying TO altitude. The results show that there is a reduction in mission fuel burn with increasing altitude. It is concluded that the benefit in climb fuel dominates and outweighs the rise in TO fuel burn resulting in an overall reduction in flight mission fuel burn. The reduction in mission fuel burn gives a proportional reduction in mission CO₂ and H₂O.

Figure 7.23 shows the ICAO LTO and TO NOx the emissions with varying altitude. The normalised ICAO LTO NOx for the reference is 1.0. The results show that the ICAO LTO and TO NOx emissions rise with increasing altitude.

The rise in TO NO_x translates into a rise in LTO NO_x. The NO_x rise for the same reason explained for the higher OATs i.e. higher operating temperatures.

Figure 7.24 shows the climb and flight mission NO_x with varying altitude. The results show that there is a reduction in climb NO_x with increasing altitude. It is concluded that the reduction in fuel burn and flight time during this segment results in a reduction in NO_x (thrust requirements and power settings being the same). Since the cruise, descent and approach/landing NO_x emissions remain essentially constant, the flight mission NO_x is influenced by the TO and climb NO_x. The reduction in climb NO_x benefits the flight mission NO_x which reduces with increasing TO altitude.

Figures 7.25 and 7.26 show the HPT blade fatigue life and the blade oxidation life (respectively) with varying TO altitude. The results show that the blade and disc lives are lower at higher TO altitudes. As explained for the other cases, this is attributed to the higher operating temperatures required, which increase both the steady state and the cyclic damage to the engine components thereby reducing the component life.

Figure 7.27 shows the engine DOC per flight with varying TO altitude. The results show that there is a reduction in the DOC with increasing TO altitude. Again as with the other two cases, the reduction in fuel costs, emissions taxes and the longer engine component lives contribute to lowering the DOC.

7.3.3 Airport Severity Factors

Airport factors such as the environment, outside air temperature (OAT) and altitude impose different power settings for the same TO thrust requirements and thus affect the engine performance and life consumption. This section presents the results of case studies conducted for take-off from different airports. The studies were carried out to assess the influence of airport factors (location and the environment) on aircraft performance and severity. As with the case studies on operational factors and as mentioned earlier, the reference airport was assumed at 0% derate and ISA SLS (15°C OAT and sea level). The same baseline trajectory was assumed i.e. a clean engine TO from the reference airport on a flight mission range of 3000km.

The various airports used in these studies are shown in table 7.3. The table also shows the conditions specific to each airport. The average high temperature for the year was chosen as the OAT for each airport. The studies were carried out for a clean engine for all the airports without considering the type and effects of the environment. For the degraded engine case studies the environment conditions and effects were considered. The degraded case considered in these studies corresponds to the health conditions of the engine after 3000 cycles of operation.

Table 7.3: Airport environmental conditions [15] [16] [17] [18] [19].

| Airport | Elevation [m] | OAT [°C] | Humidity [%] | Environment [-] |
|-----------------|--------------------------|---------------------|-------------------------|----------------------------|
| Abu Dhabi | 27 | 31 | 26 | Hot Desert |
| Ankara Esenboga | 953 | 10 | 87 | Dry Summer Continental |
| Beirut | 27 | 24 | 83 | Hot Summer Mediterranean |
| Cairo | 116 | 26 | 46 | Hot Desert |
| Dublin | 74 | 13 | 66 | Maritime |
| London Heathrow | 25 | 10 | 93 | Oceanic |
| Madrid Barajas | 610 | 20 | 72 | Mediterranean |
| Riyadh | 635 | 27 | 15 | Hot Desert |
| Reference | 0 | 15 | 55 | Mediterranean |

The effect of airport environmental conditions on engine degradation is acknowledged in this work. In this context, for the degraded engine assessments, a further step was taken to investigate the hot and sandy desert conditions at airports such as Abu Dhabi, Cairo and Riyadh. Higher levels of degradation corresponding to engine conditions after 5250 cycles of operation were assumed for these airports. Due to the unavailability of a modelling tool to model and capture the effects of the environment (e.g. sand, ice, hot) on levels of degradation, the level of degradation attributed to the environment was introduced at the discretion of the author based on information gathered from available literature. As mentioned in section 7.3.1, the values used were based on information available in [10] [11] [12] [13] and [14].

The author realizes and acknowledges that the levels of degradation in practice could vary from those chosen. In this regard, a sensitivity analysis for degradation after 4500, 5250 and 6000cycles was conducted for Abu Dhabi, Cairo and Riyadh airports. This analysis was conducted to identify the 'risk factors' of using 5250cycles that could greatly affect the evaluation. The sensitivity to the level of degradation of some chosen specific performance parameters is shown in table 7.4. The 5250cycles was chosen by the author as representative of the desert conditions at these airports as suggested by [12] that it represents harsh and severe conditions such as desert conditions.

The influence of airport factors are presented by plotting the changes to the maximum operating temperatures, EGTs, severity, mission fuel burn, engine life, DOC per flight, ICAO LTO NO_x and flight mission emissions. The results are shown in figures 7.28 to 7.35 and are presented relative to the baseline.

Table 7.4: Performance parameter sensitivity analysis.

| Airport | Performance Metric | 3000cycles [%] | 4500cycles [%] | 5250cycles [%] | 6000cycles [%] |
|-----------|--------------------------|----------------|----------------|----------------|----------------|
| Abu Dhabi | Flight Mission Fuel Burn | +3.7 | +9.1 | +13.6 | +22.2 |
| | Total Severity | +63.9 | +225.6 | +392.6 | +849.9 |
| | Blade Fatigue Life | -37.7 | -52.9 | -61.4 | -71.3 |
| | Blade Oxidation Life | -38.7 | -68.8 | -78.7 | -86.8 |
| | DOC per Flight | +1.5 | +4.0 | +5.9 | +9.1 |
| | ICAO LTO NOx | +37.5 | +85.2 | +120.8 | +171.6 |
| | Total Flight NOx | +32.2 | +89.1 | +136.0 | +241.9 |
| Cairo | Flight Mission Fuel Burn | +2.7 | +7.6 | +12.0 | +21.1 |
| | Total Severity | +61.6 | +208.4 | +347.7 | +641.1 |
| | Blade Fatigue Life | -31.4 | -47.3 | -56.7 | -67.7 |
| | Blade Oxidation Life | -38.1 | -67.6 | -77.4 | -85.2 |
| | DOC per Flight | +1.1 | +3.2 | +5.1 | +8.7 |
| | ICAO LTO NOx | +36.6 | +84.1 | +119.3 | +175.9 |
| | Total Flight NOx | +28.5 | +83.4 | +132.7 | +230.6 |
| Riyadh | Flight Mission Fuel Burn | +2.1 | +7.6 | +12.0 | +21.2 |
| | Total Severity | +64.8 | +231.6 | +434.9 | +1433.7 |
| | Blade Fatigue Life | -40.0 | -56.0 | -65.0 | -75.3 |
| | Blade Oxidation Life | -38.4 | -68.0 | -77.7 | -85.3 |
| | DOC per Flight | +0.8 | +3.4 | +5.3 | +9.0 |
| | ICAO LTO NOx | +40.2 | +90.1 | +126.3 | +177.6 |
| | Total Flight NOx | +28.7 | +84.5 | +133.1 | +231.4 |

7.3.3.1 Clean Engine Performance

The results of the studies conducted for the clean engine are summarised as follows.

- A clean engine TO from Abu Dhabi International airport was observed to require +68K higher operating temperatures which greatly impact on severity and TO fuel burn, causing an increase of +4.1% and +2.8% respectively. The blade fatigue life and blade oxidation life reduce by -19.4% and -3.7% respectively. The flight costs have a discrepancy of +0.2%.

- A clean engine TO from Ankara International airport was observed to require +20K higher operating temperatures. There is no change in severity, but the TO fuel burn increases by +2.4%. There is however benefit to the climb fuel burn, which reduces by -9.4% to give a slight reduction in flight costs of -0.5%. The blade fatigue life has a marginal change of -0.4%, with blade oxidation life relatively unchanged.
- A clean engine TO from Beirut International airport was observed to require +32K higher operating temperatures which negatively impacts on severity and TO fuel burn, causing an increase of +2.2% and +1.3% respectively. There is however little impact on flight costs which have a discrepancy of approximately +0.1%. The blade fatigue life and blade oxidation life reduce by -8.7% and -2% respectively.
- A clean engine TO from Cairo International airport was observed to require +48K higher operating temperatures with negative implications on severity and TO fuel burn, which increase by +3% and +2% respectively. There is however benefit to the climb fuel burn, which reduces by -6.2% to give a slight reduction in flight costs of -0.2%. The blade fatigue life and blade oxidation life reduce by -13% and -2.6% respectively.
- A clean engine TO from Dublin International airport was observed to require -22K lower operating temperatures which reduces severity and TO fuel burn by -1.8% and -0.8% respectively. There is however little benefit on flight costs with a discrepancy of approximately -0.1%. The blade fatigue life and blade oxidation life are better by +5.5% and +1.8% respectively.
- A clean engine TO from London Heathrow International airport was observed to require -40K lower operating temperatures, with great benefits to severity and TO fuel burn, which reduce by -3.4% and -1.6% respectively. There was however little impact on flight costs which have a discrepancy of approximately -0.1%. The blade fatigue life and blade oxidation life are better by +9.1% and +3.4% respectively.
- A clean engine TO from Madrid Barajas International airport was observed to require +50K higher operating temperatures, with negative impact on severity and TO fuel burn, which increase by +2.5% and +3% respectively. There is however benefit to the climb fuel burn, which reduces by -6.2% to give a slight benefit to flight costs of -0.3%. The blade fatigue life and blade oxidation life reduce by -10.6% and -2.2% respectively.
- A clean engine TO from Riyadh International airport was observed to require +89K higher operating temperatures, with negative impact on severity and TO fuel burn, which increase by +4.6% respectively. There is however benefit to the climb fuel burn, which reduces by -6.2% to give a slight benefit to flight costs of -0.2%. The blade fatigue life and blade oxidation life reduce by -22.1% and -3.9% respectively.

7.3.3.2 Degraded Engine Performance

The results of the studies conducted for the degraded engine are summarised as follows. The results in parentheses are for TO from the reference airport after 3000cycles.

- A TO from Abu Dhabi International airport with an engine after 3000cycles was observed to require +124K (+54K) higher operating temperatures, with negative impact on severity and TO fuel burn, causing an increase of +63.9% (+56.8%) and +6.4% (+5.4%) respectively. The impact on flight costs which have a discrepancy of +1.5% (+1.2%) is more to do with degradation rather than the airport. The blade fatigue life and blade oxidation life reduce by -37.7% (-16.6%) and -38.7% (-36.5%) respectively. A TO from Abu Dhabi with an engine after 5250cycles was observed to require +189K higher operating temperatures, with negative impact on severity and TO fuel burn, causing an increase of +393% and +11% respectively. The sandy desert conditions are harsh on the engine's health and fuel burn performance, and a large penalty is paid in flight operating costs which have a discrepancy of +6%. The blade fatigue life and blade oxidation life reduce by -61.4% and -78.7% respectively.
- A TO from Ankara International airport with an engine after 3000cycles was observed to require +72K higher operating temperatures. The severity and TO fuel burn increase by +57% and +5.7% respectively. There is benefit to the climb fuel burn, which reduces by -4.4% and the discrepancy in flight costs is +0.7%. The blade fatigue life and blade oxidation life reduce by -17.5% and -36.6% respectively.
- A TO from Beirut International airport with an engine after 3000cycles was observed to require +88K higher operating temperatures, with negative impact on severity and TO fuel burn, causing increase of +60.2% and +5% respectively. The discrepancy of +1.35% in flight costs seems to be more to do with degradation rather than the airport. The blade fatigue life and blade oxidation life reduce by -26.7% and -37.7% respectively.
- A TO from Cairo International airport with an engine after 3000cycles was observed to require +104K higher operating temperatures, with negative impact on severity and TO fuel burn, causing increase of +61.6% and +5.7% respectively. There is however benefit to the climb fuel burn of -2%, and the flight costs have a discrepancy of +1.1%. The blade fatigue life and blade oxidation life reduce by -31.4% and -38.2% respectively. A TO from Cairo with an engine after 5250cycles was observed to require +168K higher operating temperatures, with negative impact on severity and TO fuel burn, causing increase of +348% and +10.2% respectively. The engine's health and fuel burn performance suffer from the harsh sandy desert conditions, and a large penalty is paid in flight operating costs which have a discrepancy of +5.1%. The blade fatigue life and blade oxidation life reduce by -56.7% and -77.4% respectively.

- A TO from Dublin International airport with an engine after 3000cycles was observed to require +32K higher operating temperatures, causing severity and TO fuel burn to increase by +53.8% and +2.8% respectively. The flight costs have a discrepancy of +1.2%. These penalties however seem to arise from the engine degradation rather than the airport as evidenced by the airport performance of clean engine. The blade fatigue life and blade oxidation life reduce by -9.7% and -35.4% respectively.
- A TO from London Heathrow International airport with an engine after 3000cycles was observed to require +13K higher operating temperatures, causing severity and TO fuel burn to increase by +51.3% and +1.9% respectively. The discrepancy in flight costs is +1.1%. These penalties however seem to arise from the engine degradation rather than the airport as evidenced by the airport performance of clean engine. The blade fatigue life and blade oxidation life reduce by -4.5% and -38.5% respectively.
- A TO from Madrid Barajas International airport with an engine after 3000cycles was observed to require +103K higher operating temperatures, with negative impact on severity and TO fuel burn, causing increase of +60.8% and +6.4% respectively. There is however benefit to the climb fuel burn of -2.1% to give a +0.9% discrepancy in flight costs. The blade fatigue life and blade oxidation life reduce by -28.6% and -34.3% respectively.
- A TO from Riyadh International airport with an engine after 3000cycles was observed to require +143K higher operating temperatures, with negative impact on severity and TO fuel burn, causing increase of +64.8% and +8% respectively. There is however benefit to the climb fuel burn of -2.2% to give a +0.7% discrepancy in flight costs. The blade fatigue life and blade oxidation life reduce by -40.2% and -37.9% respectively. A TO from Riyadh with an engine after 5250cycles was observed to require +212K higher operating temperatures, with negative impact on severity and TO fuel burn, causing increase of +435% and +12.8% respectively. The engine's health and fuel burn performance suffer from the harsh sandy desert conditions, and a large penalty is paid in flight operating costs which have a discrepancy of +5.3%. The blade fatigue life and blade oxidation life reduce by -64.9% and -77.7% respectively.

7.3.3.3 Discussion of the Results

As with the case studies on operational factors, the parameters are presented as normalised and the baseline is 1.0 in all the figures. Since the performance trends are similar for both the clean and the degraded engines, only the clean engine results will be used for reference in these discussions.

Figure 7.28 shows the engine maximum operating temperature and EGT as a function of the TO airport. The results show that for the airports Abu Dhabi, Beirut, Cairo, Madrid and Riyadh which are at higher TO altitudes and higher OATs, the maximum operating temperatures are higher than for the reference

airport. Riyadh was found to require the highest operating temperatures, an increase of +89K for the clean engine. As discussed previously in the studies on OATs and TO altitude, the same thrust requirements push the operating temperatures up at higher TO altitudes and OATs. The higher operating temperatures at these airports translate into higher EGTs. Ankara, at a higher TO altitude and lower OAT requires a rise of +20K in operating temperatures. It is concluded that the effect of the higher TO altitude towards higher operating temperatures dominates and outweighs the effect of the lower OAT towards reduced operating temperatures. The higher operating temperatures translate into higher EGTs. The results for Dublin and London which are at higher TO altitudes and lower OATs show a reduction in the maximum operating temperatures compared to the reference. London requires the lowest operating temperatures, and has a discrepancy of -40K. It seems the lower OATs dominate the higher TO altitudes to lower the operating temperatures required at these airports. The lower operating temperatures translate into lower EGTs.

Figure 7.29 shows engine severity as a function of the TO airport. The results show that for the airports Abu Dhabi, Beirut, Cairo, Madrid and Riyadh, the severity is higher due to the higher operating temperatures and EGTs. A TO from Riyadh inflicts the most engine damage, with an increase of +4.6% in severity. The results show that the TO from Ankara has a similar level of damage as the reference airport. Dublin and London airports have a lower severity due to the lower operating temperatures and lower EGTs. London inflicts the least damage and has a discrepancy in severity of -3.4%.

Figure 7.30 shows the TO and the climb fuel burn as a function of the TO airport. The results show that for the airports Abu Dhabi, Beirut, Cairo, Madrid and Riyadh, the higher operating temperature conditions at TO result in more fuel burn. A TO from Riyadh increases TO fuel burn the most by +4.6%. Ankara also experiences an increase in TO fuel burn due to the higher operating temperatures. Dublin and London benefit from a lower TO fuel burn due to the lower operating temperatures. The results show that for Abu Dhabi, Beirut, Dublin and London with TO altitudes of +27m, +27m, +74m and +25m respectively, the climb fuel burn remains essentially the same as for the reference. This is because at these airports the climb phase begins after the initial climb (end altitude of 457.2m) and remains unchanged. Ankara, Cairo, Madrid and Riyadh with TO altitudes of 953m, 116m, 610m and 635m respectively have an initial climb that ends higher up and closer to ToC than the reference and therefore require less fuel (-9.4% for Ankara and -6.2% for the others) to reach ToC. The cruise, descent and approach/landing fuel burn remain essentially the same as for the reference.

Figure 7.31 shows the flight mission fuel burn as a function of the TO airport. The results show that for Abu Dhabi and Beirut, the rise in TO fuel burn translates into an increase in flight mission fuel burn. For Dublin and London, the flight mission fuel burn levels are similar to the reference. This is because the TO is the sole contributor to the change in flight fuel burn. For Ankara, Cairo, Madrid and Riyadh, the reduced climb fuel burn dominates the increase at TO and gives a proportional reduction in flight mission fuel burn.

Figure 7.32 shows the ICAO LTO, TO, climb and flight NO_x emissions as a function of the TO airport. The results show that for the airports Abu Dhabi, Beirut, Cairo, Madrid and Riyadh, the ICAO LTO NO_x emissions are higher than for the reference airport. Ankara was found to have a +1.2% increase in ICAO LTO NO_x emissions levels. As discussed previously, the higher operating temperatures and fuel burn at TO from these airports increases the NO_x levels produced. For Dublin and London the ICAO LTO NO_x emissions are lower than for the reference airport. This is due to the lower operating temperatures and fuel burn at TO. The results show that for Abu Dhabi and Beirut, the rise in TO NO_x translates into an increase in the total flight NO_x. For Dublin and London, the fall in TO NO_x translates into a fall in total flight NO_x. For Ankara, Cairo, Madrid and Riyadh, the reduction in climb fuel burn dominates to give a reduction in flight NO_x.

Figures 7.33 and 7.34 show the HPT blade fatigue life and blade oxidation life (respectively) as a function of the TO airport. The results show that for Abu Dhabi, Beirut, Cairo, Madrid and Riyadh the blade and disc lives are shorter due to elevated temperatures and higher severity. For Ankara the blade and disc lives are shorter, again due to the elevated temperatures. TO from Dublin and London give better blade and disc lives due to the reduced operating temperatures and lower severity.

Figure 7.35 shows the engine DOC per flight as a function of the TO airport. The results show that for Abu Dhabi and Beirut, the DOC per flight is slightly higher. For Ankara, Cairo, Dublin, London, Madrid and Riyadh, the DOC per flight are slightly lower than the reference. As previously discussed, DOC is a function of the fuel and engine maintenance costs. It is concluded that for the airports at the higher altitudes such as: Ankara, Cairo, Madrid and Riyadh, the reduction in fuel costs outweigh the increase in costs associated with engine maintenance and lower component life to benefit the DOC. For Abu Dhabi and Beirut, the increase in fuel burn and reduced component life combine to give an increase in DOC. For Dublin and London, the lower fuel burn and longer component life combine to lower the DOC.

Table 7.5 shows the rankings of each airport for selected performance parameters according to the aircraft's performance.

7.4 Summary and Conclusions

The main aim of this chapter was to present severity as a measure of life consumption. For the purposes of this work, severity was defined as the relative engine damage. The first part of the chapter therefore involved linking engine damage with severity. TO derate, OAT and altitude were identified as major parameters affecting severity and these were used as variables in the parametric analyses. Assessments were made to assess the effects of airport factors on engine component damage and aircraft performance. These were presented in the second part of the chapter with the aid of several case studies.

The case studies were conducted on the CUCCTF engine model and CUSMSA aircraft model described in chapter 2.as follows:

- Parametric studies to relate severity to operational parameters such as TO derate, OAT, altitude and the environment.
- Airport severity factors to relate severity with taking off from seven different airports including London Heathrow, Ankara International and Madrid Barajas among others.

Table 7.5: Airport performance ranking per parameter.

| Performance Metric | | Abu Dhabi | Ankara | Beirut | Cairo | Dublin | London | Madrid | Riyadh |
|----------------------|---------|-----------|--------|--------|-------|--------|--------|--------|--------|
| Fuel Burn | TO | 3 | 4 | 6 | 5 | 7 | 8 | 2 | 1 |
| | Climb | 1 | 3 | 1 | 2 | 1 | 1 | 2 | 2 |
| | Mission | 1 | 8 | 2 | 6 | 3 | 4 | 7 | 5 |
| Total Severity | | 2 | 6 | 5 | 3 | 7 | 8 | 4 | 1 |
| Blade Creep Life | | 2 | 6 | 5 | 3 | 7 | 8 | 4 | 1 |
| Disc Creep Life | | 2 | 6 | 5 | 4 | 7 | 8 | 3 | 1 |
| Blade Fatigue Life | | 2 | 6 | 5 | 3 | 7 | 8 | 4 | 1 |
| Blade Oxidation Life | | 2 | 6 | 5 | 3 | 7 | 8 | 4 | 1 |
| DOC per Flight | | 1 | 8 | 2 | 6 | 3 | 4 | 7 | 5 |
| ICAO LTO NOx | | 2 | 6 | 5 | 3 | 7 | 8 | 4 | 1 |
| Total Flight NOx | | 1 | 8 | 2 | 6 | 3 | 4 | 7 | 5 |

1 - Worst e.g. highest fuel burn, lowest life

8 - Best e.g. lowest fuel burn, highest life, lowest costs

NB: Rankings assumed for a new engine performance

A baseline performance was established to enable comparison and have a point of reference. It was assumed by matching it to the payload range performance of the Boeing 737-800 after which it was modelled. Changes were made to the health parameters so as to model the effects of engine degradation. A generic multi-disciplinary integration framework was used to make techno-economic preliminary assessments to enable analyses of airport factors and engine component degradation on engine/aircraft performance. The models used were validated and verified as described in chapters 2, 3, 4, and 5.

An important factor to note when analyzing the results, is that the numerical values presented here are not definitive (or absolute), but rather relative and indicative for the purpose of showing the trends of the effects of airport factors and aero-engine component degradation and importantly, providing insight into the engine's behaviour. The major observations made from case studies are summarised as follows (NB: The results presented in this summary and conclusions are for the clean engine, the degraded engine displayed similar trends which have not been repeated here):

- In view of the findings from the TO derate parametric analysis, it is concluded that compared to the reference engine, a derated engine

operates at lower temperatures (a 30% derated engine had a -181K reduction in the operating temperatures). The reduced temperatures caused a reduction of -7.3% in severity, in turn promoting the blade oxidation life and blade fatigue life by +15.3% and +7.8% respectively. The TO fuel burn reduces by -37.5%. The benefit from the flight operating costs seems marginal at -0.2%, but this is only because the contribution from the other phases is unchanged. The lower operating temperatures also give benefit to the ICAO LTO NOx emissions.

- It was observed that a rise in OAT caused the engine severity to increase and engine life to reduce. A clean engine TO at an OAT deviation of +20°C was found to have a +6% penalty on severity caused by a +102K rise in operating temperatures. The TO fuel also increased resulting in a marginal increase of +0.3% in flight operating costs. The blade life due to fatigue and oxidation reduce by -30% and -5% respectively. The higher operating temperatures increase the ICAO LTO and flight NOx by +13% and +1.4% respectively. A TO at an OAT deviation of -20°C was found to have -10.2% reduction on severity caused by a drop in operating temperatures of -103K. There is also a drop in TO fuel burn, ICAO LTO and flight NOx and -0.1% in flight operating costs. The blade and disc life are longer. In view of these findings, from the OAT parametric analysis, it is concluded that derating an engine at the higher OATs would benefit the engine by reducing the high operating temperatures and the severity. The fuel burn and emissions would reduce as well.
- A clean engine TO from an airport 1500m above sea level was found to have a +4.8% and +7.1% increase in severity and TO fuel burn respectively, a consequence of a +109K increase in operating temperatures. Despite these penalties, the fuel burn at climb is -12.4% less and there is a small benefit of -0.5% on the flight operating costs. The blade life due to fatigue and oxidation reduce by -22.1% and -4% respectively. The discrepancy in the ICAO LTO and flight NOx is +2.5% and -4.2% respectively. In view of the findings from the TO altitude parametric analysis, it is concluded that in the same manner as for the high OATs, derate would also benefit TO from high altitude airports.
- In view of the findings for TO from the specified airports, it is concluded that individual airports with differing environments, outside air temperatures (OAT) and altitudes impose different thrust requirements and varying effects on the engine/aircraft performance. Compared to the reference airport, higher altitude and higher OAT airports such as Abu Dhabi (+27m, +16°C) and Beirut (+27m, +9°C), impose higher operating temperatures, +68K and +32K respectively. As a consequence, engine severity is greater (+4.2% and +2.2% respectively) which implies less blade and disc component life. The higher operating temperatures and higher OATs at these airports result in more TO fuel burn (+2.8% and +1.3% respectively), higher levels of NOx emissions, and marginally (+0.2% and 0.1%) higher operating costs per flight.

Compared to the reference airport, higher altitude and higher OAT airports such as Cairo (+116m, +11°C) and Riyadh (+635m, +12°C)

impose higher operating temperatures and EGTs. As a consequence, the severity is greater by +3% and +4.6% respectively and there is more steady state and cyclic damage to blade and disc. The higher operating temperatures and higher OATs at these airports result in more TO fuel burn (+2% and +4.6%) and higher levels of NOx emissions. However, the higher TO altitudes reduce the climb fuel burn (-6.2% respectively) and marginally reduce the operating costs per flight.

Compared to the reference airport, Madrid at a higher TO altitude (+610m) and higher OAT (+5°C) imposes higher operating temperatures and EGTs. As a consequence, the severity is +2.5% greater, which implies the blade and disc life are shorter. The higher operating temperatures and higher OATs at this airport result in more TO fuel burn (+3%) and higher levels of NOx emissions. However, the higher TO altitude results in less climb (-6.2%) and marginally (-0.3%) less operating costs per flight.

Compared to the reference airport, Dublin and London with higher TO altitudes (+74m and +25m) and lower OATs (-2°C and -5°C) impose lower operating temperatures and EGTs, resulting in less severity (-1.8% and -3.4% respectively) and longer blade and disc life. The lower operating temperatures (-22K and -40K respectively), result in less TO fuel burn (-0.8% and -1.6%), and lower levels of NOx emissions, marginally reducing the operating costs per flight.

Compared to the reference airport, Ankara, with a higher TO altitude (+953m) and lower OAT (-5°C), the effect of the higher TO altitude seems to dominate and the operating temperatures and TO fuel burn increase (+20K and +2.4% respectively). The climb fuel is less at -9.4%.

In conclusion, the studies have shown that airports at higher altitudes suffer more severity due to higher operating temperatures, but benefit from less climb fuel burn and lower operating costs. The severity and fuel burn for take-off at higher OAT was found to be more due to higher operating temperatures. As a result, the higher altitude, higher OAT airports demonstrated shorter engine life. The operating costs were consequentially higher due to an increase in fuel and maintenance costs. TO derate was shown to benefit the engine and aircraft's performance parameters, giving better engine life and reducing both emissions and operating costs.

Figures for Chapter 7

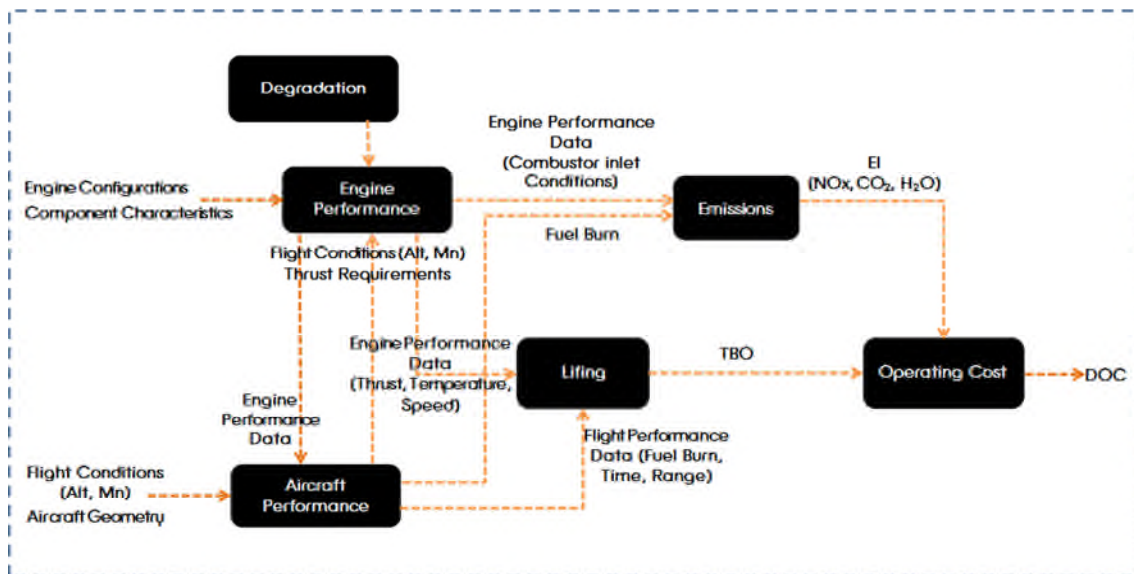


Figure 7.1: Simplified flow diagram of multi-disciplinary framework

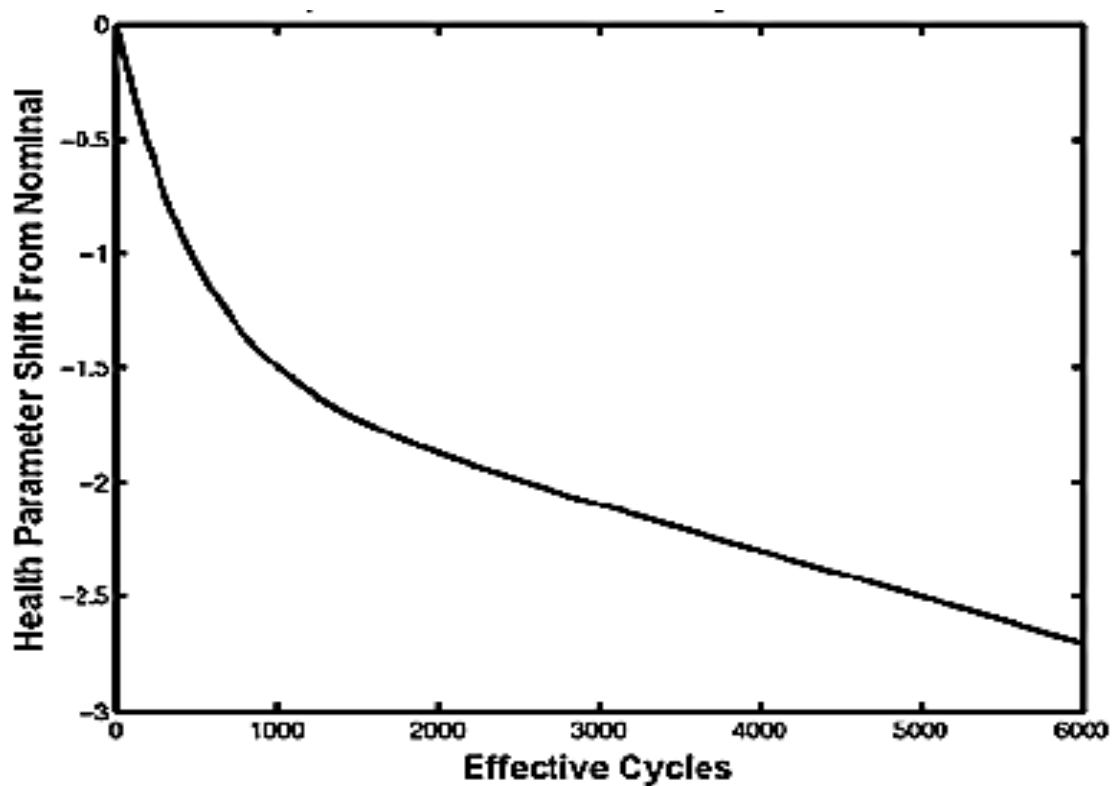


Figure 7.2: Typical degradation profile for a health parameter. Most health parameters decrease with wear, turbine flows increase with wear [11] [12].

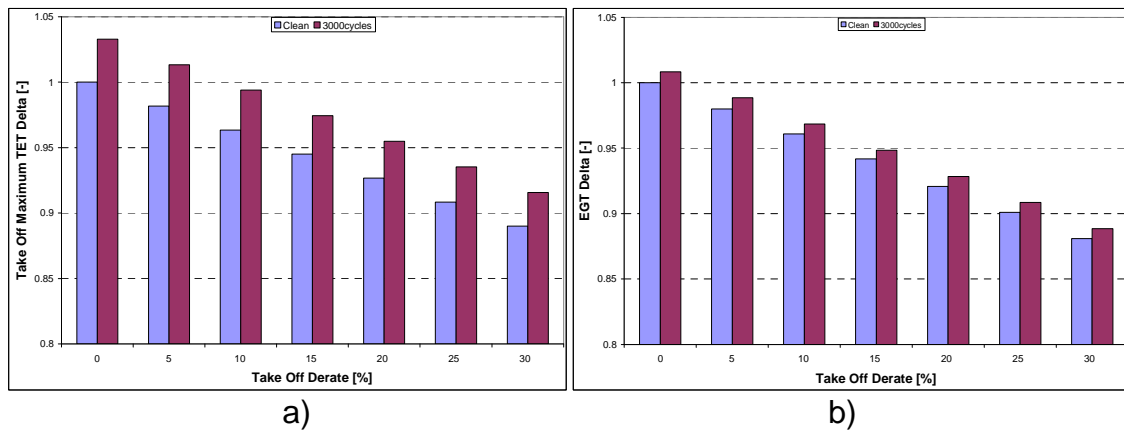


Figure 7.3: a) Maximum operating temperature (TO TET) and b) EGT with varying TO derate for clean engine and after 3000cycles.

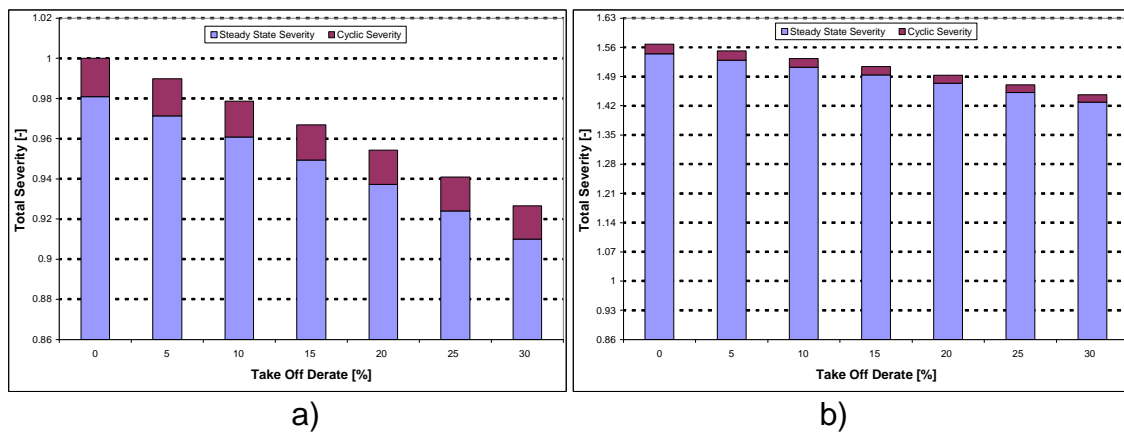


Figure 7.4: Severity with varying TO derate: a) clean engine and b) after 3000cycles.

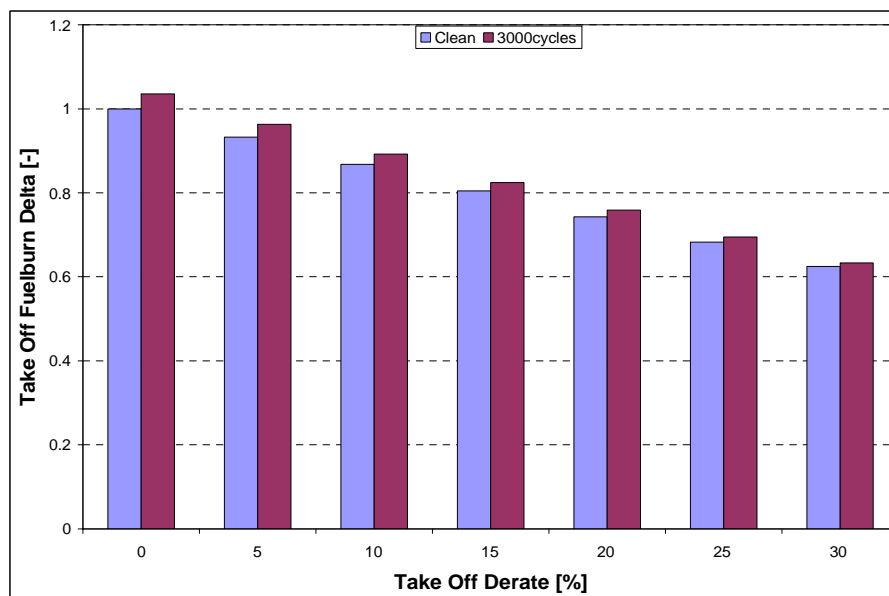


Figure 7.5: TO fuel burn with varying TO derate for the clean engine and after 3000cycles.

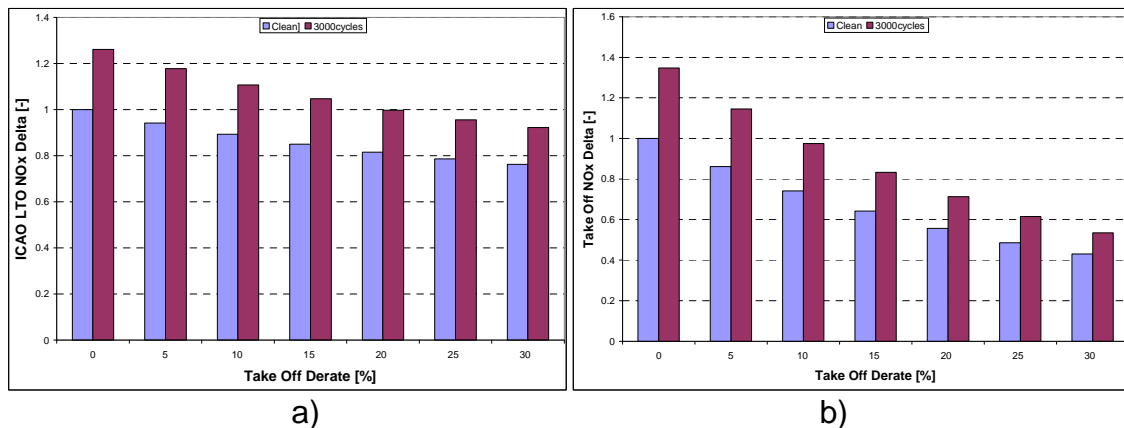


Figure 7.6: a) ICAO LTO and b) TO NOx emissions with varying TO derate for the clean engine and after 3000cycles.

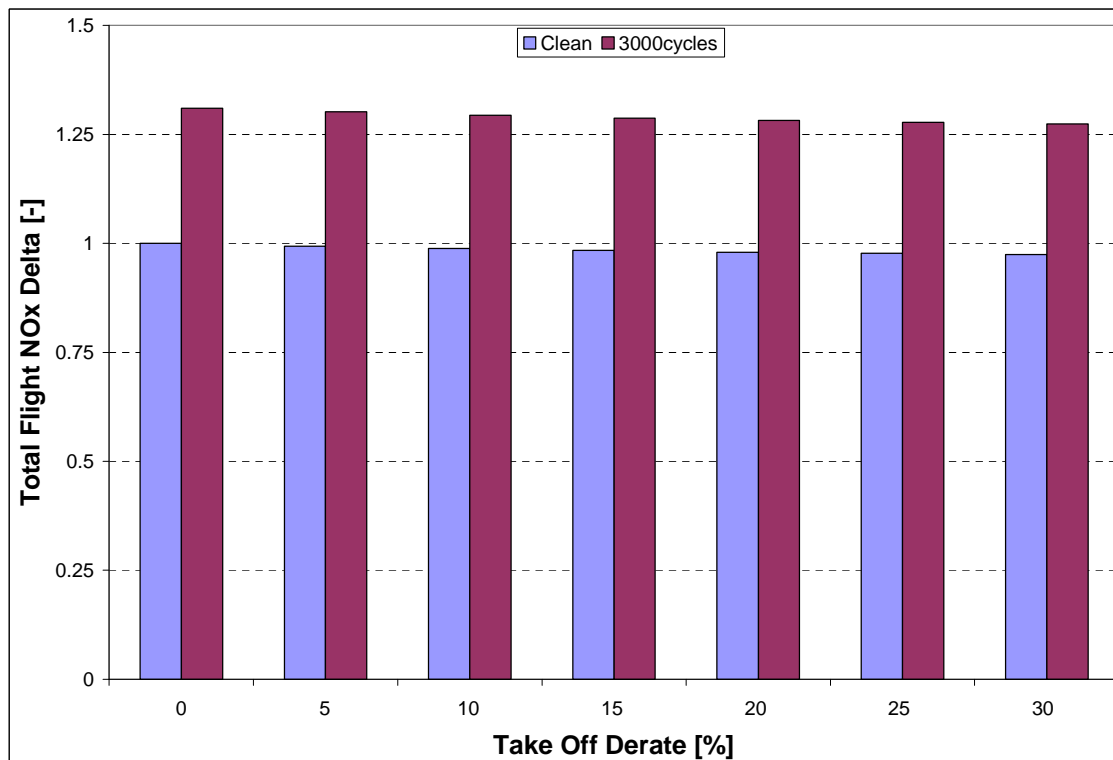


Figure 7.7: Total flight NOx emissions with varying TO derate for the clean engine and after 3000cycles.

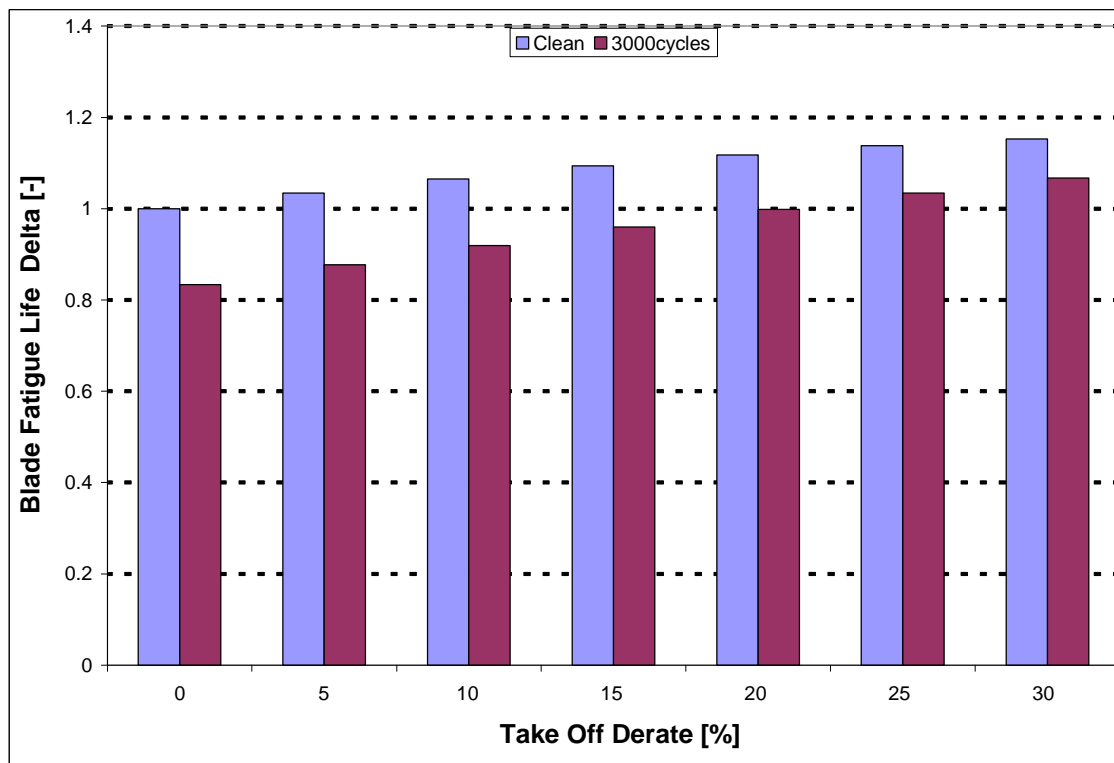


Figure 7.8: HPT blade fatigue life with varying TO derate for the clean engine and after 3000cycles.

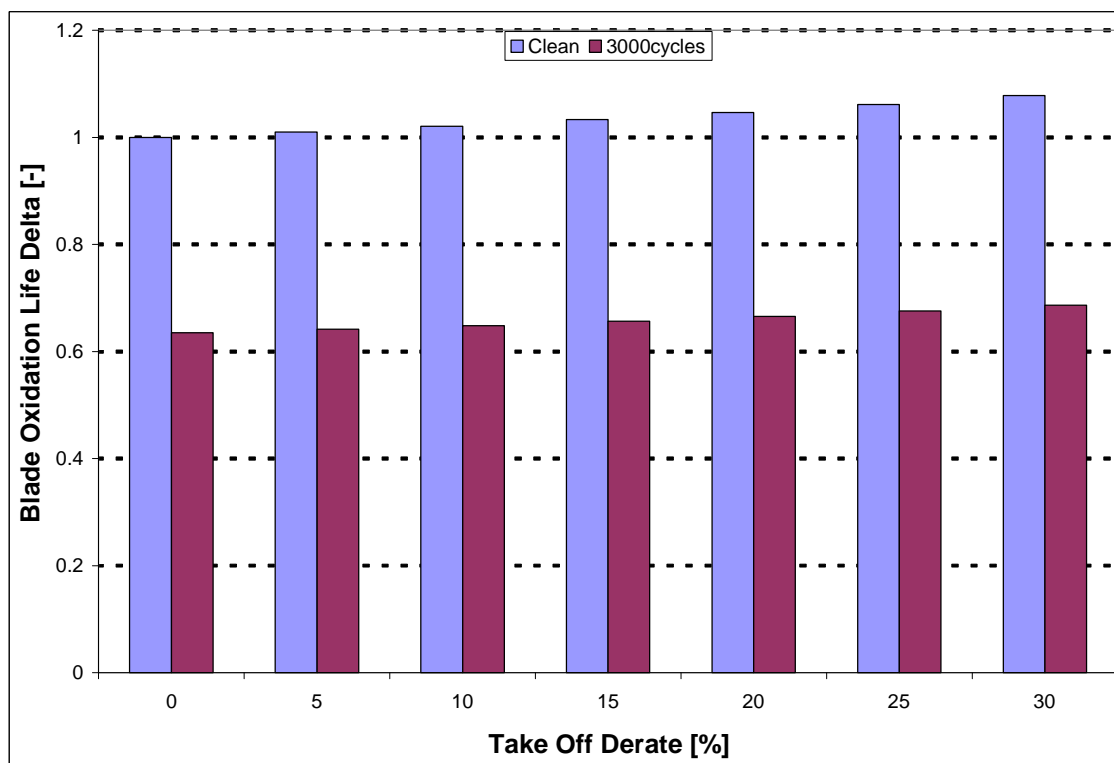


Figure 7.9: HPT blade oxidation life with varying TO derate for the clean engine and after 3000cycles.

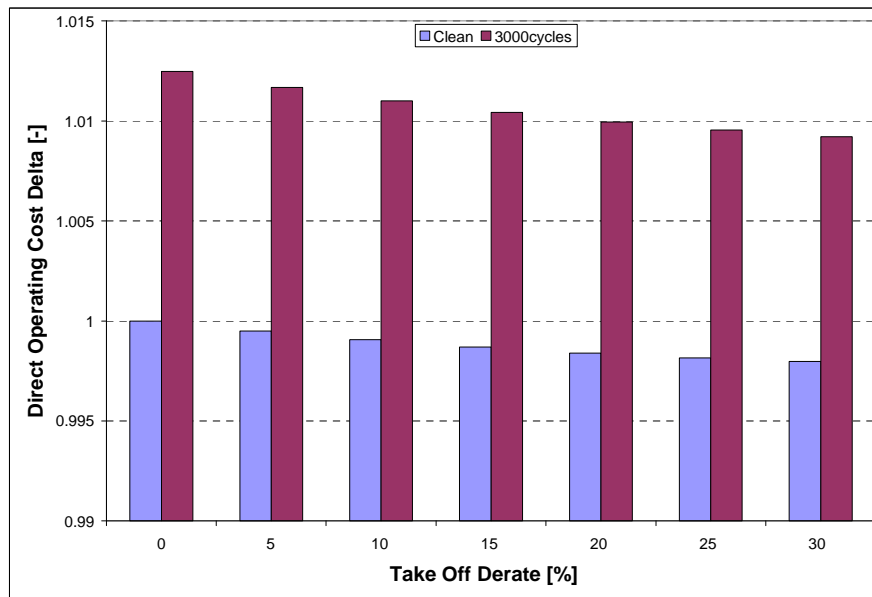


Figure 7.10: Engine DOC per flight with varying TO derate for the clean engine and after 3000cycles.

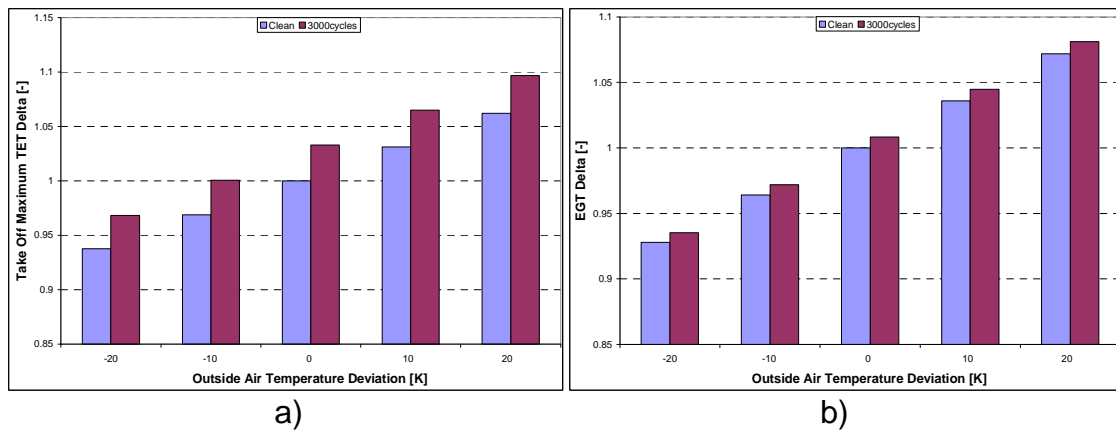


Figure 7.11: a) Maximum operating temperature (TO TET) and b) EGT with varying OAT for a clean engine and after 3000cycles.

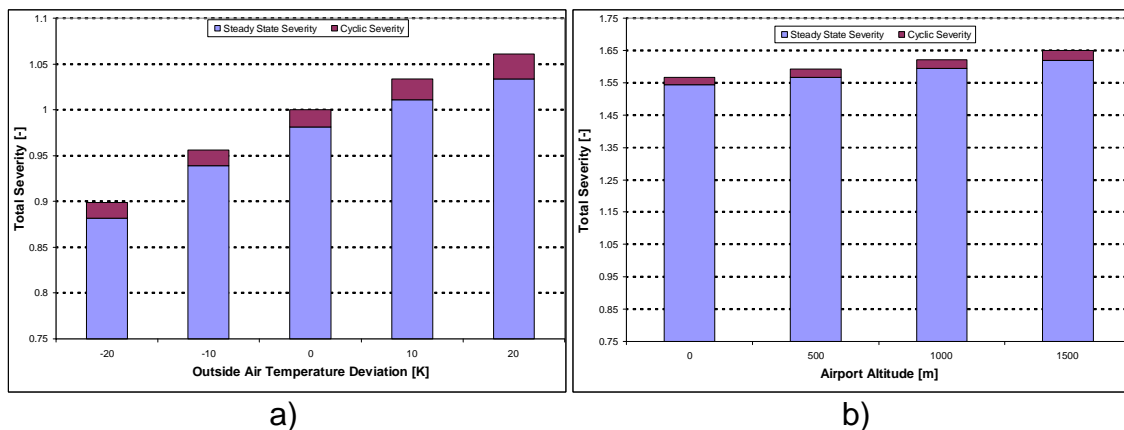


Figure 7.12: Severity with varying OAT: a) clean engine and b) after 3000cycles.

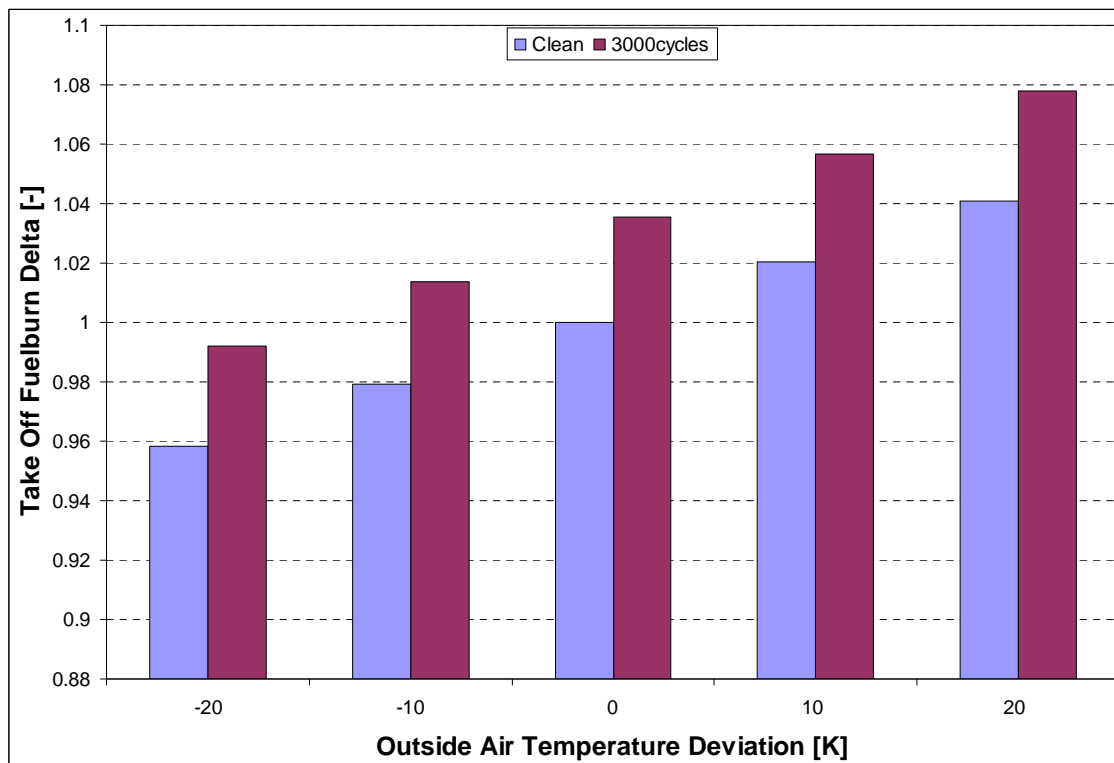


Figure 7.13: TO fuel burn with varying OAT for the clean engine and after 3000cycles.

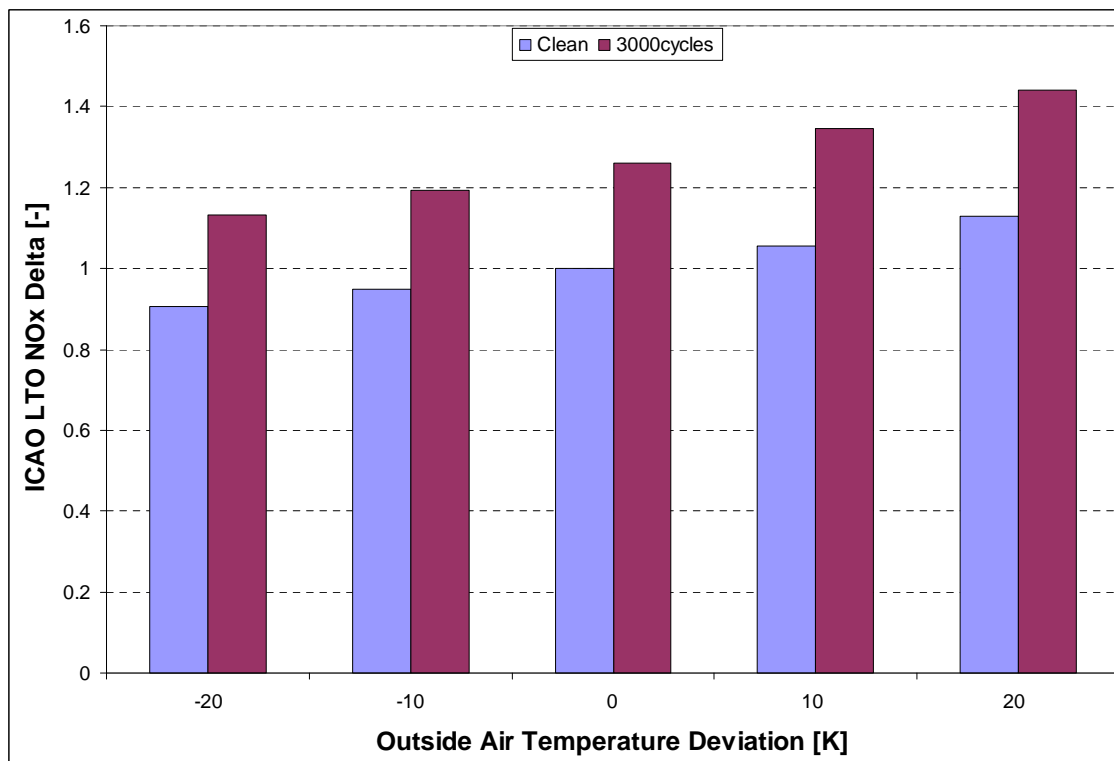


Figure 7.14: ICAO LTO NOx with varying OAT for the clean engine and after 3000cycles.

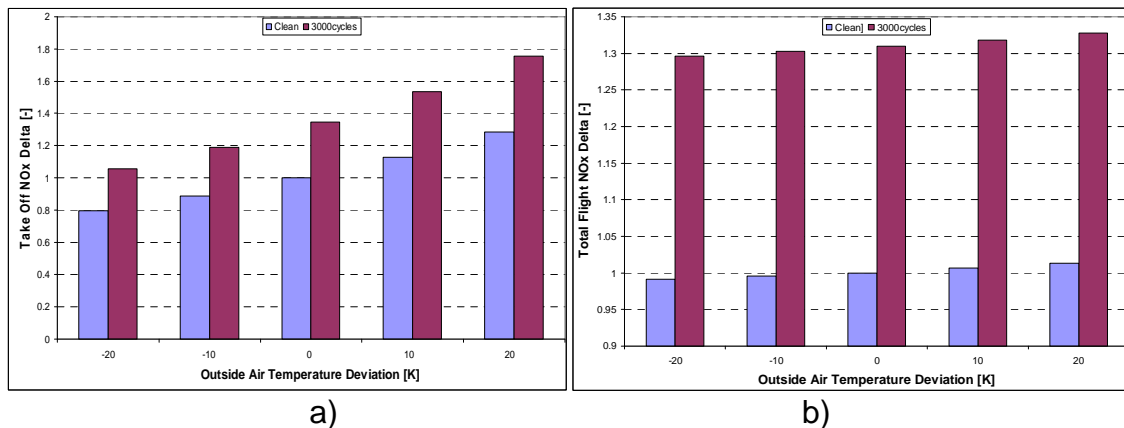


Figure 7.15: a) TO and b) Total flight NOx with varying OAT for the clean engine and after 3000cycles.

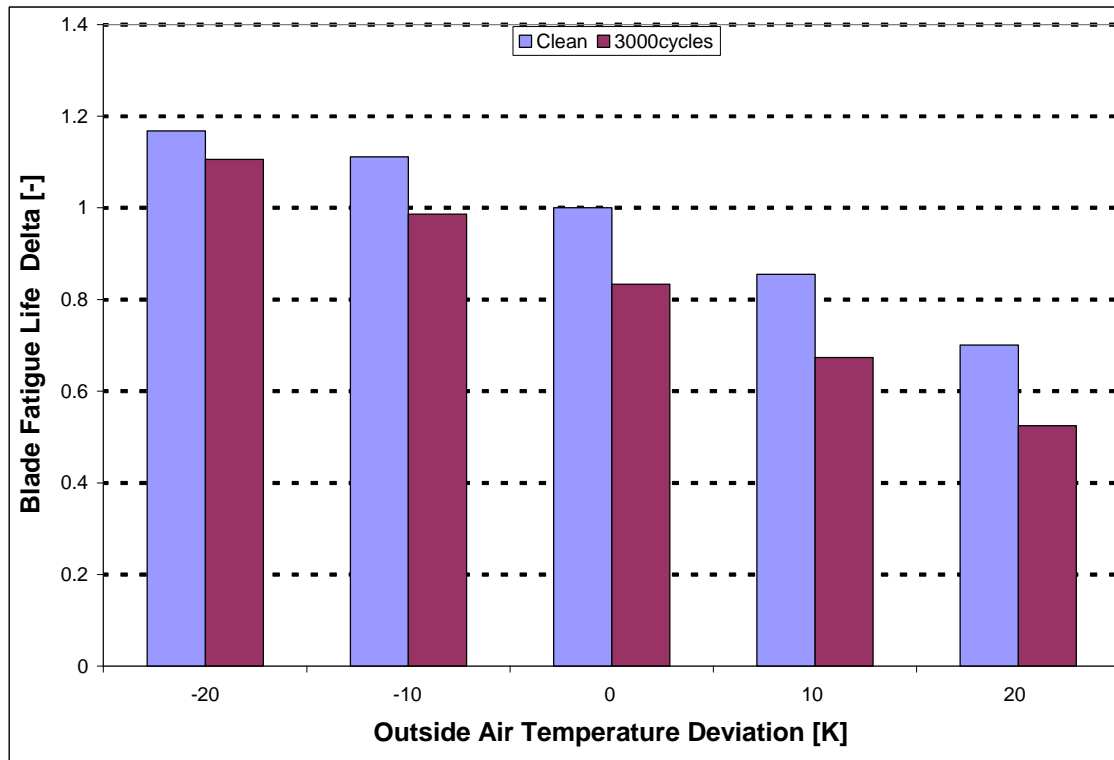


Figure 7.16: HPT blade fatigue life with varying OAT for the clean engine and after 3000cycles.

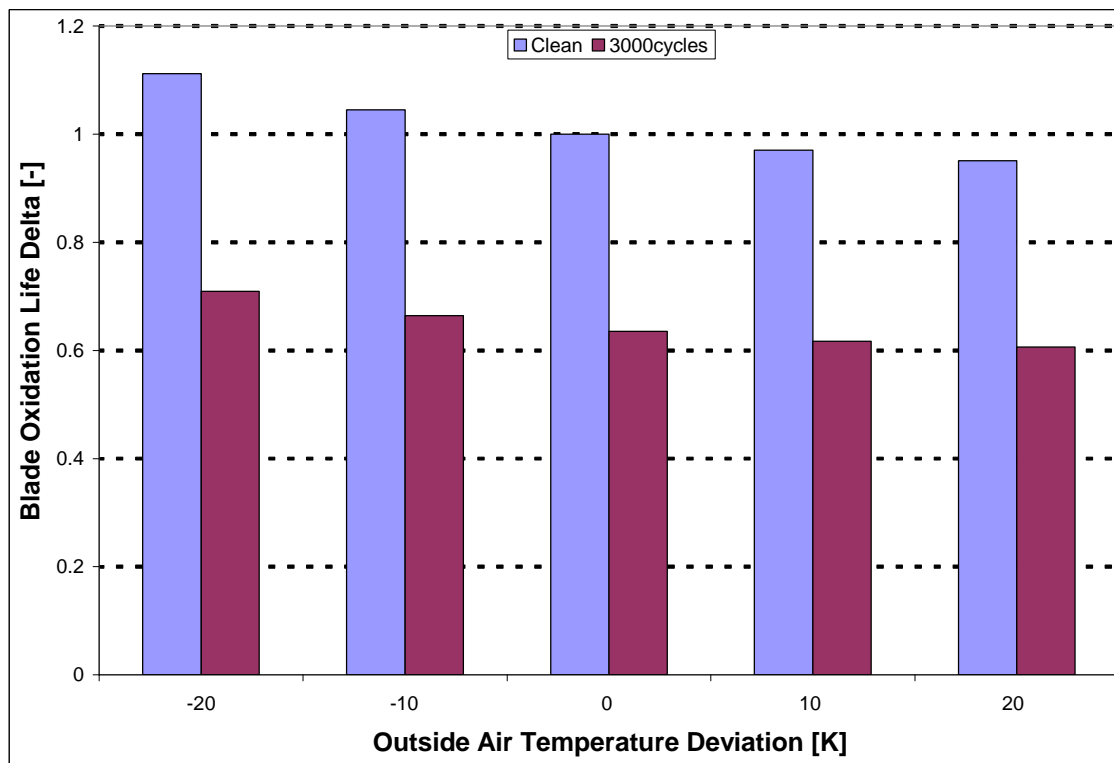


Figure 7.17: HPT blade oxidation life with varying OAT for the clean engine and after 3000cycles.

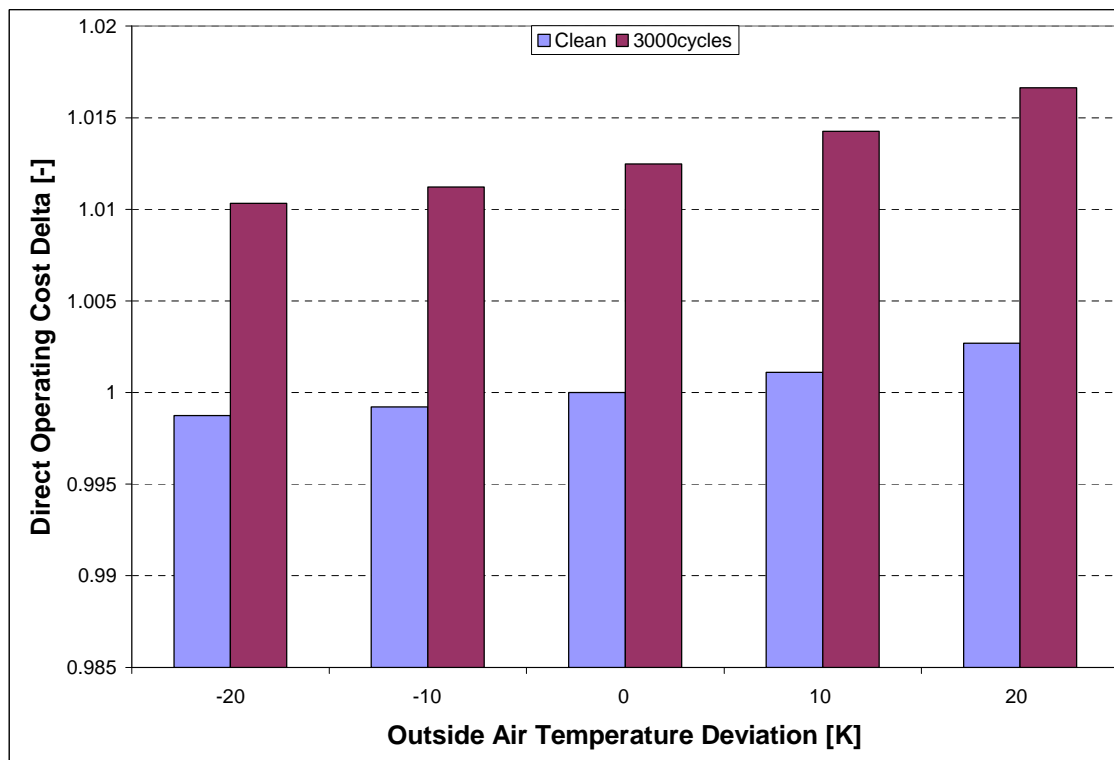


Figure 7.18: Engine DOC per flight with varying OAT for the clean engine and after 3000cycles.

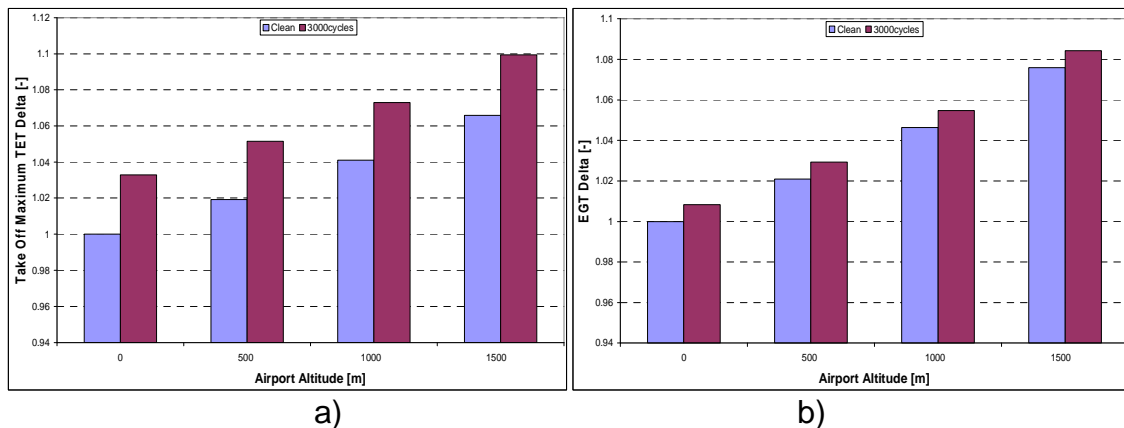


Figure 7.19: a) Maximum operating temperature (TO TET) and b) EGT with varying TO derate for clean engine and after 3000cycles.

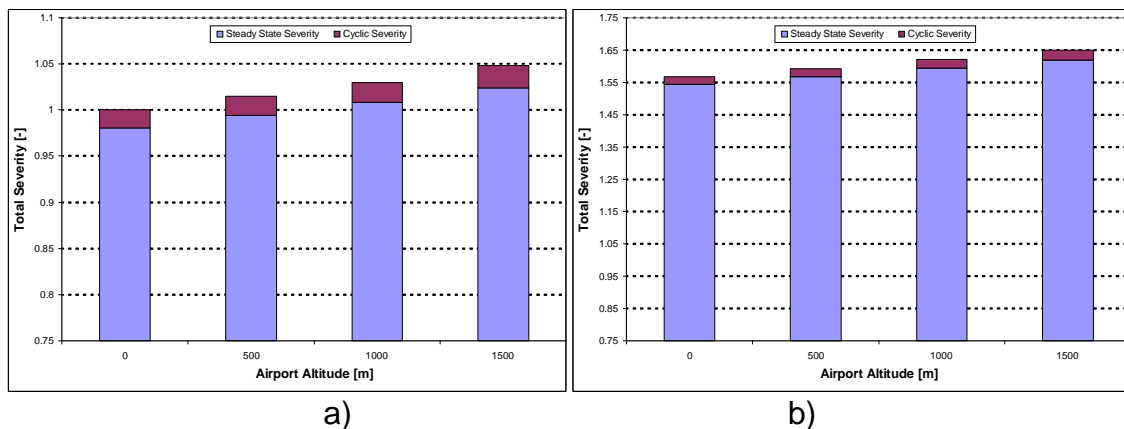


Figure 7.20: Severity with varying altitude: a) clean engine and b) after 3000cycles.

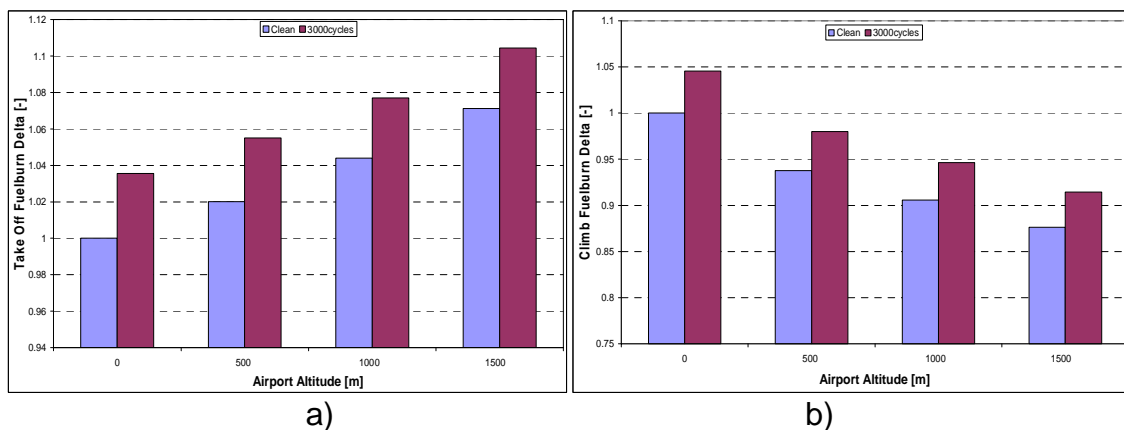


Figure 7.21: a) TO and b) Climb fuel burn with varying altitude for the clean engine and after 3000cycles.

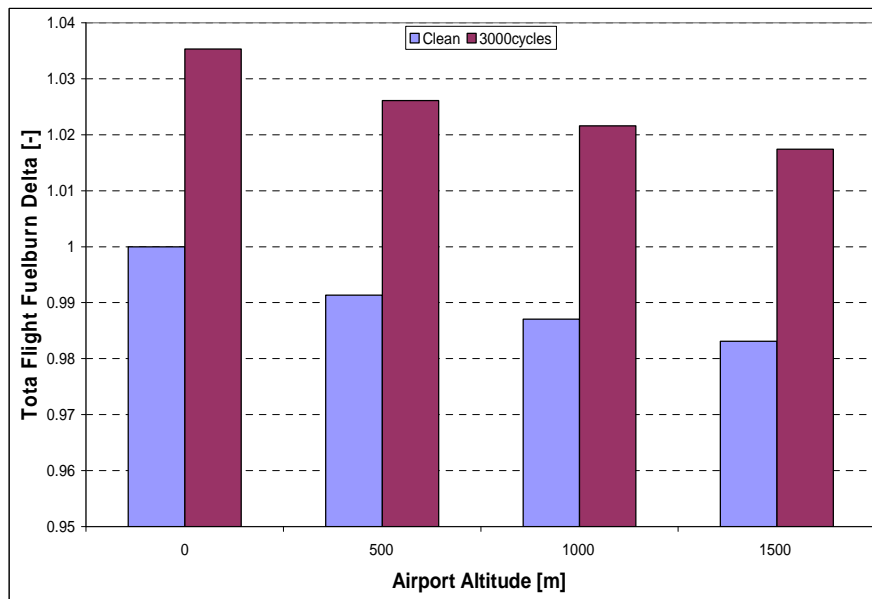


Figure 7.22: Total flight fuel burn with varying altitude for the clean engine and after 3000cycles.

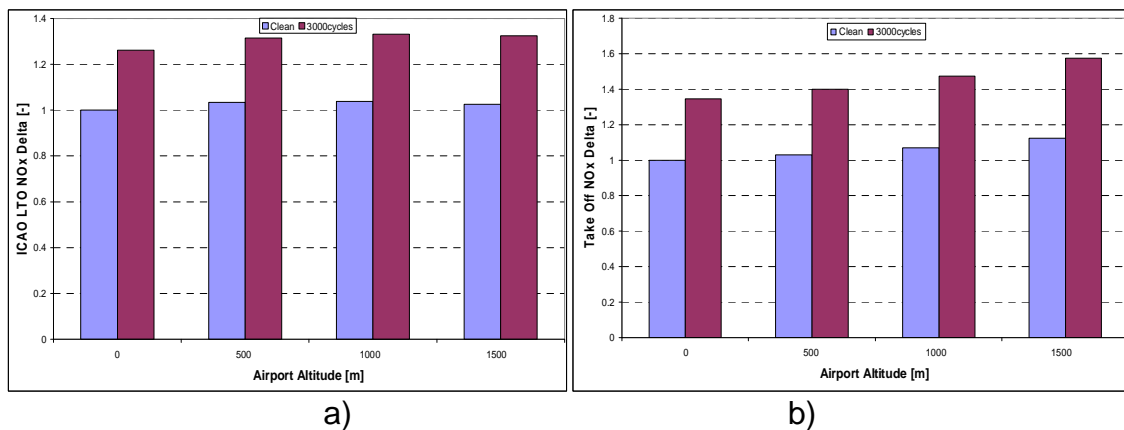


Figure 7.23: a) ICAO LTO and b) TO NOx with varying OAT for the clean engine and after 3000cycles.

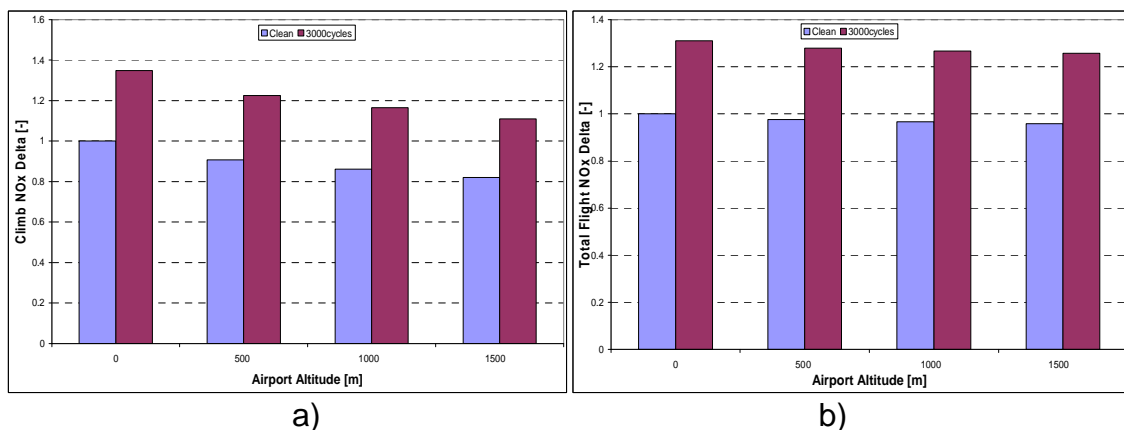


Figure 7.24: a) Climb and b) Total flight NOx emissions with varying altitude for the clean engine and after 3000cycles.

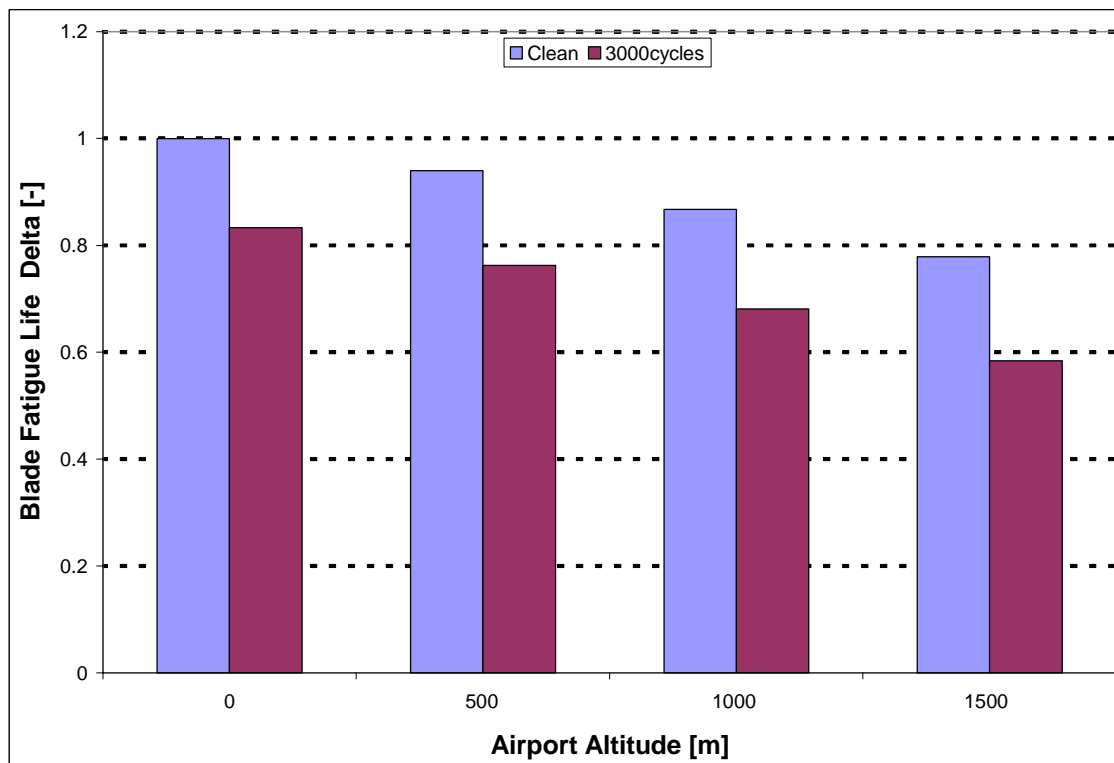


Figure 7.25: HPT blade fatigue life with varying altitude for the clean engine and after 3000cycles.

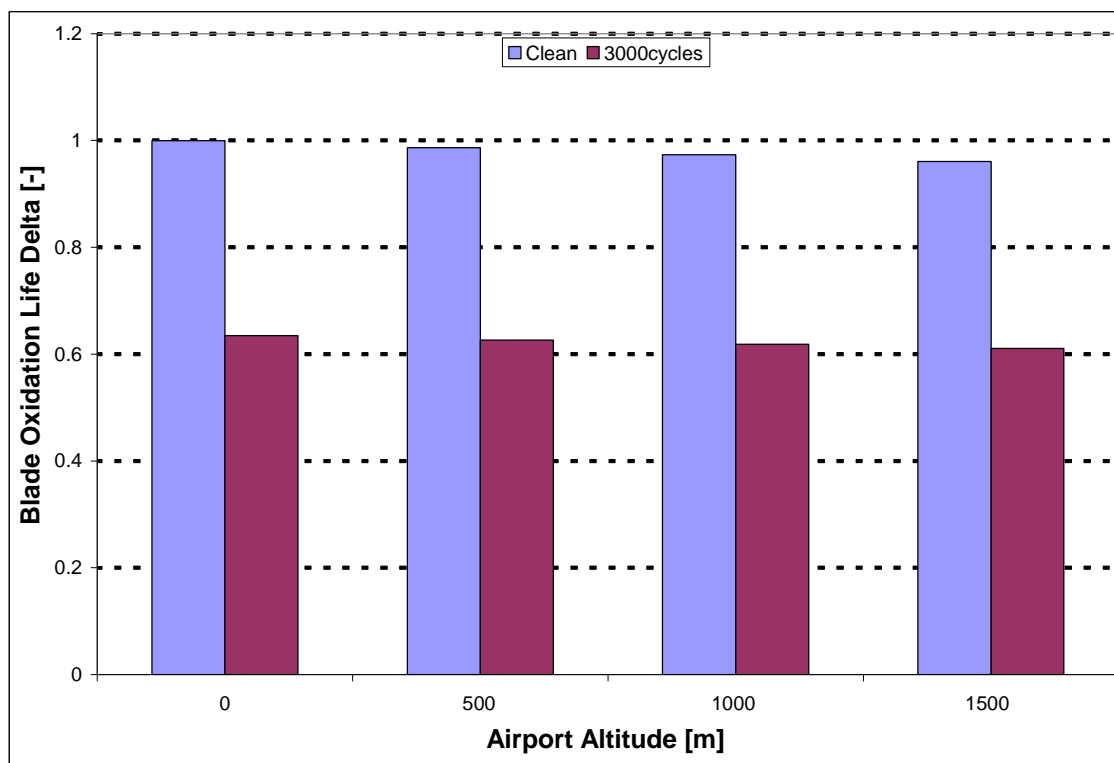


Figure 7.26: HPT blade oxidation life with varying altitude for the clean engine and after 3000cycles.

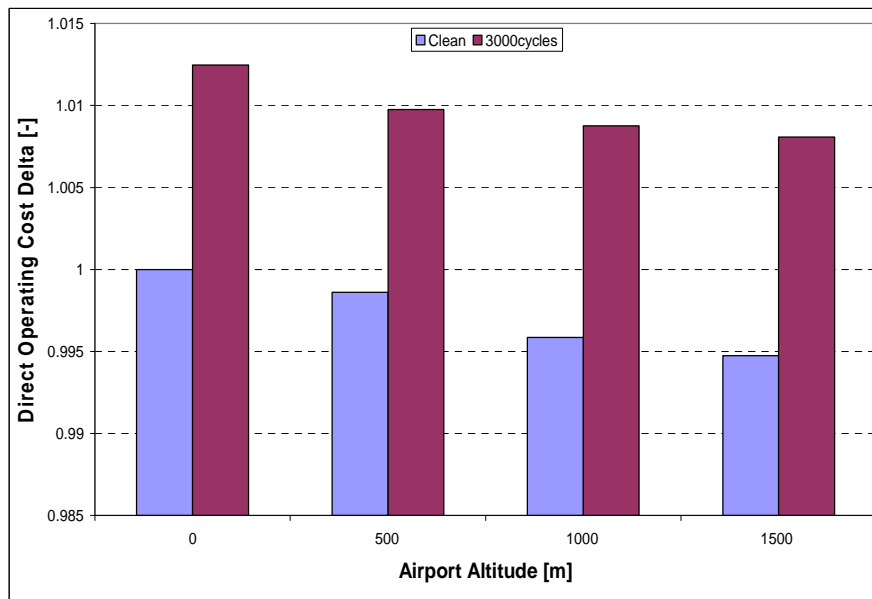


Figure 7.27: DOC with varying altitude for the clean engine and after 3000cycles.

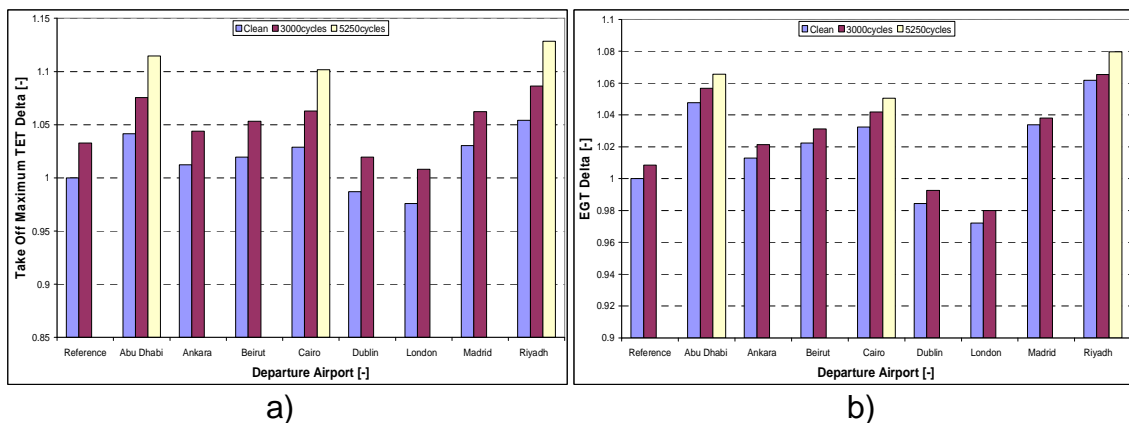


Figure 7.28: a) Maximum operating temperature (TO TET) and b) EGT variation against departure airport for clean engine, after 3000 and 5250cycles.

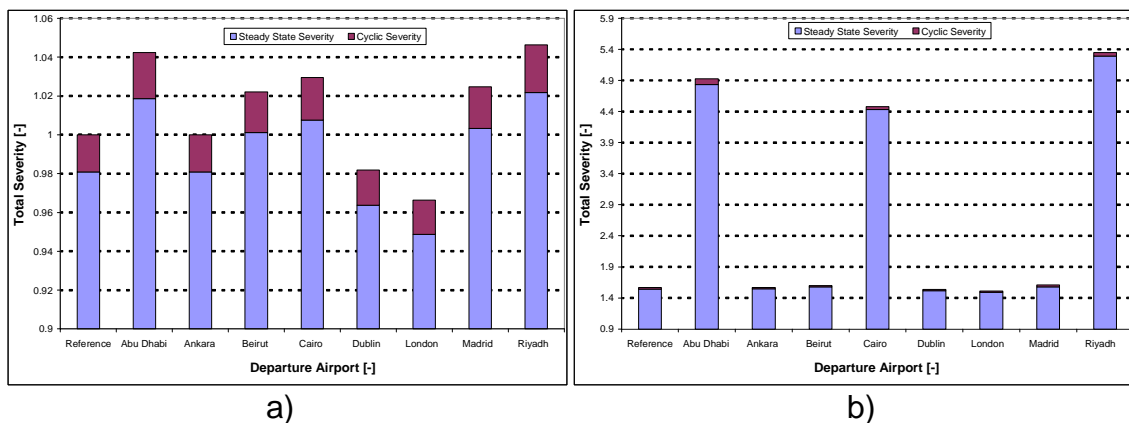


Figure 7.29: Severity with varying airport: a) clean engine and b) after 3000cycles.

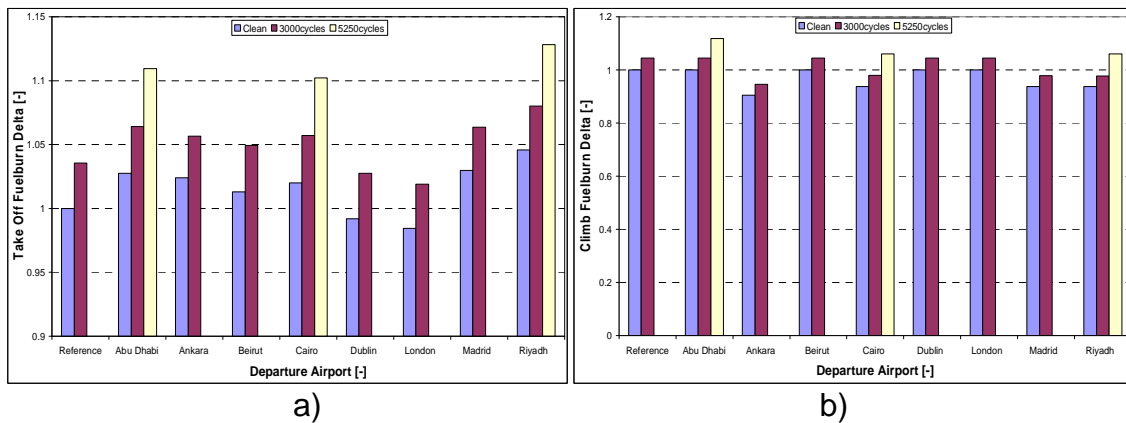


Figure 7.30: a) TO and b) Climb fuel burn with varying airport for the clean engine, after 3000 and 5250cycles.

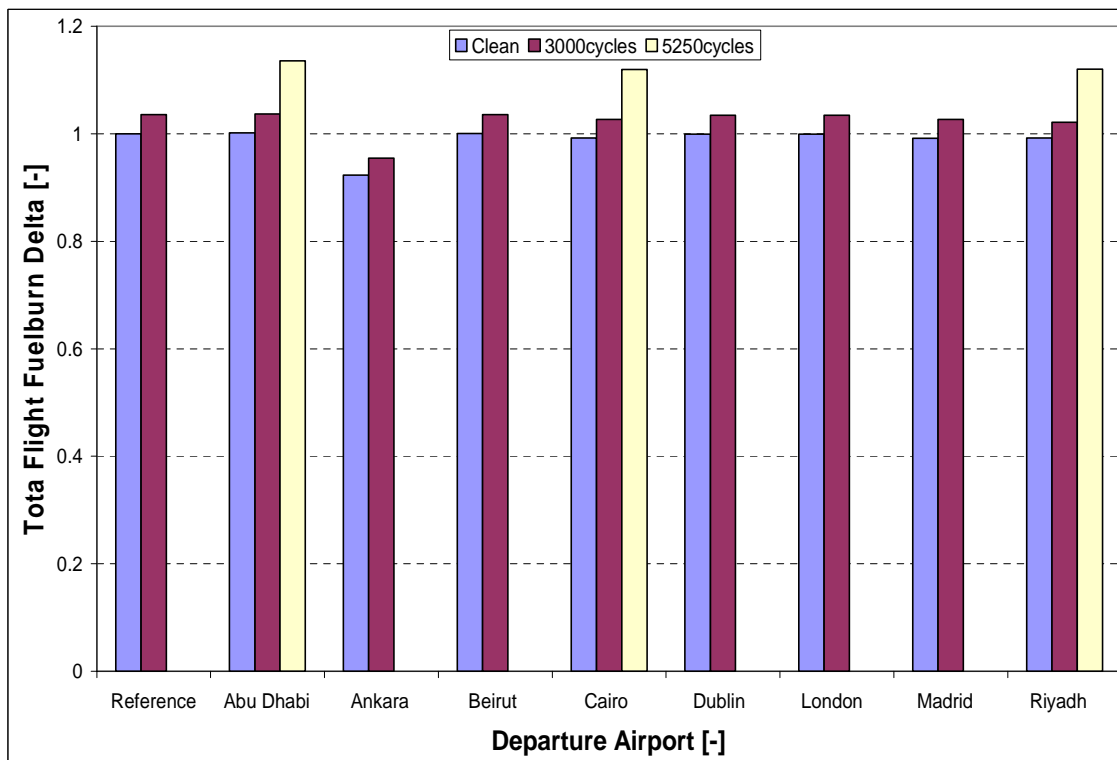


Figure 7.31: Total flight mission fuel burn with varying airport for the clean engine, after 3000 and 5250cycles.

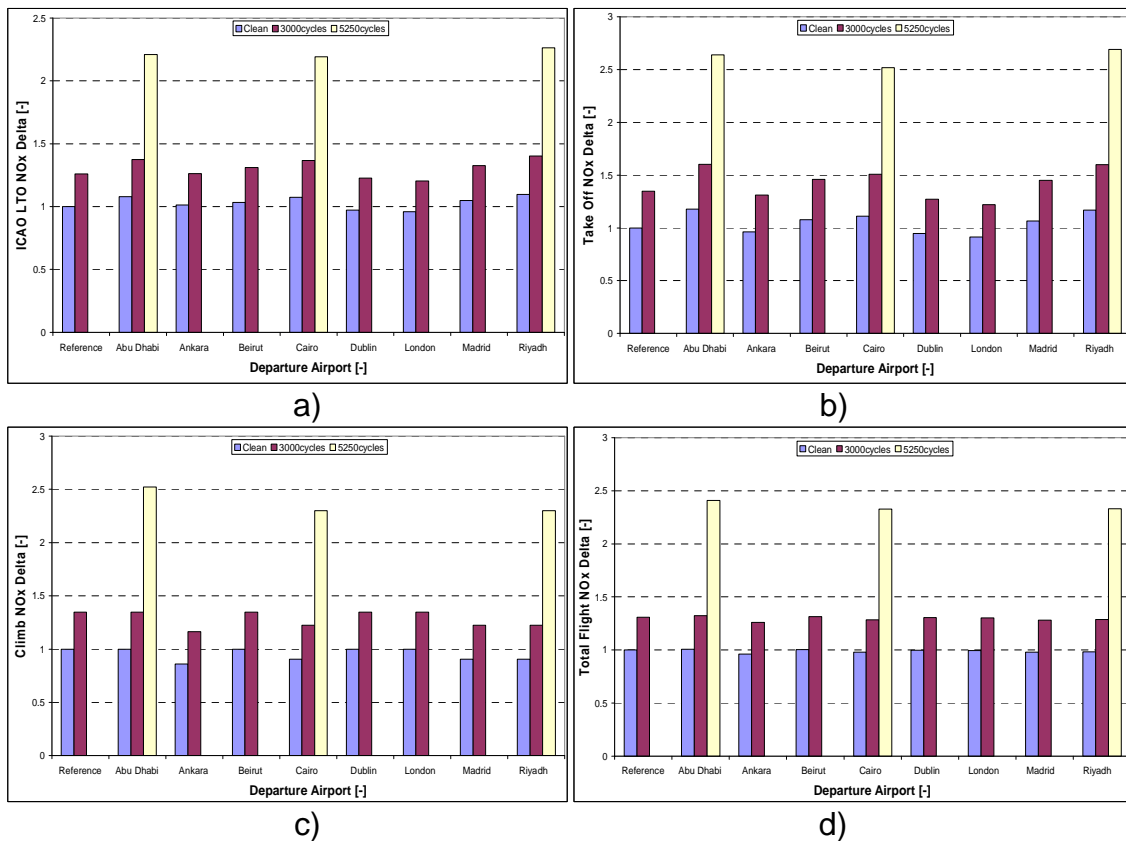


Figure 7.32: a) ICAO LTO, b) TO, c) Climb and d) Total flight NOx with varying airport for the clean engine, after 3000 and 5250cycles.

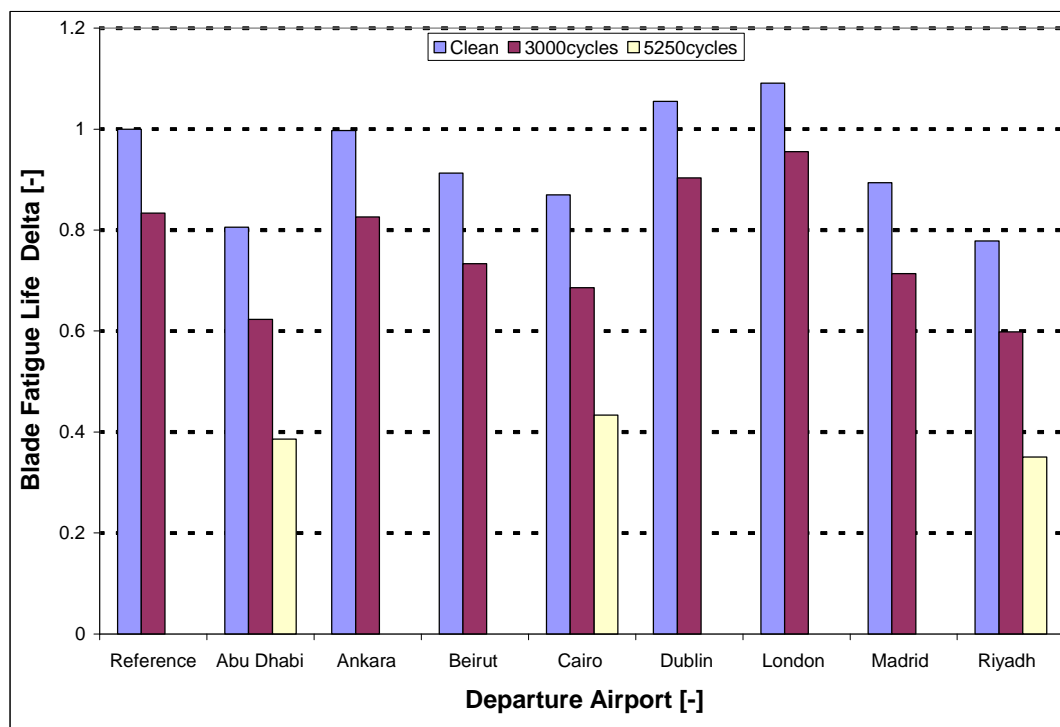


Figure 7.33: HPT blade fatigue life with varying airport for the clean engine, after 3000cycles and 5250cycles.

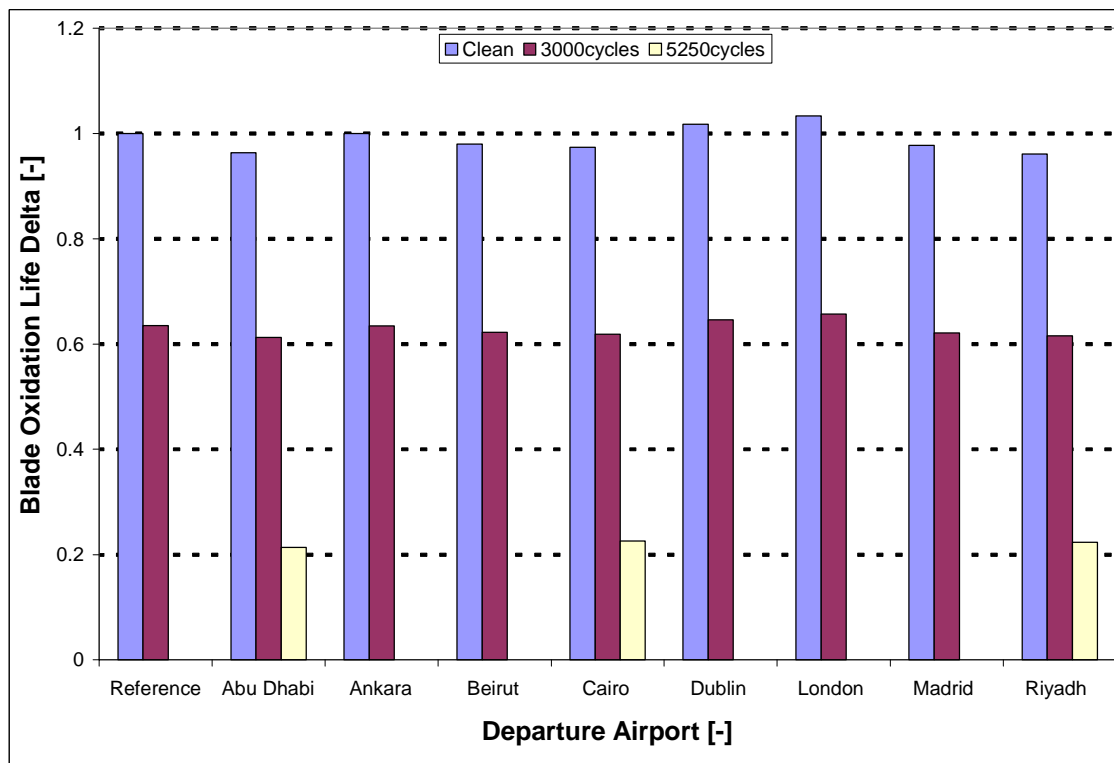


Figure 7.34: HPT blade oxidation life with varying airport for the clean engine, after 3000cycles and 5250cycles.

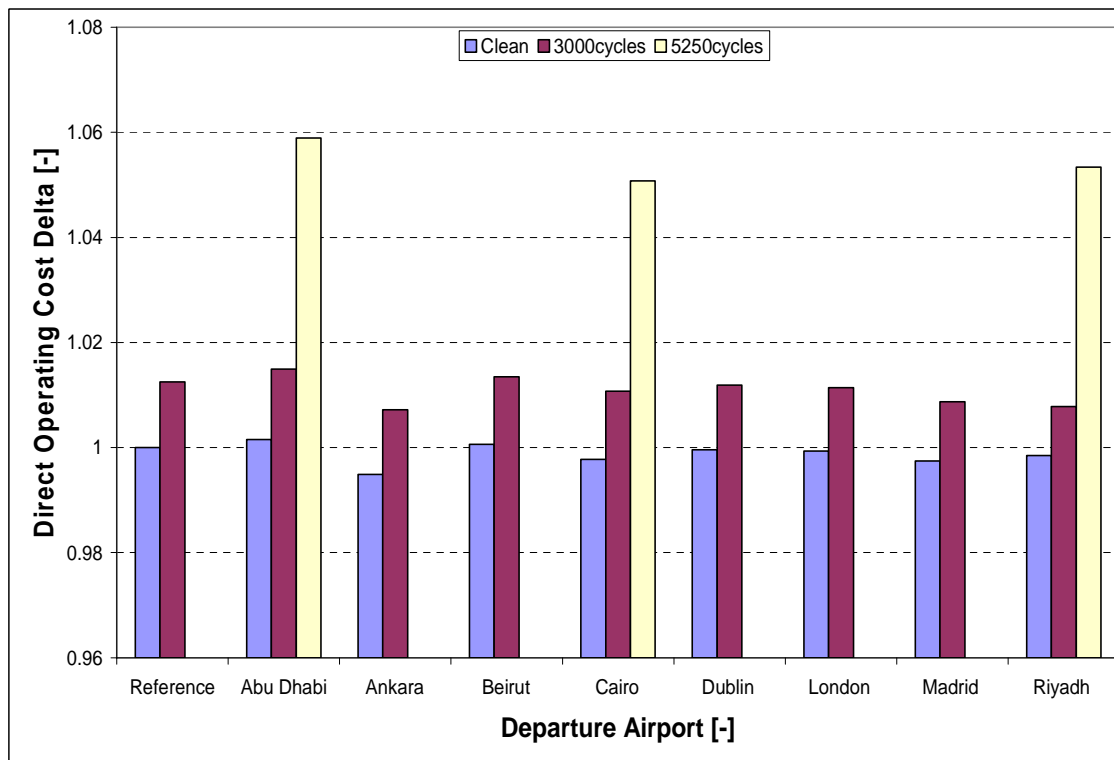


Figure 7.35: DOC with varying airport for the clean engine, after 3000cycles and 5250cycles.

References for Chapter 7

- [1] Troha, W., Stabrylla, R. (1980). Effect of aircraft power plant usage on turbine engine relative durability/life, Report no: AIAA 80-1115, American Institute for Aeronautics and Astronautics (AIAA), Reston, Virginia
- [2] Hanumanthan, H., Stitt, A., Laskaridis, P. and Singh, R. (2011). Severity estimation and effect of operational parameters for civil aircraft jet engines, Proceedings of the Institution of Mechanical Engineers, Part G: Journal of Aerospace Engineering.
- [3] Jet Engine Consulting: Our consultancy philosophy (2008), (http://www.jetengineconsulting.com/pdf/JEC_Consulting_Philosophy.pdf).
- [4] Seemann, R. (2010). 'Modelling the life cycle cost of jet engine maintenance', Students Research Project, Hamburg University of Technology.
- [5] Aircraft Commerce: Systems for engine health monitoring. (Feb/Mar 2006), (Vol. 44): pp 53–57
- [6] Devereux, B. (1992). Improving life usage of the F404 engine through thrust rating, MSc Thesis, Cranfield University
- [7] Palmer, J.R. and Pilidis, P. (2008), Gas turbine theory and performance, MSc Course Notes, Cranfield University, UK
- [8] Cookson, R.A., Haslam, A.S. (2012). Fatigue and Fracture, MSc Course Notes, Cranfield University
- [9] Aircraft performance data Boeing 737-800 (http://www.boeing.com/assets/pdf/commercial/startup/pdf/737ng_perf.pdf)
- [10] Sallee, G.P. (1980). Performance deterioration based on existing (historical) data-JT9D jet engine diagnostics program', NASA-CR-135448, Pratt and Whitney Aircraft Group
- [11] Sasahara, O. (1985). JT9D Engine/Module Performance deterioration results from back to back testing, ISABE 85-7061, Seventh International Symposium on Air Breathing Engines, Beijing, PRC, September 2–6, 1985.
- [12] Simon, D.; Simon, D.L. (2003). Aircraft turbofan engine health estimation using constrained kalman filtering, ASME-GT2003-38584, International Gas Turbine and Aeroengine Congress and Exposition, Atlanta, GA, June 2003
- [13] Litt, J., Parker, K. I. and Chatterjee, S. (2003). Adaptive gas turbine engine control for deterioration compensation due to aging, NASA/TM-2003-212607
- [14] Litt, J., Aylward, E., M. (2003). Adaptive detuning of a multivariable controller in response to turbofan engine degradation, NASA/TM-2003-212723, October 2003

- [15] http://www.flyingineurope.be/all_european_airports.htm
(accessed October 2013)
- [16] http://www.flyingineurope.be/airport_fbo_&_handlers.htm
(accessed October 2013)
- [17] <http://worldaerodata.com/> (accessed October 2013)
- [18] http://www.flyingineurope.be/peter's_airport_guide.htm
(accessed October 2013)
- [19] <http://www.azworldairports.com/cfm/homepage.cfm>
(accessed October 2013)

Chapter 8

Case Study: Flight Mission Fuel Burn and Engine Life Optimised Aircraft Trajectories

Abstract

Operational improvements such as aircraft trajectory optimisation offer a financially viable option to improve aircraft operations and contribute to achieving ACARE targets whilst remaining cost effective and competitive for existing engines and aircraft. This chapter presents the results of aircraft trajectory optimisation assessments carried out at mission level for an engine and aircraft similar to the short to medium range single aisle Boeing 737-800 aircraft powered by a CFM56-7B27. The optimisation case studies were carried out for a full flight trajectory. The case studies were applied to the representative mission ranges: 674nm, 1569nm and 2981 nm, corresponding to the city pairs: London – Madrid, London – Ankara and London – Abu Dhabi respectively. The results show that the fuel burn optimised trajectories have a negative effect on the blade life due to creep, fatigue and oxidation due to the higher maximum cruise temperatures demonstrated by these trajectories. However the reduction in fuel burn dominates the drop in life to benefit the operating costs. Optimising for blade creep life benefits the fuel burn for London–Abu Dhabi due to less fuel burn at climb dominating the cruise and descent fuel burn. The blade oxidation life optimised trajectories are detrimental to the fuel burn as the trajectories are executed at slower cruise speeds and take more time at cruise and descent, hence burning more fuel. The more fuel burn demonstrated by these trajectories translates into an increase in operating costs. The disc creep life optimised trajectories benefit the fuel burn for London – Ankara and London – Abu Dhabi due to being flown at higher altitudes and less fuel burn at cruise which dominates the climb and descent fuel burn.

8.1 Introduction

Direct operating costs have become an important concern to both the manufacturer (OEM) and the airlines. Cost effectiveness (making more money) is the perspective for both the OEM and the airlines. In view of the new model (power by hour) contracts as opposed to the older model (time and materials) contracts, the OEM's key concern is to deliver good engines that are reliable and available, whilst remaining cost effective in terms of engine maintenance. The airlines' key concern is that to remain competitive, they have to operate cost effectively by lowering operating costs whilst remaining within the constraints and operating guidelines imposed by the OEM. Engine performance and engine life are therefore important because as the engine degrades the flight mission fuel burn and maintenance costs increase, in turn translating into an increase in operating costs. This raises the need for the assessment of the

engine and aircraft at mission level with a view to optimising operational procedures.

An important aspect of this research is to understand the trade-offs between mission fuel burn and engine life and the implications on operating costs and emissions when considering the effects of engine degradation. The objective of the optimisation studies described here is to look at aircraft mission fuel burn and engine life optimised operations (as influenced by degradation) and identify the variation in the flight mission fuel burn, engine life and the operating costs and emissions and the gains that may be achievable when compared to a baseline trajectory. The engine/aircraft assessments are done at mission level to provide early visibility and identify the impact of engine component degradation on the mission fuel burn, engine life, operating costs and emissions. The assessments show the change in engine component life when flying to minimize mission fuel burn and the change in mission fuel burn when flying to maximize engine component life.

8.2 Aircraft Trajectory Definition

When optimising the aircraft trajectories in this work, the first requirement was to define the aircraft trajectory to be optimised. Only the vertical profiles were considered in the optimisations and thus the flight trajectories were defined in terms of flight altitude, aircraft speed (true airspeed (TAS), EAS or M)) and throttle setting. The trajectory was defined according to each of the flight phases as outlined below.

Take – Off: This phase is as defined in section 6.2 and starts at the airport altitude and ends at 1500ft above Mean Sea Level (MSL). This phase was divided into 13 segments and the profile followed allowed for calculation and changes in altitude, distance, speed, time and power settings. These calculations were in accordance with the progression of the TO phase through power up, ground roll, 35ft obstacle, transition and TO. The power settings increase gradually from ground idle thrust settings to full power (maximum thrust) settings. This phase was not varied.

Climb: This phase is as defined in section 6.2 and starts at the end of the TO phase (1500ft) progressing until the aircraft reaches cruise altitude. The climb phase was divided into 22 climb segments, each specified according to the absolute altitude, the temperature deviation from the ISA day, the EAS and the power setting of the engine as a percentage of the maximum thrust at the segment. The speeds were defined in accordance with ATC restrictions and the following profile was followed:

- 1) Climb at constant EAS and 250kts EAS from 1,500ft to 10,000ft.
- 2) Level flight acceleration at 10,000ft to 320kts EAS.
- 3) Climb at constant EAS (320kts) from 10,000ft until transition altitude is reached (and cruise Mach number attained).
- 4) Climb at constant Mach from transition to cruise altitude at ToC.

The altitudes and speeds were selected to correspond with those of a standard flight profile as found in [1] and are all within the design limits of the aircraft as found in [2]. This phase was varied during the optimisation, and the altitudes and speeds were used as variables within the bounds shown in table 8.1. The power settings were kept the same as for the baseline trajectory.

Table 8.1: Optimisation variable bounds.

| Phase | Decision Variable | Lower Bound | Upper Bound |
|----------------|-------------------|-----------------|-------------|
| Climb | Altitude 1 [m] | 609.6 | 913.4 |
| | Altitude 2 [m] | 914.4 | 1218.2 |
| | Altitude 3 [m] | 1219.2 | 1827.8 |
| | Altitude 4 [m] | 1828.8 | 2437.4 |
| | Altitude 5 [m] | 2438.4 | 2742.2 |
| | Altitude 6 [m] | 2743.2 | 3047 |
| | Altitude 7 [m] | 3048 | 3656.6 |
| | Altitude 8 [m] | 3657.6 | 4266.2 |
| | Altitude 9 [m] | 4267.2 | 4875.8 |
| | Altitude 10 [m] | 4876.8 | 5485.4 |
| | Altitude 11 [m] | 5486.4 | 6095 |
| | Altitude 12 [m] | 6096 | 7923.8 |
| | Altitude 13 [m] | 7924.8 | 8533.4 |
| | Altitude 14 [m] | 8534.4 | 9143 |
| | Altitude 15 [m] | 9144 | 10057 |
| | Altitude 16 [m] | 10058 | 10667 |
| | Altitude 17 [m] | 10668 | 11225 |
| | Altitude 18 [m] | 11226 | 11886 |
| | Altitude 19 [m] | 11887 | 11999 |
| | Altitude 20 [m] | 12000 | 12192 |
| Cruise | Altitude [m] | 10668 | 12192 |
| | Mach [-] | 0.68 | 0.82 |
| Descent | Speed 1 [kts] | 222.5 | 233.1 |
| | Speed 2 [kts] | 203.9 | 221.5 |
| | Speed 3 [kts] | 196 | 202.9 |
| | Speed 4 [kts] | 184.1 | 195 |
| | Speed 5 [kts] | 165.7 | 183.1 |
| | Speed 6 [kts] | 151.9 | 164.7 |
| | Speed 7 [kts] | 141 | 150.9 |
| | Speed 8 [kts] | 136 | 140 |
| | Speed 9 [kts] | Constant at 135 | |
| | Speed 10 [kts] | Constant at 135 | |

Cruise: This phase is as defined in section 6.2 and in keeping with ATM constraints was simulated for constant altitude and speed. The phase was specified according to the cruise altitude and cruise Mach number. For improved numerical accuracy, the cruise phase is divided into small time segments and in each segment the performance parameters are kept constant. This phase was varied during optimisation by changing the altitude and speed within the bounds shown in table 8.1.

Descent: For the assessments carried out in this work the approach and landing (until touchdown) phases defined in section 6.2 were considered as the descent phase. The phase starts at the cruise altitude and ends when the aircraft has landed (touched down). The descent phase was divided into 10 descent segments and each was specified according to the temperature deviation from the ISA day, the TAS and the power setting of the engine as a percentage of the maximum thrust at the segment. The altitudes at each segment are dependent on the cruise altitude and are computed within the aircraft performance code by interpolating between the cruise altitude and the landing altitude. The last three segments of descent were set at approach thrust settings. This phase was varied for the optimisation studies, with the descent speed at each descent segment used as variables within the bounds shown in table 8.1. The power settings were kept the same as for the baseline trajectory. The altitudes were not varied as these are dependent on the cruise altitude.

Landing: This phase begins at touchdown and ends when the aircraft stops and is as defined in section 6.2. This phase was divided into 11 segments and the profile followed allowed for calculation of landing airport altitude and changes in distance, speed, time and power settings. The power settings progress from the approach thrust settings at touchdown, through first a gradual increase and then a gradual decrease as a percentage of maximum TO thrust and finally return to ground idle settings. This phase was not optimised.

8.3 Case Studies: Aircraft Trajectory Optimisation

The purpose of this section is to present the main results of the optimisation studies conducted on the CUCCTF engine model and CUSMSA aircraft model described in chapter 2. According to Boeing [4], each phase of flight presents opportunities to adopt certain strategies to save fuel and minimise DOC. In the context of this work, a full flight trajectory (as described in section 8.2) optimisation in which the climb, cruise and descent phases were varied was conducted. The main variables were the flight altitude and aircraft speed. The main objectives were to minimise the flight mission fuel burn and to maximise the engine life due to creep, fatigue and oxidation. The aim was to assess and quantify the trade-offs between the fuel burn and engine life optimised trajectories and the influence of engine component degradation. The severity, NOx emissions and the DOC were also considered and assessed for the optimised trajectories.

The mission flown is important since it largely influences the LCF, creep and oxidation life of an engine component as well as the mission fuel burn. The

frequency of cyclic loading the material has to endure determine the component's LCF life; the component's creep life depends on the time it spends operating within the material's creep temperature range and the oxidation life depends on the time the component spends operating at high temperatures. Hence engine usage and the time an engine operates in various segments of the flight envelope is defined by the flight mission requirements. The engine duty cycle varies from one mission profile to another, and the changes in the duty cycle of an engine affect the life of the engine and its overall performance [5]. Hence the trade-offs between mission fuel burn and engine life optimised trajectories are presented in this section with the aid of a number of case studies. Three mission ranges were chosen for the case studies according to the available utilisation information for the Boeing 737-800 type aircraft found in [2]. The ranges 674nm, 1569nm and 2981nm correspond to the city pairs: London – Madrid, London – Ankara and London – Abu Dhabi respectively. These ranges were chosen to enable comparison of the optimised trajectory performance for a short range, short-medium range and medium-long range.

The categorisation and definition of aircraft flight length is determined by individual airlines and differs across different airlines [5] [6] [7]. Some airlines use time whereas others use the destination (or distance) served. The definitions used for this work are:

- Short range flight: less than 3hrs
- Medium range flight: 3 to 6hrs
- Long range flight: 7hrs or more

The London – Abu Dhabi route is not a typical Boeing 737-800 utilisation route, but does lie within the aircraft's maximum design range of 3,115nm [3]. A Energy to Revenue Work (ETRW) metric [8] was used to assess the energy efficiency and operational capability of the CUSMSA on the London – Abu Dhabi route. The energy efficiency of the CUSMSA was compared to the energy efficiency of an aircraft similar to the long range. The metric uses the ratio of energy liberated during a flight to the revenue work done. The ETRW is calculated using equation 8.1, and the minimum value is considered to be the optimum or most energy efficient.

$$ETRW = \frac{M_f \cdot LCV}{M_{pl} \cdot g \cdot R} \quad (8.1)$$

where

$ETRW$ = Energy to revenue work

M_f = Mass of the mission fuel actually burned on trip (kg)

M_{pl} = Maximum payload mass of the aircraft (kg)

g = Acceleration due to gravity ($\approx 9.81 \text{m/s}^2$)

R = Great circle distance for a mission (m)

LCV = Lower calorific value of fuel ($\approx 43 \text{ MJ/kg}$ for kerosene)

For each route, the clean engine trajectory was chosen as the baseline. The baseline was chosen to closely approximate the aircraft performance and

trajectory of the Boeing 737-800 aircraft as found in [2]. The effects of engine component degradation were assessed by changing the engine health parameters (as described in chapter 7) to correspond with an engine's health after 3000, 4500 and 5250 cycles of operation. As with the case study described in chapter 7, changes (corresponding to information and data found in [9] [10] and [11]) were introduced to the flow capacities and efficiencies of key engine components such as the Fan, LPC, HPC, LPT and HPT. The deviations (from the clean engine) assigned to the component characteristics (health parameters) indicate the degree of engine degradation.

The following case studies were conducted along each route:

- Case 1: Aircraft performance calculation for the clean engine (to establish baseline trajectory performance). Calculate performances after 3000, 4500 and 5250 cycles of operation along same trajectory.
- Case 2: Aircraft trajectory optimised for fuel burn and engine life for the clean engine.
- Case 3: Aircraft trajectory optimised for fuel burn and engine life after 3000 cycles of engine operation.
- Case 4: Aircraft trajectory optimised for fuel burn and engine life after 4500 cycles of engine operation.
- Case 5: Aircraft trajectory optimised for fuel burn and engine life after 5250 cycles of engine operation.

A multi-disciplinary framework coupled with an optimiser (figure 8.1) was used in the optimisation assessments. The framework combines an optimiser with the mathematical models described in previous chapters (and used in the airport severity studies described in chapter 7): engine performance, aircraft performance, emissions prediction, lifing analysis and economics. The procedure outlined below was used to predict how changes in the flight trajectory and operational conditions relatively affect the engine and aircraft performance:

- The engine performance code TURBOMATCH is used to calculate the take-off thrust, flight segment spool speeds, operating temperatures and cooling flow temperatures and specific fuel consumption (SFC).
- The aircraft performance code HERMES is used to integrate the engine and aircraft and to calculate the flight performance in terms of total mission fuel burn and flight mission time.
- The lifing code is used to estimate the life of the HPT blade and disc (LCF, creep and oxidation) based on metal temperatures, stresses and material properties. The life estimates are converted to damage fractions using the linear damage rule.
- The damage fractions calculated by the lifing code are used to estimate the severity for the HPT blade and disc. Severity was described in chapter 7 (and the reader is referred there for more detail). In the context of the optimisation studies, severity is the damage of the new mission (optimised trajectory) relative to the damage of the baseline mission.

- The economics model HESTA is used to translate the life estimation into engine/aircraft direct operating costs.
- The emissions prediction code HEHAESTUS is used to predict the emissions indices for CO₂, NO_x and H₂O for the flight mission.
- The GA optimiser was used to determine the fuel burn and engine life optimised trajectories. The optimised flight profile phases are defined in terms of flight altitudes and speeds.

Assumptions

The following assumptions were made during the assessments:

- Take off altitude is 25m above SL and -5°C temperature deviation from ISA conditions.
- For each route the same TO, climb, cruise, descent, approach and landing profiles as shown in figure 8.2 have been flown by the non-optimised clean and degraded cases.
- The aircraft performance for the clean has been assumed as the baseline trajectory against which the performances after 3000, 4500 and 5250 cycles of operation and the optimised trajectories have been compared.
- The initial climb is kept the same and ends at 457.2m (1500ft) for all the case studies.
- The range calculated is the shortest distance along the earth's surface between the two cities as the crow flies (i.e. great circle distance).
- The assumed average payload for each flight is equivalent to 162 passengers at 100kg per passenger plus bags.
- For all the routes and assessments, a full flight trajectory (climb, cruise and descent segments) optimisation has been conducted. The taxi, TO and landing phases have not been varied.
- Full mission performance assessed for all optimisations, and the phases not being optimised have followed the same altitude and speed profiles as for the baseline trajectory.

8.3.1 Route 1: London – Madrid

The first route is between London Heathrow airport and Madrid Barajas airport in Spain. It provides insight into the effects of engine aging and degradation on optimised trajectories as well as the trade-offs and changes to the fuelburn performance and engine component life for a short range operated aircraft. The fuel burn, severity (and engine component life), DOC and emissions for the optimised trajectories (clean engine, after 3000, 4500 and 5250cycles of engine operation) are compared on this route. The trajectories were optimised for fuelburn, blade creep life, disc creep life, blade fatigue life and blade oxidation life. The results are presented in figures 8.3 to 8.11. The results presented in the figures are normalised values, with the performance metrics for each engine configuration being divided by the baseline equivalent. The normalised value for the baseline is equal to 1.0 for all the metrics.

Table 8.2: London – Madrid engine/aircraft performance changes with increasing cycles of operation relative to baseline.

| Performance Metric | | 3000cycles | 4500cycles | 5250cycles |
|---------------------------------|------------------|------------|------------|------------|
| Flight Mission Fuel Burn [%] | | +3.3 | +9.5 | +12.9 |
| Total Severity [%] | | +58.3 | +164.2 | +281.5 |
| Blade Fatigue Life [%] | | -12.5 | -27.0 | -36.8 |
| Blade Oxidation Life [%] | | -37.1 | -62.5 | -74.1 |
| DOC per Flight [%] | | +1.0 | +3.0 | +4.2 |
| ICAO LTO NOx [%] | | +25.9 | +67.6 | +97.3 |
| Total Flight NOx [%] | | +28.3 | +79.6 | +118.9 |
| Maximum Operating TET [K] | Take Off | +53 | +90 | +115 |
| | Climb | +44 | +85 | +123 |
| | Cruise | +38 | +78 | +108 |
| | Descent | +60 | +105 | +129 |
| | Approach-Landing | +56 | +92 | +106 |

Table 8.2 shows the changes due to degradation in the aircraft performance after 3000, 4500 and 5250cycles of operation. Figure 8.3 shows the optimised flight profiles for the clean, after 3000, 4500 and 5250 cycles. Figure 8.4 shows the normalised mission fuelburn for each of the optimised trajectories. Figure 8.5 shows the severity. Figures 8.6 to 8.9 show the normalised blade creep, disc creep, and blade fatigue and blade oxidation life. The figures are for the clean, after 3000, 4500 and 5250cycles of operation respectively. Figure 8.10 shows the normalised DOC for each of the optimised trajectories. Figure 8.11 shows the normalised ICAO LTO and total flight NOx emissions. The main results, observations and conclusions made are summarised in the following sub-sections.

8.3.1.1 Effects of Ageing and Engine Degradation

The main results for the aircraft performance on the London – Madrid route after 3000, 4500 and 5250cycles relative to the clean engine performance are summarised in table 8.2 above.

The main conclusions drawn from the results are summarised below. They are similar to those discussed in the case study described in chapter 7.

1. The degraded and higher cycle engines must compensate for performance deterioration due to degradation and ageing. This requires the engine to run faster and burn hotter at greater SFC and fuel flow to meet the required thrust and aircraft performance. This results in more fuel burn.

2. The higher operating temperatures required to compensate for the performance losses due to degradation and ageing result in higher levels of engine severity.
3. The higher operating temperatures required to compensate for the performance losses due to degradation and ageing also result in lower HPT blade creep life, disc creep life, blade fatigue life and blade oxidation life. The high temperatures increase the steady state damage fractions (due to blade creep, disc creep and blade oxidation) and the cyclic damage fraction due to blade fatigue.
4. The higher cycles of operation and degraded engines cost more to operate because of higher fuel costs, cost of taxes on emissions and engine maintenance costs.
5. The hotter combustion temperatures required to offset the effects of performance loss due to degradation, promote an increase in the levels of NO_x produced.

NB: Since the degraded engine's performance relative to the baseline has been established and quantified, the % deltas and results presented on the optimised trajectories for the degraded case studies are relative to the non-optimised equivalents and not the baseline.

8.3.1.2 Fuelburn Optimised Trajectory

The results for the clean, after 3000, 4500 and 5250 cycles from the London – Madrid route fuelburn optimised trajectory are summarised in table 8.3. The main conclusions drawn from these results are summarised as below. In cases where the main conclusions were found to be the same, only the discussions for the clean engine are presented, and only where discrepancies exist has a summary and discussion been explicitly provided for the 3000, 4500 and 5250cycles.

1. The fuel burn optimised trajectory burns less fuel and is flown at a higher cruise altitude and speed, resulting in a reduction in the time and fuel burn at cruise. This reduction in cruise fuel burn is more than the combined rise in climb and descent fuel. Hence the optimised trajectory benefits and demonstrates a lower mission fuel burn.
2. The fuel burn optimised trajectory operates at higher maximum cruise temperatures than the baseline. The maximum cruise TET rises by +15K. The higher temperatures result in an increase in the total engine severity, largely due to an increase in the steady state severity by +2.1%.
3. The higher severity signifies greater engine component damage for the optimised trajectory, implying a lower HPT blade creep life and blade oxidation life.
4. The fuelburn optimised trajectory burns less fuel which contributes to a reduction in the cost of fuel and reduces the DOC.
5. The ICAO LTO NO_x is less because of the lower power settings and lower speeds during early climb.

Table 8.3: London – Madrid optimised trajectory results.

| Optimised Trajectory | Flight Cycles | Deltas Relative to the Non - Optimised | | | | | | | | | | | | | Cruise Parameters | |
|----------------------|---------------|--|-------------------|--------------|----|-------|-------------|---------------|-----------------|------------|---------|--------|--------------------|----------------|-------------------|------|
| | | Mission Fuel Burn % | Flight Time [min] | Severity [%] | | | Life [%] | | | | NOx [%] | | DOC per Flight [%] | Cruise TET [K] | | |
| | | | | SS | CS | Total | Blade Creep | Blade Fatigue | Blade Oxidation | Disc Creep | ICAO | Flight | | | | |
| Fuel Burn | Clean | -1.7 | +1.4 | +2.1 | ~ | +2.1 | -3.4 | -0.4 | -2.1 | +0.2 | -5.6 | ~ | -0.9 | +15 | 12172 | 0.82 |
| | 3000 | -2.3 | +1.5 | +2.0 | ~ | +2.0 | -2.3 | ~ | -2.0 | +0.2 | +2.1 | -1.5 | -0.2 | +8 | 12110 | 0.8 |
| | 4500 | -1.8 | +0.7 | +5.0 | ~ | +5.0 | -3.3 | ~ | -4.8 | ~ | +0.7 | +0.4 | -0.2 | +14 | 12192 | 0.82 |
| | 5250 | -3.6 | ~ | +3.8 | ~ | +3.8 | -5.5 | ~ | -3.7 | -0.5 | -1.6 | -1.4 | -0.7 | +8 | 12175 | 0.8 |
| Blade Creep Life | Clean | +3.6 | +9.7 | -7.0 | ~ | -7.0 | +2.5 | ~ | +7.5 | ~ | ~ | +1.6 | +3.0 | -27 | 10668 | 0.68 |
| | 3000 | +3.6 | +9.9 | -7.2 | ~ | -7.2 | +1.5 | ~ | +7.8 | ~ | ~ | +0.8 | +3.0 | -27 | 10670 | 0.68 |
| | 4500 | +3.0 | +8.0 | -8.1 | ~ | -8.0 | +3.3 | ~ | +9.0 | ~ | ~ | +0.6 | +1.6 | -28 | 10669 | 0.68 |
| | 5250 | +0.7 | +6.3 | -7.2 | ~ | -7.2 | +3.8 | ~ | +7.8 | ~ | ~ | -1.6 | +1.6 | -26 | 10668 | 0.7 |
| Blade Fatigue Life | Clean | -0.6 | ~ | +0.7 | ~ | +0.7 | +1.4 | -0.4 | -0.7 | ~ | ~ | +0.8 | -0.2 | +3 | 10674 | 0.79 |
| | 3000 | +0.2 | +0.7 | +3.5 | ~ | +3.5 | +0.1 | ~ | -13.6 | ~ | +4.4 | -0.5 | +0.2 | +13 | 10940 | 0.82 |
| | 4500 | +0.5 | +1.5 | +0.3 | ~ | +0.3 | +1.8 | ~ | +0.1 | -0.3 | +4.4 | +0.5 | +0.5 | ~ | 10668 | 0.79 |
| | 5250 | +1.4 | +7.2 | -7.0 | ~ | -7.0 | +3.8 | ~ | +7.6 | +0.9 | +8.1 | -2.9 | +1.9 | -26 | 10853 | 0.68 |
| Blade Oxidation Life | Clean | +3.8 | +7.6 | -7.1 | ~ | -7.0 | -1.2 | ~ | +7.6 | -0.2 | ~ | -1.2 | +2.5 | -28 | 10668 | 0.68 |
| | 3000 | +3.7 | +8.8 | -7.5 | ~ | -7.3 | +0.5 | ~ | +8.0 | -0.2 | +0.8 | -0.3 | +2.6 | -28 | 10668 | 0.68 |
| | 4500 | +4.2 | +7.7 | -8.7 | ~ | -8.6 | -1.6 | ~ | +9.6 | -0.3 | +0.8 | -1.2 | +2.6 | -28 | 10668 | 0.68 |
| | 5250 | +3.0 | +8.0 | -8.2 | ~ | -8.1 | +3.4 | -0.1 | +8.9 | +0.6 | +1.1 | -1.6 | +2.5 | -27 | 10668 | 0.68 |
| Disc Creep Life | Clean | +0.3 | +3.4 | -1.5 | ~ | -1.5 | +0.3 | ~ | +1.5 | +0.2 | -6.7 | -0.3 | +0.7 | +6 | 10741 | 0.77 |
| | 3000 | -0.5 | +1.8 | -0.7 | ~ | -0.7 | +0.3 | ~ | +0.7 | +0.3 | -2.7 | -2.3 | +0.3 | -3 | 10780 | 0.78 |
| | 4500 | -0.5 | +1.9 | +0.1 | ~ | +0.1 | +0.9 | -0.1 | -0.1 | +0.3 | -2.4 | -0.7 | +0.4 | ~ | 10717 | 0.78 |
| | 5250 | -0.4 | +4.6 | -6.1 | ~ | -6.1 | +4.4 | -0.1 | +6.5 | +0.9 | +0.8 | -2.0 | +1.0 | -22 | 10749 | 0.71 |

CS – Cyclic Severity

SS – Steady State Severity

Total – Total Severity

~ No Change

8.3.1.3 Blade Creep Life Optimised Trajectory

The results for the clean, after 3000, 4500 and 5250 cycles from the London – Madrid route the blade creep life optimised trajectory are summarised in table 8.3. The main conclusions drawn from these results are summarised as below. In cases where the main conclusions were found to be the same, only the discussions for the clean engine are presented, and only where discrepancies exist has a summary and discussion been explicitly provided for the 3000, 4500 and 5250 cycles.

1. The blade creep life optimised trajectory burns more fuel because it is flown at a lower cruise Mach number and same cruise altitude where it operates at a lower maximum operating TET. It spends more time and flies a longer distance during cruise and burns more fuel. The trajectory also burns more fuel during descent because it takes more time and flies a longer distance during descent.
2. The blade creep life optimised trajectory operates at lower maximum cruise temperatures than the non-optimised, reducing by -27K. The lower temperatures result in a decrease in the total engine severity, largely due to a -7% decrease in the steady state severity.
3. The reduced steady state severity manifests as a reduction in the engine component damage fractions due to blade creep and blade oxidation for the optimised trajectory, which implies a benefit of longer HPT blade creep life and blade oxidation life.
4. The blade creep life optimised trajectory burns more fuel which contributes to a rise in the cost of fuel and in DOC.
5. The ICAO LTO cycle is unchanged, whereas the flight NO_x increases largely due to the higher fuel burn and longer time.

8.3.1.4 Blade Fatigue Life Optimised Trajectory

The results for the clean, after 3000, 4500 and 5250 cycles from the London – Madrid route the blade fatigue life optimised trajectory are summarised in table 8.3. The main conclusions drawn from these results are summarised as below.

Clean Engine:

1. The fuel burn for the blade fatigue life optimised trajectory is comparable to the baseline. The trajectory is similar to the baseline but the climb is executed to reach the cruise altitude in less time and less fuel burn. At cruise it flies at a comparable altitude and speed to that of the baseline but flies a longer distance, burning more fuel and taking a longer time at this phase.
2. The severity rises because the blade fatigue life optimised trajectory operates at a marginally higher maximum cruise TET than the baseline. The cruise TET has a discrepancy of +3K. This increase though seemingly marginal, causes a rise in the oxidation damage fraction, hence increasing the steady state severity by +3.5%.

3. The increase in steady state severity due to a higher oxidation damage fraction causes a reduction in the oxidation life.
4. The blade fatigue life optimised trajectory burns less fuel which translates to a reduction in the cost of fuel thereby reducing the DOC.
5. The flight NO_x is higher due to the higher cruise TETs and more cruise fuel burn.

After 3000 cycles:

1. The blade fatigue life optimised trajectory burns more fuel because the descent is longer, burns more fuel and dominates the benefit from the cruise segment. The trajectory is flown at a slightly higher cruise altitude and a faster Mach number.
2. The severity rises for the same reasons outlined for the clean engine. In this case the cruise TET has a discrepancy of +13K and the steady state severity rises by +3.5%.
3. The steady state severity increases due to the higher oxidation damage which lowers the blade oxidation life.
4. The blade fatigue life optimised trajectory burns less fuel which translates to a reduction in the cost of fuel thereby reducing the DOC.
5. The ICAO LTO NO_x increase due to the high power high speed climb for the blade creep life optimised trajectories.

After 4500cycles:

1. The blade fatigue life optimised trajectory burns marginally more fuel for similar reasons to those discussed after 3000cycles.
2. The slightly higher cruise speed causes a marginal increase in steady state severity (+0.3%), resulting in a slight reduction in the blade oxidation life due to the slightly higher blade oxidation damage fraction.
3. The optimised trajectory is executed at less climb and cruise times which benefit the blade creep damage fraction and blade creep life.
4. The marginal increase in fuel burn for the blade fatigue life optimised trajectory translates into a proportional increase in DOC.
5. The ICAO LTO and flight NO_x emissions increase due to the higher fuel burn penalty of the shallow and longer descent.

After 5250cycles:

1. The blade fatigue life optimised trajectory is flown with a slower steep climb, a cruise that is higher and slower and a descent that is initially shallower then steeper than that of the non-optimised. The result is a fuel burn penalty at cruise that outweighs the benefits at climb and descent.
2. The blade fatigue life optimised trajectory is flown at a lower maximum cruise TET (-26K), which causes reduction in steady state severity due to the lower blade and disc creep and blade oxidation damage fractions.
3. The lower damage fractions give a better blade creep, disc creep and blade oxidation lives.

4. The blade fatigue life optimised trajectory burns more fuel which translates to an increase in the cost of fuel thereby increasing the DOC.
5. The ICAO LTO NO_x emissions increase due to the high speed and steep descent, whereas the flight NO_x reduce due to the low speed climb and low power cruise.

8.3.1.5 Blade Oxidation Life Optimised Trajectory

The results for the clean, after 3000, 4500 and 5250 cycles from the London – Madrid route the blade oxidation life optimised trajectory are summarised in table 8.3. The main conclusions drawn from these results are summarised as below. In cases where the main conclusions were found to be the same, only the discussions for the clean engine are presented, and only where discrepancies exist has a summary and discussion been explicitly provided for the 3000, 4500 and 5250cycles.

1. The optimised trajectory burns more fuel because the aircraft flies at a lower cruise Mach number and same cruise altitude where it operates at a lower operating maximum TET, spends more time and flies a longer distance during cruise and burns more fuel. The aircraft also burns more fuel during descent because it takes more time and flies a longer distance during descent.
2. The optimised trajectory operates at lower maximum cruise temperatures than the baseline, reducing by -28K. The lower temperatures result in a reduction in the total engine severity, largely due to a reduction in the steady state severity by -7%.
3. The damage fractions of each failure mode influence the benefit or detriment to the life. The steady state severity is lower due to the contribution of the blade oxidation damage fraction, which gives a better blade oxidation life whereas HPT blade creep and disc creep life are lower due to higher blade and disc creep damage fractions. The cyclic damage is unchanged hence the blade fatigue life remains the same.
4. The optimised trajectory burns more fuel which contributes to an increase in the cost of fuel and in the operating costs.
5. The LTO NO_x remains largely unchanged because the LTO cycle remains the same. The climb, cruise and descent profiles are chosen by the optimiser to maximise oxidation life. The climb is flown faster and then slower, causing a reduction in flight NO_x.

8.3.1.6 Disc Creep Life Optimised Trajectory

The results for the clean, after 3000, 4500 and 5250 cycles from the London – Madrid route the disc creep life optimised trajectory are summarised in table 8.3. The main conclusions drawn from these results are summarised as below. In cases where the main conclusions were found to be the same, only the discussions for the clean engine are presented, and only where discrepancies exist has a summary and discussion been explicitly provided for the 3000, 4500 and 5250cycles.

1. The disc creep life optimised trajectory burns more fuel because the longer descent segment burns more fuel which outweighs the benefit of a reduction in fuel burn during climb and cruise. After 3000cycles, the fuel burn is slightly less, because there is benefit of less fuel burn at climb and cruise which outweighs the penalty of more fuel burn during descent. After 5250cycles, the fuel savings at climb and descent outweigh the fuel penalty of a longer and slower cruise.
2. The disc creep life optimised trajectory is executed at lower cruise temperatures than the non-optimised equivalent. The maximum cruise TET drops by -6K. The lower temperatures result in a decrease in the total engine severity, largely due to a decrease in the steady state severity by -1.5%.
3. The lower steady severity implies reduced blade damage due to creep and oxidation, hence the longer life.
4. The disc creep life optimised trajectory burns more fuel which translates into an increase in fuel costs and the DOC.
5. The disc creep life optimised trajectory is executed with lower power settings at climb and a slower descent thereby reducing the ICAO LTO NOx. The flight NOx is lower due to less fuel burn during climb and cruise.

8.3.2 Route 2: London – Ankara

The second route is between London Heathrow airport and Ankara Esenboga airport in Turkey. It provides insight into the effects of engine aging and degradation on optimised trajectories as well as the trade-offs and changes to the fuelburn performance and engine component life for a short to medium range operated aircraft. The fuel burn and engine life optimised trajectories for the clean, after 3000, 4500 and 5250cycles of engine operation are compared on this route in terms of fuel burn, severity, engine component life, DOC and emissions. The route was optimised for each of mission fuel burn, blade creep life, disc creep life, blade fatigue life and blade oxidation life. The engine performance results for the optimised trajectories are presented in figures 8.12 to 8.20. The results presented are normalised values, with the performance metrics for each engine configuration being divided by the baseline equivalent. The normalised value for the baseline is equal to 1.0 for all the metrics. The results give an insight to the changes (deviations) from the baseline value.

Table 8.4 shows the changes in the aircraft performance after 3000, 4500 and 5250cycles of operation. Figure 8.12 shows the optimised flight profiles for the clean, after 3000, 4500 and 5250 cycles. Figure 8.13 shows the normalised mission fuelburn for each of the optimised trajectories. Figure 8.14 shows the normalised severity. Figures 8.15 to 8.18 show the normalised blade creep, disc creep, blade fatigue and blade oxidation life. The figures shown are for the clean, after 3000, 4500 and 5250cycles of operation respectively. Figure 8.19 shows the normalised DOC for each of the optimised trajectories. Figure 8.20 shows the normalised ICAO LTO and total flight NOx emissions. The main

observations and conclusions made from the results are summarised in the following sub-sections.

Table 8.4: London – Ankara engine/aircraft performance changes with increasing cycles of operation relative to the baseline.

| Performance Metric | | 3000cycles | 4500cycles | 5250cycles |
|---------------------------------|------------------|------------|------------|------------|
| Flight Mission Fuel Burn [%] | | +3.5 | +9.4 | +12.1 |
| Total Severity [%] | | +63.5. | +191.5 | +327.4. |
| Blade Fatigue Life [%] | | -12.5 | -27.0 | -36.8 |
| Blade Oxidation Life [%] | | -39.2 | -66.0 | -76.9 |
| DOC per Flight [%] | | +1.2 | +3.5 | +4.3 |
| ICAO LTO NOx [%] | | +26.5 | +68.4 | +91.5 |
| Total Flight NOx [%] | | +28.8 | +84.7 | +137.0 |
| Maximum Operating TET [K] | Take Off | +53 | +90 | +115 |
| | Climb | +44 | +85 | +123 |
| | Cruise | +39 | +80 | +111 |
| | Descent | +60 | +105 | +129 |
| | Approach-Landing | +47 | +86 | +106 |

8.3.2.1 Effects of Ageing and Engine Degradation

The main results for the aircraft performance on the London – Ankara route after 3000, 4500 and 5250cycles relative to the clean engine performance are summarised in table 8.4 above.

The main conclusions drawn from these results are similar to those from the results for the London to Madrid route presented in section 8.3.1, and will therefore not be repeated here. The only difference is in the higher magnitudes due to higher levels of degradation.

9.3.2.2 Fuelburn Optimised Trajectory

The results for the clean, after 3000, 4500 and 5250 cycles from the London – Ankara route fuelburn optimised trajectory are summarised in table 8.5. The main conclusions drawn from these results are summarised as below. In cases where the main conclusions were found to be the same, only the discussions for the clean engine are presented, and only where discrepancies exist has a summary and discussion been explicitly provided for the 3000, 4500 and 5250cycles.

Table 8.5: London – Ankara optimised trajectory results.

| Optimised Trajectory | Flight Cycles | Deltas Relative to the Non - Optimised | | | | | | | | | | | | | Cruise Parameters | |
|----------------------|---------------|--|-------------------|--------------|----|-------|-------------|---------------|-----------------|------------|---------|--------|--------------------|----------------|-------------------|------|
| | | Mission Fuel Burn [%] | Flight Time [min] | Severity [%] | | | Life [%] | | | | NOx [%] | | DOC per Flight [%] | Cruise TET [K] | | |
| | | | | SS | CS | Total | Blade Creep | Blade Fatigue | Blade Oxidation | Disc Creep | ICAO | Flight | | | | |
| Fuel Burn | Clean | -4.6 | -4.4 | +3.9 | ~ | +3.9 | -2.2 | ~ | -3.8 | +0.4 | ~ | -2.3 | -2.0 | +22 | 12192 | 0.82 |
| | 3000 | -4.7 | -3.6 | +4.8 | ~ | +4.8 | -2.7 | -0.1 | -4.9 | +0.6 | -3.1 | -2.3 | -2.1 | +16 | 12065 | 0.82 |
| | 4500 | -3.3 | -3.7 | +5.1 | ~ | +5.1 | -2.1 | ~ | -4.9 | +0.2 | +6.1 | -3.8 | -1.4 | +13 | 11649 | 0.82 |
| | 5250 | -4.2 | -1.7 | +8.3 | ~ | +8.3 | -5.8 | -0.1 | -7.7 | -0.3 | +0.7 | -7.6 | -1.5 | +19 | 12183 | 0.82 |
| Blade Creep Life | Clean | +4.9 | +22 | -4.1 | ~ | -4.0 | +2.2 | ~ | +4.3 | -0.4 | ~ | +2.8 | +4.8 | -17 | 10668 | 0.7 |
| | 3000 | +3.5 | +17.5 | -3.6 | ~ | -3.5 | +1.4 | ~ | +3.7 | -0.3 | +0.3 | +2.0 | +3.7 | -15 | 10668 | 0.72 |
| | 4500 | +2.6 | +13.3 | -4.0 | ~ | -3.9 | +2.8 | ~ | +4.1 | -0.1 | +2.8 | +1.5 | +2.7 | -14 | 10668 | 0.72 |
| | 5250 | +6.9 | +27.2 | -2.0 | ~ | -1.9 | +5.4 | ~ | +2.0 | +0.1 | +7.9 | -1.9 | +6.2 | -16 | 10675 | 0.68 |
| Blade Fatigue Life | Clean | -4.6 | -4.4 | +3.9 | ~ | +3.9 | -2.2 | ~ | -3.8 | +0.4 | ~ | -2.3 | -2.0 | +22 | 12192 | 0.82 |
| | 3000 | +2.9 | +19.9 | +5.3 | ~ | +5.2 | -2.2 | ~ | -5.0 | -0.3 | ~ | +2.0 | +3.9 | +14 | 12165 | 0.71 |
| | 4500 | +4.6 | +17.9 | -4.6 | ~ | -4.6 | -2.2 | ~ | +4.9 | -0.7 | -0.8 | ~ | +3.7 | -17 | 10668 | 0.82 |
| | 5250 | +6.2 | +22.8 | -2.5 | ~ | -2.5 | +5.0 | ~ | +2.6 | +0.2 | +2.9 | -2.4 | +5.1 | -15 | 10705 | 0.69 |
| Blade Oxidation Life | Clean | +5.9 | +25.3 | -5.3 | ~ | -4.2 | +2.0 | ~ | +4.5 | -0.5 | +5.3 | +3.4 | +5.6 | -17 | 10668 | 0.68 |
| | 3000 | +6.0 | +25.3 | -5.1 | ~ | -5.1 | +0.9 | ~ | +4.3 | -0.5 | -0.6 | +4.4 | +5.5 | -17 | 10711 | 0.69 |
| | 4500 | +5.4 | +20.4 | -4.7 | ~ | -5.7 | -3.0 | ~ | +5.0 | -0.8 | +3.3 | +1.2 | +4.7 | -20 | 10688 | 0.69 |
| | 5250 | +7.9 | +27.2 | -2.6 | ~ | -2.6 | -5.7 | ~ | +2.6 | -1.4 | +11.5 | -2.4 | +6.6 | -17 | 10688 | 0.68 |
| Disc Creep Life | Clean | -3.7 | -3.8 | +3.6 | ~ | +3.6 | -3.6 | -0.1 | -3.5 | +0.5 | -5.7 | -3.0 | -1.6 | +19 | 11865 | 0.82 |
| | 3000 | -4.7 | -3.1 | +4.7 | ~ | +4.6 | -3.1 | -0.1 | -4.5 | +0.7 | -1.9 | -3.2 | -1.8 | +10 | 12073 | 0.82 |
| | 4500 | -1.1 | -5.0 | +2.9 | ~ | +2.9 | +0.9 | -0.1 | -2.9 | +0.4 | -3.0 | -2.3 | -1.1 | +10 | 10668 | 0.81 |
| | 5250 | -0.9 | +1.0 | +1.8 | ~ | +1.8 | +2.6 | -0.2 | -1.8 | +0.8 | ~ | -7.5 | -0.1 | +3 | 10849 | 0.79 |

CS – Cyclic Severity

SS – Steady State Severity

Total – Total Severity

~ No Change

1. The fuel burn optimised trajectory burns less fuel and is flown at a higher cruise altitude and faster cruise speed. This reduces the time at cruise and the fuel burn. The fuel savings during cruise outweigh the penalty at climb and descent and give benefit to the mission fuel burn and the total flight time.
2. The fuel burn optimised trajectory operates at higher maximum cruise temperatures than the baseline. The maximum cruise TET rises by +22K. The higher temperatures result in an increase in the total engine severity, largely due to an increase in the steady state severity by +3.9%.
3. The steady state severity increases due to the higher blade creep and blade oxidation damage fractions for the optimised trajectory which shorten the HPT blade creep life and blade oxidation life.
4. The lower fuel burn demonstrated by the optimised trajectory translates into a reduction in the cost of fuel and DOC.
5. The flight NOx benefits from the low speed low power climb settings and the lower cruise fuel burn.

8.3.2.3 Blade Creep Life Optimised Trajectory

The results for the clean, after 3000, 4500 and 5250 cycles from the London – Ankara route blade creep life optimised trajectory are summarised in table 8.5. The main conclusions drawn from these results are summarised as below. In cases where the main conclusions were found to be the same, only the discussions for the clean engine are presented, and only where discrepancies exist has a summary and discussion been explicitly provided for the 3000, 4500 and 5250cycles.

1. The blade creep life optimised trajectory burns more fuel because the trajectory is executed with a faster climb to ToC for less fuel burn, a slower and longer cruise segment at more fuel burn and a longer and slower descent at more fuel burn. The fuel penalty at cruise and descent outweighs the gain in climb.
2. The blade creep life optimised trajectory operates at a lower maximum cruise temperature (-17K) than the baseline. The lower temperatures result in a reduction in the total engine severity, largely due to a decrease in the steady state severity by -4.1%.
3. The reduction in the steady state severity is due to the contribution of the blade creep and blade oxidation damage giving a better HPT blade creep life and blade oxidation life.
4. The fuelburn optimised trajectories burn more fuel which contributes to an increase in the cost of fuel and increases the DOC
5. The flight NOx is more due to the increase in the cruise and descent NOx which outweighs the reduction accrued during limb. After 5250cycles, the flight NOx reduces due to the benefit in the climb and cruise NOx which outweighs the penalty accrued at descent.

8.3.2.4 Blade Fatigue Life Optimised Trajectory

The results for the clean, after 3000, 4500 and 5250 cycles from the London – Ankara route blade fatigue life optimised trajectory are summarised in table 8.5. The main conclusions drawn from these results are summarised as below. The trajectory flown for the clean blade fatigue optimised is the same as for the clean fuel burn optimised trajectory hence the main conclusions are as those already discussed in 8.3.2.2. As discrepancies exist after 3000 and 4500cycles, a summary and discussion have been explicitly provided. The main conclusions drawn from the results for the 5250cycles assessments were found to be the same as those for the 4500cycles, except where explicitly provided.

After 3000 cycles:

1. The blade fatigue life optimised trajectory burns more fuel and is flown at a higher cruise altitude and a faster cruise Mach number. The fuel penalty accrued at climb and descent outweighs the reduction in fuel burn at cruise.
2. The higher maximum cruise TET (+14K) of the optimised trajectory increases the steady state severity by +5.3%.
3. The higher steady state severity is due to the higher blade creep and blade oxidation damage fractions which lower the HPT blade creep and oxidation lives.
4. The more fuel burn demonstrated by the blade fatigue life optimised trajectory translates into an increase in fuel costs and in the DOC.
5. The flight NOx benefits from the lower power settings and speed at climb as well as from the reduction in cruise fuel burn.

After 4500cycles:

1. The blade fatigue life optimised trajectory burns more fuel and is flown at the same cruise altitude and a faster Mach number of 0.82. The trajectory is executed by burning more fuel at climb and cruise.
2. The optimised trajectory is at lower maximum cruise TET (-17K) which reduces the engine severity due to a reduction in the steady state severity (-4.6%) contribution.
3. The optimised trajectory incurs a higher blade creep damage fraction which lowers the HPT blade creep life. The blade oxidation and disc creep damage fractions are lower and promote the blade oxidation and disc creep lives respectively. After 5250cycles, the optimised trajectory has a lower blade creep damage fraction, hence a better blade creep life.
4. The more fuel burn demonstrated by the blade fatigue life optimised trajectory translates into an increase in fuel costs and in the DOC.
5. The flight NOx benefits from the lower climb settings and the lower cruise temperatures.

8.3.2.5 Blade Oxidation Life Optimised Trajectory

The results for the clean, after 3000, 4500 and 5250 cycles from the London – Ankara route blade oxidation life optimised trajectory are summarised in table 8.5. The main conclusions drawn from these results are summarised as below. In cases where the main conclusions were found to be the same, only the discussions for the clean engine are presented, and only where discrepancies exist has a summary and discussion been explicitly provided for the 3000, 4500 and 5250cycles.

1. The blade oxidation life optimised trajectory is flown at the same cruise altitude and slower cruise Mach number. The trajectory burns more fuel because it is executed with a faster climb to ToC for less fuel burn, a slower and longer cruise segment and more fuel burn and a longer and slower descent at more fuel burn. The fuel penalty at cruise and descent outweighs the gain in climb.
2. The blade creep life optimised trajectory operates at a lower maximum cruise temperature (-17K) than the baseline. The lower temperatures result in a reduction in the total engine severity, largely due to a decrease in the steady state severity by -5.3%.
3. The reduction in the steady state severity is due to the contribution of the blade creep and blade oxidation damage, which give a better HPT blade creep life and blade oxidation life. After 4500cycles, the optimised trajectory is executed with higher blade and disc creep damage fractions, and a lower blade oxidation damage fraction which give a lower blade creep life, disc creep life and a better blade oxidation life respectively. After 5250cycles, the optimised trajectory has a higher blade creep damage fraction, which is demonstrated as a lower blade creep life.
4. The blade oxidation life optimised trajectory burns more fuel which contributes to an increase in the cost of fuel and in the operating costs
5. The optimised trajectory executes the descent at high power settings which translate into an increase in the ICAO LTO NOx. The flight NOx is more due to the increase in the cruise and descent NOx which outweighs the reduction during climb.

8.3.2.6 Disc Creep Life Optimised Trajectory

The results for the clean, after 3000, 4500 and 5250 cycles from the London – Ankara route disc creep life optimised trajectory are summarised in table 8.5. The main conclusions drawn from these results are summarised as below. In cases where the main conclusions were found to be the same, only the discussions for the clean engine are presented, and only where discrepancies exist has a summary and discussion been explicitly provided for the 3000, 4500 and 5250cycles

1. The optimised trajectory spends less time at cruise and burns less fuel due to the trajectory being flown higher and faster. The fuel burn benefit during cruise outweighs the fuel penalty at climb and descent.

2. The disc creep life optimised trajectories operates at a higher maximum cruise temperature than the baseline. The cruise TET rises by +19K. The higher temperature results in an increase in the total engine severity, largely due to an increase in the steady state severity by +3.6%.
3. The increase in steady state severity is due to the contribution of the higher blade creep and blade oxidation damage fractions. The higher damage fractions cause a reduction in the HPT blade creep life and blade oxidation life. The disc creep damage fraction is slightly lower hence the marginal gain in the disc creep life. After 4500 and 5250 cycles, the optimised trajectory experiences a reduction in blade creep damage fraction hence the better blade creep life.
4. The disc creep life optimised trajectory burns less fuel which contributes to a reduction in the cost of fuel and reduces the DOC
5. The ICAO LTO NO_x is less because of low power settings at climb, and the flight NO_x benefits from the reduction in cruise fuel burn.

8.3.3 Route 3: London – Abu Dhabi

The third route is between London Heathrow airport and Abu Dhabi International airport. It provides insight into the effects of engine aging and degradation on optimised trajectories as well as the trade-offs and changes to the fuelburn performance and engine component life for a medium to long range operated aircraft. The optimised trajectories for the clean, after 3000, 4500 and 5250 cycles of engine operation are compared on this route in terms of fuel burn, engine component life, DOC and emissions. The route was optimised for fuelburn, blade creep life, disc creep life, blade fatigue life and blade oxidation life. The engine performance results for the optimised trajectories are presented in figures 8.21 to 8.29. The results presented are normalised values, with the performance metrics for each engine configuration being divided by the baseline equivalent. The normalised value for the baseline is equal to 1.0 for all the metrics.

Table 8.6 shows the changes in the engine/aircraft performance after 3000, 4500 and 5250 cycles of operation. Figure 8.21 shows the optimised flight profiles for the clean, after 3000, 4500 and 5250 cycles. Figure 8.22 shows the normalised mission fuelburn for each of the optimised trajectories. Figure 8.23 shows the normalised severity. Figures 8.24 to 8.27 show the normalised blade creep, disc creep, and blade fatigue and blade oxidation life. The figures shown are for the clean, after 3000, 4500 and 5250 cycles of operation respectively. Figure 8.28 shows the normalised DOC for each of the optimised trajectories. Figure 8.29 shows the normalised ICAO LTO and total flight NO_x emissions. The main observations and conclusions made from the results are summarised in the following sub-sections.

8.3.3.1 Effects of Ageing and Engine Degradation

The main results for the aircraft performance on the London – Abu Dhabi route after 3000, 4500 and 5250 cycles relative to the clean engine performance are summarised in table 8.6.

Table 8.6: London – Abu Dhabi aircraft performance changes with increasing cycles of operation relative to baseline.

| Performance Metric | | 3000cycles | 4500cycles | 5250cycles |
|---------------------------------|------------------|------------|------------|------------|
| Flight Mission Fuel Burn [%] | | +3.7 | +9.0 | +13.3 |
| Total Severity [%] | | +68.9 | +207.8 | +351.5 |
| Blade Fatigue Life [%] | | -12.5 | -27.0 | -36.8 |
| Blade Oxidation Life [%] | | -41.1 | -67.8 | -78.1 |
| DOC per Flight [%] | | +1.4 | +3.6 | +5.3 |
| ICAO LTO NOx [%] | | +26.3 | +68.7 | +96.8 |
| Total Flight NOx [%] | | +32.8 | +90.0 | +139.8 |
| Maximum Operating TET [K] | Take Off | +53 | +90 | +115 |
| | Climb | +44 | +85 | +123 |
| | Cruise | +42 | +85 | +120 |
| | Descent | +60 | +105 | +129 |
| | Approach-Landing | +68 | +106 | +123 |

The main conclusions drawn from the results are similar to those from the results for the London to Madrid route presented in section 8.3.1, and therefore will not be repeated here. The only difference is in the higher magnitudes due to even higher levels of degradation.

8.3.3.2 Fuelburn Optimised Trajectory

The results for the clean, after 3000, 4500 and 5250 cycles from the London – Abu Dhabi route fuelburn optimised trajectory are summarised in table 8.7. The main conclusions drawn from these results are summarised as below. In cases where the main conclusions were found to be the same, only the discussions for the clean engine are presented, and only where discrepancies exist has a summary and discussion been explicitly provided for the 3000, 4500 and 5250 cycles.

1. The fuel burn optimised trajectory is flown at a higher cruise altitude and faster cruise speed. This reduces the time at cruise and the fuel burn. The savings accrued during the cruise phase outweigh the increase during climb and descent and give benefit to the flight time and the mission fuel burn.

Table 8.7: London – Abu Dhabi optimised trajectory results.

| Optimised Trajectory | Flight Cycles | Deltas Relative to the Non - Optimised | | | | | | | | | | | | | Cruise Parameters | |
|----------------------|---------------|--|-------------------|--------------|----|-------|-------------|---------------|-----------------|------------|---------|--------|--------------------|----------------|-------------------|------|
| | | Mission Fuel Burn [%] | Flight Time [min] | Severity [%] | | | Life [%] | | | | NOx [%] | | DOC per Flight [%] | Cruise TET [K] | | |
| | | | | SS | CS | Total | Blade Creep | Blade Fatigue | Blade Oxidation | Disc Creep | ICAO | Flight | | | | |
| Fuel Burn | Clean | -5.2 | -10.1 | +5.3 | ~ | +5.2 | -3.0 | -0.2 | -5.0 | +1.0 | +3.2 | -3.6 | -2.8 | +28 | 12190 | 0.82 |
| | 3000 | -5.5 | -8.1 | +7.3 | ~ | +6.7 | -2.7 | -0.3 | -6.3 | +1.3 | -5.2 | -30.3 | -2.7 | +26 | 12191 | 0.82 |
| | 4500 | -6.4 | -12.4 | +3.2 | ~ | +2.2 | -3.6 | -0.1 | -2.2 | +0.5 | -27.1 | -30.3 | -3.7 | +26 | 12191 | 0.82 |
| | 5250 | -7.0 | -14.4 | -2.7 | ~ | -3.7 | -6.5 | -0.2 | +3.9 | +0.5 | -6.0 | -4.6 | -4.0 | +26 | 12190 | 0.82 |
| Blade Creep Life | Clean | -0.2 | -0.5 | +0.7 | ~ | +0.6 | +2.0 | ~ | -0.7 | +0.1 | ~ | +0.4 | -0.1 | +3 | 10700 | 0.79 |
| | 3000 | -1.3 | -6.5 | +2.1 | ~ | +1.6 | +1.3 | ~ | -1.6 | +0.3 | +6.9 | -0.9 | -1.1 | +6 | 10822 | 0.81 |
| | 4500 | -1.4 | -4.2 | -2.7 | ~ | -3.5 | +3.2 | ~ | +3.6 | +0.5 | +4.7 | -26.9 | -0.8 | +20 | 10700 | 0.79 |
| | 5250 | -0.2 | -6.1 | -6.9 | ~ | -7.8 | +6.0 | ~ | +8.5 | +1.3 | +4.7 | ~ | -1.2 | +1 | 10700 | 0.79 |
| Blade Fatigue Life | Clean | -2.8 | -8.4 | +3.1 | ~ | +3.1 | -1.6 | ~ | -3.0 | +0.5 | +7.4 | -2.7 | -1.8 | +16 | 11402 | 0.82 |
| | 3000 | -2.8 | +0.8 | +5.4 | ~ | +4.8 | -2.2 | ~ | -4.6 | +0.5 | +0.4 | -3.3 | -0.9 | +18 | 11808 | 0.79 |
| | 4500 | -1.4 | ~ | -2.3 | ~ | -3.1 | +0.8 | ~ | +0.1 | +0.4 | -21.7 | -27.9 | -0.7 | +3 | 10924 | 0.79 |
| | 5250 | +0.3 | +10.9 | -7.2 | ~ | -8.1 | +2.3 | ~ | +8.9 | +0.3 | +1.4 | ~ | +1.2 | ~ | 10867 | 0.79 |
| Blade Oxidation Life | Clean | +2.3 | +18.8 | -0.7 | ~ | -0.7 | +1.1 | ~ | +0.7 | -0.2 | -6.5 | +1.5 | +2.7 | -4 | 10668 | 0.75 |
| | 3000 | +3.0 | +21.9 | ~ | ~ | -0.5 | +1.1 | ~ | +0.5 | -0.4 | +2.6 | +1.7 | +3.3 | -3 | 10680 | 0.74 |
| | 4500 | +2.5 | +22.4 | -3.7 | ~ | -4.5 | +2.2 | -0.1 | +4.7 | ~ | -26.5 | -25.3 | +3.0 | -3 | 10668 | 0.75 |
| | 5250 | +1.0 | +11.9 | -8.1 | ~ | -9.0 | +1.4 | ~ | +10.0 | ~ | ~ | ~ | +0.9 | -4 | 10677 | 0.75 |
| Disc Creep Life | Clean | -5.0 | -7.7 | +5.6 | ~ | +5.5 | -2.9 | -0.1 | -5.3 | +1.1 | -5.0 | -3.8 | -2.5 | +29 | 12190 | 0.82 |
| | 3000 | -5.5 | -8.1 | +7.3 | ~ | +6.7 | -2.7 | -0.1 | -6.3 | +1.2 | -5.2 | -4.7 | -1.4 | +26 | 12190 | 0.82 |
| | 4500 | -6.4 | -12.4 | +3.2 | ~ | +2.2 | -3.6 | -0.1 | -2.2 | +1.3 | -27.1 | -30.3 | -3.7 | +26 | 12190 | 0.82 |
| | 5250 | -3.2 | -17.9 | -7.1 | ~ | -8.0 | +4.3 | -0.1 | +8.8 | +1.6 | -8.6 | -1.9 | -3.0 | +6 | 10697 | 0.82 |

CS – Cyclic Severity

SS – Steady State Severity

Total – Total Severity

~ No Change

2. The fuel burn optimised trajectory operates at a higher maximum cruise temperature than the baseline. The maximum cruise TET rises by +28K. The higher temperature results in an increase in the total engine severity, largely due to an increase in the steady state severity by +5.3%.
3. The higher blade creep and blade oxidation damage fractions demonstrated by the optimised trajectory shorten the HPT blade creep life and blade oxidation life. The disc creep life benefits from the lower disc creep damage fraction. The slightly higher cyclic damage marginally reduces the fatigue life. After 5250cycles, the trajectory has a reduced blade oxidation damage fraction which translates into a reduction in steady state severity by -2.7%, hence the better blade oxidation life.
4. The fuelburn optimised trajectory burns less fuel which contributes to a reduction in the cost of fuel and reduces the DOC
5. The optimised trajectory is executed with a high speed initial climb which increases the ICAO LTO. The flight NOx benefits from the reduction in fuel burn during cruise. After 3000cycles, the low power settings at climb benefit the ICAO LTO NOx. After 4500cycles, the ICAO LTO and flight NOx emissions benefit from a slower speed climb and descent. After 5250cycles, the ICAO LTO NOx benefit from the slower climb and the flight NOx has added benefit from the reduced fuel burn at descent.

8.3.3.3 Blade Creep Life Optimised Trajectory

The results for the clean, after 3000, 4500 and 5250 cycles from the London – Abu Dhabi route blade creep life optimised trajectory are summarised in table 8.7. The main conclusions drawn from these results are summarised as below. In cases where the main conclusions were found to be the same, only the discussions for the clean engine are presented, and only where discrepancies exist has a summary and discussion been explicitly provided for the 3000, 4500 and 5250cycles. :

1. The blade creep life optimised trajectory is flown at a low power climb, a comparable cruise altitude and cruise speed and a shallow initial descent. This reduces the time and fuel burn at climb and cruise. The savings accrued during the climb and cruise phase dominate and outweigh the increase during descent and benefit the mission fuel burn.
2. The blade creep life optimised trajectory operates at a higher maximum cruise temperature than the baseline. The maximum cruise TET rises marginally by +3K. The higher temperature results in an increase in the total engine severity, largely due to an increase in the steady state severity by +0.7% (due to a higher blade oxidation damage fraction). After 4500 and 5250cycles, the severity reduces due to a reduction in the steady state severity, a result of lower blade oxidation damage.
3. The higher blade oxidation damage fraction demonstrated by the optimised trajectory shortens the HPT blade oxidation life. The blade creep life and disc creep life benefit from the lower blade creep and disc creep damage fractions. The cyclic damage is unchanged hence no change in the fatigue life. After 4500 and 5250cycles, the lower blade

- creep, disc creep and oxidation damage fractions contribute to give a better blade creep, blade oxidation and disc creep lives.
4. The blade creep life optimised trajectory burns less fuel which contributes to a reduction in the cost of fuel and reduces the DOC
 5. The flight NO_x is more due to a long shallow descent which burns more fuel. After 3000cycles, the flight NO_x benefits from the reduction in cruise fuel burn. After 4500cycles, the flight NO_x benefits from the low thrust settings at climb and initial descent.

8.3.3.4 Blade Fatigue Life Optimised Trajectory

The results for the clean, after 3000, 4500 and 5250 cycles from the London – Abu Dhabi route blade fatigue life optimised trajectory are summarised in table 8.7. The main conclusions drawn from these results are summarised as below. In cases where the main conclusions were found to be the same, only the discussions for the clean engine are presented, and only where discrepancies exist has a summary and discussion been explicitly provided for the 3000, 4500 and 5250cycles.

1. The blade fatigue life optimised trajectory is flown at a high speed climb, a higher cruise altitude and faster cruise speed and a steep initial descent. The benefit from the reduced fuel burn at cruise dominates the increase during climb and descent giving benefit to the mission fuel burn.
2. The blade fatigue life optimised trajectory operates at a higher maximum cruise temperature than the baseline. The maximum cruise TET rises by +16K. The higher temperature results in an increase in the total engine severity, largely due to an increase in the steady state severity by +3.1% (due to higher blade creep and blade oxidation damage fractions). After 4500 and 5250cycles, the total severity is less because there is a reduction in the steady state severity due to lower blade creep, blade oxidation and disc creep damage fractions.
3. The higher blade creep and blade oxidation damage fractions demonstrated by the optimised trajectory shorten the HPT blade creep and blade oxidation life. The disc creep life benefits from the lower disc creep damage fractions. The cyclic damage is unchanged hence no change in the fatigue life. After 4500 and 5250cycles, the lower blade creep, blade oxidation and disc creep damage fractions give better life.
4. The blade fatigue life optimised trajectory burns less fuel which contributes to a reduction in the cost of fuel and reduces the DOC. After 5250cycles, the optimised trajectory demonstrates a higher fuel burn which translates into higher fuel costs and DOC.
5. The optimised trajectory is executed with a climb at high power settings which increases the ICAO LTO NO_x. The flight NO_x benefits from the reduced fuel burn achieved during the higher altitude and high speed. After 4500cycles, the ICAO LTO NO_x benefits from a low speed climb.

8.3.3.5 Blade Oxidation Life Optimised Trajectory

The results for the clean, after 3000, 4500 and 5250 cycles from the London – Abu Dhabi route blade oxidation life optimised trajectory are summarised in table 8.7. The main conclusions drawn from these results are summarised as below. In cases where the main conclusions were found to be the same, only the discussions for the clean engine are presented, and only where discrepancies exist has a summary and discussion been explicitly provided for the 3000, 4500 and 5250cycles.

1. The blade oxidation life optimised trajectory burns more fuel because the trajectory is executed with a faster climb to ToC for less fuel burn, a slower and longer cruise segment and more fuel burn and a longer and slower descent at more fuel burn. The fuel penalty at cruise and descent outweighs the gain in climb.
2. The blade creep life optimised trajectory operates at a lower maximum cruise temperature (-4K) than the baseline. The lower temperatures result in a reduction in the total engine severity, largely due to a decrease in the steady state severity by -0.7%.
3. The reduction in the steady state severity is due to the contribution of the blade creep and blade oxidation damage fractions, which give a better HPT blade creep life and blade oxidation life.
4. The blade oxidation life optimised trajectory burns more fuel which contributes to an increase in the cost of fuel and in the operating costs
5. The optimised trajectory executes the climb at low speed and low thrust settings which translate into a reduction in the ICAO LTO NOx. The flight NOx is more due to the increase in the cruise and descent fuel burn (and NOx) which outweigh the reduction gained during climb. After 3000cycles, the ICAO LTO NOx rises due to the high power settings and speeds at climb. After 4500cycles, the flight NOx benefits from a reduction in the climb and descent fuel burn as well as the lower cruise temperatures.

8.3.3.6 Disc Creep Life Optimised Trajectory

The results for the clean, after 3000, 4500 and 5250 cycles from the London – Abu Dhabi route disc creep life optimised trajectory are summarised in table 8.7. The main conclusions drawn from these results are summarised as below. In cases where the main conclusions were found to be the same, only the discussions for the clean engine are presented, and only where discrepancies exist has a summary and discussion been explicitly provided for the 3000, 4500 and 5250cycles.

1. The disc creep life optimised trajectory is flown at a higher cruise altitude and faster cruise speed. This reduces the time at cruise and the fuel burn. The savings accrued during the cruise phase dominate the increase during climb and descent and give benefit to the flight time and the mission fuel burn.

2. The fuel burn optimised trajectory operates at a higher maximum cruise temperature than the baseline. The maximum cruise TET rises by +29K. The higher temperature results in an increase in the total engine severity, largely due to an increase in the steady state severity by +5.6%. After 5250cycles, the optimised trajectory is executed in less flight time and marginally higher cruise temperatures (+6K) resulting in a reduction in steady state severity by -7.1%.
3. The higher blade creep and blade oxidation damage fractions demonstrated by the optimised trajectory shorten the HPT blade creep life and blade oxidation life. The disc creep life benefits from the lower disc creep damage fraction. The slightly higher cyclic damage marginally reduces the fatigue life. After 5250cycles, the blade creep and blade oxidation damage fractions are lower hence the better blade creep life and blade oxidation life.
4. The fuelburn optimised trajectory burns less fuel which contributes to a reduction in the cost of fuel and reduces the DOC
5. The optimised trajectory is executed with a low speed climb which reduces the ICAO LTO NOx. The flight NOx benefits from the reduction in fuel burn during cruise.

8.4 Summary and Conclusions

The main aim of this chapter was to present the results of aircraft trajectory optimisation assessments carried out on a short to medium range aircraft similar to the Boeing 737-800 aircraft powered by a CFM56-7B27. The first part of the chapter involved defining the aircraft trajectory to be optimised. Assessments were made on three routes (London - Madrid, London - Ankara and London – Abu Dhabi) to assess the trade-offs between fuel burn and engine life optimised aircraft trajectories. These were presented in the second part of the chapter with the aid of several case studies.

The case studies were conducted on the CUCCTF engine model and CUSMSA aircraft model described in chapter 2. The case studies were conducted along each route for a clean engine and after 3000, 4500 and 5250cycles.

A baseline performance was established for each route to enable comparison and have a point of reference. It was assumed by matching it to the payload range performance of the Boeing 737-800 after which it was modelled. Changes were made to the health parameters so as to model the effects of engine degradation. A generic multi-disciplinary integration framework coupled with an optimiser was used to make techno-economic preliminary assessments to enable the analyses to be made. The models used were validated as described in chapters 2, 3, 4 and 5.

An important factor to note when analysing the results, is that the numerical values presented here are not definitive (or absolute), but rather relative and indicative for the purpose of showing the trade-offs between fuel burn optimised and engine life optimised trajectories.

The fuel burn optimised trajectories were found to be at higher operating temperatures with reduced blade (creep, fatigue and oxidation) lives. In particular, for London–Madrid, the blade creep and blade oxidation lives for the clean engine were found to reduce by -3.4% and -2.1% respectively. The blade oxidation life optimised trajectories demonstrated an increase in fuel burn of +3.6% and +4.9% for London–Madrid and London–Ankara respectively. The blade creep life optimised trajectories for London–Abu Dhabi were found to benefit from less fuel burn during climb. The disc creep life optimised trajectories showed benefit in fuel burn for London–Ankara and London–Abu Dhabi.

The conclusions from the study are:

- Fuel burn optimised trajectories have a negative effect on the blade life due to creep, fatigue and oxidation due to higher maximum temperatures. However, the reduction in fuel burn dominates the drop in life to benefit the operating costs
- Optimising for blade creep life benefits the fuel burn for London–Abu Dhabi due to less fuel burn at climb
- The blade oxidation life optimised trajectories are detrimental to the fuel burn due to slower cruise speeds and more time spent at cruise and descent
- The disc creep life optimised trajectories benefit the fuel burn for London – Ankara and London–Abu Dhabi due to higher altitudes and less fuel burn at cruise. .

Figures for Chapter 8

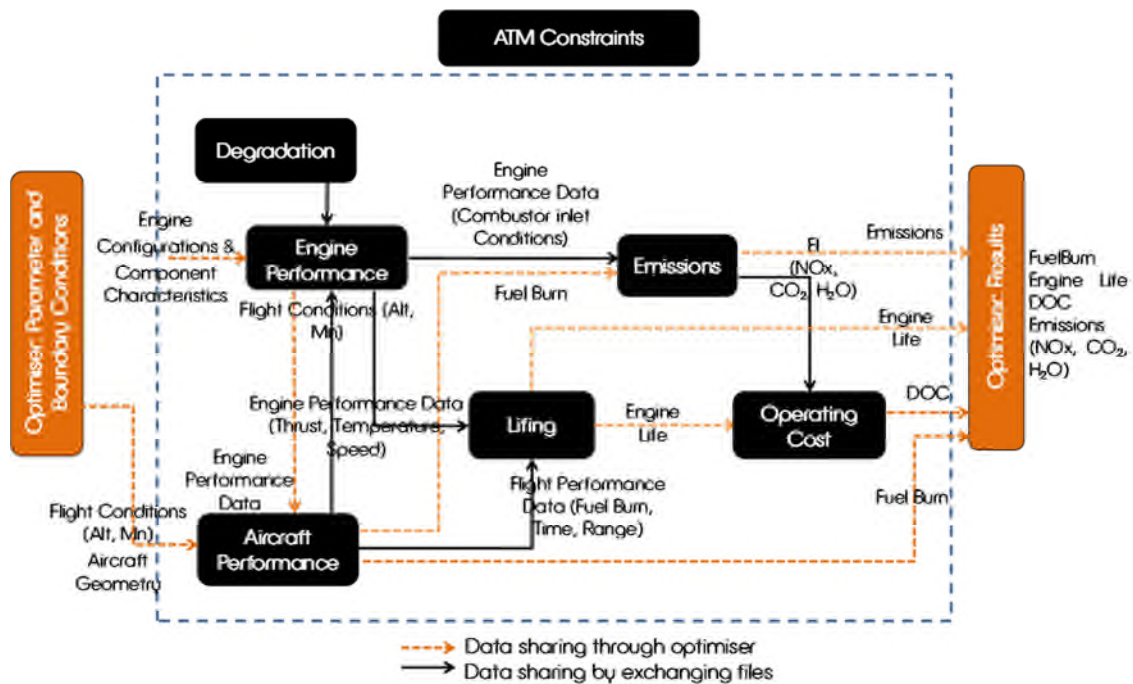


Figure 8.1: Multi-disciplinary optimisation framework.

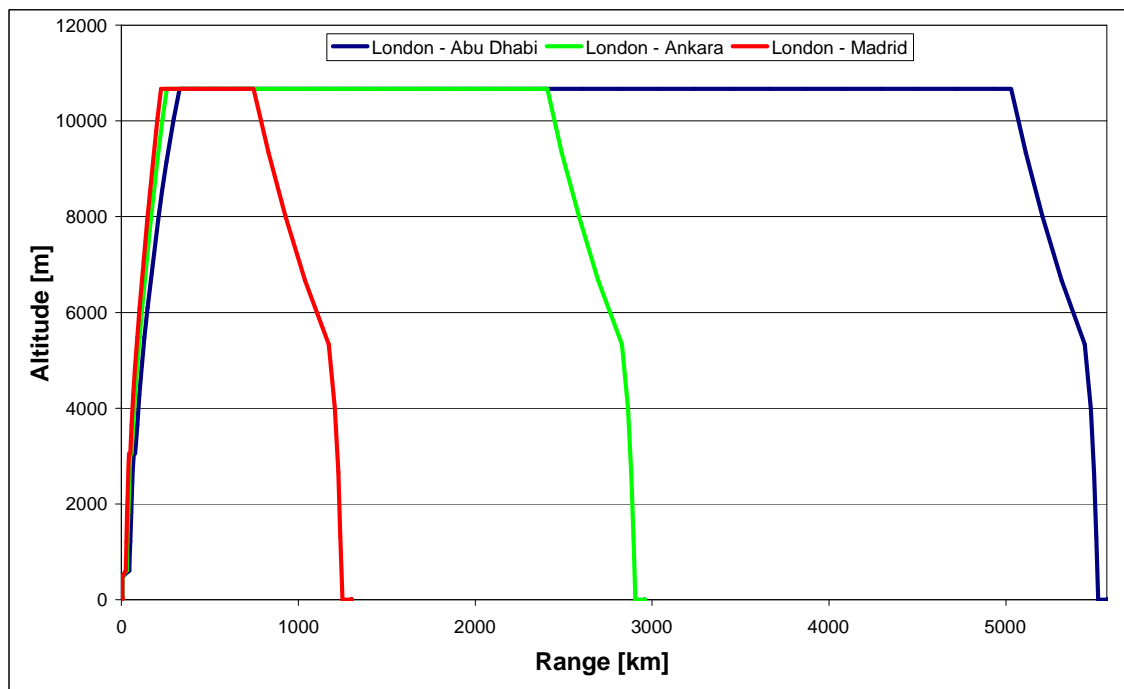


Figure 8.2: Baseline trajectory profiles for each chosen representative route.

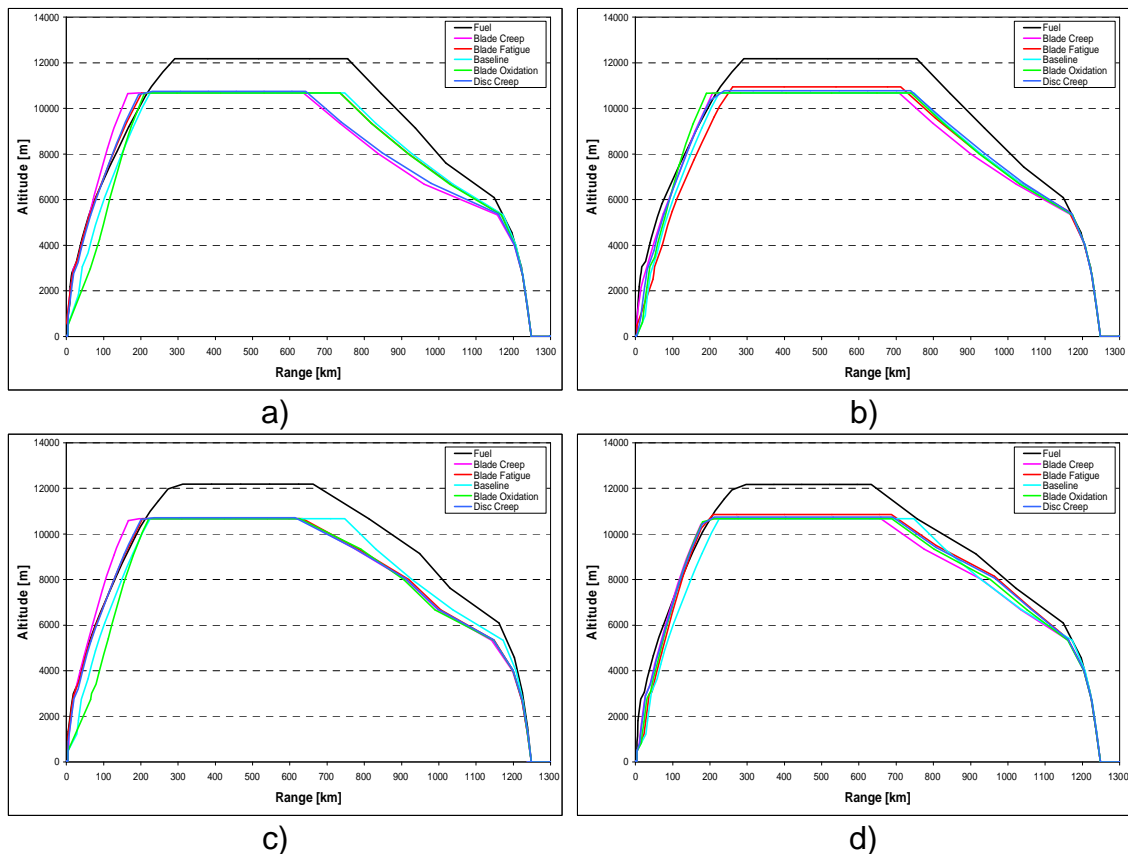


Figure 8.3: London – Madrid Optimised flight trajectories a) clean b) 3000cycles c) 4500cycles and d) 5250cycles

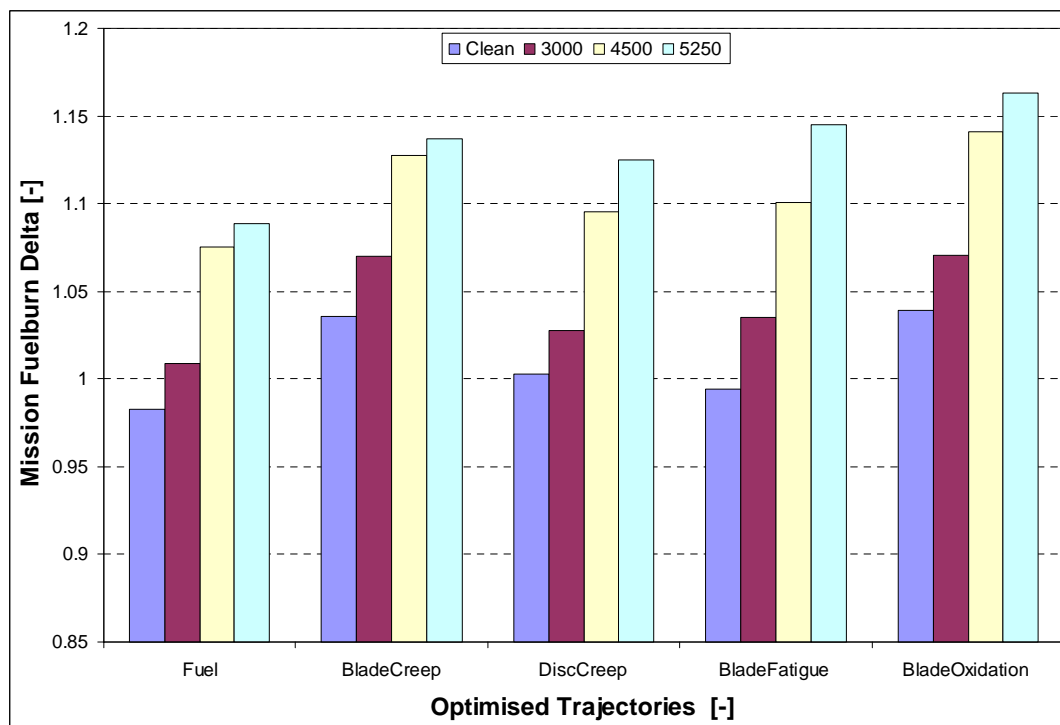


Figure 8.4: London – Madrid Flight mission fuelburn for the baseline (clean), 3000, 4500 and 5250cycles of operation.

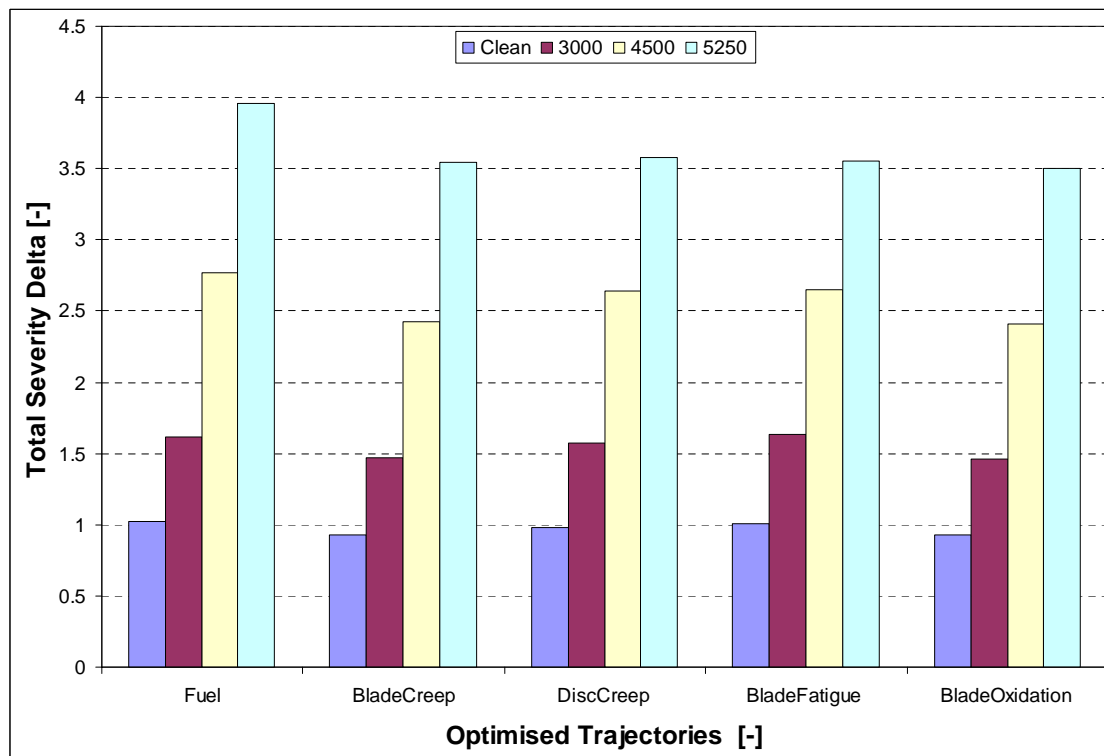


Figure 8.5: London – Madrid Total severity for the baseline (clean), 3000, 4500 and 5250cycles of operation.

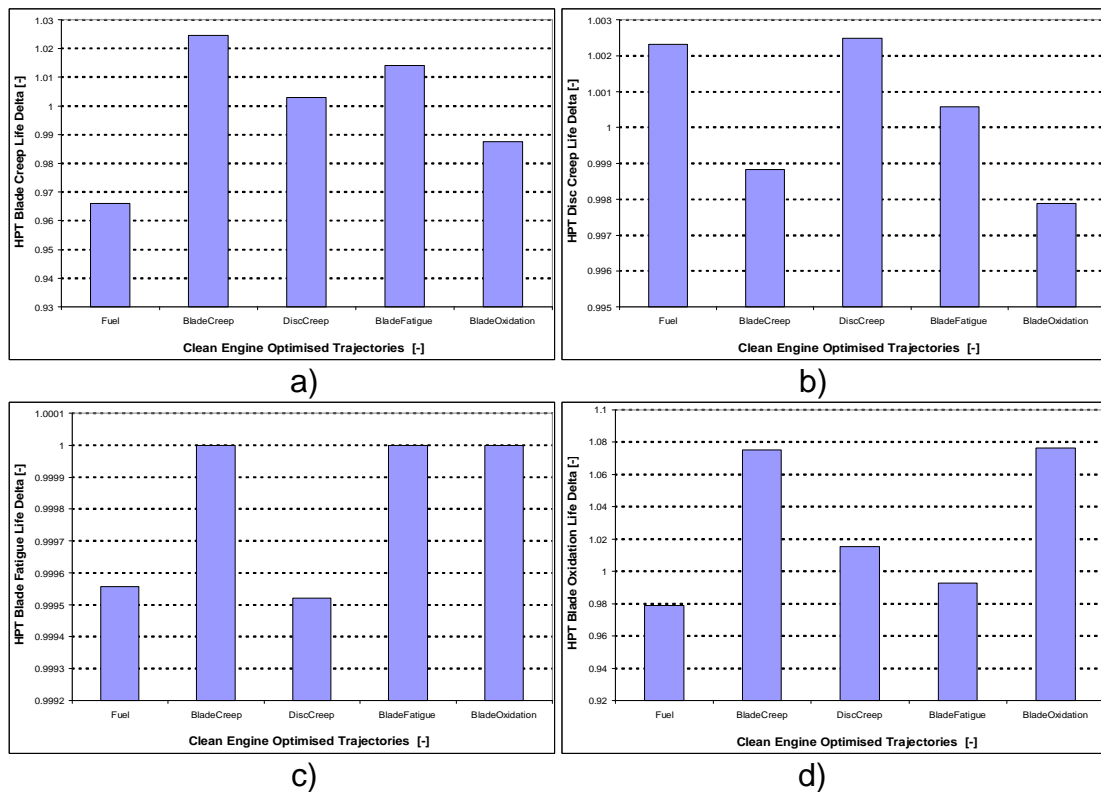


Figure 8.6: London – Madrid HPT Life for the clean engine a) blade creep b) disc creep c) blade fatigue d) blade oxidation.

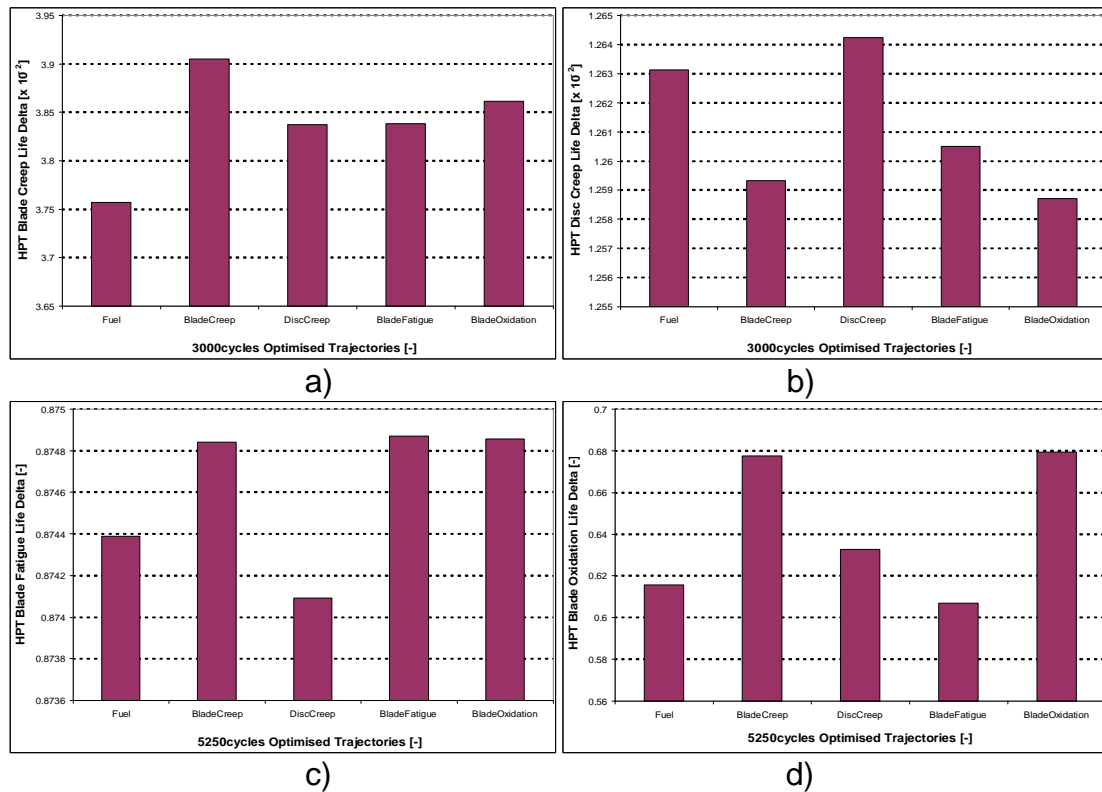


Figure 8.7: London – Madrid HPT Life for the 3000cycles engine a) blade creep b) disc creep c) blade fatigue d) blade oxidation.

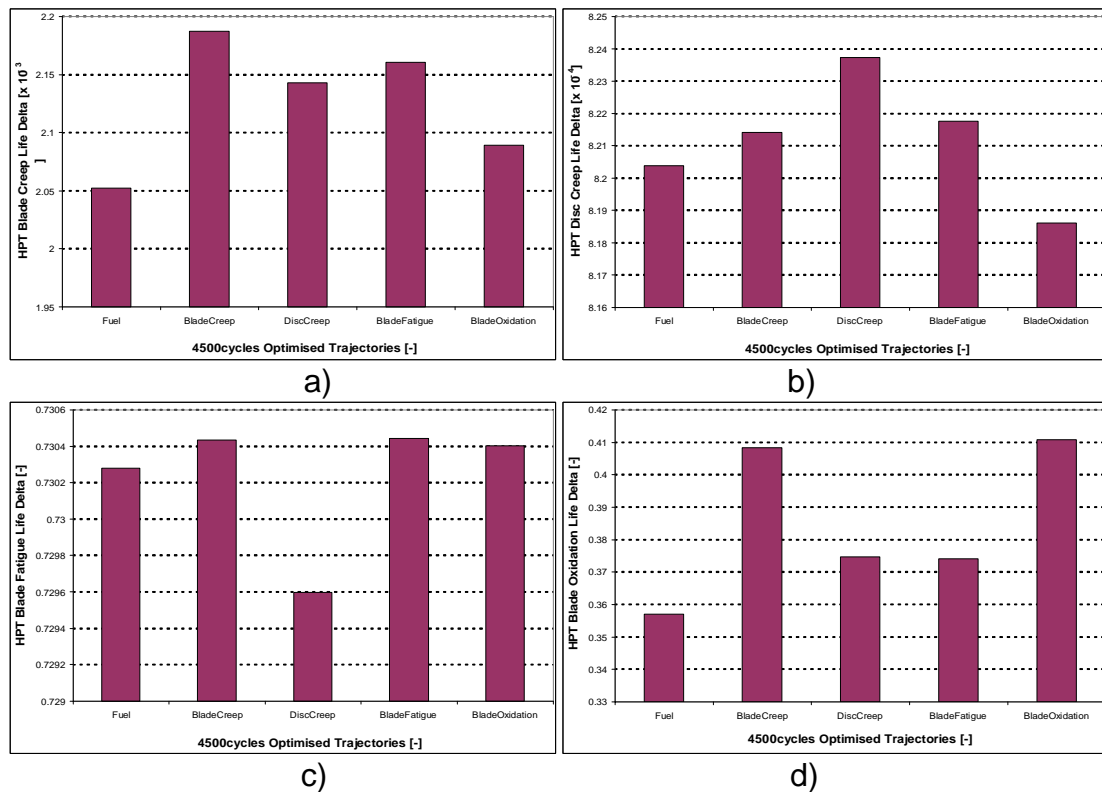


Figure 8.8: London – Madrid HPT Life for the 4500cycles engine a) blade creep b) disc creep c) blade fatigue d) blade oxidation.

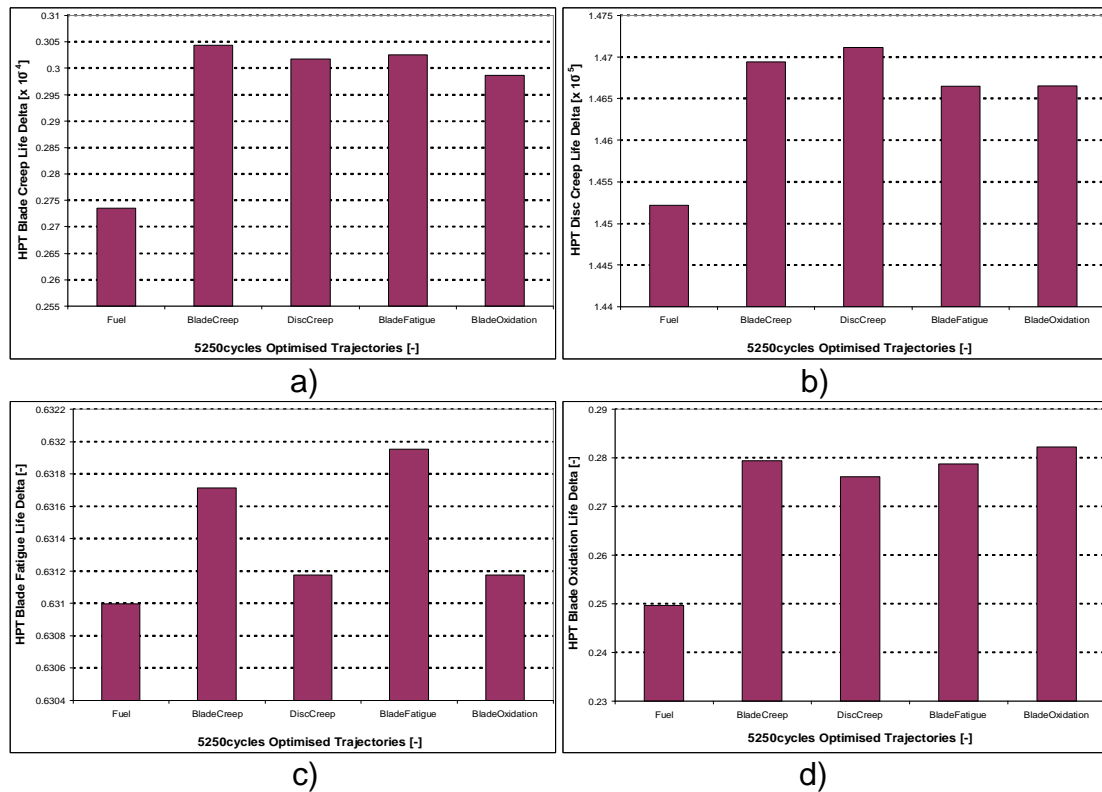


Figure 8.9: London – Madrid HPT Life for the 5250cycles engine a) blade creep b) disc creep c) blade fatigue d) blade oxidation.

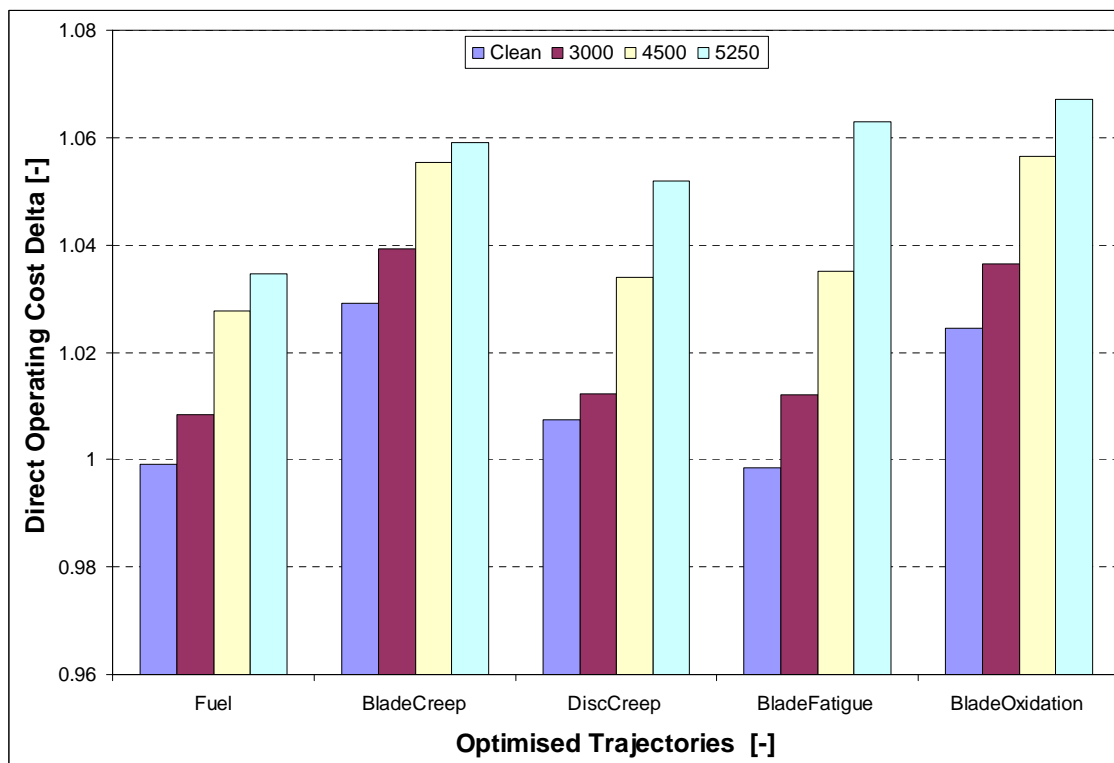


Figure 8.10: London – Madrid Engine DOC per flight for the baseline (clean), 3000, 4500 and 5250cycles of operation.

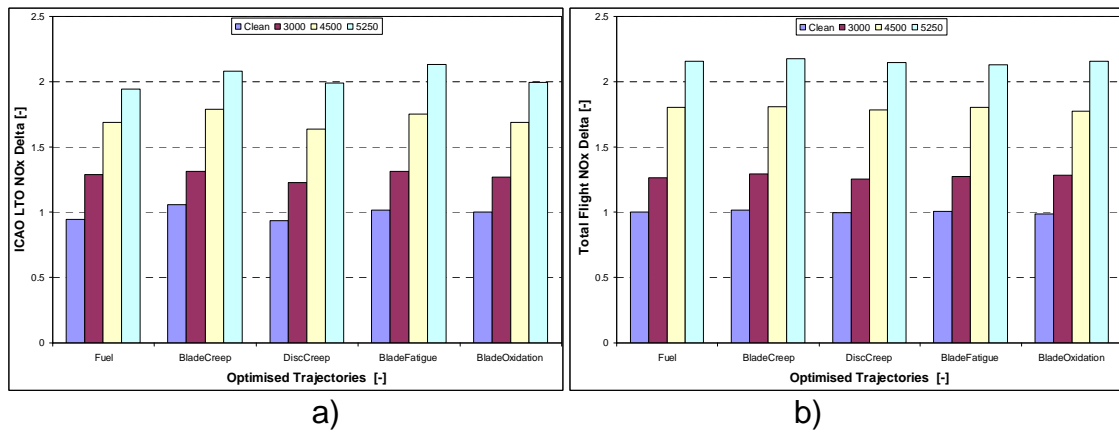


Figure 8.11: London – Madrid: a) ICAO LTO NOx and b) Total flight NOx for the baseline (clean), 3000, 4500 and 5250cycles of operation.

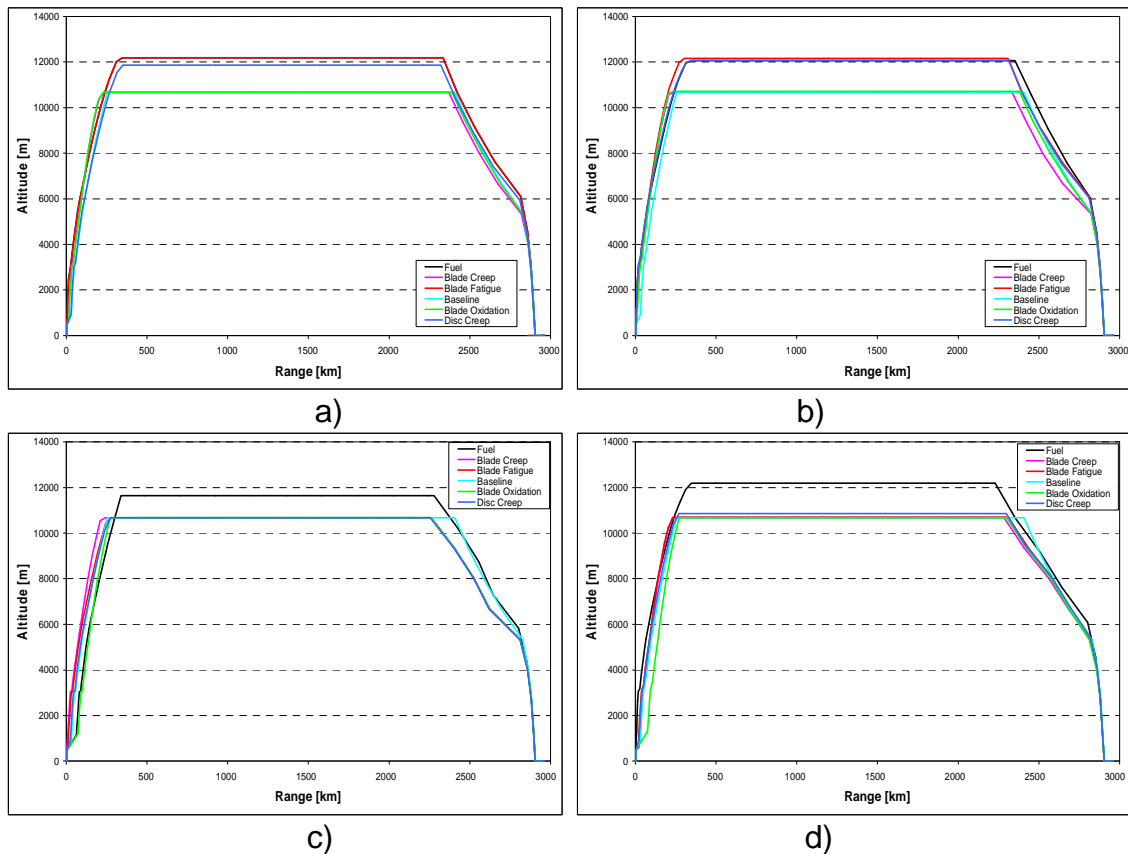


Figure 8.12: London – Ankara Optimised flight trajectories a) clean b) 3000cycles c) 4500cycles and d) 5250cycles

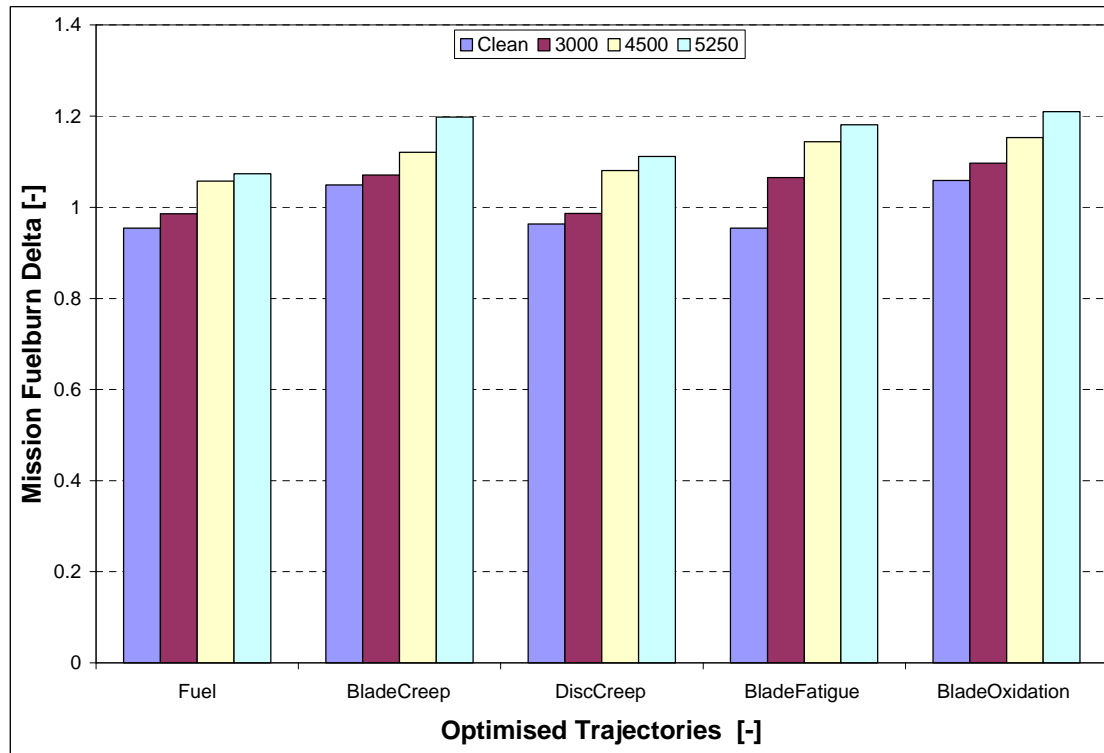


Figure 8.13: London – Ankara Flight mission fuelburn for the baseline (clean), 3000, 4500 and 5250cycles of operation.

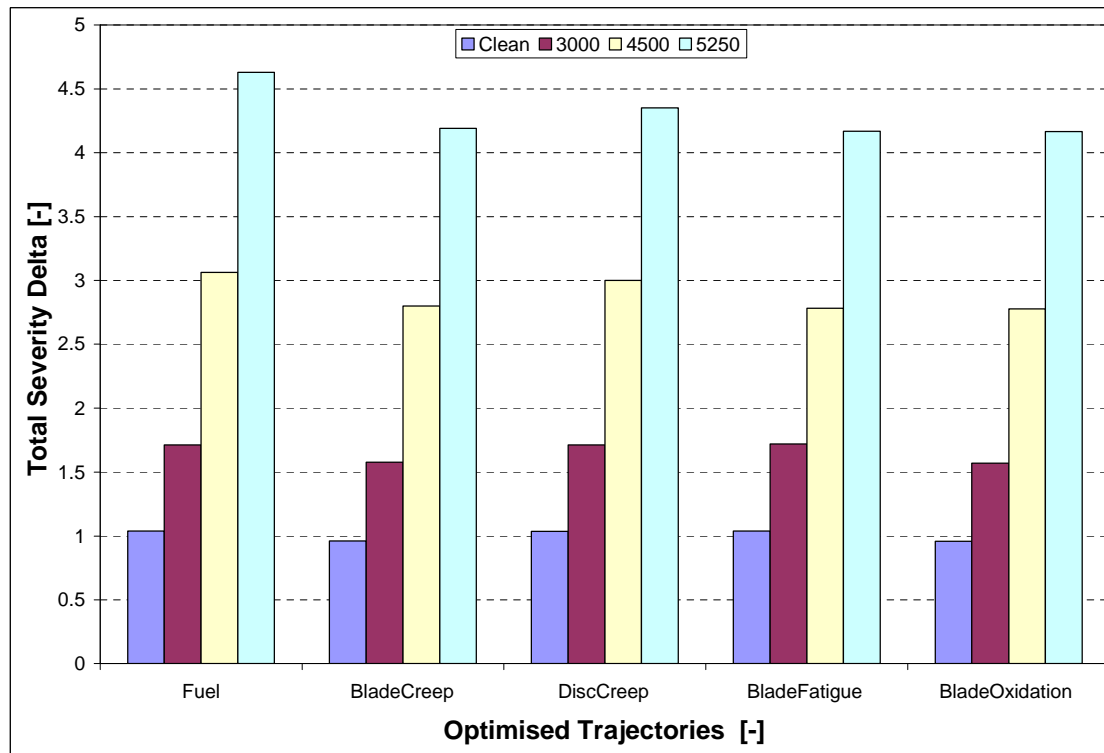


Figure 8.14: London – Ankara Total severity for the baseline (clean), 3000, 4500 and 5250cycles of operation.

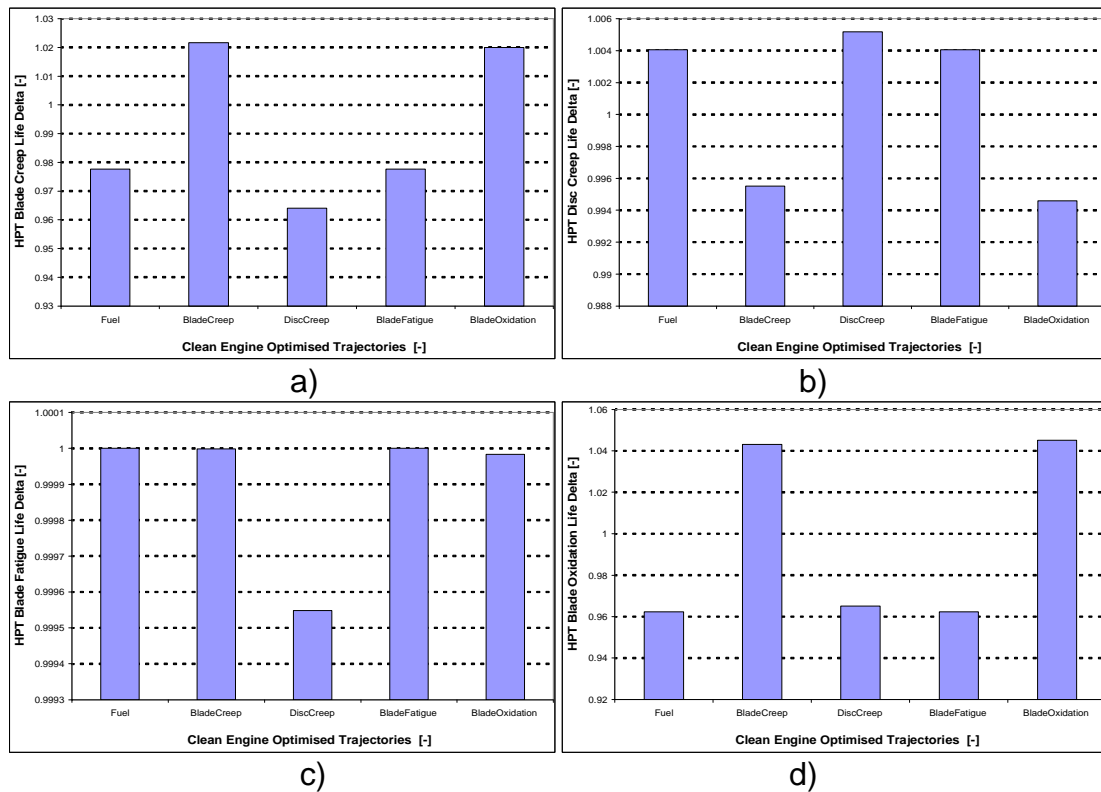


Figure 8.15: London – Ankara HPT Life for the clean engine a) blade creep b) disc creep c) blade fatigue d) blade oxidation.

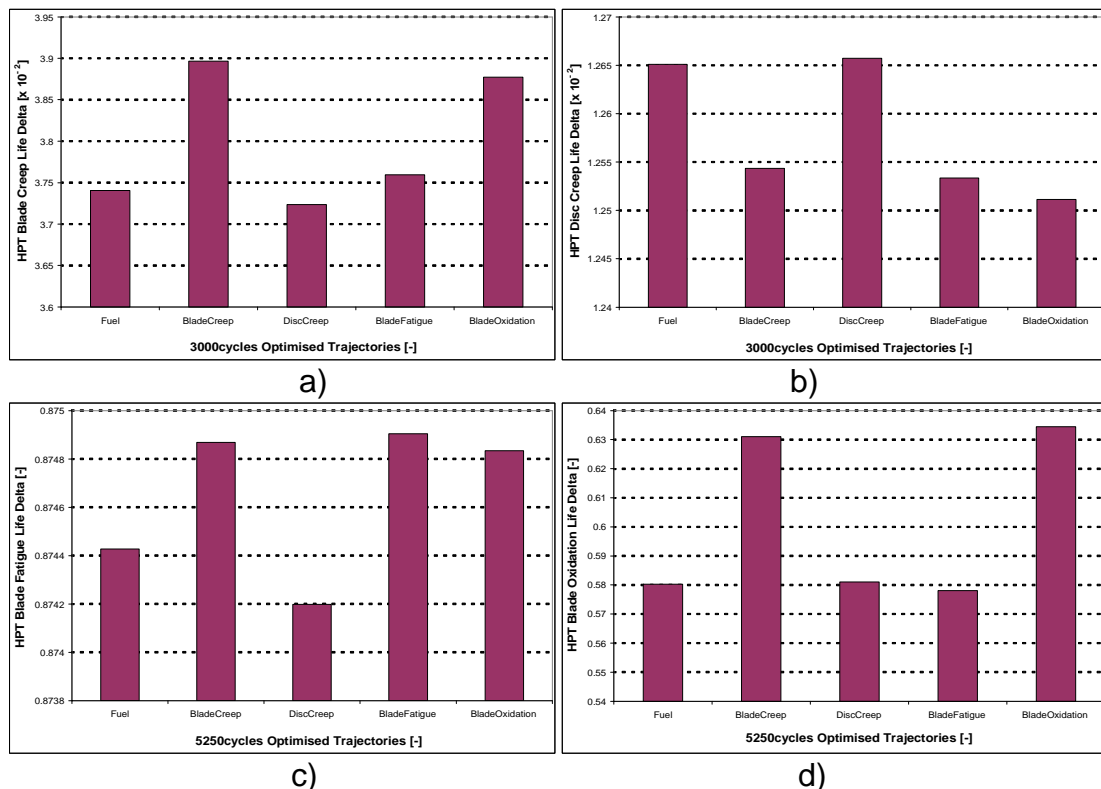


Figure 8.16: London – Ankara HPT Life for the 3000cycles engine a) blade creep b) disc creep c) blade fatigue d) blade oxidation.

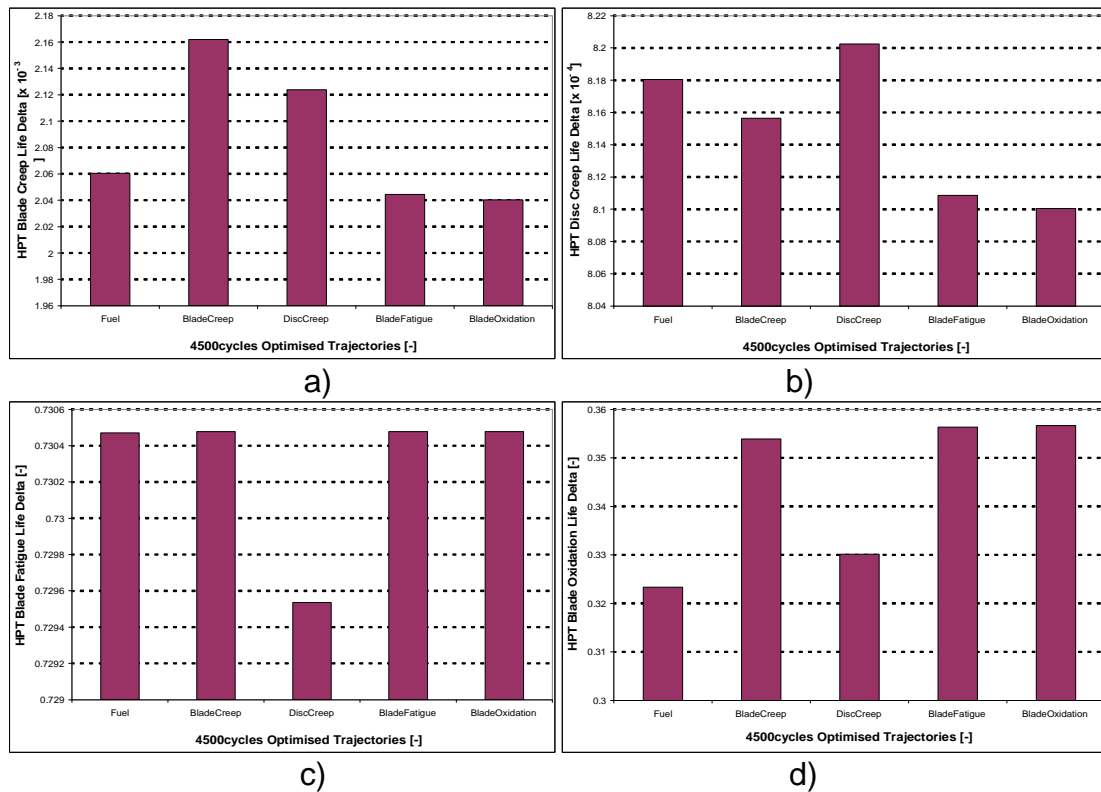


Figure 8.17: London – Ankara HPT Life for the 4500cycles engine a) blade creep b) disc creep c) blade fatigue d) blade oxidation.

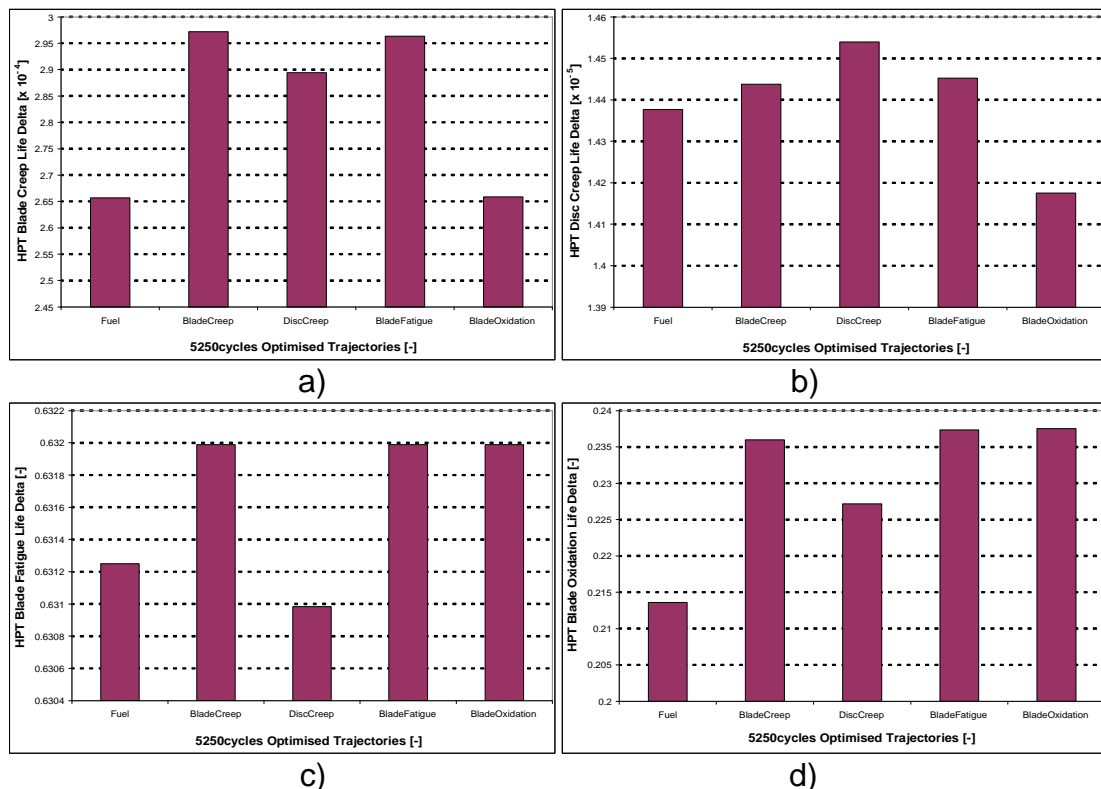


Figure 8.18: London – Ankara HPT Life for the 5250cycles engine a) blade creep b) disc creep c) blade fatigue d) blade oxidation.

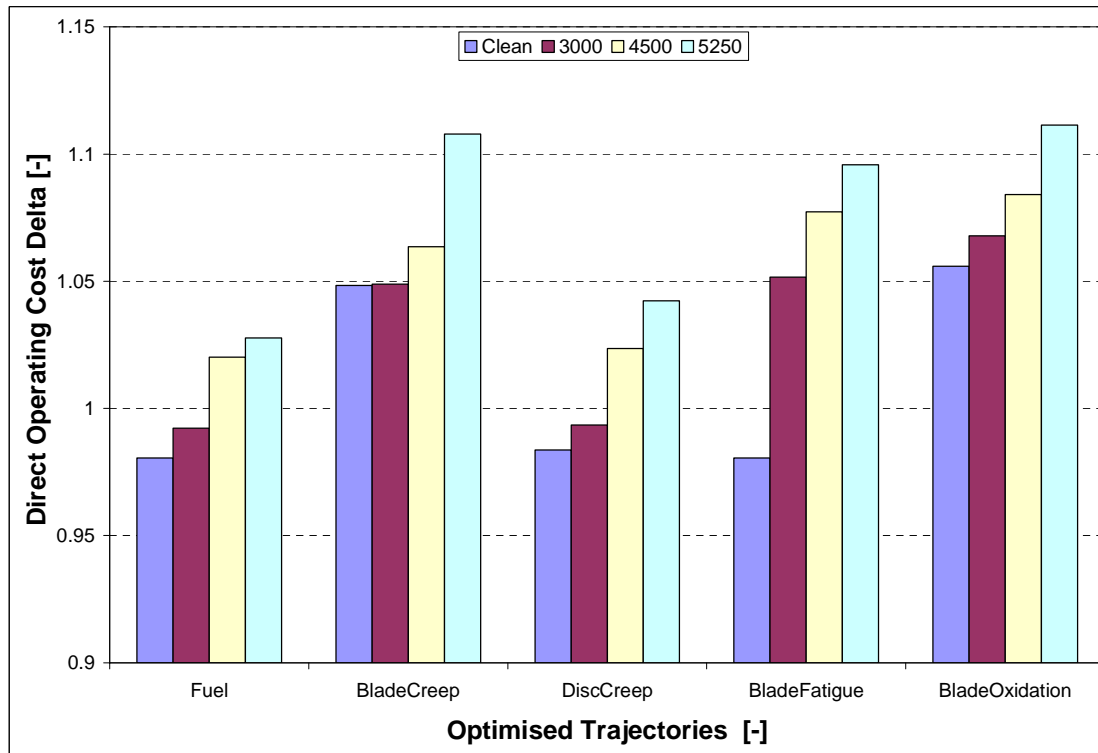


Figure 8.19: London – Ankara Engine DOC per flight (relative to the baseline) for the optimised baseline (clean), 3000, 4500 and 5250cycles.

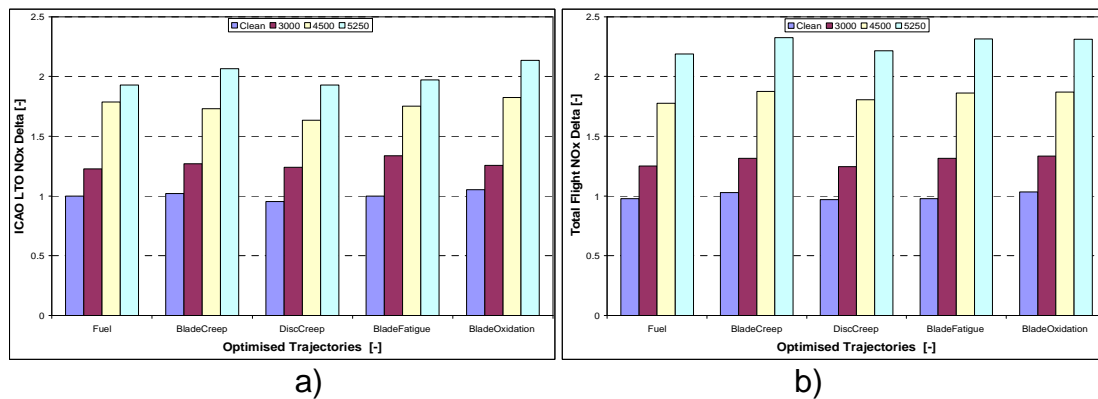


Figure 8.20: London – Ankara a) ICAO LTO NOx and b) Total flight NOx for the baseline (clean), 3000, 4500 and 5250cycles.

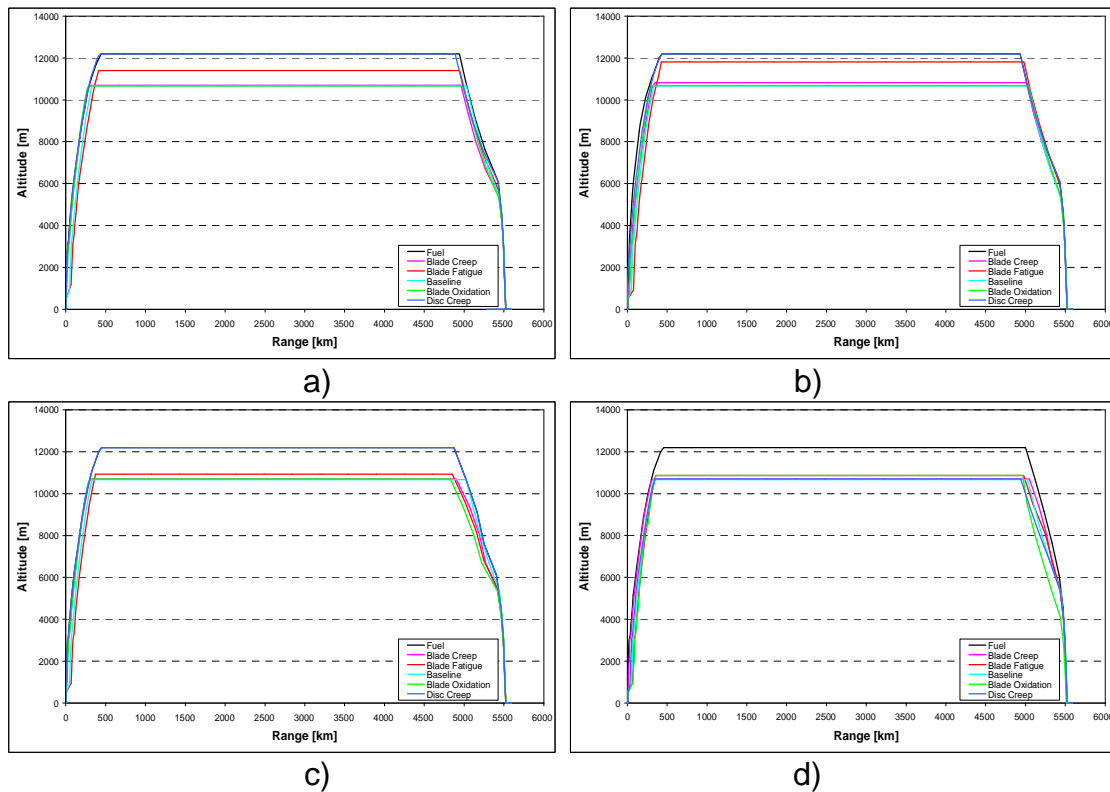


Figure 8.21: London – Abu Dhabi Optimised flight trajectories a) clean b) 3000cycles c) 4500cycles and d) 5250cycles.

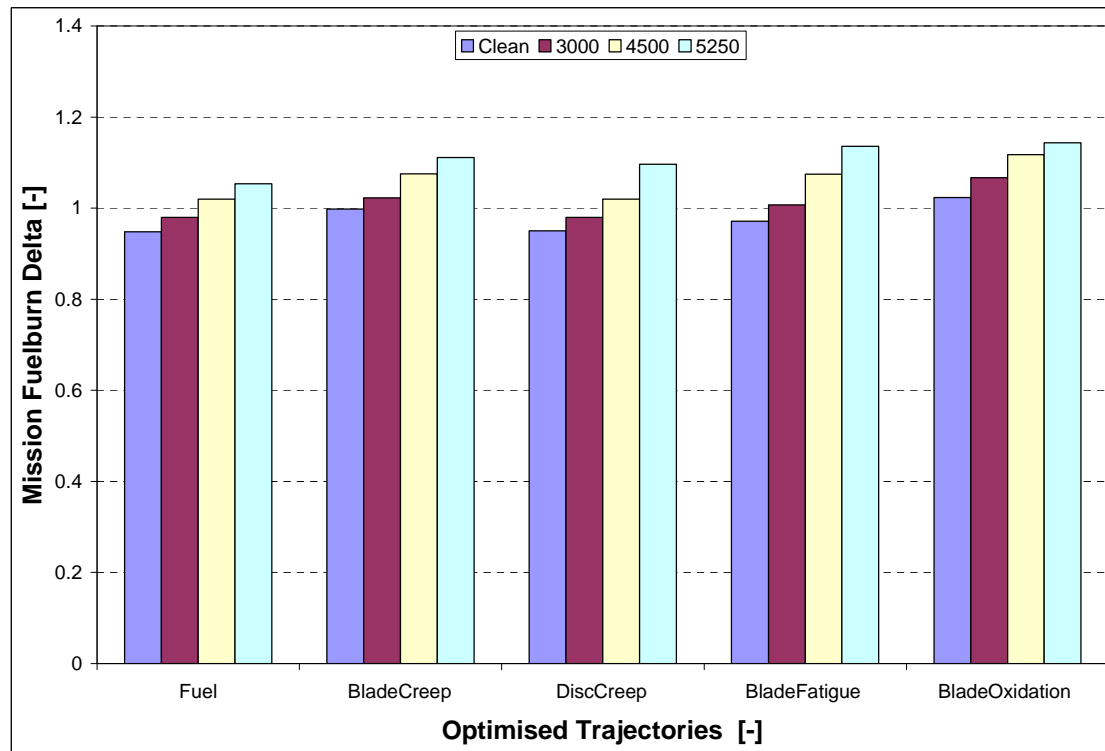


Figure 8.22: London – Abu Dhabi Flight mission fuelburn (relative to the baseline) for the optimised baseline (clean), 3000, 4500 and 5250cycles.

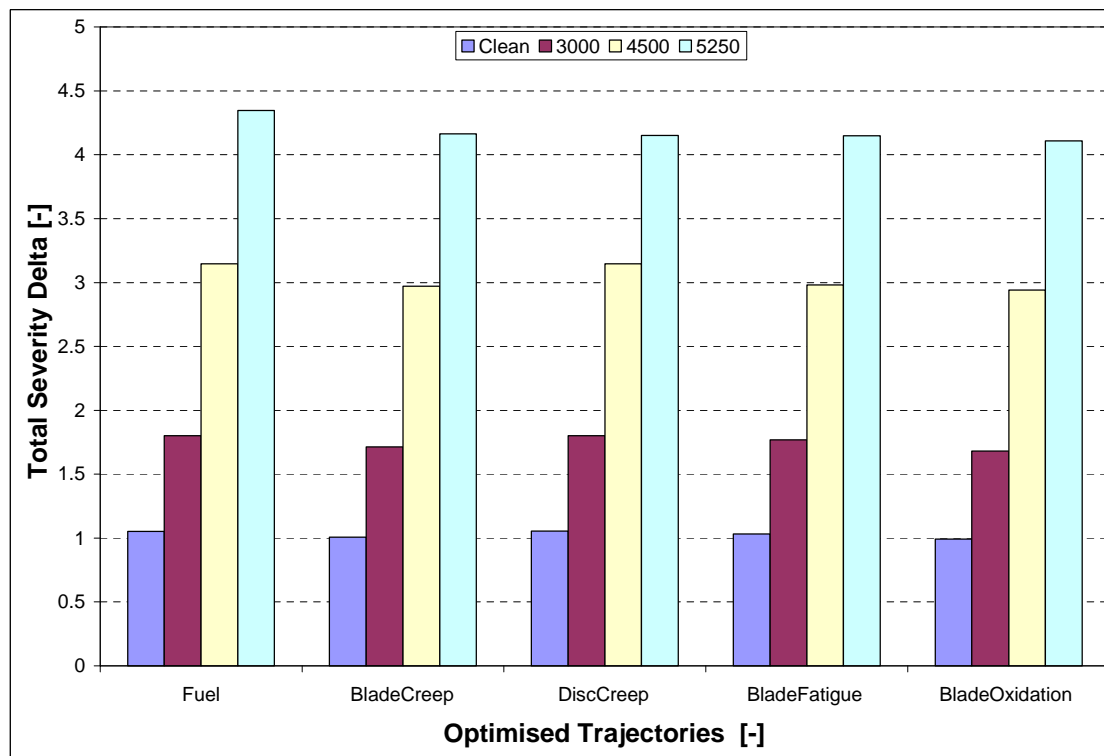


Figure 8.23: London – Abu Dhabi Total severity for the baseline (clean), 3000, 4500 and 5250cycles of operation.

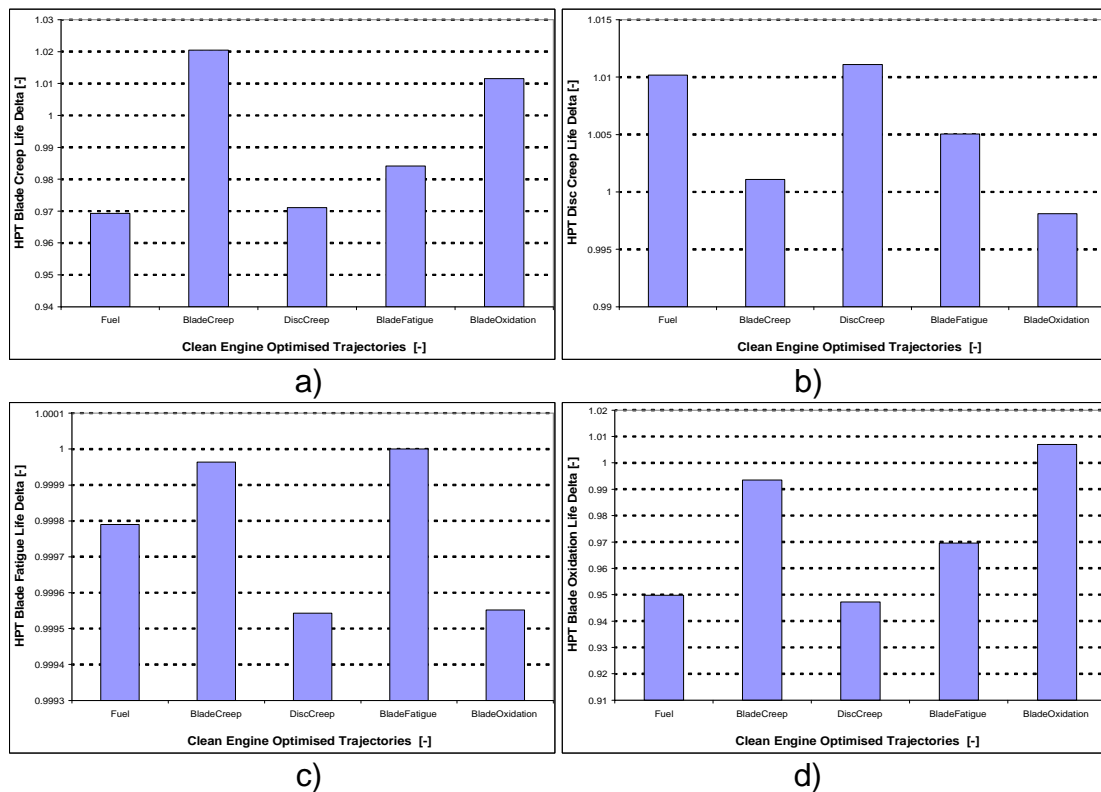


Figure 8.24: London – Abu Dhabi HPT Life for the clean engine a) blade creep b) disc creep c) blade fatigue d) blade oxidation.

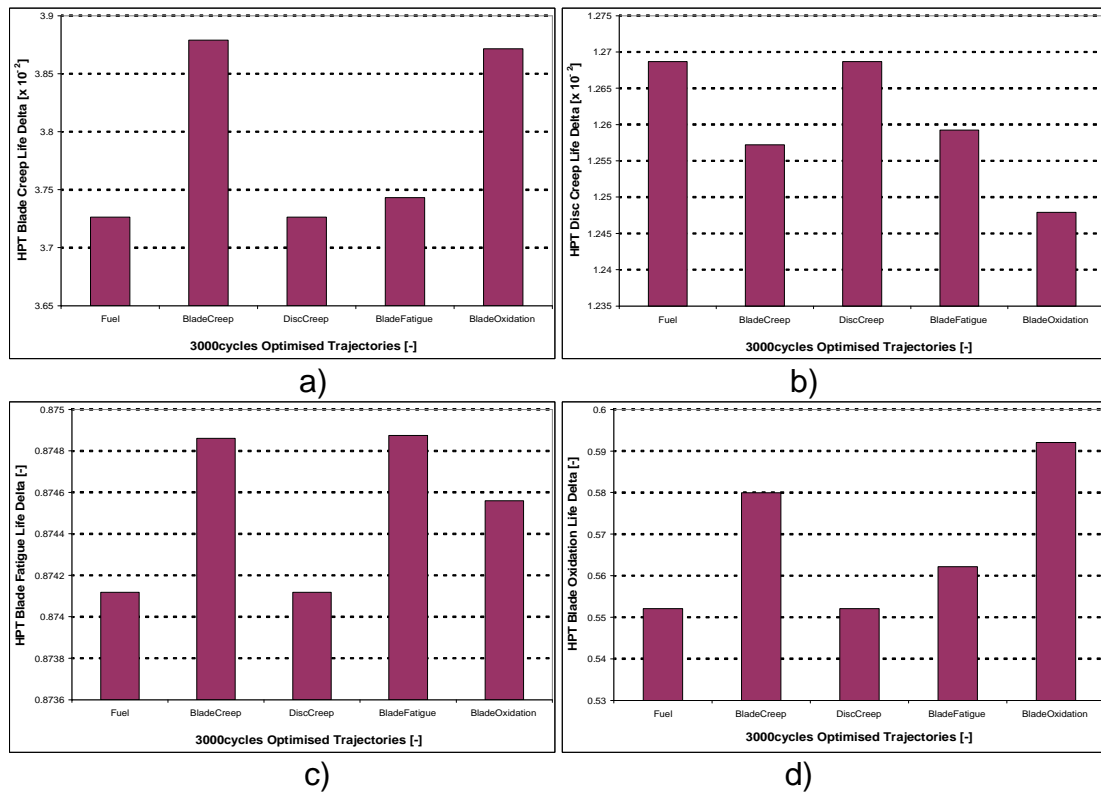


Figure 8.25: London – Abu Dhabi HPT Life for the 3000cycles engine a) blade creep b) disc creep c) blade fatigue d) blade oxidation.

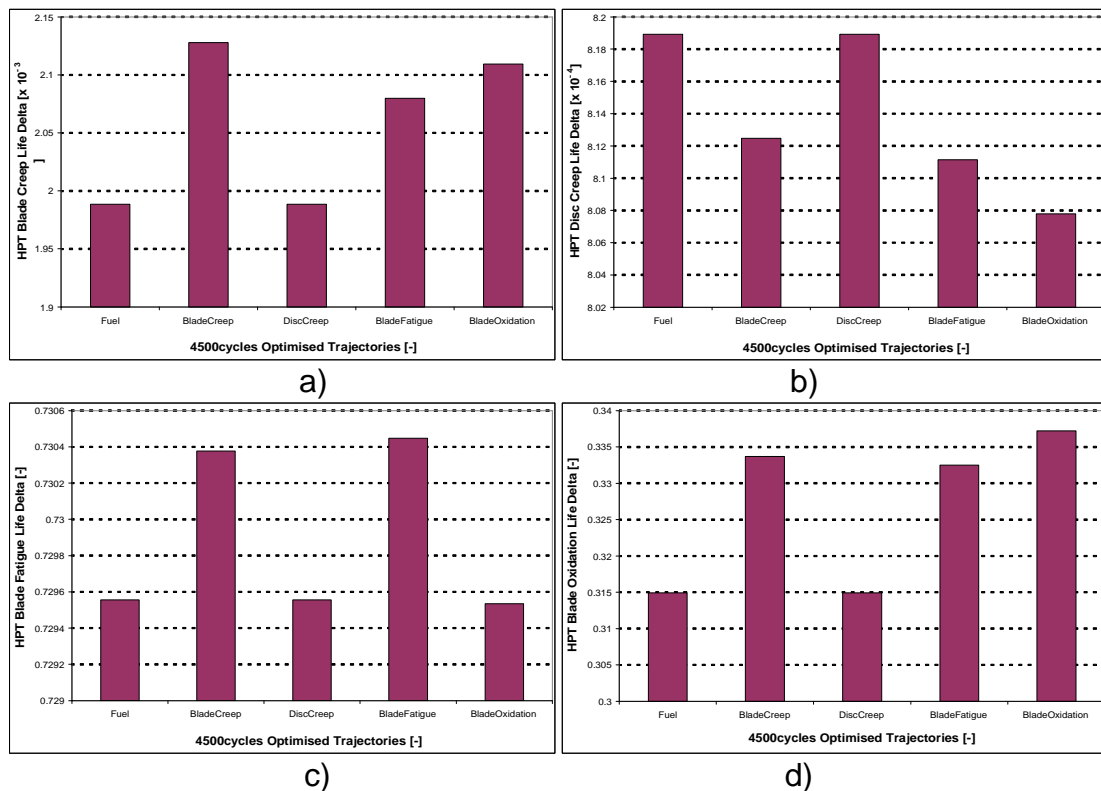


Figure 8.26: London – Abu Dhabi HPT Life for the 4500cycles engine a) blade creep b) disc creep c) blade fatigue d) blade oxidation.

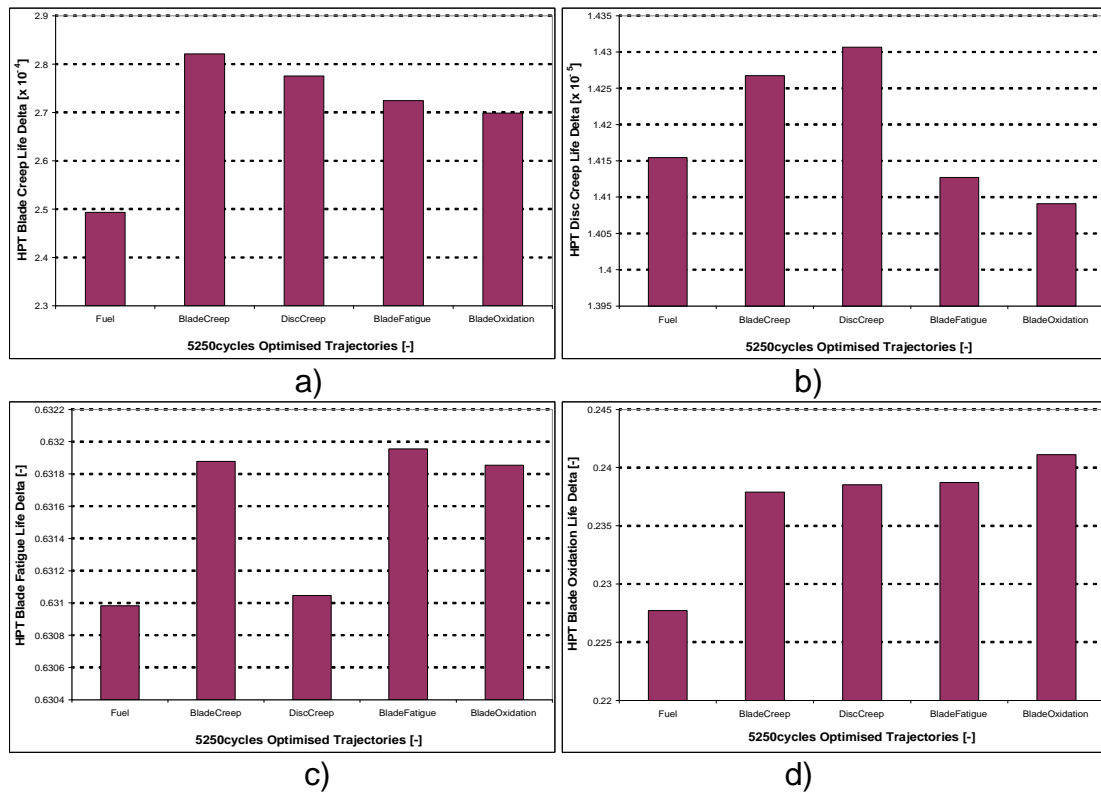


Figure 8.27: London – Abu Dhabi HPT Life for the 5250cycles engine a) blade creep b) disc creep c) blade fatigue d) blade oxidation.

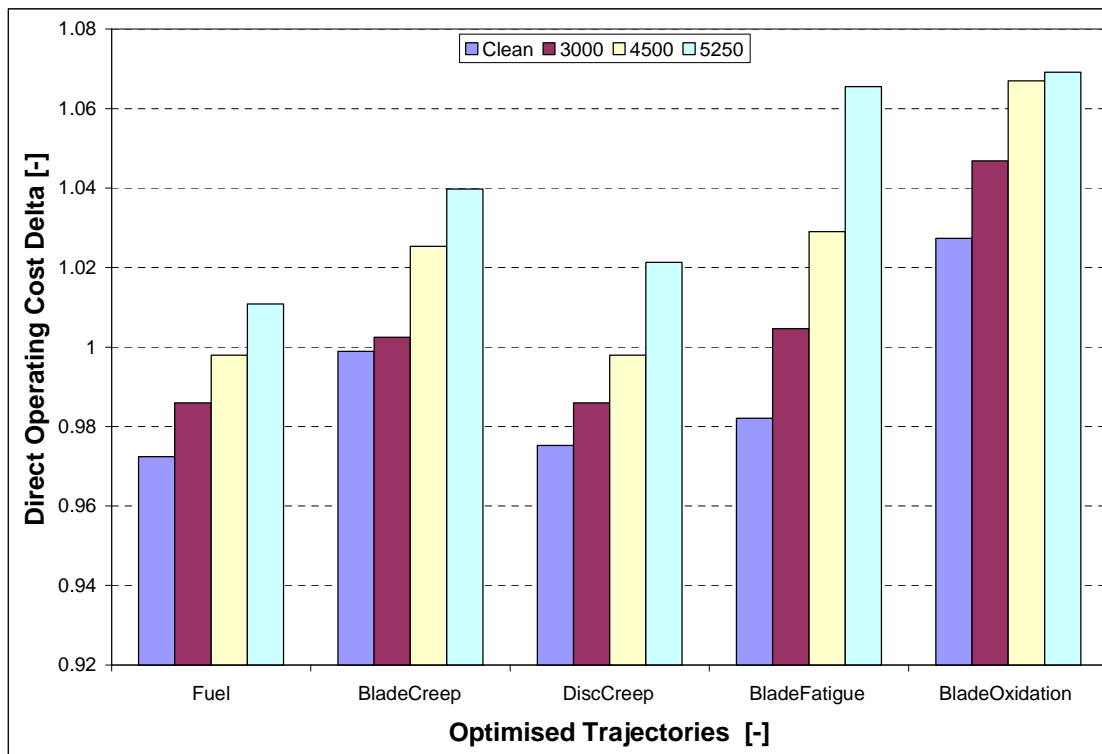


Figure 8.28: London – Abu Dhabi Engine DOC per flight for the baseline (clean), 3000, 4500 and 5250cycles of operation.

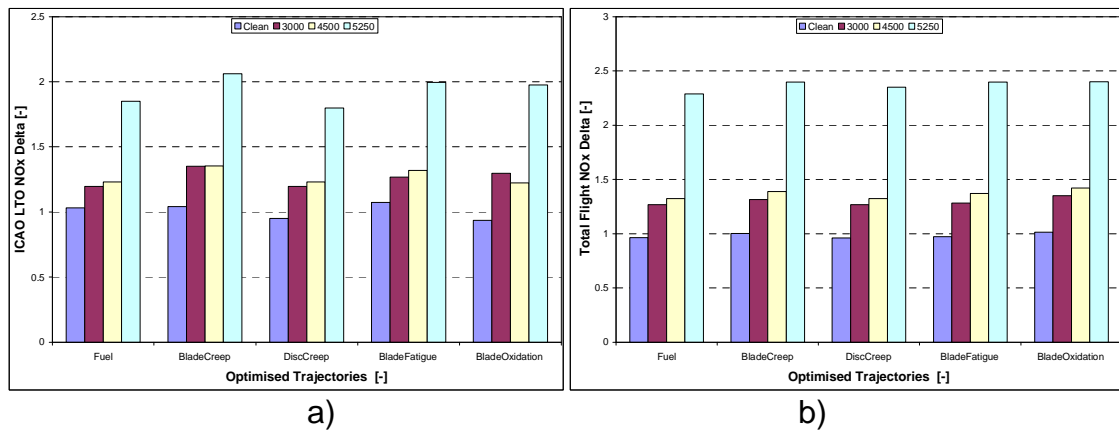


Figure 8.29: London – Abu Dhabi a) ICAO LTO NOx and b) Total flight NOx for the optimised trajectories for the baseline (clean), 3000, 4500 and 5250cycles of operation.

References for Chapter 8

- [1] Nuic, A., Poles, D. and Mouillet, V. (2010), BADA: An advanced aircraft performance model for present and future ATM systems, International journal of adaptive control and signal processing 2010, Volume 24, pg 850–866
- [2] Operator's & Owner's Guide: 737NG family(2010) Aircraft Commerce, Issue 70 June/July 2010,Nimrod Publications Limited, United Kingdom
- [3] Aircraft performance data-737, Boeing
(http://www.boeing.com/boeing/commercial/737family/pf/pf_800tech.page)
(accessed September 2013)
- [4] www.boeing.com/commercial/aeromagazine (accessed December 2013)
- [5] Flightglobal Insight (2013). Short/medium-haul widebody airliner market, Special report
- [6] Tveteras, S. and Roll, K. H. (2011). Long-haul flights and tourist arrivals, Munich Personal RePEc Archive (<http://mpra.ub.uni-muenchen.de/32157/>)
(accessed May 2014)
- [7] http://en.wikipedia.org/wiki/Flight_length (Accessed May 2014)
- [8] Nalianda D., K. (2012). Impact of environmental taxation policies on civil aviation: A techno-economic environmental risk assessment. PhD Thesis, Cranfield University
- [9] Sallee, G.P., 'Performance deterioration based on existing (historical) data-JT9D jet engine diagnostics program', NASA-CR-135448, Pratt and Whitney Aircraft Group
- [10] Litt, J., Parker, K. I. and Chatterjee, S. (2003). 'Adaptive gas turbine engine control for deterioration compensation due to aging', NASA/TM-2003-212607.
- [11] Litt, J., Aylward, E. M. (2003). 'Adaptive detuning of a multivariable controller in response to turbofan engine degradation', NASA/TM-2003-212723, October 2003.

Chapter 9

Conclusions and Recommendations

9.1 Introduction

Aircraft contribute to the ever increasing concentrations of pollutant gases in the atmosphere by emitting greenhouse gases and other pollutant emissions. The continuous growth of air transport has raised concerns about global aircraft fuel consumption, emissions and noise. Industry's concentrated effort to improve thermal efficiency and better fuel efficiency has led to higher overall pressure ratios and turbine entry temperatures. However, with the anticipated growth of air transport, global aircraft fuel consumption and emissions are expected to increase every year. The challenge to industry is to provide economic, safe and environmentally-friendly air travel in the face growing demand for air transport.

In response to the challenge and environmental impact of a growing market, international organisations such as ACARE and ICAO have set up challenging goals for 2020 (and 2050) and identified ways to best reduce the impact of aircraft operations. The environmental targets aim to: reduce CO₂ emissions by 50% (75%), reduce NO_x emissions by 80% (90%) and reduce perceived noise by 50% (65%). Achieving these goals poses significant technical challenges requiring that trade-offs be addressed. Research has indicated that to achieve these targets will require contribution from technological improvements, improved asset management and operational efficiency and greener manufacturing and recycling processes including transportation. Implementing some of these resolutions presents a range of challenges and further advances may come with high development costs. Operational improvements are a most readily implementable contributor to achieving the ACARE targets. They are financially viable, cost effective and competitive for existing engines and aircraft. One option of operational improvements is aircraft trajectory optimisation.

In the context of increasing fuel costs and the competitive nature of the airline industry profitability and safety are critical for sustainability. Direct operating costs become of concern to both the manufacturer (OEM) and the airline, thus raising the need for the assessment of the engine and aircraft at mission level and the optimising of operational procedures. Making profit is the perspective for both the OEM and the airlines.

This research falls under asset management and involves aircraft trajectory optimisation. Most aircraft trajectory optimisation studies concentrate on optimising fuel burn, emissions and noise. The aim of this research was to assess the implications of airport severity on engine life consumption and aircraft performance. Another important aspect and aim of this work was to assess and quantify the trade-offs between mission fuel burn and engine life optimised operations and the implications on operating costs when considering the effects of engine degradation.

The major achievements of this work are summarised in this chapter. The main conclusions are provided and consist of general conclusions from the work as well as those that are specific to and reflect the contribution to knowledge. The limitations of the work and directions for further study are included.

9.2 Achievements

The work presented in this thesis is a contribution towards optimising fuel burn and emissions and reducing the environmental impact and noise in the way an aircraft manages its trajectory. The contribution to knowledge from this research is a) the assessment of the impact of airport severity factors on engine life consumption and aircraft performance and b) the assessment and quantification of the change in engine life consumption when optimising for flight mission fuel burn and the change in flight mission fuel burn when optimising for engine life consumption. The influence of engine component degradation and the changes to the direct operating costs and emissions were also assessed.

Therefore, the main areas of focus in this study have been: analysis of aircraft severity factors and mission fuel burn and engine life optimisation, and these are found in chapters 7 and 8.

The trade-offs between mission fuel burn and engine life optimised trajectories are presented for a clean (new) engine for three routes (London–Madrid, London–Ankara and London–Abu Dhabi). The engine life was calculated in terms of the HPT blade and disc life due to creep, fatigue and oxidation failure modes. Mission fuel burn and engine life trajectory optimisation assessments were conducted to incorporate the effects of degradation after 3000, 4500 and 5250cycles of operation. Further assessments were made linking aircraft performance to airport severity factors for the clean engine and after 3000cycles and after 5250cycles for the hot desert conditions of Abu Dhabi, Cairo and Riyadh International airports. A multi-disciplinary framework combining various theoretical models and coupled to an optimiser was developed to make techno-economic environmental risk assessments at mission level. Each model was verified and validated. The models making up the framework are: engine and aircraft performance, emissions prediction, lifing analysis and economics. A GA optimiser was integrated to the framework.

Initial assessments were conducted for the a) airport severity factors to establish the performance for a baseline mission and for a degraded engine after 3000cycles of operation and b) optimisation assessments to establish the performance for the baseline mission for each route and for a degraded engine after 3000, 4500 and 5250cycles of operation. The engine and aircraft performance results have concurred (with literature) that when compared with the relevant baseline, the degraded cases incur a rise in the severity (severity is described in section 7.2) due to a needed increase in the maximum operating temperature for the required thrust performance. The fuel burn also rises consequentially and translates into an increase in flight costs. Due to the higher levels of severity with degradation, the remaining useful life becomes

increasingly shorter with longer cycles of operation and is always less for the higher levels of degradation.

9.3 Conclusions and Discussions

9.3.1 Airport Severity Factors

Aircraft take-off from a variety of geographical locations each demanding a different set off operational strategies and power settings for the same TO requirements. These changes in 'thrust requirements' will influence the engine's damage fractions and operational costs which are of concern to both the engine manufacturer and the operator. In recognition of this, the first aim of this study was to assess the influence of airport severity factors on the engine life consumption and aircraft performance. Airport severity estimation can serve as an aid when making decisions on operational strategies around different airports. In the context of this work, the airport severity factors were defined as those factors that influence the aircraft performance and the rate of engine life usage. To achieve the aim mentioned above, the studies were conducted in two parts:

- Parametric studies to relate severity to operational parameters such as TO derate, OAT, altitude and the environment.
- Airport factors to relate severity and aircraft performance with taking off from different airports.

A baseline performance was established to enable comparison and have a point of reference. It was assumed by matching it to the payload range performance of the Boeing 737-800 after which it was modelled. Changes were made to the health parameters so as to model the effects of engine degradation. The research question was "How do airport severity factors influence the engine's life consumption and aircraft performance?" Outlined in the following sections is what the results show.

9.3.1.1 Operational Factors

Parametric analyses were carried out by varying the TO derate from 0% to 30%, altitude from 0m to 1500m and OAT from -20°C to +20°C. The reference airport was assumed at 0% derate and ISA SLS (15°C OAT and sea level). The baseline trajectory was assumed for a clean engine TO from the reference airport on a flight mission range of 3000km.

9.3.1.1.1 Clean Engine Performance

- A clean engine TO from an airport 1500m above sea level requires a +109K increase in operating temperatures to achieve the required TO thrust. The results show that the consequences of such a rise in operating temperatures is a +4.8% increase in severity and a +7.1% increase in TO fuel burn. There is also negative impact to the blade fatigue life and the blade oxidation life which reduce by -22.1% and -4%

respectively. Despite these penalties, the results show that the climb fuel burn is less by -12.4% and there is a small benefit of -0.5% on the flight operating costs. Consequently the ICAO LTO NO_x was found to be harsh on the environment with an increase of +2.5%. The flight NO_x was however friendly on the environment, benefiting from the lower climb fuel burn to reduce by -4.2%.

- A clean engine TO at an OAT deviation of +20°C requires a +102K rise in operating temperatures, which was found to be detrimental to engine severity, incurring a penalty of +6%. There is also a rise of +4.1% in TO fuel burn and a drop in the blade fatigue life and blade oxidation life which reduce by -30% and -5% respectively. Consequently the flight operating costs rise by +0.3%.
- A clean engine TO at an OAT deviation of -20°C requires lower operating temperatures by -103K to achieve the required TO performance. This drop in temperatures gives benefit to engine severity which reduces by -10.2%. Consequently the blade fatigue life and blade oxidation life benefit, improving by +16.8% and +11.2% respectively. There is also a beneficial drop of -4.2% in TO fuel burn and a marginal -0.1% in flight operating costs is demonstrated. The lower operating temperatures reduce the ICAO LTO and flight NO_x by -9.3% and -0.8% respectively.

In concurrence with literature, the results have shown that derate can be used to minimise engine component damage. A 30% derated engine was found to have a -7.3% reduction in severity, due to a reduction of -181K in the operating temperatures. Consequently there is benefit to the blade fatigue and oxidation lives demonstrated by the derated engine, with improvements of +15.3% and +7.8% respectively. The TO fuel burn reduces by -37.5% with a small benefit of -0.2% in flight operating costs. The derated engine is shown to be beneficial to the environment with the ICAO LTO and flight NO_x reducing by -9.3% and -0.8% respectively.

9.3.1.1.2 Degraded Engine Performance (After 3000 cycles)

It was found that the trends shown for the engine after 3000 cycles were similar to those of the clean engine albeit at higher levels of magnitude. The engine operating temperatures are higher, having increased by +54K. In turn the engine severity and mission fuel burn increase by +56.8% and +3.5% respectively, translating into a rise of +1.2% in DOC.

In view of the findings from the parametric analyses, the conclusions are that the effects of derate, OAT and altitude on severity and aircraft performance cannot be ignored. High OATs and altitudes incur high damage fractions which greatly impact on the engine component life and related maintenance costs and engine availability. It is evident from the observations that derating an engine during TO would be beneficial to both the operator and the manufacturer when flying from airports at high OATs and high altitude. In the context of the power by hour contracts, and higher maintenance costs per hour, airlines may use TO derate to lower the engine operating temperatures and EGTs and minimise the damage to the engine thus prolong the engine time on wing and save on costs.

In the case of the manufacturers, they may use the flat rating concept at TO to prevent the EGT from continually rising with increasing OAT thereby preventing severe damage to the engine and prolonging time on wing. Since derate gives better engine component life and burns less fuel, it may be employed by airliners to increase savings on fuel costs. However since the results show a benefit of 0.2% for a 30% derated engine for the mission range assessed, such savings would be significantly beneficial against the impact of increasing fuel costs and large aircraft fleets. At today's jet fuel price of \$2.92 per US gallon, the 0.2% savings for the mission range assessed convert into an economic value of approximately US\$51000 per aircraft per year. Derate would also be beneficial to aging and degraded engines, allowing them to operate at the higher temperatures required to compensate for performance losses without incurring severe damage and costs. This is evidenced by the results that show a +20°C OAT with 30% derate has a downward shift of -4.3% and -0.4% in severity and costs respectively in comparison to +20°C OAT with 0% derate.

9.3.1.2 Airport Severity

Investigations were carried out on seven specific airports (see table 7.3 in chapter 7) such as Abu Dhabi, Cairo, Madrid, Dublin and Riyadh among others to assess the influence of airport location and the environment on engine severity. The baseline trajectory was assumed for a clean engine take-off from the reference airport (0% derate, ISA SLS conditions). The TO airport was the only variable in these case studies. The mission range of 3000km was assumed for each flight, and the landing airports were assumed to have the same altitude and OAT. The studies were carried out for a clean engine and for a degraded engine after 3000cycles for all the airports without considering the type of environment. A further step was taken to investigate the hot and sandy desert conditions at airports such as Abu Dhabi, Cairo and Riyadh; for these airports. A sensitivity study was conducted after 4500, 5250 and 6000cycles of operation to determine which best represented the sandy desert conditions. The degraded engine after 5250 cycles of operation was chosen based on methods used by MRO providers and also on information available from references.

9.3.1.2.1 Clean Engine Performance

- A clean engine TO from Abu Dhabi International airport requires +68K higher operating temperatures with great impact on severity and TO fuel burn, causing an increase of +4.1% and +2.8% respectively. Consequently the blade fatigue life and blade oxidation life reduce by -19.4% and -3.7% respectively. TO from this airport has marginal impact on the flight costs which change by +0.2%, which converts to approximately US\$39182 increase per aircraft per year.
- A clean engine TO from Ankara International airport requires +20K higher operating temperatures, with negative impact on severity and TO fuel burn, which increase by +1.2% and +2.4% respectively. A TO from Ankara incurs little or no change to the blade fatigue (-0.4%) and blade oxidation life respectively. There is however benefit to the climb fuel burn

which reduces by -9.4%, giving a reduction in flight costs of -0.3% which translates to savings of US\$0.13million in flight operating costs per aircraft per year.

- A clean engine TO from Beirut International airport requires +32K higher operating temperatures, with negative impact on severity and TO fuel burn, causing an increase of +2.2% and +1.3% respectively. Consequently the blade fatigue life and blade oxidation life reduce by -8.7% and -2% respectively. TO from this airport has shown little impact on flight costs which change by approximately +0.1% which translates to US\$16315 increase in flight operating costs per aircraft per year.
- A clean engine TO from Cairo International airport requires +48K higher operating temperatures with negative impact on severity and TO fuel burn, which increase by +3% and +2% respectively. The blade fatigue life and blade oxidation life reduce by -13% and -2.6% respectively. This high altitude airport demonstrates benefit to the climb fuel burn, which reduces by -6.2% to give a slight reduction in flight costs of -0.2% which translates to savings of US\$56750 in flight operating costs per aircraft per year.
- A clean engine TO from Dublin International airport requires -22K lower operating temperatures which reduces severity and TO fuel burn by -1.8% and -0.8% respectively. The blade fatigue life and blade oxidation life are better at this airport by +5.5% and +1.8% respectively. There is little benefit on flight costs with a change of approximately -0.1% which translates to savings of US\$10241 in flight operating costs per aircraft per year.
- A clean engine TO from London Heathrow International airport requires -40K lower operating temperatures, with great benefit to severity and TO fuel burn, which reduce by -3.4% and -1.6% respectively. The blade fatigue life and blade oxidation life are better by +9.1% and +3.4% respectively. There is however little impact on flight costs which have a discrepancy of approximately -0.1%, which translates to savings of US\$16217 in flight operating costs per aircraft per year..
- A clean engine TO from Madrid Barajas International airport requires +50K higher operating temperatures, with negative impact on severity and TO fuel burn, which increase by +2.5% and +3% respectively. The blade fatigue life and blade oxidation life reduce by -10.6% and -2.2% respectively. There is however benefit to the climb fuel burn, which reduces by -6.2% to give a slight benefit to flight costs of -0.3%, which approximates to US\$64157 in flight operating costs per aircraft per year.
- A clean engine TO from Riyadh International airport requires +89K higher operating temperatures, with negative impact on severity and TO fuel burn, which increase by +4.6% respectively. The blade fatigue life and blade oxidation life reduce by -22.1% and -3.9% respectively. There is however benefit to the climb fuel burn, which reduces by -6.2% to give a slight benefit to flight costs of -0.2%, which approximates to US\$38379 in flight operating costs per aircraft per year..

9.3.1.2.2 Degraded Engine Performance

- As with the operational factors assessments, the degraded engines displayed similar performance trends to the clean engine, with the difference being in higher magnitudes and less useful engine component life for the degraded cases. The results show that a TO from Abu Dhabi International airport after 3000cycles incurs a +1.5% increase in flight costs which converts to approximately US\$0.38million per aircraft per year. The blade fatigue life and blade oxidation life reduce by -37.7% and -38.7% respectively. The assessments after 5250cycles (to simulate the hot desert conditions) have shown that the sandy desert conditions are harsh on the engine's health and fuel burn performance, and a large penalty is paid in flight operating costs which have a discrepancy of +6% for a TO from Abu Dhabi. This +6% discrepancy converts into an economical value of approximately US\$1.49million per aircraft per year. The blade fatigue life and blade oxidation life reduce by -61.4% and -78.7% respectively.
- A TO from Ankara International airport with an engine after 3000cycles is shown to incur a discrepancy of +0.9% (US\$0.18million) in flight operating costs per aircraft per year. The blade fatigue life and blade oxidation life reduce by -17.5% and -36.6% respectively.
- A TO from Beirut International airport with an engine after 3000cycles is shown to incur a discrepancy of +1.35% (US\$0.34million) in flight operating costs per aircraft per year. The blade fatigue life and blade oxidation life reduce by -26.7% and -37.7% respectively.
- A TO from Cairo International airport with an engine after 3000cycles incurs a +1.1% (US\$0.27million) penalty in operating costs per aircraft per year. The blade fatigue life and blade oxidation life reduce by -31.4% and -38.2% respectively. The assessments after 5250cycles show a TO from Cairo incurs a large penalty in flight operating costs which have a discrepancy of +5.1% which converts into an economical value of approximately US\$1.28million per aircraft per year. The blade fatigue life and blade oxidation life reduce by -56.7% and -77.4% respectively.
- A TO from Dublin International airport with an engine after 3000cycles is shown to incur a discrepancy of +1.2% (US\$0.30million) in flight operating costs per aircraft per year. The blade fatigue life and blade oxidation life reduce by -9.7% and -35.4% respectively.
- A TO from London Heathrow International airport with an engine after 3000cycles is shown to incur a discrepancy of +1.1% (US\$0.29million) in flight operating costs per aircraft per year. The blade fatigue life and blade oxidation life reduce by -4.5% and -38.5% respectively.
- A TO from Madrid Barajas International airport with an engine after 3000cycles is shown to incur a discrepancy of +1.35% (US\$0.22million) in flight operating costs per aircraft per year. The blade fatigue life and blade oxidation life reduce by -28.6% and -34.3% respectively.
- A TO from Riyadh International airport with an engine after 3000cycles is shown to incur a discrepancy of +0.7% (US\$0.20million) in flight

operating costs per aircraft per year. The blade fatigue life and blade oxidation life reduce by -40.2% and -37.9% respectively. The assessments after 5250cycles show a TO from Riyadh incurs a large penalty in flight operating costs which have a discrepancy of +5.3% which converts into an economical value of approximately US\$1.35million per aircraft per year. The blade fatigue life and blade oxidation life reduce by -64.9% and -77.7% respectively.

9.3.2 Flight Mission Fuel Burn and Engine Life Optimised Aircraft Trajectories

The operation of an airline is extremely cost and cash intensive, and in the context of increasing fuel costs and the competitive nature of the airline industry, operating costs are an important concern to airlines and engine OEMs. A key to reducing lower operating costs is minimising the amount of fuel burn, and flying the optimum trajectory in terms of fuel burn becomes paramount since it translates as a saving in DOC.

According to [3] (in chapter 7), engine MRO is the highest contributor to the cost of aircraft MRO, and Aircraft MRO is a major cost driver behind flight operations. It is imperative therefore to better understand from an operator's perspective how the optimal solutions for minimising fuel burn and protecting the environment will impact on the engine useful life and engine operating costs. In recognition of these factors, the second aim of this study was the assessment and quantification of the trade-offs between the optimal solutions for fuel burn and engine life.

The optimisation studies were conducted for a full flight trajectory. The main variables were the flight altitude and aircraft speed. The optimisation objectives were a) to minimise mission fuel burn and b) to maximise engine life due to creep, fatigue and oxidation. Three mission ranges corresponding to city pairs were chosen for the case studies: London – Madrid (674nm), London – Ankara (1569nm) and London – Abu Dhabi (2981nm). A baseline was chosen and its performance established to enable comparison and have a point of reference. The baseline performance was closely matched to the payload range performance of the Boeing 737-800 aircraft. The assessments were conducted for a clean engine configuration and after 3000, 4500 and 5250cycles of operation. The multi-disciplinary framework used in the airport severity case studies, coupled with an optimiser was used. The results showing the trade-offs between mission fuel burn and engine life optimised trajectories are presented in the following sections.

9.3.2.1 Clean Engine

London – Madrid

- The results show that compared to the baseline, the fuel burn optimised trajectory demonstrates a reduction in mission fuel burn (-1.7%) at the expense of a longer flight time (+1.4min), a shorter blade creep life (-

3.4%) and a shorter blade oxidation life (-2.1%). The fuel burn optimised trajectory is achieved at a lower cost per flight (-0.9%). The fuel optimised trajectory is a high altitude high speed cruise, which achieves the fuel efficiency of a higher altitude and benefits from a shorter time at cruise. Operators use what is called a cost index (CI) to minimise operating costs. This is the ratio of the time-related cost of an airplane operation to the cost of fuel. Time related costs can be direct and hourly or be fixed over a given period. Engines and airframes can be owned or leased by the hour (e.g. power by hour total care packages) and flight crew wages can be hourly based or fixed. Where direct time costs are high, the CI is large and the operational strategy is to minimise time and hence cost. In the case where costs are fixed, the CI is low and operational strategy is to minimise fuel costs.

According to a study made for the optimal CI for a similar aircraft as modelled, a shift to a lower CI (as is the case with the fuel burn optimised trajectory) would impact on the mission by +3 minutes and the annual airline fleet operating costs would increase by US\$1,79 – \$1,97million. In contrast, the -0.9% savings in operating costs for the fuel burn optimised trajectory would convert into annual savings of approximately US\$28400 per flight at today's fuel prices of US\$2.92 per gallon. Assuming an aircraft fleet of 50 would give annual savings of US\$1.42million. This indicates that the fuel burn optimised trajectory may be the preferred choice for operators where fuel prices to rise significantly. A significant rise in the cost of the total care packages and other time related costs would require operators to decide whether they want the aircraft to fly faster or slower. The fuel burn optimised trajectory, will have a significant environmental impact due to a decrease in the ICAO LTO NO_x (-5.6%) emissions.

- In comparison, the results show that the blade creep life optimised trajectory burns more fuel (+3.6%) and takes more mission time (+9.7min) than the baseline. The blade creep life optimised trajectory demonstrates a better blade creep life (+2.5%) and blade oxidation life (+7.5%), with minimal change to the blade fatigue life and the disc creep life. The blade creep life optimised trajectory is achieved at a greater cost per flight (+3%) than the baseline, and has a higher environmental impact in terms of more and more flight NO_x (+1.6%). The +3% rise in operating costs for the blade creep life optimised trajectory would convert into an annual increase of approximately US\$0.90million per flight. Assuming that 3.16 kg CO₂ is produced for every kg of fuel burnt, the excess fuel burn would result in CO₂ emissions of approximately 720 tonnes per year per aircraft. The flight time penalty would incur increase in the time related costs.
- In comparison, the blade fatigue life optimised trajectory is shown to burn marginally less fuel (-0.6%) and takes the same time as the baseline. The blade fatigue life optimised trajectory demonstrates a better blade creep life (+1.4%) and shorter blade oxidation life (-0.7%). The blade fatigue life for the baseline was found to be the same as for the optimised

trajectory. The disc creep life has minimal change. The blade fatigue life optimised trajectory is achieved at a marginally lower cost per flight (approximately by US\$46500 annually per aircraft) than the baseline, and emits marginally more flight NO_x (+0.8%).

- In comparison the blade oxidation life optimised trajectory burns more fuel (+3.8%) and takes more time (+7.6min) than the baseline. The blade oxidation life optimised trajectory demonstrates a worse blade creep life (-1.2%) and a better blade oxidation life (+7.6%). The blade fatigue life for the baseline was found to be the same as for the optimised trajectory. The disc creep life has marginal change. The blade oxidation life optimised trajectory is achieved at a higher cost per flight (+2.5%) than the baseline, and results in lower flight NO_x (-1.2%) emissions. The trajectory is achieved at the cost of US\$0.76million annually. The excess fuel converts to 785 tonnes of CO₂ per year per aircraft.
- The results show that the disc creep life optimised trajectory burns marginally more fuel (+0.3%) and takes more time (+3.4min) than the baseline. The disc creep life optimised trajectory demonstrates a marginally better blade creep life (+0.3%) and a better blade oxidation life (+1.5%). The blade fatigue life for the baseline was found to be the same as for the optimised trajectory. The disc creep life is marginally changed. The disc creep life optimised trajectory is achieved at a marginally higher cost per flight (approximately US\$0.23million annually per aircraft) than the baseline, and emits a lower ICAO LTO NO_x (-6.7%) and marginally lower flight NO_x (-0.3%).

London – Ankara

- The results show that compared to the baseline, the fuel burn optimised trajectory demonstrates a reduction in mission fuel burn (-4.6%) and takes a shorter time (-4.4min). The fuel burn optimised trajectory has a shorter blade creep life (-2.2%) and a shorter blade oxidation life (-3.8%). The fuel burn optimised trajectory is achieved at a lower cost per flight (-2%). The fuel optimised trajectory is a high altitude high speed cruise, which achieves the fuel efficiency of a higher altitude and benefits from a shorter time at cruise. The -2% savings in operating costs convert into annual savings of approximately US\$0.49million per flight at today's fuel prices of US\$2.92 per gallon. Assuming an aircraft fleet of 50 would give annual savings of US\$24.3million. The less flight time implies a further reduction in operating costs in the form of time related costs. This indicates that the fuel burn optimised trajectory may be the preferred choice for operators, with significant savings even in scenarios where the fuel prices and time related costs rise significantly. The reduction in fuel burn converts into an annual reduction of 1040 tonnes in CO₂ per aircraft. The fuel burn optimised trajectory, will have a significant environmental impact due to lower flight NO_x emissions (-2.3%) than the baseline.
- In comparison, the results show that the blade creep life optimised trajectory burns more fuel (+4.9%) and takes more mission time (+22min) than the baseline. The blade creep life optimised trajectory demonstrates

a better blade creep life (+2.2%) and blade oxidation life (+4.3%), with minimal change to the blade fatigue life and the disc creep life. The blade creep life optimised trajectory is achieved at a greater cost per flight (+4.8%) than the baseline, and emits more flight NO_x (+2.8%). The +4.8% rise in operating costs for the blade creep life optimised trajectory converts into an annual increase of approximately US\$1.2million per aircraft. The excess fuel burn converts into approximately 1121 tonnes of CO₂ emissions per aircraft annually.

- In comparison, the results show that the blade fatigue life optimised trajectory is the same trajectory as the clean engine fuel burn optimised.
- In comparison, the results show that the blade oxidation life optimised trajectory burns more fuel (+5.9%) and takes more time (+25.3min) than the baseline. The blade oxidation life optimised trajectory demonstrates a better blade creep life (+2%) and a better blade oxidation life (+4.5%). The blade fatigue life for the baseline was found to be the same as for the optimised trajectory. The disc creep life has marginal change. The blade oxidation life optimised trajectory is achieved at a higher cost per flight (+5.6%) than the baseline, and emit more ICAO LTO NO_x (+5.3%) and flight NO_x (+3.4%). This trajectory incurs a penalty of US\$1.4million plus time related costs annually. The excess fuel burn converts into approximately 1344 tonnes of CO₂ emissions per aircraft annually.
- In comparison, the results show that the disc creep life optimised trajectory burns less fuel (-3.7%) and takes less time (-3.8min) than the baseline. The disc creep life optimised trajectory demonstrates a shorter blade creep life (-3.6%) and a shorter blade oxidation life (-3.5%). The blade fatigue life was found to be marginally changed (-0.1%) and the disc creep life by +0.5%. The disc creep life optimised trajectory is achieved at lower cost per flight (-1.6%) than the baseline, and emits lower ICAO LTO NO_x (-5.7%) and lower flight NO_x (-3%) emissions. The reduction in fuel burn converts into approximately a reduction of 837 tonnes of CO₂ emissions per aircraft annually.

London – Abu Dhabi

- The results show that compared to the baseline, the fuel burn optimised trajectory demonstrates a reduction in mission fuel burn (-5.2%) and takes less flight mission time (-10.1min). The fuel burn optimised trajectory has a shorter blade creep life (-3%) and a shorter blade oxidation life (-5%). The disc creep life is +1% more. The fuel burn optimised trajectory is achieved at a lower cost per flight (-2.8%). The fuel optimised trajectory is a high altitude high speed cruise, which achieves the fuel efficiency of a higher altitude and benefits from a shorter mission time. The -2.8% savings in operating costs convert into annual savings of approximately US\$0.60million per flight at today's fuel prices of US\$2.92 per gallon. Assuming an aircraft fleet of 50 would give annual savings of US\$30million. The less flight time implies a further reduction in operating costs in the form of time related costs. This indicates that the fuel burn optimised trajectory may be the preferred

choice for operators with savings in both fuel costs and time related costs even against any significant rise in prices. The reduction in fuel burn converts into an annual reduction of 1227 tonnes in CO₂ emissions per aircraft. The fuel burn optimised trajectory will have a significant environmental impact due to lower ICAO LTO (-27.1%) and flight NOx (-3.6%) emissions than the baseline.

- In comparison, the results show that the blade creep life optimised trajectory burns marginally less fuel (-0.2%) and takes about the same time as the baseline. The blade creep life optimised trajectory demonstrates a better blade creep life (+2%) and a marginally shorter blade oxidation life (-0.7%), with minimal change to the blade fatigue life and the disc creep life. The blade creep life optimised trajectory is achieved at a marginally lower cost per flight (-0.1%) than the baseline.
- In comparison, the results show that the blade fatigue life optimised trajectory burns less fuel (-2.8%) and takes less time (-8.4min) than the baseline. The blade fatigue life optimised trajectory demonstrates a shorter blade creep life (-1.6%) and shorter blade oxidation life (-3%). The blade fatigue life for the baseline was found to be the same as for the optimised trajectory. The disc creep life has minimal change. The blade fatigue life optimised trajectory is achieved at a lower cost per flight (approximately by US\$0.39million annually per aircraft) than the baseline, and emits more ICAO LTO (+7.4%) and less flight NOx (-1.8%).
- In comparison, the results show that the blade oxidation life optimised trajectory burns more fuel (+2.3%) and takes more time (+18.8min) than the baseline. The blade oxidation life optimised trajectory demonstrates a better blade creep life (+1.1%) and a better blade oxidation life (+0.7%). The blade fatigue life for the baseline was found to be the same as for the optimised trajectory. The disc creep life has little change. The blade oxidation life optimised trajectory is achieved at a higher cost per flight (+2.7%) than the baseline. The trajectory demonstrates a better environmental impact during the LTO cycle than across the whole flight, emitting lower ICAO LTO NOx (-6.5%) and higher flight NOx (+1.5%) emissions. This trajectory incurs a penalty of US\$0.59million plus time related costs annually. The excess fuel burn converts into approximately 552 tonnes of CO₂ emissions per aircraft annually.
- In view of the findings from the disc creep life optimised trajectory analysis, it was found that the disc creep life optimised trajectory burns less fuel (-5%) and takes less time (-7.7min) than the baseline. The disc creep life optimised trajectory demonstrates a shorter blade creep life (-2.9%) and blade oxidation life (-5.3%). The blade fatigue life and disc creep life were found to be largely unchanged. The disc creep life optimised trajectory is achieved at a lower cost per flight (which approximates to US\$0.55million per aircraft annually) than the baseline. The trajectory is more environmentally friendly, and emits lower ICAO LTO NOx (-5%) and flight NOx (-3.8%). The reduction in fuel burn converts into approximately a reduction of 837 tonnes of CO₂ emissions per aircraft annually.

9.3.2.2 After 3000 cycles

London – Madrid

- The results show that compared to the non-optimised, the fuel burn optimised trajectory demonstrates a reduction in mission fuel burn (-2.3%) at the expense of a longer flight mission time (+1.5min). The fuel burn optimised trajectory has a shorter blade creep life (-2.3%) and a shorter blade oxidation life (-2%). The fuel burn optimised trajectory is achieved at a lower cost per flight (-0.2%) than the non-optimised. The fuel optimised trajectory is a high altitude high speed cruise, which achieves the fuel efficiency of a higher altitude and benefits from a shorter cruise time. The -0.2% savings in operating costs convert into annual savings of approximately US\$36406 per aircraft at today's fuel prices of US\$2.92 per gallon. Assuming an aircraft fleet of 50 would give annual savings of US\$1.82million. The longer flight time implies a further increase in operating costs in the form of time related costs. The results indicate that the fuel burn optimised trajectory may be the preferred choice for operators where fuel prices to rise significantly compared to time related costs. The reduction in fuel burn converts into an annual reduction of 482 tonnes in CO₂ emissions per aircraft. The fuel burn optimised trajectory is harsh on the environment in terms of higher ICAO LTO NOx (+2.1%), but demonstrates a better environment performance with flight NOx which is lower (-1.5%).
- In comparison, the results show that the blade creep life optimised trajectory burns more fuel (+3.6%) and takes more mission time (+9.9min) than the non-optimised. The blade creep life optimised trajectory demonstrates a better blade creep life (+1.5%) and blade oxidation life (+7.8%), with minimal change to the blade fatigue life and the disc creep life. The blade creep life optimised trajectory is achieved at a greater cost per flight (+3%) than the non-optimised, and has a harsher environmental impact, emitting and more flight NOx (+0.8%). The +3% rise in operating costs for the blade creep life optimised trajectory would convert into an annual increase of approximately US\$0.92million per aircraft. The excess fuel burn would result in CO₂ emissions of approximately 750 tonnes per aircraft annually. The flight time penalty incurs an increase in time related costs.
- In comparison, the results show that the blade fatigue life optimised trajectory burns marginally more fuel (+0.2%) and takes about the same time as the non-optimised. The blade fatigue life optimised trajectory demonstrates a marginally better blade creep life (+0.1%) and a shorter blade oxidation life (-13.6%). The blade fatigue life for the optimised trajectory was found to be the same as for the non-optimised. The disc creep life has minimal change. The blade fatigue life optimised trajectory is achieved at a marginally higher cost per flight (approximately by US\$78584 annually per aircraft) than the non-optimised, and is harsh on the environment, emitting more ICAO LTO NOx (+4.4%).

- In comparison, the results show the blade oxidation life optimised trajectory burns more fuel (+3.7%) and takes marginally more time (+0.7min) than the non-optimised. The blade oxidation life optimised trajectory demonstrates a marginally better blade creep life (+0.5%) and a better blade oxidation life (+8%). The blade fatigue life for the optimised trajectory was found to be the same as for the non-optimised. The disc creep life had marginal change. The blade oxidation life optimised trajectory is achieved at a higher cost per flight (+2.6%) than the non-optimised, which converts to approximately US\$0.84million annually per aircraft. The optimised trajectory demonstrates marginal change to the ICAO LTO NOx (+0.8%). The excess fuel converts to 767 tonnes of CO₂ per aircraft annually.
- In comparison, the results show the disc creep life optimised trajectory burns marginally more fuel (+0.3%) and takes more time (+1.8min) than the non-optimised. The disc creep life optimised trajectory demonstrates a marginally better blade creep life (+0.7%) and blade oxidation life (+0.3%). The blade fatigue life for the non-optimised was found to be the same as for the optimised trajectory. The disc creep life is marginally changed. The disc creep life optimised trajectory is achieved at a marginally higher cost per flight (approximately US\$83153 per aircraft annually) than the baseline, and is environmentally friendly, emitting lower ICAO LTO NOx (-2.7%) and flight NOx (-2.3%).

London – Ankara

- The results show that compared to the non-optimised, the fuel burn optimised trajectory demonstrates a reduction in mission fuel burn (-4.7%) and takes a shorter flight mission time (-3.6min). The fuel burn optimised trajectory has a shorter blade creep life (-2.7%) and a shorter blade oxidation life (-4.9%). The fuel burn optimised trajectory is achieved at a lower cost per flight (-2.1%). The fuel optimised trajectory is a high altitude high speed cruise, which achieves the fuel efficiency of a higher altitude and benefits from a shorter time at cruise. The -4.7% savings in operating costs convert into annual savings of approximately US\$0.49million per flight at today's fuel prices of US\$2.92 per gallon. Assuming an aircraft fleet of 50 would give annual savings of US\$24.3million. The less flight time implies a further reduction in operating costs in the form of time related costs. This indicates that the fuel burn optimised trajectory may be the preferred choice for operators, with significant savings even in scenarios where the fuel prices and time related costs rise significantly. The reduction in fuel burn converts into an annual reduction of 1120 tonnes in CO₂ per aircraft. The fuel burn optimised trajectory, will have a significant environmental impact due to lower ICAO LTO (-3.1%) and flight NOx (-2.3%) emissions.
- In comparison, the results show the blade creep life optimised trajectory burns more fuel (+3.5%) and takes more mission time (+17.5min) than the non-optimised. The blade creep life optimised trajectory demonstrates a better blade creep life (+1.4%) and blade oxidation life

(+3.7%), with minimal change to the blade fatigue life and the disc creep life. The blade creep life optimised trajectory is achieved at a greater cost per flight (+3.7%) than the non-optimised, and emits marginally more ICAO LTO (+0.3%) and more flight NO_x (+2%). The +3.7% rise in operating costs for the blade creep life optimised trajectory converts into an annual increase of approximately US\$0.93million per aircraft. The excess fuel burn converts into approximately 825 tonnes of CO₂ emissions per aircraft annually.

- In comparison, the results show the blade fatigue life optimised trajectory burns more fuel (+2.9%) and takes more time (+19.9min) than the non-optimised. The blade fatigue life optimised trajectory demonstrates a shorter blade creep life (-2.2%) and blade oxidation life (-5%). The blade fatigue life for the optimised trajectory was found to be the same as for the non-optimised. The disc creep life has marginal change. The blade fatigue life optimised trajectory is achieved at a higher cost per flight (approximately US\$0.99million annually per aircraft) than the non-optimised. The trajectory is not environmentally friendly, and emits more flight NO_x (+2%). The excess fuel burn converts into approximately 695 tonnes of CO₂ annually per aircraft.
- In comparison, the results show the blade oxidation life optimised trajectory burns more fuel (+6%) and takes more time (+25.3min) than the non-optimised. The blade oxidation life optimised trajectory demonstrates a better blade creep life (+0.9%) and a better blade oxidation life (+4.3%). The blade fatigue life for the non-optimised was found to be the same as for the optimised trajectory. The disc creep life has marginal change. The blade oxidation life optimised trajectory is achieved at a higher cost per flight (+5.5%) than the non-optimised, which converts to approximately US\$14million annually per aircraft. The excess fuel converts to 1405 tonnes of CO₂ per aircraft annually and is harsh to the environment emitting more flight NO_x (+4.4%).
- In comparison, the results show the disc creep life optimised trajectory burns less fuel (-4.7%) and takes less time (-3.1min) than the non-optimised. The disc creep life optimised trajectory demonstrates a shorter blade creep life (-3.1%) and a shorter blade oxidation life (-4.5%). The blade fatigue life was found to be marginally changed (-0.1%) and the disc creep life by +0.7%. The disc creep life optimised trajectory is achieved at lower cost per flight (approximately US\$0.46million per aircraft annually) than the non-optimised, and is environmentally friendly demonstrating lower ICAO LTO NO_x (-1.9%) and lower flight NO_x (-3.2%) emissions.

London – Abu Dhabi

- The results show that compared to the non-optimised, the fuel burn optimised trajectory demonstrates a reduction in mission fuel burn (-5.5%) and takes less time (-8.1min). The fuel burn optimised trajectory has a shorter blade creep life (-2.7%) and blade oxidation life (-6.3%). The disc creep life is more by +1%. The fuel burn optimised trajectory is

achieved at a lower cost per flight (-2.8%). The -5.5% savings in operating costs convert into annual savings of approximately US\$0.60million per aircraft at today's fuel prices of US\$2.92 per gallon. Assuming an aircraft fleet of 50 would give annual savings of US\$30million. The longer flight time implies a further increase in operating costs in the form of time related costs. The results indicate that the fuel burn optimised trajectory may be the preferred choice for operators where fuel prices to rise significantly compared to time related costs. The reduction in fuel burn converts into an annual reduction of 1347 tonnes in CO₂ emissions per aircraft. The fuel burn optimised trajectory is friendly on the environment and emits less ICAO LTO (-5.2%) and less flight NOx (-4.7%) emissions than the non-optimised.

- In comparison, the results show the blade creep life optimised trajectory burns less fuel (-1.3%) and takes less time (-6.5min) than the non-optimised. The blade creep life optimised trajectory demonstrates a better blade creep life (+1.3%) and a shorter blade oxidation life (-1.6%), with minimal change to the blade fatigue life and the disc creep life. The blade creep life optimised trajectory is achieved at a marginally lower cost per flight (-1.1%) than the non-optimised, and emits marginally less ICAO LTO (-0.9%). The -1.1% benefit in operating costs for the blade creep life optimised trajectory would convert into an annual reduction of approximately US\$0.24million per aircraft. The reduction in fuel burn would result in CO₂ emissions reduction of approximately 326 tonnes per aircraft annually. The flight time reduction gives benefit to the time related costs.
- In comparison, the results show the blade fatigue life optimised trajectory burns less fuel (-2.8%) and takes about the same time as the non-optimised. The blade fatigue life optimised trajectory demonstrates a shorter blade creep life (-2.2%) and shorter blade oxidation life (-4.6%). The blade fatigue life for the non-optimised was found to be the same as for the optimised trajectory. The disc creep life had minimal change. The blade fatigue life optimised trajectory is achieved at a lower cost per flight (approximately by US\$0.19million annually per aircraft) than the non-optimised, and emits marginally more ICAO LTO (+0.4%) and less flight NOx (-3.3%). The reduction in fuel burn would result in CO₂ emissions reduction of approximately 696 tonnes per aircraft annually.
- In comparison, the results show the blade oxidation life optimised trajectory burns more fuel (+3%) and takes more time (+21.9min) than the non-optimised. The blade oxidation life optimised trajectory demonstrates a better blade creep life (+1.1%) and a marginally better blade oxidation life (+0.5%). The blade fatigue life for the non-optimised was found to be the same as for the optimised trajectory. The disc creep life had marginal change. The blade oxidation life optimised trajectory is achieved at a higher cost per flight (+3.3%) than the non-optimised, which converts to approximately US\$0.72million annually per aircraft. The trajectory is not environmentally friendly with higher ICAO LTO NOx (+2.6%) and flight NOx (+1.7%) emissions. The excess fuel converts to 729 tonnes of CO₂ per aircraft annually.

- In comparison, the results show the disc creep life optimised trajectory is the same trajectory that gives the fuel burn optimum performance after 3000cycles.

9.3.2.3 After 4500cycles

London – Madrid

- The results show that compared to the non-optimised, the fuel burn optimised trajectory demonstrates a reduction in mission fuel burn (-1.8%) takes about the same flight time. The fuel burn optimised trajectory has a shorter blade creep life (-3.3%) and a shorter blade oxidation life (-4.8%). The fuel burn optimised trajectory is achieved at a marginally lower cost per flight (-0.2%) and emits marginally higher ICAO LTO NOx (+0.7%) and I flight NOx (+0.4%) emissions than the non-optimised. The -0.2% savings in operating costs convert into annual savings of approximately US\$66500 per aircraft at today's fuel prices of US\$2.92 per gallon. Assuming an aircraft fleet of 50 would give annual savings of US\$3.33million. The longer flight time implies a further increase in operating costs in the form of time related costs. The results indicate that the fuel burn optimised trajectory may be the preferred choice for operators where fuel prices to rise significantly compared to time related costs. The reduction in fuel burn converts into an annual reduction of 389 tonnes in CO₂ emissions per aircraft. The fuel burn optimised trajectory is harsh on the environment in terms of higher ICAO LTO NOx (+2.1%), but demonstrates a better environment performance with flight NOx which is lower (-1.5%).
- In comparison, the results show the blade creep life optimised trajectory burns more fuel (+3%) and takes more mission time (+8min) than the non-optimised. The blade creep life optimised trajectory demonstrates a better blade creep life (+3.3%) and blade oxidation life (+9%), with minimal change to the blade fatigue life and the disc creep life. The blade creep life optimised trajectory is achieved at a greater cost per flight (+1.6%) than the non-optimised, and emits marginally more flight NOx (+0.6%). The +3% rise in operating costs for the blade creep life optimised trajectory would convert into an annual increase of approximately US\$0.78million per aircraft. The excess fuel burn would result in CO₂ emissions of approximately 671 tonnes per aircraft annually. The flight time penalty incurs an increase in time related costs.
- In comparison, the results show the blade fatigue life optimised trajectory burns marginally more fuel (+0.5%) and takes time (+1.5min) than the non-optimised. The blade fatigue life optimised trajectory demonstrates a better blade creep life (+1.8%) and a marginal change to the blade oxidation life. The blade fatigue life for the optimised trajectory was found to be the same as for the non-optimised. The disc creep life has minimal change. The blade fatigue life optimised trajectory is achieved at a higher cost per flight (approximately by US\$0.16million annually per aircraft) than the non-optimised, and emits more ICAO LTO (+4.4%).

- In comparison, the results show the blade oxidation life optimised trajectory burns more fuel (+4.2%) and takes more time (+7.7min) than the non-optimised. The blade oxidation life optimised trajectory demonstrates a shorter blade creep life (-1.6%) and a better blade oxidation life (+9.6%). The blade fatigue life for the optimised trajectory was found to be the same as for the non-optimised. The disc creep life had marginal change. The blade oxidation life optimised trajectory is achieved at a higher cost per flight (+2.6%) than the non-optimised, which converts to approximately US\$0.82million annually per aircraft. The trajectory demonstrates marginal change to the ICAO LTO NOx (+0.8%) and lower flight NOx (-1.2%) emissions. The excess fuel converts to 940 tonnes of CO₂ per aircraft annually.
- In comparison, the results show the disc creep life optimised trajectory burns marginally less fuel (-0.5%) and takes more time (+1.9min) than the non-optimised. The disc creep life optimised trajectory demonstrates a marginally better blade creep life (+0.9%) and marginal change to the blade oxidation life (-0.1%). The blade fatigue life for the non-optimised was found to be the same as for the optimised trajectory. The disc creep life is marginally changed (+0.3%). The disc creep life optimised trajectory is achieved at a higher cost per flight (approximately US\$0.13million per aircraft annually) than the non-optimised, and is environmentally friendly, emitting a lower ICAO LTO NOx (-2.4%) and flight NOx (-0.7%).

London – Ankara

- The results show that compared to the non-optimised, the fuel burn optimised trajectory demonstrates a reduction in mission fuel burn (-3.3%) and takes a shorter flight mission time (-3.7min). The fuel burn optimised trajectory has a shorter blade creep life (-2.1%) and a shorter blade oxidation life (-4.9%). The fuel burn optimised trajectory is achieved at a lower cost per flight (-1.4%) and higher ICAO LTO (+6.1%) and lower flight NOx (-3.8%) emissions than the non-optimised. The -3.3% savings in operating costs convert into annual savings of approximately US\$0.37million per flight at today's fuel prices of US\$2.92 per gallon. Assuming an aircraft fleet of 50 would give annual savings of US\$18.5million. The less flight time implies a further reduction in operating costs in the form of time related costs. This indicates that the fuel burn optimised trajectory may be the preferred choice for operators, with significant savings even in scenarios where the fuel prices and time related costs rise significantly. The reduction in fuel burn converts into an annual reduction of 818 tonnes in CO₂ per aircraft.
- In comparison, the results show the blade creep life optimised trajectory burns more fuel (+2.5%) and takes more mission time (+13.3min) than the non-optimised. The blade creep life optimised trajectory demonstrates a better blade creep life (+2.8%) and blade oxidation life (+4.1%), with minimal change to the blade fatigue life and the disc creep life. The blade creep life optimised trajectory is achieved at a greater cost

per flight (+2.7%) than the non-optimised, and emits more ICAO LTO (+2.8%) and more flight NOx (+1.5%). The +2.5% rise in operating costs for the blade creep life optimised trajectory converts into an annual increase of approximately US\$0.71million per aircraft. The excess fuel burn converts into approximately 618 tonnes of CO₂ emissions per aircraft annually.

- In comparison, the results show the blade fatigue life optimised trajectory burns more fuel (+4.6%) and takes more time (+17.9min) than the non-optimised. The blade fatigue life optimised trajectory demonstrates a shorter blade creep life (-2.2%) and a better blade oxidation life (+4.9%). The blade fatigue life for the optimised trajectory was found to be the same as for the non-optimised. The disc creep life has marginal change. The blade fatigue life optimised trajectory is achieved at a higher cost per flight (approximately US\$10.5million annually per aircraft) than the non-optimised. The excess fuel burn converts into approximately 1147 tonnes of CO₂ annually per aircraft.
- In comparison, the results show the blade oxidation life optimised trajectory burns more fuel (+5.4%) and takes more time (+20.4min) than the non-optimised. The blade oxidation life optimised trajectory demonstrates a shorter blade creep life (-3%) and a better blade oxidation life (+5%). The blade fatigue life for the non-optimised was found to be the same as for the optimised trajectory. The disc creep life has marginal change. The blade oxidation life optimised trajectory is achieved at a higher cost per flight (+4.7%) than the non-optimised, which converts to approximately US\$21million annually per aircraft. The excess fuel converts to 1355 tonnes of CO₂ per aircraft annually and is harsh to the environment emitting more ICAO LTO NOx (+3.3%) and flight NOx (+1.2%).
- In comparison, the results show the disc creep life optimised trajectory burns less fuel (-1.1%) and takes less time (-5.0min) than the non-optimised. The disc creep life optimised trajectory demonstrates a marginally better blade creep life (+0.9%) and a shorter blade oxidation life (-2.9%). The blade fatigue life was found to be marginally changed (-0.1%) and the disc creep life by +0.4%. The disc creep life optimised trajectory is achieved at lower cost per flight (approximately US\$0.29million per aircraft annually) than the non-optimised, and emits lower ICAO LTO NOx (-3%) and lower flight NOx (-2.3%) emissions.

London – Abu Dhabi

- The results show that compared to the non-optimised, the fuel burn optimised trajectory demonstrates a reduction in mission fuel burn (-6.4%) and takes less time (-12.4min). The fuel burn optimised trajectory has a shorter blade creep life (-3.6%) and a shorter blade oxidation life (-2.2%). The fuel burn optimised trajectory is achieved at a lower cost per flight (-3.7%). The -6.4% savings in operating costs convert into annual savings of approximately US\$0.83million per aircraft at today's fuel prices of US\$2.92 per gallon. Assuming an aircraft fleet of 50 would give

annual savings of US\$41.5million. The shorter flight time implies a further savings in operating costs in the form of time related costs. The results indicate that the fuel burn optimised trajectory may be the preferred choice for operators where fuel prices to rise significantly compared to time related costs. The reduction in fuel burn converts into an annual reduction of 1663 tonnes in CO₂ emissions per aircraft. The fuel burn optimised trajectory is friendly on the environment in terms of less flight NOx (-30.3%), but is harsh in terms of more ICAO LTO (+16.2%) and emissions than the non-optimised.

- In comparison, the results show the blade creep life optimised trajectory burns less fuel (-1.4%) and takes less time (-4.2min) than the non-optimised. The blade creep life optimised trajectory demonstrates a better blade creep life (+3.2%) and blade oxidation life (+3.6%), with minimal change to the blade fatigue life and the disc creep life. The blade creep life optimised trajectory is achieved at a marginally lower cost per flight (-0.8%) than the non-optimised, and emits more ICAO LTO (+27.9%) and less flight NOx -26.9%. The -1.4% benefit in operating costs for the blade creep life optimised trajectory would convert into an annual reduction of approximately US\$0.23million per aircraft. The reduction in fuel burn would result in CO₂ emissions reduction of approximately 355 tonnes per aircraft annually. The flight time reduction gives benefit to the time related costs.
- In comparison, the results show that the blade fatigue life optimised trajectory burns less fuel (-1.4%) and takes the same flight time as the non-optimised. The blade fatigue life optimised trajectory demonstrates a marginally better blade creep life (+0.8%). The blade fatigue life optimised trajectory is achieved at a lower cost per flight (approximately by US\$0.15million annually per aircraft) than the non-optimised, and is environmentally friendly, emitting less ICAO LTO (-21.7%) and less flight NOx (-27.9%). The reduced fuel burn converts into a reduction in CO₂ emissions of 370 tonnes per aircraft annually.
- In comparison, the results show that the blade oxidation life optimised trajectory burns more fuel (+2.5%) and takes more time (+22.4min) than the non-optimised. The blade oxidation life optimised trajectory demonstrates a better blade creep life (+2.2%) and blade oxidation life (+4.7%). The blade oxidation life optimised trajectory is achieved at a higher cost per flight (+3%) than the non-optimised, which converts to approximately US\$0.67million annually per aircraft. The trajectory is environmentally friendly with lower ICAO LTO NOx (-26.4%) and flight NOx (-25.3%) emissions. The excess fuel converts to 657 tonnes of CO₂ per aircraft annually.
- In comparison, the results show the disc creep life optimised trajectory is the same trajectory that gives the fuel burn optimum performance after 4500cycles.

9.3.2.4 After 5250 cycles

London – Madrid

- The results show that compared to the non-optimised, the fuel burn optimised trajectory demonstrates a reduction in mission fuel burn (-3.6%) and takes the same time. The fuel burn optimised trajectory has a shorter blade creep life (-5.5%) and a shorter blade oxidation life (-13.7%). The fuel burn optimised trajectory is achieved at a marginally lower cost per flight (-0.7%) The -0.7% savings in operating costs convert into annual savings of approximately US\$0.24million per aircraft at today's fuel prices of US\$2.92 per gallon. Assuming an aircraft fleet of 50 would give annual savings of US\$12million. The same flight time implies no change in the time related costs. The results indicate that the fuel burn optimised trajectory may be the preferred choice for operators where fuel prices to rise significantly compared to time related costs. The reduction in fuel burn converts into an annual reduction of 163 tonnes in CO₂ emissions per aircraft. The fuel burn optimised trajectory is environmentally friendly, and emits lower ICAO LTO NO_x (-1.6%) and lower flight NO_x (-1.4 %) emissions than the non-optimised.
- In comparison, the results show the blade creep life optimised trajectory burns marginally more fuel (+0.7%) and takes more time (+6.3min) than the non-optimised. The blade creep life optimised trajectory demonstrates a better blade creep life (+3.8%) and blade oxidation life (+7.8%), with minimal change to the blade fatigue life and the disc creep life. The blade creep life optimised trajectory is achieved at a greater cost per flight (+1.6%) than the non-optimised, and emits more ICAO LTO (+5.6%) and less flight NO_x (-1.6%). The +1.6% rise in operating costs would convert into an annual increase of approximately US\$0.51million per aircraft. The excess fuel burn would result in CO₂ emissions of approximately 156 tonnes per aircraft annually. The flight time penalty incurs an increase in time related costs.
- In comparison, the results show the blade fatigue life optimised trajectory burns marginally less fuel (-0.6%) and takes more flight time (+7.2min) than the non-optimised. The blade fatigue life optimised trajectory demonstrates a better blade creep life (+1.4%) and a marginally shorter blade oxidation life (-0.7%). The blade fatigue life for the optimised trajectory was found to be the same as for the non-optimised. The disc creep life has minimal change. The blade fatigue life optimised trajectory is achieved at a lower cost per flight (approximately by US\$0.64million annually per aircraft) than the non-optimised, and emits more ICAO LTO (+1.4%). The lower fuel converts into a reduction in CO₂ emissions of approximately 156 tonnes per aircraft annually.
- In comparison, the results show the blade oxidation life optimised trajectory burns more fuel (+3%) and takes more time (+8min) than the non-optimised. The blade oxidation life optimised trajectory demonstrates a marginally better blade creep life (+3.4%) and blade oxidation life (+9.5%). The blade fatigue life for the optimised trajectory was found to

be the same as for the non-optimised. The disc creep life had marginal change. The blade oxidation life optimised trajectory is achieved at a higher cost per flight (+2.5%) than the non-optimised, which converts to approximately US\$0.77million annually per aircraft. and emits more ICAO LTO NO_x (+1.1%) and less flight NO_x (-1.6%) emissions. The excess fuel converts to 686 tonnes of CO₂ per aircraft annually.

- In comparison, the results show the disc creep life optimised trajectory burns marginally less fuel (-0.4%) and takes more time (+4.6min) than the non-optimised. The disc creep life optimised trajectory demonstrates a better blade creep life (+4.4%) and blade oxidation life (+6.5%). The blade fatigue life for the non-optimised was found to be the same as for the optimised trajectory. The disc creep life is marginally changed. The disc creep life optimised trajectory is achieved at a higher cost per flight (approximately US\$0.29million per aircraft annually) than the non-optimised, and emits a marginally higher ICAO LTO NO_x (+0.8%) and lower flight NO_x (-2%) emissions.

London – Ankara

- The results show that compared to the non-optimised, the fuel burn optimised trajectory demonstrates a reduction in mission fuel burn (-4.2%) and takes a shorter flight mission time (-1.7min). The fuel burn optimised trajectory has a shorter blade creep life (-5.8%) and a shorter blade oxidation life (-7.7%). The fuel burn optimised trajectory is achieved at a lower cost per flight (-1.5%) and emits marginally more ICAO LTO (+0.7%) and less flight NO_x (-7.6%) emissions than the non-optimised. The -4.2% savings in operating costs convert into annual savings of approximately US\$0.39million per flight at today's fuel prices of US\$2.92 per gallon. Assuming an aircraft fleet of 50 would give annual savings of US\$19.5million. The less flight time implies a further reduction in operating costs in the form of time related costs. This indicates that the fuel burn optimised trajectory may be the preferred choice for operators, with significant savings even in scenarios where the fuel prices and time related costs rise significantly. The reduction in fuel burn converts into an annual reduction of 1072 tonnes in CO₂ per aircraft.
- In comparison, the results show the blade creep life optimised trajectory burns more fuel (+6.9%) and takes more time (+27.2min) than the non-optimised. The blade creep life optimised trajectory demonstrates a better blade creep life (+5.4%) and blade oxidation life (+2%), with minimal change to the blade fatigue life and the disc creep life. The blade creep life optimised trajectory is achieved at a greater cost per flight (+6.2%) than the non-optimised, and emits less flight NO_x (-1.9%). The +6.9% rise in operating costs for the blade creep life optimised trajectory converts into an annual increase of approximately US\$16.1million per aircraft. The excess fuel burn converts into approximately 1763 tonnes of CO₂ emissions per aircraft annually.
- In comparison, the results show the blade fatigue life optimised trajectory burns more fuel (+6.2%) and takes more time (+22.8min) than the non-

optimised. The blade fatigue life optimised trajectory demonstrates a better blade creep life (+5%) and blade oxidation life (+2.6%). The blade fatigue life for the optimised trajectory was found to be the same as for the non-optimised. The disc creep life has marginal change. The blade fatigue life optimised trajectory is achieved at a higher cost per flight (approximately US\$13.1million annually per aircraft), and emits more ICAO LTO (+2.9%) and less flight NO_x (-2.4%).

- In comparison, the results show the blade oxidation life optimised trajectory burns more fuel (+7.9%) and takes more time (+27.2min) than the non-optimised. The blade oxidation life optimised trajectory demonstrates a shorter blade creep life (-5.7%) and a better blade oxidation life (+2.6%). The blade fatigue life for the non-optimised was found to be the same as for the optimised trajectory. The disc creep life has marginal change. The blade oxidation life optimised trajectory is achieved at a higher cost per flight (+6.6%) than the non-optimised, and emits more ICAO LTO NO_x (+11.5%) and less flight NO_x (-2.4%). The excess fuel converts to 2029 tonnes of CO₂ per aircraft annually.
- In comparison, the results show the disc creep life optimised trajectory burns marginally less fuel (-0.9%) and takes slightly more time (+1.0min) than the non-optimised. The disc creep life optimised trajectory demonstrates a better blade creep life (+2.6%) and a shorter blade oxidation life (-1.8%). The blade fatigue life was found to be marginally changed (-0.2%) and the disc creep life by +0.8%. The disc creep life optimised trajectory is achieved at marginally lower cost per flight (approximately US\$22608 per aircraft annually) than the non-optimised, and emits less flight NO_x (-7.5%) emissions. The reduction in fuel converts to a reduction of 207 tonnes of CO₂ per aircraft annually.

London – Abu Dhabi

- The results show that compared to the non-optimised, the fuel burn optimised trajectory demonstrates a reduction in mission fuel burn (-7%) and takes less time (-14.4min). The fuel burn optimised trajectory has a shorter blade creep life (-6.5%) and a better blade oxidation life (+3.9%). The disc creep life is more by +0.5%. The fuel burn optimised trajectory is achieved at a lower cost per flight (-4%) and less ICAO LTO (-6%) and less flight NO_x (-4.6%) emissions than the non-optimised. The -7% savings in operating costs convert into annual savings of approximately US\$0.91million per flight at today's fuel prices of US\$2.92 per gallon. Assuming an aircraft fleet of 50 would give annual savings of US\$45.5million. The less flight time implies a further reduction in operating costs in the form of time related costs. This indicates that the fuel burn optimised trajectory may be the preferred choice for operators, with significant savings even in scenarios where the fuel prices and time related costs rise significantly. The reduction in fuel burn converts into an annual reduction of 1888 tonnes in CO₂ per aircraft.
- In comparison, the results show the blade creep life optimised trajectory burns marginally less fuel (-0.2%) and takes less time (-6.1min) than the

non-optimised. The blade creep life optimised trajectory demonstrates a better blade creep life (+6%) and blade oxidation life (+8.5%), with minimal change to the blade fatigue life and the disc creep life more by +1.3%. The blade creep life optimised trajectory is achieved at a lower cost per flight (-1.2%) than the non-optimised, and emits more ICAO LTO (+4.7%). The -1.2% reduction in operating costs converts into an annual reduction of approximately US\$0.28million per aircraft.

- In comparison, the results show the blade fatigue life optimised trajectory burns marginally more fuel (+0.3%) and takes more time (+10.9min) than the non-optimised. The blade fatigue life optimised trajectory demonstrates a better blade creep life (+2.3%) and blade oxidation life (+8.9%). The blade fatigue life for the non-optimised was found to be the same as for the optimised trajectory. The disc creep life had minimal change. The blade fatigue life optimised trajectory is achieved at a higher cost per flight (approximately US\$0.27million annually per aircraft) than the non-optimised, and emits more ICAO LTO (+2.5%).
- In comparison, the results show the blade oxidation life optimised trajectory burns more fuel (+1%) and takes less time (+11.9min) than the non-optimised. The blade oxidation life optimised trajectory demonstrates a better blade creep life (+1.4%) and blade oxidation life (+10%). The blade fatigue life and disc creep life are unchanged. The blade oxidation life optimised trajectory is achieved at a higher cost per flight (+0.9%), which converts to approximately US\$0.35million annually per aircraft. The excess fuel converts to 270 tonnes of CO₂ per aircraft annually
- In comparison, the results show the disc creep life optimised trajectory burns less fuel (-3.2%) and takes less time (-17.9min) than the non-optimised. The disc creep life optimised trajectory demonstrates a better blade creep life (+4.3%) and blade oxidation life (+8.8%). The blade fatigue life is unchanged, and the disc creep life more by +1.6%. The disc creep life optimised trajectory is achieved at a lower cost per flight (approximately US\$0.68million per aircraft annually) than the non-optimised, and is environmentally friendly, emitting a lower ICAO LTO NOx (-8.6%) and lower flight NOx (-1.9%).

9.3.3 Conclusion

The key contribution to knowledge from this PhD was to develop, implement and demonstrate methodologies to better understand the effect that environmental taxation in the future may have on the adaptation of optimised operation methods and novel technologies, which will be aimed specifically at reducing the aviation industry's impact on the environment. The key contribution to knowledge from this research has been a) the assessment of the impact of airport severity factors on engine life consumption and aircraft performance and b) the assessment and quantification of the change in engine life usage when optimising for flight mission fuel burn and the change in flight mission fuel burn when optimising for engine life usage, without neglecting the influence of engine component degradation.

The key conclusions from this PhD are summarised in table 9.1 and expounded in sections 9.3.3.1 and 9.3.3.2 below.

Table 9.1: Key Conclusions

| Case Study | | Flight Mission Fuel Burn | Life | DOC per Flight | NOx |
|----------------------------------|--------------------------|--------------------------|------------|----------------|-----------------------|
| Airport Severity | High Altitude | high | less | less | ICAO high Flight less |
| | High OAT | high | less | high | high |
| | Derate | less | higher | less | less |
| Aircraft Trajectory Optimisation | Flight Mission Fuel Burn | less | less | less | less |
| | Blade Creep Life | high | high | high | high |
| | Blade Fatigue Life | high | comparable | high | high |
| | Blade Oxidation Life | high | high | high | high |
| | Disc Creep Life | low | high | low | low |
| Engine Component Degradation | | high | less | high | high |

9.3.3.1 Airport Severity Factors

In conclusion, the airport studies have shown that:

- The need for different operational strategies at different airports cannot be ignored. It has been shown that high OAT and high altitude airports such as Abu Dhabi, Ankara, Beirut, Cairo, Madrid and Riyadh have an effect on the aircraft's TO performance. It has been shown that the higher operating temperatures required at these airports, have severe consequences on the engine component life, fuel burn and emissions than on operating costs. The significant rise in costs arises when degradation comes into play. Hence for the operator, if the choice is operating costs then the strategy for a clean engine operation would be 'business as usual'. If however the choice is longer engine time on wing, reduced fuel burn and emissions then a change in operating strategy would be required to minimise the impact on these metrics.
- Engine component stress levels are particularly high during TO due to high temperatures and pressure. The high temperatures will inevitably promote NOx formation. It is the author's opinion therefore that optimum TO performance is crucial towards minimising engine component damage and NOx emissions. Again as with the implications for operational factors, operational strategies such as derate would be beneficial for airports such as Abu Dhabi, Cairo, Madrid and Riyadh and others which are located at high altitude and high OAT. The airliners may use TO derate, depending on their choice in trade-off between fuel burn

(and DOC) and engine severity (life consumption) to reduce engine component damage. Engine TO derate would probably give more savings in cumulative costs because the engine would not deteriorate so quickly as to impose a fuel burn penalty. Operators may need to manage the aircraft's TO trajectory and develop optimised environmental trajectories that will have minimal impact on engine maintenance.

- As evidenced by the results when simulating the sandy desert environment conditions (represented by degradation after 5250cycles) of Abu Dhabi, Cairo and Riyadh, the environmental condition is important for engine performance and component degradation (life consumption). The environment is however difficult to manage, and a possible reprieve is avoiding high temperatures at TO, which implies use of TO derate as a strategy. Fleet management is another possibility that may be employed by operators to mitigate rapid engine damage, frequent shop visits and high maintenance costs.

9.3.3.2 Trajectory Optimisation Studies

In conclusion, the aircraft trajectory optimisation studies have shown that:

- Fuel burn optimised trajectories incur a time penalty and the higher maximum temperatures negatively impact on the blade creep and oxidation lives. These trajectories are attractive when considering fuel costs, but the benefit in operating costs seems to be somewhat eroded by the rising time dependent costs, including rising maintenance costs due to the lower engine component life on these trajectories.
- The blade creep life optimised trajectories incur a penalty on fuel burn, flight time and NO_x emissions except for the longer medium - long range (London – Abu Dhabi) route. Consequently the fuel and time dependent variables are highly influential; hence the trajectories are operated at high cost. Airline operators may be influenced to move to these trajectories along shorter routes when faced with a significant drop in fuel and time related costs.
- The blade fatigue life optimised trajectories like the blade creep life trajectory, incur a penalty on fuel burn and time except for the longer London – Abu Dhabi route. These trajectories are high cost and there is no foreseeable change in the blade fatigue life largely because the fatigue life is a function of the number of start/stop cycles and transient performance. The ICAO LTO NO_x performance of these trajectories is poor. Consequently flying these trajectories may not necessarily be attractive to operators.
- The blade oxidation life optimised trajectories are operated at higher fuel burn and more mission time. Consequently (as with the blade creep life trajectories) the fuel and time dependent variables are highly influential, resulting in high operating costs. These trajectories are also environmentally unfriendly and would incur further costs in the likelihood of emissions taxation. The improvements in blade oxidation life may not warrant operators flying these trajectories.

- The disc creep life optimised trajectories are attractive when considering fuel burn especially along the short - medium range (London – Ankara) and medium - long range (London – Abu Dhabi) routes. These trajectories also show good performance in terms of operating costs and NOx emissions.

9.4 Recommendations for Future Work

Several assumptions have been made in this work and some have been due to limitations imposed by time availability. The framework used in the studies has achieved the key requirements, there is however scope to further develop the framework and improve on the research. The area of study has not been fully exhausted and therefore warrants further research. The recommendations from this research include the following:

a) The current Lifting model calculates the engine lifting time between overhaul according to the creep, fatigue and oxidation failure modes. These are used independent of one another. The code could be developed to combine the lifting methodologies because in reality the failure modes are not entirely independent of each other but do interact.

b) The current engine performance model allows for engine degradation to be introduced into the engine model by changing the percentages of the engine health parameters. As such the levels of degradation are at the discretion of the user and do not evolve with engine use. A diagnostics and prognostics tool to predict levels of degradation and accurately capture the mechanisms of failure could be developed and incorporated to allow for the engine condition to evolve with use and better represent degradation.

c) The current framework does not include a weather and environment model and in this work, a change in the health parameters was used to simulate TO at airports with sandy environments. These health parameters were used throughout the flight mission and not just at TO. An improvement could include a weather and environment model that allows the different conditions at the TO and landing airport to be simulated. Future work can also include performance calculations based on hot and cold days.

d) The current study has focused on vertical profiles. This can be expanded to using actual waypoints on any given route and incorporating horizontal trajectory profiles.

e) Future studies can include noise as an objective, which though mentioned has not been within the scope of this work. This would allow ensuring the optimised trajectories are within the noise regulations around airports.

f) A key driver to lower operating costs is a considerable reduction in fuel burn. Maintenance costs will inevitably rise with engine life consumption. Further study of the trade-offs between fuel burn and engine life is therefore recommended.

g) A GA based optimiser has been used in this work. Future work could include the use of a hybrid optimiser to ensure the best solution is found.

Appendices

Appendix 1

Towards Development of a Diagnostic and Prognostic Tool for Civil Aero-Engine Component Degradation

N. Khani, C. Segovia, R. Navaratne, Vishal Sethi, Riti Singh and Pericles Pilidis
Department of Power & Propulsion, Cranfield University
Bedfordshire MK43 0AL United Kingdom

Abstract

A mechanical device such as an aircraft gas turbine engine will in its lifetime of service show the effects of damage and deterioration. The damage to (and deterioration of) an engine has an adverse effect on the engine's overall performance. It is therefore vitally important to predict the effects of deterioration on the performance of an engine and on the economic (fuel burn and engine life) implications from an operator's perspective. Engine component degradation leads to performance deterioration and change, which requires the engine to run hotter and faster so as to meet the required thrust and aircraft performance. Increasing engine operating temperatures and engine speed result in increased creep and fatigue damage to the hot section components and increases the engine life cycle costs. One way of reducing life cycle costs is by better usage of the engine and involves being certain about the life potential of the engine and its components and how this life evolves with use. A sound understanding of how the engine life evolves and to predict remaining life requires understanding the engine's operating environment and how component damage is sustained and accumulated. Knowledge about the engine condition and the likely stresses to which it will be subjected is required to analyse engine component usage and reduce degradation, raise safe-life limits of components and reduce maintenance requirements. This paper lays the foundation for the development of a prognostic tool that will capture and model the mechanisms of degradation, and predict levels of degradation based on engine deployment. The mechanisms that will cause degradation are assessed and integrated to establish the requirements of the tool. The paper discusses how degradation will affect component and engine performance and also the life of the engine.

Appendix 2

Effects of Aero-Engine Component Degradation on Flight Mission Fuel Burn and NOx Emissions

N. Khani, B. Venediger, C. Segovia, V. Sethi, P. Pilidis and Y. Li Department of Power & Propulsion, Cranfield University
Bedfordshire MK43 0AL United Kingdom

Abstract

Aviation contributes about 2-3% of human generated global carbon dioxide (CO₂) emissions and about 3% of the potential warming effect of the total global emissions that can affect the earth's climate. Air transport is continuously growing, and is constantly making strides to reduce its carbon footprint by reducing fuel consumption through technological and operational advances. Aviation however still contributes to the ever increasing concentrations of pollutant gases in the atmosphere including oxides of nitrogen (NO_x). At ground level and in the troposphere (up to 10km above earth's surface), the presence of NO_x results in an increase in ozone concentration, causing respiratory illness and impaired vision. In the stratosphere (10km – 50km above earth's surface), NO_x results in ozone depletion and consequently an increase in ultra-violet radiation which causes skin cancer and eye diseases. The aviation industry has been looking at ways to reduce NO_x emissions produced by aero-engines. However, industry's concentrated effort to improve thermal efficiency (better fuel efficiency) has led to higher overall pressure ratios and turbine entry temperatures which in turn promote the production of NO_x. Aero-engine components will during their life time of service suffer the effects of degradation. This results in changes in component characteristics and adversely affects the engine's overall performance, and will affect the fuel burn and NO_x emissions. In this paper, a Techno-economic, Environmental, and Risk Assessment (TERA) type aero-engine multidisciplinary optimisation tool is used to make preliminary assessments on the effects of degradation. Investigations are conducted for fuel burn and flight mission NO_x emissions. The full flight mission NO_x is considered and not just for the landing and takeoff cycle because of the effects of cruise NO_x on climate change. The fuel burn and NO_x emissions resulting from degradation are compared to those of an engine with zero degradation. The results show that to meet the required thrust and aircraft performance, the degraded engine must compensate by increasing the fuel flow rate and the turbine entry temperature. The engine is running faster and burning hotter, thus burning more fuel and emitting more NO_x. Trajectory optimisation studies are conducted for the clean engine (minimum fuel burn and minimum time) and for the degraded engine (minimum fuel burn). The fuel burn optimised trajectory burns less fuel whilst taking a longer time than the time optimised trajectory. The time optimised trajectory has significantly higher NO_x emissions. The fuel burn optimised trajectories for the clean and degraded engines are not the same. Future work will involve the effects of flow capacity degradation and the next phase optimised trajectories and the effects of engine life, flight time and fuel burn on direct operating costs.

Appendix 3

Effect of engine degradation on fuel burn optimum civil aircraft trajectories

Clara Segovia Blat: MSc Thesis
Department of Power and Propulsion
Cranfield University

Abstract

During the entire service of an engine in an aircraft, their performance is changing due to different factors such as the degradation or possible faults and breakdowns. Not all these factors are predictable since some of them are sudden events. Nevertheless, some of them can be predicted and, therefore studied, as in the case of degradation. Degradation is mainly produced by three mechanisms: • Singular events which refer to the sudden deterioration of the engine such as foreign engine damage (FOD) or engine surge. • Benign events which are those associated with the natural ageing of the engine, e.g. thermal distortion. • "Not entirely benign" events which comprise other factors different from the natural ageing that also produce degradation such as maintenance procedures or engine flight operational procedures. Since the singular events are not predictable, the scenarios that have been taken into account mainly correspond to the degradation caused by benign events and also "not entirely benign" events. This project uses a Techno-economic and Environmental Risk Assessment (TERA) approach, a multidisciplinary scenario which assess the preliminary design of gas turbine engines. The scope of this work is the study of the degradation in order to adapt the optimum flight trajectories to the level of degradation. For airlines, considering the level of degradation on optimum trajectories is very important as it is a way of reducing maintenance and operating costs. To achieve this aim a TURBOMATCH simulation code was used to calculate the uninstalled clean engine performance. Thereafter, it has been study the effects of the individual degradation of the different components, i.e. fan, low and high pressure compressors and low and high pressure turbines, selecting a 2% of degradation in flow capacity and efficiency. The degraded engine performance has been calculated, studying the effects on net thrust, SFC, mass flow, PR and TET. Degradation causes the drop of PR, mass flow and net thrust, whereas the SFC increases. Therefore, in order to achieve the required net thrust, the TET should be increased and hence, the creep life of the turbine blades will be reduced. In a further step, the aircraft simulation code HERMES has been used to obtain the flight mission fuel burn. A based line trajectory has been selected based on the public domain available data and the amount of fuel needed to meet this trajectory has been obtained. This trajectory has been optimised for the minimum fuel burn by changing the cruise altitude and Mach number, achieving a 5% reduction in fuel. Thereafter, the baseline trajectory simulation has been applied to the different degradation case studies and the amount of fuel needed in each case has been calculated. The results of this analysis show that the LPC degradation is the one which causes the greatest increase in fuel burn for the baseline trajectory. Following the same

procedure as with the clean engine, the optimum trajectory in terms of fuel burn has been obtained for each case of degradation. This study shows the benefits of flying the optimum trajectory instead of the baseline one, quantifying the reduction in fuel burn. Meanwhile, an assessment of engine life has been done using the lifing module of the Economics Model. The purpose of this step was to determine the degradation of which component causes the greatest effect on the engine life. The life of the engine is determined with respect to the life of the most demanding component, the HPT which operates at the highest temperatures. The results of the study show that the degradation in HPC shortens the most the engine life.

Appendix 4

Civil aircraft trajectory analyses: Impact of engine degradation on fuel burn and emissions

Benjamin Venediger: MSc Thesis
Department of Power and Propulsion
Cranfield University

Abstract

Commercial aviation and air traffic is still expected to grow by 4-5% annually in the future and thus the effect of aircraft operation on the environment and its consequences for the climate change is a major concern for all parties involved in the aviation industry. One important aspect of aircraft engine operation is the performance degradation of such engines over their lifetime while another aspect involves the aircraft flight trajectory itself. Therefore, the first aim of this work is to evaluate and quantify the effect of engine performance degradation on the overall aircraft flight mission and hence quantify the impact on the environment with regards to the following two objectives: fuel burned and NOx emissions. The second part of this study then aims at identifying the potential for optimised aircraft flight trajectories with respect to those two objectives. A typical two-spool high bypass ratio turbofan engine in three thrust variants (low, medium and high) and a typical narrow body single-aisle aircraft similar to the A320 series were modelled as a basis for this study. In addition, an existing emissions predictions model has been adapted for the three engine variants. Detailed parametric and off-design analyses were carried out to define and validate the performance of the aircraft, engine and emissions models. The obtained results from a short and medium range flight missions study showed that engine degradation and engine take-off thrust reduction significantly affect total mission fuel burn and total mission NOx emissions (including take-off) generated. A 2% degradation of compressor, combustor and turbine component parameters caused an increase in total mission fuel burn of up to 5.3% and an increase in NOx emissions of up to 5.9% depending on the particular mission and aircraft. However, take-off thrust reduction led to a decrease in NOx emissions of up to 41% at the expense of an increase in take-off distance of up to 12%. Subsequently, a basic multi-disciplinary aircraft trajectory optimisation framework was developed and employed to analyse short and medium range flight trajectories using one aircraft and engine configuration. Two different optimisation case studies were performed: (1) fuel burned vs. flight time and (2) fuel burned vs. NOx emitted. The results from a short range flight mission suggested a trade-off between fuel burned versus flight time and showed a fuel burn reduction of 3.0% or a reduction in flight time of 6.7% when compared to a “non-optimised” trajectory. Whereas the optimisation of fuel burn versus NOx emissions revealed those objectives to be non-conflicting. The medium range mission showed similar results with fuel burn reductions of 1.8% or flight time reductions of 7.7% when compared to a “non-optimised” trajectory. Accordingly, non-conflicting solutions for fuel burn versus NOx emissions have been achieved. Based on the assumptions introduced for the trajectory optimisation

analyses, the identified optimised trajectories represent possible solutions with the potential to reduce the environmental impact. In order to increase the simulation quality in the future and to provide more comprehensive results, a refinement and extension of the framework also with additional models taking into account engine life, noise, weather or operational procedures, is required. This will then also allow the assessment of the implications for airline operators in terms of Direct Operating Costs (DOC). In addition, the degree of optimisation could be improved by increasing the number and type of optimisation variables.

Appendix 5

Effect of engine degradation on engine and aircraft performance

Subramanian Chandran: MSc Thesis
Department of Power and Propulsion
Cranfield University

Abstract

In the recent years, tremendous growth of economy and living standard of peoples in the developed and developing countries has witnesses a significant increase in civil aviation industries which led to a raise in the number of flights undertaken globally. Due to the increase flight operation which directly related to increase pollution in environment, noise and fuel burn by the aircraft. It has been predicted that in future growth of aviation industry will be larger and have more impact to the society. In order to reduce and control the environmental pollution caused by the aviation industries strict rules was introduced by ICAO and EU. In order to control the environmental problems EU forms a group of council which led to the formation of ACARE (Advisory Council for Aeronautical Research in Europe) and also introduced different programs within the purview of framework programme of the EU. Clean Sky JTI being one such initiative and main of the project is to speed up the new greener aircraft design to reduce the environmental pollutions through its Integrated Technology Demonstrators (ITD). The System for Green Operation ITD (Clean Sky), the main aim of this work is to carry out a multi-objective optimisation for aircraft trajectory in order to minimize the fuel burn, emission and noise of the aircraft. The main objective of this thesis is to assess a parametric analysis of aircraft trajectory in cruise condition to find out minimum fuel burn and in addition to that the finding maximum Life of an engine on optimum aircraft trajectory at cruise condition both objectives are very important aspect to consider for decreasing the operating and maintenance costs. In order to achieve the above goals, TURBOMATCH is used to simulate the engine performance model for design point and for the off-design point. HERMES is used find the fuel burn and time for the given baseline trajectory. And assessment of engine life has been done using Lifting model. A parametric analysis is done for aircraft trajectory optimization in order to find a optimum fuel burn and life of the engine at cruise condition. As a result of this parametric analysis study defines that under cruise condition of altitude 12000 meters and Mach number 0.75 the engine gives optimum fuel burn and life therefore operating and maintenance costs of the engine is reduced.